U.S. Department of Energy • Office of Science

JOURNAL OF UNDERGRADUATE RESEARCH

Volume V, 2005

Office of Science
U.S. DEPARTMENT OF ENERGY

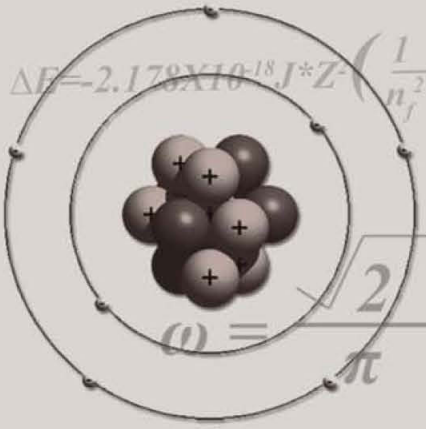

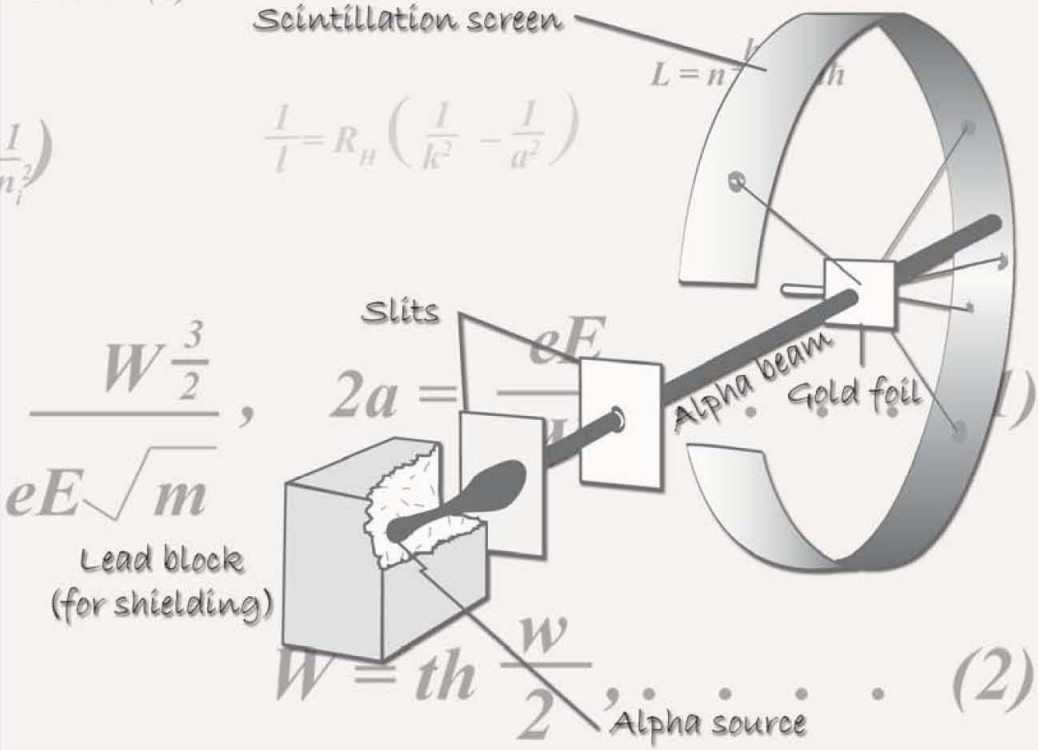

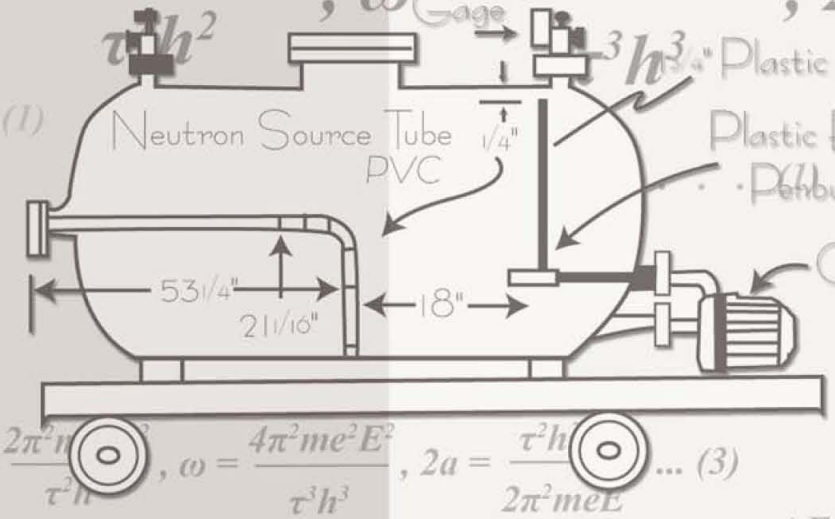

Understanding the Atom: Physics Past, Present, and Future

This year's cover for Volume 5 of the Journal of Undergraduate Research recognizes the "World Year of Physics" that celebrates the 100 years since Albert Einstein published three pivotal papers that have influenced the study and understanding of physics.

Rutherford's alpha beam experiment established the first model of the atom that distinguished between a dense, positively-charged "nucleus" and orbiting negatively-charged electrons. This schematic shows the layout of the experiment where alpha particles from a source inside a shielded lead block were directed in a beam towards a piece of gold foil. The surprising result was that some of the alpha particles deflected at large angles, almost coming directly back toward the source.

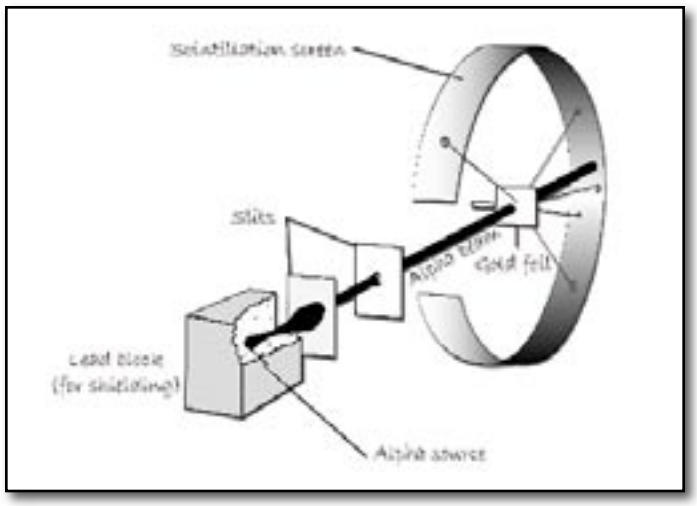

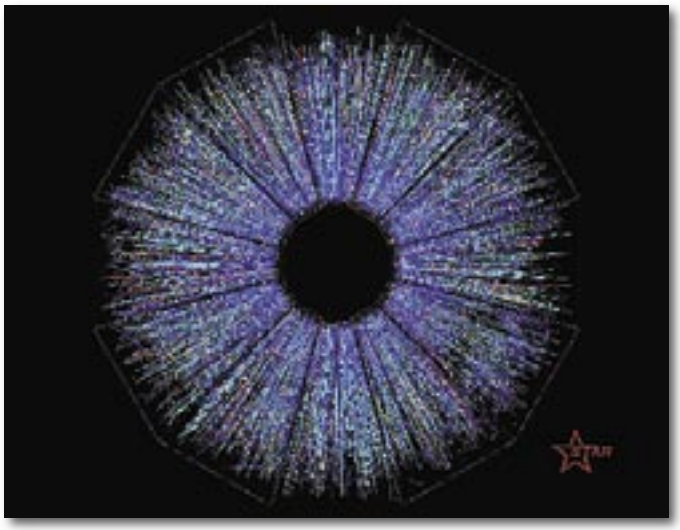

The Relativistic Heavy Ion Collider (RHIC) at the Department of Energy's Brookhaven National Laboratory (BNL) accelerates gold ions to speeds close to the speed of light and then allows them to collide. This image shows an end-view of a collision of two 30-billion electron-volt gold beams in the Solenoidal Tracker at the RHIC (STAR) detector. These experiments at BNL are searching for signatures of the form of matter that RHIC was designed to create – the quark-gluon plasma. Courtesy of Brookhaven National Laboratory-STAR Collaboration.

This image from the logbook of Dr. Ray Davis (2002 Nobel Laureate) depicts his sketch of a 500-gallon tank on a rail car with a solution of calcium nitrate in an experiment designed to detect solar neutrinos. The final experiment used a 100,000-gallon tank filled with perchloroethylene located deep beneath the earth in a former gold mine in Lead, South Dakota. This experiment led to the determination that neutrinos can change "flavors" as they travel from the sun to the earth. Courtesy of Brookhaven National Laboratory.

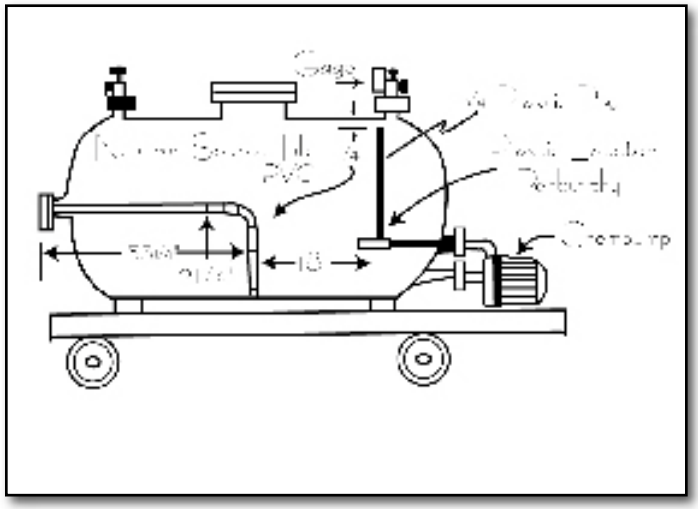

The equations in the background of the cover were derived by Niels Bohr in his paper titled, *On the Constitution of Atoms and Molecules*, published by Philosophical Magazine Series 6, Volume 26 in July 1913.

A NOTE FROM THE EDITOR:
AUDE SAPERE...DARE TO THINK INDEPENDENTLY

The earliest scientists I know of were Babylonians (probably preceded by the Sumerians in the same Fertile Crescent) who about 3,600 years ago carefully observed and charted the rising of celestial bodies. They then used these "star charts" to predict when to plant and harvest crops. Such predictions helped them establish their agriculture and their civilization. Similar progress occurred in the Yellow River Valley in ancient China. In the millennia since, the human race has steadily progressed in its understanding of nature. Looking back, the challenges that faced people eking out livings in a harsh and often unpredictable world left great opportunities for early scientists. Science would slowly take hold as it progressed in its ability to provide a level of predictability and improve the human condition.

The Babylonian star charts are an example of how early science was based on careful and direct observation of natural phenomena. If the Sumerians and Babylonians did not go far beyond the direct observation of nature, such was not the case with the Greeks, who would attempt to look beyond the human percepts and into what was not obvious. A mechanistic view of the universe began to unfold most notably from the early atomists, Leucippus and Democritus and in some sense was brought to full light by Isaac Newton. Rapid growth in scientific knowledge would be seen in the era following Galileo, who is often cited as the first modern scientist. I suppose this is largely founded on his adherence to verifying theory with experimentation.

Modern scientific process is now fully entrenched in this experimental principle and largely operates under the premise that by studying components of nature in isolation it can keep the complexity of nature from overwhelming the human intellect. It then can attempt to understand the whole from its understanding of the individual components. This sort of fragmentation has led to the divisions of scientific study and the branching of science into disciplines such as physics, chemistry, biology and the further divisions of each of these into a dizzying array of sub-disciplines. There are signs of reunification in science and there are certain scientists who by their title reveal this trend…"biophysicists" for example.

"The fragmentation of knowledge that until recently has been successful in explaining certain natural phenomena needs to change..."

The science of a hundred years from now will likely look as different as today's science does from a hundred years past. It is difficult to comprehend how far we have progressed in such a short period of time. The 2005, World Year of Physics is a celebration of a time that saw the birth and maturation of the profound descriptions of the nature of the universe expressed by both Relativity and Quantum Mechanics. Quantum

Mechanics was the first modern scientific theory to challenge the deeply entrenched notion of the mechanistic nature of the universe. During this era, the progress in all the natural sciences has been more than most could have imagined. It has allowed the human species to explore the depths of our oceans, discover the limits of outer space, and to grow its population to over 6 billion.

"Humans now have such an impact on the surface geology of the earth, that they can be considered a major geological force."

Humans now have such an impact on the surface geology of the earth, that they can be considered a major geological force. At the same time, the ability of human intellect to explain its effect on the planet as a species is quite limited. The uncertain ramifications of global warming illustrate this limitation. Furthermore, sustaining human life at the levels of comfort that much of the western world has grown to enjoy and the remaining world desires will be increasingly difficult. Providing enough clean energy for a population that will likely reach 9 billion by the next century is an immense challenge without considering the numerous other daunting problems that could equally compromise the human condition.

The fragmentation of knowledge that until recently has been successful in explaining certain natural phenomena needs to change for us to fully overcome these challenges and will likely be a growing obstacle to our understanding of the complex nature of our world. It will take more than scientists working together. It will take them thinking differently in a less compartmentalized fashion.

Although physicists have realized the limitations of a mechanistic view of the universe, where even knowing what each of the variables in a system is doing does not allow one to fully predict the outcome, biologists still approach their science largely from a mechanistic point of view. We might find that the great advancement of biological sciences will be by taking example from the physicists and establishing some sort of theory that describes living systems in a non-mechanistic fashion. This is pure speculation, but the point is that great advancements will demand new thinking and for such it will need new and fresh thinkers.

Peter Faletra, Ph.D.

Editor-In-Chief

TABLE OF CONTENTS

Selected Student Papers:

Selected Student Papers Continued:

GROWING SCIENTISTS IN THE LAB

Science cannot be learned completely from books, a set of courses, or a full undergraduate curriculum. Science has to be performed to learn it. It is true that the formalism and the foundation of science must be learned from a curriculum by anyone aspiring to work in the field. But, the excitement and captivation of science are felt best in the research laboratory. Research is the key element of a graduate degree in science or engineering, but even at the undergraduate level I am convinced that research is crucial for understanding the direction of science and appreciating the intellectual challenge that it brings.

"...the excitement and captivation of science are felt best in the research laboratory"

We live in a society that depends on rapid development of new technological tools to fuel a large part of our economic expansion. Today's average automobile contains more computer control than the first manned module that landed on the moon in 1969. The materials available now for our computers, cars, appliances, fuel cells, and such have specialized tailored properties that were thought impossible a few decades ago. But, our world leadership in new technologies is threatened by the education of too few scientists and engineers in the U.S. For example, a few years ago the number of undergraduate physics degrees in our country had shrunk to a pre-Sputnik low. We have built and maintained our world dominance in technology development in part by bringing the best and the brightest from around the globe to our graduate schools and then to careers in our country. But, the post-9/11 restriction on visas is threatening to disrupt a sufficient flow of technical talent to our shores.

"...our world leadership in new technologies is threatened by the education of too few scientists and engineers in the U.S."

The United States needs a rebirth of widespread student interest in fields of science and engineering. Yes, science can be a challenging course of study, but it is also a challenge to build a viable law practice or dig out of debt to establish a medical practice. I am convinced there is vast opportunity for trained scientists and engineers in our country, sometimes in fields that seem far from the classical ones. Undergraduate laboratory research can effectively help students appreciate more fully the beauty of science and capture their interest in building a career in science. That worked for me, as the chance to do research at my small college convinced me that this was the form of intellectual endeavor that would define my career. One of our top researchers at the Oak

Ridge National Laboratory came here as an undergraduate, became captivated by research, then received his doctorate from Yale, and returned here to lead our program in experimental nuclear astrophysics.

The undergraduate research internships supported by the Department of Energy Office of Science provide to students wonderful opportunities for a semester or a summer of research at a National Laboratory. Our National Labs are very special places that emphasize interdisciplinary research usually focused on the country's biggest technical challenges. We Americans have many questions about the future supply of energy, change of the global climate, realization of an economy based on nanotechnologies, application of genome science to the development of new drugs to cure disease on a large scale, and the next generation of clean, safe, and fuel-efficient autos. Undergraduates become involved in research programs in such areas at National Labs, and in so doing they catch the excitement of contributing to important areas of fundamental and applied science while also preparing themselves for careers. What an opportunity for the student and what a benefit for the country.

Lee L. Riedinger

Associate Laboratory Director for University Partnerships

Oak Ridge National Laboratory

AMES LABORATORY

Scientists at the Department of Energy Office of Science's Ames Laboratory seek solutions to energy-related problems through the exploration of chemical, engineering, materials and mathematical sciences, and physics.

Established in the 1940s with the successful development of the most efficient process to produce high-purity uranium metal for atomic energy, Ames Lab now pursues much broader priorities than the materials research that has given the Lab international credibility. Responding to issues of national concern, Lab scientists are actively involved in innovative research, science education programs, the development of applied technologies and the quick transfer of such technologies to industry. Uniquely integrated within a university environment, the Lab stimulates creative thought and encourages scientific discovery, providing solutions to complex problems and educating tomorrow's scientific talent.

Ames Laboratory is located in Ames, Iowa, on the campus of Iowa State University. Iowa State's 2,000-acre, park-like campus is home to approximately 25,000 students. Ames is approximately 30 minutes north of Des Moines, Iowa's capital city.

ARGONNE NATIONAL LABORATORY

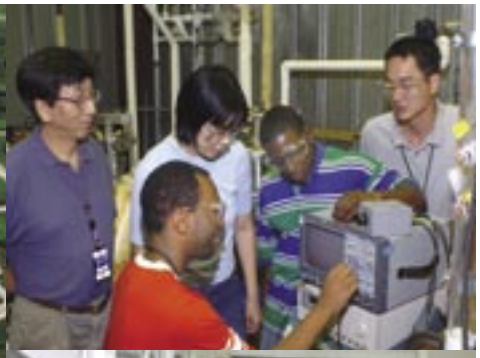

Argonne National Laboratory descends from the University of Chicago's Metallurgical Laboratory, part of the World War Two Manhattan Project. The laboratory has about 2,900 employees, including about 1,000 scientists and engineers. Argonne occupies 1,500 wooded acres in DuPage County, Il about 25 miles southwest of Chicago's Loop. Argonne research falls into broad categories:

- Basic science seeks solutions to a wide variety of scientific challenges. This includes experimental and theoretical work in biology, chemistry, high energy and nuclear physics, materials science and mathematics and computer science.
- Scientific facilities help advance America's scientific leadership and prepare the nation for the future. These facilities are used by scientists thousands of scientists and students from the U.S. and abroad. The laboratory is also home to the Advanced Photon Source, the Center for Nanoscale Materials, the Intense Pulsed Neutron Source, and the Argonne Tandem Linear Accelerator System.
- Energy resources programs help insure a reliable supply of efficient and clean energy for the future. Argonne scientists and engineers are developing advanced batteries and fuel cells, as well as advanced electric power generation and storage systems.

- Environmental management includes work on managing and solving the nation's environmental problems and promoting environmental stewardship.
- National Security has increased in significance in recent years for the nation and for Argonne research. Argonne capabilities developed over the years for other purposes are helping counter the threats of terrorism.

Argonne's Division of Educational Programs provides workforce development for faculty and students from universities to regional K-12 schools.

BROOKHAVEN NATIONAL LABORATORY

Established in 1947, Brookhaven National Laboratory is a Department of Energy, Office of Science multidisciplinary laboratory managed by Brookhaven Science Associates, a company founded by Battelle and Stony Brook University. Home to six Nobel Prizes, Brookhaven conducts research in the physical, biomedical, and environmental sciences, as well as in energy technologies and national security.

Located on a 5,300-acre site on eastern Long Island, Brookhaven builds and operates major scientific facilities available to university, industry and government researchers. Among those facilities are the world's newest accelerator for nuclear physics research, the Relativistic Heavy Ion Collider (RHIC), and the National Synchrotron Light Source (pictured here) where approximately 2,500 researchers use beams of light, from x-rays to ultraviolet and infrared, to study materials as diverse as computer chips and proteins. In the near future, the Center for Functional Nanomaterials will be built at Brookhaven, one of five proposed Department of Energy centers where researchers will study materials on the scale of a billionth of a meter, or only a few atoms.

A wide variety of both basic and applied research is conducted at Brookhaven. For instance, scientists are investigating the building blocks of matter using RHIC, the roots of drug addiction and brain metabolism using positron emission tomography, the effects of space radiation on astronauts using the newly built NASA Space Radiation Laboratory, and the effects of increased carbon dioxide in ecosystems. Brookhaven researchers also develop new technologies as varied as detectors for national security and oil burners with improved efficiency.

FERMI NATIONAL ACCELERATOR LABORATORY

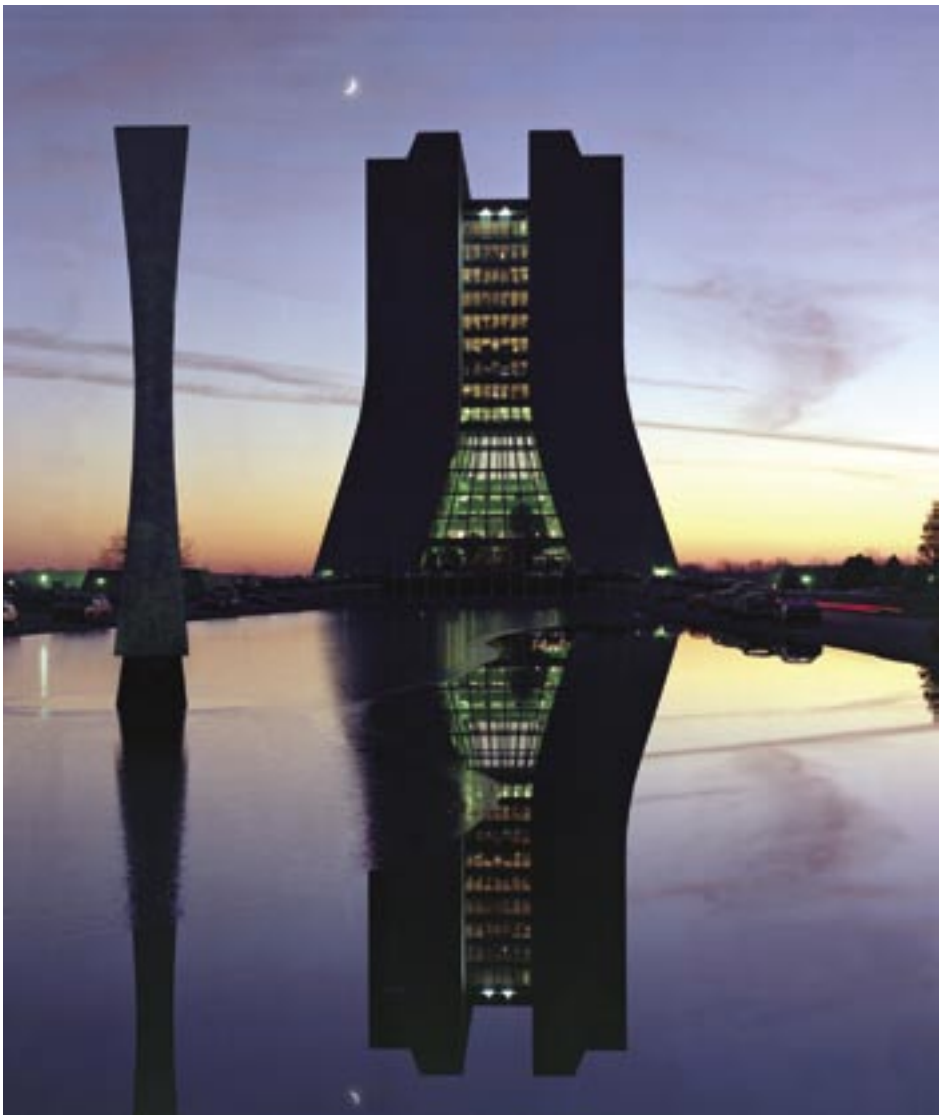

Fermi National Accelerator Laboratory (Fermilab) is one of the world's foremost laboratories dedicated to high energy physics research. The laboratory is operated for the Department of Energy, Office of Science by a consortium of 90 leading research-oriented universities primarily in the United States, with members also in Canada, Italy and Japan.

Fermilab is located on a 6,800 acre site about 35 miles west of Chicago. Fermilab is home to the Tevatron, the world's highest energy particle accelerator. Around its four-mile circumference 1,000 superconducting magnets are cooled by liquid helium to -268ºC. Two major components of the Standard Model were discovered at Fermilab—the bottom quark and the top quark—and the first direct observation of the tau neutrino, the last fundamental particle to be observed, was at Fermilab.

IDAHO NATIONAL LABORATORY

In operation since 1949, the Idaho National Laboratory (INL) is a science-based, applied engineering national laboratory dedicated to supporting the U.S. Department of Energy's (DOE) missions in nuclear and energy research, science, and national defense. The INL offers research opportunities in Generation IV Nuclear Systems, National Security, Advanced Computing and Collaboration, Subsurface Science, Biotechnology, and Engineering.

The laboratory is administered by DOE's Office of Nuclear Energy, Science and Technology. The INL is a major contributor to the international efforts to design Generation IV nuclear energy systems and advanced proliferation-resistant fuel cycle technology. It is home to one of the largest concentration of technical professionals in the northern Rocky Mountain region.

Located in southeast Idaho, the INL covers 890 miles of the Snake River Plain between Idaho Falls and Arco, Idaho. Offices and laboratories are also in the city of Idaho Falls (population 50,000), located about two hours from Grand Teton and Yellowstone national parks and other areas offering prime recreational opportunities.

LAWRENCE BERKELEY NATIONAL LABORATORY

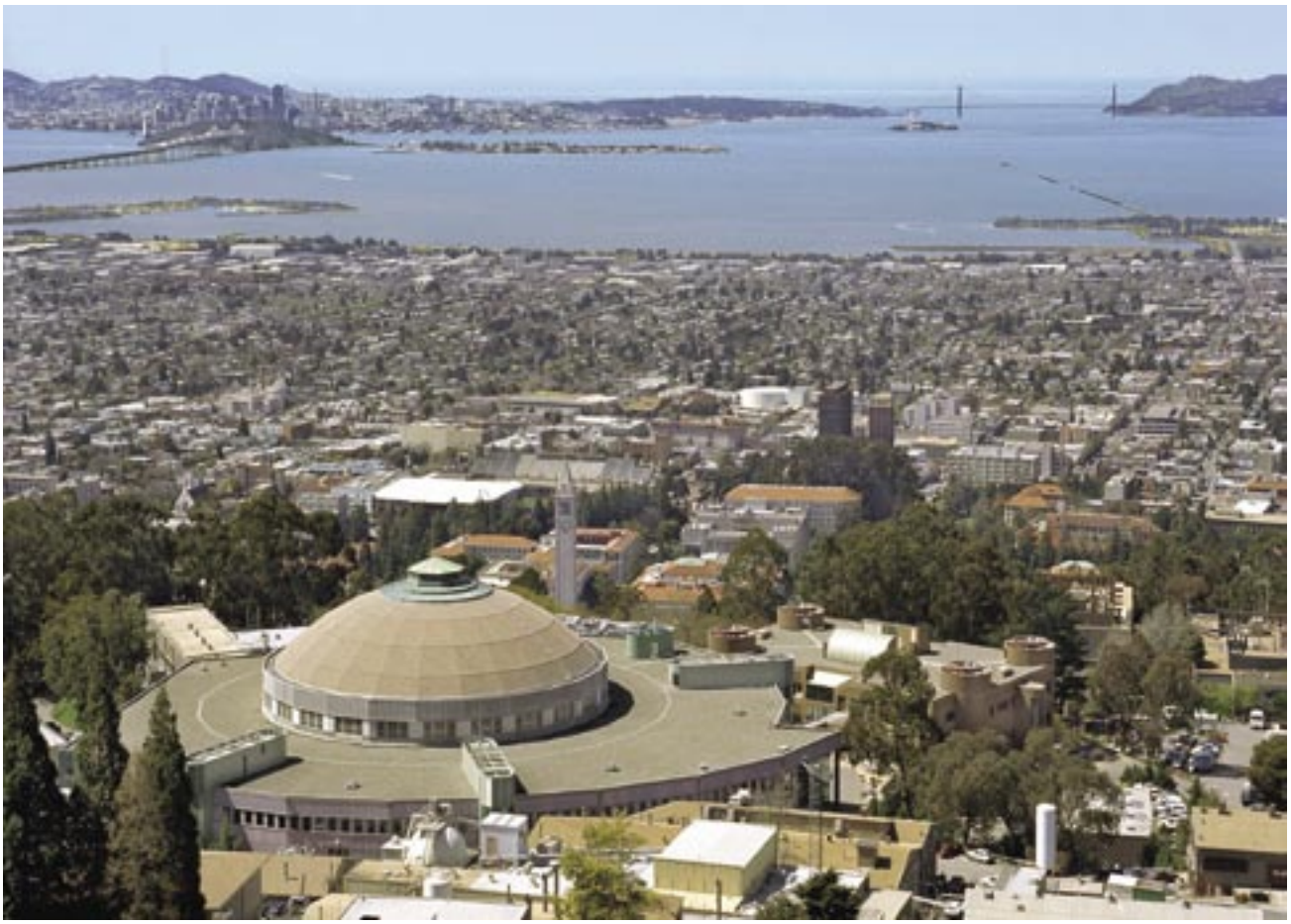

Lawrence Berkeley National Laboratory's research and development includes new energy technologies and environmental solutions with a focus on energy efficiency, electric reliability, carbon management and global climate change, and fusion. Frontier research experiences exist in nanoscience, genomics and cancer research, advanced computing, and observing matter and energy at the most fundamental level in the universe.

Ernest Orlando Lawrence founded the Berkeley Lab in 1931. Lawrence is most commonly known for his invention of the cyclotron, which led to a Golden Age of particle physics—the foundation of modern nuclear science—and revolutionary discoveries about the nature of the universe. Berkeley Lab's Advanced Light Source is its premier national user facility centrally located on the lab site overlooking the San Francisco Bay.

LAWRENCE LIVERMORE NATIONAL LABORATORY

Lawrence Livermore National Laboratory (LLNL) is a premier applied science laboratory that is part of the National Nuclear Security Administration (NNSA) within the Department of Energy (DOE). With more than 8,000 employees, LLNL is located on a one-square-mile site in Livermore, CA. A larger (10 square miles) remote explosives testing site (Site 300) is situated 18 miles to the east.

LLNL is managed by the University of California (UC) for the National Nuclear Security Administration (NNSA) within the Department of Energy (DOE). Being part of the University helps foster intellectual innovation and scientific excellence. This University connection allows LLNL to recruit and retain a diverse world-class workforce and partner with the UC's extensive research and academic community. These factors are essential to sustaining the laboratory's scientific and technical excellence.

Lawrence Livermore National Laboratory (LLNL) is a national security laboratory with responsibility for ensuring that the nation's nuclear weapons remain safe, secure, and reliable. LLNL also applies its special expertise and multidisciplinary capabilities to prevent the spread and use of nuclear and other weapons of mass destruction and strengthen homeland security.

LLNL has pioneered the application of many technologies-from high-performance computers to advanced lasers-to meet national security needs. Today, the special capabilities developed for our stockpile stewardship and nonproliferation activities enable us to also meet enduring national needs in conventional defense, energy, environment, biosciences, and basic science. Research programs in these areas enhance the competencies needed for the laboratory's national security mission.

LOS ALAMOS NATIONAL LABORATORY

The Los Alamos National Laboratory (LANL), located in the Jemez Mountains of northern New Mexico, offers the opportunity for students to work at a multi-disciplinary, world-class research facility while enjoying a truly unique environment. Long known for its artistic community, northern New Mexico also offers a variety of exciting outdoor recreational opportunities, including rock climbing and hiking in the adjacent mountains and canyons, proximity to the Rocky Mountains, and exceptional skiing opportunities at many nearby locations.

We offer a diverse research experience for undergraduate and graduate students as a means of assuring the continued vibrancy of the science, engineering, and technology at the laboratory. Serve your internship with us and you will have the opportunity to work in a team environment with some of the world's top scientists and engineers on critical issues involving our national security, environment, infrastructure, and security. We offer internship opportunities in areas that include: Biology, Chemistry, Computer Science, Physics, Mathematics, Materials Science, Environmental Science, and Engineering: Chemical, Civil, Computer, Electrical, Mechanical, Nuclear, Software.

If you are a problem solver and independent thinker, a team player, a good communicator, like a hands-on approach, and are self-motivated, we offer you the challenge of an internship at Los Alamos National Laboratory.

NATIONAL RENEWABLE ENERGY LABORATORY

The National Renewable Energy Laboratory (NREL) is the Department of Energy's primary national laboratory for renewable energy and energy efficiency research and development. From harvesting energy from the sun and wind, to advancing automotive systems, to developing biodegradable plastics form corn stalks, NREL develops renewable energy and energy efficiency technologies and practices, advances related science and engineering, and transfers knowledge and innovations to address the nation's energy and environmental goals. NREL is home to three nationals centers of excellence: the National Center for Photovoltaics, the National Bioenergy Center and the National Wind Technology Center.

NREL has been awarded 37 R& D awards with two being awarded in 2004. NREL's research programs include basic energy research, photovoltaics, wind energy, building technologies, biomass power, biofuels, fuels utilization, solar industrial technologies, solar thermal electric, hydrogen, geothermal power, superconductivity, economic and policy analysis of renewable technologies, international development of renewable energy, and advanced vehicle technologies. *Research and Development*, *Discover*, *Scientific American* and *Popular Science* magazines have ranked many of NREL's research achievements among the nation's most significant technical innovations. NREL was recognized as one of the "Scientific American 50" for their contribution to science and technology.

Innovative, challenging and dynamic—that's our culture. If you are interested in a research internship with an institution that believes creativity and individual uniqueness are at the core of our success, then explore your options at: www.nrel.gov. We value intern talent that adds to the rich pool of research findings produced by NREL each year. Intern accomplishments include:

- More than 11 students have been selected by the Office of Science to present major NREL research at the AAAS
- More than 50 past student interns have been hired on to join the NREL family
- Teacher researchers have produced over 50 renewable energy lessons for the classroom
- NREL's Office of Education partners with over 75 universities throughout the nation

NREL's main 327-acre site is in Golden, Colorado, just west of Denver. The Laboratory also operates the National Wind Technology Center on 307 acres about 20 miles north of Golden, adjacent to the Department of Energy's Rocky Flats Environmental Test Site. We are an equal opportunity employer committed to diversity.

OAK RIDGE NATIONAL LABORATORY

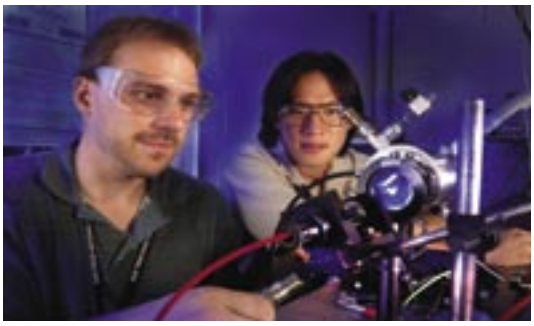

Oak Ridge National Laboratory is the Department of Energy's largest science and energy laboratory. Managed since April 2000 by a partnership of the University of Tennessee and Battelle, ORNL was established in 1943 as a part of the secret Manhattan Project to pioneer a method for producing and separating plutonium. More than 60 years later, ORNL's mission is to conduct basic and applied research that provides innovative solutions to complex problems.

ORNL, with funding that exceeds $1 billion, has a staff of more than 3,800 and approximately 3,000 guest researchers who spend two weeks or longer each year in Oak Ridge. The laboratory's six major scientific competencies, in support of DOE's Office of Science, include neutron science, energy, high performance computing, complex biological systems, advanced materials and national security.

ORNL is in the final stages of a $300 million project to provide a modern campus for the next generation of great science. A unique combination of federal, state and private funds is building 13 new facilities. Included in these new facilities will be the Functional Genomics Center, the Center for Nanophase Materials Science, the Advance Materials Laboratory, and the joint institutes for Computational Science, Biological Science and Neutron Science. ORNL has been selected as the site of the Office of Science's National Leadership Computing Facility for unclassified high-performance computing. On budget and on schedule for completion in 2006, the $1.4 billion Spallation Neutron Source will make Oak Ridge the world's foremost center for neutron science research.

UT-Battelle has provided more than $6 million in support of math and science education, economic development and other projects in the greater Oak Ridge region.

PACIFIC NORTHWEST NATIONAL LABORATORY

Pacific Northwest National Laboratory (PNNL) is a multi-purpose national laboratory dedicated to delivering innovative science-based solutions to some of the nation's most pressing problems. PNNL conducts fundamental and applied research to address important issues including securing our homeland, reducing our dependence on foreign oil, transforming the energy system, making information access easier, and protecting our natural resources.

PNNL's facilities form a world-class campus, including many laboratories recognized as best-in-class for many research areas. With an international reputation for studies in chemistry, biology, computer sciences, and a wide range of other fields, award-winning PNNL researchers rapidly translate theory into concrete solutions. Many of the laboratory's technologies have been developed into common consumer and industrial products including the compact disc (CD).

The Laboratory consistently attracts some of the world's leading scientific talents shaping the future of science through a variety of on-site educational programs. As mentors and research partners, the laboratory's staff trains young scientists and engineers to become tomorrow's inventors. Student research opportunities at PNNL include appointments in atmospheric science and global change, computational sciences, experimental chemistry, marine sciences, molecular biology, environmental studies, remediation, environmental microbiology, wildlife and fisheries biology, materials research, process science and engineering, economics and political science.

Located in southeastern Washington near the base of the Blue Mountains and the confluence of the Columbia, Snake and Yakima rivers, PNNL staff enjoy year around recreation, locally-produced fine wines, and the community's commitment to the arts.

PRINCETON PLASMA PHYSICS LABORATORY

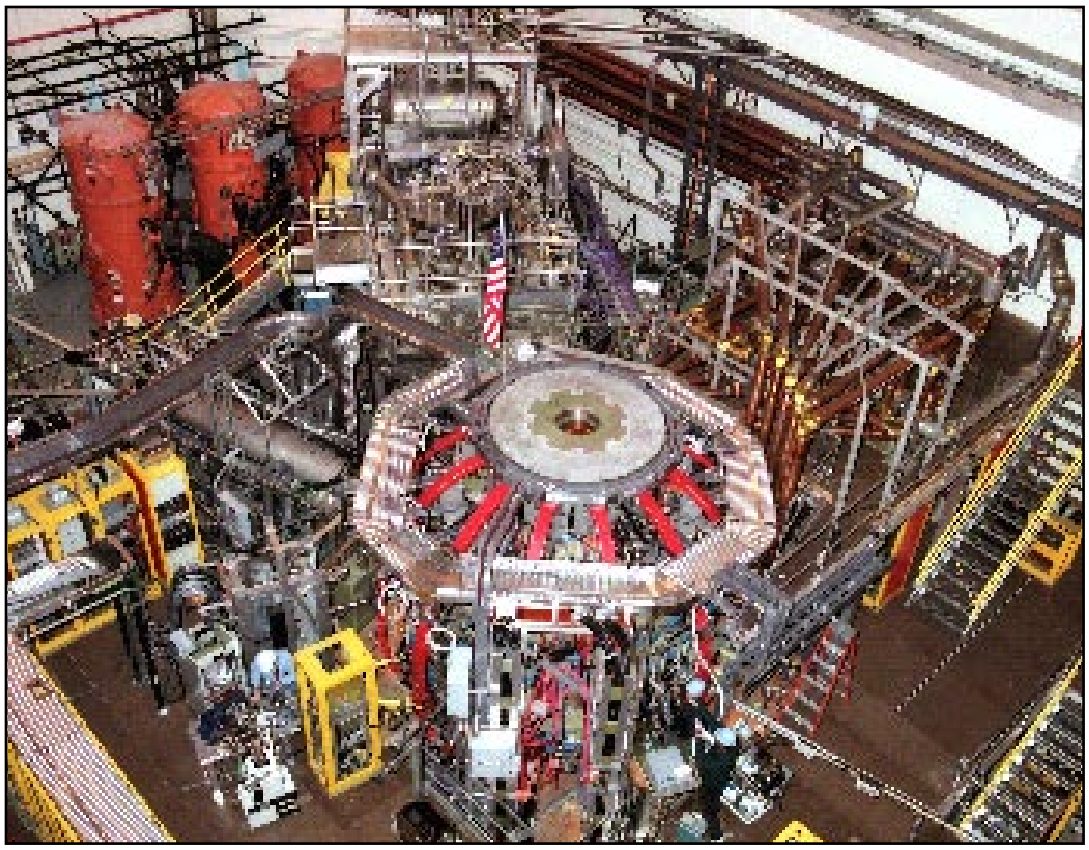

The world's reliance on fossil fuels is imperiling our environment. Fusion, the energy source of the sun and the stars, offers an inexhaustible alternative. A fusion-powered electric generator would not produce hydrocarbon emissions, greenhouse gases, or long-lived radioactive waste; nor would it emit chemicals that cause acid rain. Consequently, the U.S. Department of Energy (USDOE) Office of Science has made the development of commercial fusion power one of its highest priorities.

USDOE's Princeton Plasma Physics Laboratory (PPPL) is one of the world's leading facilities for fusion R&D. Currently the laboratory operates the National Spherical Torus Experiment (pictured above) and is designing the National Compact Stellarator Experiment, both use magnetic fields to confine hot ionized gas (plasma) that serves as the fusion fuel. PPPL's theoretical physicists are developing computational physics models that can predict how various plasma configurations will perform, saving time and money.

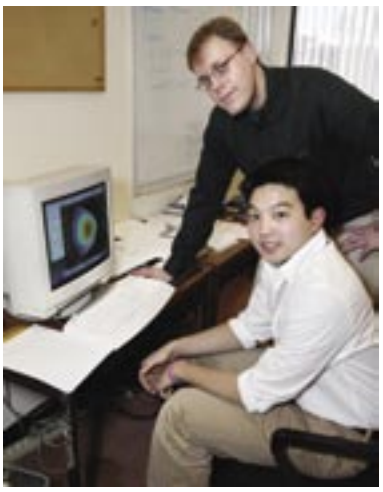

PPPL experimental physicists collaborate with their colleagues worldwide in a free, mutually beneficial, exchange of information. Princeton researchers and engineers are using knowledge and skills gained in fusion research to solve other problems, including the development of plasma-based propulsion systems for space vehicles, studies of plasma phenomena that occur in the sun's corona and the earth's magnetosphere, and research on plasma sterilization of plastic food and beverage containers. PPPL is located about three miles from Princeton University's main campus in Princeton, NJ.

STANFORD LINEAR ACCELERATOR CENTER

The Stanford Linear Accelerator Center (SLAC) is one of the world's leading fundamental science research laboratories. SLAC designs, constructs and operates state-of-the-art particle accelerators and related experimental facilities used in physics studies probing the fundamental forces and structure of matter. The Stanford Synchrotron Radiation Laboratory (SSRL), a premier national user facility at SLAC, enables research requiring ultra high-intensity x-ray beams for molecular and atomic scale studies in physics, biology, chemistry, medicine, and environmental science. The Linac Coherent Light Source, a facility to provide even more intense x-ray capability is under development.

The BABAR experiment, an international collaboration investigating matter/anti-matter asymmetry, is the current focus of the high-energy physics program. In addition a vigorous R&D program is focused on development of the Next Linear Collider, as part of a world-wide effort for this future facility for high energy physics. The Kavli Institute for Particle Astrophyics and Cosmology, which began operation this year, is a joint SLAC/Stanford program with both experimental and theoretical activity at SLAC. SLAC is operated by Stanford University for the Department of Energy, Office of Science and is located at Stanford University, about 40 miles south of San Francisco, California.

THOMAS JEFFERSON NATIONAL ACCELERATOR FACILITY

The Thomas Jefferson National Accelerator Facility (Jefferson Lab) is a U.S. Department of Energy, Office of Science national laboratory built for nuclear physics research located in Newport News, Virginia. As a user facility for university scientists worldwide, its primary mission is to conduct basic research that builds a comprehensive understanding of the atom's nucleus. With industry and university partners, it has a derivative mission as well: applied research for using Free-Electron Lasers based on technology the laboratory developed to conduct its physics experiments. As a center for both basic and applied research, Jefferson Lab also reaches out to help educate the next generation in science and technology.

Superconducting electron-accelerating technology makes the laboratory unique. Researchers use Jefferson Lab's Continuous Electron Beam Accelerator Facility (CEBAF)—the technology's first large-scale application anywhere—to conduct experiments. With high-energy electron beams from the accelerator, experimenters probe the subnuclear realm, revealing for the first time how quarks make up protons, neutrons, and the nucleus itself. Using this same superconducting electron-accelerating technology, Jefferson Lab and industry have constructed a laser of unprecedented power and versatility called a free electron laser. This laser offers unique capabilities for basic research and manufacturing processes.

Erik Garnett received his B.S. from the University of Illinois, Urbana-Champaign in chemistry in 2004. As an undergraduate, he worked on improving catalysts for direct methanol and formic acid fuel cells. Erik also was a member of the 2004 Big Ten Champion gymnastics team at Illinois. During the summers following his junior and senior years in college, he participated in the SULI program at NREL, first designing and testing a combinatorial electrochemical cell for corrosion research and second using inkjet printing of polymers for organic light emitting diodes (OLED). He presented the OLED work at the AAAS conference in 2005. Erik is currently pursuing his Ph.D. in chemistry at Cal Berkeley, where he is using inorganic nanowires to mimic the adhesion properties of gecko feet.

David S. Ginley is currently a Group Manager in Process Technology and Advanced Concepts at the National Renewable Energy Laboratory, leading activities in the applications of nanotechnology, organic electronics, transition metal oxides (ferroelectric materials, rechargeable Li batteries, and transparent conductors) and ink jet printing. He leads a team in the development of nanoparticle-based precursors to electronic materials, particularly as they apply to photovoltaic and optoelectronic technologies. Recent new activities include a program on combinatorial approaches to electronic materials and a program on polymer based photovoltaic cells and OLEDs. Over the past 25 years, he has been active in developing a basic understanding of the relationships between structure and the optoelectronic properties in a variety of materials. Dr. Ginley graduated from the Colorado School of Mines with a B.S. degree in Mineral Engineering Chemistry. He subsequently received a Ph.D. from MIT in inorganic chemistry, where he worked in inorganic photochemistry and in the emerging area of photoelectrochemistry.

ELECTRICAL AND MORPHOLOGICAL PROPERTIES OF INKJET PRINTED PEDOT/PSS FILMS

Erik Garnett, David Ginley

ABSTRACT

Organic solar cells and LEDs are becoming more popular because their low cost materials, potential manufacturability, and recent gains in efficiency make them feasible for widespread commercialization in the near future. One significant manufacturing problem, especially for OLEDs, is the cost associated with creating patterned devices with spatially non-specific deposition methods such as spincoating. Inkjet printing can remove this problem. In recent years, inkjet printed polyethylene(3,4-dioxythiophene)/ polystyrene sulfonate (PEDOT/PSS) has been incorporated into many organic devices to help charge transfer, but there has not been much research regarding the effect of different printing parameters on the electrical and morphological film properties. In this work, an atomic force microscope, four point probe, and Kelvin probe were used to study the effects of printing parameters on roughness, conductivity and workfunction. Inkjet printed PEDOT films were also compared to spincoated films to determine how the polymer deposition method affects the above properties. Generally, inkjet printing created rougher but more conductive films with a smaller workfunction. Additionally, it was demonstrated that the workfunction of PEDOT films could be tuned over a range of about 0.5 V by changing the solvent mixture or substrate surface pretreatment. All additives to the as received PEDOT/PSS suspension caused the workfunction to decrease. It was discovered that workfunction decreases as printing voltage increases, but the trend reverses after annealing the films. This phenomenon suggests that when DMSO interacts with PEDOT, the workfunction changes. Finally, the results support previous publications suggesting that DMSO increases conductivity through a screening effect and also by changing the distribution of PEDOT and PSS in the film.

INTRODUCTION

In the last several years, there has been increasing interest in organic electronics due to their low cost materials, high theoretical efficiencies, and potential manufacturability [1, 2]. Examples of organic devices range from capacitors and organic photovoltaics (OPV) to organic light emitting diodes (OLEDs)[3-5]. A recent review of manufacturing costs in organic electronics concluded that while organic devices may not become widespread in all areas of electronics, OLEDs and OPVs have enormous potential to penetrate their respective markets[2]. However, there are significant basic and manufacturing hurdles, particularly patterning issues, to overcome before organic devices can become widespread[2].

This paper reports on the use of inkjet printing as an alternative deposition technique to spincoating for OPVs and OLEDs. Even though spincoating is an inexpensive, fast and easy way to deposit

liquid precursors for organic devices, it has several major drawbacks. First, it wastes a large amount of the material. In any manufacturing process, it is preferable to waste as little as possible both for cost and disposal reasons. Perhaps a more pressing issue, is that spincoating is extremely non-specific. In other words, it is fine for coating entire surfaces, but it provides essentially no spatial resolution, which is a serious problem for electronics. Currently, lithography is used to preferentially remove the coating where it is not wanted, but this adds equipment and multiple steps to the manufacturing process, increasing cost. Also, as more complicated 3-D structured devices with more layers are required, it will become increasingly difficult to develop effective lithographic techniques. Inkjet printing has the potential to remove all of these disadvantages. It allows deposition only where desired, which minimizes wasted material and eliminates the need for extra lithographic steps. In theory, each layer of an organic device could be printed in rapid succession using different inkjet heads, which allows for effective large-scale production. Thus, inkjet printing offers a major advantage over other deposition techniques.

Contacting active polymer layers in organic opto-electronics is not a simple process and interfacial properties are critical to device performance[6]. The copolymer polyethylene(3,4-dioxythiophene)/polystyrene sulfonate (PEDOT/PSS) is currently one of the most used organic transparent conductors for making these contacts[7]. While inkjet printing has been used to deposit PEDOT/PSS for electronic devices, there has been no known study regarding the effect of inkjet printing on the electrical and morphological properties of PEDOT/PSS films[3-5, 7, 8]. This study examined the conductivity, surface roughness, and workfunction of inkjet printed PEDOT/PSS films in order to gain a better understanding of the effect of printing parameters such as solvent, temperature and voltage.

MATERIALS AND METHODS

For all experiments, the polymer Baytron P HCV2 from Bayer was employed as an aqueous suspension of PEDOT/PSS, which from now on will be referred to simply as PEDOT. It was printed both as received and diluted with various solvents. All dilutions were done by mass and for simplicity, when referring to the mass percent of PEDOT, we include the water contained in the Baytron suspension. The actual solid content in the aqueous suspension is 1.1-1.4% according to the manufacturer. Ethyl alcohol (ethanol) was 190 proof general use HPLC-UV grade from Pharmco; dimethyl sulfoxide (DMSO) was B&J brand high purity solvent from American Scientific; the surfactant used (only where specifically mentioned) was Surfynol 2502 from Air Products. Solutions were filtered with the smallest nylon filter for which the suspension remained stable, either 0.2, 0.45 or 2.7 μm, before being used for printing to avoid clogging the inkjet head. The piezoelectric inkjet head, Teflon tubing, connectors, and holder were supplied by MicroFab and controlled by a Gateway Pentium III computer using LabView. The substrates were Fisherbrand plain glass microslides and were translated using a Newport X-Y stage controlled by a Newport Universal Driver programmed in LabView. Substrates were pre-cleaned using either a water and ethanol rinse, or a 10 min sonication in isopropanol followed by oxygen plasma cleaning for 5 minutes at about 157 watts power and approximately 0.57 torr oxygen pressure. Films were printed within a few hours of the cleaning procedure. Printing temperatures refer to the metal heating element directly below the substrate. Since glass is not a good thermal conductor, the actual substrate surface could be significantly lower than the programmed temperature. However, for all experiments substrates were placed on the heating element several minutes before printing in an attempt to produce consistent results.

Sheet resistances were measured using a Signatone four point probe connected with a Keithley programmable current source and system DMM. Film thickness was determined using a Dektak profilometer and surface roughness was determined using a Park Scientific atomic force microscope (AFM) with a 100 μm stage in contact mode. The relative workfunction of various films were compared by measuring their contact potential difference (CPD) with a McAllister Technical Services KP6500 Kelvin probe. A more negative contact potential difference translates to a larger workfunction (further from vacuum). The uncertainty in the CPD was set at 0.1 V, which was the maximum variation seen in the calibration Indium Tin Oxide (ITO) standard throughout the entire study.

RESULTS

Initial work focused on the printing of as received PEDOT to determine nominal thickness, roughness, and conductivity to use as control to compare against all other ink permutations. Compared to typical spincoated films (literature and this work), the initial inkjet printed films of PEDOT were significantly thicker and rougher but more conductive (Table 1). Since the desired thickness for the PEDOT layer in OLEDs and OPVs is between 80 and 150 nm all subsequent printing was performed with diluted solutions[9]. This also allowed us to easily see the effect of modifying the solvent and additives. As expected, film thickness scaled roughly to the PEDOT content. Diluting the PEDOT with water did not have a significant effect on the film's roughness or conductivity (Table 1).

DMSO was added to the PEDOT films to see if it would increase the conductivity. This effect has been recorded previously with spincoated films, although the mechanism is still under some debate [10, 11]. An addition of 5% DMSO increased the conductivity by approximately a factor of 10 (Table 1). Adding DMSO caused the ink droplets to bead up and made printing films difficult. This effect was thought to be from an increase in surface

Sample description	Thickness (nm)	Roughness (nm)	Conductivity (S/cm)
Inkjet Printed PEDOT	350	8-10	4.3
Spincoated PEDOT	160	3	3.1
Inkjet - 1:1 PEDOT/water	150	10-12	4.7
Spincoat – 1:1 PEDOT/water	60	3	3.7
Inkjet – 1:1 PEDOT/water +5% DMSO	300	Very rough and non-uniform	33
Inkjet – 1:1 PEDOT/water + 5% DMSO +1% Surfynol	300	31	51
Inkjet – 1:1 PEDOT/water + 1% DMSO +1% Surfynol	180	25-28	31

Table 1. Properties of various inkjet printed and spincoated films.

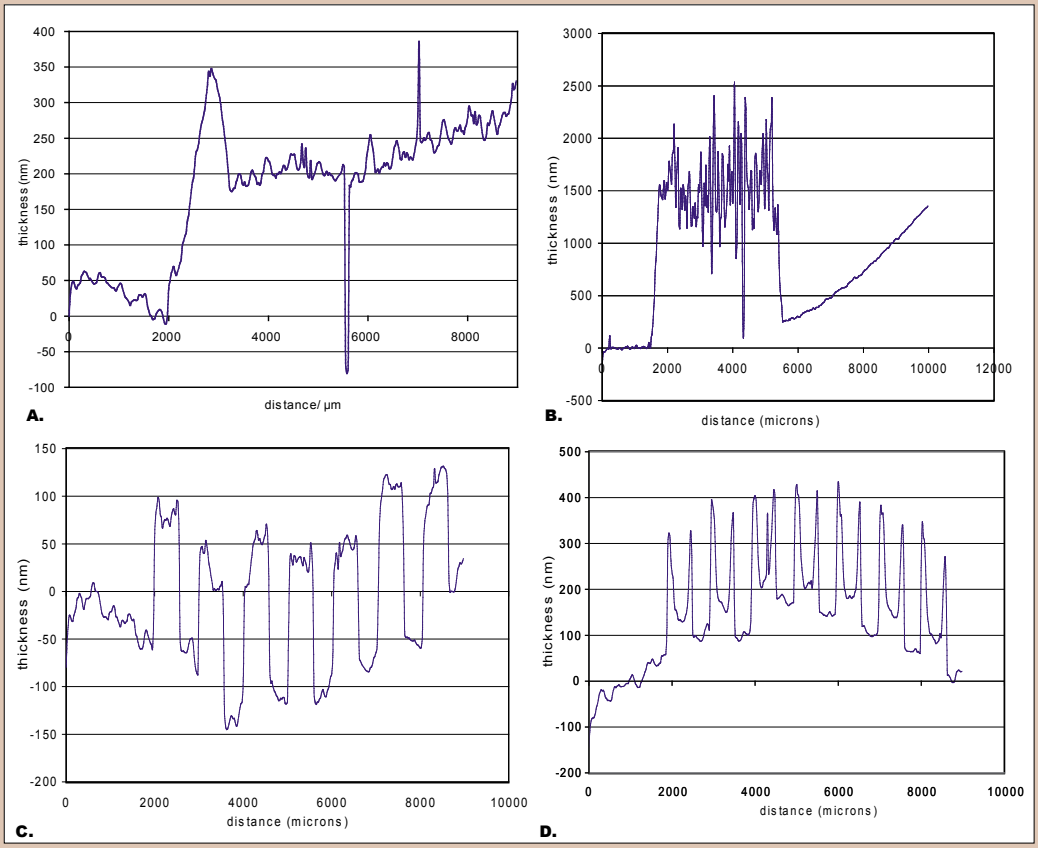

Figure 1. Profiles of PEDOT films printed at a) 50°C, b) 60°C and PEDOT lines printed at c) 50°C and d) 60°C.

tension, so the surfactant Surfynol 2502 was added to the ink to lower the surface tension and facilitate spreading. This addition not only created visibly more uniform and smoother films, but also increased conductivity by a factor of about 1.5 (Table 1). When Surfynol was used alone, it still increased conductivity, but also increased roughness (Table 1). Overall, adding DMSO also increased the roughness by about a factor of 2-3 (Table 1).

Several inkjet printing parameters were explored in an attempt to create smoother films. It was found that increasing the substrate temperature increased film roughness and thickness (Fig. 1). Increasing printing voltage also increased film roughness and thickness. The printing voltage could not be tested above 90V because of concerns about damaging the jet and below 30V most solutions would not print reliably. Printing frequency (drops per second) was held constant at 800 Hertz throughout all experiments and thus it is not known how that parameter affects film characteristics.

The workfunction of PEDOT films is an important consideration for making contact in organic electronic devices, so its sensitivity to solvent and printing parameter was explored. It was found that workfunction could be tuned over a range of about 0.5 V simply by adjusting the solvent mixture or changing the surface pretreatment (Fig. 2). There were several key results. First, pre-treating the glass surface with oxygen plasma increased the workfunction by a little over 0.1 eV. Secondly, inkjet printed PEDOT films had a smaller workfunction than spincoated films from the same solvent. Thirdly, addition of various solvents and surfactants including ethanol, DMSO, and Surfynol all reduced the workfunction. Fourth, for PEDOT diluted only with water, the printing voltage had no effect on workfunction, but when DMSO and Surfynol were added, as the printing voltage increased, the workfunction decreased (Fig. 3). After annealing the films containing DMSO and Surfynol, this effect reversed (Fig. 4). Finally, it was found that varying the DMSO concentration between 1 and 5% or varying the Surfynol concentration between 0.33 and 1% had no appreciable effect on the workfunction.

DISCUSSION AND CONCLUSION

From Table 1 it is clear that there is a difference between inkjet printed and spincoated PEDOT films. The difference in thickness can reasonably be attributed to the fact that all of the deposited material in inkjet printing remains on the substrate to form a film. A small increase in roughness may be expected from the longer drying time, which allows the material to agglomerate and couples to possible uneven solvent evaporation. However, a four-fold increase probably cannot be explained by this phenomenon alone. From microscope images, inkjet films had visible "pot holes" while individually printed lines did not. This suggests that subsequently printed lines somehow roughen the previous lines. We suspect that this is from micro-splashing that occurs when the droplets hit the substrate surface, although it may also be caused by the burst of air accompanying each droplet. As mentioned earlier, increasing voltage also increased roughness, which would be expected from either of the two previous explanations, because a higher printing voltage essentially translates to a faster droplet ejection. If splashing is the main problem, then incorporating highly dynamic surfactants with the ink should help reduce the roughness. This will be explored in future research. It is also possible that the above mentioned effects could be explained by charged droplet interactions. However, if this were the case, we would expect to see little or no difference in roughness between individually printed lines and printed films, which does not fit with the results.

The increased conductivity of the inkjet versus spincoated films is not entirely understood, but may be due to preferential polymer alignment or orientation that occurs with the longer drying time. Attempts to look at surface ordering of the films to confirm this hypothesis were inconclusive, but the smaller workfunction for

inkjet compared to spincoated films also supports a more ordered film. It is also possible that the coordination of PEDOT to its stabilizing copolymer PSS, or the distribution of the two is different in inkjet printed versus spincoated films, which may explain both the conductivity and workfunction effects. Several groups have reported that spincoated PEDOT/PSS films are phase separated with a lower ratio of PEDOT to PSS near the surface than in the bulk film [10, 12]. In particular, Jonsson et al. found that as they increased the surface ratio of PEDOT through addition of solvents, they also increased the conductivity[10]. It is possible that inkjet printing mixes the copolymers more effectively than spincoating, which would produce a higher surface ratio of PEDOT to PSS compared to the spincoated films. Compositional analysis of the films was not performed, but would be necessary to confirm this hypothesis. It is also possible that inkjet printing creates more ordered films by promoting the formation of micro-spheres representing different droplet domains. Upon annealing, these domains might be mixed or destroyed to create a more disordered film.

Figure 1 shows that there is a dramatic difference between PEDOT films printed at 50°C and 60°C. Looking at the single lines of PEDOT printed at the two temperatures, it is clear that the increased roughness and film thickness that accompany the higher temperature are caused by a difference in drying dynamics. At higher temperature, when the solvent evaporates more rapidly, suspended material conglomerates at the edges of the line. As the film is printed line by line, these differences become even more exaggerated leading to a very rough film. This supports that to achieve the smoothest film, it is preferable to maintain a low printing temperature or to control the solvent removal kinetics, such as with surfactants.

As noted earlier, the increase in conductivity of PEDOT films with the addition of DMSO has been well documented but the mechanism is still uncertain. However, an increase in conductivity from adding Surfynol has not to our knowledge been previously reported. This effect was initially presumed to be due to better connectivity between adjacent lines of the film, caused by the increase in spreading. However, films without Surfynol showed equal sheet resistance along the axis of the printed lines and in the direction perpendicular to the lines, which would not be expected if there were poor connectivity between lines. Since Surfynol is a surfactant, composed of a long chain ester, it is not likely to be acting as a dopant; rather, it probably acts as a dispersing agent, mixing the PEDOT and PSS more thoroughly. This explanation is corroborated by the fact that adding Surfynol to a pristine PEDOT suspension increased the conductivity by about a factor of 1.5 (Table 1).

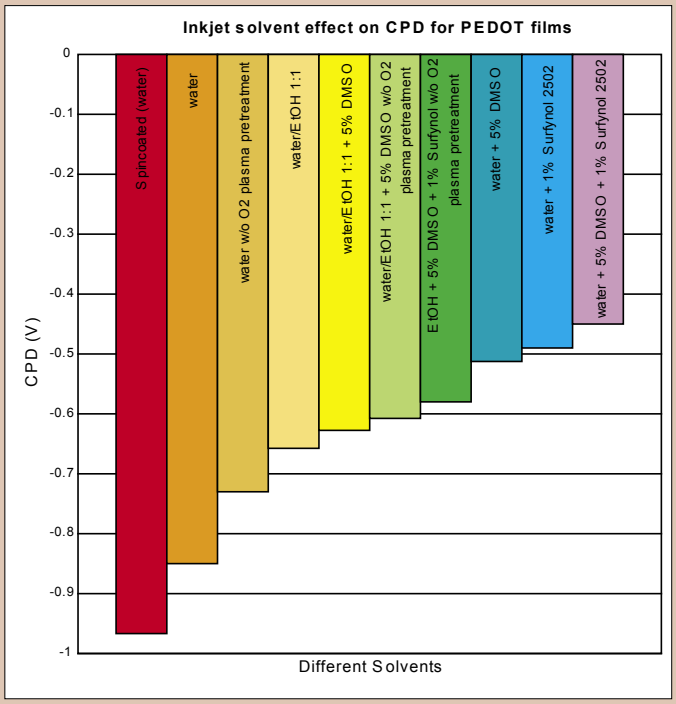

Figure 2. Contact Potential Difference (CPD) of 50% PEDOT films printed under identical conditions with various solvents and substrate pretreatments.

If Surfynol does in fact change the PEDOT film morphology by acting as a mixing agent, then it would not be surprising to see a change in the film's workfunction. Interestingly, Surfynol and DMSO seem to have an equal effect on the film's workfunction despite the fact that DMSO has a much greater effect on conductivity (Fig. 3, Table 1). Actually, as mentioned earlier, the amount of DMSO and Surfynol did not affect the workfunction – their presence at all tested levels caused a significant decrease in workfunction. However, workfunction is not simply a function of the conductivity of a film. Like DMSO and Surfynol, addition of ethanol decreased the workfunction, but unlike the other additives, the presence of ethanol decreased the conductivity. Therefore, we suggest that there are at least two different effects: the uniformity of PEDOT throughout the film, and some other phenomenon, possibly an interaction of the PEDOT with the DMSO, both of which may affect the conductivity and workfunction of the film. The similarity of effects from surfynol and DMSO may imply that DMSO acts like a surfactant for the polymer mixing but not for wetting the substrate.

There are several results that may help elucidate the unknown phenomenon mentioned above. First, increasing the printing voltage did not significantly alter the workfunction of the PEDOT film diluted in water, but it did cause a decrease in the workfunction for the films containing DMSO. Voltage did not seem to have a consistent effect on films with only Surfynol (Fig. 3). These results suggest that DMSO may have stronger interactions with PEDOT as the voltage increases, reducing the workfunction. Stronger interactions mean DMSO would be incorporated more completely into the film at higher voltages, which seems reasonable since a higher voltage causes a stronger impact of the ink with the substrate, causing more thorough mixing. A second result is that after annealing films containing DMSO at 180°C for 10 minutes, the workfunction trend reverses (Fig. 4). Since adding DMSO reduces the workfunction, the augmented workfunction upon annealing suggests that DMSO is being driven out of the film – reasonable given the boiling point of DMSO is 189°C. The post-anneal workfunction trend is also reasonable, since the films with weaker DMSO-PEDOT interactions (lower printing voltages) should not be affected much by DMSO leaving.

It is important to note that after annealing the PEDOT/DMSO/Surfynol films, the sheet resistance went up by about a factor of two. This increase was fairly consistent across the printing voltage range, which suggests that the conductivity of a film is not affected by

the strength of PEDOT-DMSO interactions. Since the conductivity of a film is moderately affected by the DMSO concentration (Table 1), it is likely that strength of PEDOT-DMSO interactions and DMSO concentration are not related. In other words, increasing the DMSO concentration will not necessarily increase the PEDOT-DMSO interactions. This agrees with previously discussed results, which showed that increasing the DMSO concentration had no effect on the workfunction, while strengthening the PEDOT-DMSO interactions by increasing the printing voltage did affect the workfunction.

Finally, it is important to note that annealing DMSO doped films creates two conflicting effects. First, it has been shown that annealing PEDOT films generally increases conductivity by increasing the PEDOT to PSS surface ratio as discussed earlier [10, 12]. It has also been suggested that the presence of DMSO itself has a significant effect on conductivity, independent of film morphology[11]. Considering the above, and the fact that annealing the films increased sheet resistance, we can conclude that the presence of DMSO affects conductivity more than the film morphology.

In conclusion, inkjet printed PEDOT films are more conductive, rougher, and have a smaller workfunction than spincoated films. It was suggested that these differences arise from a better mixing of PEDOT and PSS in inkjet printed versus spincoated films. Additionally, the increase in conductivity when DMSO is added to spincoated films also is seen in inkjet printed films. Furthermore, the surfactant Surfynol was observed to also increase the conductivity of PEDOT films to a lesser extent than DMSO, while affecting the workfunction in a similar manner. The changes in film properties after annealing various films suggest that DMSO increases conductivity both by the screening effect and by altering the film morphology. These same experiments coupled with the fact that DMSO concentration does not affect workfunction, suggest that the strength of PEDOT-DMSO interactions increases as printing voltage increases, which in turn causes the workfunction to go down. Finally, the workfunction of PEDOT films can be tuned over a range of about 0.5 V by altering the solvent mixture and substrate surface pretreatment. This is a very important result because it may allow for energy level matching with a variety of different (even yet undiscovered) light emitting or absorbing polymers for OLEDs and

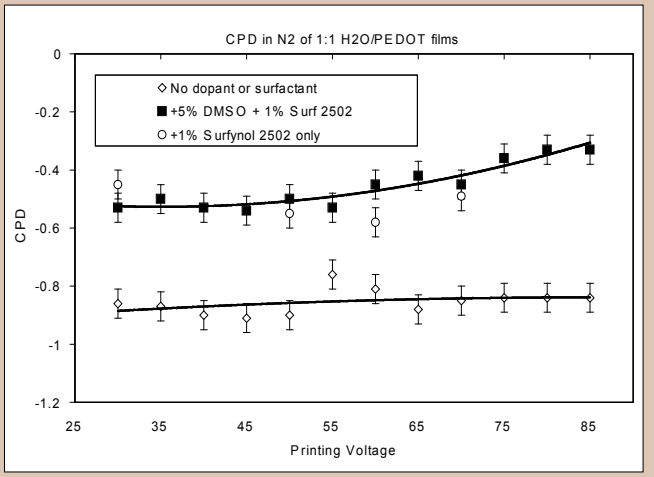

Figure 3. CPD as a function of printing voltage for PEDOT films using various solvent systems.

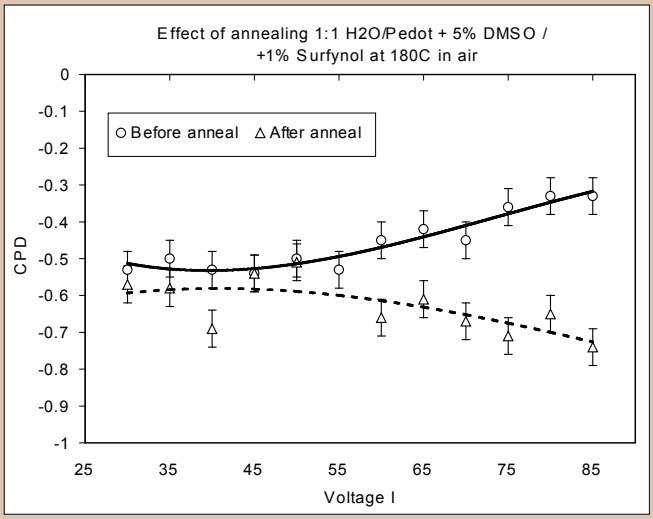

Figure 4. Effect of annealing PEDOT films on the CPD as a function of printing voltage.

OPVs. This work clearly demonstrates the viability of inkjet printing of PEDOT with the inherent advantages of patterning, efficient materials usage and 3-D structure development. Future work will focus on examination of other surfactants and additives with lower boiling points and better wetting properties.

ACKNOWLEDGEMENTS

I would like to thank my mentor Dr. David Ginley for his guidance, Lee Smith for his assistance in using the inkjet printing software and hardware, Dr. Sean Shaheen for his help with the workfunction studies and theory, the National Renewable Energy Laboratory for hosting me during the summer and the Department of Energy for funding my research.

REFERENCES

[1] C. Adachi, M. A. Baldo, M. E. Thompson, and S. R. Forrest, "Nearly 100% internal phosphorescence efficiency in an organic light-emitting device," *Journal of Applied Physics*, vol. 90, pp. 5048-5051, 2001.

[2] J. R. Sheats, "Manufacturing and commercialization issues in organic electronics," *Journal of Materials Research*, vol. 19, pp. 1974-1989, 2004.

[3] M. Shibusawa, M. Kobayashi, J. Hanari, K. Sunohara, and N. Ibaraki, "A 17-inch WXGA full-color OLED display using the polymer ink-jet technology," *Ieice Transactions on Electronics*, vol. E86C, pp. 2269-2274, 2003.

[4] Y. Liu, T. H. Cui, and K. Varahramyan, "All-polymer capacitor fabricated with inkjet printing technique," *Solid-State Electronics*, vol. 47, pp. 1543-1548, 2003.

[5] T. Kawase, T. Shimoda, C. Newsome, H. Sirringhaus, and R. H. Friend, "Inkjet printing of polymer thin film transistors,"

Thin Solid Films, vol. 438, pp. 279-287, 2003.

[6] T. M. Brown and F. Cacialli, "Contact optimization in polymer light-emitting diodes," *Journal of Polymer Science Part B-Polymer Physics*, vol. 41, pp. 2649-2664, 2003.

[7] B. J. de Gans, P. C. Duineveld, and U. S. Schubert, "Inkjet printing of polymers: State of the art and future developments," *Advanced Materials*, vol. 16, pp. 203-213, 2004.

[8] B. Chen, T. H. Cui, Y. Liu, and K. Varahramyan, "All-polymer RC filter circuits fabricated with inkjet printing technology," *Solid-State Electronics*, vol. 47, pp. 841-847, 2003.

[9] H. Frohne, D. C. Muller, and K. Meerholz, "Continuously variable hole injection in organic light emitting diodes," *Chemphyschem*, vol. 3, pp. 707-+, 2002.

[10] S. K. M. Jonsson, J. Birgerson, X. Crispin, G. Greczynski, W. Osikowicz, A. W. D. van der Gon, W. R. Salaneck, and M. Fahlman, "The effects of solvents on the morphology and sheet resistance in poly (3,4-ethylenedioxythiophene)-polystyrenesulfonic acid (PEDOT-PSS) films," *Synthetic Metals*, vol. 139, pp. 1-10, 2003.

[11] J. Y. Kim, J. H. Jung, D. E. Lee, and J. Joo, "Enhancement of electrical conductivity of poly(3,4-ethylenedioxythiophene)/poly(4-styrenesulfonate) by a change of solvents," *Synthetic Metals*, vol. 126, pp. 311-316, 2002.

[12] G. Greczynski, T. Kugler, M. Keil, W. Osikowicz, M. Fahlman, and W. R. Salaneck, "Photoelectron spectroscopy of thin films of PEDOT-PSS conjugated polymer blend: a mini-review and some new results," *Journal of Electron Spectroscopy and Related Phenomena*, vol. 121, pp. 1-17, 2001.

Nathan Justis recently graduated from Brigham Young University (BYU) in Physics Teaching and Math Education. He is currently a full-time Physics teacher at Riverton High School, Riverton, Utah. After graduating from BYU, Nathan completed an internship in Physics at the Thomas Jefferson National Accelerator Facility in Newport News, Virginia. After finishing his first year of teaching Nathan began work on a master's degree at Arizona State University in Modeling Physics. He hopes to continue teaching in high school throughout graduate school and then move on to complete a PhD in order to train future teachers.

Jian-ping Chen is a staff physicist at Jefferson Lab in Newport News, Virginia. He got his PhD in 1990 from the University of Virginia in experimental nuclear physics. After postdoctoral appointments at University of Virginia and Massachusetts Institute of Technology, he joined the physics division at Jefferson Lab as a staff scientist. He has worked at a number of accelerator laborotaries, including Jefferson Lab, SLAC, CERN, MIT Bates, Las Alamos and Mainz. His research has been focussed on the study of the nucleon and nuclear structure with electron scattering, including the electromagnetic form factors, the strangeness in nucleon, nucleon properties in nuclear medium and in particular, the study of the nucleon spin structure using polarized beams on polarized targets. His research also covers the test of the standard model with parity violating experiments.

MEASURING GLASS THICKNESS OF A REFERENCE CELL USED IN A POLARIZED ^{3}HE EXPERIMENT

Nathan Justis, Jian-ping Chen

ABSTRACT

Studies of the spin structure of the neutron are often conducted using a polarized ^{3}He target due to its close spin resemblance to that of a free neutron. Experiments are conducted by bombarding polarized ^{3}He nuclei with high-energy electrons from a linear accelerator. The polarized ^{3}He gas is contained in a glass tube-like cell called the *target cell*. In addition to the target cell, a *reference cell* is also used for calibration purposes. The thickness of each cell must be accurately determined for the analysis of the scattering data of the experiment. The thickness of a reference cell was determined by using a tunable infrared laser to create a thin-film interference pattern by reflecting the laser light off of the glass cell. The intensity of the pattern is known to vary sinusoidally as the wavelength of the laser changes. Such variation was recorded as an array of numbers by a LabView program at 26 different points on the cell. Each of the 26 sets of data were fit to an equation containing the thickness variable to determine the thickness of the glass. The cell side, or *wall,* thickness ranged from 1.42 mm to 1.65 mm, with an uncertainty of less than 5% in every case. End, or *window*, thickness measurements were also successfully taken, but have yet to be fitted to the derived equation.

INTRODUCTION

Reference cells in a polarized ^{3}He experiment are needed because electron scattering results from more than just the electron/^{3}He interaction. The total electron scattering must be described in terms of scattering due to the ^{3}He nuclei, the glass, and the small amount of N_2 molecules that are in the target cell.

During an experiment, the reference cell sits below the target cell on a mobile ladder system. By moving the ladder up and down, the system can move the target cell, the reference cell, or any other target into the beam line for measurements. In this apparatus, the reference cell is attached to a vacuum pump, as well as to ^{3}He and N_2 gas bottles, which allows the cell to be filled with either of the two gases, or placed in a vacuum state [1]. When the cell is filled with ^{3}He or N_2 gas, researchers can measure the amount of electron scattering due to these gases in a target cell. With the cell vented and evacuated, measurements reveal how much electron scattering is due to the glass itself.

In addition to assisting in the characterization of the scattering data, the reference cell can be used to interpolate the pressure in the target cell. Because the pressure can be varied when filling the reference cell with either of the two gases, and most importantly, the ^{3}He gas, the amount of electron scattering can be observed at many different pressures in the reference cell. The pressure at which the amount of scattering in the reference cell matches that of the target cell can be used to estimate the pressure in the target cell [2].

Radiative Corrections

The thickness of a reference cell must be known to correct for energy loss of both the incoming and scattered electrons. As an electron passes through matter, such as glass, it loses energy in the form of electromagnetic radiation. If one can characterize the type and amount of matter the electrons passed through before and after the scattering, the necessary mathematical corrections, or *radiative corrections*, are possible [3].

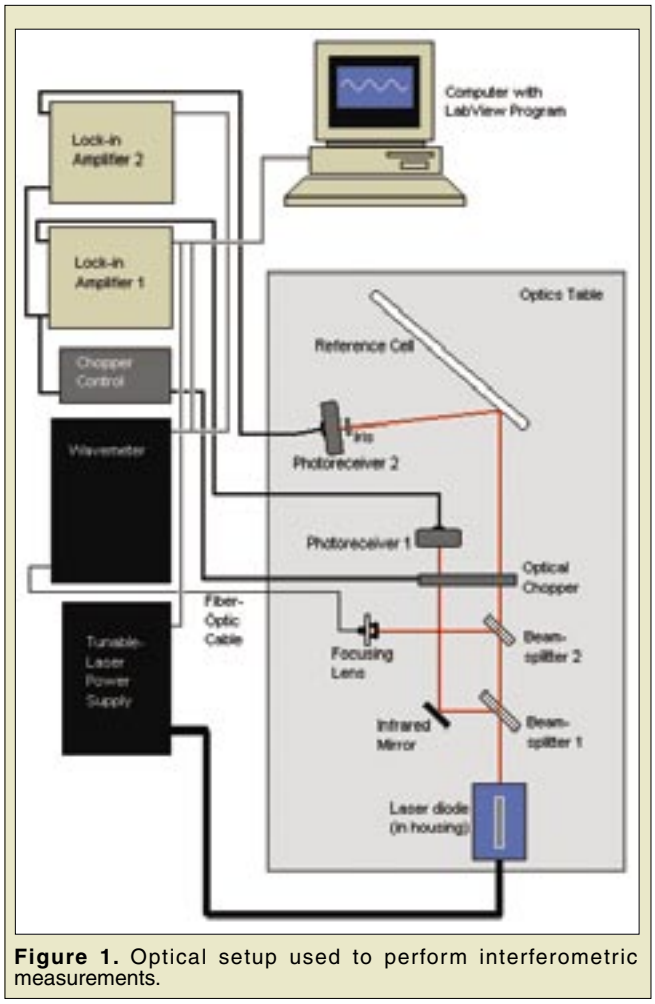

Figure 1. Optical setup used to perform interferometric measurements.

MATERIALS AND METHODS

Interferometry Review

When two sources of light are incident on the same surface, they interfere with each other either constructively, or destructively, depending on their relative phase. Interferometry is the application of coherent light interference principles to determine values such as thickness of a thin transparent material and surface integrity of a smooth surface.

In determining the thickness of a transparent material, or thin-film, laser light is set incident on the thin-film. As one wave front reflects off of the front surface, another will pass through the film and reflect off of the back surface of the film. This second wave front will then travel back through the film and the first surface and interfere with the first wave. Whether constructive or destructive interference occurs at a certain point depends on the optical path difference of the two waves, and hence, their relative phase [4].

Optical Setup

Applying principles of interferometry to actually measure the thickness of the glass cell was fairly complex and involved a number of steps. Twenty-six measurements were taken on the sides of the cell and analyzed. The instrumental setup used to take these measurements is shown in figure 1. This setup was used because of its previous success in measuring cell glass thickness at Jefferson Lab.

Infrared laser light from a tunable laser (New Focus 6300) was directed through a beam-sampler where ~10% was split off to an infrared mirror and then reflected through an optical chopper (New Focus 3501). The chopper converted the laser light to pulsed laser light with a pulse frequency of 1.4 kHz. After passing through the chopper, the light reached a photoreceiver (New Focus 2031) that was connected to a lock-in amplifier (PerkinElmer 7265) referenced to the chopper frequency. The remaining ~90% of the light was directed to a beam-splitter where ~50% of the light was split off and channeled down a fiber-optic to a wave-meter (Burleigh WA-1100) for wavelength measurement. The remaining ~50% from this beam-splitter continued through the same optical chopper set at 1.4 kHz. After passing through the chopper the light finally reached the glass cell.

An additional photoreceiver was placed in line of the interference pattern to measure its intensity. An optical iris was placed in front of this photoreceiver to assist in focusing on the small portion of the interference pattern desired for the measurement.

The signals from the two photoreceivers, each after passing through a lock-in amplifier, were sent to a computer and read by a LabView program. The measured wavelength of the light was also read by the computer through the wavemeter. Perhaps the key element of the setup was the tunable laser. As the wavelength of the laser was increased, the intensity of the interference pattern varied sinusoidally, going from wavelengths that provided for destructive interference to wavelengths that provided for constructive interference. A plot of Signal vs. Wavelength was created where "Signal" represents roughly the ratio of reflected light (measured by photoreceiver 2) to incident light (measured by photoreceiver 1) (see fig. 2).

The above setup was used to record data at 26 different points on the right and left walls of the cell. For each measurement, a location from the center of the cell was recorded in centimeters, as well as the angle of incidence used when taking the measurement. This angle was later used with Snell's Law to calculate the angle of refraction in the glass. Figure 3 displays the various points at which measurements were recorded.

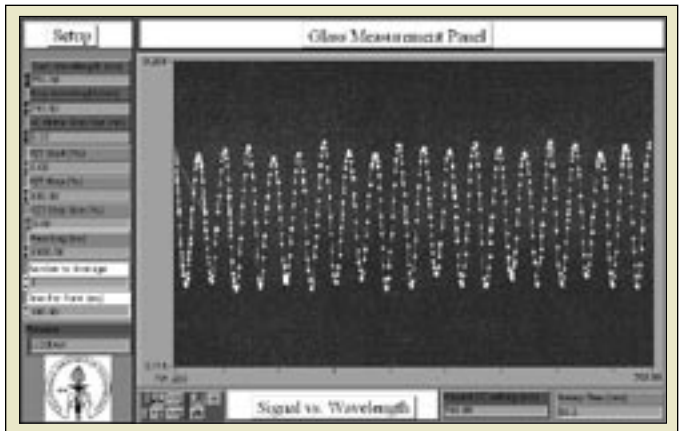

Figure 2. Graphical user interface of LabView program used to collect thickness data.

To take a measurement, many things had to be checked and verified in the system. For example, it had to be verified that the lock-in amplifiers were picking up and correctly reading the 1.4 kHz signals coming from the photoreceivers. This was done by checking that the amplifiers had settled on the signal of that frequency. Also, laser temperature stability had to be achieved before recording any data. Laser temperature was stable within 0.1 degrees Fahrenheit after just a few minutes of turning it on. The data collection software reminded the user to check for laser temperature stability before proceeding. Effects of changing the laser temperature were not studied.

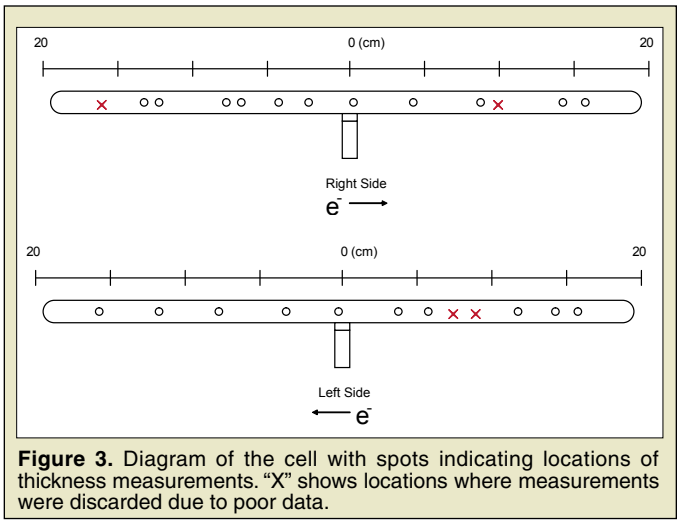

Figure 3. Diagram of the cell with spots indicating locations of thickness measurements. "X" shows locations where measurements were discarded due to poor data.

Once the instrumentation was functioning properly, preliminary measurements were taken. Because the search for a good signal often required many trials, the size of laser wavelength increments was increased to decrease the scan time required. To do this, a piezoelectric ceramic made from oxides of Lead (Pb), Zirconium (Zr) and Titanium (Ti), or PZT, step size was temporarily increased to 6.00%, and a DC motor step size to 0.30 nm [5]. The DC motor step size indicates the rough increment at which the wavelength was increased. The PZT step size is a percentage of the DC motor step size—basically a finer increment at which the laser wavelength was increased. When a final measurement was performed, the PZT step size was set at 3.00% and the DC motor step size at 0.15 nm. This final measurement took about 15-16 minutes to perform.

Obtaining a good signal required finding a good thin-film interference image. Clear interference images were found by slowly moving the cell in both a rotational and linear manner until distinct fringes in the image were discovered. The clearer the fringes were, the easier it was to obtain a good signal with the photoreceiver. The photoreceiver was placed in such a way that the fringes fell upon the photocell. Shifting the iris and photoreceiver around behind the image helped in discovering a section of the image that provided a good signal. When a good signal seemed particularly difficult to obtain, the iris and photoreceiver were pulled further away from the cell to allow the interference fringes to spread out. This way, the photoreceiver could be placed in a more specific area of the fringes. After each attempt, the iris and receiver were shifted a very small amount (approximately 1 mm) from left to right behind the image and a new practice signal was recorded.

Taking preliminary measurements involved taking a reading, shifting the cell and/or photoreceiver and iris, taking another reading, shifting again, taking another reading, etc., until the desired signal was discovered. A perfect signal would be one that is perfectly sinusoidal. Normally, however, an acceptable signal included some slight variation in the amplitude as the signal was recorded. A poor signal looked nothing like a sine wave. At this point, quality of a signal was simply determined by eyeballing it.

Once a good signal was found and recorded as a final measurement, the location measurements were recorded. A ruler was used to measure the location of the measurement from the center of the cell within +/- 0.3 cm, and a protractor was used to measure the angle of incidence within +/- 2 degrees. After the data were recorded along with a location and angle of incidence, they were fit to the following equation [4] by a computer program described below:

$$\frac{I_R}{I_i} = \frac{\dfrac{4\left(\dfrac{n-1}{n+1}\right)^2}{\left(1-\left(\dfrac{n-1}{n+1}\right)^2\right)^2}\sin^2\left(\dfrac{2\pi nd\cos\theta}{\lambda}\right)}{1+\dfrac{4\left(\dfrac{n-1}{n+1}\right)^2}{\left(1-\left(\dfrac{n-1}{n+1}\right)^2\right)^2}\sin^2\left(\dfrac{2\pi nd\cos\theta}{\lambda}\right)} \quad (1)$$

Here, I_R is the intensity of the reflected light, I_i is the intensity of the incident light, n is the refractive index of the glass, d is the thickness of the glass, θ is the angle of refraction, and λ is the wavelength. The refractive index for the cell, which was made of GE-180 Aluminosilicate glass, is known to be 1.536 [3].

The fit was improved by adjusting the thickness value in the programming code until the fit was reasonable; the fit was judged by the χ^2/ndf ratio. A fit was considered reasonable if this ratio was less than 6. Minimizing this ratio to improve quality of fit is a standard procedure in any fitting process. Using this method, the thickness associated with a measurement was determined to within 5% of the actual width.

Window Thickness Measurements

Only a few differences need to be noted concerning the measurement of the window thickness. Because the window thickness is about a factor of ten smaller than the wall thickness, the sinusoidal signal had a much longer period. The signal period for a window measurement was typically a little more than ten times the signal period for a wall thickness measurement. The original scanning range of 791 nm to 793.5 nm was increased to 791 nm to 799 nm in order to capture more than one signal wavelength. This

range typically provided for about four to five signal wavelengths in a window thickness measurement.

Another difference in measuring the window thickness involved the search for a good signal to record. The search for a good signal in performing a wall thickness measurement involved finding a clear vertical band of horizontal fringes, but the search for a good signal in performing a window thickness measurement required finding a circular pattern of interference fringes, which was expected because of the hemispherical shape of the windows. A clear circular pattern was discovered for each of the cell's two windows, and sinusoidal signals were obtained by placing the photoreceiver and iris at the center of these signals. Because the scan for a window thickness measurement covered 8 nm, as compared to the 2.5 nm for the wall measurements, recording signals took much longer—about 45 minutes. Practice scans were performed with a PZT step size of 40.0%, and a DC motor step size of 0.35 nm. Final measurements were performed using a PZT step size of 3.00%, and a DC motor step size of 0.15 nm, the same as when measuring the wall thickness.

Error Analysis

An uncertainty of less than 5% was desired to properly understand the error in calculating the radiative corrections for the associated experiments. Calculating the uncertainty required consideration of both systematic and statistical errors. The dominant systematic error involved determining the angle of incidence, and subsequently, the angle of refraction. The angle of incidence in (1) is the angle of refraction, however, so Snell's Law was used to calculate the angle of refraction. Afterwards the uncertainty was adjusted appropriately by finding the largest deviation in angle of refraction due to an increase or decrease of 2° in the angle of incidence. This value, 1°, was then used to find the largest deviation in thickness due to an increase or decrease of 1° in the angle of refraction when fitting the data. The largest deviation was 0.005 mm, or approximately 0.3% of the thickness. An uncertainty of 0.5% was used to be conservative.

Calculating the statistical error involved many steps. The data recorded by the optical setup was in a text file format. The program used to record the data performed two measurements with the laser at each step in the wavelength scan of the laser. A series of programs developed by Vince Sulkosky and Aidan Kelleher of the College of William and Mary, read the text files and output an array of the differences between the two values recorded at each wavelength and then produced a histogram of these differences and output a sigma value for the histogram. This sigma was later used as the signal error in the fitting the data to (1). Part of the fitting program found the minima and maxima of the fit and used these values to calculate the thickness. This was done by taking the difference between two adjacent minima (or maxima). The difference was then used to create another plot with all minima and maxima separated by this difference. The wavelength of this plot determined thickness. For example, a plot of the data with a fit equation containing five minima and five maxima would calculate eight different thickness measurements. A plot of these measurements with their statistical error bars was made and an average of these values was calculated. This average was the thickness of the glass at the specific location of measurement. The standard deviation of these values from the average was the statistical uncertainty of that thickness.

The systematic error was roughly 4% of the thickness, and the systematic error due to the angle measurement was 0.5%. Any other systematic error was considered negligible. When added in quadrature to give the overall error, the systematic error dominated. Only once was the overall error more than 5% of the thickness (see Table 1).

Wall Thickness Measurement Data

No.	File Name	Distance from center (cm)	Side	Thickness Uncertainty (mm)	Thickness Uncertainty (Percentage)	Notes
1	JanineL9up	8.6 up	L	-	-	discarded
2	JanineL8up	7.5 up	L	-	-	discarded
3	JanineL6up	5.5 up	L	-	-	discarded
4	JanineL6upII	5.5 up	L	1.421	0.056	
5	JanineL14up	14.4 up	L	1.55	0.048	
6	JanineL8down	8.0 down	L	1.484	0.061	
7	JanineL12down	11.8 down	L	1.517	0.058	
8	JanineL4down	3.7 down	L	1.437	0.059	
9	JanineL16down	15.7 down	L	1.497	0.073	
10	JanineLcenter	0.5 down	L	1.48	0.061	
11	JanineL12up	11.7 up	L	1.469	0.056	
12	JanineL16up	15.7 up	L	1.496	0.053	
13	JanineL3up	3.0 up	L	1.468	0.056	
14	JanineR14down	14.3 down	R	1.516	0.056	
15	JanineR2up	2.2 up	R	1.594	0.054	discarded
16	JanineR10down	9.8 down	R	1.556	0.149	discarded
17	JanineR9down	8.5 down	R	1.513	0.058	
18	JanineR4down	4.0 down	R	1.505	0.055	
19	JanineR16down	15.7 down	R	1.553	0.059	
20	JanineRcenter	0.0 up/down	R	1.603	0.055	
21	JanineR4up	4.4 up	R	1.605	0.055	
22	JanineR7up	7.0 up	R	1.555	0.057	
23	JanineR13up	12.5 up	R	1.654	0.055	
24	JanineR8up	8.0 up	R	1.571	0.06	
25	JanineR14up	13.5 up	R	1.622	0.056	

Table 1. Thickness measurements of the cell with associated locations.

RESULTS

Wall Results

Thirteen thickness measurements were taken on the left side of the cell, and thirteen were taken on the right side (see fig. 3). Five of these were not used due to the difficulty of fitting the sinusoidal equation to the data recorded at these five points. Wall thickness of the cell ranged from 1.421 mm to 1.55 mm on the left side, and

from 1.505 mm to 1.654 mm on the right side. Table 1 gives a complete listing of the thickness measurements acquired.

Window Results

Two thickness measurements were recorded on the down window of the cell, and one thickness measurement was recorded on the up window of the cell. These three sets of data have yet to be fit to the equation aforementioned. As displayed by the data recording program, the data recorded at these points appeared generally sinusoidal.

Comparison With Mechanical Measurements

Wall and window thicknesses of the cell had been previously measured mechanically at the University of Virginia (UVa) using a micrometer before the various sections of the glass tube were fused together. However, in order to make a more precise measurement, interferometric methods were required. The mechanical measurements give a range on the left side of 1.524 mm to 1.702 mm and an unweighted average of 1.592 mm (+/- 0.007 mm), whereas the interferometric measurements give a range of 1.421 mm to 1.55 mm and an unweighted average of 1.482 mm (+/- 0.058 mm). On the right side, the mechanical measurements give a range of 1.549 mm to 1.778 mm and an unweighted average of 1.676 mm (+/- 0.007 mm), whereas the interferometric measurements give a range of 1.505 mm to 1.654 mm and an unweighted average of 1.571 mm (+/- 0.064 mm). Furthermore, the mechanical measurements show that the right side is somewhat thinner near the down end. This difference is also seen in the interferometric measurements (see table 1). Difference between thickness on the right and left sides can be attributed to the different effects on the two sides from fusing the glass tubing together.

The window thickness measurements were also measured mechanically at UVa—0.137 mm on the upstream window (with unknown uncertainty), and 0.135 mm on the downstream window (with unknown uncertainty). No comparison is possible until the interferometric data taken on the windows is fit to the sinusoidal equation.

DISCUSSION AND CONCLUSION

Using interferometry and data-fitting to measure the thickness of thin glass is an adequately accurate method. Despite the uncertainty of the interferometric method, it still proves more reliable than the mechanical measurements taken before the completion of the cell because of the effects of the fusing during cell construction on glass thickness. This method involves many steps, however, and takes a fairly long time to complete. If a faster method were developed, just as accurate, it should be employed over the use of interferometry and data-fitting. However, the current setup at JLab can now be considered capable of performing both wall and window thickness measurements. This setup is highly convenient, since in the past cells were moved to another lab to perform window thickness measurements.

Finally, the author gives two simple recommendations. First, that the optics table upon which the measurements were performed be stabilized with pneumatic dampening legs in order to reduce vibration of the setup and background noise in the signal. Second, that a focusing lens be placed in the incident beam line to decrease the size of the beam spot and assist in obtaining a good sinusoidal signal for recording measurement data, especially when recording the window thickness, which is much smaller and more difficult to measure.

ACKNOWLEDGMENTS

I would like to thank the U.S. Department of Energy and Jefferson Lab for giving me the opportunity to participate in this internship. I would also like to thank my mentor, Jian-ping Chen, for all of his assistance. I also thank Vince Sulkosky and Aidan Kelleher of the College of William and Mary. These two doctoral candidates patiently responded to my unceasing questioning with valuable answers and insights. I thank Jan Tyler and Lisa Surles-Law as well, for assisting in the construction of this paper.

REFERENCES

[1] Polarized ^{3}He Target Operational Safety Procedure, Thomas Jefferson National Accelerator Facility, Hall A, Newport News, VA, 2001.

[2] Vince Sulkosky, Private Communication, College of William and Mary, Williamsburg, VA, 2004.

[3] Kevin M. Kramer, "A Search for Higher Twist Functions in the Neutron Spin Structure Function $g_2^n(x,Q^2)$," Ph.D. dissertation, Dept. of Physics, College of William and Mary, Williamsburg, VA, 2003.

[4] Eugene Hecht, Optics, San Francisco: Addison-Wesley, pp. 416-420, 2002.

[5] CTS Coporation, Burbank, CA, 2003, Available HTTP: http://www.ctscorp.com/techtalk/vol3no2/page2.htm.

Jacqueline Tio is a rising senior at the Massachusetts Institute of Technology currently pursuing a Bachelors of Science in Chemistry. Over the past two summers, she has conducted research in the Environmental Sciences Division of Oak Ridge National Laboratories under the supervision of Dr. Baohua Gu. Her work at ORNL, funded by the Department of Energy and Office of Science, has explored using surface-enhanced Raman spectroscopy to detect perchlorate anion at low concentrations. Since 2003, she has also been actively involved in the Chemistry Source Reduction Project under the supervision of Professor Jeffrey I. Steinfeld. This project, also entitled Encouraging Toxic Use Reduction in Academic Laboratories, recently received the P3 Student Design for Sustainability Award from the EPA for phase II of project development and implementation. At present, she is also conducting research on fluorescence-based sensors for detecting nitric oxide under the supervision of Professor Stephen J. Lippard.

Baohua Gu is a senior research scientist at Oak Ridge National Laboratory and also an Adjunct Professor at University of Tennessee, Knoxville with more than 15 years of experience in environmental research and development. He has been a principal investigator responsible for a number of research projects such as perchlorate detection and remediation, biogeochemical interactions of contaminants, neutron-scattering studies at silica nanoparticle-water interfaces, and permeable reactive barriers. He is the inventor of three patents and winner of the 2004 R&D 100 Award related to the development of highly-selective bifunctional anion exchange resin, its regeneration and the destruction of perchlorate. He has over 70 peer-reviewed journal or book publications and currently serves as an editorial board member for the international Journal of Water, Air, and Soil Pollution. He received his Ph.D. from the University of California, Berkeley in 1991 and his M.Sc. from the University of British Columbia in 1986.

DETECTION OF PERCHLORATE ANION ON FUNCTIONALIZED SILVER COLLOIDS USING SURFACE-ENHANCED RAMAN SCATTERING

Jacqueline Tio, Wei Wang, and Baohua Gu

ABSTRACT

Perchlorate anion interferes with the uptake of iodide by the human thyroid gland and consequently disrupts the regulation of metabolism. Chronic exposure to high levels of perchlorate may lead to the formation of thyroid gland tumors. Although the Environmental Protection Agency (EPA) has not set a maximum contaminant level (MCL) for perchlorate, a draft drinking water range of 4-18 ppb based on 2 liter daily consumption of water has been established. The current EPA approved method for detecting perchlorate uses ion chromatography which has a detection limit of ~1ppb and involves lengthy analytical time in the laboratory. A unique combination of the surface-enhanced Raman scattering (SERS) effect and the bifunctional anion exchange resin's high selectivity may provide an alternative way to detect perchlorate at such low concentrations and with high specificity. SERS, which uses laser excitation of adsorbed perchlorate anions on silver nanoparticles, has been shown to detect perchlorate anions at concentrations as low as 50 ppb. Normal micro-Raman analysis of perchlorate sorbed onto the resin beads has detected an even lower concentration of 10 ppb. In an effort to integrate these two effects, silver nanoparticles were coated with N-trimethoxysilylpropyl-N,N,N-trimethylammonium chloride, a functional group similar to that found on the resin bead, and subsequently inserted into different perchlorate concentration environments. This method has resulted in perchlorate detection down to ~10 ppb and a more consistent detection of perchlorate anion at ~50 ppb than that of earlier methods. As suggested by the direct insertion of functionalized silver colloids into perchlorate samples, this technique may potentially allow for the development of a probe using on-site Raman spectrometry to detect significantly low concentrations of perchlorate *in situ* rather than in the laboratory.

INTRODUCTION

Perchlorate anion (ClO_4^-) is a kinetically inert, nonvolatile, water soluble anion that is found in rocket propellants, munitions, fireworks, and some nitrate fertilizers [1,2]. Traces of ClO_4^- are increasingly being detected in soil, groundwater, drinking water, and irrigation water systems, and it is suspected to threaten human health by competitively inhibiting iodide uptake by the thyroid gland. The thyroid gland plays an important role in regulating metabolism, and changes in its hormone production may especially affect the proper development of children and fetuses [2].

The Environmental Protection Agency has not yet set a maximum contaminant level (MCL) for ClO_4^-, but a draft drinking water range of 4-18 ppb (based on a 2 liter daily consumption of water for a 70 kg adult) has been established [3]. The current EPA Method 314 uses ion chromatography to detect ClO_4^- at low concentrations by its chromatographic retention time. Other techniques utilize mass spectrometry and detect ClO_4^- based on its mass ratio, *m/z*.

A unique combination of the surface-enhanced Raman scattering (SERS) effect and the bifunctional anion exchange resin's high selectivity may provide an alternative way to detect ClO_4^- at

even lower concentrations and with higher selectivity based on the Raman active vibrational frequency of ClO_4^-. SERS, which uses laser excitation of adsorbed analyte molecules on silver nanoparticles, has been shown to detect molecules with enhancement factors reaching up to 10^{14} [4]. Bao et al. reported a detection limit of 8.5 x 10^{-8} M for uranyl ions on silver- doped silica sol-gel films [5]. In addition, bifunctional anion exchange resin beads that are coated with quaternary ammonium functional groups of large (C_6) and small (C_2) trialkyl groups have been shown to selectively adsorb ClO_4^- in the presence of competing anions commonly found in groundwater [6].

In our previous study, SERS of Ag colloids aggregated by the addition of NaCl detected ClO_4^- down to concentrations of ~50 ppb (µg/L), and Raman analysis of bifunctional anion-exchange resin beads detected even lower concentrations of 10 ppb [7]. In an effort to integrate the SERS effect of Ag nanoparticles with the selectivity of the bifunctional anion exchange resin, silver nanoparticles and silver-doped silica sol-gels were coated with N-trimethoxysilylpropyl-N,N,N-trimethylammonium chloride, an organosilane with a functional group similar to that found on the resin bead. Through hydrolysis and subsequent condensation reactions shown below, the functional groups of this layer formed silicon-oxygen-silicon bridges that allowed attachment to Ag coated glass slides.

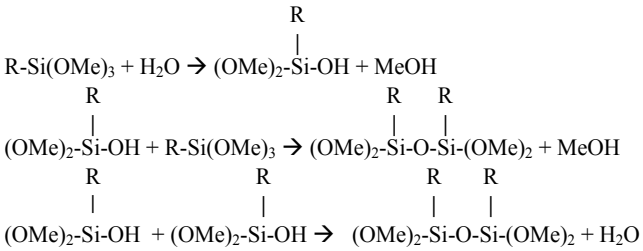

These methods resulted in a more consistent detection of ClO_4^- at ~50 ppb than that of earlier methods, and detection of ClO_4^- at ~10 ppb using the silver-doped silica sol-gel. This technology may eventually lead to the development of a probe using on-site Raman spectrometry to detect significantly low concentrations of ClO_4^- *in situ* rather than in the laboratory.

MATERIALS AND METHODS

Of the several different methods that exist for preparing Ag colloids suitable for observing the SERS effect, this study used a modified method of Creighton et al. [8]. In brief, 25 ml of freshly prepared 0.01M $NaBH_4$ (EM Science) were added to 12.5 ml of 0.01M $AgNO_3$ (J.T. Baker) and stirred vigorously for ~1 hour at room temperature to create a yellow, Ag sol. Sample slides were prepared by applying one drop of the Ag sol to the surface of a glass slide and dried in a 70°C oven. Particle size and size distribution of the Ag colloids were measured by means of dynamic light scattering using a ZetaPlus particle size analyzer (Brookhaven Instruments Corporation, Holtsville, New York). Ag-doped silica sol-gels on frosted glass slides were obtained from Bao et al. [5].

A layer of N-trimethoxysilylpropyl-N,N,N-trimethylammonium chloride (Gelest, Inc.) diluted in chloroform (EM Science) was added to the surface of Ag colloids and Ag-doped silica sol-gel samples and was allowed to hydrolyze with water in the air. Excess organosilane was gently washed off with ethanol (Aldrich). The functionalized slides were then placed in 100 ml of Milli-Q deionized water (EASYpure, Barnstead) and background Raman spectra were obtained.

Perchlorate solutions of 1000 ppm and increasingly dilute concentrations were made from $NaClO_4 \cdot H_2O$ (EM Science). Samples were then placed in 100 ml of aqueous ClO_4^- solution and allowed to equilibrate for 24 hours, whereupon Raman spectra of the samples were obtained while samples were still wet. These steps were repeated for non-functionalized Ag sol samples.

Raman spectra were obtained using a Renishaw micro-Raman system equipped with a 300 mW near-infrared diode laser at a wavelength of 785 nm operating at 10% power (Renishaw Inc., New Mills, UK). The laser beam was set in position through a Leica Raman Imaging Microscope objective (50x) set at a lateral spatial resolution of ~2 µm and a depth of field of ~1 to 5 µm depending on the sample. A charge-coupled device (CCD) array detector was used to achieve signal detection from a 1200 grooves/mm grating light path controlled by Renishaw WiRE software and analyzed by Galactic GRAMS software. Polarization optics was set perpendicular to the laser with an intensity of ~60 mW at the exit of the 50x objective.

RESULTS

Particle size and size distributions of synthesized Ag colloids were routinely analyzed by means of the dynamic light scattering technique. Particle sizes of the Ag sol remained stable and ranged from 10-30 nm over a period of ~30 days (data not shown). Upon drying of the Ag sol on a glass slide, aggregated Ag nanoclusters formed on the micrometer scale. Although several clusters fell off the sample slides during sample preparation, a sufficient amount remained to obtain Raman spectra. Background Raman spectra verifying the absence of major peaks between 910-960 cm^{-1} for

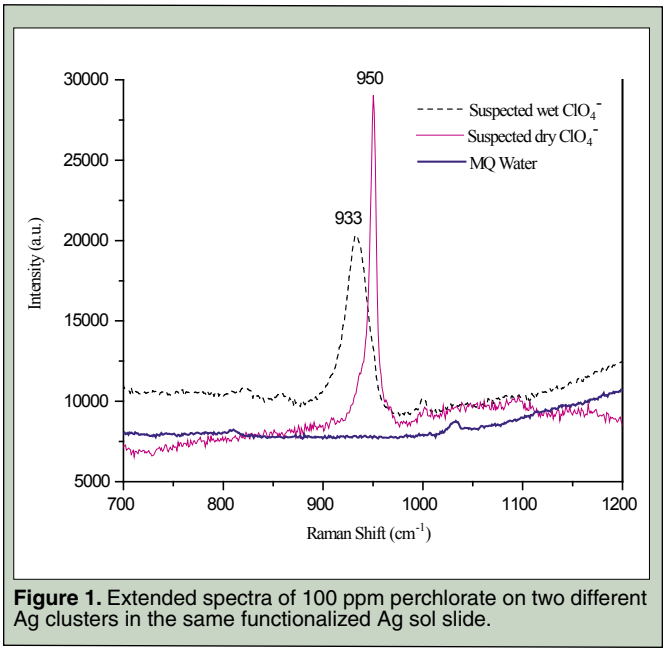

Figure 1. Extended spectra of 100 ppm perchlorate on two different Ag clusters in the same functionalized Ag sol slide.

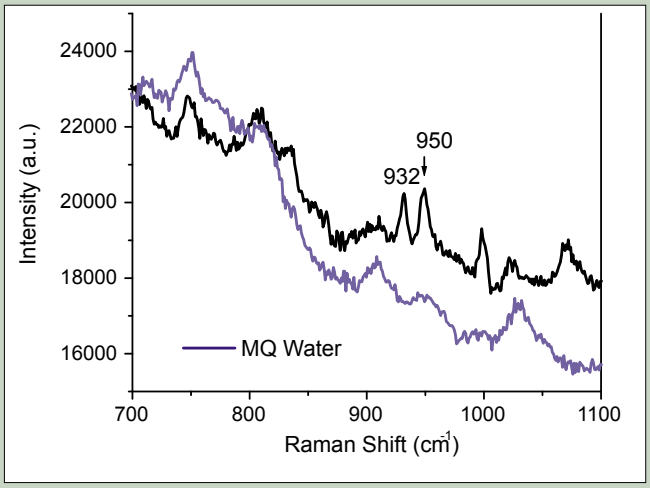

Figure 2. Extended spectra of 50 ppb perchlorate on functionalized Ag sol slide.

all samples were taken prior to placing the samples in the ClO_4^- solution.

Frequently, wet samples would appear to dry during spectral acquisition, giving sharp peaks at ~933 cm^{-1} and 950 cm^{-1}. Figure 1 shows 100 ppm ClO_4^- detection giving peaks at ~933 cm^{-1} on one Ag cluster and ~950 cm^{-1} on another cluster in the same Ag sol sample. Figure 2 shows 50 ppb ClO_4^- detection of another Ag sol sample where both ~932 cm^{-1} and ~950 cm^{-1} peaks are present in the same spectrum.

Figure 3 shows sample images of the functionalized Ag colloids and the functionalized Ag-doped silica sol-gel that were used to detect ClO_4^- under a 50**x** objective. Perchlorate detection occurred most frequently on clusters thinly covered by moisture leftover from equilibration, whereas thick wet layers yielded Raman spectra with small signal to noise ratios.

The lowest detection limit for non-functionalized Ag sol was 1000 ppm, with the characteristic ClO_4^- peak occurring at ~933 cm^{-1} (data not shown). Adding the quaternary ammonium functional group layer enabled both the Ag sol and the Ag-doped silica sol- gel to detect ClO_4^- down to 50 ppb with more consistency than that of our past studies and enabled the Ag-doped silica sol-gel to detect down to 10 ppb [7]. Figure 4 shows spectra of ClO_4^- detection on functionalized Ag sol substrates at concentrations of 100 ppm, 10 ppm, 500 ppb, 100 ppb, 50 ppb and 0 ppb. Figure 5 shows spectra of ClO_4^- detection on functionalized Ag-doped silica sol-gel substrates at concentrations of 10 ppm, 1 ppm, 100 ppb, 50 ppb, 10 ppb, and 0 ppb. Figure 6 is an illustration of quaternary ammonium groups adsorbing ClO_4^- on both functionalized Ag colloids and Ag-doped silica sol-gel. For both functionalized media, Raman peak intensities decreased with decreasing perchlorate concentration until reaching the part per billion range. Here ClO_4^- signal intensities did not consistently decrease with the concentration. Moreover, at lower concentrations, samples were subjected to more spectral acquisitions, and subsequent increased exposure to the laser prompted the tendency for remaining analyte moisture to recede and concentrate in one area of the slide before drying completely.

Figures 7 shows the SERS enhancement effects of using functionalized Ag colloids as compared to functionalized Ag-doped silica sol- gel for ClO_4^- concentrations at 50 ppb and 100 ppb. Although both Ag substrates had Raman ClO_4^- peaks of similar intensity, the ClO_4^- peaks detected using Ag colloids were sharper and less red-shifted than those detected using the Ag-doped silica sol-gel.

DISCUSSION AND CONCLUSIONS

Characteristic Perchlorate Peaks

Our past studies have shown dry ClO_4^- to have a Raman peak at ~950 cm^{-1} and ClO_4^- detection on bifunctional resin beads to occur at ~930 cm^{-1}. The latter ~20 cm^{-1} shift was expected to be the result of strong interactions between the ClO_4^- and positively charged quaternary ammonium functional groups [7]. However, in the absence of any quaternary ammonium functional groups, the characteristic ClO_4^- peak from analysis of wet non-functionalized Ag samples in this study was ~933 cm^{-1}. Therefore the ~933 cm^{-1} peak is most likely characteristic of ClO_4^- in its aqueous form, as other studies have reported the normal Raman peak of aqueous ClO_4^- solutions to occur at ~935 cm^{-1} [9]. Figures 1 and 2 show how both peaks were observed in this study, most likely indicating the presence of wet and dry ClO_4^-, with the wet peak predominantly observed in the beginning of sample analysis and the dry peak appearing toward the end of the analysis when the samples had dried.

Aggregation of Nanoparticles

The probability of detecting ClO_4^- was higher in the presence of nanoclusters that were not too heavily clustered or isolated. Figure 3a shows strings of clusters that exhibited the SERS effect in the Ag colloid samples. Nanoclusters showing the SERS effect on the Ag-doped silica sol-gel samples were found both on the sol-gel surface and in crevices, as seen in Figure 3b. The affinity for SERS detection of molecules on Ag clusters has been observed before and may be explained by a large electromagnetic enhancement attributed to interactions between neighboring Ag particles in a fractal cluster

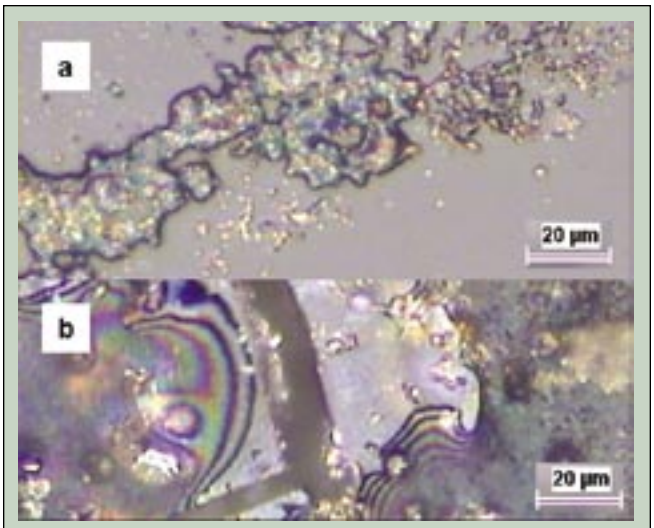

Figure 3. Functionalized Ag colloids (a) and functionalized Ag-doped silica sol-gel (b) during 50 ppb analysis under 50x objective.

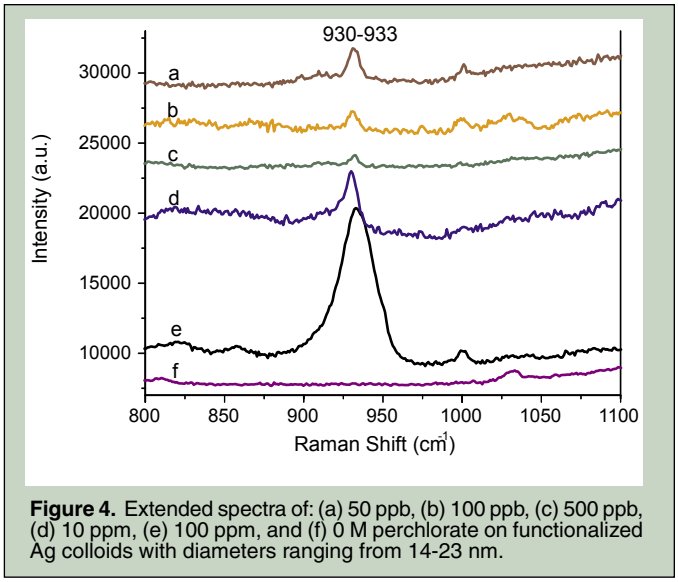

Figure 4. Extended spectra of: (a) 50 ppb, (b) 100 ppb, (c) 500 ppb, (d) 10 ppm, (e) 100 ppm, and (f) 0 M perchlorate on functionalized Ag colloids with diameters ranging from 14-23 nm.

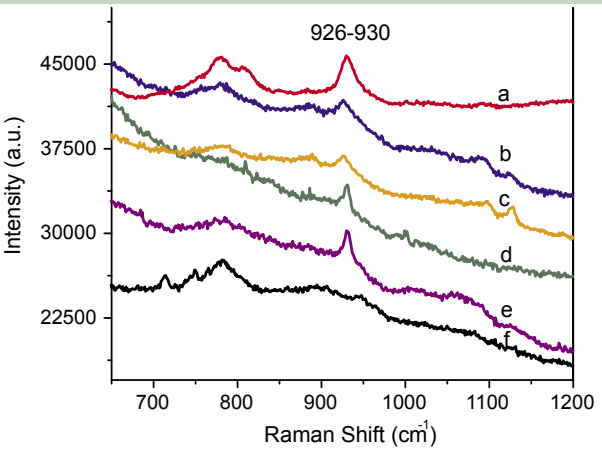

Figure 5. Extended spectra of: (a) 10 ppb,(b) 50 ppb,(c) 100 ppb, (d) 1 ppm, (e) 10 ppm, (f) 0 M perchlorate on functionalized Ag-doped silica sol-gel films.

[4,10]. Moreover, as demonstrated by Hu et al. and Kralchevsky et al. [11, 12], no chemical was needed to induce aggregation because capillary forces present during the drying of the Ag colloid solution seemed to cause particles to aggregate.

Although some studies have cited irreproducibility of results using Ag aggregates for SERS enhancement [13], our results showed that detecting ClO_4^- on aggregated Ag colloids even at 50 ppb was reproducible in different trials. This result may be explained by previous studies that have shown Ag aggregates to absorb radiation most intensely in the near-infrared region of the electromagnetic spectrum, especially in the presence of ClO_4^- [14].

The detection of ClO_4^- was relatively homogenous per sample until concentrations entered the part per billion range, where ClO_4^- detection only occurred on certain parts of the sample. Moreover, the Ag-doped silica sol-gel, with a more consistent Ag cluster composition, did not yield a significantly more homogeneous detection of ClO_4^- per sample than the Ag sol. Also in the ppb range, as seen for both substrates in Figures 4 and 5, ClO_4^- peak intensities did not decrease with concentration. At such low concentrations and given the ~1 cm breadth of functionalized Ag sites available for ClO_4^- adsorption, it is likely that ClO_4^- signal intensities were more dependent on the probability of finding an SERS active, ClO_4^- adsorbed Ag cluster rather than on the number of ClO_4^- molecules present in one site.

Functional Group Enhancement

Figures 4 and 5 also show how the addition of the quaternary ammonium functional group layer allowed detection of concentrations 10^5 lower than on non-functionalized Ag sol particles. The application of the functional group layer, as depicted in Figure 6, was expected to have formed Si-O-Si bridges in between silver nanoparticles on the glass slide and in between silver nanoparticles embedded in the Ag-doped silica sol-gel, allowing the quaternary ammonium group to bring ClO_4^- anions into close proximity of Ag particles for SERS enhancement. Moreover, the short alkyl chains (C_2) capped with a trimethylammonium group used in this study were sufficiently selective in adsorbing ClO_4^- molecules. Further studies should use trihexylammonium and triethylammonium functional groups with both short (C_2) and long (C_6) alkyl chains to detect ClO_4^- since these groups were the primary components of the bifunctional anion-exchange resin that had previously detected ClO_4^- down to 10 ppb [7,15].

Ag Colloid versus Ag-doped Silica Sol-Gel Enhancement

As seen in Figure 7, the Raman signals detected on Ag colloids were sharper than those detected using the Ag-doped silica sol-gel although peak intensities and integral ratios were relatively the same. This may be due to the thinner layer of nanoparticles and more isolated clusters formed when Ag colloids were applied using the drop method as opposed to Ag doping in the Bao et al. method [5]. Calculations have predicted that to achieve high enhancement

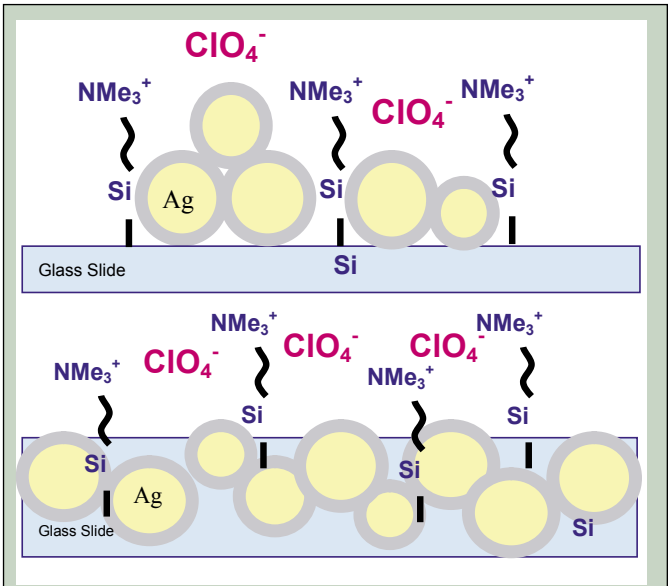

Figure 6. Quaternary ammonium groups adsorbing perchlorate anions on Ag colloids (top) and Ag-doped silica sol-gel films (bottom).

factors, either the average cross section per molecule must be very small or the number of SERS active molecules must be very small [16]. The Ag colloid method had a smaller density of Ag particles than the Ag-doped silica sol-gel method, which may explain why at 50 ppb, a greater enhancement is observed for the Ag colloid method.

During analysis, however, wet Ag colloid samples dried quicker than the Ag-doped silica sol-gel samples. The Ag-doped silica substrate, pictured in Figure 3b, may have concentrated ClO_4^- within its many cracks and crevices, and therefore allowed for better sensitivity in detecting ClO_4^- at 10 ppb than the Ag colloid sample. For the Ag-doped silica sol-gel, however, some ClO_4^- peaks were broader and red-shifted to ~926 cm^{-1}; this may indicate either more robust interactions with the quaternary ammonium functional group layer were occurring with the Ag-doped silica sol-gel or interactions with other molecules present in the substrate were occurring and, therefore, changing the vibrational frequency of ClO_4^-.

Future research on ClO_4^- detection using SERS of Ag colloids or Ag-doped silica sol-gels should focus on simulating real on-site analysis of surface water or groundwater samples. This work would include studying the effect of detecting ClO_4^- in the presence of competing ions such as chloride, nitrate, sulfate, carbonates, and even chlorite; improving the stability of the SERS substrate; and finding the optimal alkyl chain length and functional groups that could be used in SERS detection of ClO_4^-. Improvements in the homogeneity of detecting ClO_4^- on a given sample slide could also be made if the functionalized SERS substrate were micro-prepared at a much smaller scale, forming much fewer functionalized Ag aggregates and increasing the likelihood of ClO_4^- detection at even lower concentrations. Considering the portable Raman systems now available, the SERS approach to ClO_4^- detection may allow for the development of a probe that can be used directly at groundwater and surface water sites for *in situ* detection of significantly low concentrations of ClO_4^-.

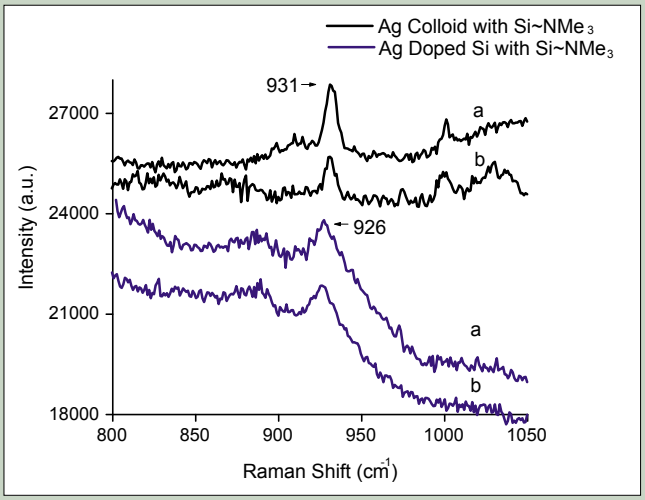

Figure 7. Extended spectra of: (a) 50 ppb and (b) 100 ppb perchlorate on functionalized Ag colloids and Ag-doped silica sol-gel.

ACKNOWLEDGEMENTS

This research was conducted in the summer of 2004 under the auspices of the Science Undergraduate Laboratory Internship program and would not have been possible without the support of the Department of Energy and Oak Ridge National Laboratory to whom I extend my many thanks. Thanks also to Dr. Lili Bao and Dr. Sheng Dai for providing silver-doped sol-gel films, Dr. Wei Wang for his expert advice, and Dr. Baohua Gu, my mentor, for his encouragement and guidance.

REFERENCES

[1] B. Gu, G. M. Brown, L. Maya, M. J. Lance, and B. A. Moyer, "Regeneration of Perchlorate-Loaded Anion Exchange Resins by a Novel Tetrachloroferrate Displacement Technique," *Environmental Science Technology*, vol. 35, pp. 3363-3368, 2001.

[2] Center for Food Safety and Applied Nutrition, "Perchlorate Questions and Answers," *U.S. Food and Drug Administration*, [Online Document], June 2004, [cited 2004 August 7], Available at HTTP: http://www.cfsan.fda.gov/~dms/clo4qa.html.

[3] Office of Solid Waste and Emergency Response, "Perchlorate Questions and Answers Document," *United States Environmental Protection Agency*, [Online Document], March 2003, [cited 2004 August 7], Available at HTTP: http://www.epa.gov/swerffrr/documents/perchlorate_qa.htm.

[4] K. Kneipp, H. Kneipp, R. Manohuran, I. Itzkan, R. R. Dasari, and M. S. Feld, "Near-Infrared Surface-Enhanced Raman Scattering Can Detect Single Molecules and Observe 'Hot' Vibrational Transitions," *Journal of Raman Spectroscopy*, vol. 29, pp. 743-747, 1998.

[5] L. Bao, S. M. Mahurin, R. G. Haire, and S. Dai, "Silver-Doped Sol-Gel Film as a Surface-Enhanced Raman Scattering Substrate for Detection of Uranyl and Neptunyl Ions," *Anal. Chem.*, vol. 75, pp. 6614-6620, 2003.

[6] B. Gu, Y. Ku, and G. Brown, "Treatment of Perchlorate-Contaminated Groundwater Using Highly Selective Regenerable Ion-Exchange Technology: A Pilot-Scale Demonstration," *Remediation*, vol. 12, pp. 51-68, Spring 2002.

[7] B. Gu, J. Tio, W. Wang, Y. Ku, and S. Dai, "Raman Spectroscopic Detection for Perchlorate at Low Concentrations," *Applied Spectroscopy*, vol. 58, pp. 741-744, 2004.

[8] J. A. Creighton, C. G. Blatchford, and M. G. Albrecht, *Trans. Faraday Society*, vol. 75, 790, 1979.

[9] P. A. Mosier-Boss, and S. H. Lieberman, "Detection of Anions by Normal Raman Spectroscopy and Surface-En-

hanced Raman Spectroscopy of Cationic-Coated Substrates," *Applied Spectroscopy*, vol. 57, pp. 1129-1137, 2003.

[10] M. Stockman, V. M. Shalaev, M. Moskovits, R. Botet, and T. F. George, "Enhanced Raman scattering by fractal clusters: Scale-invariant theory," *Physical Review B*, vol. 46, pp. 2821-2830, 1992.

[11] Hu, B. Zhao, W. Xu, Y. Fan, B. Li, and Y. Ozaki, "Simple Method for Preparing Controllably Aggregated Silver Particle Films Used as Surface-Enhanced Raman Scattering Active Substrates," *Langmuir*, vol. 18, pp. 6839-6844.

[12] P. A. Kralchevsky, N. D. Denkov, V. N. Paunov, O. D. Velev, I. B. Ivanov, H. Yoshimura, and K. Nagayama, "Formation of two-dimensional colloid crystals in liquid films under the action of capillary forces," *J. Phys.: Condens. Matter*, vol. 6, pp. A395-A402, 1994.

[13] F. Ni, and T. M. Cotton, "Chemical Procedure for Preparing Surface-Enhanced Raman Scattering Active Silver Films," *Anal. Chem.*, vol. 58, pp. 3159-3163, 1986.

[14] S. Sanchez-Cortes, J. V. Garcia-Ramos, G. Morcillo, and A. Tinti, "Morphological Study of Silver Colloids Employed in Surface-Enhanced Raman Spectroscopy: Activation when Exciting in Visible and Near-Infrared Regions," *Journal of Colloid and Interface Science*, vol. 175, pp. 358-368, 1995.

[15] B. Gu, G. Brown, L. Maya, M. Lance, and B. Moyer, "Regeneration of Perchlorate Loaded Anion Exchange Resins by a Novel Tetrachloroferrate Displacement Technique," *Environ. Sci. Technol.*, vol. 35, pp. 3363-3368, 2001.

[16] K. Kneipp, Y. Wang, H. Kneipp, I. Itzkan, R. R. Dasari, and M. S. Feld, "Population Pumping of Excited Vibrational States by Spontaneous Surface-Enhanced Raman Scattering," *Physical Review Letters*, vol. 76, no. 14, pp. 2444-2447, 1996.

Tanya B. Ostapenko is an undergraduate physics/mathematics double major who will be receiving her BS from Gettysburg College in May 2006. She participated in the DOE Science Undergraduate Laboratory Intern program two years at Thomas Jefferson National Accelerator Facility and conducted research for Hall C on electron/positron rates during summer 2003 and research in Hall B during summer 2004. Tanya's summer 2004 research of mass constraint usage for improvement of mass resolution was presented at the AAAS National Conference in February 2005. During the fall of 2004, Tanya worked on the vacuum system used in Gettysburg College's proton accelerator laboratory, and devised methods for modifying the beamline so that a leakage problem was fixed. In the spring of 2005, she was inducted into Sigma Pi Sigma, the national physics honor society. Tanya was awarded a 2005 Summer Undergraduate Research Fellowship at the National Institute of Standards and Technology, where she is working in the Ionizing Radiation division of the Physics Laboratory on industrial radiation processing and temperature dependencies on alanine dosimeter readings. She plans on entering an MS/PhD program in either physics or forensic science in the Fall of 2006.

Mac Mestayer is a staff physicist at Jefferson Lab. He received his Ph.D. from Stanford University in 1978 for analysis of deep-inelastic scattering. He has worked at Fermilab, CLEO and now Jefferson Lab on research into baryonic structure using electromagnetic probes. At Jefferson Lab his interest has focussed upon understanding the angular momentum state of quark-anti-quark pairs created in the course of hyperon production.

USE OF CONSTRAINED FITS TO IMPROVE MASS RESOLUTION IN PARTICLE PHYSICS

TANYA B. OSTAPENKO, M.D. MESTAYER

ABSTRACT

The Hall B Physics Division at Thomas Jefferson National Accelerator Facility (JLab) uses the CEBAF Large Acceptance Spectrometer (CLAS) and offline techniques to identify reactions by detecting all outgoing particles but one; this last one is identified by the missing mass of the reaction. For our purposes, we specifically examined the reaction $e\ p \rightarrow e'\ K^+\ \Lambda(1405)$, where $\Lambda(1405) \rightarrow \Sigma^-\ \pi^+$ and $\Sigma^- \rightarrow (n)\ \pi^-$. Our analysis requires that there is good resolution on the missing mass to minimize background and we achieve a better resolution if a formula is used in which one variable is constrained to the accepted value; for the aforementioned reaction, this would be the neutron mass. We proved this by using two different methods of calculating the reaction's Σ^- mass, either using the experimental neutron mass or the known neutron mass. For both methods, we plotted histograms of the calculations, as well as deriving the propagated error equations. From our methods and analysis, we conclude that there is a smaller experimental error on the Σ^- mass which uses the accepted neutron mass, rather than the experimentally determined neutron mass. In general, this is a technique that can be applied to other physics analyses and shows that a fit constrained by external information yields a better result than an unconstrained fit.

INTRODUCTION

Thomas Jefferson National Accelerator Facility (JLab) in Newport News, Virginia conducts scattering experiments to understand the structure of the sub-nuclear world. Each experimental hall at JLab is equipped with spectrometers to study a wide variety of areas pertaining to particle physics. Hall B uses a large acceptance spectrometer called CLAS, the acronym for CEBAF Large Acceptance Spectrometer. The main difference between CLAS and the other spectrometers at JLab is that CLAS's solid angle is 4π radians, about 2π steradians, and much larger than the solid angles of the other spectrometers. The advantage of a larger solid angle is that multi-particle final states typical of reactions, where excited mesons and baryons are produced, are more easily seen [1]. Such observations and studies are the focus of Hall B's experiments.

CLAS is a magnetic spectrometer; its magnet is comprised of six superconducting coils arranged azimuthally around the electron beamline. The magnetic field inside CLAS is calculated directly from the current flow in the coils. This design is ideal for good momentum resolution over a large solid angle in covering large areas of charged particles in polarized-target experiments. Electronics provide CLAS with its trigger system and data acquisition (DAQ) capabilities. The detectors used in CLAS are arranged circularly around the beamline in successive layers, each of which plays a role in tracking a particle's path [1].

The main use of CLAS is for measuring cross sections for several strange final states; for this project, we studied the specific reaction $e\,p \rightarrow e'\,K^+\,\Lambda(1405)$, where $\Lambda(1405) \rightarrow \Sigma^-\,\pi^+$ and $\Sigma^- \rightarrow (n)\,\pi^-$. The parentheses around the neutron symbol indicate that the neutron is not detected directly, whereas the e', K^+, π^+ and π^- 4-momenta are detected and their energies computed. Detection of hyperons in similar reactions is done by means of the missing mass of the reaction, which increases our statistics and ensures that our acceptance is smooth and easily calculable. In addition, there exists background to the missing mass, which is a common experimental situation, so the goal is to eliminate as much of the background as possible. Graphically, we want to make the missing mass peak as narrow as possible.

One way to improve the resolution on the missing mass is to use a constrained calculation, where the missing energy and momentum of an intermediate state are constrained as per the known missing mass from the Particle Data Group's (PDG) tables. In this calculation, there are two methods used: the first uses the missing momentum and missing energy from the event as the momentum and energy of the neutron; the second uses the event's missing momentum, but uses the accepted value of the neutron's mass instead of the event's missing energy [2]. In using the accepted value for the neutron's mass, we place a mass constraint on the data, thus using our prior knowledge of the neutron's accepted mass.

The motivation for using successive mass constraints is based on eliminating as many background signals as possible and narrowing down the amount of data that fits all the cut requirements. Any signals that do not fulfill all the constraints are cut out of the sample, whereas signals that meet the prerequisites are kept. Therefore, a narrower peak width will have less background contamination than a wider peak width [2].

For this reason, our error analysis sought to prove that more constraints on the data will ultimately generate smaller error than data that does not have as many or no constraints in effect. Specifically, we focused on the calculation of the missing neutron mass and the invariant $n\pi^-$ mass resulting from $\Lambda(1405)$'s decay, although this analysis can apply to any physics analysis. In order to prove our conjecture, we decided to analyze the missing neutron mass, the invariant $n\pi^-$ mass without constraining the neutron mass and the invariant $n\pi^-$ mass after using a neutron mass constraint, both graphically and deriving the propagated error equations.

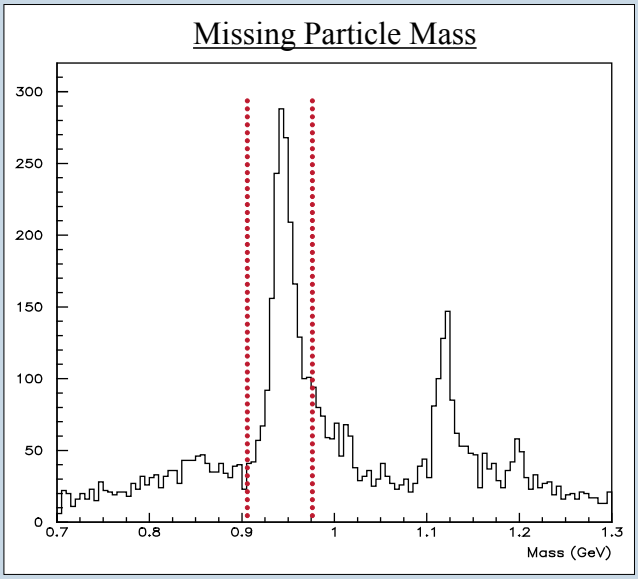

Figure 1. Missing particle mass of the reaction, with the neutron cut marked at 0.915 and 0.98.

METHODS

The first step in finding the invariant $n\pi^-$ mass is to make a cut on the identification of the neutron. To do this, we calculate the missing mass of the reaction from:

$$M^2 = E^2 - P^2 \qquad (1)$$

where M is the missing mass of the reaction, E is the missing energy and P is the missing momentum.

Next, we create a plot of this missing mass to determine what the reaction's missing particle is. As can be seen in Figure 1 [3], the peak at about 0.94 GeV is statistically identified as a neutron, so we place a cut at 0.915 and 0.98 for further analysis.

Since we want to exclusively study the $n\pi^-$ in this project, we define the invariant $n\pi^-$ mass in terms of 4-momenta as:

$$|M_{\Sigma^-}|^2 = |\vec{P}_{\Sigma^-}|^2 = (\vec{P}_{\pi^-} + \vec{P}_n)^2 \qquad (2)$$

where we introduce the shorthand for the Σ^-, π^- and neutron 4-momenta.

In turn, the 4-momentum is defined as:

$$\vec{P} = [E,P] = (E,P_x,P_y,P_z) \qquad (3)$$

where P is the 3-momentum vector and P_x, P_y and P_z are the x-, y- and z- components of the 3-momentum vector respectively.

The most important point to remember is as follows; the 4-momentum of the neutron candidate, called so because it is only statistically identified as a neutron, can be calculated two ways, with and without the mass constraint. These calculations are done only for events with e', K^+, π^+ and π^- detected and the event's missing mass approximately that of a neutron. For our purposes, we found the error in terms of the 4-momentum of each detected particle. We used histograms that were previously made of the missing neutron mass and the two invariant $n\pi^-$ masses for the reaction [3].

We can also explicitly derive the propagated error equations for each method and compare in order to determine which error is smaller, starting with the 4-momentum conservation equation of the situation:

$$\vec{P}_{\Sigma^-} = \vec{P}_{\pi^-} + \vec{P}_n \qquad (4)$$

where we have the 4-momenta of Σ^-, π^- and the neutron. Next, we square the equation, which gives us:

$$\vec{P}_{\Sigma^-}{}^2 = (\vec{P}_{\pi^-} + \vec{P}_n)^2 = \vec{P}_{\pi^-}{}^2 + 2\vec{P}_{\pi^-}\vec{P}_n + \vec{P}_n{}^2 \qquad (5)$$

Therefore, the general error propagation equation is:

$$\delta(M_{\Sigma^-}^2) = 2M_{\Sigma^-}\delta M_{\Sigma^-} = 2M_{\Sigma^-}\sqrt{\sum_i \left(\frac{\partial(M_{\Sigma^-}^2)}{\partial(P_i)}\delta(P_i)\right)^2} \quad (7)$$

where we have the sum of the squares of all the partial derivatives.

Given the following unconstrained 4-momentum:

$$\vec{P}_{n,\text{unconstr}} = \vec{P}_{e^-} - \vec{P}_{K^+} - \vec{P}_{\pi^+} + \vec{P}_{\pi^-}$$

we can substitute into Equation 4:

$$\vec{P}_{\Sigma^-,unconstr} = \vec{P}_{\pi^-} + \left(\vec{P}_{e^-} - \vec{P}_{K^+} - \vec{P}_{\pi^+} - \vec{P}_{\pi^-}\right) = \vec{P}_{e^-} - \vec{P}_{K^+} - \vec{P}_{\pi^+} \quad (8)$$

Therefore, squaring Equation 8 will yield $M^2_{\Sigma^-}$:

$$\begin{aligned} M^2_{\Sigma^-,unconstr} &= \vec{P}^2_{\Sigma^-,unconstr} = \left(\vec{P}_{e^-} - \vec{P}_{K^+} - \vec{P}_{\pi^+}\right)^2 \\ M^2_{\Sigma^-,unconstr} &= \vec{P}^2_{e^-} + \vec{P}^2_{K^+} + \vec{P}^2_{\pi^+} - 2\vec{P}_{e^-}\vec{P}_{K^+} - 2\vec{P}_{e^-}\vec{P}_{\pi^+} + 2\vec{P}_{K^+}\vec{P}_{\pi^+} \end{aligned} \quad (9)$$

The error on the unconstrained $M^2_{\Sigma^-}$ will be the partial derivatives with respect to each momentum term, multiplied by the error on it. These partial derivatives are:

$$\frac{\partial(M^2_{\Sigma^-,unconstr})}{\partial(\vec{P}_{e^-})}\delta(\vec{P}_{e^-}) = \left(2\vec{P}_{e^-} - 2\vec{P}_{K^+} - 2\vec{P}_{\pi^+}\right)\delta(\vec{P}_{e^-}) \quad (10a)$$

$$\frac{\partial(M^2_{\Sigma^-,unconstr})}{\partial(\vec{P}_{K^+})}\delta(\vec{P}_{K^+}) = \left(2\vec{P}_{K^+} - 2\vec{P}_{e^-} + 2\vec{P}_{\pi^+}\right)\delta(\vec{P}_{K^+}) \quad (10b)$$

$$\frac{\partial(M^2_{\Sigma^-,unconstr})}{\partial(\vec{P}_{\pi^+})}\delta(\vec{P}_{\pi^+}) = \left(2\vec{P}_{\pi^+} - 2\vec{P}_{e^-} + 2\vec{P}_{K^+}\right)\delta(\vec{P}_{\pi^+}) \quad (10c)$$

Hence, the total error on the unconstrained invariant $n\pi^-$ mass is:

$$\delta(M^2_{\Sigma^-,\text{unconstr}}) = 2M_{\Sigma^-,\text{unconstr}}\delta M_{\Sigma^-,\text{unconstr}}$$

$$\delta(M^2_{\Sigma^-}) = 2M_{\Sigma^-,unconstr}\sqrt{\begin{aligned}&\left\{\left(2\vec{P}_{e^-} - 2\vec{P}_{K^+} - 2\vec{P}_{\pi^+}\right)\delta\vec{P}_{e^-}\right\}^2 + \\ &\left\{\left(2\vec{P}_{K^+} - 2\vec{P}_{e^-} + 2\vec{P}_{\pi^+}\right)\delta\vec{P}_{K^+}\right\}^2 + \\ &\left\{\left(2\vec{P}_{\pi^+} - 2\vec{P}_{e^-} + 2\vec{P}_{K^+}\right)\delta\vec{P}_{\pi^+}\right\}^2\end{aligned}} \quad (11)$$

where:

$$M_{\Sigma^-,\text{unconstr}} = (\vec{P}_{e^-} - \vec{P}_{K^+} - \vec{P}_{\pi^+})$$

The uncertainty in $M^2_{\Sigma^-}$ when the neutron mass is constrained to its known value is given by:

$$M^2_{\Sigma^-,\text{constr}} = (M_n + \vec{P}_{\pi^-})^2$$

$$M^2_{\Sigma^-,\text{constr}} = M_n^2 + 2M_n\vec{P}_{\pi^-} + \vec{P}^2_{\pi^-} \quad (12)$$

Therefore, the partial derivative gives the following:

$$\frac{\partial\left(M^2_{\Sigma^-,constr}\right)}{\partial\left(\vec{P}_{\pi^-}\right)}\delta\left(\vec{P}_{\pi^-}\right) = \left(2M_n + 2\vec{P}_{\pi^-}\right)\delta\left(\vec{P}_{\pi^-}\right) \quad (13)$$

Hence, the total error is:

$$\begin{aligned}\delta(M^2_{\Sigma^-,constr}) &= 2M_{\Sigma^-,constr}\sqrt{\left\{\left(2M_n + 2\vec{P}_{\pi^-}\right)\delta\left(\vec{P}_{\pi^-}\right)\right\}^2} \\ &= 2M_{\Sigma^-,constr}\left(2M_n\delta\vec{P}_{\pi^-} + 2\vec{P}_{\pi^-}\delta\vec{P}_{\pi^-}\right)\end{aligned} \quad (14)$$

where:

$M_{\Sigma^-,\text{constr}} = (M_n + \vec{P}_{\pi^-})$

RESULTS

Figure 2 illustrates the invariant $n\pi^-$ mass without the neutron mass constraint applied, marking the width of the peak between two dotted lines and Figure 3 shows the invariant $n\pi^-$ mass with the neutron mass constraint applied.

Equation 11 from above is the error on the unconstrained invariant $n\pi^-$ mass:

$$\delta(M^2_{\Sigma^-}) = 2M_{\Sigma^-,unconstr}\sqrt{\begin{aligned}&\left\{\left(2\vec{P}_{e^-} - 2\vec{P}_{K^+} - 2\vec{P}_{\pi^+}\right)\delta\vec{P}_{e^-}\right\}^2 + \\ &\left\{\left(2\vec{P}_{K^+} - 2\vec{P}_{e^-} + 2\vec{P}_{\pi^+}\right)\delta\vec{P}_{K^+}\right\}^2 + \\ &\left\{\left(2\vec{P}_{\pi^+} - 2\vec{P}_{e^-} + 2\vec{P}_{K^+}\right)\delta\vec{P}_{\pi^+}\right\}^2\end{aligned}}$$

where:

$$M_{\Sigma^-,\text{unconstr}} = (\vec{P}_{e^-} - \vec{P}_{K^+} - \vec{P}_{\pi^+})$$

and Equation 14 is the error on the constrained invariant $n\pi^-$ mass:

$$\delta(M^2_{\Sigma^-,constr}) = 2M_{\Sigma^-,constr}\left(2M_n\delta\vec{P}_{\pi^-} + 2\vec{P}_{\pi^-}\delta\vec{P}_{\pi^-}\right)$$

where:

$M_{\Sigma^-,\text{constr}} = (M_n + \vec{P}_{\pi^-})$

DISCUSSION & CONCLUSIONS

In analyzing the aforementioned results, it is important to remember the purpose of the project. Intuitively, we know that using the neutron mass's known value, rather than the experimental value, should give us less error.

Generally, the accepted rule of a physics analysis is to use all of the information known in order to make a better decision on which direction to proceed in the analysis. Sometimes, this may not help, because it is possible for data to conflict with one another, thus making it difficult to decide which data is correct.

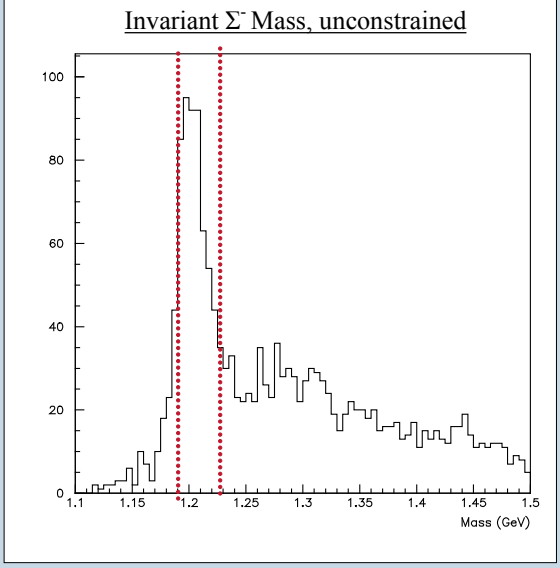

Figure 2. Peak width (1.179 < width < 1.235) of unconstrained invariant $n\pi^-$ mass (between the dotted lines).

Nonetheless, all the prior knowledge is used, since knowing more information about a particular reaction should help to decrease the amount of error.

In comparing Figure 2 and Figure 3, it appears that the constrained invariant mass yields a narrower peak width than the unconstrained invariant mass. In comparing the background of each, it is seen that the constrained invariant $n\pi^-$ has a smaller background, hence it has a better experimental resolution than the unconstrained case.

Although we can show this graphically, it is necessary to prove it mathematically by propagating the error for each situation; our derivations show that the smaller error is indeed on the constrained invariant mass. This is a specific example of a general finding that using external data improves the final results.

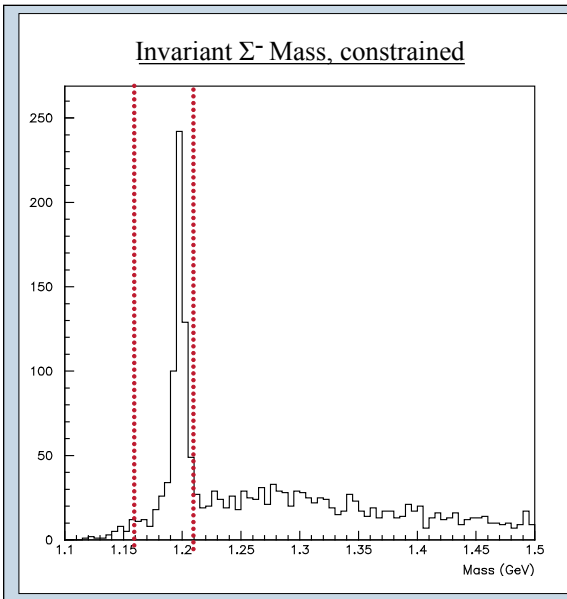

Figure 3. Peak width (1.179 < width < 1.235) of constrained invariant $n\pi^-$ mass (between the dotted lines).

ACKNOWLEDGEMENTS

First of all, I want to acknowledge my mentor, Dr. M.D. Mestayer, and $\Lambda(1405)$ data analysis group for overseeing and assisting me in my project this summer. Next, I want to thank the Gettysburg College physics department for their continued support and advice in aiding my development towards a career in physics.

I also want to thank my supervisors in the Science Education department and all the other SULI/PST interns for making this summer a truly enjoyable experience.

Finally, I want to thank the Office of Science, United States Department of Energy (DOE) and Jefferson Lab for providing the opportunity to work at Jefferson Lab for another summer. I certainly enjoyed the academic and social atmosphere that the DOE's SULI program creates for its interns and I look forward to continuing along the path created by the DOE and Jefferson Lab program en route to my future graduate studies and professional livelihood.

REFERENCES

[1] E.S. Smith, "The CEBAF Large Acceptance Spectrometer (CLAS)," Nuclear Instruments and Methods in Physics Research, vol. 503, section A, pp. 514-553, 2003.

[2] M.D. Mestayer (private communication), 2004.

[3] Daniel S. Carman, "$\Lambda(1405)/\Sigma(1385)$ Analysis – CLAS e1c 4 GeV Data Sets", Thomas Jefferson National Accelerator Facility, Newport News, 2003.

Kevin W. Reynolds is a junior at Norfolk State University where he is pursuing a BS in physics with a minor in mathematics. Reynolds worked at Stanford Linear Accelerator Center where he tested high-resolution silicon and germanium analyzers to be used in a X-Ray Raman Spectrometer for probing the fundamental structure of liquid water. At the conclusion of his research, he was awarded the Ernest Coleman Award by SLAC for outstanding initiative and citizenship as a young researcher. Kevin presented at the 2005 Annual AAAS meeting and was recognized as a winner of the Physical Science poster session. This coming summer he plans to do an internship through the MURF program at Caltech where he will build microfluidic channels with possible medical application. Reynolds plans to attend graduate school in aerospace engineering.

Uwe Bergmann is a Staff Scientist at the Stanford Synchotron Radiation Laboratory which is part of the Stanford Linear Accelerator Center. He received his Ph.D. in Physics from Stony Brook University, NY in 1994. Following a 2-year postdoc at the European Synchrotron Radiation Facility in Grenoble, France he joined Lawrence Berkeley National Laboratory (LBNL), first as a postdoc then as a scientist. Before joining SSRL in 2003 he held a joint appointment LBNL and University of California, Davis. His current research interests include the development and application of novel x-ray spectroscopic techniques to study transition metal complexes and low Z materials including water. The particular techniques are non-resonant x-ray Raman scattering, resonant inelastic x-ray scattering, x-ray emission spectroscopy and selective x-ray absorption spectroscopy. Most recently he has started work on x-ray fluorescence imaging of the Archimedes Palimpsest.

TESTING OF HIGH-RESOLUTION SI AND GE ANALYZERS FOR X-RAY RAMAN SCATTERING AND X-RAY EMISSION SPECTROSCOPY

KEVIN W. REYNOLDS, UWE BERGMANN

ABSTRACT

A project at Stanford Linear Accelerator Center (SLAC) is currently underway for the building of a new multi-crystal x-ray spectrometer that will be used to probe the fundamental structures of light elements, including water, as well as 3d transition metals, such as metalloproteins, in dilute systems. Experimentation for determining the focal lengths for the prospective high-resolution, spherically-curved silicon (Si) and germanium (Ge) analyzers for the instrument and the energy resolutions at their respective focal points is described. The focal lengths of the Si and Ge analyzers being sampled were found by minimizing the focal size made from a diffused helium-neon (HeNe) gas laser operating at 632 nm (0.95 meV). Afterwards, the energy resolutions were determined by using synchrotron radiation (SR), in the range from 6-16 keV energies. The experiments were performed at Beamline 10-2 at the Stanford Synchrotron Radiation Laboratory (SSRL), a division of SLAC. This data, along with the energies of the incident beams, was used to determine which samples are most effective at focusing x-rays to the highest spatial and energy resolution. Sample Si (440)A, with a focal length of 1015.2 mm, had the best energy resolution. Furthermore, a new multi-crystal goniometer was tested and commissioned. As part of this work, the device was prealigned into Rowland geometry, in order to facilitate the process of finding a single high-energy resolution x-ray focus for all 7 analyzers.

INTRODUCTION

As strange as it may seem, water, taken to be one of nature's most fundamental elements, has been and still is, in large part, a mystery. For the past 20 years, scientists have maintained a consensus that a typical water molecule forms, on average, 3.5 hydrogen bonds with nearby water molecules at any moment in time. But recent research, based partly on X-ray Raman scattering (XRS), suggests that there might be only two hydrogen bonds per molecule [1-3]. The confirmation of such an assignment would have dramatic consequences in the whole field of water research. Therefore efforts are under way to build a new, more efficient, instrument for future X-ray Raman studies. The device will also be used for other studies including X-ray Emission spectroscopy (XES) on 3d transition metals.

In prototyping for a new instrument, several innovations will be made and compared to a previous design [4]. An essential requirement for the instrument is the ability to diffract one particular energy back to a focal point in order to obtain information about the scattered/emitted x-ray energy. At the same time, a large solid angle should be captured to make the measurement efficient. Bragg diffraction, as used in this paper, underlies the mechanism of how the instrument works. Each analyzer needs to be capable of good energy resolution and large angular acceptance. To achieve the highest energy resolution and smallest focus possible, a variety of

Si and Ge crystals are tested. In order to characterize analyzers appropriately both the focal sizes and energy resolution spectra are measured and compared. The first experimental setup uses a HeNe gas laser to measure the respective focal lengths and focal sizes of the analyzers. The second arrangement incorporates the found values by using synchrotron radiation to study the energy resolutions found at those lengths. In this report, we show which crystals will provide the best resolution for the new X-ray spectrometer. This data has been used to determine from which provider the analyzer crystals for the new instrument will be purchased.

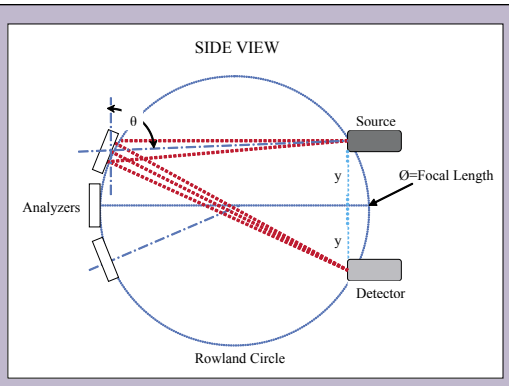

Figure 1. Left: Side view of a Rowland Geometry that shows how a diffused radiation source is focused back to a detector through elastic scattering at a Bragg angle θ. Right: Photo of Experiment I setup showing the superimposed path of the diffused laser as it hits the analyzer.

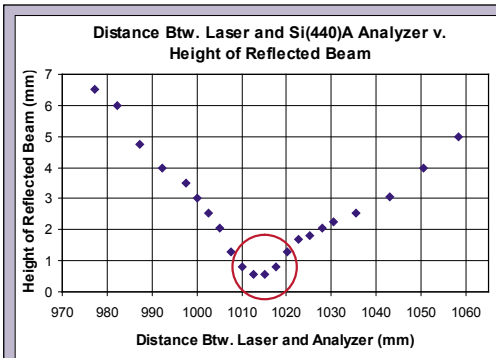

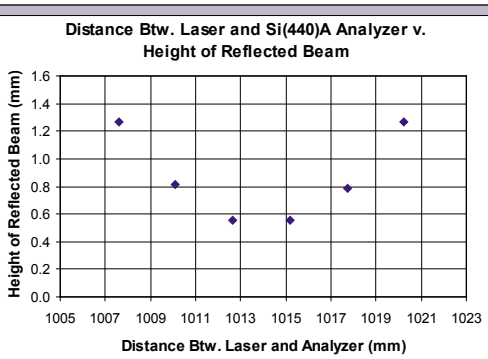

Figure 2. *Left:* Graph showing relationship between distance and height of beam. *Right:* Graph showing magnified view of the region containing the focus.

MATERIALS AND METHODS

Bragg's Law

To effectively monochromatize, or make of a single frequency, radiation being scattered from a point source, a special geometry, called Rowland geometry, serves as a means for capturing a large portion of the solid angle of scattered light without significant energy resolution loss. Still, even in Rowland geometry the energy resolution is limited, mainly due to stresses in the crystal structure, geometric effects related to the beam size, and non-perfect spherical bending of the silicon and germanium wafers into the concavity of each different analyzer. When collimated x-rays hit a crystalline solid, their approximately energy upon reflection can be obtained from Bragg's Law,

$$2\,d \sin\theta = n\,\lambda, \qquad (1)$$

where θ is the Bragg angle or angle of incidence, λ is the wavelength of the incident x-rays, *n* is an integer describing multiples of the wavelength, and *d* is the spacing between sequentially planes in the crystal [5, 6]. The distance $d = a / (h^2 + k^2 + l^2)^{1/2}$, where *a* is the lattice parameter and *h*, *k*, and *l* are Miller indices, or coordinates defining the orientation of the intrinsic crystalline planes. Since the *d*-spacing is extraordinarily minute, monochromators often are used to make beams having energies well above 1 keV uniform in wavelength. The inverse relationship between wavelength λ and energy *E* is shown by

$$E = \hbar c / \lambda \quad \rightarrow \quad E[\text{keV}] = 12.3985 / \lambda[\text{Å}] \qquad (2)$$

with wavelength being given in Å and energy being obtained in keV. As can be drawn from Eq. 1, the wavelength of the incident beam has to be less than two times the distance between sequential planes in the crystal in order for the wave to be diffracted.

To estimate the energy resolution of Bragg optics, we form the derivative of Eq. 1 shown by

$$|\Delta E/E| = |\Delta\lambda / \lambda| = \Delta\theta \cot\theta. \qquad (3)$$

Equation 3 shows that for a given angular spread Δθ, the smallest energy resolution $\Delta E/E$ can be achieved at Bragg angles close to 90° where *cot* θ becomes very small. This is why high-energy resolution Bragg optics is operated in back scattering, where θ is close to 90°.

Rowland's Geometry

Focusing of a radiation source can be achieved by either employing a spherical arrangement of a large number of small flat crystals, which ultimately results in the best focus, or by bending Miller planes in the structure of a single crystal. Our instrument utilizes a unique combination of the two; it calls for eventually positioning 28 spherically-curved crystals on intersecting Rowland circles with a diameter equal to the established focal length (Figure 1). This compromise of energy resolution and capturing of a large solid angle of the scattered radiation has become a promising means of obtaining an efficient analyzer. In Rowland geometry, analyzers source and detector are positioned on a circle (Rowland circle), with both source and detector at a distance *y* above and below the diameter (see Figure 1) [4]. Once completed, the analyzer system should capture ~1.75 % of the total 4π solid angle, a factor 4 improvement over the previous x-ray spectrometer [4]. By covering

greater portions of the solid angle, higher efficiency can be achieved for examining unsolved aspects of the light elements and 3d transition metals.

Experiment I

In order to characterize the eight different analyzers for the highest energy resolution, the focal length of each of the analyzers was experimentally determined. The crystals ranged from thicknesses of 0.15 to 0.5 mm. They were glued or ionically bonded on spherically-curved glass substrates with radii of curvature ranging from 850 to 1020 mm. The diameters of the substrates ranged from 90 mm to 100 mm.

The focal length of each of the analyzers was found using a HeNe laser diffused radially by a simple scatterer, a piece of clear tape, placed overtop of the front lens. One at a time, each analyzer was fastened into a metal frame holder mounted vertically on a manually-operated, screw-transitioned table. The distances traveled closer to and farther away from the laser source were recorded in increments of 2.54 mm. This distance was the calculated horizontal distance traveled during one revolution of the turning screw. The analyzer was positioned 5 mm vertically below the laser's focal point to fulfill the Rowland condition (see again Figure 1) so that the reflected laser beam appeared 10 mm below the laser source on a white piece of paper attached to the front of the encasement for the laser.

The height of the focus was measured using a micro telescope, leveled off at horizontal, which assigned number values on a scale of 0.01 of an inch, to the vertical extremes of the diffracted beam. These numbers were added, divided by 1000, and multiplied by 25.4 to find the height of the beam in millimeters. Heights larger than 4.5 mm were measured with a ruler. Graphs were produced for all of the analyzers and related the horizontal distance between the laser and analyzer and the size of the diffracted beam as shown in Figure 2. The region surrounding the minimum of the graph was magnified and used to identify a minimum focal size. The distance corresponding to the focal size was recorded.

Since these measurements only accounted for the horizontal distance R to the outer edges of the analyzer, the focal length F was calculated using a right triangle diagram as shown in Figure 3. Later, the concavity Δx was determined by subtracting distance R from distance F.

Experiment Ii

At SSRL, electrons are accelerated in a circular vacuum loop, known as booster, to nearly the speed of light were they form packets of electrons known as bunches. These bunches are approximately the diameter of a human hair. From the synchrotron, the bunches are then fed into a storage ring where bending magnets change the direction of the beam at twelve different locations. At these selected turns, the fast-moving electrons lose some of their energy in the form of emitted photons, or electromagnetic radiation known as synchrotron radiation. In addition, to these bending magnets SSRL also employs arrays of magnets known as wigglers. Because the electrons undergo multiple lateral accelerations these wigglers produce even more intense synchrotron radiation. The electrons continue through the storage ring where electromagnetic kickers replenish their lost energy so a constant energy can be maintained. The radiation emitted by the electron bunches produces a broad spectrum of synchrotron light ranging from infrared to x-rays. Conveniently, tangential ports channel the radiation into beamlines which end at experimental stations. Horizontal and vertical focusing mirrors increase the spatial resolution of the beam. A monochromator selects a specific wavelength, and thus a specific energy. In our experiments, the slit width in front of the scatterer was set to 0.12 mm horizontal X 1.00 mm vertical.

Experiment II used synchrotron radiation to identify the highest energy resolutions produced by the analyzers at their measured focal lengths. Upon entering the experimental hutch, or end station, at wiggler Beamline 10-2, the x-rays were directed through an ion chamber filled with nitrogen gas. As the x-rays passed through the chamber, they knocked

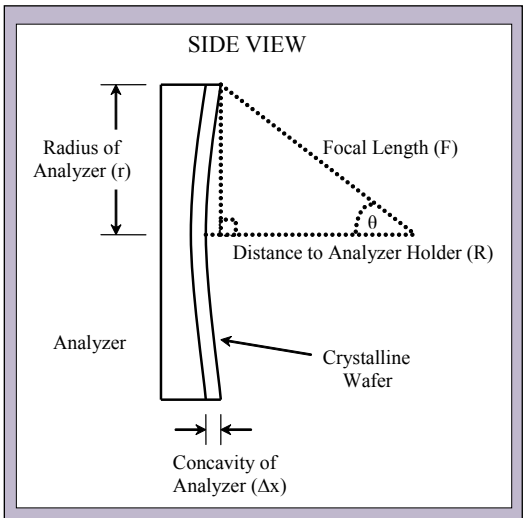

Figure 3. Detailed side view schematic for calculating the focal length F of an analyzer and determining its concavity x. As noted in *Fig.1 Left*, the distance R on the Rowland circle is half of the focal length.

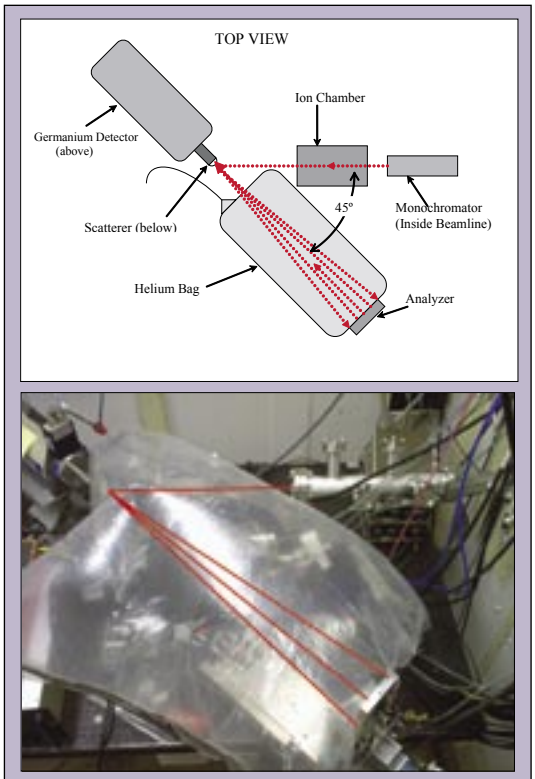

Figure 4. *Above* Top view of the schematic setup for Experiment II demonstrating the 45˚ chosen for back scattering. *Below:* Photo showing Experiment II setup and a superimposed path of the invisible synchrotron radiation as it hits the analyzer.

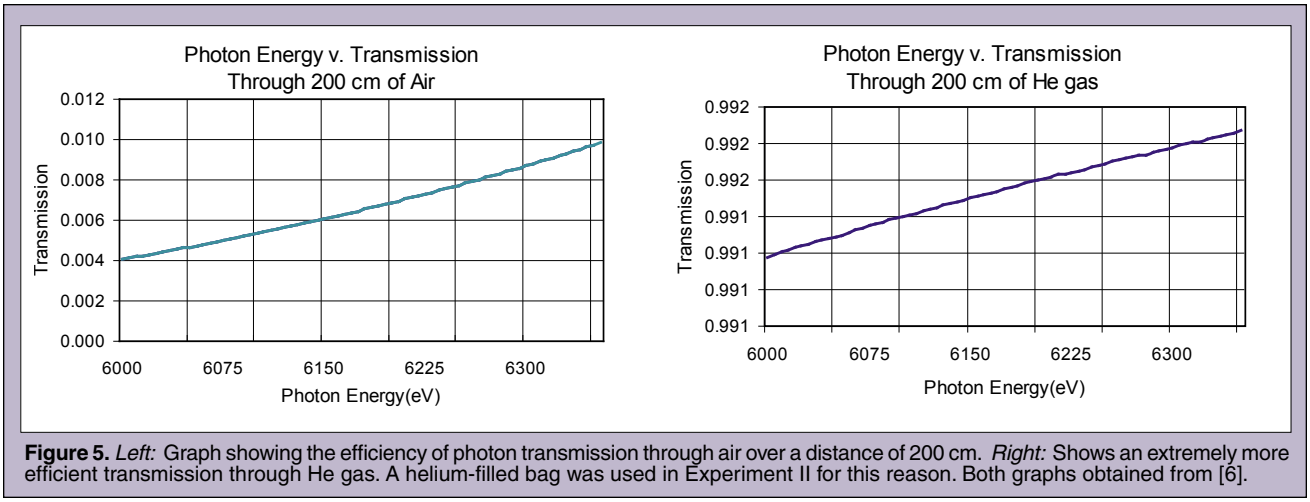

Figure 5. *Left:* Graph showing the efficiency of photon transmission through air over a distance of 200 cm. *Right:* Shows an extremely more efficient transmission through He gas. A helium-filled bag was used in Experiment II for this reason. Both graphs obtained from [6].

electrons out of the nitrogen atoms and produced a cloud of free electrons. A high voltage across two plates inside of the chamber pulled away the electrons to a positively charged anode. In turn, the measured current was proportional to the intensity of the x-rays passing through the chamber.

After passing through the ion chamber, the beam was scattered by a piece of paraffin taped to a metal column. The instrument holding the analyzer was placed at a 45˚angle adjacent to the incoming x-ray (see Figure 4). For purposes of limiting the attenuation of x-rays from air, a plastic bag was filled with helium gas and placed between the scatterer and analyzer. The difference in the absorption of photons as they propagate through the two gases is depicted in the graphs contained in Figure 5. According to the figures, transmission of 6.46 keV x-rays through helium gas is about 100 times in magnitude better than transmission through air over the same 200 cm distance. In fact, the transmission through the helium gas is nearly 100%, and loss in the plastic of the bag is also negligible. This compliment to our experiment drastically increased the signal that reached the detector and enabled us to perform much improved studies.

After being diffracted by the analyzer, the beam was refocused into a germanium detector positioned directly above the scatterer as shown in Figure 4. A piece of lead tape was placed around the front beryllium window to minimize unwanted scattering background. Inside of the detector, the x-ray beam interacted with semi-conducting Ge diodes sensitive to the ionizing radiation. As a result, electrons were knocked out of the semi-conducting material. Finally, the electrons were drawn to an anode similar to the one in the ionizing chamber. A pulse proportional to the energy of the photons was produced, and a ~400 eV discriminator window around the wanted energy provided an additional background removal. The detector was then operated in photon-counting mode.

RESULTS

In Experiment I, a spreadsheet comparing the horizontal distance between the analyzer and laser and the vertical size of the diffracted beam just below the laser was created for each of the eight analyzers tested. Measurements of the diffracted beam were taken at distance intervals of 2.54 mm along the region containing the smallest focal size. Farther away from the focus, multiples of this distance were utilized for their efficiency at covering space as well as for their structural reinforcement in the graphs that were to be created later (see Table 1 and Figure 2). Although the smallest focal sizes were easily identified with the numbers collected, graphs were made so that the minimum regions could be examined in greater detail. Points along these regions were then scaled to a larger size so that a smooth best-fit curve could be drawn in by hand. This method allowed for the focal distances to be even more accurately depicted (see Figure 2). A chart containing both the manufacturers' quoted and experimentally determined focal lengths is shown in Table 2.

Our measured values for the focal lengths were then used by us in Experiment II where the energy resolution of the analyzers was studied. This was done by scanning the incident x-ray energy through the energy range of the analyzer. We then obtained the total energy resolution which is the convolution of both monochromator and analyzer resolutions. The graphs produced by the detector (see Figure 6) relating the energy of the incident beam and the intensity of the photons reaching the detector were used to determine these resolutions using Full Width Half Maximum (FWHM). This method found the total energy resolution of the system by the measured width of the line at half the vertical height of the curve.

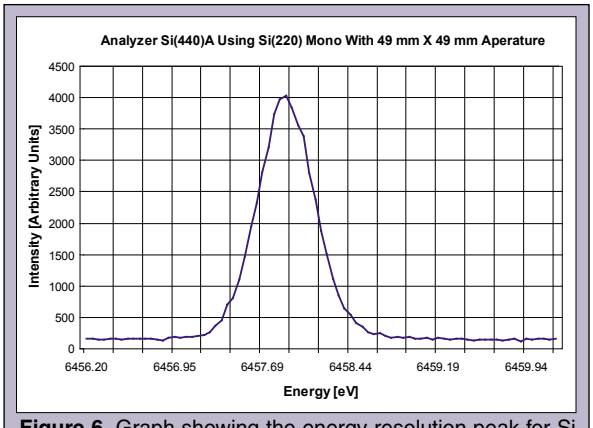

Figure 6. Graph showing the energy resolution peak for Si (440)A which, overall, had the best resolution.

Distance from Laser to Front Edge of Analyzer [mm]	Reading From Telescope	Size of Reflected Beam [mm]
1058.19	NA	5.00
1050.60	NA	4.00
1043.01	120.00	3.05
1035.42	100.00	2.54
1030.36	89.00	2.26
1027.83	80.00	2.03
1025.30	71.00	1.80
1022.77	66.00	1.68
1020.24	50.00	1.27
1017.71	31.00	0.79
1015.18	22.00	0.56
1012.65	22.00	0.56
1010.12	32.00	0.81
1007.59	50.00	1.27
1005.06	80.00	2.03
1002.53	100.00	2.54
1000.00	NA	3.00
997.47	NA	3.50
992.41	NA	4.00
987.35	NA	4.75
982.29	NA	6.00
977.23	NA	6.50

Table 1. Example spreadsheet relating distance to size of focus for Si(440)A.

Assuming that the resolution profiles were of Gaussian shape, the total resolution ΔE_{TOT} is given by the formula

$$\Delta E_{TOT} = (\Delta E_{MONO}{}^2 + \Delta E_{ANAL}{}^2)^{1/2} \qquad (4)$$

where ΔE_{ANAL} refers to the analyzer resolution and ΔE_{MONO} to the monochromator resolution. Using a theoretical value for ΔE_{MONO} of 0.40 eV, we then solved Eq. 4 for the analyzer energy resolution ΔE_{ANAL}. Since this value for ΔE_{MONO} describes the best possible monochomator resolution, our derived values for ΔE_{ANAL} are the worst case scenario and likely to be somewhat better. The experiment employed the analyzers of 90-100 mm diameter being tested fully exposed to the scattered radiation. Soon after, more readings were taken with an aperture of lead tape containing a 49 mm X 49 mm cutout being centered over the front of the analyzer. Table 3 and Table 4 were recorded.

DISCUSSION AND CONCLUSION

Overall, the eight analyzers performed similarly. Each of the eight analyzers tested was concluded to have a focal length within 3 cm of what was suggested by the manufacturer. Furthermore, seven of the eight were within 1.52 cm of those figures (see Table 2). We speculate that most of the focal lengths being slightly longer than what was quoted by the manufacturer was a result of less stress in the center regions of the Si and Ge wafers after being mounted to the glass substrates via glue or ionic bonding. Very slight bumps behind the wafers as some were mounted with glue may have been potential causes of imperfect energy resolutions.

Analyzer	Manufacturer's Quote Focal Length [mm]	Experimental Focal Length [mm]
Si(111)A	850	861.2
Si(111)B	1000	1015.2
Ge(111)C	850	860.2
Si(440)A	1000	1015.2
Si(440)B	1000	971.8
Si(440)C	850	848.5
Si(440)D	850	860.2
Ge(440)E	1000	1002.1

Table 2. Chart with results from Experiment I comparing experimentally determined focal lengths to manufacturers' quote focal lengths.

Si (440)A was found to have the best resolution at an energy range around 6.46 keV (See Tables 3 and 4). Its resolution increased by about a factor of two after the lead aperture was positioned over it to hide more than 2/3 the original surface area of the crystal wafer. It performed the best in 4 of 5 experiments done using 4 different Si(440) samples. Our speculations are that Si(440)A gave the best resolution because it used a slightly thicker silicon wafer (0.50 mm) and ionic bonding as compared to glue for the other three tested for resolution.

The usefulness of the experiments in accomplishing resolution in the new X-ray Raman spectrometer to be assembled at a later date was quite evidenced. Soon after the Si (440)A sample was determined to have the best energy resolution, the sample was used to prealign a goniometer for 7 analyzers into a Rowland geometry. Meanwhile, the orders for the analyzers of model Si (440)A were placed. Future projects include the assembly of the complete spectrometer employing 28 such analyzers, and testing of more

Using Si(220) Beamline Monochromator, 0.12 mm X 1.0 mm Beam Size, Full Analyzer Exposure	Si(440)A	Si(440)B	Si(440)C	Si(440)D
Diameter [mm]	100	100	100	90
Experimental Focal Length [mm]	1015.2	971.8	848.5	860.2
Total Resolution FWHM [eV] Beam Energy [eV]	0.91 6457.9	1.0 6458.5	1.1 6458.5	0.87 6458.7
Analyzer Resolution Assuming Mono Res = 0.40eV	0.82	0.92	1.02	0.88

Table 3. Chart with results from Experiment II. The total resolution was recorded in the detector, the monochromator resolution was given, and the analyzer resolution was derived from the two using Eq. 4.

Using Si(220) Beamline Monochromator, 0.12 mm X 1.0 mm Beam Size, 49 mm X 49 mm Aperture	Si(440)A	Si(440)B	Si(440)C	Si(440)D
Diameter [mm]	100	100	100	90
Experimental Focal Length [mm]	1015.2	971.8	848.5	860.2
Total Resolution FWHM [eV] Beam Energy [eV]	0.56 6457.9	0.59 6458.5	0.61 6458.9	0.64 6458.9
Analyzer Resolution Assuming Mono Res = 0.40eV	0.39	0.43	0.46	0.50

Table 4. Chart with second set of results from Experiment II. An aperture was used to limit the exposure of the analyzer.

analyzers at different energies. This instrument is expected to be the most efficient of its kind world wide.

ACKNOWLEDGEMENTS

I would like to thank the U. S. Department of Energy for providing me the opportunity to participate in the SULI summer internship program at Stanford Linear Accelerator Center and for giving me the chance to experience such an intellectually-stimulating research environment. A special thanks goes to my mentor, U. Bergmann, a noteworthy researcher and scientist for whom I have developed great respect. Thank you again for all the knowledge you were willing to share. I would also like to thank Mike Toney and Apurva Mehta for starting me out on the project. Greetings go out to A. Pierce.

REFERENCES

[1] Castelvecchi, Davide. "Favorite Liquid Revisited," SLAC Press Release, April 2004 <http://www.slac.stanford.edu/slac/media-info/20040402/>.

[2] Wernet, Ph; Nordlund, D; Bergmann, U; Ogasawara, H; Cavalleri, M; Näslund, LÅ; Hirsch, TK; Ojamäe, L; Glatzel, P; Odelius, M; Pettersson, LGM; & Nilsson, A. "The Structure of the First Coordination Shell in Liquid Water," Science, vol. 304, 2004, pp. 995.

[3] Bergmann, U; Wernet, Ph; Glatzel, P; Cavalleri, M; Pettersson, LGM; Nilsson, A; Cramer; SP. "X-ray Raman Spectroscopy at the Oxygen K-edge of Water and Ice: Implications on Local Structure Models." Phys. Rev. B, vol. 66, 092107, 2002.

[4] Bergmann, U. & Cramer, S.P. "A High-Resolution Large-Acceptance Analyzer for X-ray Fluorescence and Raman Spectroscopy," SPIE-Proceedings, vol. 3448, July 1998, pp. 198-209.

[5] Goodhew, Peter. "Diffraction," Matter Universities, July 2000 <http:// www.matter.org.uk/diffraction/>.

[6] Eric Gullikson. "X-ray Interactions With Matter: X-ray Transmission of a Gas," Center for X-ray Optics at Lawrence Berkeley Labs, 2004 <http://www. cxro.lbl.gov/optical_constants/gastrn2.html>.

Johannes Norrell participated in the SULI program in the fall of 2003, working at the Oak Ridge National Laboratory in the field of X-Ray spectroscopy. In 2004, he graduated from Birmingham-Southern College with a BS in physics. His research while at BSC included the development of nonlinear optical materials and the analysis of the dynamics of Jupiter's torus. Currently Johannes is working toward his Ph.D. at Duke University, where his research will focus on atomic trapping and cooling.

Ian M. Anderson has been the Leader of the Microscopy, Microanalysis, Microstructures Group at the Oak Ridge National Laboratory (ORNL) since 1999. He received his BSc in 1985 from the California Institute of Technology and his PhD in 1993 from Cornell University, both in Applied Physics. Ian's research interests are in the development of electron optical techniques for materials characterization and their applications to materials science. Techniques of particular focus have been ALCHEMI, spectral imaging and multivariate statistical analysis techniques. These methods have been used to understand strengthening mechanisms in ordered intermetallic alloys, oxidation phenomena, bonding in ceramics, and interface structures in semiconductors. Ian is currently Director of the Shared Research Equipment (SHaRE) User Facility, co-Leader of the Electron Microscopy and Spectroscopy Scientific Theme of the Center for Nanoscale Materials Sciences (CNMS), and leads the ORNL contribution to the multi-laboratory transmission electron aberration-corrected microscopy (TEAM) project.

HIGH RESOLUTION X-RAY SPECTROSCOPY WITH A MICROCALORIMETER

JOHANNES NORRELL, IAN ANDERSON

ABSTRACT

Energy-dispersive spectrometry (EDS) is often the preferred choice for X-ray microanalysis, but there are still many disadvantages associated with EDS, the most significant of which is the relatively poor energy resolution, which limits detection sensitivity and the ability to distinguish among closely spaced spectral features, limiting even qualitative analysis. A new type of EDS detector that operates on the principle of microcalorimetry has the potential to eliminate this shortcoming, reaching resolutions an order of magnitude better. The detector consists of an absorber in thermal contact with a transition edge sensor (TES). An X-ray from the specimen hits the absorber and manifests itself as a change in temperature. Because the system is kept at 80 mK, the heat capacity is low and the temperature spike is observable. The TES responds to the increase in temperature by transitioning from its superconducting to its normal conducting state, thus sharply raising the overall resistance of the circuit. The circuit is kept at a constant voltage, so the increase in resistance is manifested as a decrease in current flow. This decrease in current is measured by a superconducting quantum interference device (SQUID), and by integrating the current over time, the energy of the incident X-ray is determined. The prototype microcalorimeter was developed by NIST, and this technology is now available commercially through a partnership between Vericold Technologies and EDAX International. ORNL has received the first of these commercial microcalorimeters in the United States. The absorber in this detector is gold, and the TES consists of a gold-iridium bilayer. It is designed to offer spectral resolution of 10-15 eV at a count rate of ~150 s^{-1}. The goal of this project was to analyze and document the performance of the detector, with particular attention given to the effects of an X-ray optic used to improve collection efficiency, the multiple window system and any other sources of spectral artifacts. It was found that the detector is capable of distinguishing many Lα and Lβ spectral lines, with a resolution between 13 and 17 eV. It was also observed that the background has an unusual shape, and this is largely being attributed to the variable transmission coefficient of the X-ray optic. These preliminary results suggest that the microcalorimeter has a high potential for use in microanalysis, but more work to quantify its capabilities must still be done.

INTRODUCTION

Energy-dispersive X-ray spectroscopy (EDS) is often preferred over wavelength-dispersive X-ray spectroscopy (WDS) because it is possible to collect the entire spectrum at once, with consequently shorter acquisition times and more uniform sensitivity to spectral features across a wide range of photon energies. However, there are many disadvantages associated with EDS, the most significant of which is the relatively poor energy resolution, which limits detection sensitivity and the ability to distinguish among closely spaced spectral features, limiting even qualitative analysis. A new type of EDS detector that operates on the principle of microcalorimetry has the potential to eliminate this shortcoming, reaching resolutions comparable to, and perhaps even superior to, WDS detectors. The prototype microcalorimeter was developed by the National Institute of Standards and Technology (NIST) [1], and this technology is

now available commercially through a partnership between Vericold Technologies and EDAX International. ORNL has received the first of these commercial microcalorimeters in the United States. It has been installed within the past two months, so the results presented here are preliminary, but timely.

MATERIALS AND METHODS

Operating Principles

The microcalorimeter is designed for X-ray microanalysis with conventional scanning electron microscopy (SEM) techniques. The detector consists of an absorber in thermal contact with a transition edge sensor (TES) thermometer. The TES is a metallic bilayer consisting of a superconductor and a normal conductor. By varying the thickness of the layers, one can "tune" the transition temperature of the TES between its normal and superconducting states. When an X-ray from the specimen hits the absorber, the energy of the photon is deposited as heat and manifests itself as a change in temperature. The heat sink quickly returns the absorber to its initial temperature. Because the system is kept at a very low temperature (< 0.1 K), the heat capacity is small ($C \propto T^3$), allowing for a more sensitive response. The TES responds to the increase in temperature by transitioning from its superconducting to its normal conducting state, thus sharply raising the overall resistance of the circuit of which it is a part. The circuit is kept at a constant voltage, so the increase in resistance is manifested as a decrease in current flow. This decrease in current is measured by a superconducting quantum interference device (SQUID), and by integrating the current as a function of time, the energy of the incident X-ray is determined [1,2,3].

Establishing the Baseline Temperature

As mentioned before, it is important that the heat capacity of the absorber be small so that the temperature change will be more noticeable. This also allows the system to return to the baseline temperature more quickly, thereby improving the count rate capability. The small heat capacity is obtained by operating at a very low temperature, approximately 80 mK. The cryogenic system used to achieve this temperature is comprised of three stages. The first, outermost stage is a nitrogen refrigerator that will drop the temperature of the system to below 77 K. A second stage helium refrigerator in series with the first stage will drop the temperature to below 4 K. The third stage uses an adiabatic demagnetization refrigerator (ADR), which uses a paramagnetic salt pill capable of reaching temperatures below 100 mK. The salt is in thermal contact with the second heat sink (T < 4 K). The spins of the paramagnetic atoms within the salt are randomly oriented. A magnetic field is applied, aligning the spins along the field direction. The increase in energy necessary to align the spins (drawn from the field) generates heat that flows to the heat sink. The salt is then isolated from the heat sink and the magnetic field is removed. The spins will randomize to increase entropy, and this change of polarity requires energy. Because the salt is now thermally isolated from the heat sink (i.e., adiabatic), the energy used must come from the internal energy of the particles, thus reducing the temperature from ~ 4 K to less than 100 mK. The ADR in the ORNL microcalorimeter operates at 70 mK, but perfect thermal equilibrium is difficult to achieve, so the absorber itself has a baseline temperature of 80 mK.

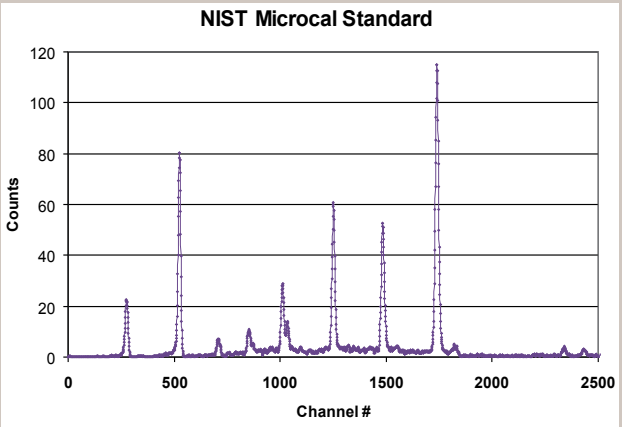

Figure 1. Spectrum of a NIST glass standard acquired with the microcalorimeter.

Line	Energy	Resolution (eV)
C	282	16
O	523	14
Mg	1254	15
Al	1487	17
Si	1740	19

Table 1. Resolution data determined from the NIST glass standard spectrum.

The Absorber

The absorber in the ORNL microcalorimeter is made of gold. It has lateral dimensions of 250 μm × 250 μm and a thickness of 1 μm. Because the lateral dimensions of the absorber are small in comparison to the distance between the absorber and the specimen, which is approximately 45 mm, the solid angle subtended by the detector is extremely small, on the order of 10^{-5} steradians. Because characteristic X-ray emission occurs isotropically, the small solid angle results in a proportionately small X-ray collection efficiency, and a poor count rate [4]. This is one of the primary limitations of the microcalorimeter.

The TES Thermometer

The TES in the ORNL microcalorimeter is made of a gold-iridium bilayer. At very low temperatures, gold is a normal conductor and iridium is a superconductor. The TES has lateral dimensions of 300 × 500 μm and a thickness of 1 μm. The thickness ratio of gold to iridium is adjusted so that the TES will transition between its normal conducting state to its superconducting state at a temperature of 94 mK, 14 mK above the baseline temperature. The TES never goes fully normal conducting as energy sensitivity would be lost. The temperature increases stay within the temperature range of the

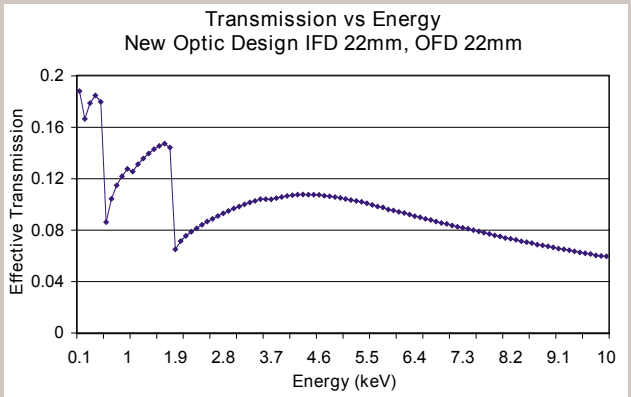

Figure 2. Transmission coefficient of the X-ray optic.

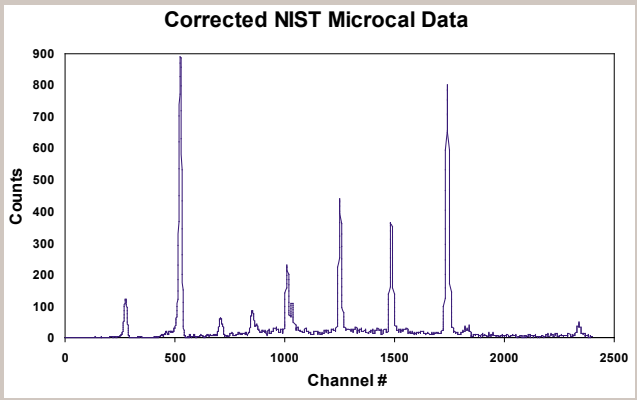

Figure 3. NIST glass standard spectrum corrected for X-ray optic transmission effects.

normal-to-superconducting transition. After an X-ray increases its temperature, the TES returns to its baseline temperature of 80 mK in less than 2 ms. To unambiguously identify the energies of detected X-rays, i.e. to avoid pulse pile-up, if two pulses are detected within 2 ms of one another, both are discarded. Under these operating conditions, the detector achieves a maximum theoretical output count rate of 500 s^{-1}, although the maximum practical count rate is considerably smaller, ~150 s^{-1}. The rejection of overlapping pulses creates an effect somewhat analogous to dead time in a conventional EDS detector.

The X-Ray Optic

To improve collection efficiency, a polycapillary X-ray optic has been inserted between the specimen and the absorber. While the optic does increase the collection efficiency by a factor of 100, it also introduces a nonlinear transmission coefficient that can obscure the interpretation of the data. The prototype microcalorimeter developed by NIST initially had an X-ray optic [2], but because of the nonlinearity it was eventually removed. The ORNL microcalorimeter continues to take advantage of the focusing effects of the optic, and the nonlinear transmission is accounted for mathematically.

The Multiple Window System

The ORNL microcalorimeter has a series of six windows, a noticeable difference from both a conventional EDS detector, which has one window, and the NIST microcalorimeter, which has four. The multiple window system is necessary to screen the background of room temperature infrared (IR) radiation as well as to protect the vacuum. The first (outermost) window is a Moxtek film on a silicon membrane at room temperature. The remaining five windows are made of parylene. The second and third windows are kept at the temperature of the first cooling stage, < 77 K; the fourth and fifth are kept at the temperature of the second cooling stage, < 4 K; the sixth (innermost) window is kept at the temperature of the detector, ~ 80 mK. All six windows have a thickness of approximately 100 nm, and all are reinforced with aluminum to mitigate electrostatic charging and to reflect light and heat. The second and fourth windows have a copper grid reinforcement as well.

Research Goals

It is the goal of this research to analyze and document the performance of the microcalorimeter, with particular attention given to the effects of the X-ray optic used to improve collection efficiency, the multiple window system used to safeguard the cryogenic temperature of the detector, and any other sources of spectral artifacts. The eventual goal is to obtain a thorough understanding of the detector, its electronics and software, to optimize energy resolution and thereby achieve high detection sensitivity, to distinguish low-intensity M and N-shell X-ray spectral lines for high-Z elements, to resolve low-Z elements, and potentially to observe chemical shifts. We are also interested in raising the count rate for improved collection efficiency. This is still a work in progress, but much has already been learned from the preliminary data presented below. The spectra presented in this paper were collected using a glass standard prepared by NIST and an iridium alloy.

RESULTS

Figure 1 presents a spectrum acquired from a NIST glass standard with the ORNL microcalorimeter. It is immediately evident upon inspection that the count rate is very low; this is described in more detail in the discussion section. As desired, the energy resolution of this spectrum is significantly better than that of conventional EDS. However, before the resolution can be accurately quantified, the transmission effects of the X-ray optic must be addressed. The transmission data were determined experimentally by Vericold Technologies and are presented in figure 2. Because of the obvious dependence on X-ray energy, it is important to account for this variation. The relevant relationship is

Counts (observed) = Counts (real) × Transmission Coefficient

Thus, calculating the real counts is as simple as multiplying the observed counts by the reciprocal of the transmission coefficient. The result of this correction is presented in figure 3, the corrected spectrum of the NIST glass standard. Energy resolution is defined as the FWHM of the spectral lines; the resolution of the peaks in this spectrum were determined with a fitting program and are presented in table 1. The resolution range of 14 to 19 eV is close to the 15 eV provided by Vericold Technologies. To corroborate this result, one can examine the peak separations that would not be distinguishable

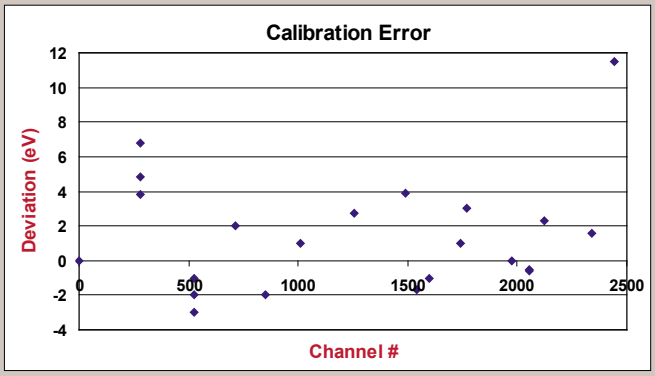

Figure 4. Calibration Error in the NIST glass standard spectrum.

with conventional EDS. The Lα peak for nickel occurs at 849 eV, and the Lβ peak occurs at 866 eV, a difference of 17 eV. It is possible to discriminate between these two peaks, thus suggesting that the microcalorimeter is resolving at least 17 eV. The Lα peak for iron occurs at 704 eV, and the Lβ peak occurs at 717 eV, a difference of 13 eV. Because these two peaks are not distinguishable on the spectrum, this suggests that the microcalorimeter is not currently resolving at 13 eV. These findings are consistent with the FWHM measurements.

In addition to quantifying the energy resolution, it is important to determine how accurately the experimental spectral lines reflect the real energies of the characteristic X-rays. Figure 4 presents the deviation of the microcalorimeter peak centers from those documented in the NIST database. The error is less than the resolution of the detector, and the values in the NIST database are not known with absolute certainty, so the deviations are statistically acceptable. However, it might still be desirable to try to enhance the accuracy of the measurements, and it will be necessary to do so if the resolution of the microcalorimeter can be improved to 10 eV or better. This can be done by using a fifth order polynomial calibration of the X-ray energy.

Another feature of the corrected spectrum (figure 3) is the more expected shape of the background over the initial spectrum (figure 1). In the initial spectrum, there is a clear discontinuity in the background at the silicon absorption edge, ~1.8 keV. Beyond this point, it simply flattens out rather than falling inversely with energy as expected. Examining the X-ray optic data, there is a large drop in transmission at this point, beyond which the transmission is significantly less efficient. The corrected spectrum is much smoother and exhibits a background shape more like the expected bremstrahlung background. To further investigate the effects of the X-ray optic on the background, a spectrum of an iridium alloy was taken. Figure 5 presents the initial spectrum collected by the microcalorimeter, and figure 6 presents the same spectrum after the transmission correction. While the drop at the silicon edge is not completely eliminated by the correction, it is noticeably reduced. Furthermore, the overall shape of the background is dramatically improved. This indicates that future work with the microcalorimeter/X-ray optic system will require that this kind of correction be made for quantitative analysis.

DISCUSSION AND CONCLUSIONS

The preliminary results are promising: the microcalorimeter generates spectra with a resolution almost an order of magnitude better than conventional EDS, which generally gives an optimum resolution of 135 eV. However, there are still many issues to be addressed. Perhaps the most apparent shortcoming of the microcalorimeter is the extremely low collection efficiency. Even with the X-ray optic, count rates typically have not exceeded 70 counts per second, twenty to fifty times lower than conventional EDS. If it takes a long time to collect a statistically quantifiable spectrum, the potential uses for microanalysis may be limited. Operating at high beam currents will help increase the count rate, but depending on how sensitive the specimen is to contamination or beam damage, this may create other problems. Another problem that must be addressed is that the transmission effects of the multiple window system are as of yet unknown. The windows could have as significant an impact as the X-ray optic, although whereas the X-ray optic transmits most efficiently at low energy due to its polycapillary structure, the windows will likely transmit most efficiently at higher energies. The transmission of the windows must be quantified for the microcalorimeter to be used for microanalysis.

Also of interest is the manner in which the spectra are constructed from the raw data. The spectra presented in this paper were not binned in the traditional manner. Instead, each data point was given an artificial line width, a Gaussian curve with a spread of 1 eV and unit area. This is the technique preferred by Vericold Technologies, but it gives rise to some concerns about the interpretation of the spectra where counts are few. Because each

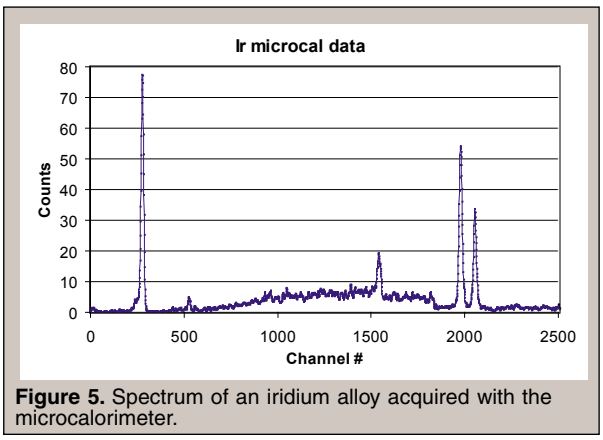

Figure 5. Spectrum of an iridium alloy acquired with the microcalorimeter.

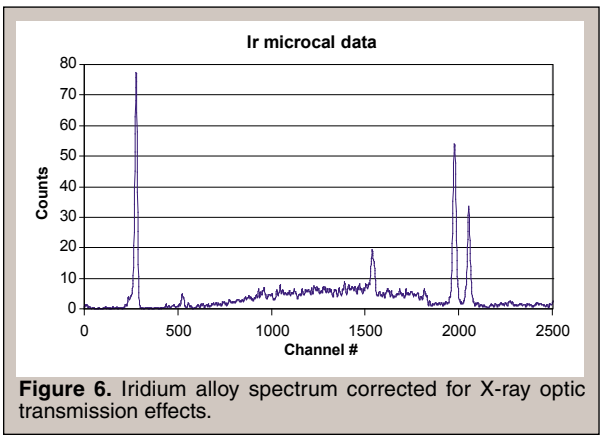

Figure 6. Iridium alloy spectrum corrected for X-ray optic transmission effects.

count is represented by a curve of unit area distributed over several channels instead of a count of unit height assigned to a single channel, the final spectrum contains a fractional number of counts within each channel. Also, it is currently unknown how much of the background can be attributed to the spread of the artificial curves. If this technique continues to be used, more investigation into the statistical implications will be necessary. Alternatively, if conventional step-function binning is used, it will be necessary to determine what size bins are most appropriate.

Finally, there is some concern regarding the shape of the X-ray lines: the statistical intensity distribution within the characteristic peaks is such that they appear to be noticeably sharper than a Gaussian distribution. Although the peaks in the microcalorimeter spectra are better than expected, it is unknown why this is so. Further investigation will be necessary to explain this result before microcalorimetry can be used for quantitative compositional analysis. The natural intrinsic line-width of an X-ray is determined by the lifetime of the ionization event which created the X-ray. A long-lived event will create a sharper peak, whereas a short-lived event will create a peak with more spread. Typical values range between 2 and 8 eV. Because the detector resolution is still significantly larger than the natural line-widths, the sharper distribution observed is characteristic of either the detector response or the method of data rendering.

ACKNOWLEDGEMENTS

I thank Ian Anderson, Edward Kenik and David Joy for all their guidance and assistance with this project. Many thanks go to Teresa Lazarz for her part in this work and her companionship throughout the semester. I would also like to thank the US Department of Energy, Oak Ridge National Laboratory, the Division of Metals and Ceramics and the ACM/GCLA ORSS program for making my time here at ORNL possible. I thank NIST, Vericold Technologies and EDAX International for their immense contributions to this work. Finally, I would like to thank Birmingham-Southern College for providing me with the scientific background needed to qualify for this kind of internship.

REFERENCES

[1] D.A. Wollman, K.D. Irwin, G.C. Hilton, L.L. Dulcie, D.E. Newbury, J.M. Martinis, "High-Resolution, Energy-Dispersive Microcalorimeter Spectrometer for X-ray Microanalysis," Journal of Microscopy, vol. 188, no. 3, Dec. 1997, 196-223.

[2] D.A. Wollman, S.W. Nam, D.E. Newbury, G.C. Hilton, K.D. Irwin, N.F. Bergren, S. Deiker, D.A. Rudman, J.M. Marinis, "Superconducting Transition-Edge-Microcalorimeter X-ray Spectrometer with 2 eV Energy Resolution at 1.5 keV," Nuclear Instruments & Methods in Physics Research A, vol. 444, 2000, 145-150.

[3] D.E. Newbury, D.A. Wollman, S.W. Nam, G.C. Hilton, K.D. Irwin, J. Small, J.M. Martinis, "Energy Dispersive X-Ray Spectrometry by Microcalorimetry for the SEM," Mikrochimica Acta, vol. 138, 2002, 265-274.

[4] D.A. Wollman, S.W. Nam, G.C. Hilton, K.D. Irwin, N.F. Bergren, D.A. Rudman, J.M. Martinis, D.E. Newbury, "Microcalorimeter Energy-Dispersive Spectrometry Using a Low Voltage Scanning Electron Microscope," Journal of Microscopy, vol. 199, no. 1, July 2000, 37-44.

Jessica Baumgaertel is a senior at the University of Washington (UW) in Seattle majoring in physics and mathematics. During the summer of 2004, she held a Science Undergraduate Laboratory Internship at the Princeton Plasma Physics Laboratory in Princeton, NJ. Her project involved using linear simulations of drift waves to study microturbulence and stability of drift wave modes. This work was presented at the APS Division of Plasma Physics Annual Conference in 2004 and at the AAAS Annual Conference in 2005. At UW this year, Jessica worked on the Steady Inductive Helicity Injected Torus experiment in the Plasma Dynamics Group, studied various quantum mechanical paradoxes and elements of quantum computing, and was a teaching assistant for freshman physics classes. She will finish her B.S. degrees next year and hopes to then earn a PhD in physics.

Martha Redi is Principal Research Physicist at Princeton Plasma Physics Laboratory, Princeton University. She recieved a B.S. in physics from MIT (1964) and a Ph.D. in physics from Rutgers University (1969). She has published over 100 papers in superconductivity theory, theoretical biophysics, and oceanography as well as plasma physics. Since 1982 she has concentrated on computational plasma physics, testing theoretical ideas against experiment and planning new magnetic fusion devices. Her present interests center on astrophysical plasmas.

MARGINAL STABILITY STUDIES OF MICROTURBULENCE NEAR ITB ONSET ON ALCATOR C-MOD

JESSICA BAUMGAERTEL, M.H. REDI, R.V. BUDNY, D.C. MCCUNE, W. DORLAND, AND C.L. FIORE

ABSTRACT

Insight into microturbulence and transport in tokamak plasmas is being sought using linear simulations of drift waves near the onset time of an internal transport barrier (ITB) on Alcator C-Mod. Microturbulence is likely generated by instabilities of drift waves and causes transport of heat and particles. This transport is studied because the containment of heat and particles is important for the achievement of practical nuclear fusion. We investigate nearness to marginal stability of ion temperature gradient (ITG) modes for conditions in the ITB region at the trigger time for ITB formation. Data from C-Mod, analyzed by TRANSP (a time dependent transport analysis code), is read by the code TRXPL and made into input files for the parallel gyrokinetic model code GS2. Temperature and density gradients in these input files are modified to produce new input files. Results from these simulations show a weak ITG instability in the barrier region at the time of onset, above marginal stability; the normalized critical temperature gradient is 80% of the experimental temperature gradient. The growth rate increases linearly above the critical value, with the spectrum of ITG modes remaining parabolic up to a multiplicative factor of 2. The effect of varying density gradients is found to be much weaker and causes the fastest growing drift mode to change from ITG to trapped electron mode character. Simulations were carried out on the NERSC IBM 6000 SP using 4 nodes, 16 processors per node. Predictive simulations were examined for converged instability after 10,000-50,000 timesteps in each case. Each simulation took approximately 30 minutes to complete on the IBM SP.

INTRODUCTION

Insight into microturbulence and transport in tokamak plasmas is being sought using linear simulations of drift waves near the onset time of an internal transport barrier (ITB) on Alcator C-Mod [1]. Microturbulence is widely believed to be generated by drift wave instabilities causing transport of heat and particles. This transport is studied because the containment of heat and particles is important for the achievement of practical nuclear fusion. If transport was better understood, then it would be possible to design a better fusion reactor.

A tokamak is an experimental device which uses high magnetic fields to contain the charged particles of the plasma which may one day lead to energy from a practical fusion reactor. An ITB is a location

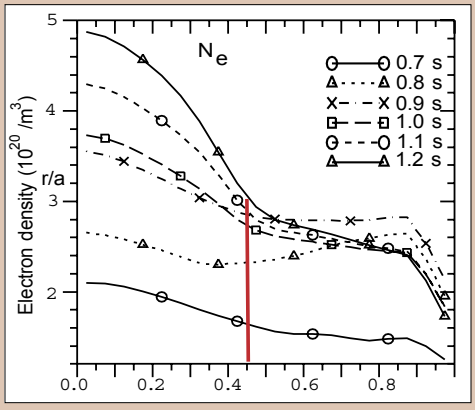

Figure 1. Electron density profile for the C-Mod experiment. Electron density for radial locations in the plasma, given in r/a ≡ the radial distance, *r*, from plasma magnetic axis divided by the minor radius, *a*. Simulations were carried out at the ITB trigger time, 0.9 seconds; the ITB forms at r/a≅0.45.

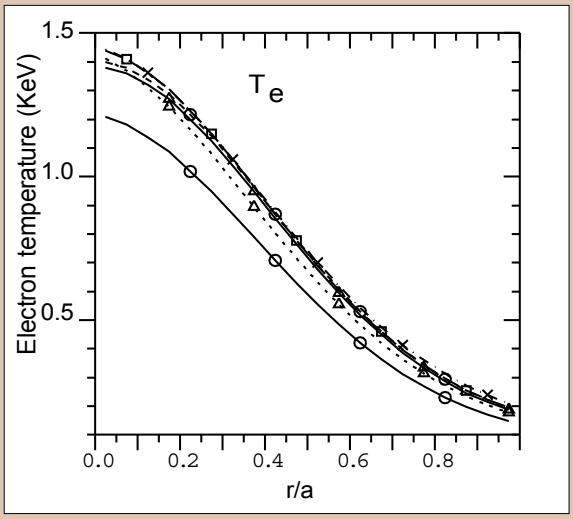

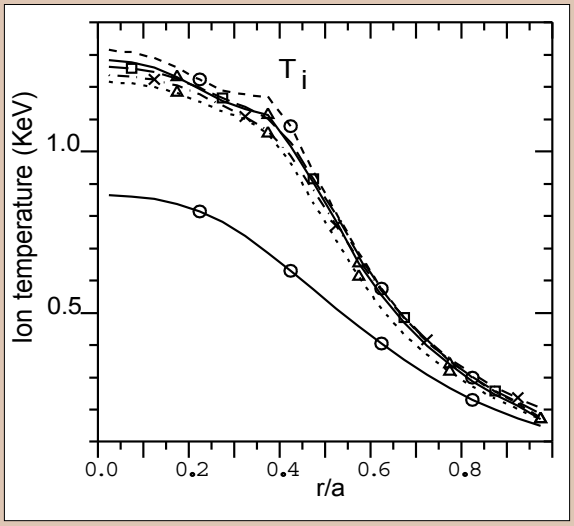

Figures 2. and 3. Temperature profiles for electrons and ions vs. r/a. Notice that the temperature profiles do not change much with time.

were undertaken to learn about the conditions in the plasma just before ITB formation, for possible ITB control.

A drift wave is an oscillation of plasma particle densities and currents and their electrostatic and electromagnetic fields. They are caused by particle drifts due to the electric and magnetic fields in the tokamak plasma, such as the **E** ×**B** drift of particles (Ref. [2], chapter 2). Charged particles move in a helical fashion around magnetic field lines, and in the presence of an electric field, they drift out of their helical orbits in a direction perpendicular to both **E** and **B**. Drifts can also arise from curvature of magnetic field lines and magnetic field gradients.

Components of the microturbulent electrostatic and electromagnetic fields may be written as $\{S(k,\omega)e^{i(kx-\omega t)}\}$, each mode described by frequencies, ω, and wave vectors, **k**. $k_\perp$ is perpendicular to the magnetic field line which wraps around a magnetic flux surface. Further details about drift wave physics may be found in reference [2], chapter 8.

Three types of drift waves are believed to affect plasma confinement: the ion temperature gradient (ITG) mode, the trapped electron mode (TEM), and the electron temperature gradient (ETG) mode. The normalized wave vectors, $k_\perp\rho_s$, of the ITG are in the range of $k_\perp\rho_s$ ~0.1-0.8; of the TEM, $k_\perp\rho_s$ ~1-8; and of the ETG, $k_\perp\rho_s$ ~10-80, where $\rho_s \equiv (\sqrt{(m_i T_e)})/eB$. Because the ITG mode has the longest wavelength ($\lambda = 2\pi/k$), it is most dangerous for causing plasma transport; such instabilities could cause a loss of heat or plasma on a larger scale than would the shorter wavelength modes. Therefore, we wish to see if our experiment is above or below marginal stability of the ITG (i.e., whether it has a positive or negative growth rate), and determine the critical temperature gradient so as to compare with standard models used in reactor design.

The experiment being studied is an off-axis radio frequency (RF) heated high performance plasma (H-mode) which develops an ITB near the time of 0.9 seconds (Figures 1-4) [3]. The ITB forms at a radius for which the ratio to the minor radius is r/a ≅ 0.45. All of the simulations are based on data taken at the ITB trigger time, 0.9 seconds. Table I shows plasma parameters for the experiment.

MATERIALS AND METHODS

To investigate the drift wave microturbulence, linear simulations of drift wave stability were carried out using the massively parallel code GS2 [4]. The time dependent transport analysis code TRANSP was used to analyze data from C-Mod and TRXPL was used to create GS2 input files from the TRANSP output [5]. These input files contain such information as the plasma equilibrium configuration, the plasma location of interest, and parameters for each of the plasma species, including density, temperature, gradients of the density and temperature, and collisionalities. The C-Mod

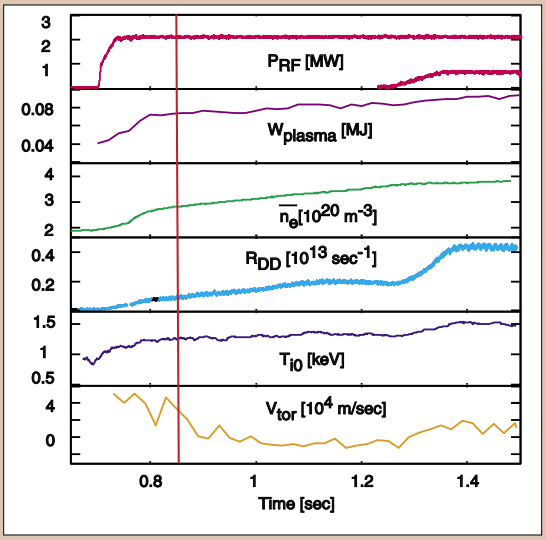

Figure 4. Time dependence of some parameters for the C-Mod experiment. The plasma was heated initially with off-axis radio frequency (RF) heating; at 1.25 seconds on-axis RF heating is added. W_{Plasma} is the stored energy of the plasma, $\overline{n_e}$ is line averaged electron density, R_{DD} is the rate of production D-D of neutrons, T_{i0} is the ion temperature, and v_{tor} is the toroidal velocity (it goes through zero at the time of interest, 0.9 seconds). [Figure from S. Wukitch, R. L. Boivin, P. T. Bonoli, *et al.,* Phys. Plas. **9**, 2149 (2002), used with permission.]

plasma was modeled with four species: electrons, deuterons, boron ions, and trace amounts of hydrogen ions. The neutral gas used was deuterium; the boron and hydrogen ions are present as impurities in the plasma.

GS2 solves the perturbed distribution function of the plasma particles, given by

$$f = f_0 + \left[e_j \phi \frac{\partial f_0}{\partial K} + g \exp\left(i \frac{\mathbf{v}_\perp \times \mathbf{b} \cdot \mathbf{k}_\perp}{\omega_{cj}} \right) \right] \quad (1)$$

where $g(\mu, K, x)$ satisfies the gyrokinetic equation:

$$\frac{\partial g}{\partial t} + v_\parallel \mathbf{b} \cdot \nabla g + i \mathbf{k}_\perp \cdot \mathbf{v}_g g = -\left[\omega \frac{\partial f_0}{\partial K} - \frac{\mathbf{b} \times \nabla f_0 \cdot \mathbf{k}_\perp}{\omega_{cj}} \right] \left[J_0(z) e_j (\phi - v_\parallel A_\parallel) + \frac{2 J_1(z)}{z} \mu B_\parallel \right] \quad (2)$$

K is the kinetic energy of the particles, ϕ and $A_\parallel$ are perturbed potentials, **b=B/|B|**, e_j is the charge of the particle j, $\omega_{cj} = e_j B/m_j$ is the cyclotron frequency of particle j, $J_0(z)$ and $J_1(z)$ are Bessel functions, $v_\parallel$ and $v_\perp$ are components of the particle velocity, $k_\perp$ is the perpendicular wave vector (inversely proportional to the wavelength of the drift wave), v_g is the guiding center velocity, and $z = k_\perp v_\perp / \omega_{cj}$. (Reference [2], chapter 2.)

The simulations were carried out on the Department of Energy National Energy Research Scientific Computing Center's (NERSC) IBM 6000 SP, nicknamed Seaborg. Hundreds of linear stability simulations were carried out, scaling normalized density and temperature gradients for each case. Each simulation used 4 nodes, 16 processors per node and took approximately 30 minutes to complete on the IBM SP.

GS2 simulations yield growth rates, γ, and real frequencies, ω, for each wave vector of the simulated drift wave. These values were examined for converged instability (positive γ and corresponding ω) after 10,000-50,000 time steps in each case, and plotted with EXCEL. GS2 also calculates eigenfunctions of the electrostatic and electromagnetic fields for each wave vector.

RESULTS

A. Instabilities in Three Regions of the Plasma

For each run, EXCEL was used to plot the growth rates and real frequencies as functions of normalized wave vectors, $k_\perp \rho_s$. Wave vectors, which correspond to the ITG, TEM, and ETG mode drift waves, were plotted for three locations in the plasma: the plasma core, the ITB region, and outside of the ITB. Negative growth rates denote damped modes ($e^{-\gamma t}$) and are set to zero in the plots. Figures 5 and 7 show the growth rates, γ, and the frequencies, ω, as a function of wave vector, $k_\perp \rho_s$, for all three drift wave mode ranges, while Figure 6 shows γ for only the ITG range of $k_\perp \rho_s$ [6]. It was found that there are positive growth rates for ITG and ETG modes at and outside of the ITB, but no strongly unstable modes inside the plasma core. The real frequencies describe the mode rotation direction around the field line and are typically positive when the drift wave is an ITG mode, and negative for TEM and ETG modes.

B. At the ITB Region: Temperature Gradient Scaling

Next, the ITG range of wave vectors at the ITB region was considered and the normalized temperature gradients ($a\nabla T/T$, Table I) of each of the plasma species were scaled in order to obtain the dependence of growth rate on temperature gradient. The gradient was varied by factors of 0.1 to 10. Figure 8 shows γ versus $k_\perp \rho_s$ for each case. From this, the maximum growth rate for each case was plotted as a function of the scaling factor on the normalized temperature gradient (Figure 10). The real frequencies, ω, versus $k_\perp \rho_s$ are shown in Figure 9, and the real frequency corresponding to the maximum growth rate per run is plotted as a function of scaling factor in Figure 11.

C. At the ITB Region: Density Gradient Scaling

Next, the normalized density gradients ($a\nabla n/n$, Table I) of the plasma species were scaled to examine the ITG growth rate dependence on normalized density gradient. The scaling factors of the density gradient ranged from 1/6 to 10. Figures 12 and 13 shows γ and ω versus $k_\perp \rho_s$ and Figures 14 and 15 show the maximum γ and corresponding ω as functions of the scaling factor of the density gradients.

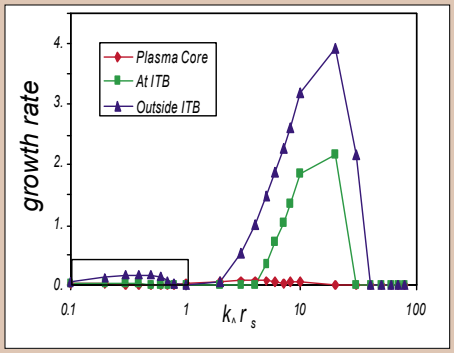

Figure 5. Growth rates of ITG, TEM, and ETG drift wave modes as a function of normalized wave vector, for the three regions of interest.

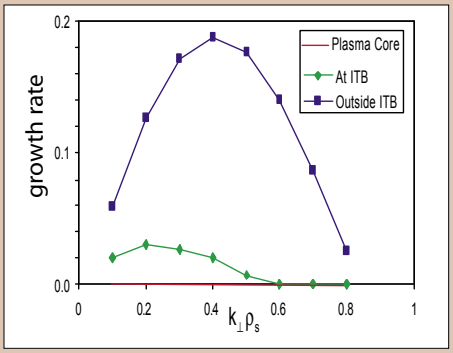

Figure 6. ITG growth rate as a function of normalized wave vector, for three regions in the plasma.

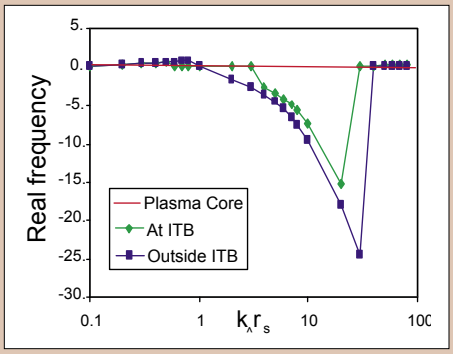

Figure 7. ITG, TEM, and ETG real frequencies as a function of normalized wave vectors at three regions in the plasma.

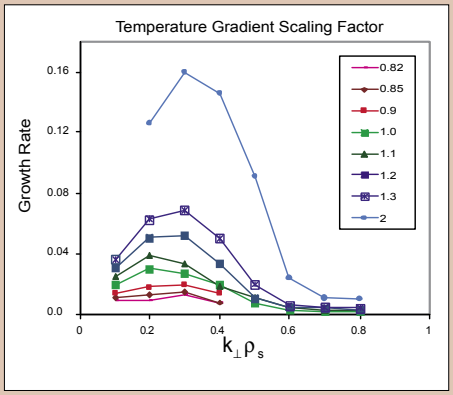

Figure 8. ITG growth rates at the ITB region.

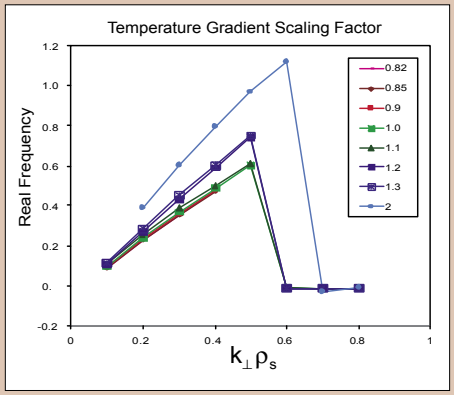

Figure 9. ITG real frequencies at the ITB region.

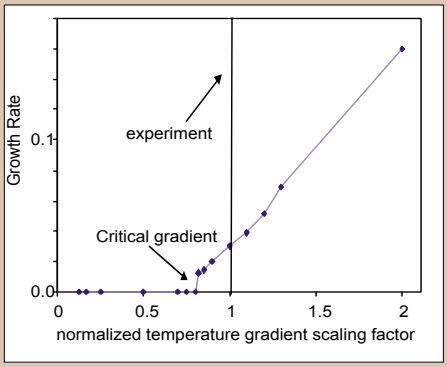

Figure 10. ITG growth rate as a function of normalized temperature gradient.

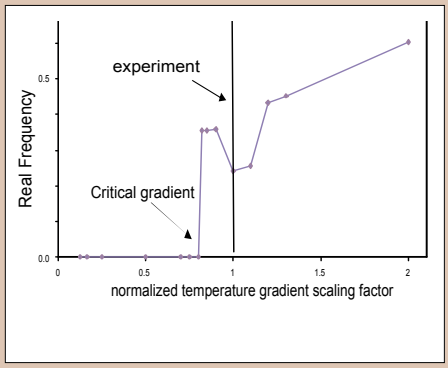

Figure 11. ITG real frequency as a function of normalized temperature gradient.

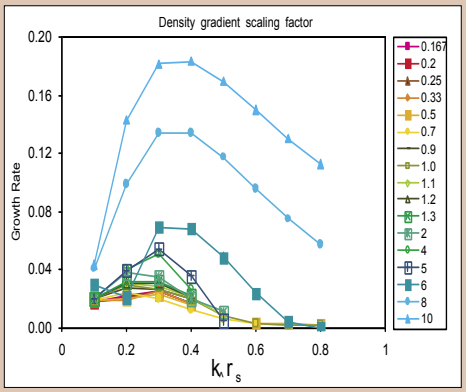

Figure 12. Drift wave mode growth rates at the ITB region.

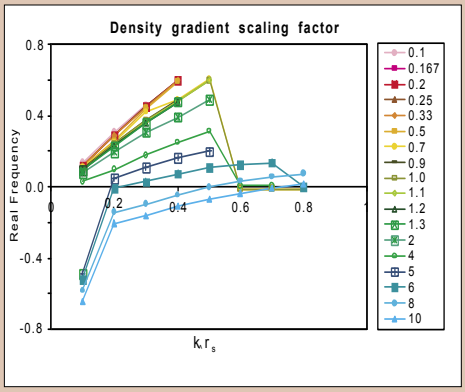

Figure 13. Drift wave mode real frequencies at the ITB region.

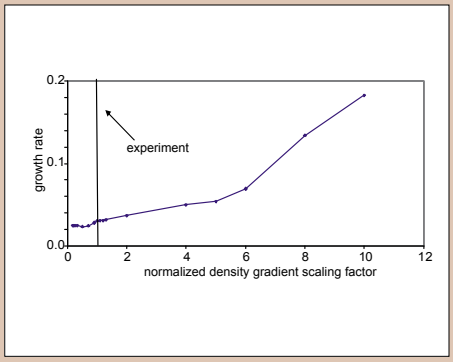

Figure 14. Drift wave mode growth rate as a function of normalized density gradient.

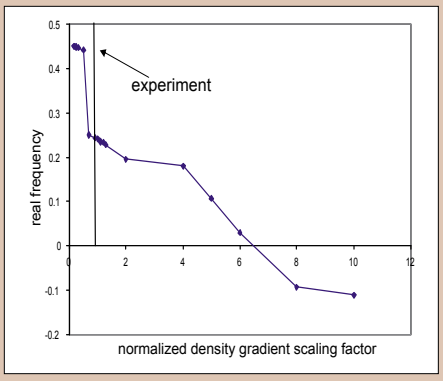

Figure 15. Drift wave mode real frequency as a function of normalized density gradient.

DISCUSSION AND CONCLUSIONS

A. Instabilities in Three Regions of the Plasma

GS2 solutions of the gyrokinetic equation were examined for drift wave instability, that is, a positive growth rate. If the simulated modes are stable, then no transport would be driven by these modes. All drift wave modes were stable in the plasma core (Figure 5) [6, 7]. In the ITB region, however, the ITG is unstable, which could cause some transport of heat and particles. However, Figure 5 shows that the ITG instability in the barrier region is significantly weaker than that found outside the ITB. This is likely the cause of the developing good confinement (i.e., lack of transport) within the barrier. There are also strong ETG instabilities both at and outside of the ITB, but because the ETG has the shortest wavelengths of the drift wave modes, it is unlikely that it will have much effect on ion transport. ETG is thought to be important in heat transport mediated by electrons.

B. At the ITB Region: Temperature Gradient Scaling

Figure 10 indicates that at small normalized temperature gradients, the ITG is stable in the ITB region until the temperature gradient reaches a critical value, then it becomes approximately linearly unstable. The bump in the linear region of the graph, which corresponds to the dip in Figure 11, is due to the fact that the value of $k_\perp \rho_s$ at which the maximum growth rate occurs changes from 0.2 to 0.3, as can be seen in Figure 8. The simulation's critical temperature gradient is 0.80 of the experimental value. Thus, the experiment is well above marginal stability; recall that the ITG was found to be unstable in this region (Figure 6).

C. At the ITB Region: Density Gradient Scaling

The GS2 simulations showed that the ITG growth rates cannot be made zero in the barrier region by scaling the normalized density gradients (Figure 14). The growth rate has a relatively weak

dependence on normalized density gradient—the experimental gradient had to be scaled by a factor of ten to increase the growth rate by a factor of about nine, as opposed to the temperature gradient, which only had to be scaled by a factor of two to increase the growth rate by a factor of eight.

There is a transition in the character of the most unstable ITG range drift waves as the normalized density gradient increases. Compare the real frequencies as a function of scaling factor in Figure 15 with the real frequencies for our base cases of ITG, TEM, and ETG modes in Figure 7. The most unstable drift wave starts as an ITG mode, but then shifts to a TEM mode at about 6.5 times the normalized experimental density gradient, as seen by the real frequency becoming negative and a development of discontinuity in the slope of the growth rate. This is to be expected from the stability diagram in Figure 16, showing the effects of the temperature and density gradients on drift wave instability [8]. A high enough shift in the normalized density gradient changes the mode from ITG to TEM.

In conclusion, it was found that at the barrier region, just before ITB onset, transport is likely caused primarily by weak instabilities of the ITG, the drift wave mode of longest wavelength. Transport can be further reduced by decreasing the species' temperature gradients, which stabilizes the ITG. In addition, increasing the density gradients will induce a shift from the ITG to a potentially less dangerous mode at shorter wavelength, the TEM, which may also reduce ion transport. Nonlinear simulations are needed to verify these conclusions.

Parameter	r/a~0.25	0.45	0.65
q	0.99	1.32	2.00
ŝ	0.51	0.96	1.48
$T_d/T_e = T_b/T_e$	0.99	1.16	1.06
T_h/T_e	1.30	3.96	1.59
$-a_{ref}\nabla n_e/n_e = -a_{ref}\nabla n_s/n_s$	0.71	0.42	0.04
$-a_{ref}\nabla T_e/T_e$	1.47	2.35	2.83
$-a_{ref}\nabla T_d/T_d = -a_{ref}\nabla T_b/T_b$	0.67	2.75	3.41
$-a_{ref}\nabla T_h/T_h$	-3.13	15.4	5.69
$v_e a_{ref}/(c_s\sqrt{2})$	0.30	0.56	1.54
$v_d a_{ref}/(c_s\sqrt{2})$	0.01	0.02	0.05
$v_b a_{ref}/(c_s\sqrt{2})$	0.07	0.11	0.33
$v_h a_{ref}/(c_s\sqrt{2})$	0.01	0.01	0.04
$T_{ref}(keV) = T_e$	1.15	0.77	0.45
$n_{ref} = n_e$ (m-3)	3.1x1020	2.8x1020	2.7x1020
β_{ref}	0.75%	0.45%	0.25%
Freq norm= $(T_{ref}/m_{ref})0.5/a_{ref}$ (sec-1)	1.07x106	0.88x106	0.67x106

Table I. Plasma parameters for C-Mod simulations at 0.9 sec. q is the safety factor, ŝ is the magnetic shear, T_s are the species (electron, deuteron, hydrogen, and boron) temperatures, n_s are the species densities, ∇T_s are the species temperature gradients, ∇n_s are the species density gradients, v_s are the species collisionalities in units of $c_s\sqrt{2}/a_{ref}$, where a_{ref} is a reference length and c_s is the sound speed, β_{ref} is a reference beta, T_{ref} is a reference temperature, n_{ref} is a reference density, Freq norm is a frequency normalization. The ratios of densities are: n_d/n_e =0.8, n_b/n_e=0.03, n_h/n_e=0.04, and a_{ref}=0.22m.

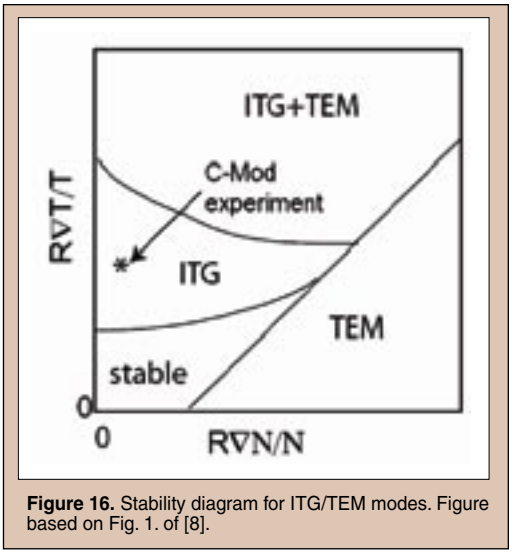

Figure 16. Stability diagram for ITG/TEM modes. Figure based on Fig. 1. of [8].

Much of the study described here will appear in a forthcoming publication [7].

FUTURE RESEARCH

Many lines of future research would be interesting. For example, future research could include investigation of marginal stability conditions in the plasma core and outside the ITB region, as well as the effect on the critical temperature of density and temperature perturbations for each species separately. Critical gradients can be compared to standard models [9]. In addition, nonlinear ITG studies in the barrier region would deepen our understanding of ITB formation; shifts in critical temperatures have been found from nonlinear microturbulence studies[10].

ACKNOWLEDGEMENTS

We would like to thank the U.S. Department of Energy and the Princeton Plasma Physics Laboratory for the opportunity to participate in the SULI program. We thank James Morgan for his enthusiastic and energetic work with the SULI students, and the Alcator C-Mod group at MIT for the data and analysis of the experiment. Work also supported by U. S. DOE Contract DE-AC02-76CH03073.

REFERENCES

[1] I. H. Hutchinson, R. L. Boivin, F. Bombarda *et al.*, Phys. Plas. **1**, 1511 (1994).

[2] J. A. Wesson, *Tokamaks,* Oxford University Press, New YYork, NY (1997).

[3] C. L. Fiore, *et. al.* Phys. Plas. 8, 2023 (2001).

[4] M. Kotschenreuther, *et. al.*, Comp.Phys. Com. 88, 128

(1995).

[5] R. J. Hawryluk, in *Physics of Plasmas Close to Thermonuclear Conditions*, edited by B. Coppi, G. G. Leotta, D. Pfirsch, R. Pozzoli, and E. Sindoni (Pergamon, Oxford, 1980), Vol. 1, p.19.

[6] M. H. Redi, *et. al*. EPS-2004, London, UK, paper P2-163.

[7] M. H. Redi , *et. al*. "Microturbulent drift mode stability of before internal transport barrier formation in the Alcator C-Mod radio frequency heated H-mode", Physics of Plasmas (2005).

[8] X. Garbet, P. Mantica, C. Angioni, *et al.*, "Physics of Transport in Tokamaks", to appear in Proceedings of the 31th EPS Conference on Plasma Physics and Controlled Fusion, London, England (2004), and Plasma Physics and Controlled Fusion (2005).

[9] F. Jenko, W. Dorland, G. W. Hammett, Phys. Plas**. 8**, 4096 (2001).

[10] A. M. Dimits, G. Bateman, M. A. Beer *et al.*, Phys. Plasmas **7**, 969 (2000).

Juliana Olmstead is currently an undergraduate student at the Massachusetts Institute of Technology. She will graduate in June 2006 with a B.S. in materials science and engineering. She researched chalcogenide nanowire formation at Pacific Northwest National Laboratory during the summer of 2004 as a participant in the DOE Student Undergraduate Laboratory Internship program. For the summer of 2005, she is traveling to Bangalore, India for an internship at DaimlerChrysler Research and Technology India Private Limited, where she is working to reduce engine emissions. After graduation, Juliana hopes to do research work in industry before eventually returning to school for a graduate degree.

SK Sundaram is a Chief Materials Scientist at Pacific Northwest National Laboratory (PNNL) in Richland, Washington. He received his Ph.D. in Materials Science & Engineering from the Georgia Institute of Technology in 1988. He began his career as a senior scientist at PNNL in 1996 following a postdoctoral appointment at PNNL 1994-1996. Sundaram had thirteen years of various technical/research experiences in India at Indira Gandhi Centre for Atomic Research at Kalpakkam, Indian Institute of Technology at Kharagpur, and Tata Research Development & Design Centre at Pune. Sundaram has studied corrosion/protection of materials in melts and extreme environments, electronic materials, infrared optic/photonic materials, laser modification of materials, and nanoscale materials. Sundaram has also developed millimeter wave diagnostic tools for novel characterization of materials, melts, and surfaces. Most recently his work has involved ultrafast (femtosecond/attosecond) processing of/processes in materials. Aside from materials science, Sundaram enjoys his family, reading, international cinema, and writing.

Brian Riley is a Research Scientist at Pacific Northwest National Laboratory (PNNL) in Richland, Washington. He received his B.S. in Chemistry and Biology from Eastern Washington University in 2003. He began his career at PNNL in 1998 where he assisted with oxide glass processing and characterization for the bulk vitrification project. In 2002, he began work on non-oxide glass processing, manufacture, characterization, and purification of various chalcogenide chemistries. Brian has also done extensive research on chalcogenide nanowire formation within different pressure and temperature regimes. His most recent work has been in biophotonics studying the biomarker pathways of cellular response to environmental stimulus. Brian finds his joy in Christianity, his family, and cinema.

Bradley R. Johnson is a Sr. Research Scientist at Pacific Northwest National Laboratory where he has investigated processing science and photonic sensitivity in chalcogenide systems, developed ceramic solutions for high temperature catalytic reactions, and has used analytical transmission electron microscopy to study stress corrosion cracking phenomena in nickel-based alloys. He received his M.S. and Ph.D. in Materials Science and Engineering from the University of Illinois at Urbana-Champaign in 1996 and 2001, respectively. Prior to commencing graduate studies, Dr. Johnson had graduated from the U.S. Naval Academy in 1986 with a B.S in Mechanical Engineering and had served as a naval officer with several different commands at sea and on land.

ARSENIC SULFIDE NANOWIRE FORMATION ON FUSED QUARTZ SURFACES

JULIANA OLMSTEAD, BRIAN J. RILEY, BRADLEY R. JOHNSON, AND S.K. SUNDARAM

ABSTRACT

Arsenic sulfide (As_xS_y) nanowires were synthesized by an evaporation-condensation process in evacuated fused quartz ampoules. During the deposition process, a thin, colored film of As_xS_y was deposited along the upper, cooler portion of the ampoule. The ampoule was sectioned and the deposited film analyzed using scanning electron microscopy (SEM) to characterize and semi-quantitatively evaluate the microstructural features of the deposited film. A variety of microstructures were observed that ranged from a continuous thin film (warmer portion of the ampoule), to isolated micron- and nano-scale droplets (in the intermediate portion), as well as nanowires (colder portion of the ampoule). Experiments were conducted to evaluate the effects of ampoule cleaning methods (e.g. modify surface chemistry) and quantity of source material on nanowire formation. The evolution of these microstructures in the thin film was determined to be a function of initial pressure, substrate temperature, substrate surface treatment, and initial volume of As_2S_3 glass. In a set of two experiments where the initial pressure, substrate thermal gradient, and surface treatment were the same, the initial quantity of As_2S_3 glass per internal ampoule volume was doubled from one test to the other. The results showed that As_xS_y nanowires were only formed in the test with the greater initial quantity of As_2S_3 per internal ampoule volume. The growth data for variation in diameter (e.g. nanowire or droplet) as a function of substrate temperature was fit to an exponential trendline with the form $y = Ae^{kx}$, where y is the structure diameter, $A = 1.25\times10^{-3}$, $k = 3.96\times10^{-2}$, and x is the temperature with correlation coefficient, $R^2 = 0.979$, indicating a thermally-activated process.

INTRODUCTION

Chalcogenide glasses are formed by combining chalcogen elements (S, Se, or Te) with Group IV or V elements (e.g., As). Arsenic sulfide (As_2S_3) is an important material belonging to this chalcogenide glass family. It is infrared (IR) transparent (700 nm-11.5 μm) and can be used in many IR applications such as sensors, waveguides, photonic crystals, and photolithography [1]. Recent studies [2] have revealed that, under specific

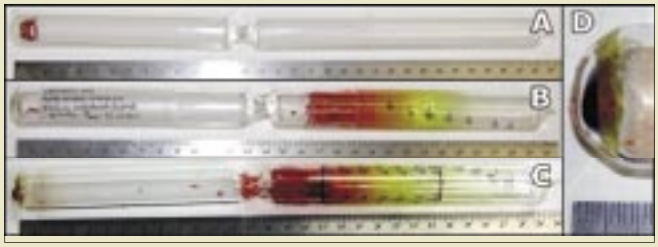

Figure 1-A, -B, -C, & -D: Examples of As2S3 deposition ampoules for nanowire growth. (A) As2S3 glass in the bottom of a fused quartz ampoule sealed at specified pressure pressure, before the heating process. (B) Picture of AEB1 following heat treatment. (C) Picture of AEB2 following heat treatment. (D) Close-up of the ampoule bottom of AEB2. The scale is in centimeters.

conditions, As_xS_y can form nanowires. These wires have diameters ranging from tens of nanometers to several hundred nanometers. They have been examined via transmission electron microscopy (TEM), scanning electron microscopy (SEM), x-ray diffraction (XRD), and Raman spectroscopy which revealed that they are amorphous in nature [2]. Their successful formation depends upon a variety of processing variables (i.e., pressure, temperature, duration of deposition, As_2S_3 glass purity level, quantity of As_2S_3 per internal volume and surface area of ampoule, substrate surface states, etc). As_2S_3 has also formed micro- and nanoscale droplet structures. The goal of the present study was to explore the effects of substrate surface chemistry and initial quantity of As_2S_3 glass on the formation of As_xS_y nanowires.

MATERIALS AND METHODS

The As_2S_3 used in this study was synthesized at PNNL. It was made by combining stoichiometric quantities of high purity elemental arsenic and sulfur (Alfa Aesar®, Ward Hill, MA) in evacuated and argon-purged fused quartz or borosilicate glass ampoules. The sealed ampoules were heated to a temperature between 480°C and 500°C and agitated in a rocking furnace (Deltech, Denver, CO) for up to 18 hours to ensure uniform mixing of the two components. After rocking, the ampoules were quenched in air down to approximately 200°C. The quenched glass was then annealed by placing

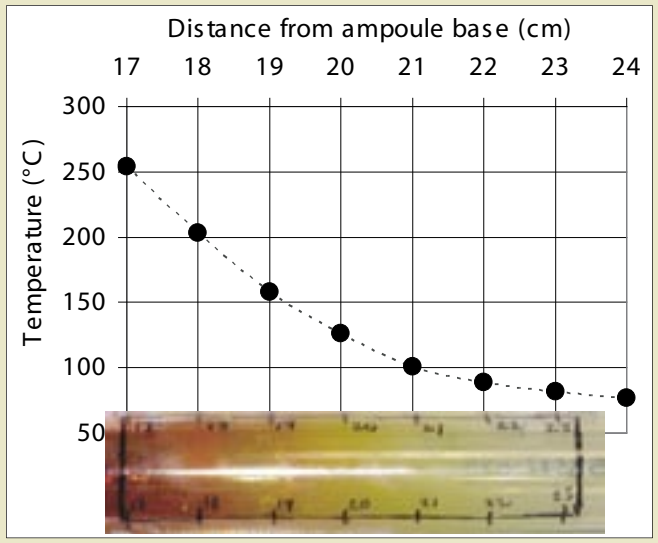

Figure 2. External substrate temperature profile of AEB2 (initial pressure of 70 torr) with accompanying picture of ampoule, demonstrating color variation with substrate temperature.

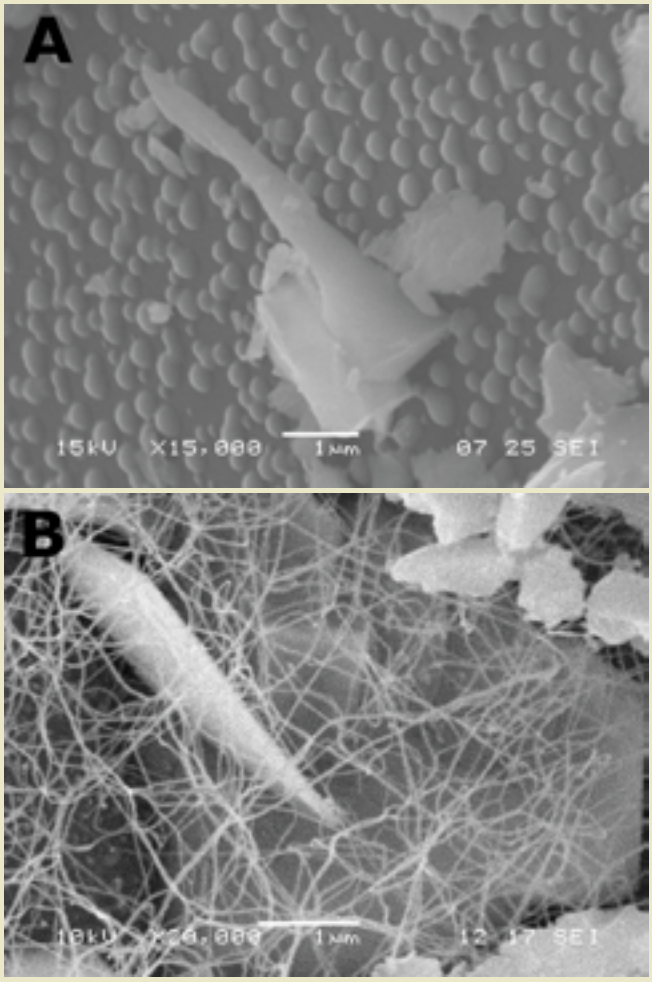

Figure 3. (A) SEM micrograph of nanodroplets from AEB1 at 94.1°C. (B) SEM micrograph of nanowires from AEB2 at 94.2°C. Initial ampoule pressure = 70 torr for both ampoules.

the ampoules in a furnace pre-heated to 170°C. The ampoules were held at that temperature for at least 2 hours, and then the furnace was turned off and allowed to slowly cool to ambient temperatures [2].

The experiments followed the general procedure established in previous work [2]. Deposition ampoules for nanowire growth were prepared from fused quartz tubes (GE 214 tubing, 1.9 cm ID, approximately 30 cm long internal volume of ~ 85 cm^3). The surfaces of the interior walls (deposition substrate) were cleaned using an acid etching procedure with a solution of HF, HNO_3, and deionized water (DIW) in a 5:5:90 volume ratio, respectively, for 20 minutes. The ampoule was then rinsed with DIW and heat treated at 1000°C for 1 hour. This cleaning protocol had been selected from a number of different procedures, based on characterization data from atomic force microscopy (AFM – Nanoscope III, Veeco - formerly Digital Instruments) and x-ray photoelectron spectroscopy (XPS – PHI Quantum 2000). This cleaning protocol was termed "AEB" for acid-etched and baked.

After cleaning the deposition ampoule, a small mass of As_2S_3, usually about 1 gram (4.1×10^{-3} moles), was placed in it. A neck was created, ~ 13.5 cm from the bottom of the tube, by drawing the glass wall inward using an oxy-propane torch. The tube was then attached to a vacuum system, evacuated and back-filled with argon gas several times, and finally regulated to a pressure of 70 torr. The pressure was monitored with an

in-line pressure gauge during this process. Then the top of the deposition ampoule was sealed off using the torch. This created a closed system at the chosen starting pressure (Figure 1-A). The ampoule was instrumented with up to 17 K-type thermocouples (Omega Engineering, Inc., Stamford, CT) positioned at 1 cm intervals along the length of the deposition region of the ampoule. They were used to monitor the substrate temperature during the deposition process.

This ampoule was inserted into a secondary containment vessel (5 cm ID, fused quartz tube), and placed inside a top-loading furnace, with the upper region of the ampoule remaining outside the furnace. The ampoule was heated in the furnace at a rate of 5°C/min. to ~ 470°C, held at this temperature for 17.2 hours, and cooled back to room temperature at 5°C/min. The configuration of having the top half of the ampoule outside the furnace created a thermal gradient within the upper regions of the ampoule. The As_2S_3 glass evaporated from the bottom of the ampoule (the hottest region) and condensed along the upper wall of the ampoule at lower temperatures.

During the deposition process, a thin film of As_xS_y was deposited on the interior of the ampoule which was about 13 cm in length, starting from near the neck and continuing upwards (Figure 1-B, -C). The film varied in color from a deep red, at the bottom (warmer region), to pale yellow, at the top (cooler region). The detailed temperature range for these different regions was obtained using the data from the thermocouples (Figure 2). A portion of the ampoule within the colored thin film deposit region was sectioned from the ampoule, sputter coated with gold (Polaron Range SC7640, Quorum Technologies, England), and analyzed using an SEM (JEOL 5900 LV, Amherst, MA).

A plot was made of the thermal gradient (based on thermocouple data) along the wall of the ampoule where the sectioned piece was located (Figure 2). Also, etch marks were made on the specimen to designate the original thermocouple locations along the ampoule wall. The motorized stage on the SEM was used to measure distances between marks of known temperatures, and based on these distances and the thermal profile, the temperature at each point could be interpolated. Micrographs were taken of various microstructures, with an emphasis placed on wires and droplets. Their diameters were then semi-quantitatively measured in Adobe Photoshop CS®. In this particular study, micrographs were taken from ~ 30 different temperature zones on a single sample, sometimes with multiple micrographs from a single area. Ten measurements were taken from each micrograph, and then these measurements were averaged together to give a single data point with a corresponding standard deviation.

Two experiments were performed to test the effect of the initial quantity of As_2S_3 per internal volume of the ampoule on nanowire formation in AEB cleaned deposition ampoules. The experiments were conducted using the same ampoule dimensions, initial pressure, cleaning method, and thermal treatment as described above, but with different amounts of As_2S_3 loaded into the ampoules. The first, AEB1, used 4.14×10^{-3} moles (1.02 grams) of As_2S_3, corresponding to 4.96×10^{-5} mol As_2S_3/cm^3. The second, AEB2, used 8.41×10^{-3} moles (2.07 grams) As_2S_3, corresponding to 1.01×10^{-4} mol As_2S_3/cm^3.

RESULTS

Experiment AEB1 produced nano/micro droplets only. The diameters of these droplets ranged from 175 ± 25 nm to 2.35 ± 0.61 µm, between the temperatures of 86°C and 156°C, respectively. The average standard deviation of the data points was 0.19 µm [3]. Figure 3-A shows a typical SEM micrograph from this experiment.

Experiment AEB2, on the other hand, produced a large number of nanowires as illustrated in Figure 3-B. Wire diameters ranged from 31 ± 6.1 nm to 86 ± 7.6 nm, between the temperatures of 84.0°C and 109.4°C, respectively. The average standard deviation for the wire diameter data was 7.7 nm. Microdroplets were also seen with diameters ranging from 2.0 ± 0.3 µm to 5.5 ± 0.3 µm, between the temperatures of 184.2°C and 220.6°C. The average standard deviation for the droplet diameter data was 1.8 µm. Figure 4 shows various SEM micrographs from AEB2, representing both wires and droplets. The wire diameter vs. temperature data fits an exponential trendline with an R^2 value of 0.912. The size (diameter) vs. temperature data for both wires and droplets also fits an exponential trendline, with an R^2 value of 0.979 (Figure 5). The trendlines for Figure 5-A and Figure 5-B fit the form, $y = Ae^{kx}$, where A and k are 9.32×10^{-4} and

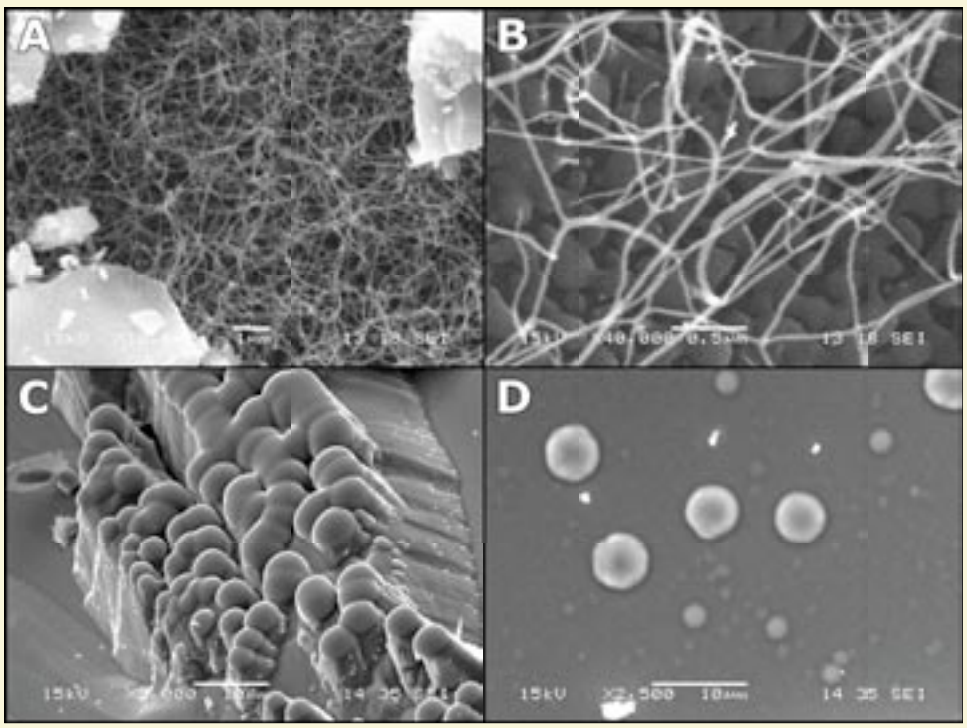

Figure 4. SEM micrographs of As2S3 deposits on the interior wall of AEB2. Micrographs A, B, C, & D were from different areas along length of ampoule wall (21.30, 22.00, 17.85, & 18.41 cm from bottom, respectively) with approximate substrate temperatures of 95.6°C, 89.0°C, 210.7°C, & 184.1°C, respectively.

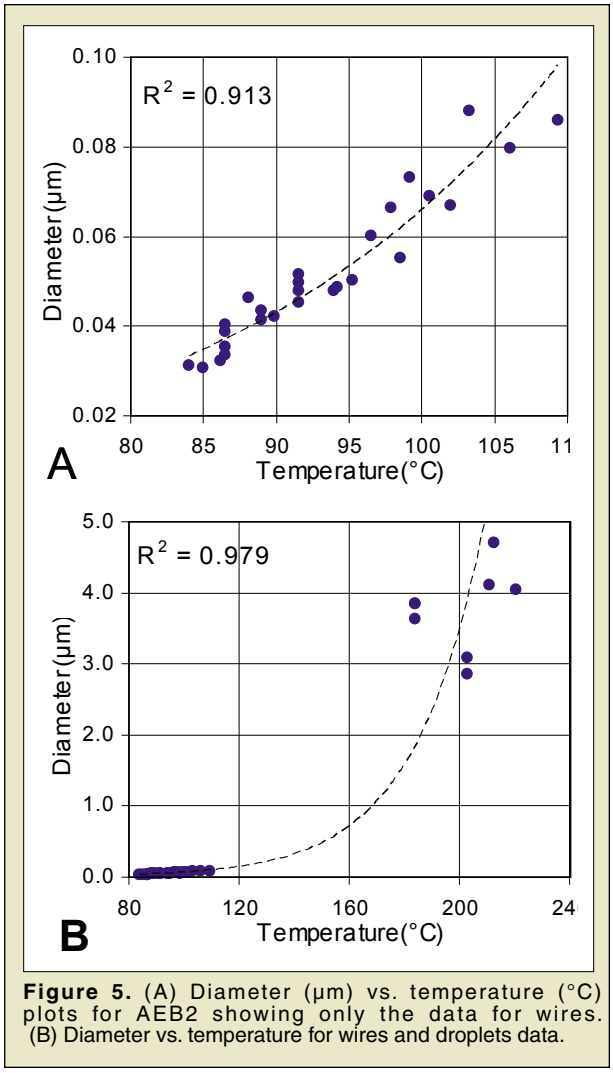

Figure 5. (A) Diameter (µm) vs. temperature (°C) plots for AEB2 showing only the data for wires. (B) Diameter vs. temperature for wires and droplets data.

4.26×10^{-2} for Figure 5-A, respectively, and 1.25×10^{-3} and 3.96×10^{-2} for Figure 5-B, respectively.

Additionally, there was a qualitative difference between the way the As_2S_3 deposited in AEB1 and AEB2. In AEB1, all the glass in the ampoule deposited on the upper walls (Figure 1-B). A couple of small pieces of As_2S_3 glass are visible near the bottom of the ampoule, but those appear to have fallen off the ampoule walls after the heating process. In AEB2, however, a small portion of the glass remained at the bottom of the ampoule after the evaporation-condensation process. The As_2S_3 also appears to have dripped down from the upper walls of the ampoule into the neck before it solidified (Figure 1-C, -D).

DISCUSSION

Experiments AEB1 and AEB2 had significantly different results, although the only parameter that was varied between the experiments was the quantity of As_2S_3 used per internal volume of the ampoule. Figure 6 shows a comparison of the diameter (size) vs. temperature plots for the two experiments, which highlights the difference between the structures formed. Mathematical curve fitting to the data suggests an exponential growth mechanism. A more systematic study is needed to determine the precise mechanism. In Figure 6, the trendlines fit the form $y = Ae^{kx}$ where y is the structure diameter and x is the temperature. For AEB1, A and k are 1.42×10^{-2} and 3.34×10^{-2}, respectively, and for AEB2, A and k are 1.25×10^{-3} and 3.96×10^{-2}, respectively.

The differences between AEB1 and AEB2 could be due to a couple of factors. First, the pressure in AEB2 during the experiment was most likely higher than the pressure in AEB1. Even though both ampoules had the same initial pressure of 70 torr, AEB2 could have had up to twice the As_2S_3 vapor pressure during the deposition process, since it had twice the quantity of initial As_2S_3 per internal volume of the ampoule. This is consistent with the results from previous studies [2] which showed that nanowire formation was sensitive to pressure. Second, since the volume and internal surface area of the two experiments was approximately the same, the ratio of moles of As_2S_3 to the ampoule volume and surface area for AEB2 was double that for AEB1. In AEB1, there was no visible residual glass in the bottom of the ampoule, and the region of glass deposition did not extend down as far into the hotter regions of the ampoule as in AEB2. Thus, all of the As_2S_3 may have deposited quickly on the substrate walls during the AEB1 experiment and then no further structures would have formed due to depletion of the material supply. However, there was an apparent excess of As_2S_3 in the AEB2 experiment (glass in the bottom of the ampoule and near the neck) that possibly facilitated reflux and circulation of the As_2S_3 vapors, thereby providing sufficient material to allow nanowire growth to occur. Though we did not perform mass-balance, it is reasonable to postulate that the increase in the amount of available material would allow more interaction with the available surface, facilitating growth of complex microstructures (e.g. nanowires). Additional experiments are needed to verify this postulate.

The success of the second AEB2 experiment also showed that nanowires potentially can be deposited on a wider variety of silica surfaces than was previously known. This is a significant result, because in previous studies nanowires were only successfully formed on fused quartz ampoules that were cleaned using traditional laboratory cleaning methods (wash with water and rinse with DIW – "water-washed" surfaces) [2]. The effects of substrate surface modification are further discussed in detail elsewhere [3].

AFM analysis was used to conduct a detailed surface roughness characterization on an as-received fused quartz surface and on an AEB

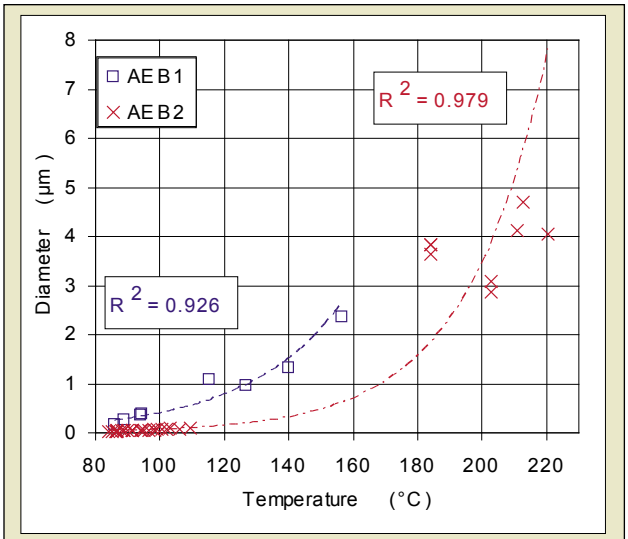

Figure 6. Size (diameter in µm) vs. temperature (°C) plots for AEB1 (droplets) and AEB2 (wires and droplets).

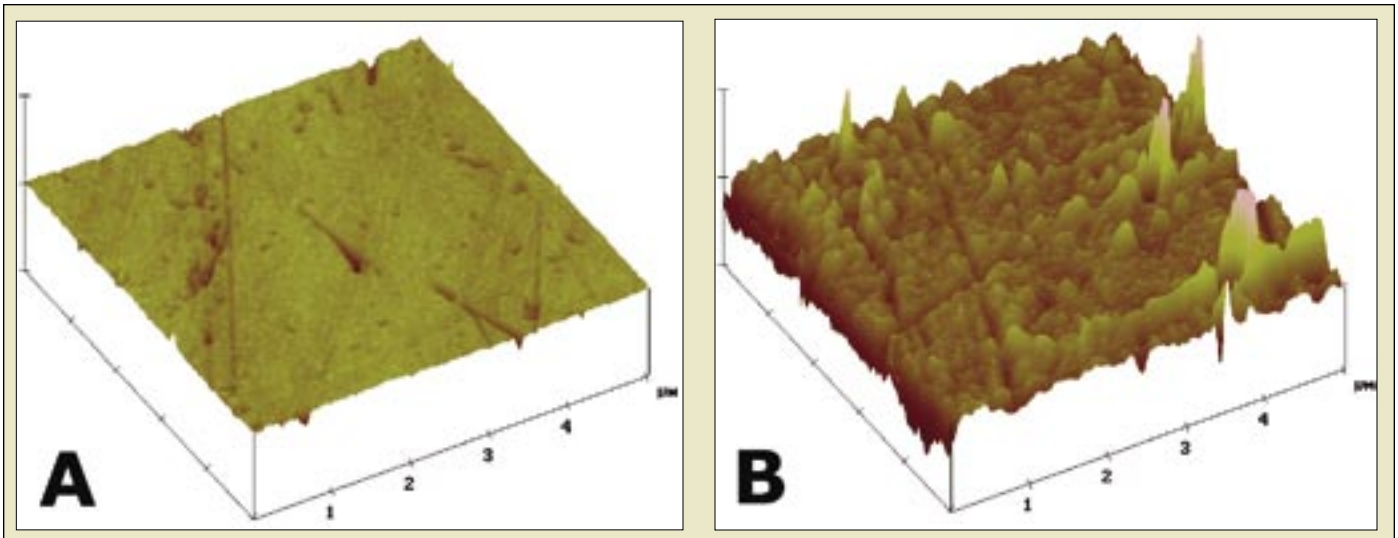

Figure 7. (A) AFM micrograph of as-received quartz surface. (B) AFM micrograph of acid-etched and baked (AEB) quartz surface. X-axis scale bar is 5 μm long with divisions every 1 μm; Z-axis scale bar is 100 nm long with divisions every 50 nm.

fused quartz surface (Figure 7). The results showed that AEB treatment significantly increased the roughness of the fused quartz surface. The Z range of the as-received sample, Figure 7-A, was 21.65 nm, whereas the Z range of the AEB sample, Figure 7-B, was 310.68 nm, increasing the peak-to-valley height difference by an order of magnitude. The root mean square (RMS) value also increased significantly, from 1.15 nm for the as-received sample to 9.06 nm for the AEB sample. In addition to the number of moles of As_2S_3 per available internal ampoule volume, the available deposition surface area also likely influences droplet/nanowire formation.

Additionally, XPS was performed on an as-received fused quartz sample and an AEB fused quartz sample. The results showed that the carbonaceous content of the surface was reduced from 21.9 ± 1.6 atomic % on the as-received sample to 0.7 ± 0.1 atomic % on the AEB sample, a decrease of nearly two orders of magnitude. Therefore, the AEB surface contains significantly less carbonaceous contamination than the as-received sample. It is likely that this difference also affects the way As_xS_y deposits on an AEB surface versus a water-washed one. Further detailed investigation will be needed to determine the precise roles of carbonaceous contamination as well as molar surface area in the formation of nanowires and other features.

CONCLUSION

Several main conclusions can be drawn from this study. First, nanowire formation on an AEB surface has been demonstrated, which is a new finding. Second, the initial quantity of As_2S_3 has been shown to be a crucial variable in nanowire formation on AEB surfaces. Under identical initial conditions, there is a minimum quantity of As_2S_3 required for nanowire synthesis, below which nanowires do not form. Third, the growth of nanowires and nano/micro droplets as a function of substrate temperature has been fitted to an exponential curve. And finally, the surface chemistry and roughness of AEB cleaned fused quartz surfaces have been characterized and shown to create a significantly cleaner, yet rougher surface than initially present. In summary, we have presented a process that can be replicated more consistently and accurately which is expected to lead to standardized nanowire synthesis, a major step towards commercial production.

ACKNOWLEDGEMENTS

The authors would like to thank the U.S. Department of Energy Office of Science for creating and maintaining this internship program and providing students the opportunity to learn about science-based careers. Pacific Northwest National Laboratory (PNNL) is a multi-program national laboratory operated by Battelle Memorial Institute for the United States Department of Energy under contract DE-AC06-76RLO 1830. A portion of the research described in this paper was performed in the Environmental Molecular Sciences Laboratory, a national scientific user facility sponsored by the Department of Energy's Office of Biological and Environmental Research and located at Pacific Northwest National Laboratory. The authors would also like to express their gratitude towards Rick Williford for his contribution with AFM analysis and towards Mark Engelhard for performing XPS analysis and providing suggestions as to optimum surface cleaning and sample preparation methods. The authors also thank everyone at the Applied Process Engineering Laboratory, especially Evan Jones (managerial support), Teresa Schott (secretarial support), and James Martinez (SEM support).

REFERENCES

[1] P. Klocek, Handbook of Infrared Optical Materials, Marcel Dekker, Inc., 1991.

[2] B. R. Johnson, M. J. Schweiger, S. K. Sundaram. "Chalcogenide Nanowires by Evaporation-Condensation," *Journal of Non-Crystalline Solids* (in press).

[3] B. J. Riley, B. R. Johnson, S. K. Sundaram, and M. H. Engelhard, R.E. Williford and J. Olmstead. "Pressure-Temperature Dependence of Nanowire Formation in Arsenic-Sulfur System." In press, *Chem and Phys of Glass*. (http://www.ceramics.org/meetings/glass2004/default.asp).

Daniel L. Rokusek held his Science Undergraduate Laboratory Internship at Argonne National Laboratory in Argonne, IL during the summer before his senior year at the University of Illinois at Urbana-Champaign. His work was a continuation of the previous summer's work in ANL's Student Research Participation program. Under the direction of Ahmed Hassanein and Jean Paul Allain, Dan investigated the erosion of candidate mirror materials for use in extreme-ultraviolet lithography devices. This work was presented at the AAAS Annual Meeting in Washington D.C., and received first place in the Technology & Engineering category of the student poster competition. Since his time at ANL, Dan received a B.S. in nuclear engineering and a minor in mathematics. He is ready to begin his Ph.D. work in nuclear engineering at the Massachusetts Institute of Technology in the fall of 2005. While at MIT, Dan plans to study plasma-material interactions with applications in fusion science and plasma technology. After he leaves MIT, Dan plans to remain in academia and aspires to one day become an educator.

Jean Paul Allain is a staff scientist in the Computational Physics and Hydrodynamics section of the Energy Technology division at Argonne National Laboratory. He obtained his Ph.D. degree from the Department of Plasma, Radiological and Nuclear Engineering at the University of Illinois Urbana-Champaign in 2001. He also earned a Masters degree from the same department in 1999 and a B.S. degree in Mechanical Engineering with a minor in Physics from the California State Polytechnic University in 1996. Dr. Allain specializes in the areas of plasma-material interactions with applications in nanolithography using EUV radiation and fusion science. He has designed and built a state-of-the-art facility at Argonne named PRIME. The PRIME facility conducts experiments in the area of intense particle/radiation – material interactions. His most recent work and interests include: low-energy ion scattering spectroscopy, synergistic photon and ion irradiation on thin-films, surface charge dynamics and multi-component surface evolution under threshold energy-level ion irradiation.

Ahmed Hassanein is Senior Nuclear Engineer at Argonne National Laboratory. Has five engineering and physics degrees including a Ph.D. (1982) and two Masters from the university of Wisconsin, Madison. Internationally recognized as one of the world's foremost lead persons in the area of modeling material response to different radiation sources. Has developed unique models and comprehensive computer package to predict materials behavior, lifetime issues, and fluid hydrodynamics under various irradiation conditions. Created the PRIME "Particle Radiation Interaction with Material Experiments" facilities at Argonne. These facilities now conduct research for DOE fusion program, Intel, SEMATECH, Philips, ASML, and others. Dr. Hassanein is author of more than 270 journal publications and technical reports in heat transfer, thermal hydraulics, radiation damage, hydrodynamics, particle diffusion and transport, atomic physics, and photon and radiation transport. He presented numerous invited talks and chaired international conferences and workshops as well as keynote speaker to universities and world-class institutions.

EROSION STUDIES OF EUVL CANDIDATE COLLECTOR MIRROR MATERIALS IN THE IMPACT EXPERIMENT

Daniel L. Rokusek, Jean P. Allain, Ahmed Hassanein, and Martin Nieto

ABSTRACT

The IMPACT (Interaction of Materials with charged Particles And Components Testing) experiment at Argonne National Laboratory was used to expose Pd, Ru, and Re-capped Ru candidate EUV light collector mirror materials to conditions similar to extreme-ultraviolet (EUV) lithography source devices, in particular high-energy singly-charged Xe ions. Experiments measured both the time-dependent atomic surface concentration evolution of candidate single-layer mirror (SLM) samples and the Xe^+-induced sputtering yield. Elemental surface information was acquired using low-energy ion scattering spectroscopy (LEISS) and sputtering yields were acquired using an in-situ quartz crystal microbalance. Sputtering results show large erosion rates between 0.5 and up to 7.0 for Pd and Ru SLM samples for energies between 500 and 1000 eV of Xe^+ irradiation at grazing incidence. Re-capped Ru SLM samples also demonstrated very high sputter yields. Time-dependent erosion rate measurements used with LEISS resulted in a high depth-resolution profile and led to the discovery of ion-induced recoil implantation of oxygen atoms to the Ru mirror surface. High concentration of oxygen throughout the Ru SLM may be detrimental to the reflectivity response of the collector mirror.

INTRODUCTION

Deep-ultraviolet lithography (DUVL), the industry's standard for manufacturing microprocessors, is projected to reach its limits in 2009. DUVL is limited by the minimum wavelength of light, 193-nm, that can be used to etch circuits on silicon wafers. Thus, a new technique is needed to create smaller microprocessors with more transistors. Extreme-ultraviolet lithography (EUVL), using a wavelength of 13.5-nm, is a process undergoing intense research and one of the leading candidates for emerging lithography techniques of next generation microprocessors [1,2]. To generate EUV light, hot, dense plasmas are required [3]. Two main configurations are used:

gas-discharge-produced plasmas (DPPs) and laser produced plasmas (LPPs). Both configurations require the collection of EUV light at the first condenser optics to an intermediate focus downstream from the high-intensity plasma. Figure 1 shows schematically both the DPP and LPP configurations showing the use of grazing incidence collector mirrors and near-normal incidence mirrors, respectively. Scaling to higher EUV powers hinders the application of EUV light for high-volume manufacturing lithography in the near future due to lifetime limits on critical components in EUV sources, in particular the plasma-facing collector mirror. Lifetime is currently defined as loss of EUV photon reflectivity of about 10% after operation with about 10^{11} shots or about 2.5 years.

In LPP EUVL sources, EUV light is collected at near normal incidence with respect to the mirror surface [3] compared to DPP sources, at grazing incidence. Multilayer mirrors (MLMs) with dissimilar EUV optical constants made of Si/Mo with a period of about $\lambda/2$ are used as LPP collector optics [4]. The conventional EUV light fuel used in both configurations is currently Xe, although Sn is also under consideration [5]. The high-intensity plasma pinch produces fast ions and neutrals that bombard and erode nearby components, including the collector optics. The collector optics surface will also be exposed to off-band radiation (outside 13.5-nm) inducing heat, debris (i.e., electrode material in DPP devices), highly charged ions, and background impurities (i.e., H, C, N, O). This paper studies in particular the interaction of intense, energetic Xe singly-charged ions with single-layer (grazing incidence) mirror materials including: palladium, ruthenium, and rhenium.

The IMPACT (Interaction of Materials with charged Particles And Components Testing) experiment at the Argonne National Laboratory studies the interaction of highly energetic and intense particles with various candidate mirror materials for EUVL, such as Pd and Ru. IMPACT features a well-collimated ion source to conduct erosion studies of the candidate mirror materials [6]. The source is capable of producing ions with energies between 50 and 5000 eV, fluxes ranging from 10^{11} to 10^{17} ions/cm^2/s, and incident angles ranging from 0 to 60-degrees with respect to normal. Temperature dependent studies up to 1000 ^{o}C can also be performed, as the system includes an in-situ heating element to vary sample temperature. Another feature of IMPACT is the capability of performing in-situ low-energy ion scattering spectroscopy (LEISS) to facilitate the characterization of multi-component surfaces as they erode.

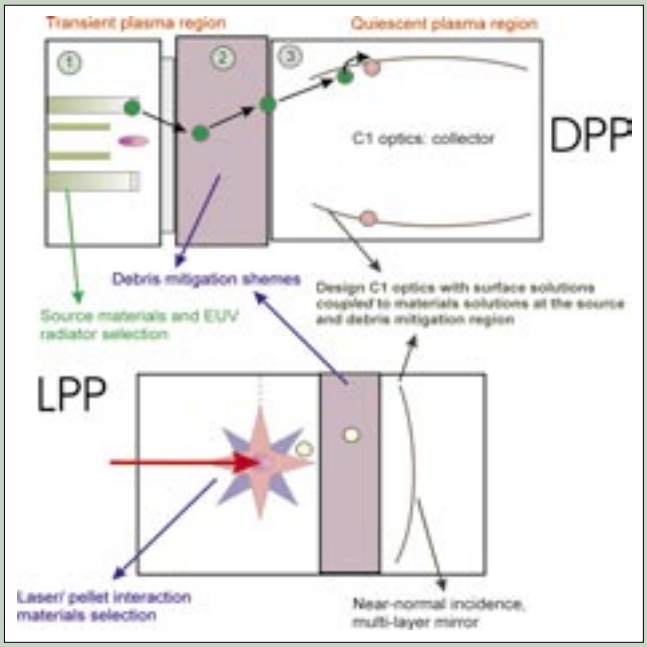

Figure 1. Schematic describing competing candidate configurations to generate EUV light in EUV lithography sources and their respective components. In discharge produced plasma (DPP) sources, grazing incidence collectors are used; whilst in laser produced plasma (LPP) devices near-normal incidence collector mirrors are applied.

MATERIALS AND METHODS

The samples used in IMPACT are single-layer mirrors (SLMs) of palladium, ruthenium, and rhenium were fabricated at the Materials Research Laboratory at the University of Illinois at Urbana-Champaign. SLMs were grown on SiO_2 substrates, with the thin films deposited via magnetron sputtering. The composition of each sample consists of a thin film of the candidate mirror material (10 – 50-nm) on top of a 5-nm layer of Ti on top of the SiO_2 substrate. This Ti layer is deposited to minimize silicide formation of the top-most layer. Identification of samples follows the form of Xy-Z, where Xy is the element of the topmost thin film and Z is the sample number (assigned according to samples original position on a 6-in SiO_2 wafer).

Samples, generally 1-cm^2, are transferred in and out of the IMPACT chamber via a custom designed transfer-lock system. While isolated and vented, the transfer-lock chamber is opened and a sample is placed on two forks that are fixed to the end of a linear feedthrough. Once the sample is in place, the chamber is sealed and pumped down to the pressure of the main chamber (IMPACT experiments are conducted in an ultra-high vacuum (UHV) environment). A typical base pressure of 10^{-8} Torr can be achieved through the use of a magnetically-levitated turbo-molecular pump backed by a scroll pump. When an acceptable pressure is reached, a valve is opened to allow the transportation of the sample from the transfer-lock into the main chamber. Using the linear feedthrough, the sample is transferred from its position on the forks onto a boron-nitride sample holder in the main chamber. This sample holder is fixed to a rotatable, linear motion feedthrough. The axis of rotation of the feedthrough lies in the plane of the sample's surface, allowing angle-of-incidence measurements to be conducted. The linear manipulation of the sample allows for moving the sample in and out of the ion beam path.

IMPACT uses a differentially-pumped Model 1401 Ion Gun, commercially manufactured by Nonsequitur Technologies, Inc. (NTI) Beams of inert gas ions are generated by means of electron impact ionization; gases used include Xe, He, Ne, and Ar. Beams are characterized by four factors: gas species, beam energy, beam current, and spot size. The first two are relatively easy to obtain, however beam current and spot size require the use of optics contained inside of the ion gun. Varying these optical settings will focus and/or condense the beam, with an overall effect of changing beam current and beam diameter, allowing full control of the particle

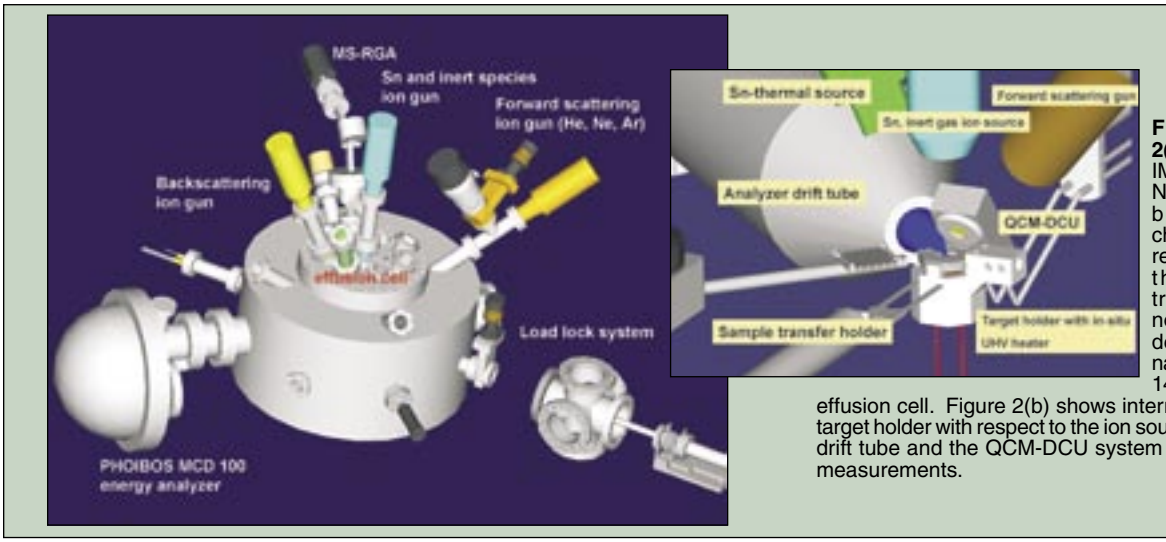

Figures 2(a) and 2(b). Diagram of the IMPACT experiment. Note that the section between the two chambers has been removed to illustrate the path of the transfer arm. Also note that additional devices are shown, namely two additional 1401 ion guns and an effusion cell. Figure 2(b) shows internally location of the target holder with respect to the ion sources, the PHOIBOS drift tube and the QCM-DCU system used for sputtering measurements.

flux level reaching the sample. A Faraday Cup is used to measure the beam current. The Faraday Cup is a device that allows for direct measurement of collected ions by having a picoammeter in series with ground. The beam's diameter is also measured with the Faraday Cup, coupled with beam profiling software. The software serves as a virtual instrument (VI), programmed with National Instrument's LabVIEW software package. The VI rasters the beam across five pinholes inside the Faraday Cup to create a spatial beam profile using the NTI ion source's octopole lenses. Profiles are cataloged for future reference and use. Once the desired beam current and diameter are obtained, the sample is positioned under the beam for irradiation. Figure 2(a) shows a schematic for both the overall IMPACT geometry and multiple ion sources along with figure 2(b) showing the internal components of the experiment. Multiple ion sources are used for LEISS and irradiation of sample SLMs.

Erosion experiments collect sputtered target atoms from the mirror sample induced by the incident, highly-intense energetic Xe (or other) ions. IMPACT uses a quartz crystal microbalance – dual crystal unit (QCM-DCU) diagnostic system for in-situ real-time erosion measurements and is shown in figure 2(b). The quartz crystal microbalance technique is a powerful, well-developed diagnostic metrology tool measuring mass loss from materials irradiated by the incident ions [7]. It can measure monolayer-level erosion of surfaces irradiated by charged-particle bombardment. This technique utilizes one crystal oscillator to measure the deposition of sputtered particles, while the other crystal oscillator is shielded from the sputtering flux and measures the background ambient only. The measured frequency difference between the two crystals (proportional to the mass of material sputtered onto the unshielded crystal) is then correlated to the amount of eroded material from the sample. Total sputtering data is extracted from the measured frequency difference using some graphical software and is used to calculate sputtering rates. Points of inflection represent changes in the total sputtering rate due to changes in surface interfaces, compounds, and ion-induced mixing. The sputtering yield is calculated from the reduced data, which is then used to calculate sputtering rates.

Beam irradiation time is determined on an individual experiment basis. The convention used to determine exposure time was based on the desire to deliver a common dose of irradiation for each trial in a set of experiments. The LEISS technique is used with multiple NTI ions sources in forward and backscattering modes with a PHOIBOS 100-MCD hemispherical energy analyzer. The LEISS technique is one of several in-situ metrology techniques in IMPACT to study the sample surface under particle bombardment. In addition, sputter rates measured with the QCM-DCU are used in conjunction with LEISS for in-situ depth profiling.

RESULTS

Figures 3(a) and 3(b) show the frequency difference on the two QCM crystals during Xe^+ bombardment of Pd-15 and Ru-46 samples, respectively, irradiated at 45-degrees incidence and 2.6×10^{14} $cm^{-2}s^{-1}$ flux at room temperature. Both samples were irradiated varying incident Xe^+ ion energies to study the effect of ion energy on sputtering yield. The curve in each figure was generated by inserting the sample under the beam and irradiating, then removing the sample to measure the beam current. After each irradiation, the beam energy was decreased and the sample was re-inserted under the beam and irradiated again. The flat sections seen in figures 3(a) and 3(b) correspond to no sputtering during the time the sample is removed from the beam while the beam current was measured with the Faraday Cup. Each drop in frequency measured corresponds to a particular incident Xe^+ energy, and is used to obtain the energy-dependent sputtering yield. These sputtering yields are plotted in figures 4(a) and 4(b) for Pd-15 and Ru-46 respectively. These figures show the behavior of sputtering yield as a function of energy. The sputtering yields were calculated using the following equation [7]:

$$Y = \frac{1}{D f_i S^{QCM} \Omega m_{avg}} \frac{\Delta f}{f} M_{crystal} \quad (1)$$

Here, D represents total ion dose, S^{QCM} represents a sticking coefficient, $M_{crystal}$ represents the mass of the crystal (provided by manufacturer), Δf represents the change in frequency during sputtering, f represents background after sputtering, Ω represents the collected fraction, m_{avg} represents the mass of the deposited species, and f_i represents the dose correction factor for secondary electrons and sputtered ion current.

Figure 5(a) shows the surface composition evolution for the Ru-107 sample obtained by the LEISS technique, using 1000 eV

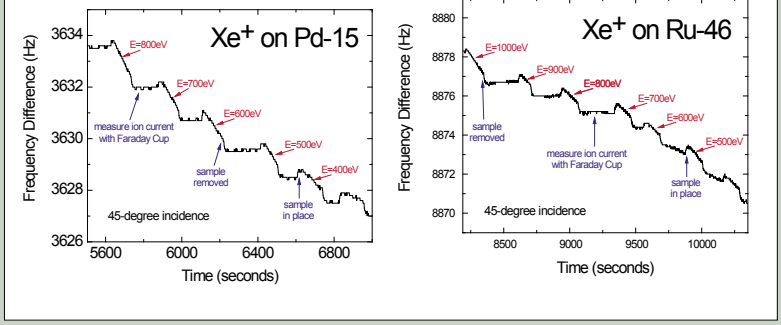

Figures 3(a) and 3(b). Frequency difference measurements from QCM-DCU diagnostic in IMPACT for Xe^+ bombardment of Pd-15 and Ru-46, respectively, at 45-degree incidence for varying energies.

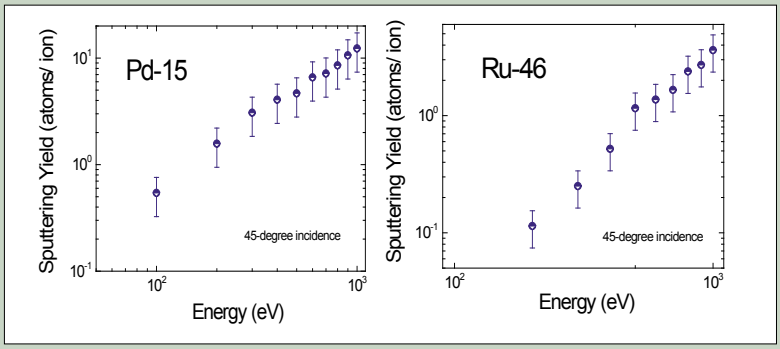

Figures 4(a) and 4(b). Sputtering yield of Pd-15 and Ru-46, respectively, on 5-nm of Ti/SiO_2 bombarded by Xe^+ at 45-degree incidence for various energies.

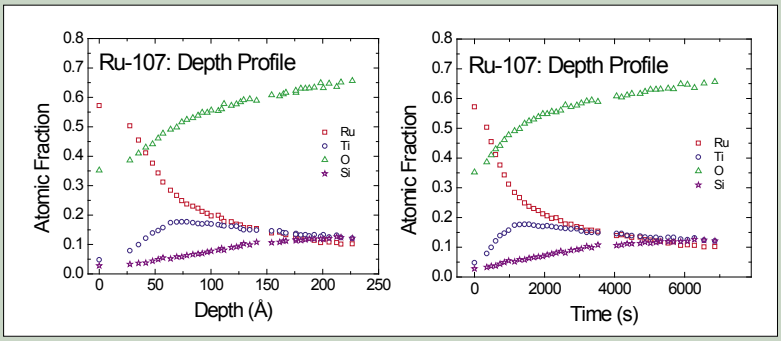

Figures 5(a) and 5(b). Evolution of atomic fraction of species in Ru-107 over time and depth, respectively. Note that the profile on the right is a true depth profile.

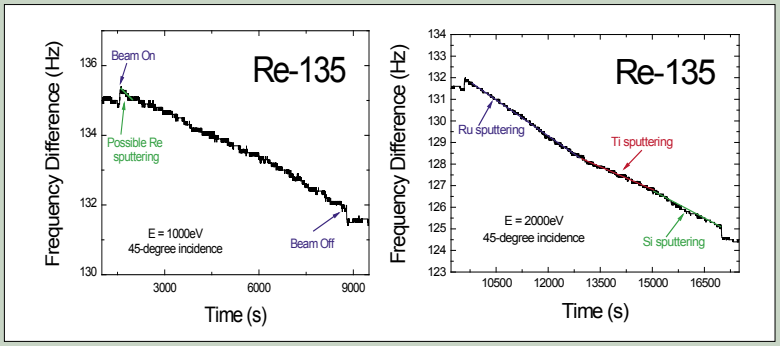

Figures 6(a) and 6(b). Frequency difference measurements from QCM-DCU diagnostic in IMPACT for Xe+ bombardment of Re-135, at 45-degree incidence for 1000 and 2000 eV cases, respectively. Note in figure 6(a) that there may be a small region of Re sputtering. Note the high-flux sputtering in figure 6(b) shows the different layers of materials in the sample.

He^+ as the probing ions at normal incidence and room temperature. The flux of He ions was varied so that during LEISS data collection it was minimized and then increased to sputter material, thus resulting in a profile through the SLM depth. The architecture of the Ru-107 SLM was 10-nm Ru / 5-nm Ti / Si substrate. This sample was irradiated for approximately 120 minutes. The species observed in figure 5(a) correspond to Ru, Ti, Si, and O surface atom fractions measured with LEISS as a function of depth. The depth profile illustrated in figure 5(b) was obtained by multiplying the time evolution of the peaks by the sputtering rate as a function of time. The transformation of figure 5(a) to figure 5(b) required smoothing the QCM sputtering data with a Fast Fourier Transform (FFT) filter to eliminate intrinsic noise. The smoothed curve was then fit with a third-degree polynomial, which was subtracted from the original signal. The difference was fit with a cosine function, which was then removed from the original signal to obtain the true signal. The resulting curve was quite linear, with a slope corresponding to the total change in frequency of the two QCM crystals due to the sputtering. This value was incorporated into a constant, along with equation (1), giving the following for sputtering rate [8]:

$$\frac{\partial x}{\partial t} = \frac{K}{\sum y_i \rho_i} \qquad (2)$$

where K represents a constant involving current and yield values, and y_i and ρ_i represent the atomic fraction (intensity) and mass density for i=Ru,Ti,Si,O. Now, to obtain depth as the unit of measurement of the x-axis, time is simply divided by sputtering rate, that is, [s]/[Å/s]=[Å]. Knowledge of the energy corresponding to each target mass and the cross section σ for the corresponding projectile-target pair allows the calculation of surface composition of the sample. Suppose that during an energy scan with the detector, N number of peaks each with area A_i, are observed. The atomic fraction of each component y_i can be calculated by:

$$y_i = \frac{A_i \sigma_i^{-1}}{\sum_{k=1}^{N} A_k \sigma_k^{-1}} \qquad (3)$$

Therefore, the surface atomic fraction can be determined from knowledge of the elastic scattering cross section and use of the LEISS intensity spectra [9].

Re is another EUV collector mirror candidate along with Pd and Ru. Figure 6(a) shows data for 1000 eV Xe^+ bombardment of Re-135, irradiated at 45-degrees incidence and 3.3×10^{13} $cm^{-2}s^{-1}$ flux at room

temperature. The architecture of the Re-135 SLM sample is Re/Ru/Ti/SiO_2, with layer thicknesses of 2-nm / 10-nm / 5-nm / substrate, respectively. The data shows immediate and rapid sputtering of the Re layer, represented by the first downward sloping segment in the figure during the first three minutes of irradiation. At the end of this region there exists a point of inflection representing the end of the Re layer and the beginning of the Ru layer. The bombarding flux was predetermined, based on a calculation for a fixed sputtering time of five minutes.

To illustrate the different regions of the sample, the same experiment was performed at new location on Re-135, this time with 2000 eV Xe^+ ions. The results of this experiment are shown in figure 6(b). Notice three distinct regions, corresponding to the Ru, Ti, and Si layers. Also note that no Re layer is observed, as the Xe^+ flux is too large for such a thin layer to be detected by the frequency difference measured on the QCM-DCU in the short time interval.

Figure 7 shows LEISS data for Re-133 obtained with a 1000 eV He^+ beam. The architecture of the Re-133 SLM sample is the same as that of Re-135. Here, Re-133 was bombarded with 1000 eV He^+ ions at normal incidence and room temperature. The scans do not distinguish the Ru peak from the Re peak since they are very close in energy (868.8 eV and 902.9 eV, respectively). Since the use of He^+ ions as scattering particles limits the identification between Ru and Re atoms, Ne^+ ions were chosen as scattering particles to achieve better mass resolution due to higher energy coupling between incident and target masses.

Figure 8 shows a LEISS scan of Re-135. This scan was performed using 1000 eV Ne^+ ions incident on Re-135 at normal incidence and room temperature. The peak observed on the left at E = 608 eV corresponds to Ru, while the peak on the right at E = 749 eV corresponds to Re. Ne^+ ions were used because they are heavier than He^+ ions and therefore better resolve the two peaks based on the principles of LEISS [9], as evident in the figure. The disadvantage with using Ne^+ beams, however, is that impurities such as oxygen and carbon (i.e. M = 16 or 12 amu) cannot be detected.

DISCUSSION AND CONCLUSIONS

In order for a candidate mirror material to be used in a EUV-light generation device, its behavior while being irradiated must be understood and potential degradation mechanisms mitigated. Because different energy particles can exist in practical applications, it was necessary to study the sputtering yields of candidates Pd, Ru, and Re with variation in incident particle energy. The plots shown in figures 4(a) and 4(b) illustrate such behavior for energies ranging from 100 to 1000 eV. The data shows that as incident particle energy increases, the sputtering yield also increases. Figures 3(a) and 3(b) show that the higher energy cases have a larger change in frequency vs. time than that of the lower energies. This correlates to larger sputter rates and calculated sputter yields presented in figures 4(a) and 4(b). These sputtering yield measurements have two important results. The first is that at energies greater than 500 eV, Ru will sputter more than Pd-based collector mirrors; therefore any fast ions generated from the creation of EUV light will have to be mitigated if Ru mirrors are used. The second finding is that for either Pd or Ru, 1000 eV particles cannot be tolerated since both will have over unity sputter yields induced by Xe^+ bombardment. Recall, Xe is used as a light generator for EUV light in plasma-based EUVL sources.

Figures 5(a) and 5(b) graphically illustrate the composition of the Ru-107 SLM sample as a function of time. The ability to profile a sample with LEISS while measuring the sputter rate in-situ is quite powerful, as individual monolayers of a sample can be examined. In addition, knowing how the surface composition changes in time will allow for design decisions of EUVL collector mirrors as they are irradiated by Xe^+ particles. In the case of Ru-107, the known composition was verified, however mixing between layers was observed. Such mixing was assumed to occur, however the level of oxygen at the surface was higher than anticipated. The time behavior of oxygen suggests that oxygen is present throughout the sample. As oxygen is diffuses from the SiO_2 substrate, it mixes with the other metals and oxides are formed. In addition, ion-induced recoil implantation of oxygen atoms to the surface is also found. This is an important result and the first time this phenomenon has been discovered for an SLM collector mirror. Such oxygen segregation could be detrimental to EUV reflectivity and degrade the collector mirror.

The curve in figure 6(a) shows the possibility of Re sputtering in the first four minutes. It is difficult to conclude whether there is a point of inflection suggesting the transition from Re to Ru. Because the slope is not linear, it is concluded that the layer is not purely Re. Rather, Re and Ru mixing has occurred as sputtering

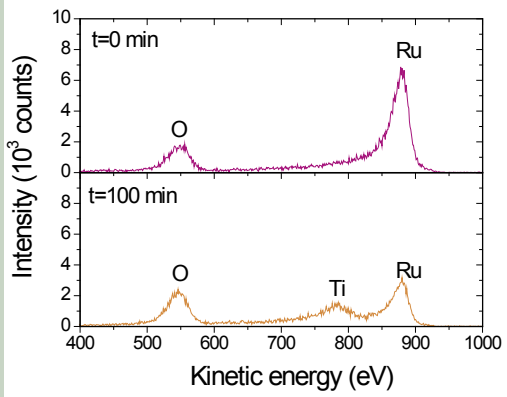

Figure 7. Intensity of species of Re-133 for increasing time. Note that this plot shows intensity, and not atomic fraction. Because Re is not observed in the profile, atomic fractions cannot be assigned to the Ru, Ti, and O species.

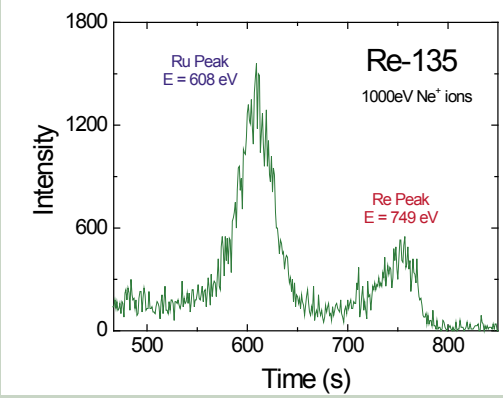

Figure 8. LEISS scan of 1000 eV Ne^+ bombardment of Re-135. Note that the Ru and Re peaks are now clearly resolved.

of the two components gives the non-linear slope. Even with the low-flux Xe^+ beam, the Re layer was eroded too quickly to obtain useful data, and therefore it is concluded that the Re layer appears to be too thin to be studied at the incident flux level used. In order to obtain meaningful data, future experiments should be performed on a sample that has a thicker Re layer and/or performed at much lower ion flux levels. This result does however point to the propensity for Re to erode under Xe^+ bombardment. Therefore, collector mirrors designed with Re cap layers should be avoided.

Another important result is the time evolution of the Re-capped SLM. The time scans shown in figure 7 of Re-133 show the evolution of various species on the sample surface. It was known that the mirror sample's architecture was Re/Ru/Ti/Si. The scans show a large Ru peak, an ever-present O peak, and eventually a Ti peak. It is not explicitly obvious that Re is present. The main result here is that oxygen again is found to preferentially segregate to the surface. This seems to be a dominant mechanism for Ru-based mirrors and thus may make Ru a poor candidate EUV collector mirror material.

The Re peak was not clear in the LEISS spectra, and this is probably due to the closeness of energy of the Re and Ru peaks. To support this claim, it is noted that 1000eV He^+ ions in an LEISS scan will resolve a Re peak at E = 902.9 eV and a Ru peak at E=868.9 eV. The difference in energy of these two peaks is only 34 eV equivalent to the full-width-at-half-maximum of the scattered peak, and therefore it is concluded that the larger Ru peak is effectively hiding the Re peak. To acquire data with better mass resolution, Ne^+ ions were used. The heavier ions will profile the surface more accurately than the He^+ ions, however because Ne^+ ions are heavier than oxygen the O peak will not be seen. Figure 8 shows the case for LEISS spectra using a Ne^+ beam. Note the good separation in energy peaks for both Re and Ru. Thus the ability for IMPACT to use a variety of source gases allows flexibility and versatility for identification of various candidate EUV mirror materials whose masses may not be that much different.

In summary, Pd, Ru and Re-capped Ru candidate EUVL collector mirror materials have been tested in IMPACT under various bombardment conditions. All experiments using relatively high-energy Xe^+ ions led to large erosion levels of candidate EUVL collector mirror materials (i.e. Pd, Ru and Re). Therefore, high energy Xe ions must be avoided and mitigated. Oxygen segregation induced by ion-bombardment and oxygen diffusion from SiO_2 interface regions present another challenge to collector mirrors, especially Re and Ru-based systems, which have a high affinity for oxygen. Therefore, selection of a collector mirror with low oxygen affinity, low erosion yields and high EUV reflectivity is preferred.

ACKNOWLEDGEMENTS

Major parts of this work are supported by the Intel Corporation. The US Department of Energy, the Office of Science, and the SULI program for support of D. Rokusek at Argonne National Laboratory. M.M.C. Allain and Prof. B.J. Heuser for fabrication and characterization of the SLM samples. Surface characterization measurements on SLM samples prior to delivery to ANL were performed at the University of Illinois Center for Microanalysis of Materials, which is partially supported by the U.S. Department of Energy under grant DEFG02-91-ER45439.

REFERENCES

[1] Sematech, *The National Semiconductor Roadmap* (Sematech and Semiconductor Industry Association, Austin, TX, 2004.

[2] John E. Bjorkholm, Intel Technology Journal Q3, (1998) 1.

[3] U. Stamm, J. Phys. D: Appl. Phys. 37, (2004) 3244.

[4] S. Bajt et al., Optical Engineering 41 (8), (2002) 1797.

[5] V. Banine and R. Moors, J. Phys. D: Appl. Phys. 37, (2004) 3207

[6] J.P. Allain et al., "Xe^+-Irradiation effects on multilayer thin-film optical surfaces in EUV lithography", Nucl. Instrum. Methods B, Submitted 2004.

[7] J.P. Allain and D.N. Ruzic, Nucl. Fusion 42, (2002) 202.

[8] S. Hoffman, Rep. Prog. Phys. 61, (1998) 827.

[9] J.W. Rabalais, Principles and Applications of Ion Scattering Spectrometry. Hoboken, NJ: John Wiley & Sons, (2003).

Ryan Reed received his B.S. in Chemical Engineering from the University of Washington in the spring of 2004. As an undergraduate, Ryan worked with Dr. Stuart Adler on solid oxide fuel cell cathode materials. Their work focused mainly on chemical expansion of ceramic materials in high vacuum. Following graduation, he participated in the Science Undergraduate Laboratory Internship (SULI) at the National Renewable Energy Laboratory (NREL). While at NREL, the focus of his project was testing new proton exchange membrane materials for use in fuel cell. Specifically, the project was looking at ionic conductivity. Advising him on the project was Dr. John Turner (NREL). Ryan is currently a graduate student at the University of Washington under the tutelage of Dr. John Berg, who specializes in colloidal and interfacial science. Ryan is currently devoting his research time to looking at the mechanical optimization of composite materials through chemical modification.

John A. Turner, Ph. D., is a Principal Scientist at the National Renewable Energy Laboratory. He received his B.S. degree from Idaho State University, his Ph.D. from Colorado State University, and completed a postdoctoral appointment at the California Institute of Technology before joining the Laboratory (then the Solar Energy Research Institute) in 1979. His research is primarily concerned with enabling technologies for the implementation of hydrogen systems into the energy infrastructure. This includes direct conversion (photoelectrolysis) systems for hydrogen production from sunlight and water, advanced materials for high temperature fuel cell membranes, and corrosion studies of fuel cell metal bipolar plates.

CONDUCTIVITY ANALYSIS OF MEMBRANES FOR HIGH-TEMPERATURE PEMFC APPLICATIONS

R. Reed, J.A. Turner

ABSTRACT

Low-temperature operation requirements for per-fluorinated membranes are one factor that limits the viability of current fuel cell technology for transportation and other uses. Because of this, high-temperature membrane materials are being researched. The protonic conductivity of organic/inorganic hybrid composites, Nafion® analog material, and heteropoly acid doped Nafion membranes were studied using a BekkTech® conductivity test cell as a hydrogen pump. The goal was to find a high-temperature membrane with sufficient enough conductive properties to replace the currently implemented low-temperature membranes, such as Nafion. Four-point conductivity measurements were taken using a hydrogen pump experiment. Results showed that one of the organic/inorganic membranes that we tested had similar protonic conductivity to Nafion. Nafion analog membranes were shown to have similar to slightly better conductivity than Nafion at high-temperatures. However, like Nafion, performance dropped upon dehydration of the membrane at higher temperatures. Of the heteropoly acid doped Nafion membranes studied, silicotungstic acid was found to be, overall, the most promising for use as a dopant.

INTRODUCTION

Proton exchange membrane fuel cells (PEMFC) have been shown in the literature to be viable options for replacing petroleum-based power generation applications such as diesel generators and internal combustion engines [1-8]. However, economic competitiveness, fuel choice, and system integration difficulties are hurdles that must be cleared in order for the technology to become widely accepted. One factor that addresses all of these issues is membrane material technology.

A majority of commercially available fuel cell systems today use Nafion®, produced by DuPont®. Nafion is a perfluorinated sulfonic acid polymer that is manufactured into a membrane. As a fuel cell membrane, Nafion has long been known to produce high power densities at low-temperature operation (< 100°C). One reason for the high power density is that, at low-temperatures (e.g. 80°C) and high relative humidity, Nafion conducts protons very efficiently, 75 mS/cm (Nafion 117) [9, 10]. Because of this, Nafion currently is the most common fuel cell electrolyte. However, due to the dependence of hydration for conductivity, Nafion is not designed for high-temperature (low relative humidity) operation [11]. At high relative humidity (high water activity), water is absorbed into hydrophilic regions of Nafion, which in turn conduct protons, necessary for generating the PEMFC reactions [12]. When the water required for proton conduction is eliminated from the system, membrane proton conductivity decreases rapidly [13].

The need to maintain a high relative humidity makes high temperature operation difficult due to the energy losses associated with humidifying feed streams. The need for low-temperature operation poses a problem when attempting to integrate current fuel cell and automotive technologies. Automotive cooling systems are designed to operate at temperatures around 120°C. Lowering

the operating temperature to accommodate a Nafion PEMFC stack requires either a retrofit or a complete redesign of the automotive cooling system. In both cases, the total system cost could increase significantly. Ideally, membrane materials that could conduct at higher temperatures (120°C) and lower relative humidity could be employed so that current automotive cooling systems could be employed without excessive energy losses due to reactant stream humidification.

In addition to the system costs associated with low-temperature integration, fuel choice is also limited by operation with Nafion and other perfluorinated membranes. The low-temperature requirements of these systems cause the catalyst to be highly sensitive to carbon monoxide (CO) poisoning [14]. Because of this, a system using Nafion requires that the CO content of the fuel be extremely low. In most cases, the fuel must be additionally filtered after production, as in the case of hydrogen obtained via reformation of hydrocarbons [14]. Post-reformation filtration also increases the overall system cost. Higher temperature operation decreases the poisoning effect of CO on the catalyst [14], and eliminates some, if not all, of the need for post-reformation filtration of fuel. For these reasons and more, high-temperature membrane materials are being studied.

Conductivity analysis of alternative membrane materials at high-temperature operation was the focus of this paper. Specifically three types of membranes were studied. The first were organic/inorganic hybrid composite membranes. Secondly, an analog of Nafion was studied. Finally, Nafion doped with various heteropoly acid proton-conductors were investigated. In each of these studies Nafion control samples were also compared to our test membranes.

Organic/Inorganic hybrid composite membranes of the type studied here are defined as having polymer complexes (organic) that have been doped with a proton-conducting material (inorganic) in order to obtain an optimized combination of physical and chemical properties. The synergy between the thermo-mechanical stability of the polymer "backbone" and the conductive properties of the dopant provide a possibility for higher efficiency, high-temperature, proton exchange membranes to be developed [11, 17-21]. Heteropoly silicotungstic acid and sulfonic acid were the two groups of conductors studied. They were chosen because both display high protonic conductivity in their solid states compared to Nafion. A special type of polypropylene oxide named BSPPO was used as the polymer complex in both cases. The composition of BSPPO is proprietary. In addition to the membrane compositions discussed here, other organic/inorganic composite membrane studies can be found in the literature [15, 16].

Analog membranes are materials that have similar composition to an existing membrane; however, they are different enough to be categorized as their own material. Two thicknesses of a Nafion analog that were designed and manufactured in Russia were tested under high-temperature operation. The purposes of these tests were to see if the slight modification to the composition yielded improved performance at high-temperatures.

The third membrane type studied was Nafion doped with proton-conducting inorganic heteropoly acids. Membranes of these types have been studied elsewhere and have shown promising results [13]. By doping Nafion with highly conductive heteropoly acids it is theorized that conductivity will be increased and become less dependent on hydration. This lack of dependence on hydration would open the door for high-temperature operation. The specific membrane/dopant combinations studied were Nafion 112 doped with the following: heteropoly silicotungstic acid (HSiW), heteropoly arsenotungstic acid (HAs_2W), and both Dawson and Keggin structures of heteropoly phosphotungstic acid (12-HPW and HP_2W, respectively). In addition to the membranes studied in this paper, Savadogo has provided a summary of other types of high-temperature membranes currently being researched [14].

MATERIALS AND METHODS

Hydrogen pump experiments were performed on three types of membranes, organic/inorganic hybrids, Nafion analogs, and heteropoly acid doped Nafion. Organic/Inorganic hybrid membranes were solution-cast consisting of a polymer host and a SiO_2-based proton-carrier composite that was synthesized via a sol gel approach using a functional silane and tetraethoxysilane (TEOS) in acidic conditions [22]. In total, two organic/inorganic membranes were studied. The first organic/inorganic hybrid membrane was composed of a polymer backbone of special polypropylene oxide (BSPPO) and doped with heteropoly silicotungstic acid (W12-STA). Sulfonic acid (SFA) that was thermo-oxidatively converted from a mercapto (-SH) group was used along with the same BSPPO backbone in the second organic/inorganic hybrid membrane. These membranes have been characterized in previous work, using diffusion reflectance Fourier transform infrared spectroscopy (DRIFT), differential scanning calorimetry (DSC), thermo-gravimetric analysis (TGA), scanning electron microscopy (SEM), and electron probe microanalysis (EPMA) [22].

Analog membranes were provided from an Armenian company; however, the membranes themselves were designed and produced in Russia. Membranes of multiple thicknesses were supplied for the study; samples of 80 μm and 150 μm were tested. Exact composition of the membranes is proprietary.

Heteropoly acid (HPA) doped Nafion membranes were prepared by submersing pure Nafion membranes in aqueous solutions of HPA or HPA salts for 24 hours at 80°C. The amount of acid in solution varied according to the amount of material available and the solution density. A more detailed description of the fabrication method may be found in literature [26]. Membranes were characterized using attenuated total reflectance Fourier transform infrared spectroscopy (ATR-FTIR), diffusion reflectance Fourier transform infrared spectroscopy (DRIFTS), small-angle x-ray scattering (SAXS), and thermo-gravimetric analysis (TGA). The procedure and results of these tests have been published elsewhere [10].

Four-point conductivity measurements were taken of all three types of membranes using the BekkTech® conductivity test cell in conjunction with a PGZ 301 Dynamic EIS Voltammeter®. The BekkTech cell functioned as the hydrogen pump with sense wires set up along the transverse direction. Temperature and humidification were controlled using the Globe Tech CompuCell® GT fuel cell test stand. Strips of membrane material approximately 5 cm x 2 cm were cut and placed into the BekkTech conductivity test cell in order to test for protonic conductivity.

Four-point conductivity measurements involved the use of four electrodes placed around the cell to obtain resistance values. First, two electrodes were attached to the current collectors of the test cell. Two additional electrodes were then attached directly to the membrane material via platinum sense wires in the BekkTech cell. The electrodes being attached directly to the membrane material allowed for compensation of the interfacial and material resistances due to the existing fuel cell hardware. Current was then measured as a function of applied voltage; from this, a membrane resistance could be calculated via Ohm's Law. Length, width, and thickness of samples were then recorded in order to calculate conductivity. While the length and width could always be accurately determined using calipers, the thickness of the membranes was found to vary occasionally upon inspection with a micrometer. When this was the case, average thickness values were recorded. Conductivity was then calculated using the equation was provided with the BekkTech test cell manual.

RESULTS

Figure 1 shows the conductivity verses cell temperature results obtained for the organic/inorganic hybrid composite membranes using the BekkTech cell. Membrane materials were cut and placed in the conductivity test cell, as mentioned above. All measurements were obtained in a pure hydrogen (99.999%) environment, keeping with the standard operating procedure of the BekkTech cell provided in the manual. Values were taken at a constant humidification temperature of 80°C, a hydrogen flow rate of 0.2 slpm, and a hydrogen backpressure of 30 psig. Results are presented along with a conductivity sweep of Nafion 117, to provide a baseline for comparison. Nafion 117 was chosen due to the similarity that the membranes shared in thickness. Results were consistent with those of a typical hydrogen pump experiment using the BekkTech cell.

Figure 2 compares the conductivity verses cell temperature of the Russian analog membrane to Nafion 117. Again, Nafion 117 was chosen because of the similarity in thickness to the analog membranes. Measurements were obtained in a pure hydrogen (99.999%) environment, keeping with the standard operating procedure of the BekkTech cell provided in the manual. Values were taken at a constant humidification temperature of 80°C, a hydrogen flow rate of 1.0 slpm, and a hydrogen backpressure of 30 psig.

Figure 3 displays the conductivity verses cell temperature of various heteropoly acid doped Nafion membranes. The membrane base in each case was Nafion 112. For that reason, results are shown along with a control membrane of pure Nafion 112. Measurements were obtained in a pure hydrogen (99.999%) environment, keeping with the standard operating procedure of the BekkTech cell provided in the manual. Values were taken at a constant humidification temperature of 80°C, a hydrogen flow rate of 1.0 slpm, and a hydrogen backpressure of 30 psig.

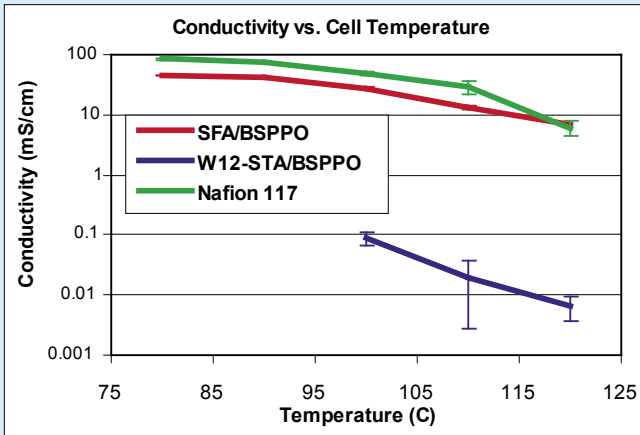

Figure 1. Conductivity measurements obtained for SFA/BSPPO 0.41wt% and W12-STA/BSPPO 0.44wt% at various cell temperatures ranging from 80-120°C. All measurements were taken at a humidification temperature of 80°C, hydrogen flow rate of 0.2 slpm, and a hydrogen backpressure of 30 psig. Note that units of conductivity are in milli-Siemens/cm.

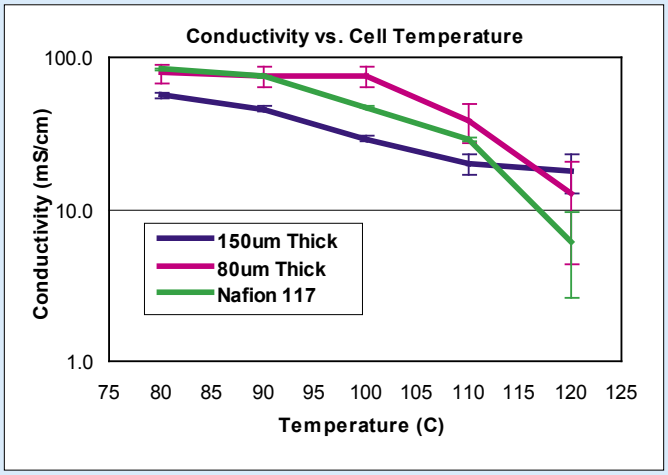

Figure 2. Conductivity verses operating temperature results for Russian analog membranes at varying thicknesses. All measurements were taken at a humidification temperature of 80°C, hydrogen flow rate of 1.0 slpm, and a hydrogen backpressure of 30 psig. Note that units of conductivity are in milli-Siemens/cm.

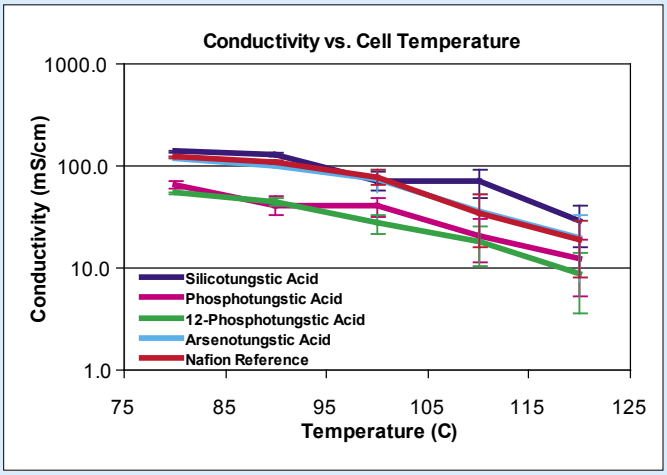

Figure 3. Conductivity verses operating temperature results for heteropoly acid doped Nafion membranes. All measurements were taken at a humidification temperature of 80°C, hydrogen flow rate of 1.0slpm, and a hydrogen backpressure of 30psig. Note that units of conductivity are in milli-Siemens/cm.

DISCUSSION AND CONCLUSIONS

Conductivity results of the organic/inorganic hybrid membranes showed that SFA/BSPPO has a much higher protonic conductivity than W-12 STA/BSPPO at all temperatures measured. As discussed in the literature, the decreased performance of W-12 STA as a dopant for organic/inorganic hybrid membranes is likely due to the fabrication process of the membrane [20]. Further research on membrane fabrication has been undertaken. SFA/BSPPO was not as conductive as Nafion at 80°C; however, there are multiple reasons for considering it a viable replacement option. First, at 80°C, the normal operating temperature of Nafion, SFA/BSPPO showed conductivity near 50 mS/cm, two-third the values of Nafion. This conductivity gap became smaller as temperature was increased. Secondly, SFA/BSPPO showed increased thermo-mechanical and conductive stability at elevated temperatures when compared to Nafion. These are promising results when compared to current literature on organic/inorganic hybrid composite membranes [15, 16]. It is suspected that by continuing research on the effect of dopant concentration and by optimizing the fabrication method, that overall performance of organic/inorganic hybrid composite membranes can be increased to a point that may make them a viable replacement material in the future.

Conductivity results for the Nafion analog appeared to show that as membrane thickness increased, the conductivity of the material decreased. Most likely, the higher performance was caused by superior water retention in the thicker analog membrane. Evidence of this increased performance can be seen in Figure 2. At +100°C operation the 150 μm thick membrane had a slower drop in conductivity than the 80 μm sample, most likely corresponding to better water retention. However, it is believed that the superior performance is to be the due to the transient nature of water retention at short operating times. Long term operation would need to be performed to confirm this theory. Regardless, both samples showed similar to slightly better conductive properties compared to reference Nafion samples. Both the 150 μm and 80 μm membranes had superior high-temperature conduction values than Nafion, as can again be seen from Figure 2. Additionally, the thermo-mechanical properties of the analog membranes were superior to Nafion in the sense that the material did not disintegrate at 120°C, as was the case with the Nafion studied. Increased conductivity performance and improved thermo-mechanical properties make this material another possible option for replacement of Nafion in high-temperature applications.

Heteropoly acid doped Nafion 112 membranes showed promising results when compared to pure Nafion 112 at elevated temperatures. Specifically, the membrane doped with heteropoly silicotungstic acid (HSiW). At 120°C, the HSiW doped Nafion had a recorded conductivity of 12.6 mS/cm, a 17% improvement over Nafion 112. In addition to the membrane doped with heteropoly silicotungstic acid, the membrane doped with heteropoly arsenotungstic acid (HAs_2W) also showed slightly better conductivity at 120°C, when compared to Nafion 112. From theses results, heteropoly acid doped Nafion membranes certainly seem to be a viable possibility for use as high-temperature proton exchange fuel cell membranes.

Analysis of the high-temperature conductivity for the various membranes shows that, at temperatures at or near 120°C, many are still relatively conductive. Stable performance at or near 120°C is promising given that system integration problems between the fuel cell and automotive system would be alleviated at this temperature. While the performance of most of the membranes in this temperature range were quasi-stable, it can be seen from error bars in Figures 1, 2, and 3 that reproducibility of results does become increasingly difficult at +100°C operation. It has been theorized in literature [9], that the irreproducibility of conductivity could be caused from the effect of hydration on activation energy for heteropoly acids. The theory points out that activation energy of heteropoly acids change in the presence of even small amounts of water. Building on this theory, instability in conductivity at elevated temperatures could be caused by uneven dopant distribution throughout the membrane. Because the dopants are more capable of retaining water, the variation in concentration would lead to heterogeneous hydration across the membrane and varied conduction pathways. Heterogeneous conduction pathways would lead to irreproducible conductivity values. The theory seems reasonable when considering that the varying dopant concentration would have less effect on the overall conduction when in the presence of highly conductive water, i.e. below 100°C operation, as can be seen in Figure 1, 2, and 3 from the decreased magnitude of the error bars below 100°C.

In conclusion, the organic/inorganic membrane, SFA/BSPPO, while still inferior to Nafion, appears to show promise as a possible replacement for Nafion and other low-temperature per-fluorinated membranes. In general, for organic/inorganic hybrid composite membranes, the issue of dopant heterogeneity needs to be addressed in order to improve the material. Russian analog membrane samples showed superior conduction compared to Nafion at high-temperature operation. Most promising of the materials types studied were the heteropoly acid doped Nafion membranes. Among them, heteropoly silicotungstic acid and heteropoly arsenotungstic acid showed the most promising results; exceeded the conductivity of the control Nafion 112. Overall, in order to advance the technology of high-temperature membranes, further research is recommended on the effect of dopant levels to conductivity, in order to obtain the optimal balance of mechanical strength and membrane conductivity. Conductivity measurements under long-term operation (above 100 hours) are also recommended to test the durability and consistency of the material properties at high-temperatures. These tests could further validate the possibility of the membranes studied as replacement materials in high-temperature fuel cell applications.

ACKNOWLEDGEMENTS

I would like to thank the U.S. Department of Energy, Office of Science for giving me the opportunity to participate in the SULI program. Special thanks go to my mentor, Dr. John Turner, for all of his patience and advice. Additionally, I would like to thank Dr. John Pern for supplying the organic/inorganic membrane samples for testing and Dr. Andrew Herring of the Colorado School of Mines for providing the heteropoly acid doped Nafion 112 membranes for this study.

REFERENCES

[1] T. Oi, K. Wada, "Feasibility study on hydrogen refueling infrastructure for fuel cell vehicles using the off-peak power in Japan," International Journal of Hydrogen Energy, vol. 29, 2004, pp. 347-354.

[2] D. Hissel, M.C. Péra, J.M. Kauffmann, "Diagnosis of automotive fuel cell power generators," Journal of Power Sources, vol. 128, 2004, pp. 239-246.

[3] K. Agbossou, M. Lal Kolhe, J. Hamelin, É. Bernier, T. Bose, "Electrolytic hydrogen based renewable energy system with oxygen recovery and re-utilization," Renewable Energy, vol. 29, 2004, pp. 1305-1318.

[4] A. Mills, S. Al-Hallaj, "Simulation of hydrogen-based hybrid systems using Hybrid2," International Journal of Hydrogen Energy, vol. 29, 2004, pp. 991-999.

[5] "DaimlerChrysler begins deliveries in Japan, US," Fuel Cells Bulletin, vol. 2003 (12), Dec. 2003, pp. 9.

[6] "Honda FCX demonstrates cold-start performance," Fuel Cells Bulletin, vol. 2004 (4), April 2004, pp. 5.

[7] "Ebara Ballard 1 kWe generator for field trials, unveils kerosene system," Fuel Cells Bulletin, vol. 2004 (6), June 2004, pp. 3-4.

[8] "Have Power to install ReliOn fuel cells in Ohio," Fuel Cells Bulletin, vol. 2004 (6), June 2004, pp. 8.

[9] E.L. Hahn, "Spin Echoes," Phys. Rev. vol. 80, 1950, pp.580-594.

[10] M.A. Sweikart, "Heteropoly Acids for Use as Proton Conductors in High Temperatures Proton Conducting Membrane Fuel Cells," M.S. Thesis. Golden, CO: Colorado School of Mines, 2004.

[11] I. Honma, H. Nakajima, S. Nomura, "High temperature proton conducting hybrid polymer electrolyte membranes," Solid State Ionics, vol. 154-155, 2004, pp. 707-712.

[12] J.J. Fontanella, M.C. Wintersgill, R.S. Chen, Y. Wu, S.G. Greenbaum, "Charge Transport and water molecular motion in variable molecular weight Nafion membranes: high pressure electrical conductivity and NMR," Electrochimic Acta, vol. 40, no. 13-14, 1995, pp. 2321-2326.

[13] V. Ramani, H.R. Kunz, J.M. Fenton, "Investigation of Nafion®/HPA composite membranes for high temperature/low relative humidity PEMFC operation," Journal of Membrane Science, vol. 232, 2004, pp. 31-44.

[14] O. Savadogo, "Emerging membranes for electrochemical systems Part II. High temperature composite membranes for polymer electrolyte fuel cell (PEFC) applications," Journal of Power Sources, vol. 127, 2004, pp.135-161.

[15] Mary Ann Sweikart, Andrew M. Herring, John A. Turner, D. L. Williamson, Bryan D. McCloskey, Sukritthra R. Boonrueng, and Maria Sanchez,"12-Tungstophosphoric Acid Composites with Sulfonated or Unsulfonated Epoxies for High-Temperature PEMFCs", Journal of The Electrochemical Society, vol. 152, 2005, A98-A103.

[16] D. Vernon, F. Meng, D.L. Williamson, J.A. Turner, A.M. Herring, "Synthesis, Characterization, and Conductivity Measurements of Hybrid Membranes Containing a Lacunary Heteropolyacid for PEM Fuel Cell Applications," Journal of the Electrochemical Society, in Press.

[17] I. Honma, S. Hirakawa, K. Yamada, J.M. Bae, "Synthesis of organic/inorganic nanocomposites protonic conduction membrane through sol-gel processes," Solid State Ionics, vol. 118, 1999, pp.29-36.

[18] I. Honma, Y. Takeda, J.M. Bae, "Protonic conducting properties of sol-gel derived organic/inorganic nanocomposite membranes doped with acidic functional molecules," Solid State Ionics, vol. 120, 1999, pp. 255-264.

[19] I. Honma, S. Nomura, H. Nakajima, "Protonic conducting organic/inorganic nanocomposites for polymer electrolyte membrane," Journal of Membrane Science, vol. 185, 2001, pp. 83-94.

[20] H. Nakajima, I. Honma, "Proton-conducting hybrid solid electrolytes for intermediate temperature fuel cells," Solid State Ionics, vol. 148, 2002, pp. 607-610.

[21] I. Honma, H. Nakajima, O. Nishikawa, T. Sugimoto, S. Nomura, "Organic/inorganic nano-composites for high temperature proton conducting polymer electrolytes," Solid State Ionics, vol. 162-163, 2003, pp. 237-245.

[22] F.J. Pern, J.A. Turner, A.M. Herring, "Hybrid Proton-Carrier Polymer Composites for High-Temperature FCPEM Application," Proceeding of Symposium S: Nanostructured Materials in Alternative Energy Devices, 2004, in Press.

[23] V. Ramani, H.R. Kunz, J.M. Fenton, "Electrochemical Characterization of Stabilized Heteropolyacid/Ionomer Composite Membranes for High Temperature PEMFCs," Abs. 983, 2004 Meeting, © 2003 The Electrochemical Society, Inc.

[24] S. Hocevar, P. L. A., V. Antonucci, N. Giordano Fuel Cell Seminar: San Diego, CA, 1994, p 329.

Joseph Piacentine was senior at California State University, Chico, majoring in Physics, when attending a summer internship at the Stanford Linear Accelerator Center, where he worked on the detection of galaxy clusters with the use of X-ray telescopes. This work was presented at the AAAS National Conference in 2005. He has since graduated and moved to Pasadena, where he hopes to pursue a Master's Degree in Astronautical Engineering.

Phil Marshall is a postdoctoral research fellow at the Kavli Institute for Particle Astrophysics and Cosmology, Stanford University. Primarily based at SLAC, he works on data analysis techniques in optical, radio and X-ray astronomy, focusing on clusters of galaxies and gravitational lenses and insisting on probabilistic methodology throughout. Phil obtained a Masters degree in Physics at the University of Cambridge, and then remained at the Cavendish Laboratory for his PhD in astrophysics (entitled "Bayesian Analysis of Clusters of Galaxies"). Since October 2003 he has continued this work, and branched out into both investigating the available strong lensing information in large-scale optical surveys such as SNAP and LSST, and the analysis of X-ray spectro-imaging data.

A NEW METHOD FOR THE DETECTION OF GALAXY CLUSTERS IN X-RAY SURVEYS

J.M. Piacentine, P.J. Marshall, J.R. Peterson, and K.E. Andersson

ABSTRACT

For many years the power of counting clusters of galaxies as a function of their mass has been recognized as a powerful cosmological probe; however, we are only now beginning to acquire data from dedicated surveys with sufcient sky coverage and sensitivity to measure the cluster population out to distances where the dark energy came to dominate the Universe's evolution. One such survey uses the XMM X-ray telescope to scan a large area of sky, detecting the X-ray photons from the hot plasma that lies in the deep potential wells of massive clusters of galaxies. These clusters appear as extended (not point-like) objects, each providing just a few hundred photons in a typical observation. The detection of extended sources in such a low signal-to-noise situation is an important problem in astrophysics: we attempt to solve it by using as much prior information as possible, translating our experience with wellmeasured clusters to define a "template" cluster that can be varied and matched to the features seen in the XMM images. In this work we adapt an existing Monte Carlo analysis code for this problem. Two detection templates were dened and their suitability explored using simulated data; the method was then applied to a publically avalable XMM observation of a "blank" field. Presented are the encouraging results of this series of experiments, suggesting that this approach continue to be developed for future cluster-identication endeavours.

INTRODUCTION

Galaxy clusters are of interest because they are the largest gravitationally bound structures in the Universe; their composition is believed to be dominated by dark matter. The number density of clusters as a function of mass and redshift is a sensitive probe of cosmology: the detection of clusters is important to the study of the evolution of large scale structure.

To date, X-ray observations have provided the highest precision measurements of galaxy clusters. The heated gas trapped within the gravitational potential well of the dark matter emits strongly in the X-ray band: much has been learned about the physics of galaxy clusters through pointed X-ray observations. However, to discover new clusters via their X-ray emission a "blank sky" survey is needed. For surveys where the detection of X-ray photons occurs less than 1 per second, it would be useful to be able to construct an approach to distinguish galaxy clusters from other astronomical objects using as much information as possible. The angular position on the sky and the energy spectrum of the X-ray emission are observable quantities: we will use both.

Objects may be identified based on their angular size; it is important to understand the parameters that may affect this observed spatial extent. The smearing of a point source to appear wider is due to the telescope's point spread function (PSF): a point source is understood to have the spatial extent of the PSF. Any source observed to be larger is by definition extended (Figure 1). The physical sizes of the two most abundant X-ray sources, active galactic nuclei (AGN) and galaxy clusters, are such that, when placed at cosmological distances (100's of Mpc) the former appear point-like, and the latter extended. Typical cluster sizes are ~100 Kpc at the cluster, and appear with arcminute angular diameters. However, some clusters are smaller than this and the X-ray emission is more concentrated than the physical extent of the cluster gas so that there is some possibility of confusion, especially if the PSF is large.

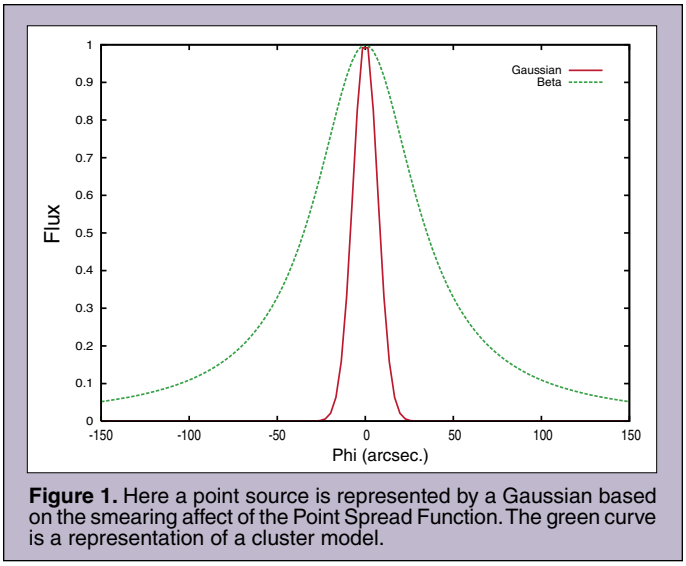

Figure 1. Here a point source is represented by a Gaussian based on the smearing affect of the Point Spread Function. The green curve is a representation of a cluster model.

The AGN emission comes from a comparatively very small region around the black hole at the center of the galaxy and always appear point-like. It is important to keep in mind that it is possible for two AGN to be aligned and may appear as a single extended source.

The classification of an object can also be determined by spectral analysis. AGN are known to have power law spectra, whereas cluster spectra go as $\propto \exp(-h\nu/kT)$ [1], with distinct line features produced by ions in the intracluster gas. To some extent it is possible to mimic a cluster spectrum with a AGN spectrum, and vice versa: one of the aims of this work is to investigate this degeneracy.

We use data from the XMM Newton observatory; this telescope currently provides the largest collection area and field of view, making it the present instrument of choice for blank sky surveys. Specifically we focus on spectroimages taken with XMM-Newton's European Photon Imaging Camera (EPIC). EPIC has three cameras, two Metal Oxide Semiconductor (MOS) charge-coupled devices (CCDs) and one PN CCD. As photons strike the CCDs, the location of the event and the photon energy is recorded. The analyzed observation data is simply a list of photon CCD coordinates and energies.

We are interested in detecting and classifying objects in previously unobserved areas of sky: the XMM-Newton Large Scale Structure survey is a large program designed with this end in mind [2]. The observations cover an 8x8 deg^2 section of sky centered at 2h 18m 00s, -7° 00' 00" , and are comprised of 24 x 24 obervations each with a field of view of some 30 arcminutes in diameter.

The PSF of all X-ray telescopes is energy dependent: the chromatic aberrations in the optics are significant. To properly correct for this the data must be simulated using Monte Carlo methods; the analysis code for doing this is called X-ray Monte Carlo (XMC) [3]. While used extensively in the analysis of single cluster observations, here we apply this "forward folding" approach to the analysis of survey data containing both AGN and clusters, and use both the spectral and spatial information to distinguish the objects. We do this by defining a flexible template for each object (or part-object), and then fitting the parameters of these templates to the data.

In the first section we discuss the experiments performed on simulated data to test our ability to locate and identify objects based on their spatial and spectral properties; in the second section we present results from an analysis of an XMM blank field. We discuss our findings and draw brief conclusions in the final section.

METHODS

In this section we give a brief description of the analysis code used, and then outline a number of experiments designed to explore the suitability of the template-fitting approach.

A. Overview of XMC

Given noise-free data, the inferences drawn using XMC would extend to all parameters of all the astronomical objects in the eld. How well this task can be accomplished depends on the quality of the dataset; X-ray data are typically quite noisy, with very few photons per bin in energy and detector position.

It is first necessary to provide XMC with input, either a previously created simulation or data from an observation. A model is then created to test against the data. The model's parameters will be set with initial trial values and a range that the parameters are allowed to explore. XMC generates a set of simulated data, which are compared with the real data using a two-sample multinomial likelihood function, adjusts the simulated data and repeats. For each iteration it returns a set of all parameters being explored and the mist statistic(χ^2). The lower the value of this mist, the closer the mock data is to that of the real data. The parameter space is explored using the Markov Chain Monte Carlo technique [4], the end result of which is an ensemble of parameter sets that define models which all fit the real data acceptably well. For each model a mock sky can be plotted; by averaging these maps, deconvolved images can be reconstructed. This can be done separately for the AGN and cluster parts of the model: combining these images in different color channels (for instance, plotting AGN photons in green and cluster photons in red) allows the user, at a glance, to get an idea of the nature of objects analyzed.

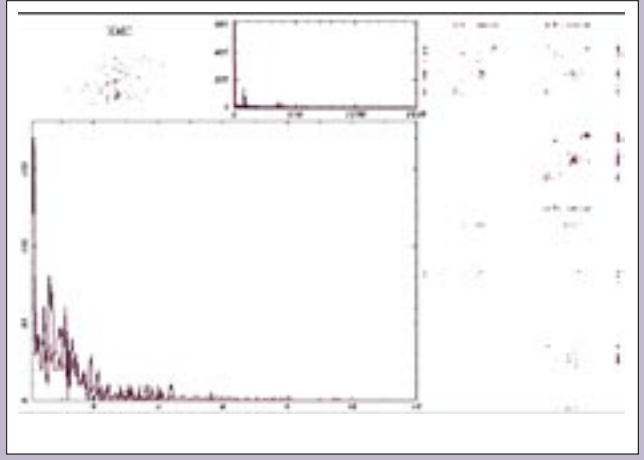

Figure 2. The main window of the XMC windows shows the spectra (real and fitted). The upper right shows the locations of the input data and the bottom right XMC's inferred location.

Figure 2 shows the real time progress window displayed by XMC, allowing a user to monitor the evolution of the spatial and spectral analysis. This display shows the user the location of the input data as well as the location of the tted objects. The main windows displays the spectral analysis.

B. Experiment 1

First a simulation was dened using a pointlike AGNspectrum object centered in the field of view. This simulated data was then analysed assuming the same model. All parameters of the model were xed at the true values save one, so that the object and the model were identical except for the object location. This one coordinate was then allowed to vary, to see if XMC could locate an object in a single spatial direction.

The simulation object's location parameter, Phi, was set at a value of -60. The variation in mist as the model Phi value was changed is shown in Figure 3. As shown in the plot the lowest misfitt value corresponds with the correct parameter value.When applying this same technique to the Psi coordinate, an error was discovered and corrected in the XMC code when the program failed to locate the object. It is interesting to note the slope of the curve in this plot. As XMC's estimation of the parameter value approaches that of the simulation, the slope sharpens drastically, while the slope levels out the further away one gets from the true value. From this we can better understand the burn in time required for XMC. For the first few hundred iterations the program simply "guesses" parameter values in the specied allowed range and records a misfit value until it has enough data points to recognize sloping curves, making it possible to hone in on the parameter value. However, to some extent XMC is always guessing; the χ^2 simply helps XMC judge when and how much to adjust a parameter.

C. Experiment 2

The purpose of this second experiment is to determine whether or not XMC can recover the nature of a simulated object at fixed position. The spectral signatures of AGN and clusters are fairly well-defined; we use the community standard analysis code XSPEC to calculate predicted spectra given model parameters. We also need to define a spatial model for the emission from each object, and here we investigate two approaches. Both entail the superposition of two spatial models, one for each spectral type. The centroids of the two components are tied together, and the fraction of flux associated with each is allowed to vary: this parameter encodes the "clusterness" of the object. We refer to these two-component models as "blobs".

In the first approach we envisage fitting one two-component model to each object in the field: in this case it makes sense to make the spatial emission distribution as close to what is already known about clusters and AGN as seen in X-ray observations. Hence, we assign the AGN flux component a delta-function spatial distribution (making it a true point source). For the cluster we use the surface brightness given by Sarazin [1],

$$I(r) \propto \frac{1}{\left[1+\left(\frac{r}{r_c}\right)^2\right]^{3\beta-\frac{1}{2}}} \qquad (1)$$

where r is the radius of the cluster and r_c is the core radius and is the parameter allowed to vary within XMC. The parameter β has been calculated for many pointed observations and for the simplicity of the simulation was set to 0.66 in accordance to these findings.

In the second approach we admit the possibility of more complex objects, and attempt to build these from superpositions of many models, each of some general spatial model. We choose a Gaussian distribution,

$$I(r) \propto \exp\left(\frac{-r^2}{2\sigma^2}\right) \qquad (2)$$

where σ is the parameter allowed to vary within XMC. For a truly point-like source the delta function model is at first sight the better option, but allowing in the spatial Gaussian model to become arbitrarily small achieves the same aim. When combining many blobs to represent an object, do the Gaussians do a better job of dealing with the smearing effect of the PSF on a point source?

Experiment 2 consisted of two tests. In the first, a point-like AGN object was simulated, centered on the exposure map. This simulated data was then fitted using XMC with a blob of the first kind (beta model plus delta function). The core radius of the beta model component and the spectral parameters of both were allowed to vary. In the second test, the simulation was identical, but the blob used in the analysis was of the second kind (two Gaussian spatial models, with equal extent, one with AGN spectrum and and one with cluster spectrum). In both tests, XMC was used to explore the spatial and spectral parameters of the model and return the fraction of photons that were "AGN-like" and "cluster-like".

As can be seen in Figure 4, XMC has correctly inferred that the simulation object was an AGN. The spatial extent corresponds

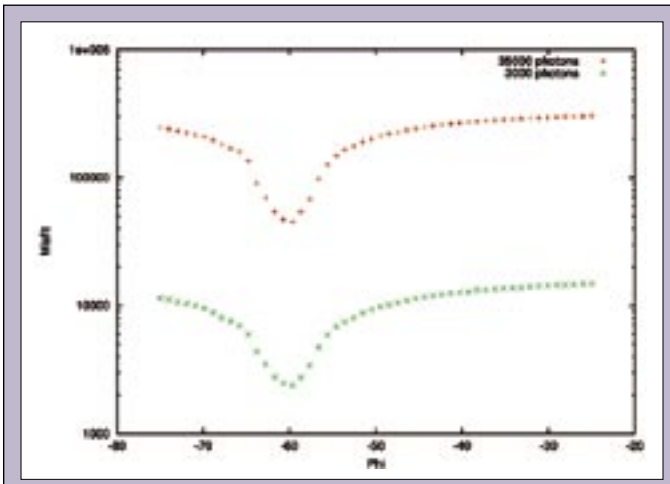

Figure 3. Plot of misfit χ^2 vs. Phi. XMC located the AGN simulation with 3000 photons and again with 35000 photons.

closely to the XMM PSF, with a diameter of about 6 arcseconds. The blobs of this run consisted of a point source model and Beta model. The number of photons XMC determined to be of AGN origin is approximately 1000 times greater than cluster photons. This information can be used to give a rough estimate on the probability of being an AGN. The results of the blobs with two spatial Gaussians tied together were similar. However, the ratio of AGN to cluster flux was not as extreme. This can be understood in terms of the different spatial models used: if the data are well represented by a beta model plus delta function, then we would expect this model to perform better in the classification of the object from noisy simulated data. We shall see in section III that real astronomical objects are less clear-cut cases.

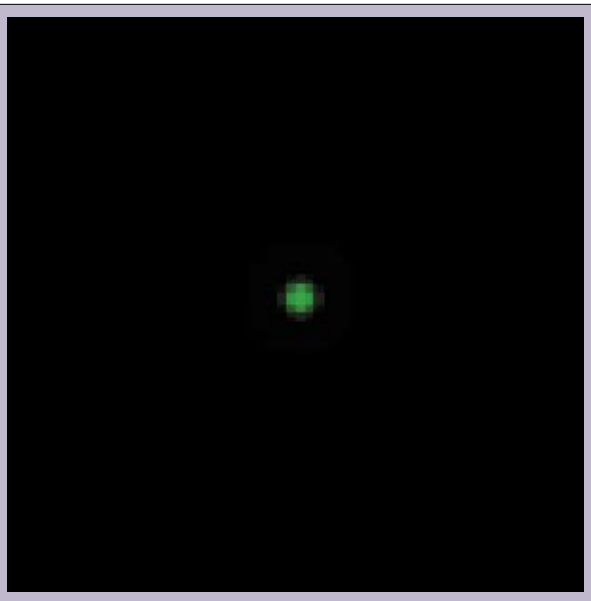

Figure 4. The simulation was set as an AGN located at the center of the field. The model was allowed to vary between AGN and cluster parameters. XMC determined that the simulation photons consisted that of only AGN to one part in 1000.

D. Experiment 3

A final simulation was created using a mixture of AGN and cluster objects (three of each) placed in various locations on the sky. Again two tests were run. The analysis blobs were the same as the ones used in experiment 2. Six blobs were used to match the six simulation objects. The objective of this experiment was to ascertain the ability of XMC to track the location, spatial and spectral parameters of each object simultaneously. Knowing that XMC can locate and distinguish simulation objects, it is necessary to evaluate how well XMC can distinguish objects in close proximity of one another. In the upper right corner of this simulation two AGN were placed near one another, and both were located within the radius of a cluster object, so that XMC must distinguish between three tightly packed objects. In the center of the field was placed a cluster. A cluster was placed in the bottom left and an AGN in the top left.

The results (Figure 5) show our ability to identify the two AGN and cluster in the upper right corner. However, there seems to be

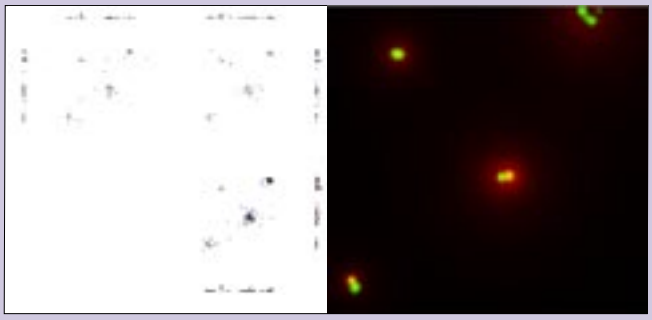

Figure 5. The left picture shows the locations and sizes of the objects before analysis. The more spread out objects are the clusters. In the right picture the 3 cluster & 3 AGN objects can be seen. The central and bottom left corner objects are clusters, in the top right two AGN and top left another AGN. XMC located every object but the two clusters still have significant AGN flux.

some ambiguity with XMC's classification of the other objects. The two remaining cluster objects appear to have just as much AGN flux as cluster flux.

The upper right conglomeration of three objects has some cluster (red) but is dominated by AGN (green). This indicates that XMC can distinguish objects near or overlapping one another. However, the purely cluster object has a significant amount of AGN flux to it. This effect is analyzed in the final section.

XMM DATA

We now go on to apply the methodology introduced and demonstrated in the previous section to real XMM data. A dataset from the Large Scale Structure survey was retrieved from the on-line archive, and reduced to a list of photon locations and energies readable by XMC. It is interesting to note some features of the EPIC cameras. We can see (Figure 6) the PSF affects the objects in the exposure map. The central objects all have a width of about 6 arcseconds and up to 20 arcseconds at the edges of the field of view. In the upper left corner there is an object which is much larger than any other object. This could be the PSF greatly smearing the object near the edge of the camera or this could be an extended source. The gaps between the CCDs is also noticeable in the exposure map (only the data from the PN CCDs were used).

For simulations, the number of objects is known and creating the number of model objects to be the same is simple enough. However when analyzing real data, the number of objects will not be known, so it is necessary to take a somewhat different approach. Experience with pointed observations suggests that a combination of Gaussian components (typically ~100) is a good way of characterising a complex image. For this analysis we used blobs of the second kind; to recap, these are two concentric Gaussians of equal size, that differ in their spectral properties. The fraction of the flux assigned to each spectral component is an indication of the "clusterness" of that blob. Bright objects in the data can then be built up from collections of blobs, whose clusterness fraction should change during the XMC analysis to reflect the spectral type of the object.

When dealing with real data, the background emission has to be taken into account. This was modelled as a spatially uniform distribution, composed of a variable fraction of high energy particles

and the remainder detector noise. The flux from this background can be predicted and fitted to the data at the same time as the blobs. Note that the astronomical X-ray background was not included in this way: the X-ray background is made up of clusters and AGN and is in fact what we are trying to detect.

It can be seen that in areas between the CCDs, XMC assumes there is flux, although no data is actually recorded by the telescope in these regions. When the data from the MOS detector along with the PN is used the gaps between the CCDs will be resolved.

Comparing the raw photon counts map (Figure 6) with the output from XMC, we see that the majority of features in the former are detected in the latter. In a survey such as this, it was expected that 70% of the objects would be AGN. As is shown in Figure 7, all the objects have some AGN component associated with them. However, a significant number of objects seem to have a considerable amount of cluster flux as well.

Focusing on the object in the top left hand corner of the field, which seems to be smeared, we see both AGN and cluster flux. Also, the elongation of the reconstructed object is much greater than that of the object in the data. This could possibly be the greater PSF of the telescope at the edges, smearing the object. However, one would expect the reconstructed image to be similar to that of the exposure map. Considering that this object is the brightest in the field of view, it is possible that XMC positioned a majority of the 100 blobs on this one object; with the averaging process comes some variance, which is seen as a smearing in the recontructed image. Further work should include study of this dilution effect, especially in regard to the classification of objects.

DISCUSSION AND CONCLUSIONS

The test runs provided some level of confidence in our ability to locate and distinguish astronomical objects using template-fitting with XMC. The accuracy achieved for simple simulation was encouraging. When complicating a test run by introducing a larger number of blobs, the program became slower, because of the greater number of parameters to be varied.

In experiment 2, there seemed to be some ambiguity of the nature of the object when using the spatial Gaussian blobs. However, some ambiguity is to be expected when allowing the spatial parameters of the Gaussians to vary. By tying the parameter of each Gaussian, the model with AGN spectrum would be allowed to grow to the size of a cluster, whereas the model with cluster spectrum would also be allowed to shrink to the size of the telescope's PSF. The extra degree of freedom allowed provides us with useful information on the ability of the program to determine astronomical objects.

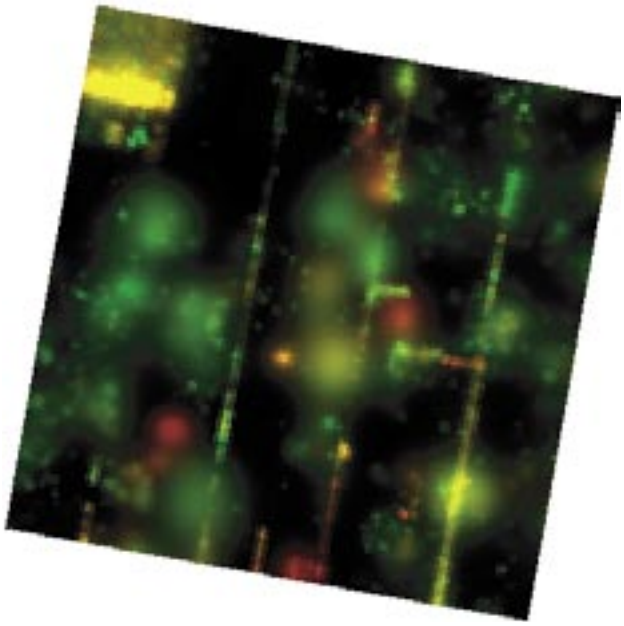

Figure 7. The results of the LSS-20 analysis with green representing AGN flux and red representing that from clusters.

The six blobs in experiment 3 successfully matched the location of the simulated objects. However, the nature of the objects was not determined accurately. Whilst this may be due to the relatively low number of iterations XMC was allowed to make, there is also some considerable degeneracy between the different spectral and spatial signatures of the two classes of objects considered. The spectra of the mock data are suffieciently similar to allow for the fitting of cluster spectra to a power-law within the uncertanties of the data, so that a power-law spectrum seems to be an acceptable fit to a cluster image, leading to the question of spatial extent. Given the wide range in the variable assigned to the size of a cluster, may indicate that extended source distributions fit poorly to AGN images, leaving the purely green AGN spots in Figure 5. However when analyzing a cluster image, the PSF of a point source may be large enough to fit both photon ditributions to the image.

This was also seen in the analysis of the XMM data: Figure 7 shows many objects with ambiguous classifications for reasons seen in experiment 3. However, this image clearly contains an incredible amount of information. A large number of objects are detected, and the range of colors is impressive: the objects are not all yellow!

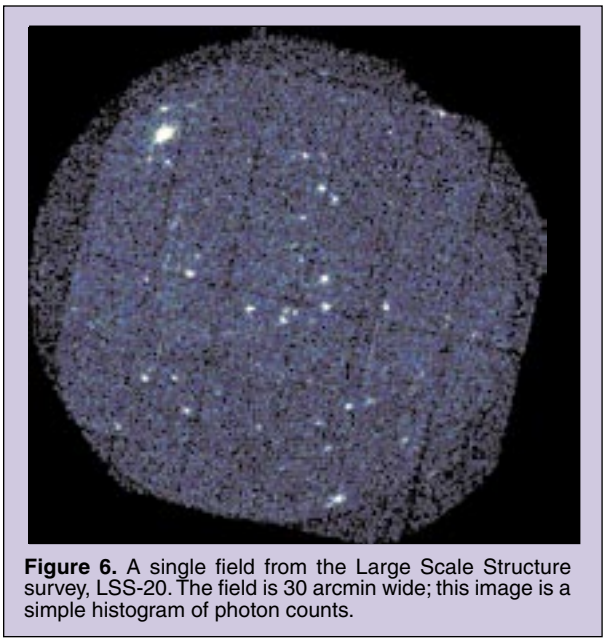

Figure 6. A single field from the Large Scale Structure survey, LSS-20. The field is 30 arcmin wide; this image is a simple histogram of photon counts.

The results of the LSS data suggest that using multiple blobs to reconstruct a single object is a viable procedure for distinguishing objects. Averaging the ensemble of models generated by XMC to make a deconvolved map demonstrates the effectiveness of the program's ability to locate objects. The color representation of AGN and cluster flux has allowed rough estimates of the object classification probability to be made.

The methodology demonstrated in this work, whilst not without teething problems, seems to us to deserve further effort in its development. The major benefits it brings include full propagation of errors from noisy data to reconstructed image, correct treatment of a PSF that varies both spectrally and across the image, the input of sensible prior knowledge (via the choice of blob surface brightness distributions and spectra), and the separation and visualisation of the two putative image components without the need for isolation of individual objects (which often lie in close proximity to each other).

ACKNOWLEDGMENTS

We thank Alex Refregier for bringing our attention to the problem of LSS analysis. J. Piacentine was supported by funding from the Department of Energy, Office of Science during a summer internship at Stanford Linear Accelerator Center. This work was supported in part by the U.S. Department of Energy under contract number DE-AC02-76SF00515.

REFERENCES

[1] C. L. Sarazin, X-ray emission from Clusters of Galaxies, Cambridge University Press (2004)

[2] M. Pierre et al, J. Cosmol. Astropart. Phys., 9, 11 (2004)

[3] J.R. Peterson, J.G. Jernigan, and S.M. Kahn, Multivariate Monte Carlo Methods for the Reflection Grating Spectrometers on XMM-Newton, ApJ, 615, 545 (2004)

[4] W.R. Gilks, S. Richardson, and D.J. Spiegelhalter, Markov-Chain Monte-Carlo In Practice, Cambridge: Chapman and Hall (1996)

Melisa Carpio is currently a graduating senior at the University of California, Berkeley majoring in Chemical Engineering with an emphasis in Biotechnology. Prior to her appointment in SULI, Melisa held research positions at UCSF's Department of Pathology studying the parasite Trichomonas vaginalis and at LBNL's Physics Department modeling solar funnels. Through SULI, Melisa began working in LBNL's Environmental Energy Technology Division under the guidance of Dr. John Kerr. She still works for the Kerr group researching rhodium catalyst complexes and their application to sensing devices. This research received first place at the 2005 AiChE Western Regional Conference and honorable mention at the 2005 AAAS National Conference. In the future, Melisa aspires to attend graduate school and continue researching in the fields of chemical and bioengineering.

John Kerr is Program Manager in the Advanced Energy Technologies Department, Environmental Energy Technologies Division of Lawrence Berkeley National Laboratory where he has been on staff since 1994. He received his Ph.D. in organic chemistry from the University of Edinburgh in 1978 and has held a number of research and management positions in large companies (Union Carbide, PPG Inductries, Inc.) and small start-up stage companies where he worked on organic electrochemistry for synthesis and energy conversion as well as separation technologies, including the Artificial Gill which used artificial blood systems to extract oxygen from the ocean for underwater power. Since coming to LBNL he has worked on development of polymer membrane separators for lithium batteries, fuel cells and polymer LED systems in addition to combining polymer systems with chemical and biochemical catalysts for synthesis, sensing and separation purposes.

EXAMINING RHODIUM CATALYST COMPLEXES FOR USE WITH CONDUCTING POLYMERS DESIGNED FOR FUEL CELLS IN PREPARING BIOSENSORS

Melisa M. Carpio, John B. Kerr

ABSTRACT

Biosensing devices are important because they can detect, record, and transmit information regarding the presence of, or physiological changes in, different chemical or biological materials in the environment. The goal of this research is to prepare a biosensing device that is effective, quick, and low cost. This is done by examining which chemicals will work best when placed in a biosensor. The first study involved experimenting on a rhodium catalyst complexed with ligands such as bipyridine and imidazole. The rhodium catalyst is important because it is reduced from Rh^{III} to Rh^{I}, forms a hydride by reaction with water and releases the hydride to react with nicotinamide adenine dinucleotide (NAD^+) to selectively produce 1,4-NADH, the reduced form of NAD^+. The second study looked at different types of ketones and enzymes for the enzyme-substrate reaction converting a ketone into an alcohol. Preliminary results showed that the rhodium complexed with bipyridine was able to carry out all the reactions, while the rhodium complexed with imidazole was not able to produce and release hydrides. In addition, the most effective ketone to use is benzylacetone with the enzyme alcohol dehydrogenase from baker's yeast. Future work includes experimenting with bis-imidazole, which mimics the structure of bipyridine to see if it has the capability to reduce and if the reduction rate is comparable to the bipyridine complex. Once all testing is completed, the fastest catalysts will be combined with polymer membranes designed for fuel cells to prepare biosensing devices that can be used in a variety of applications including ones in the medical and environmental fields.

INTRODUCTION

Biosensors are commonly used for the food industry, health care, and even by the government for security purposes [1]. Biosensing devices are used because they can detect, record, and transmit information regarding the presence of, or physiological changes in, different chemical or biological materials in the environment. A basic biosensing device is composed of three parts (Figure 1). The first two steps involve a hydride-forming reduction reaction and a cofactor transformation. The final step is an enzymatic reaction to produce the desired products. In this study, the rhodium in the catalyst complex is reduced chemically or electrochemically from Rh^{III} to Rh^{I}, producing hydrides by reaction with water. The hydrides then react with nictotinamide adenine dinucleotide (NAD^+) to selectively

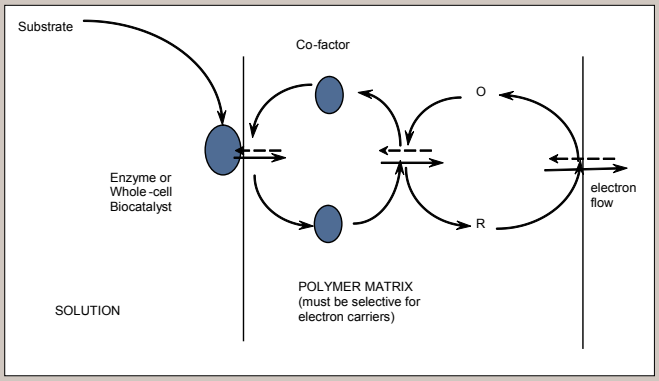

Figure 1. Schematic of a typical biosensor.

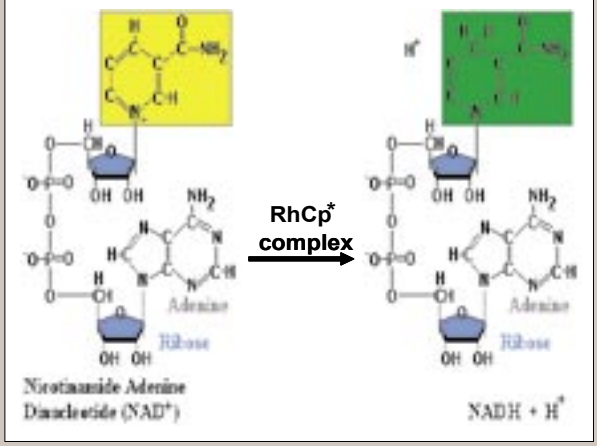

Figure 2. The conversion of nicotinamide adenine dinucleotide (NAD+) to its reduced form, 1,4-NADH using a hydride from the rhodium catalyst complex.

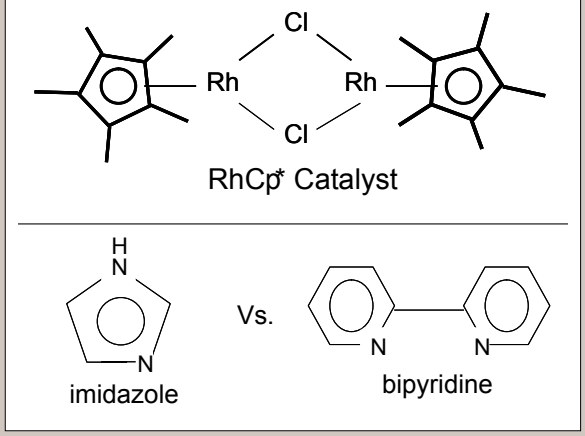

Figure 3. The rhodium catalyst can be complexed with ligands such as imidazole and bipyridine.

produce 1,4-NADH, the reduced form of NAD^+ (Figure 2). Lastly, the 1,4-NADH reacts through an enzyme catalyst with a ketone to make an alcohol and regenerate NAD^+. The goal of this research is to prepare a quick, efficient, and low cost electrochemical biosensor. Such biosensors can be used in environmental applications to detect trace amounts of harmful chemicals in the air or in medical applications to measure amounts of glucose present in a person's bloodstream. This is done by examining different rhodium catalyst complexes as well as different ketones and enzymes to see which one works the best.

Previous experiments have complexed the rhodium (Rh) catalyst with polypyridine or phosphine ligands. Such ligands are necessary for the Rh^{III} complex to get reduced to the Rh^{I} complex which produces a hydride ion by reaction with water [2]. Without the rhodium complex present, NAD^+ would react to form $(NAD)_2$ and NADH isomers that are not active with enzymes. 1,4-NADH is the preferred form because it is a biochemically active compound that is a hydride donor in enzymatic reactions, such as the conversion of a ketone into an alcohol or pyruvate to lactate [3,4].

During the reduction of ketone (substrate) into alcohol (reduced product), the 1,4-NADH cofactor donates a hydride to permit reduction of the substrate into the reduced product [5]. Under the same conditions, different ketones reduce at different rates depending on their structure. The oxygen atom must be at a position where it avoids both steric interaction with its own side chains as well as other molecules. During this process, NADH loses a hydride and at the end of the reaction, NADH is oxidized to form NAD^+. Then, the process must be reversed, and the NADH must be regenerated. NAD^+/1,4-NADH regeneration is a low cost alternative to continually adding NAD^+ or 1,4-NADH until the reaction goes to completion [6].

By adding an enzyme like alcohol dehydrogenase to the system, the catalyzed reaction exhibits chemo-, region-, and stereo-selectivity [7]. The chiral alcohols produced are important in pharmaceuticals and in making specialty chemicals. Such chirality can be detected using gas chromatography (GC) and capillary electrophoresis (CE). Proper separation of the enantiomers of chiral compounds requires that the GC and CE be operated at right temperatures, the correct buffer is used, and the solutions are at the appropriate concentrations [8].

Once the reaction is complete and the product has been formed it must be separated from the other parts of the system, which can be difficult if the reaction is done in solution. One possible way to isolate the product is to immobilize one or more components. This can be done by putting some parts, like the electrode, cofactors, and enzymes in a "membrane reactor," whose walls are permeable only to the substrates and products [9]. It is important for a biosensor that biomolecules are immobilized on conducting surfaces so that their properties remain intact [1]. This is especially important in this study because the conducting surfaces are the core of the reduction reactions. In addition, the three parts of the biosensor depend upon each other, so if one part fails, the whole sensor will not function.

One proposed "membrane reactor" involves using ionically conducting polymers designed for fuel cells. Conducting polymers have a number of properties that allow them to act as effective mobilizers of biomolecules [1]. One such property is that they

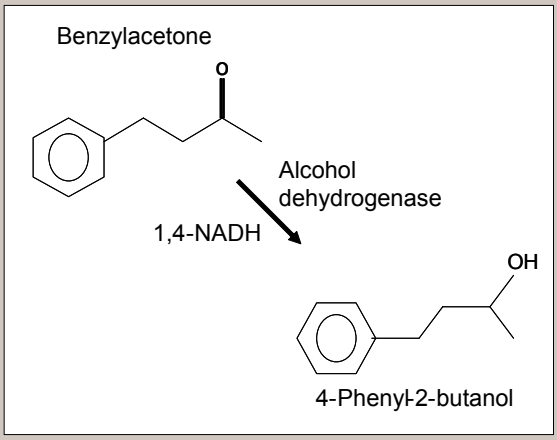

Figure 4. The conversion of a ketone to an alcohol using alcohol dehydrogenase as an enzyme and a hydride from 1,4-NADH.

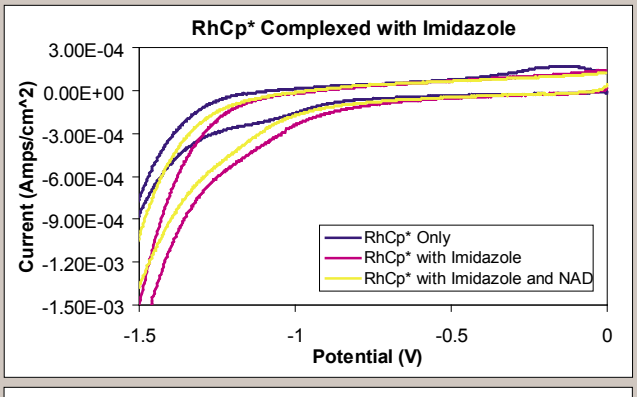

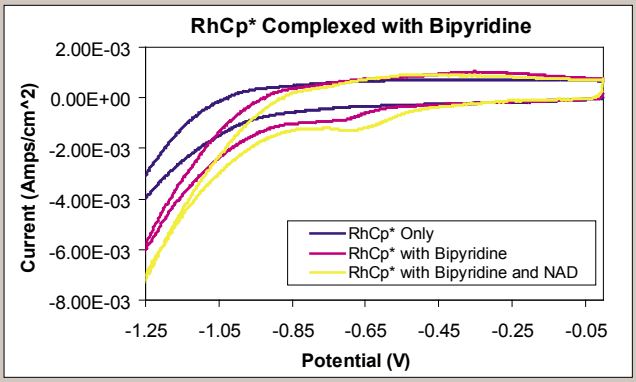

Figure 5. Cyclic voltammograms testing the reduction of the RhCp* catalyst complexed with imidazole versus that with bipyridine. The sweep rate is 50mV/s.

transfer charge rapidly through the polymer membrane. It is ideal to use polymers designed for fuel cells because those are also used with isolation of products [7, 10].

One part of this study will examine rhodium catalysts complexed with bipyridine and imidazole to compare reduction rate (Figure 3). The prediction is that the imidazole complex will work faster because imidazole is often what nature uses when it needs a base. In addition, the imidazole complex has unbound nitrogen atoms that may participate in the reduction reaction through hydrogen bonding to solvent water molecules as well as attract and bind the complex to the conducting polymer. The other part of the study deals with examining four different types of ketones and two different types of enzymes to determine which combination will work the fastest and have the highest conversion (Figure 4).

By preparing biosensing devices using regenerated NAD^+ and NADH in a system incorporating the rhodium complex to catalyze enzymatic reactions, benefits of both electrochemical and enzymatic strategies can be obtained. Such benefits include high selectivity when producing 1,4-NADH, readily controlled redox potential, easy product isolation, and easy monitoring of reaction progress [11]. In addition, by combining the reaction in a conducting polymer membrane, the product is easily separated and used.

MATERIALS AND METHODS

Chemicals

All chemicals were used as received. The chemicals include $[Cp^*RhCl_2]_2$ (Colonial Metals); β-nicotinamide adenine dinucleotide (NAD) and β-nicotinamide adenine dinucleotide, reduced form (1,4-NADH) (Sigma); benzylacetone, 4-phenyl-2-butanol, 2,2'-dipyridyl , alcohol dehydrogenase (both from baker's yeast and equine liver), dichloromethane, HPLC grade water, acetophenone, and 2-pentanone (Aldrich); and sodium phosphate (JT Baker).

Instrumentation

Electrochemical measurements were made by means of cyclic voltammetry using a PAR173 Potentiostat equipped with a Model 276 Computer Interface connected to a standard three electrode cell with a glassy carbon electrode as the cathode, a platinum gauze counter electrode as the anode, and a silver (Ag) reference electrode. Argon gas was bubbled through each sample to deoxygenate the solution before measurements were taken, and a stream of argon was passed over the solution during measurements.

Potentiostatic experiments were done under the same conditions as cyclic voltammetry except a carbon felt electrode replaced the glassy carbon electrode as the cathode. In addition, the argon gas was bubbled throughout the solution for the duration of the experiment. Both the cyclic voltammetry and potentiostatic experiments were controlled by computer software, CorrWare and CorrView (Scribner Associates).

A Hewlett Packard ^{3D}Capillary Electrophoresis (CE) System and an Aglient 6890 Series Gas Chromatography (GC) System coupled with the Aglient 5973*Network* Mass Selective Detector were used for separating and identifying products from solution. The samples for CE were injected straight from the reaction cell. The samples for GC were extracted with dichloromethane before injection.

The pH was monitored using a VWR pHastchek pH meter. Phosphoric acid and sodium hydroxide were used to either lower or raise the pH as necessary.

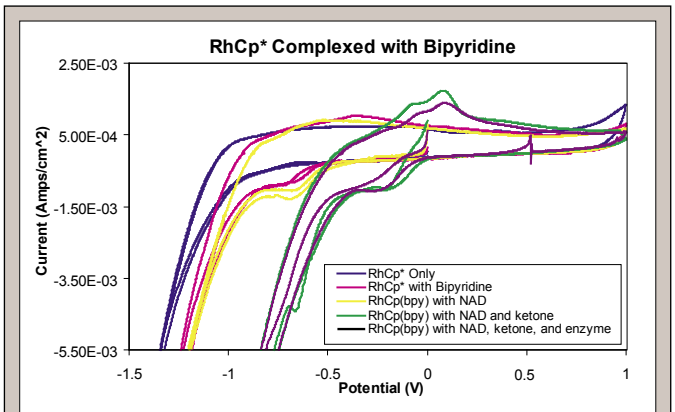

Figure 6. Cyclic voltammogram monitoring the reduction of each step leading up to the enzymatic reaction.

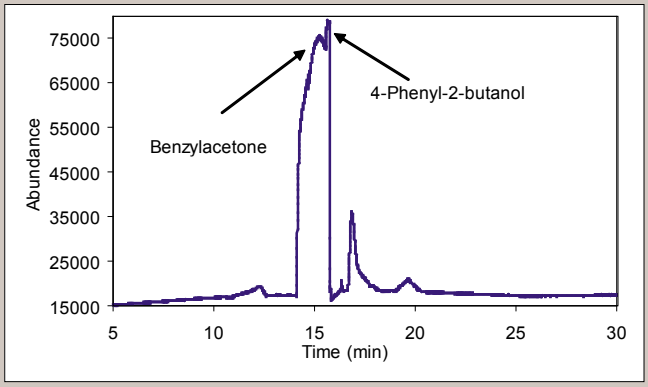

Figure 7. Resulting plot from gas chromatography (GC) analysis of the cyclic voltammetry solution. The identity of the peaks comes from the mass spectrophotometer attached to the GC.

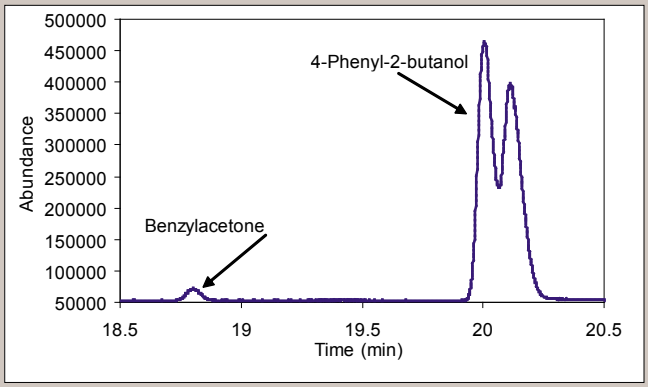

Figure 8. Resulting plot from the GC using a column with cyclodextrin.

UV-Spectra were measured with a Hewlett Packard model 8452A diode-array UV-vis spectrophotometer. Solutions were diluted to 0.25 mM and deoxygenated with argon gas before being placed in the spectrophotometer.

*General procedure for the enzymatic reaction converting ketone to alcohol using NAD+/NADH regeneration and the [Cp*RhCl2]2 catalyst*

An electrochemical cell was set up with 100 mL of 50 mM phosphate buffer. One millimolar $[Cp^*RhCl_2]_2$ catalyst, two equivalents 2,2'-dipyridyl, and one equivalent NAD^+ were added to the solution. Between each addition, a cyclic voltammogram was taken and 1 mL of sample was removed for CE and UV-Vis analysis. A one hour potentiostatic experiment was run at a constant voltage corresponding to the cyclic voltammetry peak to get complete conversion of NAD^+ to 1,4-NADH. Ten equivalents of benzylacetone (ketone) and one equivalent alcohol dehydrogenase (enzyme) were then added. Cyclic voltammetry was performed and 1 mL was removed for analysis between each addition. A three hour potentiostatic experiment was run to completely convert the ketone to alcohol (Figure 4). A final cyclic voltammetry was performed and another sample was taken before the remaining solution was extracted with dichloromethane for GC analysis. This procedure was repeated with imidazole instead of 2,2'-dipyridyl. The entire reaction was done at room temperature and at a pH of seven.

General procedure for measuring reaction kinetics and enzyme activity

In a reaction cuvette, enough 1,4-NADH was added to 5 mL of 50 mM phosphate buffer to make a 0.25 mM solution, and a UV-Vis spectrum was taken. Next, an equivalent of enzyme was added, and another spectrum was taken. After 10 minutes, an equivalent of ketone was mixed into the solution. Oxygen was removed by holding the solution under vacuumfor 5 minutes, then capping the cuvette. A spectrum was then taken every 10 minutes until the 1,4-NADH peak at an absorbance of 340nm disappeared. Tests were done on four different types of ketones, benzylacetone made in lab, benzylacetone purchased commercially, acetophenone, and 2-pentanone, and two different types of enzymes, alcohol dehydrogenase from baker's yeast and alcohol dehydrogenase from equine liver.

RESULTS

Cyclic voltammograms comparing the rhodium complexed with bipyridine versus the rhodium complexed with imidazole is shown in Figure 5. The voltammogram in Figure 6 tracks the complete enzymatic reaction from the addition of the rhodium catalyst to the conversion of the alcohol. Figures 7 and 8 are gas chromatographs of a successful ketone to alcohol conversion. In Figure 7, a regular GC column coupled with a mass spectrophotometer was used, while in Figure 8, a column with cyclodextrin was used to separate the chiral alcohol products.

A typical UV-Vis spectrum is shown in Figure 9, with the 1,4-NADH peak at 340 nm highlighted. Figure 10 is a plot of the natural log of the absorbance at 340 nm as shown by the spectra versus the elapsed reaction time. The slope of the resulting linear regression line is the rate of 1,4-NADH appearance/disappearance, which is directly related to the rate of alcohol product production. Tables 1 and 2 list the rates of ketone and enzyme activity as determined by plotting spectral data from each sample as described in Figure 10.

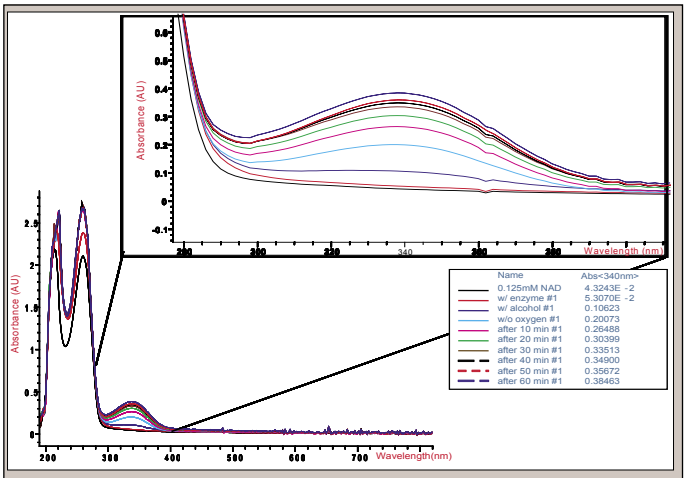

Figure 9. A typical UV-Vis spectrophotometer plot of absorbance versus wavelength. 1,4-NADH peak appearance or disappearance can be monitored as the characteristic peak is at 340 nanometers (nm).

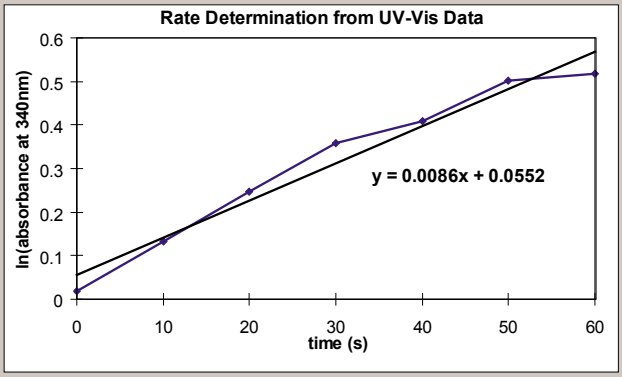

Figure 10. By plotting the natural log of the absorbance at 340nm versus the elapsed reaction time, the slope of the resulting linear regression line is the rate of 1,4-NADH appearance/ disappearance.

DISCUSSION AND CONCLUSIONS

As shown clearly in Figure 5, the catalyst complexed with bipyridine has a clear reduction peak at -0.9V, and the peak grows with the addition of NAD^+. The catalyst complexed with imidazole does not have a reduction peak, and there is also no reduction peak when NAD^+ is added to the solution. One explanation for the imidazole failing to reduce is that it does not have strong enough bonds with the rhodium catalyst, so the amines from the NAD^+ attract the catalyst rather than the amines from the imidazole. Since the bipyridine was successful in reducing, it is possible that a bis-imidazole compound will have stronger binding than NAD^+, therefore having the ability to reduce the rhodium compound. Another solution is to put the imidazole compounds directly onto the conducting polymer as a chelate effect may mimic the bis-imidazole/bipyridine structure.

Based on the data from Tables 1 and 2, the best ketone to use is benzylacetone prepared in lab and the most efficient enzyme is alcohol dehydrogenase from equine liver. The cyclic voltammetry experiments confirmed that benzylacetone is the best ketone to use. It appears to have the right bulk of carbon atoms and a strategically placed oxygen atom adequate for binding in the enzyme reaction center. However, the only enzyme that successfully converted the ketone into alcohol was the alcohol dehydrogenase from baker's yeast, which contradicts the results from the UV-Vis experiments. It could either be that the alcohol dehydrogenase from baker's yeast only works when a current is passed though the sample, while the one from equine liver does not need current. However, the activities of the enzymes are so sensitive to small variations in the conditions that it is hard to make a definite conclusion.

Ketone Name	Structure	Rate (s-1)
Benzylacetone (made in lab)	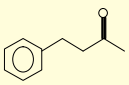	0.044
Benzylacetone (from Aldrich)	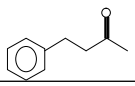	0.009
Acetophenone		0.0027
2-Pentanone		0.0001

Table 1. This table lists four different types of ketones and their rates of 1,4-NADH disappearance. Benzylacetone (made in lab) is the fastest of the four.

Preliminary results show that the rhodium complexed with bipyridine is effective in reducing a ketone to an alcohol using enzymatic catalysis and NAD^+/1,4-NADH regeneration. In addition, the ketone benzylacetone and the enzyme alcohol dehydrogenase from baker's yeast is the only successful substrate-enzyme combination that produced a product.

Future work includes repeating the cyclic voltammetry with bis-imidazole ligands on the RhCp* catalyst complex to determine if has the ability to reduce and release hydrides, or trying to put the imidazole directly onto the conducting polymer to test if the chelate effect works. If reduction does occur, the rate of reduction of the bis-imidazole complex or the imidazole on polymer complex will be compared against the bipyridine complex. Finally, the quickest and most effective of the catalyst complexes will be combined with polymer membranes designed for fuel cells to prepare a biosensor device like the one shown in Figure 1.

Enzyme Name	Rate (s-1)
Alcohol Dehydrogenase (from Baker's Yeast)	0.0024
Alcohol Dehydrogenase (from Equine Liver)	0.0325

Table 2. This table lists two different types of enzymes and their rates of 1,4-NADH disappearance. Alcohol dehydrogenase (from equine liver) is the faster of the two.

ACKNOWLEDGEMENTS

I would like to thank my mentor, Dr. John Kerr, for his help and guidance this summer. Thanks also go out to my co-workers in the Kerr Group for being so kind and supportive. Lastly, thanks to the Department of Energy and the Office of Science for allowing me to participate in the Science Undergraduate Laboratory Internship (SULI) program. It has been a very rewarding experience. This work was supported by the Director, Office of Science, Office of Basic Energy Sciences, of the U.S. Department of Energy under Contract No. DE-AC03-76SF00098.

REFERENCES

[1] M. Gerard, A. Chaubey, B.D. Malhotra, "Application of conducting polymers to biosensors," *Biosensors and Bioelectronics*, vol. 17, pp. 345-359, 2002.

[2] A. Heller, "Electrical Wiring of Redox Enzymes," *Acc. Chem.*

Res., vol. 23, pp. 128-134, 1990.

[3] E. Steckhan, S. Herrmann, R. Ruppert, E. Dietz, M. Frede, E. Spika, "Analytical Study of a Series of Substituted (2,2'-Bipyridyl)(pentamethylcyclopentadienyl)rhodium and –Iridium Complexes with Regard to Their Effectiveness as Redox Catalysts for the Indirect Electrochemical and Chemical Reduction of $NAD(P)^+$," *Organometallics*, vol. 10, pp. 1568-1577, 1991.

[4] M. Beley and J. Collin, "Electrochemical regeneration of nicotinamide cofactor using a polypyrrole rhodium bis-ter-pyridine modified electrode," *Journal of Molecular Catalysis*, vol. 79, pp. 133-140, 1993.

[5] R.H. Fish, J.B. Kerr, H.C. Lo, "Agents for Replacement of NAD^+/NADH System in Enzymatic Reactions," U.S. Patent 6 716 596 B2, April 6, 2004.

[6] R. Ruppert, S. Herrmann, E. Steckhan, "Efficient Indirect Electrochemical In-Situ Regeneration Driven Enzymatic Reduction of Pyruvate Catalyzed by D-LDH," *Tetrahedron Letters*, vol. 28, pp. 6583-6586, 1987.

[7] E. Höfer, E. Steckham, B. Ramos, W.R. Heineman, "Polymer-modified electrodes with pendant $[Rh^{III}(C_5Me_5)(L)Cl]^+$-complexes for by -irradiation cross-linking," *Journal of Electroanalytical Chemistry*, vol. 402, pp. 115-122, 1996.

[8] S. Kodama, et. Al, "Direct chiral resolution of lactic acid in food products by capillary electrophoresis," *Journal of Chromatography A*, vol. 875, pp. 371-377, 2000.

[9] A.J. Fry, S.B. Sobolov, M.D. Leonida, K.I. Voivodov, "Electroenzymatic Synthesis (Regeneration of NADH Coenzyme): Use of Nafion Ion Exchange Films for Immobilization of Enzyme and Redox Mediator," *Tetrahedron Letters*, vol. 53, pp. 5607-5610, 1994.

[10] H.C. Lo, C. Leiva, O. Buriez, J.B. Kerr, M.M. Olmstead, R.H. Fish, "Regioselective Reduction of NAD^+ Models, 1-Benzylnicotinamde Triflate and -Nicotinamide Ribose-5'-methyl Phosphate, with in Situ Generated $[Cp^*Rh(bpy)H]^+$: Structure-Activity Relationships, Kinetics, and Mechanistic Aspects in the Formation of the 1,4-NADH Derivatives," *Inorg. Chem.*, vol. 40, pp. 6705-6716, 2001.

[11] H.K. Chenault and G.M. Whitesides, "Regeneration of Nicotinamide Cofactors for use in Organic Synthesis," *Applied Biochemistry and Biotechnology*, vol. 14, pp. 147-197, 1987.

Nathan Castro is an undergraduate student at El Paso Community College in El Paso, Texas majoring in Biology with a minor in Chemistry. In the summer of 2004 he was awarded an internship at Pacific Northwest National Laboratory (PNNL) through the Office of Science Workforce Development Program to help study the interaction between the globular protein albumin and cotton. After finishing his internship he stayed on at PNNL and helped with further investigations through the fall of 2004 and has returned to PNNL this summer. Future plans include applying to medical or graduate school and ultimately specializing in a field of medicine pertinent to the region from where he originated.

Steve Goheen is a Staff Scientist in the Chemical and Biological Sciences Group at Pacific Northwest National Laboratory (PNNL) in Richland, Washington. He received his Ph.D. in Biomaterials Engineering from Northwestern University in 1978. He began his career at PNNL as a senior scientist in 1988 following his appointment as a senior research scientist at Bio-Rad Laboratories in the Chromatography Division (Richmond, California). There, he examined the separation of membrane proteins and studied hydrophobic-interaction chromatography (HIC). His appointment at Bio-Rad was followed by a scientist position at the Martinez VA Medical Center where he worked on nutrition, alcoholic liver disease, and lipid biochemistry. Steve has also worked in the areas of chemical and biological effects of corona discharge, complex chromatographic separations, waste characterization, the dynamics of surface-mediated protein unfolding, wound healing, and has published some books on the sampling and analytical methods used for waste characterization.

COTTON STUDY: ALBUMIN BINDING AND ITS EFFECT ON ELASTASE ACTIVITY IN THE CHRONIC NON-HEALING WOUND

NATHAN CASTRO, STEVE GOHEEN

ABSTRACT

Cotton, as it is used in wound dressings is composed of nearly pure cellulose. During the wound-healing process, cotton is exposed to various blood components including water, salts, cells, and blood proteins. Albumin is the most prominent protein in blood. Elastase is an enzyme secreted by white blood cells and takes an active role in tissue reconstruction. In the chronic non-healing wound, elastase is often over-expressed such that this enzyme digests tissue and growth factors, and interferes with the normal healing process. Our goal is to design a cotton wound dressing that will sequester elastase or assist in reducing elastase activity in the presence of other blood proteins such as albumin. The ability of cotton and various cotton derivatives to sequester elastase and albumin has been studied by examining the adsorption of these two proteins separately. We undertook the present work to confirm the binding of albumin to cotton and to quantify the activity of elastase in the presence of various derivatives of cotton. We previously observed a slight increase in elastase activity when exposed to cotton. We also observed a continuous accumulation of albumin on cotton using high-performance liquid chromatography methods. In the present study, we used an open-column-absorption technique coupled with a colorimetric protein assay to confirm losses of albumin to cotton. We have also confirmed increased elastase activity after exposure to cotton. The results are discussed in relation to the porosity of cotton and the use of cotton for treating chronic non-healing wounds.

INTRODUCTION

Decreasing the negative effects of chronic non-healing wounds on a patient's comfort level, improving the economic relief, and exploring potential commercial benefits are all justifiable bases for continuing the research efforts to develop treated cotton gauze that will help expedite the wound-healing process. Although many individuals suffer from non-healing wounds, those who are diabetic are especially susceptible to such wounds which, in some cases, lead to the amputation of the affected limb. More than 60% of non-traumatic lower-limb amputations occur among people with diabetes. In 2000-2001 that percentage corresponded to approximately 82,000 cases. Medical costs related to amputation can exceed $13,000 per patient and the overall indirect medical costs, including loss in productivity, are as high as $39.8 billion per year [1].

Another segment of the U.S. population, some 200,000 people, lives with a disability related to spinal cord injuries. This segment's medical care costs the nation approximately $9.7 billion per year. Of that amount, $1.2 billion is attributed to the secondary condition of pressure sores [2]. The costs and care of pressure ulcers is so significant that advances in chronic wound research and fiber dressing design for accelerated healing is clearly needed.

During the normal healing process, elastase and other proteases help digest unwanted proteins, thereby removing them from the wounded region. Wound fluid from chronic non-healing wounds

Solution	Buffer (mL)	BSA (mL)	BSA (µg)
1	0.5	0	0
2	0.4	0.1	60
3	0.3	0.2	120
4	0.2	0.3	180
5	0.1	0.4	240
6	0	0.5	300

Table 1. Volume of solutions used in constructing BSA standard curve.

Elastase (µg/mL)	Elastase (mL)	Saline Solution (mL)
0	0	0.5
1.14E+02	0.1	0.4
2.28E+02	0.2	0.3
3.42E+02	0.3	0.2
4.56E+02	0.4	0.1
5.70E+02	0.5	0

Table 2. Volume of solutions used in constructing elastase activity standard curve.

contains elevated levels of elastase activity, which has been associated with the debasement of important growth factors and fibronectin necessary for wound healing [3,4]. We suspect a direct correlation lies between the inability of a wound to heal naturally and an increase in elastase activity. Elastase activity is the rate at which this enzyme catalyzes the digestion of elastin, a connective tissue protein, whose role is critical in the healing process.

Serum albumin is expected to be far more concentrated (by at least one order of magnitude) than any of the proteases in wound fluids. Insufficient data have been collected from patients suffering from chronic non-healing wounds to determine actual concentrations of the various proteases. We are interested in the interactions between elastase and wound dressings in the wound site so we quantified the binding interaction between serum albumin and cotton fiber. Serum albumin is the most prominent globular protein found in blood. Even though elastase is present in healing and non-healing wounds, its over-expression in chronic non-healing wounds has been associated with the degradation of important growth factors necessary for wound healing.

It can be said that the local chemistry of the wound fluid is responsible for governing elastase activity. Chemically modifying cotton cellulose while retaining its basic properties, may help to accelerate the healing process of chronic wounds by sequestering over-expressed elastase in wound fluid through the arbitration of elastase activity. This may assist in avoiding the degradation of extracellular elastin and growth factors, thus hastening the healing of chronic wounds.

Our focus is on the design of a synthesized cotton dressing that will enisle, or aid in the reduction of elastase activity as it is expressed in wound fluid to facilitate the body's natural healing ability. The formulation of a wound dressing that potentially has the ability to lower the amount of over-expressed elastase activity merits additional research. Before formulating better dressings, however, a better understanding of the mechanisms involved in cotton-wound dressing and wound-site interactions with key wound-fluid biomolecules merits further exploration.

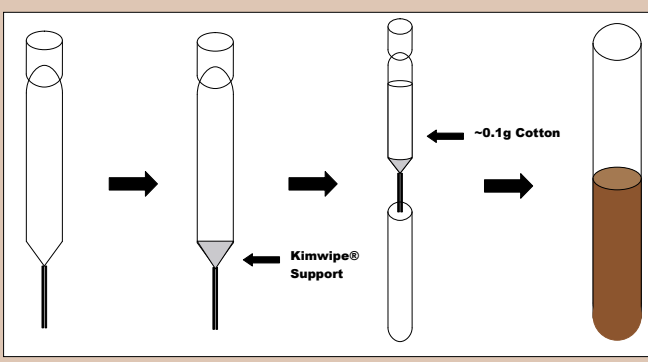

Figure 1. Open-column used in Protein and Enzyme Assay.

MATERIALS AND METHODS

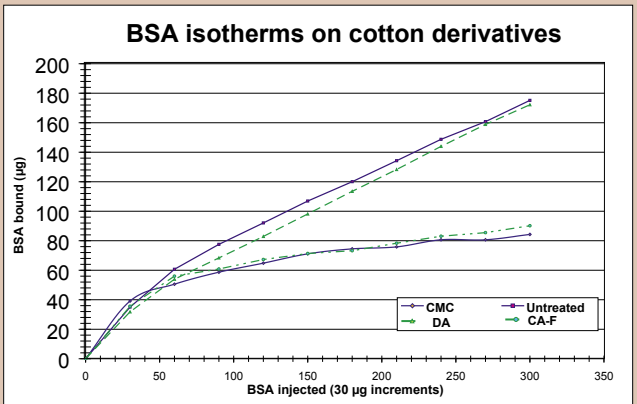

Figure 2. Results of protein assay involving BSA absorption in treated and untreated cotton samples per 0.1g sample. Each data point represents the average of four samples measured.

Protein Assay

Bovine serum albumin (BSA) obtained from Sigma Chemical Co. (St. Louis, MO) was used throughout this study because of its similarity to human serum albumin in structure, molecular weight, and other properties. We believe both forms of albumin have analogous influences on elastase activity. Through the modification of a Bio-Rad protein assay procedure, the following solution was primed: 4:1 dye reagent concentrate (from Bio-Rad Laboratories, Hercules, CA) consisting of 20 mL dye reagent and 80 mL MilliQ water that was processed through a Millipore MilliQ Plus system (from Millipore, Billerica, MA) such that the resistance was greater than 18.2 ohms. A 5 mM buffer solution was made by measuring 0.6055 g of Trizma® (Tris[hydroxymethyl]aminomethane-HCl) salt (Tris) obtained from Sigma Chemical Co. (St. Louis, MO) and placing it in a one-liter volumetric flask brought to volume with MilliQ water. The solution was brought to a pH of 7.4 by adding 1.0 M HCl and using a magnetic stir rod and pH meter. A 0.2 M salt solution was created by adding 2.9220 g of NaCl to a 250-mL volumetric flask and brought to volume with MilliQ water. A 10-mL

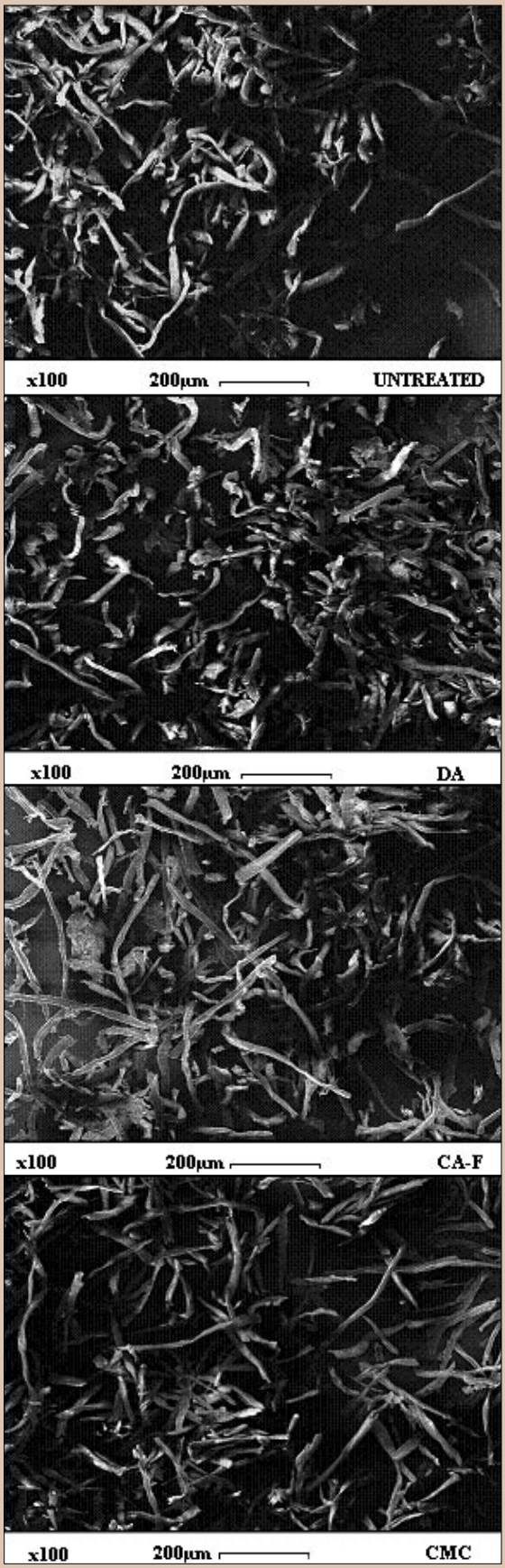

Figure 3. Scanning electron microscope photos of untreated and treated cotton samples.

sample of a 300 µg/mL solution of BSA in 5 mM Tris solution was then prepared by adding 0.003 g of BSA to a 10-mL volumetric flask brought to volume with 5 mM Tris.

The Bradford protein assay [5] was used to measure protein concentrations. Cotton derivatives consisted of carboxymethyl cellulose (CMC), dialdehyde (DAQ), citrate-fructose cellulose (CA-F), and an untreated control sample. All treated and untreated cotton samples were ground and sifted to pass through a –80 mesh screen. All cotton samples were supplied by J. Vincent Edwards at the U.S. Department of Agriculture, ARS Laboratory (New Orleans, LA). Before conducting the open-column assay, a standard curve was created using the volumes of our buffer and BSA solutions found in Table 1.

All experiments were done independently as follows. The masses of all Pasteur pipets used were taken and recorded. A Kimwipe® plug was inserted into each pipet and the mass was recorded. Approximately 0.1 g of cotton sample was placed in each pipet. Actual masses varied and were recorded. Figure 1 depicts the configuration of these open columns.

A collection of 12 test tubes was used per experiment. A blank sample was first made with 0.5 mL salt solution; next a 0.5 mL injection of salt solution was eluted through the open column, followed by the first of ten 100 µL injections of 300 µg/mL BSA in 5mM Tris buffer solution. Elutions were collected in numbered test tubes. Preceding the collection of all eluted samples, 5 mL of the 4:1 dye reagent in MilliQ water was added to each sample and spectrophotometric measurements were taken seven minutes after the dye reagent was added. Spectrophotometric measurements were taken from a Cole Parmer 1200 spectrophotometer. The wavelength was kept constant at 595 nm.

Enzyme Assay

The procedure used to determine the activity of elastase in the presence of treated and untreated cotton samples was similar. The enzyme assay experiment was conducted on only CMC and untreated cotton samples. The 570 µg/mL elastase in 0.2 M NaCl solution was primed by measuring 0.0057 g of porcine pancreatic elastase, which was placed in a 10-mL volumetric flask followed by the addition of 0.0584 g NaCl brought to volume with MilliQ water. A saline solution of 0.15 M Tris, 0.2 M NaCl was made by measuring 0.6055 g Tris and 11.7 g NaCl, which were set in a one-liter volumetric flask brought to volume with MilliQ water and to a pH of 7.4 1.0 M HCl and a magnetic stir rod and pH meter. A 0.6 mM substrate solution was prepared by placing 0.0035 g N-(methoxysuccinyl)-ala-ala-pro-val 4-nitroanalide in a 10-mL volumetric flask and bringing to volume with 100% dimethylsulfoxide (DMSO).

Following a procedure similar to the Bradford protein assay, a standard curve was created using the volumes found in Table 2 of our elastase and saline solutions. Open columns were prepared in the same manner as above. A collection of eight test tubes was used per experiment. A blank sample was first created by pipeting 1.0 mL saline solution in the first of our test tubes. Then, 0.5 mL of the 570 µg/mL elastase solution was injected in each column and subsequent 1.0-mL injections of saline solution were administered. Upon completion of the final elution, a 0.5-mL aliquot of each elution was pipeted into a cuvette. A 100-µL injection of substrate was administered to each cuvette and 20 seconds elapsed between initial exposure and actual reading measurement for each sample in order to incite the release of p-nitroanaline from the enzymatic hydrolysis of MeOSuc-Ala-Ala-Pro-Val-pNA measured at a constant wavelength of 410 nm.

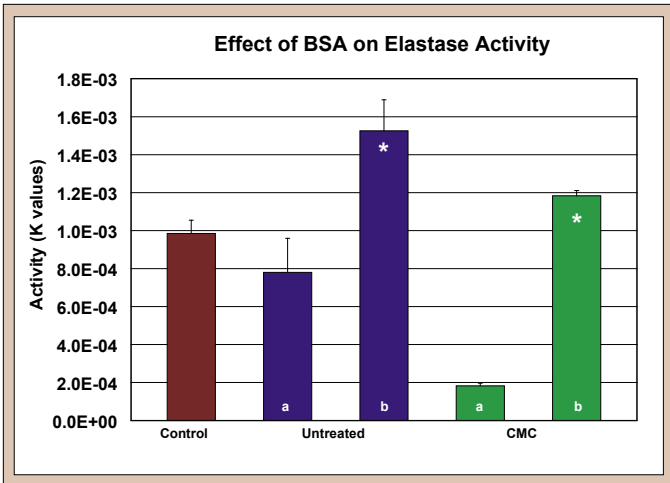

Figure 4. Overall elastase activity of CMC and untreated cotton samples in comparison to initial elastase activity with respect to the presence or absence of BSA. Elastase activity as measured without the presence of BSA (a), elastase activity as measured in the presence of BSA (b). A minimum of two samples per condition were measured.

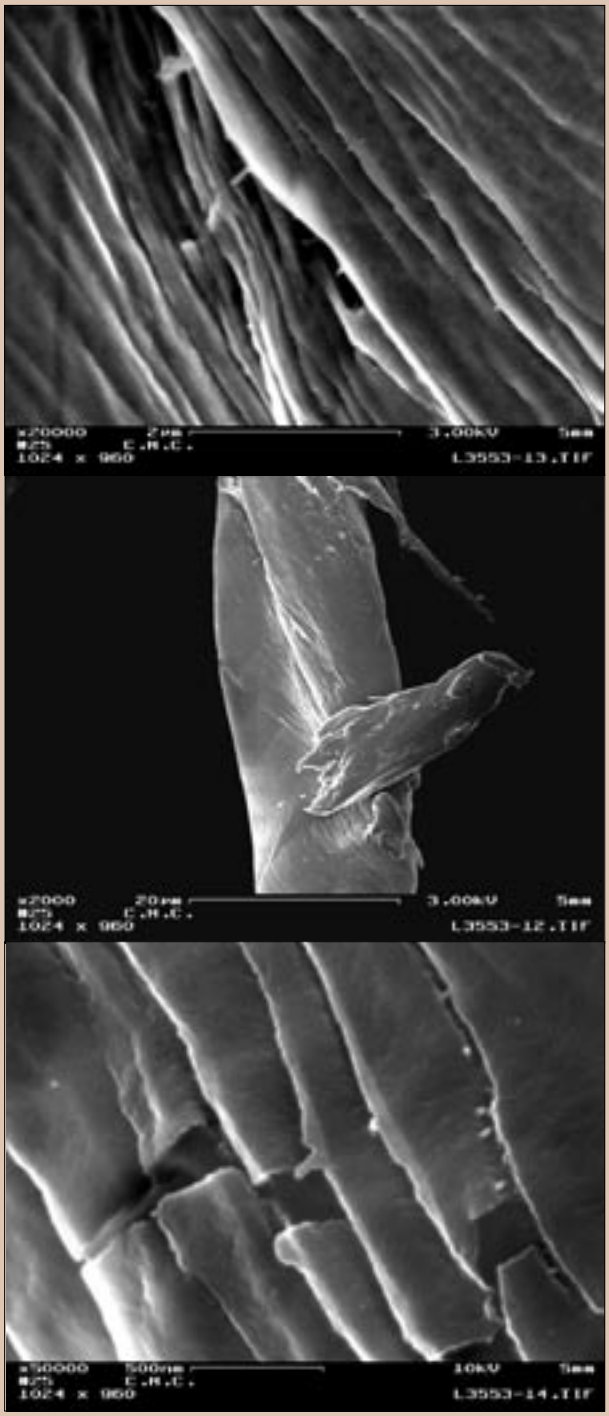

Figure 5. Scanning electron microscope photos of cotton surface depicting porosity of cotton fibers.

Scanning Electron Microscopy Sample Preparation

All four cotton fiber samples were prepared for viewing in a field emission scanning electron microscope in the same manner. A 13-mm scanning electron microscopy (SEM) stub was cleaned and a small piece of graphite tape was placed on the top of the stub. A small amount of the cotton fiber sample was placed on top of the graphite tape. The material that had not adhered to the graphite tape was removed with a small discharge of air from a filtered air source. The sample was placed in an Edwards S150B Sputter Coater under partial vacuum for one hour to allow the small particles to settle on the graphite tape. After the particles had settled, the samples were sputter-coated with carbon for 10 seconds. The samples were removed from the sputter coater and placed in a nitrogen-gas-fed dry box for storage.

The samples were viewed on the LEO 982 FESEM with varying magnifications. The LEO 982 FESEM has resolution capabilities of 1.0 nm at 30 kv. High- and low-magnification images were taken of the particles with the majority of the images being taken of abnormal structures or contamination. The samples were then removed from the FESEM and placed back in the dry box for storage and further examination.

RESULTS AND DISCUSSION

Protein assay results show that all cotton forms (untreated, dialdehyde, CMC, and CA-F) bound about 70 µg BSA per 0.1 g cotton in the first few elutions. The results are depicted in Figure 2. The untreated and dialdehyde samples continued to bind approximately 14 µg BSA per 0.1 g cotton with each subsequent elution. CMC and CA-F bound approximately 4 µg BSA with subsequent elutions. The treated and untreated cotton samples are shown in Figure 3.

One explanation of the results shown in Figure 2 is that the 70 µg of BSA filled pores in the cotton particles and subsequent adsorption was from the accumulation of monolayers (CMC/CA-F) or multilayers (dialdehyde/untreated) of BSA over the exterior of the cotton particles. The inability of the CMC and CA-F to bind additional BSA is likely related to the structure or ionic character of the derivatives. Overall elastase activity increased with elution through both CMC and untreated cotton (Figure 4). Several fractions were collected after injecting elastase and eluting with mild buffer. The earliest eluting elastase fraction was the most active. Typically, no activity was exhibited in the next few fractions. In the seventh fraction, we typically saw additional activity. This confirmed

no activity was present in any of these fractions when elastase was absent. Reasons for the increased activity remain unknown.

CONCLUSIONS

Both CMC and CA-F are negatively charged whereas dialdehyde and untreated cotton samples are neutral. Particles that pass through a –80 mesh sieve are approximately 100 μ in diameter. If we assume all particles were 100 μ in diameter and were perfect cubes, they would have a surface area of approximately 11.1 nm^2/molecule (the density of cotton is 0.3849 g/cm^3). Therefore, it is unlikely the other components of cotton (lignin, protein, etc.) are responsible for this adsorption. The differences in continual binding of BSA to cotton may be related to the orientation of BSA bound to the various derivatives. We suggest the possibility that BSA has a cationic binding site directly opposite a region that resists subsequent binding. If BSA has a region of positively charged amino acids, those are more likely to bind to the anionic cellulose. Then, the remaining exposed surface of BSA would oppose additional binding, by some unknown mechanism. Therefore, by controlling the chemical structure of cotton, bandages can be designed to maximize or minimize the absorption of albumin. All the forms of cotton studied activated elastase. The mechanism by which the activity increased has not been identified. However, future work should be carried out to determine with greater certainty, how the use of cotton can inhibit healing in chronic non-healing wounds by stimulating elastase activity. It may be, for example that albumin will mask this activation effect, or other materials may activate elastase more extensively. Regardless of the answers to these important questions, the results of this study clearly show that bandage materials can play an important role in the biochemistry of wound healing. More research is needed to find the ideal bandage material for chronic non-healing wounds.

ACKNOWLEDGMENTS

I would like to thank the U.S. Department of Energy, Office of Science for giving me the opportunity to participate in the Community College Institute Program at Pacific Northwest National Laboratory. I would also like to thank my mentor, Steve Goheen, for the support and guidance he has given me throughout my internship, and J. Vincent Edwards with the USDA in furnishing the necessary materials to conduct the experiments. Special thanks go to Rachel Davis for her generous assistance in showing me around the laboratory and making sure projects were running smoothly, and to Brian Pultz for supplying SEM images and preparation procedure for the analysis of the cotton samples studied. Lastly, I want to thank Royace Aikin and Dale Johns for being excellent program directors in helping me this summer.

REFERENCES

[1] National Center for Chronic Disease Prevention and Health Promotion, Center for Disease Control, "National Diabetes Fact Sheet." (2003). http://www.cdc.gov/diabetes/pubs/pdf/ndfs_2003.pdf.

[2] National Center for Injury Prevention and Control, Center for Disease Control, "Spinal Cord Injury: Fact Sheet." (August 2004). http://www.cdc.gov/ncipc/factsheets/scifacts.htm.

[3] Edwards, J.V., G. Eggleston, D. R. Yager, I. K. Cohen, R. F. Diegelmann, A. F. Bopp, "Design, preparation and assessment of citrate-linked monosaccharide cellulose conjugates with elastase-lowering activity," Carbohydrate Polymers, 2002, pp. 305-314.

[4] Edwards, J. V., S. L. Batiste, E. M. Gibbins, S. C. Goheen, "Synthesis and activity of NH_2- and COOH-terminal elastase recognition sequences on cotton," Journal of Peptide Research, 1999, pp. 536-543.

[5] Bradford, M. M., Analytical Biochemistry, 1976 72, pp. 248.

Erika Zink graduated from Washington State University with a B.S. in Biology with minors in Chemistry and Psychology in 2004. While an undergraduate, she conducted research in the analysis of the components of noble fir oil and its antibacterial properties at Columbia Basin College. Her work in this area was presented in poster form at the 60th annual regional meeting of the ACS. In her senior year she participated in the DOE Faculty and Student Team internship program at Pacific Northwest National Laboratory, where she worked with a professor and a fellow student to determine if saliva could be used as a medium to test for chemical exposure. This work was presented at the AAAS National Conference in 2005.

Ryan Clark is a sophomore attending Columbia Basin College (CBC) where he is currently pursuing pharmacy with intent to go into pharmacology research. He is involved in undergraduate research on natural resource chemistry, which is being presented at the national American Chemical Society meeting (2005). During his student research appointment at Pacific Northwest National Laboratory as a member of a Faculty and Student Team (FaST), he helped work on developing a method for recovering the metabolites of pesticides and other compounds of interest for creating a process to test for exposure of these chemicals non-invasively.

Karen Grant serves as head of the new joint Bachelor of Science in Chemistry program currently being developed between Columbia Basin College and Washington State University – Tri-Cities. She obtained B.S. degrees in chemistry and in physics from Bates College in 1967 and an M.S. degree in chemistry from the University of Wisconsin in 1969. She has more than ten years experience as a Faculty Research Fellow in the Advanced Organic Analytical Methods Group at the Pacific Northwest National Laboratory and has developed a successful undergraduate research program at Columbia Basin College, a community college in Pasco, WA. In 2001, she was awarded the American Chemistry Council's National Catalyst Award. Her research interests include natural product chemistry and development of analytical methods for analysis of trace organic species in non-invasive biological matrices.

Jim Campbell is a Laboratory Fellow at Pacific Northwest National Laboratory (PNNL) in Richland, Washington. He received his Ph.D. in Analytical Chemistry from Montana State University in 1983. Jim has studied the development of analytical techniques for the detection and quantification of organic components in difficult matrices, both environmental and biological. Most recently his work has involved evaluating saliva as a non-invasive biomonitoring matrix for the determination of exposure to organophosphate insecticides and other hazardous chemicals. In addition, his interests lie in the area of metabolomics.

Eric Hoppe is a Senior Research Scientist in the Chemical and Biological Sciences Group at Pacific Northwest National Laboratory (PNNL) in Richland, Washington. He received his B.S. in chemistry from Colorado State University. His research interests include gas and liquid chromatographic techniques using various inlets, interface systems, and detectors including mass spectrometry and infrared spectroscopy. Other interests include analytical methods development for components of radioactive mixed waste and other highly complex matrices, ordnance compounds, and EPA priority pollutants in a variety of materials. He has developed real-time analytical systems for monitoring of air, gaseous process effluents, engine exhausts, off-gas of in-situ remediation techniques involving thermal and oxidative destruction methods. He regularly tests and develops materials used in advanced engineering programs.

ANALYTICAL METHODOLOGIES FOR DETECTION OF GAMMA-VALEROLACTONE, DELTA-VALEROLACTONE, ACEPHATE, AND AZINPHOS METHYL AND THEIR ASSOCIATED METABOLITES IN COMPLEX BIOLOGICAL MATRICES

Erika Zink, Ryan Clark, Karen Grant, James Campbell, and Eric Hoppe

ABSTRACT

Non-invasive biomonitoring for chemicals of interest in law enforcement and similar monitoring of pesticides, together with their metabolites, can not only save money but can lead to faster medical attention for individuals exposed to these chemicals. This study describes methods developed for the analysis of gamma-valerolactone (GVL), delta-valerolactone (DVL), acephate, and azinphos methyl in saliva and serum. Liquid chromatography/mass spectrometry (LC/MS) operated in the negative and positive ion mode and gas chromatography/mass spectrometry (GC/MS) were used to analyze GVL and DVL. Although both analytical techniques worked well, lower detection limits were obtained with GC/MS. The lactones and their corresponding sodium salts were spiked into both saliva and serum. The lactones were isolated from saliva or serum using newly developed extraction techniques and then subsequently analyzed using GC/MS. The sodium salts of the lactones are nonvolatile and require derivatization prior to analysis by this method. N-methyl-N-(t-butyldimethylsilyl)-trifluoroacetamide (MTBSTFA) was ultimately selected as the reagent for derivatization because the acidic conditions required for reactions with diazomethane caused the salts to undergo intramolecular cyclization to the corresponding lactones. *In vitro* studies were conducted using rat liver microsomes to determine other metabolites associated with these compounds. Azinphos methyl and acephate are classified as organophosphate pesticides, and are known to be cholinesterase inhibitors in humans and insects, causing neurotoxicity. For this reason they have both exposure and environmental impact implications. These compounds were spiked into serum and saliva and prepared for analysis by GC/MS. Continuation of this research would include analysis by GC/MS under positive ion mode to determine the parent ions of the unknown metabolites. Further research is planned through an *in vivo* analysis of the lactones and pesticides. These methodologies could be extended for further analysis of other similar compounds.

INTRODUCTION

Non-invasive biomonitoring for chemicals of interest in law enforcement and similar monitoring of pesticides together with their metabolites can not only save money but can lead to faster medical attention for individuals exposed to these chemicals. This study describes methods developed for the analysis of gamma-valerolactone (GVL), delta-valerolactone (DVL), acephate, and azinphos methyl (structures are shown in Figure 1) in saliva and serum with extension to metabolic studies. Currently, studies are being done on these chemicals and their toxicities, but very little is known about their metabolism.

Approximately five billion tons of pesticides were used in the United States in 1997 [1]. Azinphos methyl and acephate are classified as organophosphate pesticides, and are known to be cholinesterase inhibitors in humans and insects, causing neurotoxicity [2, 3]. For this reason they have both exposure and environmental impact implications. Farm workers are often exposed to these pesticides and therefore, it has been recommended that they be tested for the accumulation of these chemicals. In Washington State, bioassays on individuals are required after fifty hours of exposure over a thirty-day span [1]. Currently, these pesticides are

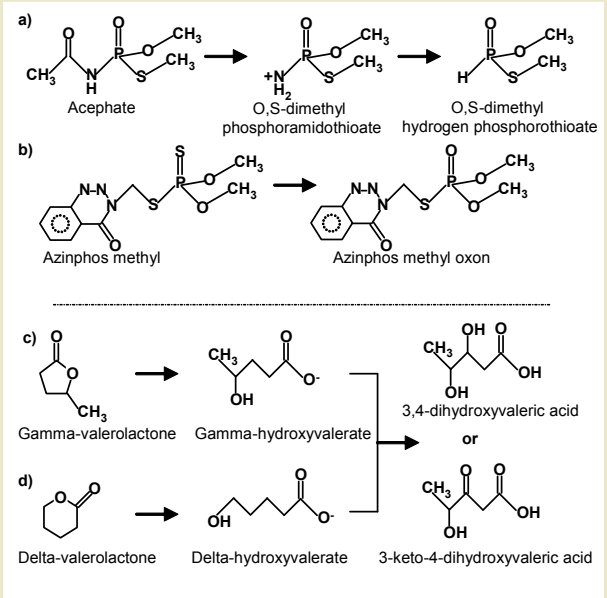

Figure 1. Metabolism possibilities for a) acephate, b) azinphos methyl, c) gamma-valerolactone and d) delta-valerolactone.

GC/MS Conditions		
Parameter	Lactones	Pesticides
Inj. Port Temp	220 C	250 C
Initial Temp	50 C	80 C
Initial Time	2.00 min.	1.00 min.
Solvent Delay	5.00 min.	5.00 min.
Rate	10 deg/min.	20 deg/min.
Final Temp	300 C	300 C

Table 1. General settings for GC/MS for analysis of lactones and pesticides.

monitored by analysis of their metabolites in biological matrices (i.e. blood and urine). These metabolites degrade very quickly and leave the body within a short-time period [4, 5]. The cost to the farmer in terms of testing and time lost per field worker is estimated to be two to three thousand dollars. Detection of the metabolites (see Figure 1a and 1b for possible metabolic routes) could lead to real-time analysis of exposure to these chemicals, resulting in a substantially lower cost.

The lactones, GVL and DVL, have physiological effects similar to those of certain controlled substances of interest to law enforcement agencies. Based on the structure of these compounds and the environment created by ingestion, it is believed that these compounds would first metabolize to the anion (Figure 1c and 1d). Since this structure is similar to that of a fatty acid, a good prediction is that they would undergo beta-oxidation as well, producing the metabolites shown in Figure 1. If analytical techniques could be developed for the detection of GVL, DVL, and their metabolites, the results would provide more effective drug enforcement and litigation, as well as the required first aid due to exposure.

Due to the short-lived nature of these analytes, the development of techniques for their detection will eventually lead to more immediate analysis, particularly if obtained from a non-invasive sampling such as saliva. This would enable agricultural industries to save money on exposure testing for pesticides and allow first aid to be administered within the narrow window of opportunity for such chemicals.

The objective of this study was to determine if any unique metabolites exist and if saliva is a viable matrix for non-invasive biomonitoring. This was done by initially developing techniques for the detection of the analytes in standard solutions. This was followed by the development of techniques for the detection of GVL, DVL, azinphos methyl, and acephate in complex biological matrices, in this case, saliva and serum. Ultimately, an *in vitro* study with rat liver microsomes was conducted where the analytes were spiked into the S-9 fraction, incubated, and then analyzed for possible metabolites. Comparisons of recoveries and different techniques were then drawn between the analytes. Further research is planned through an *in vivo* analysis of the lactones and pesticides.

Methods have been developed for the analysis of GVL, DVL, acephate, and azinphos methyl in blood, saliva, and the S-9 fraction from rat livers. Preliminary results indicate no metabolism occurring in rat blood. However, for DVL and azinphos methyl, there are differences between the control (no metabolism) and the sample undergoing metabolism with the S-9 fraction. The metabolic products are in the initial stages of identification.

MATERIALS AND METHODS

The chemicals used in this study included gamma-valerolactone, GVL (Sigma-Aldrich), delta-valerolactone, DVL (Lancaster Synthesis, Inc.), acephate (Chem Services, Inc), and azinphos methyl (Chem Services, Inc). The serum used was ordered through Sigma-Aldrich and saliva was collected. The livers used for the *in vitro* study were extracted from rats ordered from Charles River Laboratory (Hollister, CA).

The sodium salts of the two lactones were prepared through saponification of 0.001 M solutions of GVL or DVL by adding a solution of 0.001 M of sodium hydroxide in a methanol solvent to the sample. The resulting salts were dried under a nitrogen stream for 30 minutes and then dried overnight with silica beads before purifying by washing the crystals with acetone. Once purified, they were once again blown down to dryness under nitrogen gas and dried overnight as before [6]. The derivatizing agent used, N-methyl-N-(t-butyldimethylsilyl)-trifluoroacetamide (MTBSTFA) was ordered from Pierce Biotechnology, Inc.

All samples were analyzed by gas chromotagraphy/mass spectrometry (GC/MS) using an HP5890 gas chromatograph with a 30 m x 0.25 mm x 0.25 µm DB5 column (Agilent) and a JEOL SX-102/SX-102 tandem, four sector, high resolution mass spectrometer. The parameters for the analysis of the lactones and the pesticides can be found in Table 1, unless otherwise stated. For those samples that were lyophilized, a Labconco Lyph·Lock 4.5 Freeze Dry System was utilized. The samples that were analyzed by liquid chromatography/mass spectrometry (LC/MS) were done using a ThermoFinnigan TSQ 7000 triple-quadrupole mass spectrometer equipped with an Agilent LC binary pump to perform separations using a variety of different columns. A Harvard Apparatus Model '22' syringe pump was used for direct infusion of the sample into the mass spectrometer. All samples were run under electrospray ionization (ESI) in both the positive ion and negative ion modes.

The dosing solutions of the analytes for the *in vitro* studies were prepared by making 40,000-ppm solutions. Approximately 0.040 mg of GVL or acephate was added to 1 mL of Milli Q water. In the

BCA Protein AssayStandards 081604					
desc.	mg/mL protein	absorbance protein	Avg. absorbance	mg/mL Calculated	analyzed/ calc (%)
Std 1	0.000	0.235	0.235	-0.091	
Std 2	0.212	0.392	0.392	0.255	120.085
Std 3	0.530	0.547	0.547	0.595	112.322
Std 4	1.060	0.813	0.813	1.180	111.324
Std 5	1.590	0.937	0.937	1.453	91.360
Std 6	2.120	1.049	1.049	1.699	80.133

Table 2. BCA protein assay standards.

case of DVL and azinphos methyl, the solubilities in water were low, so 0.040 g of DVL was added to 2 mL ethanol and 0.040 g of azinphos methyl was added to 2 mL of methanol and each were sonicated to aid solvation.

The buffer solutions used in the preparation of the liver microsomes were prepared prior to the extraction of the rat livers. The phosphate buffered saline (PBS) was prepared by adding 1 tablet (Sigma cat#P-4417) to 200 mL of water (distilled, de-ionized). The homogenization buffer was prepared by measuring 250 mL of stock phosphate buffer in a 500 mL graduated cylinder and adding to this 42.78 g of sucrose. To this was also added 0.190 g of ethylenediam-inetetraacetic acid (EDTA) and enough water to make a total volume of 470 mL. The pH was then adjusted to 7.4-7.5 with 1 N NaOH. The solution was then brought up to 500 mL with water. Lastly, the stock phosphate buffer was prepared by measuring 400 mL of water in a graduated cylinder and adding to this 5.77 g K_2HPO_4 (potassium phosphate, DIBASIC, Fisher/Acros Cat#42419-5000), then 2.08 g KH_2PO_4 (potassium phosphate, MONOBASIC, Fisher/Acros Cat#42420-5000). The pH was then adjusted to 7.4-7.5 using either monobasic or dibasic crystals (slowly), the solution was then brought up to a total of 500 mL with water.

Eight male Spraque Dawley rats were received on 07/27/04 and acclimated to the lab for 7 days. They were euthanized with CO_2 and their body weights were recorded. Blood was extracted from each animal and the livers were first perfused with cold PBS via the vena cava prior to extraction. With some it was necessary to perform an external perfusion by rinsing each lobe of the liver with cold PBS after it had been extracted. The weight of the liver was recorded after removing any extraneous tissues and were found to vary from 11.6 to 15.0 grams. The livers were then rinsed with cold PBS prior to being submersed in 30 mL of ice-cold homogenization buffer. The tissue was then minced into small pieces with scissors while keeping it in the buffer and on ice. The tissues were then homogenized with a Teflon/glass homogenizer (10 strokes) on a drill press. The homogenate was then spun for 20 min at 4°C at 9000 x g (~11,000 rpm). The supernatant was saved and stored at -80°C until used.

The protein content of the S-9 fractions that were isolated from the rats was found to be around 30 mg/ml (Tables 2-4). About 1680 µL of the phosphate buffer solution was added to 330 µL of the S-9 fraction to create a solution with approximately 10 mg of protein per mL. This solution was warmed for approximately two minutes before 10 µL of the dosing solutions described previously were added. Once spiked with the analytes, microsomes were incubated for one hour in a 37°C water bath, and vortex mixed every ten minutes. The reactions were quenched with 2 mL of ethyl acetate, after which they were vortexed and centrifuged. After removing the top organic layer, each sample was washed two more times with 2 mL of ethyl acetate to extract the analytes. The combined organic layers were then blown down to approximately a 1 mL volume under nitrogen and dried with anhydrous sodium sulfate.

S-9 protein assay: 20 x dilution

sample	absorbance	average absorbance	diluted mg/mL protein	final mg/mL protein	Average protein mg/ml
#1	0.867	0.867	1.299	25.975	29.134
#2	0.756	0.756	1.055	21.095	22.627
#3	0.783	0.783	1.114	22.282	24.320
#4	0.894	0.894	1.358	27.162	25.221
#5	0.919	0.919	1.413	28.261	24.672
#6	1.095	1.095	1.800	35.999	29.640
#7	0.9	0.9	1.371	27.426	27.112
#8	1.006	1.006	1.604	32.086	35.157

Table 3. Analysis of samples at 20x dilution.

S-9 protein assay: 50 x dilution

sample	absorbance	average absorbance	diluted mg/mL protein	final mg/mL protein
#1	0.57	0.57	0.646	32.29
#2	0.496	0.496	0.483	24.16
#3	0.516	0.516	0.527	26.36
#4	0.488	0.488	0.466	23.28
#5	0.468	0.468	0.422	21.08
#6	0.488	0.488	0.466	23.28
#7	0.52	0.52	0.536	26.80
#8	0.624	0.624	0.765	38.23

Table 4. Analysis of samples at 50 x dilution.

A control was created with the analyte present by first adding 2 mL of ethyl acetate to the microsome-buffer solution to prevent any metabolism from occurring and then allowing them to heat for 2 minutes before adding the analyte. These were incubated for one hour before the compounds of interest were extracted using the same technique as described for the samples above. Adding 2 mL of ethyl acetate to the microsome-buffer solution and extracting three times (just as the previous samples) created a method blank. The microsome samples that were left after being extracted were then lyophilized and derivatized with MTBSTFA to test for any other possible metabolites. The extracted samples were analyzed by GC/MS for acephate, azinphos methyl, and GVL. The derivatized sample extracts containing azinphos methyl and GVL were also analyzed by GC/MS.

To verify that the enzymes in the microsomes were functioning properly, they were tested with chlorpyrifos (CLP). This was done by creating a sample, a duplicate, an analyte blank and a solvent blank using a similar method to that used for the analytes of interest. One of the samples was derivatized with MTBSTFA to determine if the metabolite, trichloropyridinol (TCP), was present and compared to a standard of TCP derivatized with MTBSTFA. The results showed that metabolism had occurred and that the microsomes were functioning as expected [10].

The blood that was extracted previously was used for incubation with the metabolites, using a method similar to that used for the microsome incubations. In this case, the dosing solutions were prepared by adding approximately 10 mg of the GVL, DVL, and acephate to 10 mL of Milli Q water, and 10 mg of azinphos methyl to 10 mL of methanol. A sample, duplicate and a method blank were created using 40 µL of the water solutions and 20 µL of the methanol solution. Also, for these samples, ethyl acetate was used as the quenching solvent, except for GVL, which was quenched with dichloromethane. Two method blanks were also created using ethyl acetate and dichloromethane. All the samples were extracted three times and analyzed by GC/MS.

RESULTS AND DISCUSSION

GVL and DVL.

Saponification of the lactones to produce the sodium salts produced 89.7 mg of Na-GHV, giving about a 63% yield. A similar yield was observed with the formation of Na-DHV from DVL. Analysis by GC/MS of the analyte standards produced reasonable responses, as shown in Figure 2. The responses of the lactones were found to be low compared to that of the derivatized sodium salts. This could have been due to the elevated injection port temperature, which was consistent with studies done on the acids of the analogs of the lactones. The lactones are reported to be thermally labile [8]; the effects of which could be tested using lower temperatures and by on-column analysis. The base ion for GVL is believed to result from the loss of the methyl group attached to the ring; whereas the base ion for DVL is the lactone (Figure 3c and 3d). The derivatized sodium salts produced mass spectra that had the same base ion with an m/z of 189, shown in Figure 3e and 3f.

When GVL was analyzed by LC/MS, it was found that the pH of the analyte solution could have a tremendous effect on the results. When deionized water was used, which had a pH of around 8.6, the lactone appeared to open up and polymerize with a mass difference of 140 between each increment. It was also found that at this pH, the NIM for GVL was the same as the NIM for Na-GHV and the PIM for GVL was the same as the PIM for Na-GHV. However, when Milli-Q water was used, which had a pH of around 7.9, the NIM for GVL was found to show no recognizable results, but the PIM showed a small amount of the sodium adduct (m/z 122.7) and no polymerization. When the electrospray capillary temperature was increased from 200°C to 250°C the main response was at m/z 122.7.

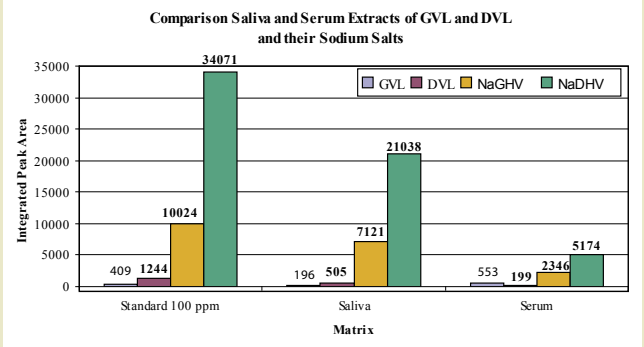

Figure 2. Results of the lactones and their sodium salts in saliva and serum.

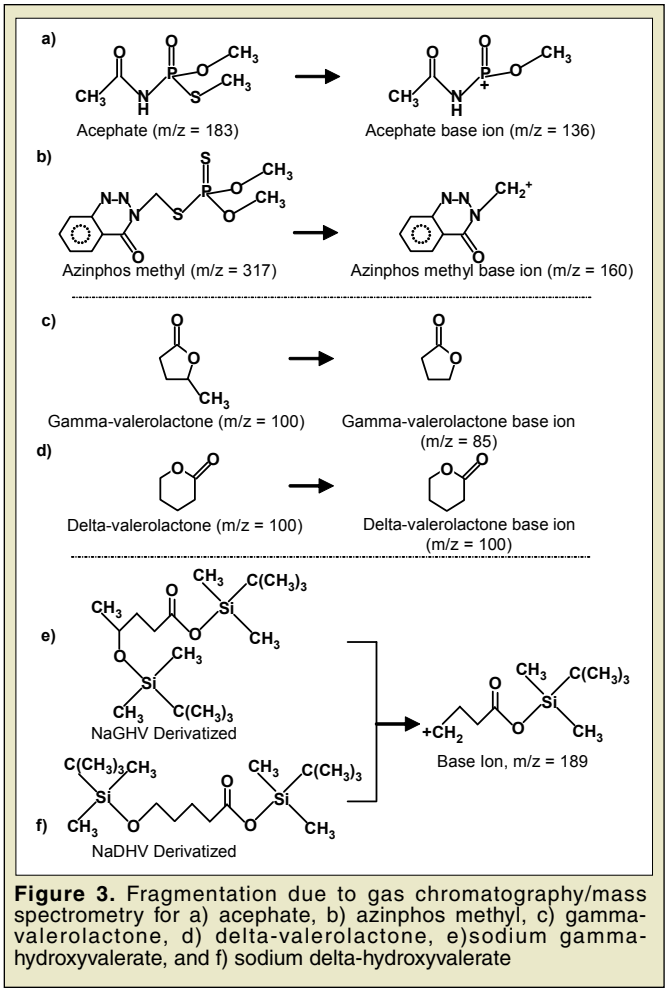

Figure 3. Fragmentation due to gas chromatography/mass spectrometry for a) acephate, b) azinphos methyl, c) gamma-valerolactone, d) delta-valerolactone, e)sodium gamma-hydroxyvalerate, and f) sodium delta-hydroxyvalerate

Analysis of the lactones spiked into human saliva collected from volunteers produced reasonable results by GC/MS (Figure 5). At an injection port temperature of 220°C, the response was lower for GVL than when the injection port temperature was lowered to 150°C. For DVL, an injection port temperature of 220°C was used, which showed good results. A saliva blank, extracted with dichloromethane was analyzed by GC/MS, showed a fairly clean sample with no large peaks. The GVL and Na-GHV saliva samples that were analyzed by LC/MS gave a weak signal under NIM with a peak at m/z 116.8, while nothing was seen under PIM conditions. The sodium salts of the lactones, when analyzed by GC/MS after lyophilization and derivatization with MTBSTFA for the saliva samples, showed an adequate response (Figure 2).

Serum was initially found to have a pH between 8 and 9, which initially produced a weak response when the lactones were extracted with dichloromethane. When the pH was lowered to between 7 and 8, a better recovery was achieved. The pH was further adjusted to between 6 and 7 and the use of ethyl acetate as an alternative solvent each produced improved results, as shown in

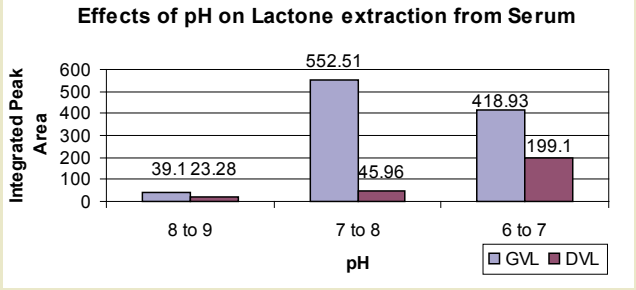

Figure 4. Effects of pH on the lactones in serum.

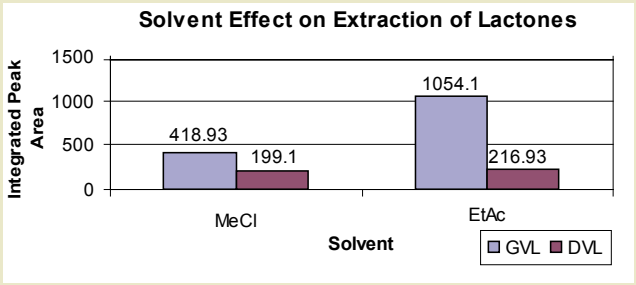

Figure 5. Results of the lactones in saliva and serum.

Figures 4 and 5. It was found with both lactones that ethyl acetate proved to be the better extraction solvent. Lyophilization followed by derivatization with MTBSTFA of the serum samples proved to produce good responses for the sodium salts of the lactones when analyzed by GC/MS (Figure 2).

Azinphos methyl and acephate.

Analysis of the standards showed reasonable responses, which are shown in Figure 6. The base ion of azinphos methyl (m/z = 160) is thought to be due to the loss of the -SPS(OCH_3)$_2$ group from the parent compound, and the base ion for acephate (m/z = 136) is believed to be due to the loss of the –SCH_3 group from the phosphate (Figures 3a and 3b). The results for acephate spiked into saliva and serum produced reasonable results. The response for azinphos methyl in saliva was not nearly as prominent; however the serum extract showed good results (Figure 6).

The overall comparison of metabolized and unmetabolized results for each analyte is illustrated in Figure 7. Results of the *in vitro* tests and comparison the chromatograms from the metabolized and non-metabolized samples showed there were potential nonpolar metabolites for azinphos methyl. A comparison of the chromatograms from metabolized and non-metabolized extracted samples of acephate and GVL showed no unique peaks. Therefore, if a metabolite is being created, it is not being derivatized under these conditions. However, a possible metabolite near 14 minutes was observed for the GVL sample that was derivatized

CONCLUSIONS

The initial results of this study show that unique metabolites may exist for these compounds and that saliva could be a possible matrix for the analysis of exposure to these chemicals. Gas chromatography/mass spectrometry was found to be an effective tool for analyzing the samples although derivatization was required in some cases.

It was found during development that certain solvents worked better than others at extracting the analytes. The use of ethyl acetate was more effective because it is more polar than dichloromethane. It was also determined that the use of diazomethane as a derivatizing agent was inferior for the lactones. This was due to the acidic conditions required for the derivatization reaction which also causes an intramolecular cyclization of the lactones. Also the use of N-methyl-bis(trifluoroacetamide) MTBFA was not as effective as MTBSTFA because it appeared to be affected by the presence of residual water, which caused it to no longer derivatize the sodium salts of the lactones.

The formation of a lactone (cyclic ester) from the corresponding hydroxyl acid is an equilibrium process. Significant amounts of product are usually only obtained when a five- or six-membered ring would result; since these have angles closest to the optimum open chain value and, therefore, less ring strain. In fact, gamma-lactones and delta-lactones undergo intramolecular esterification from their hydroxyl acid counterparts so readily that an acid catalyst is often not needed. However, data presented from a study of hydrolytic equilibria of lactones shows that alkyl substitution on the ring increases the amount of lactone present at equilibrium (demonstrated in Figure 8) [9]. This may explain why there is a reversal in the relative amounts of the gamma- and delta-lactones recovered from serum (shown in Figure 4 for lactone extraction) compared to the

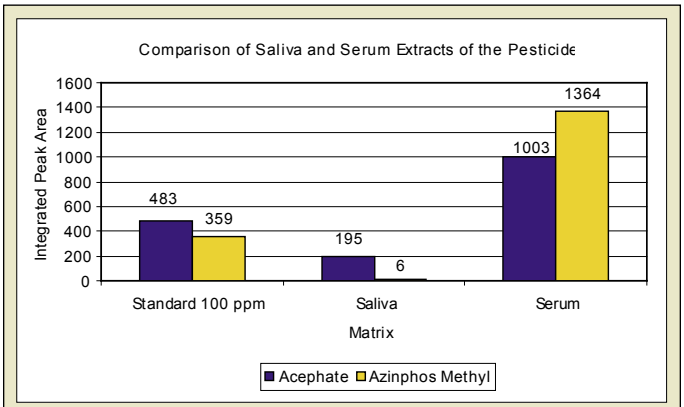

Figure 6. Results of the pesticides in saliva and serum.

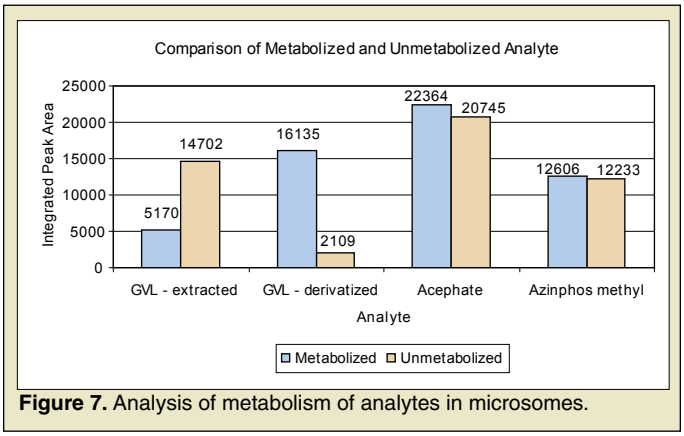

Figure 7. Analysis of metabolism of analytes in microsomes.

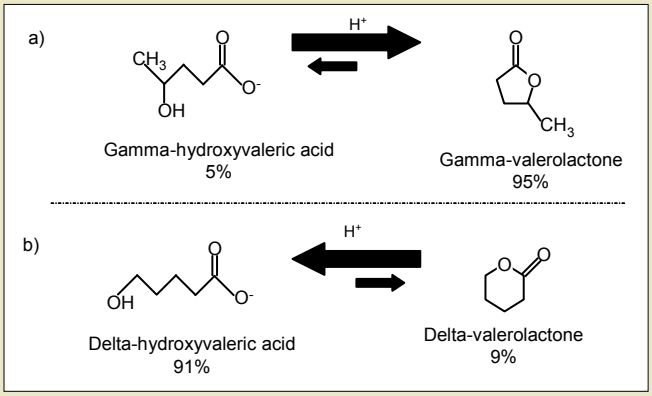

Figure 8. Demonstration of the unequal distribution of gamma- and delta-valeric acid with the corresponding lactones in solution due to the methyl side chain.

gamma- and delta-hydroxyl acids recovered from saliva and serum (shown in Figure 2).

Continuation of this research would also include analysis with GC/MS under positive ion mode. This would help to determine the parent ion (molecular weight) of the unknown metabolites, which would aid in their identification. On-column injection techniques for GC/MS analysis of the lactones would also verify whether thermal lability is affecting the recovery results.

Future work in this research line will also include moving from *in vitro* studies to *in vivo* studies. This research will create techniques that could be used for advance warning tests for other hazardous chemicals, and detection for the use of illegal drugs. This could also be used forensically to determine if particular suspects were either making the warfare agents or the drugs in question. Economically this will create more cost-effective techniques for farmers who must monitor workers for exposure to pesticides and decrease the medical costs for those individuals exposed to such chemicals.

Safety note

MTBSTFA has significant safety risks. These risks include violent reactivity with water which could produce hydrofluoric acid. MTBSTFA is highly flammable and the resulting toxic fumes consist of carbon monoxide, carbon dioxide, silicon oxides, nitrogen oxides and hydrogen fluoride gas. Ingestion, inhalation and contact with the skin must be avoided by using proper measures and precautions found in the material safety data sheet.

ACKNOWLEDGMENTS

We would like to thank Pacific Northwest National Laboratory and DOE for the use of their facilities during the research appointment. Special thanks go to our mentors Jim Campbell and Eric Hoppe for their guidance and their support on this project. We would like to thank Torka Poet, Richard Gies, and Allison Cartmell in the Biology Department for their assistance with the *in vitro* studies. We also thank Royace Aikin and Dale Johns for encouraging us to apply for the FaST program and for supplying the means in which we were able to accomplish the research conducted.

REFERENCES

[1] Campbell, et al. "Negative ion chemical ionization mass spectrometry for the analysis of trichloropyridinaol in saliva of rats exposed to chlorpyrifos." Battelle, Pacific Northwest Division. Accepted for publication in Analytical Letters.

[2] http://www.pesticideinfo.org/Docs/ref_general3.html#ChemClassDescr .

[3] Buratti, et. al. "CYP-specific bioactivation of four organophosphorothioate pesticides by human liver microsomes." Toxicology and Applied Pharmacology. Vol 186:3, Feb. 2003, pg. 143-154.

[4] Kosiainen, et. al. "Liquid chromatography/atmospheric pressure ionization-mass spectrometry in drug metablolism studies", Journal of Mass Spectrometry, vol. 38, 2003, pp 357-372.

[5] Hines, et al. "Biological Monitoring for Selected Herbicide Biomarkers in the Urine of Exposed Custom Applicators: Application of Mixed-effect Models," Annals of Occupational Hygiene, Vol 47, No. 6, 2003, pp 503-517.

[6] GHB (Gamma-Hydroxybutyrate) Synthesis FAQ. Rhodium. http://www.rhodium.ws/chemistry/ghb.html.

[7] Handbook of Analytical Derivatization Reactions. Knapp, Daniel R, John Wiley & Sons, Inc. 1979, p. 32.

[8] Garcia. "Quantitation of gamma-hydroxybutyric acid and gamma-butyrolactone using capillary electrophoresis and high performance liquid chromotagraphy." http://www.fiu.edu/~almirall/students.htm.

[9] Streitwieser. Introduction to Organic Chemistry. University of California, Berkley, MacMillan Publishing Co., New York, 1985, 3rd ed., pg. 860.

[10] Campbell, et. al. "*In Vitro* Metabolism Study with a mixture of the organosphosphate insecticides chlorpyrifos and diazinon", In: Proceedings of the American Society of Mass Spectrometry and Allied Topics, Long Beach, CA., 2000.

Jessica Blanton is a biology major at Amherst College. During the summer of her senior year, she conducted research at Lawrence Berkeley National Laboratory as a participant in the DOE Science Undergraduate Laboratory Internship program. For her internship she worked on a transformation system for the archae Sulfolobus solfataricus. This research was presented as a poster at the 2005 AAAS Meeting in Washington, DC. The following fall she stayed on at LBNL working on in vitro expression of human DNA repair proteins. She is now conducting her undergraduate thesis in the field of plant molecular phylogenetics, and will graduate in the winter of 2005. After graduating she plans to spend a year as a Research Assistant before pursuing a doctorate in the biological sciences.

Steve Yannone is currently a staff scientist at Lawrence Berkeley National Laboratory in the department of Molecular Biology. He completed his undergraduate studies in biochemistry at the University of California at Riverside, his Ph.D. in biochemistry at UC Irvine, and his postdoctoral training at Los Alamos National Laboratory. Steve began his research career with an undergraduate research scholarship to study insect kairomones in the department of entomology at UC Riverside. His graduate work was focused on cellular stress responses and redox status in the nitrogen fixing bacteria Azotobacter vinelandii. His graduate studies lead him into the field of DNA repair and he now leads an active research program at LBNL studying the biochemistry of mammalian DNA repair enzymes.

Jill Fuss is a postdoctoral fellow at Lawrence Berkeley National Laboratory in the laboratories of Priscilla K. Cooper and John A. Tainer. She received her Ph.D. in Molecular and Cell Biology from the University of California, Berkeley in 2001. Jill first became interested in basic science research as an undergraduate during a summer internship at the National Institutes of Health in Bethesda, MD. As a graduate student, Jill worked mainly in the field of DNA replication using biochemistry and cell biology to characterize a mammalian DNA polymerase. She is currently studying the structural biology of DNA repair. Jill is an NIH Ruth L. Kirschstein National Research Service Award Fellow and is a recipient of the 2002 Department of Energy Office of Science Outstanding Mentor Award. When not in the lab, Jill enjoys driving her diesel Volkswagen that runs on vegetable oil.

MODELING DNA REPAIR: APPROACHING *IN VIVO* TECHNIQUES IN THE HYPERTHERMOPHILE *SULFOLOBUS SOLFATARICUS*

Jessica Blanton, Jill Fuss, Steven M. Yannone,
John A. Tainer, Priscilla K. Cooper

ABSTRACT

Archaea are found in some of the most extreme environments on earth and represent a third domain of life distinct from Eukarya and Eubacteria. The hyperthermophilic archaeon *Sulfolobus solfataricus*, isolated from acidic hot springs (80°C, pH 3) in Yellowstone National Park, has emerged as a potential model system for studying human DNA repair processes. Archaea are more closely related to Eukarya than to Eubacteria, suggesting that archaeal DNA repair machinery may model the complex human system much more closely than that of other prokaryotes. DNA repair requires coordinated protein-protein interactions that are frequently transient. Protein complexes that are transient at extreme temperatures where archaea thrive may be more stable at room temperature, allowing for the characterization of otherwise short-lived complexes. However, characterization of these systems in archaea has been limited by the absence of a stable *in vivo* transformation and expression system. The work presented here is a pilot study in gene cloning and recombinant protein expression in *S. solfataricus*. Three genes associated with DNA repair were selected for expression: MRE11, PCNA1, and a putative CSB homologue. Though preparation of these recombinant genes followed standard methods, preparation of a suitable vector proved more challenging. The shuttle vector pSSV64, derived from the SSV1 virus and the *E. coli* vector pBSSK+, was most successfully isolated from the DH5α *E. coli* strain. Currently, alternative vectors are being designed for more efficient genetic manipulations in *S. solfataricus.*

INTRODUCTION

If left unrepaired, damage to an organism's DNA from both exogenous sources, such as UV radiation, and endogenous sources, such as the reactive oxygen species produced from metabolism, can cause permanent genetic changes. Mutations and chromosomal changes are often detrimental, leading to defects in function. It is because of these defects that understanding DNA maintenance and repair mechanisms is important for medical research, notably in studying cancer and degenerative diseases.

One means of investigating repair mechanisms is through comparative organismal studies. This is especially applicable for

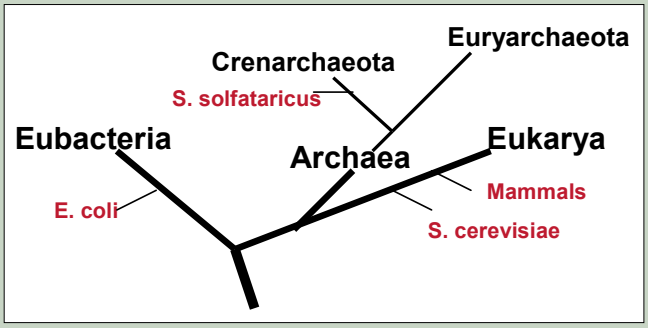

Figure 1. Phylogenetic relationship between the three domains of life. Archaea and Eukarya diverge after the split from Eubacteria.

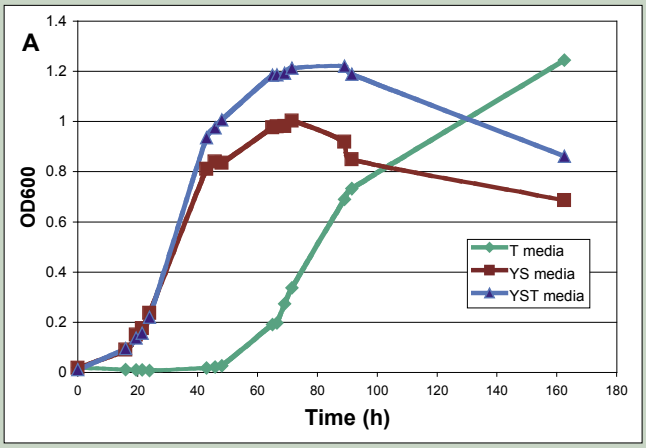

Figure 2. (A) *S. solfataricus* growth during 170h. (B) Semi-logarithmic plot of *S. solfataricus* growth during 170 h at 80°C.

DNA repair research, since genome maintenance is of such high importance that these mechanisms are found highly conserved or analogous across all life. These studies can also provide clues as to the evolutionary path of mammalian DNA repair and damage response. One such model organism under study is *Sulfolobus solfataricus*, a species representing the third domain of life—the archaea.

Archaea are prokaryotes, but the divergence between Archaea and Eukarya lies after the split from Eubacteria (Figure 1), therefore archaea are more closely related to eukaryoes than bacteria [1]. Many of these microbes are extremophiles, living in some of the harshest conditions on earth, up to temperatures of 113°C and to pHs below 1.0 [2]. Though they maintain internal pHs much closer to 7.0, the internal temperature matches that of the environment [3]. In this extreme heat, archaea perform cellular functions, including the difficult task of keeping their genome intact at temperatures shown ordinarily to drastically increase the error rate during DNA replication [4,5].

Archaeal repair mechanisms are of high interest to the scientific community for a number of reasons. Archaeal DNA transcription shares characteristics with that of both Eubacteria and Eukarya [1]. This implies archaea may be an intermediate system that could illuminate the evolution of eukaryotic DNA repair [6,7,8]. Also, some archaea are hyperthermophiles and employ arsenals of proteins that function at high temperatures. These proteins should be very stable at room temperature, relative to those of mesothermophiles, and working with such proteins may allow researchers to more easily trap their dynamic complexes [6].

S. solfataricus is a hyperthermophilic archaeon found in Yellowstone hot springs that has optimum growing conditions of 80°C, pH 3 [2]. This organism is a good candidate for a model archaeal system because it is practical for laboratory use relative to other extremophiles (growth temperature below boiling and pressure at 1 atmosphere) and the annotated genome has been published [9,10]. Previous studies have characterized *S. solfataricus* DNA repair pathway genes by expressing and extracting the proteins from *E. coli* hosts. This is in part because of the high degree of knowledge, experience, and molecular biological tools developed for the *E. coli* system, but more pointedly because of the absence of a stable archaeal transformation system.

In order to clone genes into archaea, viral vectors are currently being developed that are infective, expressible, and stable. SSV1 is one such archaeal virus that has been highly characterized, from which the vector pSSV64, inducible with either UV radiation or mitomycin C, has been produced [11, 12, 13].

The research presented here represents a series of pilot studies of *in vivo* expression of supposed *S. solfataricus* DNA repair genes, with the intent to extract *S.so* protein complexes. Three genes associated with DNA repair were selected for study. The first gene, an MRE11 homologue, is involved with DNA double-strand break repair. The protein structure has been solved from the archaeon *Pyrococcus furiosus* [14]. PCNA-1 is a well-characterized "DNA

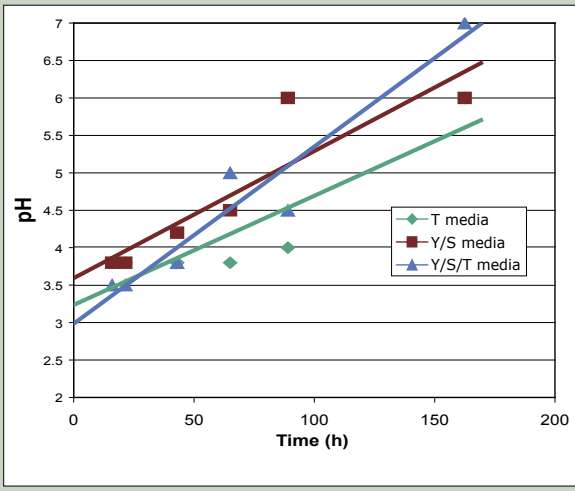

Figure 3. Acidity of *S. solfataricus* cultures over 170 h at 80°C. Lines represent a linear regression of the data.

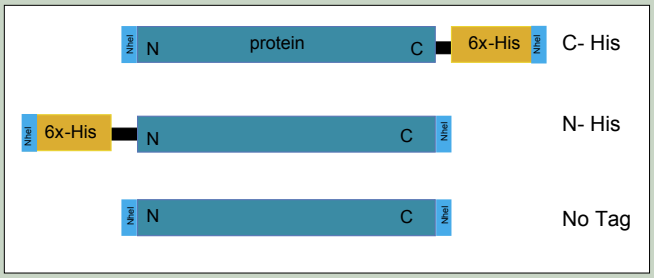

Figure 4. Orientation of the histidine tag (6xhis) for each insert. NheI restriction endonuclease sites will be used to clone the genes into the pSSV64 shuttle vector.

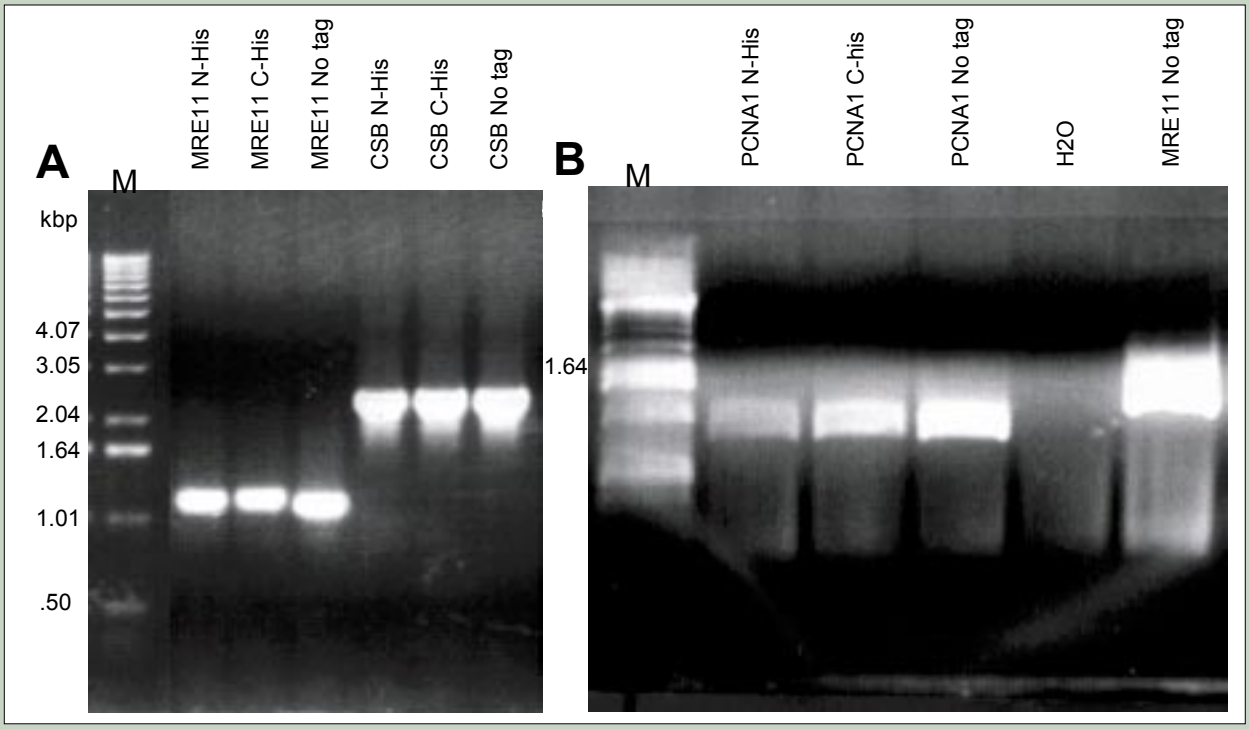

Figure 5. (A) PCR of MRE11 and CSB constructs performed at 65°C. (B) PCR of PCNA-1 construct performed at 60°C. Controls using either no primers or Mre11 primers were performed as negative and positive controls, respectively.

clamp" from *S. solfataricus,* of which the homologues increase the processivity of DNA polymerase in other organisms and has been well characterized from expression in *E. coli* but not yet expressed in *S. solfataricus* [15]. Lastly, a SWI/SNF ATPase (putatively a CSB-like protein referred to here simply as CSB) was chosen. It is a critical protein for transcription-coupled repair in mammals, and of which little is known in archaea [16]. These studies will contribute to developing *S. solfataricus* as a model organism, opening the door for the study of many thermostable proteins. Because of the phylogenetic relationship of archaea to eukaryotes, characterization of these proteins will in turn aid in understanding the dynamic protein complexes of our own repair systems.

MATERIALS AND METHODS

Materials

Archaeal strain *S. solfataricus* P2 and pSSV64 viral vector were provided by Ken Stedman. Five bacterial *E. coli* cell lines were used: TOP10F', GeneHOG, Stbl3, DH5α (all four Invitrogen) and SURE 2 (Stratagene). A shuttle vector pCR2.1-TOPO (Invitrogen) was used for *E. coli* transformation of PCR products. One restriction enzyme, Nhe1 (NEB), was used.

S. solfataricus cell growth

S. solfataricus P2 cells were grown aerobically in 50 ml liquid cultures at 80°C. Media was prepared in accordance with Zillig *et. al* [17]. Three different media were used containing either 0.2% tryptone, 0.1% yeast extract and 0.2% sucrose (Y/S/T media); or 0.1% yeast extract and 0.2% sucrose (Y/S/T media); or only 0.2% tryptone (T media) as a carbon source. All media contained 0.3% ammonium sulfate, 0.07% glycine, 0.05% potassium hydrogen phosphate, 0.01% potassium chloride, 0.01% magnesium chloride, and 0.005% calcium nitrate. To a final volume of 1L, the following volumes of 1% solutions were added: 244µl sodium borate, 90 µl manganese chloride, 11 µl zinc sulfate, 2.5 µl cupric sulfate, 1.5 µl sodium molybdate, 1.5 µl vanadyl sulfate, 0.5 µl cobalt chloride, and 0.5 µl nickel sulfate. The carbon source was added, the media was adjusted to pH 3.2 with a 1:1 dilution of sulfuric acid in water, autoclaved, and stored at 4°C after opening. All solutions were prepared as percent weight volume (w/v) except where indicated.

Cell growth and culture pH was monitored by Optical Density measurements at 600nm (OD_{600}) and indicator paper respectively.

S. solfataricus total DNA isolation

Total DNA was prepared by phenol extraction as according to Stedman *et al.*, 1999 [12], using 50 ml of *S. solfataricus* growing at log phase (OD_{600}=0.323). Purity and concentration were determined by $OD_{260/280}$ measurements.

Construction of MRE11, CSB and PCNA1 inserts

A six-histidine tag and NheI restriction sites were introduced to MRE11, CSB and PCNA1 genes during Polymerase Chain Reaction (PCR) amplification with Taq polymerase, using *S. solfataricus* genomic DNA as template. The primers were checked against hairpins and dimers, and for ideal annealing temperature with

DNASTAR. All PCR products were confirmed on a 1% agarose gel with 0.5µg/ml ethidium bromide.

PCR products were adenylated for TOPO TA cloning by adding 1µl of 100mM dATP, 0.5µl Taq polymerase to each reaction in a total volume of 50µl (Invitrogen). Each insert was cloned into the pCR2.1-TOPO vector and transformed into One Shot TOP10F' *E. coli* cells (Invitrogen).

Transformed cells were plated on LB plates selecting for ampicillin resistance and grown overnight. Overnight liquid cultures were inoculated from single colonies and the plasmid DNA was isolated as described using Wizard *Plus* SV Minipreps DNA Purification System as per the manufacturer's instructions (Promega). All constructs were verified by restriction digest with Nhe1 and by sequencing.

Inserts were cut from the plasmid by NheI digestion, and purified by gel extraction (GeneClean - Bio 101).

Preparation of pSSV64

The pSSV64 vector was transformed into the four *E. coli* strains, which were plated on LB + 100µg/ml ampicillin and grown overnight. Liquid cultures of LB + 50µg/ml ampicillin were inoculated with single colonies and grown overnight at 25°C for 24 hours. Isolation of pSSV64 was performed by an alkaline lysis extraction. Pellets from overnight cultures were lysed with 300µl of a 1% SDS, 200mM sodium hydroxide solution and neutralized with 300µl of a 3M potassium acetate (pH 5.5) solution. Cell debris and genomic DNA was pelleted out by a 15 min centrifugation at 14000 x g. The aqueous phase (850 µl) was centrifuged again and a final volume of 800µl supernatant containing the pSSV64 vector was extracted. The pSSV64 vector was precipitated with 800µl isopropanol and centrifuged 30 min at 14000 x g. After removing the supernatant the pellet was washed with 500µl 70% (v/v) ethanol and centrifuged 5 min at 14000 x g. This ethanol wash and centrifugation was repeated three times to extract salts. The pellet was dried overnight and dissolved in 40µl H_20. The vector was verified on a 0.5% agarose gel with 0.5µg/ml ethidium bromide.

RESULTS

Culture growth

S. solfataricus grew faster in Y/S and Y/S/T media (peak OD_{600} at 80 h) than the T media (peak OD_{600} at final timepoint at 170 h) (Figure 2A). Though the peak density of the Y/S media (OD_{600} = 1.0) did not reach that of the Y/S/T media (OD_{600} = 1.2), the T media surpassed both with a final OD_{600} of 1.3. The doubling times calculated from the growth curve (Figure2B) were 6.7 h for the Y/S/T media, 5.8 h for the Y/S media, and 6.0 h for the T media. No significant difference in generation times between media or correlation with carbon abundance was noted**.** Over time, all three cultures rose in pH. The Y/S/T media showed the most drastic increase while the T was the slowest to rise (Figure 3).

Insert construction

Design of the MRE11, CSB and PCNA1 primers involved the insertion of a six-histidine tag. To ensure accessibility of the histidine tag on the protein, three constructs were made of each protein, changing the orientation of the tag (Figure 4). The PCR reaction was run with an annealing temperature of 65°C. The MRE11 and CSB reactions produced product (figure 5A), but the PCNA1 reactions were successful only when the annealing temperature was lowered to 60°C (figure 5B). Sequences are shown in Table 1.

For more efficient cloning into the viral vector, the PCR products were adenylated and cloned into the pCR2.1-TOPO vector, amplified and then liberated by Nhe1 digestion. These digests

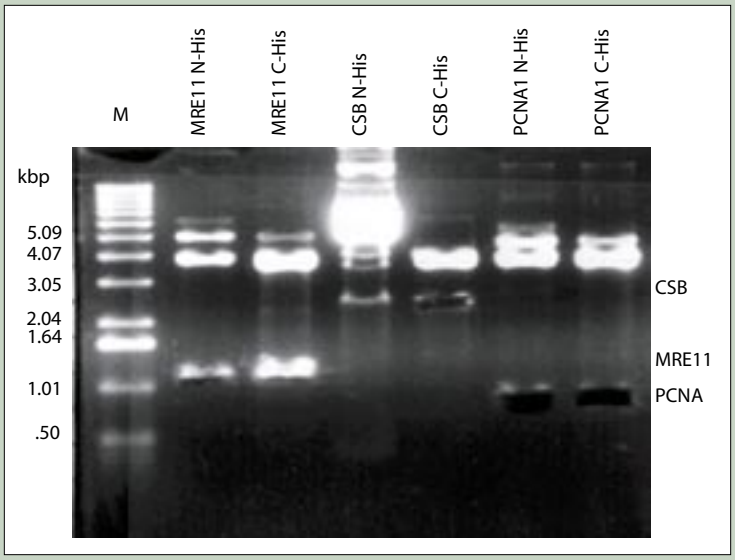

Figure 6. Gel separation of NheI digestion. Inserts were removed from gel for gel purification. Fragments were resolved on a 1.0 % agarose gel with 0.5µg/ml EtBr.

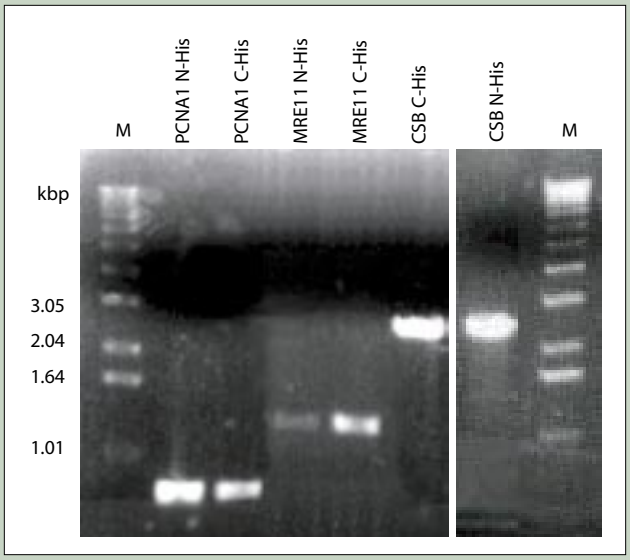

Figure 7. GeneClean gel purification confirmation of inserts. Purified fragments were resolved on a 1.0 % agarose gel with 0.5µg/ml EtBr.

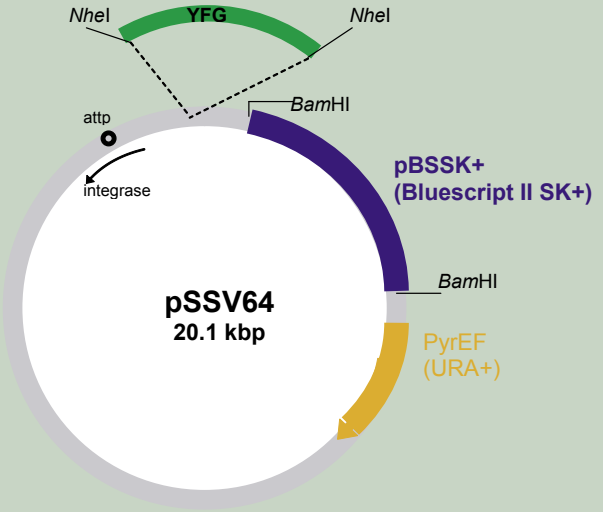

Figure 8. pSSV64 vector. Bluescript plasmid was inserted for bacterial replication, ampicillin resistance, blue/white screening. URA+ complementation from the pyrEF gene [13].

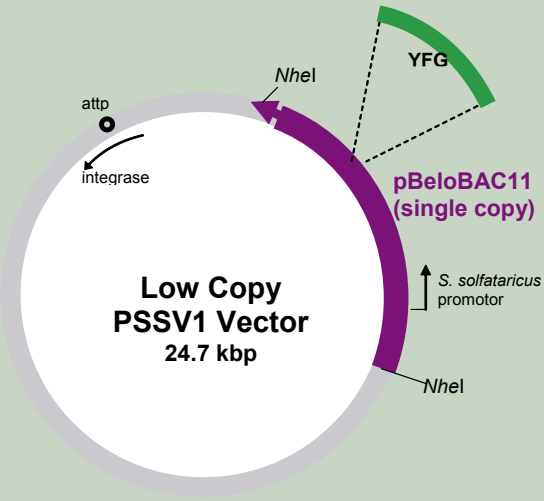

Figure 10. Proposed single copy viral shuttle vector designed with pBeloBAC11 bacterial plasmid and SSV1 virus for future insert expression of your favorite gene (YFG).

were run out on a 1.0% agarose gel (figure 6) to isolate the inserts. These bands were cut from the gel and purified (figure 7).

pSSV64 isolation

The pSSV64 vector (Figure 8) is a large construct comprised mainly of the archaeal virus, SSV1. The plasmid pBSSK+ was inserted for replication in bacteria, ampicillin resistance and blue/white selection [13]. The *pyr*EF gene provides complementation for *S. solfataricus* URA- mutants.

Because of the large size of this vector, pSSV64 has a much higher recombination rate than the smaller, commonly used bacterial plasmids. To ensure isolation of full-length vector four strains of *E. coli* GeneHOG, Stbl3, SURE 2 and DH5α were selected for transformation and extrachromosomal DNA isolated from these *E. coli* strains was run against a Hind λ DNA digest marker. Only the DH5α showed significantly more product in the 20.1 kbp band than

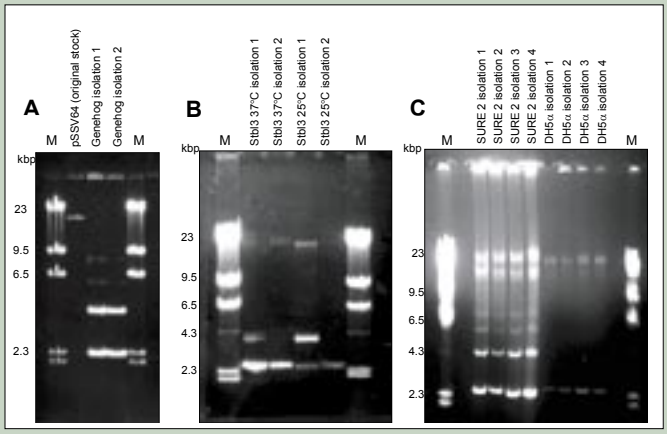

Figure 9. Isolation of pSSV64 from E. coli. (A) GeneHOG grown at 37°C, (B) Stbl3 grown at 37°C and 25°C, (C) SURE 2 and DHFα grown at 25°C. Run against a HIND λ DNA marker on a 0.5% agarose gel with 0.5μg/ml EtBr.

in any smaller band. The GeneHOG cells produced no noticeable amount of the full 20.1 kbp vector; instead, four smaller bands were seen (Figure 9A). The other three cell lines produced similar small bands to the GeneHOG but also produced the full-length pSSV64 (Figures 9B,C).

DISCUSSION AND CONCLUSIONS

Growing S. solfataricus

Overall it was found that the richer media (Y/S and Y/S/T) provided faster culture growth, though the T media may potentially reach the highest densities. Growth in the Y/S and Y/S/T media began to fall off immediately after peaking, which may be due to the rise in pH over time, making the environment too neutral for *S. solfataricus*. This rise may be caused by the accumulation of waste products and from cell lysis, which would release internal cell contents (maintained at a neutral pH in living cells) into the media. Continually buffering growth media with 10 mM citrate could counter this effect.

Insert preparation follows standard methodologies

In preparing the selected gene for ligation into the shuttle vector, standard genomic template isolation, PCR, cloning, and purification methods were performed successfully. This indicates that preparation of *S. solfataricus* genes requires no more development than is normally used for bacterial gene preparation.

Vector isolation is ill suited to E. coli hosts

Four strains of E. coli were transformed with the pSSV64 vector, and extrachromosomal DNA isolated from these cultures were too small to be the full viral vector. This indicates a high recombination

Gene	Direction	Tag	Sequence (5' to 3')
Mre11	For.	N-term 6x-His	GAGCTAGCATGCATCATCATCATCATCATGTACAAATTTTACATATTTCTGATACTC
	Rev.	-	GAGCTAGCTTATAAGTTAACACCTGTTAACTTTTTTAATATC
	For.	-	GAGCTAGCATGGTACAAATTTTACATATTTCTGATACTC
	Rev.	C-term 6x-His	GAGCTAGCTTAATGATGATGATGATGATGTAAGTTAACACCTGTTAACTTTTTTAATATC
CSB	For.	N-term 6x-His	GAGCTAGCATGCATCATCATCATCATCATTGGATAGTCCATGGCGTATGGGAC
	Rev.	-	GAGCTAGCTTATATGATATCGAATAAGATGACTGCATGAG
	For.	-	GAGCTAGCATGTGGATAGTCCATGGCGTATGGGAC
	Rev.	C-term 6x-His	GAGCTAGCTTAATGATGATGATGATGATGTATGATATCGAATAAGATGACTGCATGAG
PCNA-1	For.	N-term 6x-His	GAGCTAGCATGCATCATCATCATCATCATATATATCTTAAATCTTTTGAAAGG
	Rev.	-	GAGCTAGCTTAAACTTTTGGAGCTAATAAATAAG
	For.	-	GAGCTAGCATGATATATCTTAAATCTTTTGAAAGG

Table 1. Primer oligonucleotide sequences.

rate by the bacteria, producing smaller sized plasmids. Of these four strains, the DH5α strain proved most successful in producing substantial amounts of full-length viral DNA (20kbp) versus any smaller recombinant isolates. This difficulty in isolation, even when using strains constructed specifically for use with large or unstable DNA (Stbl3 and SURE 2) was probably due to the extremely large size of the pSSV64 vector (4 times the size of average bacterial vectors) and also to the high copy nature of the pBSSK+ bacterial plasmid insert. Though DH5α is a standard laboratory strain, it does carry the *recA1* mutation, reducing homologous recombination ability and presumably aiding the retention of the full size of the pSSV64 vector. However, the other three strains as well carry *rec* mutations, leaving their high recombination rate unexplained.

Further Directions

It will be possible to continue with protein expression using the vector isolated from the DH5α strain by ligating the genes of interest directly into an NheI digested vector sample. The 2kbp contaminant fragment seen in the isolation will likely not interfere with protein expression because it will be insufficient to support viral growth. The resulting construct will be electroporated into *S. solfataricus* DS522 cells, complementing the URA- defect of the strain for transformant screening. This is a self-spreading vector that should propagate through a culture entirely, not causing cell death but retarding growth. Replication and expression of this vector will be induced with UV radiation and protein purification will be attempted by standard purification methods.

A second method of obtaining sufficient quantities of pSSV64 will be to infect a *S. solfataricus* population and isolate the vector directly from the archaea. Alternatively, a second vector has been designed to alleviate some of the complications of pSSV64 (Figure 10). This vector would use the single copy plasmid pBeloBAC11, instead of the high copy pBSSK+, requiring less energy from the bacterium to maintain it. This vector will contain a *S. solfataricus* promoter for gene expression and lack the *pyr*EF nutritional marker.

If these three proteins can be successfully expressed in *S. solfataricus*, it will open the door for further protein expression and characterization of not only the DNA repair pathways, but other processes as well.

ACKNOWLEGEMENTS

I would like to thank my mentor, Dr. Jill Fuss, for her knowledge and her patience. Thanks also to Priscilla Cooper, the Cooper lab, and Steve Yannone, for their time and the enthusiasm with which they taught me. Lastly, thanks to the Department of Energy and the Office of Science for this wonderful opportunity to participate in the Science Undergraduate Laboratory Internship (SULI) program.

REFERENCES

[1] P.J. Keeling and W.F. Doolittle, "Archaea: Narrowing the gap between prokayotes and eukaryotes," *Proc. Natl. Acad. Sci. USA*, vol. 92, pp. 5761-5764, June 1995.

[2] D. W. Grogan, "Phenotypic Characterization of the Archaebacterial Genus *Sulfolobus*: Comparison of Five Wild-Type Strains," *Am. Soc. Microbiol.*, vol. 171, pp. 6710-6719, 1989.

[3] S.V. Albers, J.L. van de Vossenberg, A.J. Driessen, W.N. Konings, "Adaptations of the archaeal cell membrane to heat stress," *Front. Biosci.*, vol. 1, no. 5, pp. D813-D820, 2000.

[4] T. Lindahl, "Instability and decay of the primary structure of DNA," *Nature*, vol. 362, pp. 709-715, 1993.

[5] J. Marmur, P. Doty, "Determination for the base composition of deoxyribonucleic acid from its thermal denaturation temperature," *J. Mol. Biol.*, vol. 5, pp109-118, 1962.

[6] D.W. Grogan, "Hyperthermophiles and the problem of DNA

instability," *Mol. Microbiol.*, vol. 26, no. 6, pp. 1043-1049, 1998.

[7] M.F. White, "Archaeal DNA repair: paradigms and puzzles," *Biochem. Soc. Trans.*, vol. 31, pp. 690-693, 2003.

[8] D.W. Grogan, "Stability and repair of DNA in hperthermophilic archaea," *Curr. Issues Mol. Biol.*, vol. 6, no. 2, pp. 137-144, July 2004.

[9] Q. She, R.K. Singh, F. Confalonieri, Y. Zivanovic, G. Allard, M.J.Awayez, C.C. Chan-Weiher, I.G. Clausen, B.A. Curtis, A.D. Moors, G. Erauso, C. Fletcher, P.M. Gordon, I. H.-d. Jong, A.C. Jeffries, C.J. Kozera, N. Medina, X. Peng, H.P. Thi-Ngoc, P. Redder, M.E. Schenk, C. Theriault, N. Tolstrup, R.L. Charlebois, W.F. Doolittle, M. Duguet, T. Gaasterland, R.A. Garrett, M.A. Ragan, C.W. Sensen, and J.V. d. Oost, "The complete genome of the crenarchaeon *Sulfolobus solfataricus* P2," *Proc. Natl. Acad. Sci. USA*, vol. 98, pp.7835-7840, 2001b.

[10] M. Ciaramella, F.M. Pisani, M. Rossi, "Molecular biology of extremophiles: recent progress on the hyperthermophilic archeon *Sulfolobus*," *Antonie van Leeuwenhoek,* vol. 81, pp. 85-97, 2002.

[11] C. Schleper, K. Kubo, W. Zillig, "The particle SSV1 from the extremely thermophilic archaeon *Sulfolobus* is a virus: Demonstration of infectivity and of transfection with viral DNA," *Proc. Natl. Acad. Sci. USA*, vol. 89, pp. 7645-7649, August 1992.

[12] K.M. Stedman, C. Schleper, E. Rumpf, W. Zillig, "Genetic Requirements for the function of the archael virus SSV1 in *Sulfolobus solfataricus*: Construction and Testing of Viral Shuttle Vectors," *Genetics*, vol.152, pp. 1697-1405, August 1999.

[13] M. Jonuscheit, E. Martusewitzch, K.M. Stedman, C. Schleper, "A reporter gene system for the hyperthermophilic archaeon *Sulfolobus solfataricus* based on a selectable shuttle vector," *Mol. Microbiol.*, vol, 48, no. 5, pp. 1241-1252, 2003.

[14] K.P. Hopfner, A. Karcher, D. Shin, C. Fairley, J.A. Tainer,J. P. Carney, "Mre11 and Rad50 from Pyrococcus furiosus: cloning and biochemical characterization reveal an evolutionarily conserved multiprotein machine," J. Bacteriol., vol. 182, pp. 6036–6041, 2000a.

[15] I. Dionne, R.K. Nooklala, S.P. Jackson, A.J. Doherty, S.D. Bell, "A heterotrimeric PCNA in the Hperthermophilic Archaeon Sulfolobus Solfataricus," Mol. Cell, vol. 11, pp. 275-282, January 2003.

[16] C.L. Licht, T. Stevnsner, V.A. Bohr, "Cockayne syndrome group B cellular and biochemical functions," Am. J. Hum. Genet., vol. 73, no. 6, pp. 1217-1239, November 2003.

[17] W. Zillig, A. Kletzin, C. Schleper, I. Holtz, K. Janekovic, J. Hain, M. Lansendorfer, and J. K. Kristjansson, "Screening for *Sulfolabales*, their plasmids and their viruses in Icelandic Solfataras.," *System. Appl. Microbiol.*, vol. 16, pp. 609-628, 1994.

ABSTRACTS

TABLE OF CONTENTS

BIOLOGY

Grassland Birds at Fermi National Accelerator Laboratory: A Study of Bird Populations with Respect to Habitat, Humidity, Temperature, Atmospheric Pressure, and Time of Day. *AMANI ABUHABSAH (University of Illinois at Chicago, Chicago, IL 60612) RODNEY WALTON (Fermi National Accelerator Laboratory, Batavia, IL 60510).* Nationwide, grassland birds are suffering the most abrupt population declines of any habitat-specific group. Fermilab has dedicated over 1,000 acres of land to reconstruction of natural grasslands. Seven sites on Fermilab property were included in this study investigating species preferences of habitats. Each site was visited four times at four different periods of the day. One- half hour was spent at each site making observations of bird presence. In order to determine if there was a correlation between bird populations and different sites, an Analysis of Variance (ANOVA) was carried out. The result of the analysis showed that there is no evidence to support the notion that the areas are significantly different with respect to their use by birds. A one-way ANOVA comparing the time of day that the data was collected was also carried out, and was also not significant. Statistical tests conducted to examine the influences of temperature, humidity, and wind on bird presence revealed a statistically significant relationship between humidity and bird presence. Further studies can be conducted to see how humidity affects birds, and whether this correlation is significant. The last test that was performed was a t-test to see if birds prefer recently burned sites or sites that have not been burned for over two years. The result of this test was not significant. Further research may be conducted to determine species preference for burned versus non-burned sites and the land management implications.

Isolating Aptamers that Bind to ATP. *NADIA AHMED (University of Illinois at Chicago, Chicago, IL 60607) MICHELLE BENIG ARORA (Argonne National Laboratory, Argonne, IL 60439).* The study of disease requires an understanding at the cellular level. Therefore, tracking intracellular targets will prove to be beneficiary. The result of this is that intracellular function may be monitored under different stresses and thus allow in the future, better diagnosis and treatments of diseases. Since intracellular molecules are so small, found at the nano and pico scale, locating them is very difficult. Using aptamers is a promising and efficient way. Aptamers are small, artificially created nucleic acids that selectively bind to molecules. Aptamers can be easily made, very stable (do not denature easily), and can be created to bind to a specific molecule. Aptamers are created using the Systemic Evolution of Ligands by Exponential Enrichment, or SELEX process. Using this process is a proven method to upscale production of aptamers very quickly. The focus of this project is to use the SELEX method to find aptamers that will bind to adenosine triphosphate (ATP).

Synthesis of Magnetic Microspheres and Nanospheres for Controlled Drug Delivery and Toxin Removal Systems. *ADETOWUN ALIMI (University of Illinois at Chicago, Chicago, IL 60612) MICHAEL KAMINSKI (Argonne National Laboratory, Argonne, IL 60439).* The main object of focus is to vary the magnetic fraction of the microspheres and determine the resulting effect on the magnetic moment, surface charge, and microsphere size distribution. The ultimate goal of drug delivery is to incorporate drugs without damaging them, release drugs at its target location such as cells and tissue, and retain the microspheres within circulation without being recognized as a foreign object by the immune system. The spheres are coated with poly-ethylene glycol. This polymer gives the particles a stealth property, a characteristics which inhibits the immune system to recognize the particles as foreign objects. In a controlled drug delivery system, large spheres with adequate drug capacities are necessary. Specifically, we desire microspheres with a size range approximately or greater than several hundred nanometers. Contrarily, in the toxin removal system, small particles between 200-400 nanometers will be produced. The size range will ensure larger surface area, which will enhance many surface receptors to bind to numerous toxins. Being magnetic, the nanospheres can be filtered from the blood using an extra corporeal magnetic filter being designed under this program.

Utilizing the CreA Gene to Better Understand Carbon Flux in Fungi. *MATT ANNECHARICO (Middlesex Community College, Middletown, CT 06345) SCOTT BAKER (Pacific Northwest National Laboratory, Richland, WA 99352).* Carbon catabolite repression (CCR) is a system which represses the synthesis of enzymes required for certain carbon sources when more favored carbon sources are present. Fungal enzymes are useful in various industrial applications such as the degradation of bi-product biomass produced in many areas of manufacturing and production. For example, the basidiomycete, Phanerochaete chrysosporium, a filamentous fungus, produces a number of lignin peroxidases (LiPs) such as an extra-cellular lignin-modifying protein and manganese-dependent peroxidase (MnPs). The LiPs secreted by P. chrysosporium are able to break down lignin, one of the main substances of wood, while leaving the cellulose behind. These enzymes are capable of degrading toxic waste as well as biomass waste. Through polysaccharide hydrolysis and lignin utilization, biobased products and biofuels can be processed from biomass instead of petroleum, which is more environmentally sound than current fuel options. Previous research in the fungal phylum, Ascomyces has shown that the creA gene is an important gene that controls various enzymes which have key roles in controlling carbon utilization by fungi. We hypothesize that there are similarities across all fungi in the mechanism by which carbon flux is controlled and that orthologs of the creA gene exist in all fungal phyla. A COnsensus-DEgenerate Hybrid Oligonucleotide Primers (CODEHOP) polymerase chain reaction (PCR) strategy was used to isolate genomic fragments of the creA gene from a variety of fungi with the objective to design and utilize a method for isolation of the creA gene from a wide range of fungi.

Adenovirus Proteinase: Characterization of the DNA Binding Site. *NEIL BAJPAYEE (The Pennsylvania State University, State College, PA 16802) WALTER F. MANGEL (Brookhaven National Laboratory, Upton, NY 11973).* The human Adenovirus Proteinase (AVP) is a target for potential antiviral drug therapies. For maximal activity, AVP requires two cofactors, whose binding domains have become the focus for biochemical inhibition. The sequence specific binding site of the cofactor pVIc, an 11-amino-acid peptide, has been determined by crystallographic analysis. However, the binding position of the second cofactor, Adenovirus DNA, remains unknown due to insolubility of the AVP-pVIc-DNA complex at low concentrations. The binding of DNA to AVP is known to occur nonspecifically. In response, similarly anionic polymers of glutamic acid (polyE) were characterized for DNA-like binding properties as a tool for crystallization. Activity assays measuring the rate of substrate hydrolysis of a fluorogenic rhodamine derivative specific to AVP-pVIc cleavage demonstrated stimulation of 2 to 33-fold in the presence of polyE of sizes 1.1 kD to 66 kD. A plateau of stimulation occurs after 18.1 kD polyE, suggesting a length dependency on the AVP for poly-anion. Utilizing fluorescence anisotropy, direct competition was seen between a 1.1 kD polyE and 12-mer DNA, indicating an equivalent binding site on the AVP protein for polyE and DNA. Upon binding of 10.6 kD polyE one ionic pair formation was recorded. A calculated ΔG^0 of -5.8 kcal for the nonelectrostatic free energy of binding signified a considerable element of the binding free energy results from nonspecific interactions. Comparably, DNA gave a ΔG^0 of -4.6 kcal and exhibited formation of two ion pairs. This study provides substantial evidence that polymers of glutamic acid not only bind to the identical site as the cofactor DNA on AVP but also can also stimulate the cleavage activity of the proteinase similar to DNA. The additional binding studies between DNA and polyE depict similar energies of nonelectrostatic binding and a small difference in ion pair formation upon binding. With this knowledge, crystallographic data from an AVP-pVIc-polyE complex will provide relevant information on the regional binding by the DNA cofactor.

Adenovirus Protienase: Interaction with Protein Cofactors of High Negative Charge. *NEIL BAJPAYEE (Pennsylvania State University, State College, PA 16802) WALTER F. MANGEL (Brookhaven National Laboratory, Upton, NY 11973).* The human Adenovirus Proteinase (AVP) is a target for potential antiviral drugs therapies. For maximal enzyme activity, AVP requires two cofactors, whose binding domains have been the focus for biochemical inhibition studies. The sequence specific binding site of the cofactor, pVIc, an 11-amino-acid peptide, has been determined by crystallographic analysis. However, the binding position of the second cofactor, Adenovirus DNA, remains unknown due to insolubility of the AVP-pVIc-DNA complex at concentrations required for crystallization. In response, anionic polymers of glutamic acid (polyE) were characterized for their DNA-like binding properties to AVP-pVIc as a tool for crystallization. Activity assays measuring the rate of substrate hydrolysis of a fluorogenic rhodamine derivative specific to AVP-pVIc cleavage demonstrated enzyme stimulation upon addition of increasing concentrations of the glutamic acid polymers. Using fluorescence anisotropy, direct competition was seen between the 1.1 kD polyE and a fluorescein-labeled 12-mer DNA, indicating an equivalent binding site on the AVP protein for both polyE and DNA. The dissociation constant, Kd, for the binding of 1.1 kD polyE was 56.2 nM at 25 C. From enzyme activity assays at tight binding conditions, stoichiometries were calculated for the binding of AVP-pVIc to each length of polyE. The stoichiometries were 1:1, 6:1, 15:1, 34:1, and 38:1 for 1.1 kD, 10.6 kD, 18.1 kD, 51.3 kD, and 66 kD polyE, respectively. Among the five polymers of glutamic acid assayed, AVP-pVIc binding spanned from 8.5 to 13.6 Glu

residues on the polymers. Enzyme kinetic constants, Km and kcat, were determined for AVP-pVIc with none, 1.1 kD, and 18.1 kD polyE. These data illustrated lower Km values and higher kcat values for AVP-pVIc in the presence of either polyE. Solubility tests have shown that equal molar solutions of AVP, pVIc, and 1.1 kD polyE are soluble to at least 200 μM, where as AVP, pVIc, and DNA become insoluble at 50 μM. This study has provided substantial evidence that polymers of glutamic acid not only bind to the identical site as the cofactor DNA on AVP, but can also stimulate the cleavage activity of the proteinase similar to DNA.

Fluctuation-Dissipation Theorem Predicting Microcantilever Noise. *SARIT BARHEN (Emory University, Atlanta, GA 303221) THOMAS THUNDAT (Oak Ridge National Laboratory, Oak Ridge, TN 37831).* The past few years have shown an incredible growth in micromechanical sensor development. As more demands are placed upon these sensors, the quality and accuracy of their sensing ability has become critically important. No longer can the implications of white noise be avoided, as sensors have become too receptive, and are significantly affected by the presence of white noise. Such is the case of the microcantilever system, where simple thermal fluctuations drive the system into Brownian motion. However, this natural phenomenon has been exploited and is now a key component of a new methodology that uses amplified thermal vibrations to drive the cantilever via a delayed feedback loop. With a variety of implications, this technique has improved the system's Q-factor by several orders of magnitude. To better understand and improve the effects of this phenomenon, the Fluctuation-Dissipation Theorem is applied to a theoretical microcantilever model. Dependent on components such as the temperature and damping magnitude of the model, it has the power to predict the strength of the thermal vibrations affecting the system. The theorem is analytically applied to a mass-spring model of the cantilever system, and implemented in a computer simulation on the program XPPAUT. XPPAUT allows experimentation with temperatures oscillation patterns. The theorem's ability to predict white noise as well as confirm improved Q-factor is then verified.

Understanding the Incident Ion Energy Effects on "Ridge" Like Structures Formed During the High-Energy Gold Ion Implantation on $SrTiO_3$ Single Crystal Surfaces. *JEREMY BARTON (Salt Lake Community College, Salt Lake City, UT 84321) VAITHIYALINGAM (SHUTTHA) SHUTTHANANDAN (Pacific Northwest National Laboratory, Richland, WA 99352).* Formation and nucleation of "ridge" like structures synthesized using MeV Au^2 implantation in $SrTiO_3$ single crystals was investigated using Rutherford backscattering spectrometry (RBS), scanning electron microscopy (SEM), energy dispersive x-ray emission (EDX), atomic force microscopy (AFM) and high-resolution transmission electron microscopy (HRTEM). Influence of incident ion energy on these "ridge" structures was investigated in detail. Approximately 333 Au^2/nm^2 with energies between 0.5 to 7 MeV were implanted at 60 off normal to the surface at 300 K in $SrTiO_3$ (100) single crystal substrates. SEM micrographs obtained from these samples clearly show that the surface of the implanted region underwent substantial rearrangement and formed "ridge" like structures. These "ridge" like structures are periodic in nature with wavelengths ranging from 0.5 to 4 microns and formed throughout the implanted region with the average heights of 0.2 to 4 microns. It was further found out that there is a distinct energy dependence on the ridge height as well as the ridge wavelength and both ridge amplitude and wavelength increased linearly with energy. However, between 2 to 4 MeV incident energies, the ridge wavelength did not change significantly. Implanted gold depth profiles obtained from RBS measurements clearly show two distinct regions at energies greater than 2 MeV. Some of the implanted gold atoms are concentrated near the surface region. It was further found out that both Sr and Ti concentrations levels in these ridges are depleted little bit compared to the bulk $SrTiO_3$.

Purification and Crystallization of a Zinc Transporter, YiiP, from *Escherichia coli*. *MICHELE BENDER (Mount Saint Mary College, Newburgh, NY 12550) DAX FU (Brookhaven National Laboratory, Upton, NY 11973).* When concentrations of zinc are too high in the cell it has been proven to be toxic, therefore maintaining appropriate zinc concentrations in cells are important to all living organisms. Cation diffusion facilitators (CDF) are membrane proteins that are important in maintaining zinc concentration in a narrow range by regulating zinc movement in and out of the cells. YiiP is a member of the CDF family that acts as a transporter of zinc through the cell membrane of *Escherichia coli*. The mechanism of the zinc transport is still unknown therefore studies determine appropriate crystallization conditions for the YiiP protein to obtain crystals for X-ray crystallographic studies. Crystallization trials were performed at 10°C and 20°C utilizing varying PEG 1K and PEG 2K concentrations and additives. Small Crystals were present in trays containing PEG 1K. This work produced highly purified YiiP and outlined a number of promising additive compounds for creating crystals suitable for X-ray diffraction.

Capture and Concentration of Waterborne Pathogens Using Lectin and Antibody Coupled Magnetic Beads. *ALENA BENNETT (University of Puget Sound, Tacoma, WA 98027) RICHARD M. OZANICH, JR. (Pacific Northwest National Laboratory, Richland, WA 99352).* The primary challenge of the surveillance of natural and introduced biological threats in large water samples is the purification and concentration process. A method for simultaneously capturing many types of biological pathogens is desired. Lectins coupled with magnetic beads were studied due to their ability to bind to the carbohydrates on the surfaces of cells. With lectin coupled beads we attempted to trap *Escherichia coli*, Bacillus subtilis, and Brevundimonas diminuta. Also *E. coli* antibody coupled beads were tested for their effectiveness at concentrating *E. coli* cells. Bench top indirect and direct cell capture methods were studied for both lectins and antibodies. The indirect method was found to be more effective for cell concentration. Experiments are underway to understand the differences in the two approaches and improve the direct capture method for implementation on an online automated system.

Predicting the Drying Rate of Western Hemlock Lumber as a Method to Presort Lumber and Improve Wood Quality. *KELLY BENNETT (Mesa State College, Grand Junction, CO 81501) STEPHEN KELLY (National Renewable Energy Laboratory, Golden, CO 89401).* The need for better lumber products, and the pressure to conserve energy and money while maintaining quality have spurred industry to seek help in finding more efficient methods for drying lumber. The drying process is the most costly and time-intensive part of the lumber manufacturing process. The research objective for this project is to develop analytical tools to make the drying process more efficient and less expensive. Several studies have shown that a dependable presorting system can help schedule drying times for wood with different moisture content (MC), thereby making the overall drying process more effective in the following ways. First, there would be less energy wasted in drying wood products with lower MC in the same process, or drying schedule, as wood with high MC. Second, a higher quality product can be obtained by avoiding damage caused by over drying. Last, under-dried wood has the potential to serve as a site for fungal infection. Fungal infections from a variety of sources have caused numerous lawsuits and claims of health problem related to mold growth. This research investigated whether any differences in the chemical composition of wood impact its drying rate and if these differences allow for prediction of the drying rate, thus making drying more efficient. Wet and dry wood samples were analyzed by collecting lumber samples with known differences in drying rates and grinding them to a uniform particular size. Then, near-infrared spectroscopy was used to collect spectra of the ground wood. Pyrolysis molecular beam mass spectroscopy was also used to analyze the chemical composition of the wood samples. The ground wood was extracted with a Soxhlet extraction system using 200 proof ethanol to remove organic substances (extractives). Finally, the spectral information was analyzed using multivariate statistical tools(The Unscrambler®). It was evident that there was a measurable difference in the chemical composition of the fast-drying and slow-drying wood. These differences appear to be related to the amount and type o extractives in the wood.

Modeling DNA Repair: Approaching in vivo Techniques in the Hyperthermophile *Sulfolobus solfataricus*. *JESSICA BLANTON (Amherst College, Amherst, MA 01002) JILL FUSS (Lawrence Berkeley National Laboratory, Berkley, CA 94720).* Archaea are found in some of the most extreme environments on earth and represent a third domain of life distinct from Eukarya and Eubacteria. The hyperthermophilic archaeon Sulfolobus solfataricus was isolated from acidic hot springs (80°C, pH 3) in Yellowstone National Park. Archaeal DNA repair mechanisms are more similar to those of eukaryotes than prokaryotes. This similarity, together with its relatively simple genome, make *S. solfataricus* an ideal model system for characterizing these eukaryal processes. DNA repair is essential to all domains of life and requires coordinated protein-protein interactions that are frequently transient. Protein complexes that are transient at extreme temperatures where archaea thrive may be more stable at room temperature, allowing for the characterization of otherwise short-lived complexes. However, characterization of these systems in archaea has been limited by the absence of a stable in vivo transformation and expression system. The work presented here is a pilot study in gene cloning and recombinant protein expression in *S. solfataricus*. Three genes associated with DNA repair were selected for expression: MRE11, a putative CSB homologue, and PCNA1. Though preparation of these recombinant genes followed standard methods, preparation of a suitable vector proved more challenging. The shuttle vector pSSV64, derived from the SSV1 virus and the *E. coli* vector

pBSSK+, was most successfully isolated from the DH5a *E. coli* strain. Currently, alternative vectors are being designed for more efficient genetic manipulations in *S. solfataricus*.

Use of 28S rRNA gene D1/D2 Domain Sequences for the Identification and Phylogenetic Analysis of Filamentous Fungi Isolated from Extreme Environments. *ERICA BOUDREAU (University of New Hampshire, Durham, NH 03824) TAMAS TOROK (Lawrence Berkeley National Laboratory, Berkley, CA 94720).* Microorganisms have been found to thrive in some of the most extreme environments on earth, exposed to high radiation, chemical contamination, high salinity, acidic or alkaline pH conditions, or exceptionally low or high temperatures. Due to the vast diversity of extremophillic microorganisms, they have become a valuable bioprospecting target. An important aspect of bioprospecting is the taxonomic identification of these microorganisms, for this provides a greater understanding of their diversity, unique metabolism, and ecological function. An ongoing study in this laboratory focuses on the taxonomic characterization by molecular comparison of thousands of filamentous fungi isolated from sediments of Lake Baikal and geothermal sites in Kamchatka, Russia, and from the 30-km "exclusion zone" surrounding the failed nuclear power plant in Chernobyl, Ukraine. Pure cultures of the filamentous fungi were grown under standardized conditions. The genomic DNA was extracted using the BIO 101 FastDNA kit and protocol (Q-BIOgene, CA). The D1/D2 domain of the 28S rRNA gene was amplified by polymerase chain reaction (PCR). Amplicons were separated by gel electrophoresis in a 1.2 % agarose in a 1x TBE buffer. Prior to sequencing, PCR products were run through MicroSpin™ silica gel columns (Amersham Pharmacia, NJ) and ethanol precipitated. The University of California at Berkeley DNA Sequencing Facility sequenced the PCR products. Raw sequences were edited with EditView Ver. 1.0.1.1 (ABI, CA), aligned using the online site MultAlin (http://prodes.toulouse.inra.fr/multalin/multalin.html), and blasted against the National Center for Biotechnology Information database (http://www.ncbi.nlm.nih.gov/BLAST) to determine taxonomical relatedness of the filamentous fungi.

Characterization of Xylanase from a Thermoacidophilic Organism. *MORGAN BRUNO (University of Idaho, Moscow, ID 83844) VICKI THOMPSON (Idaho National Engineering & Environmental Laboratory, Idaho Falls, ID 83415).* Xylanase catalyzes the depolymerisation of Xylan. Xylan and Cellulose are major constituents of ligno-cellulosic waste materials such as straw, grain husks, and wood. To be used as a fuel source, these wastes must initially be broken down to simple sugars. Traditionally this has been achieved by either concentrated or dilute acid hydrolysis. These methods have large chemical costs associated with them. An enzymatic method of breaking down these materials could be much more cost effective. Xylanase produced by a thermoacidophilic organism was characterized and studied as a possible means of breaking these wastes down to their composite sugars. The organism was grown in liquid media with Wheat Arabinoxylan. After growing up to 1L, the cultures were allowed to grow for 2 days and then harvested. Centrifugation at six thousand rpm yielded supernatant that was decanted and concentrated 50 times using a 10-kiloDalton molecular weight cutoff filter. Activity of concentrated solution was visualized by running it in 12.5% SDS-PAGE gel at 25 milliamps for 4.5 hours. Enzyme activity of concentrated solution was studied over a temperature range of 20 to 90° Celsius and over a pH range of 2.0 to 9.0 using a modified Somogyi Reducing sugar assay (Megazyme). This was done for depolymerisation of both Xylan and Cellulose with a 1% Wheat Arabinoxylan substrate and a 0.25% Carboxy Methyl Cellulose substrate. A study was begun of enzyme kinetics. This was done by performing the modified Somogyi assay and Wheat Arabinoxylan substrate concentrations of 0.01, 0.1, 0.5, 1.0, 2.0, 5.0, and 10.0 percent. Calculated micromoles of Xylose converted per minute will be graphed versus substrate concentration to produce an enzyme kinetic curve. Thin Layer Chromatography (TLC) was also begun to study how long it takes the enzyme to break both Xylan and Cellulose down to their composite sugars. Results for the kinetics and TLC studies are pending. The temperature assay revealed that as temperature increased, activity of the enzyme on both Xylan and Cellulose increased. The pH assay revealed that as pH decreased, enzyme activity on both substrates increased. These results are consistent with expected trends for thermoacidophilic organisms.

Automated RNA Extraction and Purification for Multiplexed Pathogen Detection. *AMY BRUZEK (Carroll College, Waukesha, WI 53186) CYNTHIA BRUCKNER-LEA (Pacific Northwest National Laboratory, Richland, WA 99352).* Pathogen detection has become an extremely important part of our nation's defense in this post 9/11 world where the threat of bioterrorist attacks are a grim reality. When a biological attack takes place, response time is critical. The faster the biothreat is assessed, the faster countermeasures can be put in place to protect the health of the general public. Today some of the most widely used methods for detecting pathogens are either time consuming or not reliable. Therefore, a method that can detect multiple pathogens that is inherently reliable, rapid, automated and field portable is needed. To that end, we are developing automated fluidics systems for the recovery, cleanup, and direct labeling of community RNA from suspect environmental samples. The advantage of using RNA for detection is that there are multiple copies of mRNA in a cell, whereas there are normally only one or two copies of DNA. Because there are multiple copies of mRNA in a cell for highly expressed genes, no amplification of the genetic material may be necessary, and thus rapid and direct detection of only a few cells may be possible. This report outlines the development of both manual and automated methods for the extraction and purification of mRNA. The methods were evaluated using cell lysates from *Escherichia coli* 25922 (nonpathogenic), Salmonella typhimurium (pathogenic), and Shigella spp (pathogenic). Automated RNA purification was achieved using a custom sequential injection fluidics system consisting of a syringe pump, a multi-port valve and a magnetic capture cell. mRNA was captured using silica coated superparamagnetic beads that were trapped in the tubing by a rare earth magnet. RNA was detected by gel electrophoresis and/or by hybridization of the RNA to microarrays. The versatility of the fluidics systems and the ability to automate these systems allows for quick and easy processing of samples and eliminates the need for an experienced operator.

Computational Methods for Determination of Functional Sites in Proteins of a Fold. *JONATHAN BRYAK (University of Illinois at Urbana-Champaign, Champaign, IL 61820) RICHARD VILIM (Argonne National Laboratory, Argonne, IL 60439).* There are many proteins in the non-redundant protein database that have unknown fold or function. It can be time consuming to try to identify the fold or function of these proteins by pure inspection with little knowledge about them. To facilitate this process, a computational method for determining both fold-conserved and functional sites in previously known proteins must be used. A database of protein sequences is made either by searching for protein regions similar to proteins of the same fold and aligning these proteins with each other. Because of the importance of sites that confer fold and sites that confer function, these sites are preserved evolutionarily. However, functional sites functional sites may not be preserved in proteins that are in the same fold yet are functionally dissimilar. We look to identify positions that are conserved in one class but not preserved over all proteins in the database. We also seek to take an unknown or unseen protein and place it in the appropriate class thus helping to identify its function. Results from proteins in the cupredoxin fold show that, by computing constancy metric for each position, it may be possible to pick out sites of function for classes in a given fold. However, results of placing hypothetical proteins into a class were not what as expected. This could be due to the difficulty in determining the exact scope of a class and further investigation will be needed.

Studying Gene Function by Identifying Mutations in Mice Through RNA Analysis. *GENEVA BURCH (Bethune-Cookman College, Daytona Beach, FL 32114) MITCHELL KLEBIG (Oak Ridge National Laboratory, Oak Ridge, TN 37831).* With the recent analysis and completion of the mouse and human genome, scientist have been able to use the DNA sequence of mice to allow further exploration of disease and other gene related disorders that occur in humans. The DOE's Joint Genome Institute sequenced chromosomes 5, 16, and 19. To help determine the functions of the human genes on these chromosomes, ORNL's Mammalian Genetics group is mutagenizing the mouse orthologs of the genes. In order to do this, DNA, tissue, and sperm of 4,000 C57Bl/6JRn male mice carrying chemically induced mutations, referred to as the Cryopreserved Mutant Mouse Bank (CMMB), have been isolated and cryogenically archived. Currently the entire bank of DNA is being screened for mutations. In addition to looking for mutations in DNA, RNA can be isolated from the tissue of the mice and cDNA can be screened for mutations. Screening for mutations in cDNA covers more coding region per amplicon and thus more efficiently identify mutations. During this summer's research project, an additional 110 samples of RNA were extracted from CMMB tissues and used to make first-strand cDNA templates. The first 368 CMMB cDNA templates are now being screened for mutations in two genes, dynamin 2 (Dmn2) and p21-activated kinase (Pak4), by heteroduplex analysis of reverse transcription-polymerase chain reaction (RT-PCR) products derived from these genes. In the future, any RT-PCR products that are found to contain heteroduplexes by a technique called Temperature Gradient Capillary Electrophoresis (TGCE) will be sequenced to confirm the presence of the mutation and define the extract nucleotide change. Any significant mutations identified (e.g., amino acid substitution) will be introduced into live stocks of mice by Intracytoplasmic Sperm Injection (ICSI) using the

frozen sperm from the mouse in which the mutation was identified. The amplicons of the two genes are presently being analyzed by RT-PCR amplification and TGCE and the results will be reported.

In Vitro Inhibition of Chlorpyrifos Metabolism by Diazinon in Rat Hepatic Microsomes. *ANDREA BUSBY (Trinity Western University, Langley, BRITISH COLUMBIA) CHARLES TIMCHALK (Pacific Northwest National Laboratory, Richland, WA 99352).* Chlorpyrifos (CPF) and diazinon (DZN) are two commonly encountered organophosphate insecticides whose toxicity lies in their respective oxon metabolites' (CPF-oxon and DZN-oxon) abilities to strongly inhibit acetylcholinesterase, an enzyme responsible for the breakdown of acetylcholine at nerve synapses. CPF-oxon and DZN-oxon are highly unstable compounds that degrade via hepatic, peripheral blood, and intestinal metabolism to the more stable metabolites, TCP (3,5,6-trichloro-2-pyridinol) and IMHP (2-isopropyl-6-methyl-4-pyrimidinol), respectively. Studies are currently underway to characterize binary exposure interactions of CPF and DZN and the purpose of this study was to determine the inhibitory nature of DZN on CYP-mediated in vitro microsomal metabolism of CPF to TCP and CPF-oxon. In this study, in vitro incubations were carried out using 1 mg/mL rat microsomal protein in 1 mL of 0.1 mM Tris, 1 mM EDTA/HCl buffer in the presence of varying concentrations of CPF substrate at three different DZN inhibitor concentrations (60, 160, 350 mM DZN). A second type of experiment was performed in which samples were pre-incubated in the presence of DZN for 1, 3, 6, 9, and 15 minutes before undergoing incubation with 22 mM CPF substrate. Preliminary data suggest that CPF competitively inhibits the DZN to IMHP pathway and non-competitively inhibits the DZNàDZN-oxon pathway. Traditional Michaelis-Menten and Lineweaver-Burke plots were constructed for this study, strongly suggesting a mixed inhibition mechanism for the CPF to TCP pathway and indicating an uncompetitive inhibition mechanism for the CPF to CPF-oxon pathway at low DZN concentrations. The pre-incubation experiment revealed a dramatic increase in CPF-oxon production at high DZN concentrations suggesting greater AchE toxicity at these levels. This is presumably due to more CPF being available for conversion to CPF-oxon due to complete inhibition of the CPF to TCP pathway at high DZN concentrations. Further inhibition studies are required to characterize CPF-oxon kinetics at high DZN concentrations.

Cotton Study: Albumin Binding and its Effect on Elastase Activity in the Chronic Non-healing Wound. *NATHAN CASTRO (El Paso Community College, El Paso, TX 79915) STEVE GOHEEN (Pacific Northwest National Laboratory, Richland, WA 99352).* Cotton, as it is used in wound dressings is comprised of 80-90% cellulose, along with 3-3.3% lignin, 0.5-1% waxes and fats, and 2-5% other components (proteins and etc.). During the healing process, cotton is exposed to various blood components, including water, salts, cells, and blood proteins. Albumin is the most prominent protein in blood. Elastase is an enzyme secreted by white blood cells that takes an active role in tissue reconstruction. In the chronic non-healing wound, elastase is often over-expressed, such that this over-active enzyme digests tissue and growth factors, interfering with the normal healing process. Our goal is to design a cotton wound dressing that will sequester elastase or assist in reducing elastase activity in the presence of other blood proteins, such as albumin. The ability of cotton and various cotton derivatives to sequester elastase and albumin have been studied by examining the adsorption of these two proteins separately. The present work was undertaken to confirm the binding of albumin to cotton, and to quantify the activity of elastase in the presence of various derivatives of cotton. We previously observed a slight increase in enzyme activity when elastase was exposed to cotton. We have also observed a continuous accumulation of albumin on cotton using HPLC methods. In the present study, we used an open column absorption technique coupled with a colorimetric protein assay to confirm losses of albumin to cotton. We have also confirmed increased elastase activity after exposure to cotton. The results are discussed in relation to the porosity of cotton and the use of cotton for treating chronic non-healing wounds.

Diversity of Archaeal Communities in Crater Hills Monitoring Site. *RACHEL CICHOWSKI (Calvin College, Grand Rapids, MI 49546) DEBORAH NEWBY (Idaho National Engineering & Environmental Laboratory, Idaho Falls, ID 83415).* Estimates place prokaryotic diversity in the range of 4x105-4x106 species, yet only a few thousand species of prokaryotes are known and classified. Of those that are known, Eubacteria represent the majority. The lesser known domain of Archaea is gaining interest in the scientific community. Many archaea are capable of growth at extremes of temperature and pH. Since archaea can thrive in the harshest conditions, it is possible that they possess unusual metabolic capabilities which could make them economically and environmentally useful in emerging industries like biomining. Research was conducted in collaboration with Montana State University to develop a phylogenetic understanding of archaeal hosts and their interactions with viruses recently discovered from samples taken from the Crater Hills monitoring site in Yellowstone National Park (YNP). These archaea serve as hosts for thermophilic viruses, the primary focus of the NSF-supported research. The Idaho National Engineering and Environmental Laboratory (INEEL) is interested in the characterization of novel archaea that could be used in biomining. The DNA was isolated at MSU, and sent to the INEEL where PCR was performed on the samples to amplify the 16S ribosomal RNA (rRNA) gene. The PCR product was gel purified and ligated into a plasmid vector, which was used to transform E. coli host cells for the purpose of creating a clone library. The transformation reactions were plated on S-gal plates, which allowed for black-white screening. The white colonies were picked, and the plasmid DNA was isolated and purified from cells grown from each colony. Each plasmid was sequenced through Big Dye Terminator version 3.0 cycle sequencing, and a BLAST (Basic Local Alignment Search Tool;) search was conducted to identify the archaeal sequences recovered from the samples. Results indicated that *Caldococcus noboribetus* was the most common archaeon in the samples taken from Crater Hills monitoring site. Four other identified archaea were present in small numbers. However, 17.4% of the BLAST sequences indicated less than a 90% similarity to *C. noboribetus*. These data indicate a more diverse sample containing uncultured and unidentified Archaea.

Analytical Methodologies for Detection of Gamma-valerolacone, Delta-valerolactone, Acephate, and Azinphos Methyl and Their Associated Metabolites in Complex Biological Matrices. *RYAN CLARK (Columbia Basin College, Pasco, WA 99301) JAMES A. CAMPBELL (Pacific Northwest National Laboratory, Richland, WA 99352).* Non-invasive biomonitoring for chemicals of interest in law enforcement and similar monitoring of pesticides together with their metabolites can not only save money but can lead to faster medical attention for individuals exposed to these chemicals. This study describes methods developed for the analysis of gamma-valerolactone (GVL), delta-valerolactone (DVL), acephate, and azinphos methyl in saliva and serum. Liquid chromatography/mass spectrometry (LC/MS) operated in the negative ion mode and in the positive ion mode and gas chromatography/mass spectrometry (GC/MS) were used to analyze GVL and DVL. Although both analytical techniques worked well, lower detection limits were obtained with GC/MS. The lactones and their corresponding sodium salts were spiked into both saliva and serum. The lactones were isolated from saliva or serum using newly developed extraction techniques and then subsequently analyzed using GC/MS. The sodium salts of the lactones are nonvolatile and require derivatization prior to analysis by this method. N-methyl-N-(t-butyldimethylsilyl)-trifluoroacetamide (MTBSTFA) was ultimately selected as the reagent for derivatization because the acidic conditions required for reactions with diazomethane caused the salts to undergo intramolecular cyclization to the corresponding lactones. In vitro studies were conducted using rat liver microsomes to determine other metabolites associated with these compounds. Azinphos methyl and acephate are classified as organophosphate pesticides, and are known to be cholinesterase inhibitors in humans and insects, causing neurotoxicity. For this reason they have both exposure and environmental impact implications. These compounds were spiked into serum and saliva and prepared for analysis by GC/MS. Continuation of this research would include analysis by GC/MS under positive ion mode to determine the parent ions of the unknown metabolites. Further research is planned through an in vivo analysis of the lactones and pesticides. These methodologies could be extended for further analysis of other similar compounds as well as chemical and biological warfare agents.

Investigation of the Role of Algal H2-Production Under Sulfur Deprivation. *ZUZANNA CZERNIK (Scripps College, Claremont, CA 91711) MARIA GHIRARDI (National Renewable Energy Laboratory, Golden, CO 89401).* Due to the growing concern over shortages and reliance on foreign sources of oil, the interest in alternative fuels such as H_2 is rising. The green alga, Chlamydomonas reinhardtii is capable of sustained H_2 photoproduction under anaerobic conditions. H_2 production in algae by the enzyme hydrogenase is believed to act as a temporary release for accumulated reductants. However, not all algal strains have hydrogenases. In order to investigate whether H_2 production is important for algal survival, the differences between the metabolism of mutant cc103-9, which cannot produce H2, and its parental wild type cc425 (requiring exogenous arginine for growth) were studied and compared to previous data on the wild-type cc124 under anaerobiosis induced by sulfur deprivation. The two strains were deprived of sulfur and suspended in computer-monitored photobioreactors. Samples of various metabolic indicators were taken every day. The chlorophyll and starch concentrations, oxygen evolution rates, and ATP levels all

drop more quickly in cc103-9 than in cc425. Protein concentrations stay constant in the mutant while increasing in the wild-type. The level of fermentation products in both strains increase at comparable rates. These results suggest that mutant cc103-9 has lower viability than the wild type cc425 under prolonged sulfur deprivation. However, the mutant's response is very similar to that of the wild-type cc124 strain. This demonstrates that the hydrogenase pathway is not essential for algal survival, at least not under sulfur stress. Future work will determine whether alternative pathways are activated to utilize accumulated reductants in the mutant. Our work also revealed significant metabolic differences between the two wild-type strains that are probably related to the arginine requirement of cc425.

Purification of Human Adenovirus and Its Active Site Mutant. *ANN MARIE DEGRUCCIO (Long Island University-Southampton College, Southampton, NY 11968) WALTER F. MANGEL (Brookhaven National Laboratory, Upton, NY 11973).* Adenovirus proteinase (AVP) is an enzyme essential for the synthesis of infectious virus. Adenovirus is a virus associated with infections such as a common cold and pink eye. Prior work on the wild type (WT) AVP gene involved mutating the nucleophilic cysteine 122, to an alanine(C122A). This gene was ligated into a unknown vector and parked in One Shot Top 10 cells. The unknown vector was identified as pET3a and contained the AVP cysteine to alanine mutation. The plasmid was isolated from the Top 10 cells and electroporated into the BL21(DE3)pLysS expression host. The AVP gene was analyzed and the mutation confirmed using DNA sequencing. After transformation, cells were plated on 2X-YT ampicillin plates and grown overnight at 37°C. Resistant colonies were selected and were grown in PO.5G media overnight. Five mL of PO.5G was used to innoculate 500ml of ZYP-5052 auto induction media containing 100mg ampicillin and 25mg chloroamphenicol at 37°C overnight. Cells were harvested by centrifugation at 5000 x g for 10 min. The cell pellet was resuspended in 25mM Tris, pH7.5, buffered BugBuster supplemented with Benzonase at 2% of the original culture volume and incubated with rocking for 20 minutes at room temperature. After cell lyses, the lysate was separated by centrifugation at 15000 x g for 20 minutes. The supernatant was then analyzed by a SDS-PAGE for expression of the Adenovirus C122A proteinase. Purification of this protein was done using ion exchange and chelating sepharose chromatography. C122A is an important mutation of the WT AVP gene because cysteine 122 is the amino acid that makes this enzyme active. Through mutation of the cysteine to alanine this enzyme becomes inactive. This inactive form of the enzyme will allow us to investigate where the substrate will bind in the active site and how this complex will interact with its cellular cofactor, actin. Knowing how the substrate reacts with the inactive form of the enzyme will lead to a better understanding of substrate binding and identifying targets for new drug therapies.

Tumor Necrosis Factor-Dependent Regulation of Inducible Nitric Oxide Synthase Activity during the Host-Pathogen Immune Response. *MICHELLE DESIMONE (Northeastern University, Boston, MA 02115) BRIAN D. THRALL (Pacific Northwest National Laboratory, Richland, WA 99352).* During the host-pathogen response, immune cells such as macrophages release tumor necrosis factor-a (TNF), a signaling molecule whose primary role includes the recruitment of other cells to the site of infection. TNF causes an array of biological effects, but elevated levels of circulating TNF can lead to chronic inflammation, which has been implicated in many disease states such as Alzheimer's, multiple sclerosis, arthritis, and cancer. In part, tissue damage during inflammation is due to the generation of free radicals, including nitric oxide. In this study, an in vitro macrophage model system was used to study the relationship between TNF and inducible nitric oxide synthase (iNOS), the enzyme responsible for the generation of nitric oxide. RAW 264.7 mouse macrophages were stimulated with Escherichia coli lipopolysaccharide (LPS) over a 24hr time course to induce signaling cascades and gene expression associated with the immune response. The response curve showed that LPS caused the induction and shedding of TNF prior to the induction of iNOS protein expression. In addition, the results show that iNOS activity does not contribute to TNF release in activated macrophages and that TNF treatment is not sufficient to cause iNOS expression. Further studies using short-interfering RNA revealed that inhibiting TNF induction had no effect on iNOS protein expression in response to LPS, but led to >80% reduction in iNOS activity. This suggests that TNF or TNF-stimulated pathways play a role in the regulation of iNOS activity. Future studies will examine the mechanism of iNOS activation and TNF's role in the regulation of this important inflammatory mediator.

A New Technical Approach To The Study Of Radiation-Induced "Bystander Effect" Using An X-Ray Microbeam. *ANDREA DRAGER (City College of San Francisco, San Francisco, CA 94110) KATHLEEN BJORNSTAD (Lawrence Berkeley National Laboratory, Berkley, CA 94720).* Exposure to radiation can cause "bystander effects" in neighboring cells that are outside of the radiation field. Significant levels of genetic changes, molecular damage and lethality have been observed in bystander cells of varying genetic background, lineage and organ origin. While evidence for such effects has been well established, a clear understanding of the basic biochemical and molecular processes by which they occur is only beginning to emerge. The goal of this project is to investigate the bystander effect in human mammary epithelial cells, using an X-ray Microbeam and serine -15 phosphorylation of TP53 as a marker of radiation-induced DNA damage (specifically, a double-strand break) in irradiated and neighboring cells in a time course after irradiation. To do this we have quantitated the fluorescence signal associated with the TP53 ser15phosphorylation in a stripe of dose in a time course after irradiation. The ALS X-ray microbeam is a novel method to evaluate bystander effects that has potential for the evaluation of large cell numbers for statistical power. The effects of X-ray microbeam dose stripes broaden with time up to 3 hours to include bystander cells not in the radiation field. Intensity of fluorescence also increases with dose. Further statistical evaluation of the bystander effect is in progress using BioSig. Work is in progress to analyze this bystander effect at lower doses.

Thermal Electrochemical Synthesis Of Silver Nanocrystals. *CAMERON ERICSON (Lawrence University, Appleton, WI 54911) MICHAEL HU (Oak Ridge National Laboratory, Oak Ridge, TN 37831).* A thermal electrochemical synthesis (TECS) process has been developed to create "naked" (free from organic molecule capping) silver nanocrystals of approximately 10 nm or smaller in diameter suspended in an aqueous solution. The ultimate goal is to achieve a monodisperse silver nanocrystal sol of a given concentration. Dr. C. Easterly (Life Sciences Division, ORNL) suggests that silver nanocrystals have potential applications in medicine. A systematic study of various silver TECS process factors has been performed to develop a general understanding of formation of naked silver nanocrystals in order to improve the yield of synthesis. Studies were conducted using different types of reaction containers with varying temperature, electrode distance, and reaction time with applied electrical potential. Light scattering measurements are conducted with a Dynamic Light Scattering (DLS) setup to determine nanocrystal size and size distribution. Scanning Tunneling Electron Microscope (STEM) is used to visualize the images of nanocrystals. UV/ Vis Spectrophotometer is used to quantify silver concentration in solutions as well as provide information in size. Our studies developed preliminary correlation between particle size, growth kinetics, and process factors. This relationship will allow process optimization, which could provide small (<10 nm) nanocrystals for further investigation of properties of monodispersed nanocrystals.

Assembling the Complex of Adenovirus 2 Knob Domain and D1 Domain of Human Coxsackievirus and Adenovirus Receptor (CAR). *FARRAH FAN (University of Missouri- Columbia, Columbia, MO 65211) YIAN-BIAO ZHANG (Brookhaven National Laboratory, Upton, NY 11973).* Many viral infections are initiated by the binding of virus particles to specific host cellular receptors. Although the crystal structure of the adenovirus 12 knob domain (Ad12 knob) complex with the CAR D1 domain has been solved, there are more than fifty serotypes of adenovirus. The majority of adenovirus serotypes can bind to the coxsackievirus and adenovirus receptor (CAR) on human cells, despite only limited conservation of amino acid residue that comprise the receptor-binding sites of these viruses. In order to understand the molecular structural basis for variation in adenovirus affinity for the cellular receptor CAR, the knob domain for Ad serotype 2 and the NH2-terminal domain of human CAR (CAR D1) were cloned in pET15 vector of the pET system. Both proteins were over expressed in *Escherichia coli* as soluble protein fragments. The recombinant protein of Ad2 knob domain was purified using DE52 ion exchange column followed by using Ni-NTA agarose column. The D1 domain of human cellular receptor was purified from *Escherichia coli* bacteria by a combination of DE52 ion exchange chromatography and affinity column chromatography of knob domain of Ad12 coupled with CNBr-activated Sepharose 4B. Both proteins were proteolysed separately with trypsin to remove tags and complex was formed at room temperature in vitro. A native electrophoresis gel confirmed complex formation of these two proteins and crystals of complex Ad2 knob and CAR D1 were grown at room temperature with the sitting drop vapor diffusion method. The crystals of knob-CAR complex have been found growing at two different buffer conditions. Our future work will focus on testing those growing conditions of the crystal complex determining the molecular structure of knob-CAR complex.

Characterization of the Microbial Community in a Methane-Driven Denitrifying Bioreactor. *ANA FERNANDEZ (University of Florida, Gainesville, FL 32611) WILLIAM STRINGFELLOW (Lawrence Berkeley National Laboratory, Berkley, CA 94720).* Denitrification is an important step of the wastewater bioremediation process. It involves the removal of nitrogenous compounds from wastewater, known to cause adverse effects to human health and the environment. Because denitrification is the last step in the wastewater bioremediation process, a supplemental source of organic carbon must be added at a significant cost to wastewater treatment plants. Methane may be an inexpensive alternative source of organic carbon for denitrification. Previous studies suggest that coupled anaerobic methane oxidation and denitrification may be an effective, low cost alternative to facilitate the denitrification process in wastewater treatment plants. Understanding the microbial community present in a coupled anaerobic methane oxidation denitrifying system may allow for optimization of denitrification in wastewater treatment facilities. In this study, a low oxygen, methane-oxidizing denitrifying bioreactor (MOR) is used to emulate a coupled anaerobic methane oxidation denitrifying system. Methanotrophic and denitrifying bacteria are expected to be the major constituents of the MOR. 16S rDNA sequencing via microarray hybridization is used to identify the microbial community of the MOR. Results show that five bacterial subgroups represent the major constituents of the microbial community of the MOR, including members of the Bacillus subdivision known to reduce nitrate to nitrite. Denitrifying bacteria are indeed the major constituents of the microbial community of the MOR. However, 16S rDNA microarray technology is unable to detect the presence of known methanotrophic bacteria in the MOR. The 16S rDNA microarray must be optimized to detect methanotrophic bacteria. Additionally, the microarray technology is used to identify the microbial communities of an ammonia-oxidizing bioreactor (AOR) and a hydrogen membrane bioreactor (HMBR). As expected, distinct microbial communities are found in each of the three bioreactors using the 16S rDNA microarray. Results show that the 16S rDNA microarray is effective for the identification of distinct microbial communities in different bioreactors.

Up-Regulating Plant Defenses In Populus Increases Their Phytoremediation Capacity For Carbon Tetrachloride Contaminant In Groundwater. *ABIGAIL FERRIERI (College of the Holy Cross, Worcester, MA 01610) MICHAEL THORPE (Brookhaven National Laboratory, Upton, NY 11973).* There is a growing concern over continued increases in groundwater contamination by chlorocarbon compounds such as trichloroethylene and carbon tetrachloride, which present health risks as potential carcinogens and pollutants capable of depleting the ozone layer. Although the use of poplar trees to cleanup groundwater has proven to be cost-effective, we still face the challenge of minimizing foliar emissions of chlorocarbons. It was recently reported that CCl_4 is metabolized to nonvolatile trichloroacetic acid (TCA) in leaves, but the mechanism for this process is unknown. We hypothesized that recently fixed carbon plays a role in this mechanism. Labeling intact leaves with $^{11}CO_2$ (t½ 20.4 m) can test this hypothesis because the extremely short half-life of the tracer reflects only those processes involving recently fixed carbon. Using radio-HPLC analysis, we did indeed observe radiolabeled [^{11}C]TCA from leaf tissue extracted from poplar clones (OP637) whose roots were exposed to 500 ppm of CCl_4. Autoradiography of [^{11}C]photosynthate showed increased leaf export and partitioning to the apex within 24 hours of exposure to CCl_4 suggesting that changes in plant metabolism and partitioning of recently fixed carbon occur upon exposure to the contaminant. Additionally, foliar emissions of CCl_4 were found to be the highest in the morning when carbon pools were low suggesting a link between emission and plant carbon metabolism. Further, we tested the hypothesis that it is possible to amplify leaf CCl_4 metabolism, thereby lowering leaf emissions, by altering recently fixed carbon stores. We recently showed that an exogenous treatment with jasmonate, a hormone implicated in signal transduction within the plant's defense train, increases sugar intermediates in leaves at the expense of starch storage. Indeed, when the entire foliage of a cut stem of poplar was treated with a 1 mM solution of jasmonate, leaf CCl_4 emissions were reduced 2-fold while TCA levels were increased 1.7-fold. Future work will explore whether persistent up-regulation of a plant's defenses through continuous jasmonate treatment will continue to have beneficial phytoremediation effects. This research was supported by a BNL LDRD seed grant, the DOE Office of Biological and Environmental Research and the DOE SULI program.

Characterization of receptor interaction in bacterial chemotaxis. *ISRAEL FIGUEROA (University of California, Berkeley, Berkeley, CA 94720) ADAM P. ARKIN (Lawrence Berkeley National Laboratory, Berkley, CA 94720).* Bacterial chemotaxis is the motion of bacteria toward chemical attractants or away from chemical repellents. It is one of the most studied biological systems, most notably in E.coli. Chemotaxis is a model system for signal transduction with its relative simplicity, wide dynamic range, high sensitivity and robustness. It remains unknown how *E.coli* is able to sense such a wide dynamic range of chemicals, while still maintaining such high sensitivities. We have studied the interactions between different chemical receptors types to find a possible answer. It is hypothesized that receptors synergistically interact to amplify signals and increase chemical sensitivity. *E.coli* strains were constructed that allow the number of Tar and Tsr receptors to be controlled via the PBAD promoter. Motility plate assays were then conducted with varying chemical conditions and receptor numbers. The expression of the Tar receptor was successfully controlled in the engineered strain, but the Tsr receptor was not - probably due to medium plasmid copy numbers and expression leakage inherent of the PBAD promoter. Preliminary results from motility plate assays show that the Tar and Tsr chemoreceptors do not interact.

Assessment of Vegetation Along Peconic River Post Remediation. *WENDY FINN (Community College of Rhode Island, Warwick, RI 02886) TIMOTHY GREEN (Brookhaven National Laboratory, Upton, NY 11973).* The Peconic River running through the property of Brookhaven National Laboratory is the focus of a remediation process to eliminate contaminated sediments inadvertently created by the laboratories past practices. An assessment of planted vegetation from April 2002 is being conducted to monitor how reintroduced vegetation has thrived. The methods used to assess the vegetation's progress includes 1) identifying native and invasive plant species, 2) mapping various plant species with a Thales Navigational Mobile Mapper GPS unit and 3) comparing present results with the original revegetation planted in April 2002. The data collected will be used to determine how different species adjust after the remediation process has occurred.

Seasonal Food Intake Affecting ^{137}Cs Levels in White-tailed Deer at Brookhaven National Laboratory. *ESPERANZA FLORENDO (Los Angeles Mission College, Sylmar, CA 91342) TIMOTHY GREEN (Brookhaven National Laboratory, Upton, NY 11973).* Food intake by ruminants is mainly controlled by photoperiod, meaning that food intake is higher during the summer months when days are longer than in the winter months. While ^{137}Cs continues to be present in the environment due to radioactive fallout at Brookhaven National Laboratory (BNL), there are increased levels of ^{137}Cs levels due to soil contamination. From 2000 to 2003, ^{137}Cs levels were obtained in deer killed at three different areas: BNL, within a mile's distance from BNL (1 mile). Data from all the years were compressed and divided into the first half and second half of the year. T-tests showed that deer >1 mile from BNL had significantly lower ^{137}Cs levels than the other three groups (BNL, <1 mile, and BNL and <1 mile combined). Deer <1 mile from BNL also had significantly higher ^{137}Cs levels than BNL deer. Within each group, there were significantly higher ^{137}Cs levels for the second half of the year, which was expected since there was an increase in food intake during the summer months and equilibrium levels were reached within 100 days.

Isolation and Characterization of Carbon Catabolism Regulators Exploitable in Carbon Sequestration. *KYLE FOWLER (Columbia Basin College, Pasco, WA 99301) SCOTT BAKER (Pacific Northwest National Laboratory, Richland, WA 99352).* Carbon sequestration by fungi may prove to be an invaluable process in limiting atmospheric CO_2 buildup. One method to better understand and possibly facilitate limiting atmospheric accumulation of CO_2 is the identification, isolation, and sequencing of genomes from microorganisms which produce and capture these gases or have prospective use producing bioproducts or biofuels. Here we attempt to isolate the carbon catabolite repressor gene creA and the transcriptional activator xlnR from numerous fungi spanning several phyla. These gene products are global regulators that mediate the expression of genes encoding a variety of glycosyl hydrolases, enzymes of interest in the production of bioproducts and biofuels and the basis of a bottleneck in these industries. Furthermore, we aimed to discover novel gene homologues that may fulfill these same roles mediating this metabolic pathway. To accomplish this we designed degenerative PCR primers and utilized a number of different PCR procedures followed by agarose gel electrophoresis. Compared to standard PCR which involves very selective primer bonding and amplification, binding by our degenerate primer was achieved with more ambiguity to tolerate subtle gene variation. Subsequent gel electrophoresis allowed us to clone and sequence the product. Comparatively analyzing these sequences from various fungi will help to identify conserved proteins and novel proteins possibly possessing conserved domains. This information is vital to ascertaining if a common carbon regulatory protein or domain is conserved throughout the fungal kingdom. Improved understanding of the carbon cycle in fungi is important in both

the use of biomass for alternative fuels and increasing our knowledge of atmospheric carbon sequestration.

Applications for Duralco 4538N Epoxy Resin. *KENDALL FRUCHEY (A&M University, College Station, TX 77840) ANDREW MADDISON (Argonne National Laboratory, Argonne, IL 60439).* Analytical techniques for determining metal distribution in an epoxy matrix were studied. A flame ashing technique coupled with ICP-OES for quantification was found to be capable of measuring incorporated cerium levels to within 13%. The process can be extended to test uranium distribution, which was simulated in this testing by a cerium surrogate. This technique will allow for the analysis of epoxy encapsulated standards for a nondestructive assay gamma-ray spectrometer for homogeneity in the distribution of the nuclear material, as required by the spectrometer.

Sage Sparrow Breeding Territory Sizes in Relation to Habitat Characteristics. *JESSE FRUCHTER (State University of New York College of Environmental Science and Forestry, Syracuse, NY 13210) COREY DUBERSTEIN (Pacific Northwest National Laboratory, Richland, WA 99352).* Shrub-steppe is listed as a priority habitat by the Washington State Department of Fish and Wildlife because it is an important breeding habitat for many species of fish and wildlife and has declined 98% since European settlement. There is a large tract of relatively pristine shrub-steppe habitat on the Hanford Site in Eastern Washington. In order to preserve this habitat, the Hanford Site Biological Resources Management Plan (BRMaP) explicitly states that the United States Department of Energy - Richland Operations Office (DOE-RL) must monitor habitat mitigation and restoration actions. The sage sparrow *Amphispiza belli* is a Washington State Candidate - a species whose status may meet the listing criteria for State Endangered, Threatened or Sensitive - making it worthy of study, as well as a sagebrush obligate species, making it a good indicator species for sagebrush habitat quality. This study was conducted to determine the relationship between habitat characteristics and sage sparrow territory size. The breeding territories of 22 sage sparrows were mapped to characterize understory and overstory vegetation in each territory on the Hanford Site. Preliminary analyses indicate no significant correlation between the measured habitat characteristics and territory size, indicating that the measured habitat characteristics may not be related to territory size. Coupled with data on fecundity, clutch size and nesting success, these findings will eventually aid us in creating a habitat suitability index (HSI) to determine relative value of sagebrush habitat, consequently refining sagebrush mitigation guidelines.

UVA-Melanin Interactions, a Possible Cause of Cutaneous Malignant Melanoma. *SEBASTIAN GALAZKA (Housatonic Communtiy Colge, Bridgeport, CT 06604) RICHARD SETLOW (Brookhaven National Laboratory, Upton, NY 11973).* Significant evidence exists to point to sunlight exposure, due to its highly genotoxic effects on DNA, as the principle cause for skin cancer, amongst which cutaneous malignant melanoma (CMM) accounts for almost all of the invasive, metastatic skin cancers. Studies with Xiphophorus backcross hybrid fish have demonstrated that the melanoma action spectrum is within the same range as UVA and visible light, with UVB having only some effects. However, since UVA accounts for 90% of the UV spectrum it is though to be the main initiator for melanoma. Because UVA wavelengths are not significantly absorbed by DNA, the deleterious effects of UVA must be indirect. It is therefore believed that reactions with endogenous cellular chromophores, such as melanin, are responsible for causing DNA damage, either through to formation of free radical oxygen species or though the formation of DNA-melanin adducts. Such damage would normally be repaired through repair processes such as nucleotide excision repair (NER). However, individuals deficient in enzymes involved in NER show a 1000 fold increase in cancer. Albino blacks, since they lack a built-in sun screen, show lots of damage from sun exposure, sunburns and nonmelanoma skin cancer. However, their incidences of melanoma were almost nonexistent pointing to a UVA-melanin interaction as the chief cause for melanoma. To test this possibility, a strain of *Escherichia coli* containing a plasmid (pJOE 810) that allows the cell to synthesize the melanin pigment was used. The cells were irradiated with UVA, B, or C light, and their survivals were compared to an amelanotic strain of *E. coli* (pUC 19). The results obtained from the UVB and C irradiation were identical, showing a slightly greater sensitivity of the mel+ cell at those wavelengths. However, the UVA irradiation showed a large difference between the survival rates of the two strains, with the mel+ cells being reduced by about 50% at a dose that only reduces the pUC19 cells by 25%. Even though *E. coli* are not susceptible to cancer, their survival acts as a model of the UVA induced damage and should point a way for further studies using mammalian cells. That being the case, these findings seem to support to the hypothesis that a UVA-melanin interaction may promote cutaneous malignant melanoma and shed light on the possible risks of recreational tanning which consists of solariums comprising of >90% UVA lights.

UVA-Melanin Interactions a Possible Cause of Cutaneous Malignant Melanoma. *SEBASTIAN GALAZKA (Housatonic Community College, Bridgeport, CT 06604) RICHARD SETLOW (Brookhaven National Laboratory, Upton, NY 11973).* Cutaneous malignant melanoma (CMM), accounts for almost all of the invasive, metastatic skin cancers. Since UVA accounts for 90% of the UV spectrum it is though to be the main initiator for melanoma. Because it is not absorbed by DNA, the deleterious effects of UVA must be indirect and occur though endogenous cellular chromophores, such as melanin. This damage would normally be repaired through numerous cellular repair processes. However, individuals deficient in enzymes involved show a 1000 fold increase in cancer. Albino blacks, since they lack a built-in sun screen, show lots of damage from sun exposure. However, their incidences of melanoma were almost nonexistent pointing to a UVA-melanin interaction as the chief cause for melanoma. To test this possibility, pigment producing mouse cells S91/mel, I3, amel as well as human melanoma cells were used. The cells were irradiated with UVA, and UVB light. Heavy molecular sized DNA was isolated and, as a result of the irradiation, damage was detected using UVrABC and compared to cells treated with *M. luteus* and untreated cells on Alkaline gel electrophoresis. The gels demonstrated that UVrABC was not able to from the complex required to detect the damage. At least not at a high detectable level, some detection was visible but not at a high enough resolution.

Frequency Domain Analysis of Noise in Cellular Systems. *BRYCE GALEN (University of Virginia, Charlottesville, VA 22903) MICHAEL SIMPSON (Oak Ridge National Laboratory, Oak Ridge, TN 37831).* Signals within cellular systems have an inherent degree of variability or “noise,” which cannot accurately be modeled by purely deterministic differential equations. We have created a more accurate model by employing a frequency domain Langevin approach, which adds noise terms to the differential equations that correspond to the points of molecular synthesis and decay. We are attempting to verify this model experimentally by tracking selected single cells of *Escherichia coli* K-12 transfected to constitutively express Green Fluorescent Protein (GFP) during the log phase of growth. An *E. coli*-GFP system is suitable for the measurement of cellular noise because transcription and translation variance is manifest in protein fluorescence levels over time. Our technique involves the capture of cellular images over an extended period of time using a laser confocal microscope fitted with photomultiplier detectors. Images are digitized by a data acquisition computer, and imaging software is used to measure fluorescence intensity values per unit area within the boundaries of a single cell. Second-order (Fourier) analysis of this experimental data identifies the frequency components of the noise, which can readily be compared to the analytical results of our Langevin-based model. Focusing on a signal from a single cell in the frequency domain allows us to directly perceive relevant noise, free from the first-order variance among an entire group of cells. It is our hope that insights arising from this work will eventually give clues as to how cellular systems maintain robust functionality despite high levels of noise.

Using Image Analysis in 3D to Quantify the Relative Gene Expression in *Drosophila melanogaster* Blastoderms. *BENJAMIN GARMAN (Shasta College, Redding, CA 96080) DAVID W. KNOWLES (Lawrence Berkeley National Laboratory, Berkley, CA 94720).* While many studies of the genome and of specific genes of the organism *Drosophila melanogaster* have been conducted, there is a lack of available information to explain the connection between gene expression and the transcription network. As part of the Berkeley Drosophila Transcription Network Project (BDTN), we are aiding in the understanding of gene transcription in D. *melanogaster* by providing three-dimensional spatial data sets of gene expression for stage 5.8 blastulae, at cellular resolution. Based on biological and developmental factors, embryos are being staged and stained to provide flourescent samples that are within a tight 2-3 minutes developmental period. Staining is done through an intensive in-situ hybridization process using tyramide signal amplification protocols to attach the fluorophores coumarin, cy3 or cy5 to multiple gene products within the same embryo. Nuclear stain, sytox green, is also attached to reveal all nuclei. The resulting fluorescent embryo is then imaged using multi-channel 2-photon confocal microscopy to produce three-dimensional images, acquired at 1024x1024x100 pixels. The dimensions of each data point resolves to approximately one micron of real spatial distance. These images are then stored in a database and analyzed. Analysis techniques include mapping of each cell and its nuclei, creation of a mesh model of the embryo surface for projection and comparison analysis, figuring percentage expression of specific gene patterns in any individual cell, and future developments. Currently,

the gene expression patterns snail, fushi tarazu, even skipped, sloppy paired 1, rhomboid, and knirps are being acquired and studied, but the list will slowly be expanded to include all active gene expression patterns within, and then beyond, this stage of the organisms development. The overall goal is to map the early transcription network of *Drosophila melanogaster*.

Gene-driven Mutagenesis by RNA-based Mutation Scanning of the Cyropreserved Mutant Mouse Bank. *RACHEL GOLDSTON (Cedarville University, Cedarville, OH 45314) MITCHELL KLEBIG (Oak Ridge National Laboratory, Oak Ridge, TN 37831).* Since the human genome has been sequenced, efforts are now focused on determining the function of the approximately 30,000 human genes. The Mammalian Genetics program at ORNL is determining the function of the genes on human chromosomes 5, 16 and 19, the three chromosomes sequenced by the Department of Energy, using analysis of induced single-nucleotide mutations in the orthologous mouse genes. They developed a unique resource called the Cyropreserved Mutant Mouse Bank (CMMB), a collection of DNA, frozen tissues, and sperm from 4,000 male progeny of N-ethyl-N-nitrosourea (ENU) mutagenized mice that contain many point mutations throughout their genome. The genes to be studied are chosen based on four criteria: either no reported mutations or existing mutations are embryonic lethal, conservation over distantly related genomes, well-defined protein domains, and restricted patterns of expression. Because of its large scale, the protocols for this functional-genomics initiative must be fine-tuned to ensure high-throughput screening for mutant genes. In this project, an RNA component of the CMMB is being developed and screened for mutations in the following way: (1) RNA is extracted from the frozen tissue, (2) first-strand cDNA is synthesized, (3) regions of the gene are PCR amplified in a 96-well format, and (4) the PCR products are screened for possible point mutations and size alterations by Temperature Gradient Capillary Electrophoresis (TGCE) and gel electrophoresis, respectively. Currently two genes are being studied: Dnm2 and Pak4. RNA extraction and cDNA preparation have been initiated (about 250 samples completed) and the protocols optimized for large-scale work. It has been shown that PCR and TGCE multiplexing with up to three different amplicons are successful, which will save time and resources. Three possible mutants have been flagged by TGCE analysis, but at this point no size-altering mutations have been found. The putative mutants are being sequenced to confirm and characterize the mutations. If the mutations are predicted to have a significant effect on the structure of the protein, then live mutant mice will be recovered by intracytoplasmic sperm injection using the cryopreserved sperm. These heterozygous mice, as well as homozygous mutant progeny from intercrossing, will be evaluated for phenotypes. This gene-driven approach to mutagenesis can be used to study any gene of interest, including genes suspected of involvement in human diseases.

Simulating and Examining the Radiation Damage due to Alpha Decay of Radioactive Actinide Elements by Au2+ Ion Implantations in $SrTiO_3$ at 150 K. *DANIEL HADLAND (Creighton University, Omaha, NE 68178) YANWEN ZHANG (Pacific Northwest National Laboratory, Richland, WA 99352).* One technique of immobilizing actinide nuclear waste is to use the crystalline matrix of several classes of compounds. In order for these materials to be considered for actinide waste immobilization, the physical characteristics and durability must be studied under simulations of α-decay and β-emitter recoil using a variety of procedures. In this analysis in particular, strontium titanate, $SrTiO_3$, from the class of ABO_3 oxides, was studied. During the course of this research a constant temperature of 150 K was maintained while the two samples were implanted with several doses of 1.0 MeV Au^{2+} ions at 60 off channeling normal with each dose applied to a virgin area of the sample. Following each dose of Au^{2+} ions a RBS spectrum was taken from irradiated sample area using 2.0 MeV He^{+} ions. As predicted and theorized, with each subsequent dose of Au^{2+} ions the disorder on both the Ti and Sr sublattices had increased. The study concluded that the $SrTiO_3$ crystal had a critical dose of $2x10^{13}$ Ions/cm^2 at 150K before complete amorphization of the crystal had taken place. As the dpa rose above the critical dose, the amorphous layer within the crystal became thicker.

Insectivorous Birds Hatching Success: Evaluating the Use of Indicator Species for Non-invasive Monitoring of Environmental Quality. *EMILY HAMBLEN (Lane Community College, Eugene, OR 97405) BRETT TILLER (Pacific Northwest National Laboratory, Richland, WA 99352).* Nesting success in birds is often used to monitor environmental quality because avian species are widely distributed and occupy a wide range of habitats. This study focused on assessing the nesting success of four insectivorous birds: American robin (Turdus migratorius), Bullock's oriole (Icterus bullocki), western kingbird (Tyrannus verticalis), and eastern kingbird (Tyrannus tyrannus) using a new video surveillance technique. Two components of nesting success, hatching success and nest fate, was monitored in eastern Washington in riparian treed habitats along the Columbia River on the U.S. Department of Energy's 100-D Hanford Site and at a reference study area near Vernita Bridge. Our objectives were to test the utility of the video monitoring system, provide baseline information on nesting success for these species, and determine which species are easiest to monitor. Eleven nests were located at the Vernita Bridge site compared to five nests found near the 100-D study area. Preliminary monitoring results indicate that predation largely affected nest fate of species at the study sites. Approximately 40% of the nests at the Vernita bridge site and 60% of the nests near the 100-D study site were predated. Five nests located at the Vernita bridge site had 100% hatching success, while one Bullock's oriole nest had a nesting success of 83%. None of the five nests found and monitored near the 100-D Area hatched eggs because of predation by other avian species. Our study suggests that kingbirds are the most easily monitored species. Future work will focus on obtaining a larger sample of bird nests and investigating the use of migratory birds as efficient indicator species.

Measuring the Radiocarbon of Three Soil Density Fractions. *ERIN HANLON (St. John's College, Santa Fe, NM 87505) MARGARET S. TORN (Lawrence Berkeley National Laboratory, Berkley, CA 94720).* Measuring carbon-14 isotopes (^{14}C) in different soil components is a useful technique for tracing the pathways of carbon in soil. This study investigates the incorporation of ^{14}C into different soil C pools at the 0-15cm depth. Soil samples were taken from Walker Branch Watershed in Oak Ridge, Tennessee. Soil samples were processed using physical fractionation techniques and separated using 1.7 g/mL sodium polytungstate (NaPT) into three density fractions; free light, occluded light and heavy. Each density fraction was assayed for ^{14}C content using an accelerator mass spectrometer and for carbon and nitrogen with an elemental analyzer. The carbon in the occluded light fraction was found to be older than the carbon in the free light fraction. These results support the idea that organic matter that is occluded within aggregates is protected from decomposition, leading to longer turnover times and increased stabilization of carbon. Understanding the role soil aggregates play in stabilizing soil organic carbon can increase our knowledge of the methodology of carbon sequestration in a particular environment.

Water Stress Impacts on the Net Leaf ^{18}O Isoflux: Experimental Results and Model Predictions. *ERIN HANLON (St. John's College, Santa Fe, NM 87505) MARGARET S. TORN (Lawrence Berkeley National Laboratory, Berkley, CA 94720).* Water-stressed leaves have lower stomatal conductance and a lower photosynthetic rate than leaves not subjected to water stress. The Isotope Land Surface Model (ISOLSM) was developed from the Land Surface Model (LSM) to predict the isotopic fluxes of CO_2 and H_2O (isoflux) from vegetation and soil. Previous publications revealed ISOLSM's effectiveness at predicting the isoflux from plants under normal conditions. Until now the model had not been used to predict the consequences of water stress on the isoflux from photosynthesizing plants. We examine both causes and effects of water stress in the leaf. The model was set up to predict the effects of drought stress and we looked at the results from that prediction.

Whole Gland Hormone Receptor Analysis of Mammary Development. *ABBEY HARTLAND (Shasta College, Redding, CA 94049) CARLOS ORTIZ DE SOLÓRZANO (Lawrence Berkeley National Laboratory, Berkley, CA 94720).* Steroid hormones, signaling through their cognate cellular receptors, are known to play an important role in the development of the breast and its tendency to become carcinogenic. Both the number of cells that express hormone receptors and their distribution throughout the gland contribute to the homeostatic equilibrium that allows normal development, maintenance and function of the gland. Many recent developments in diagnostic tools have provided for quick assessment of the receptors in clinical specimens, but do not account for the rich cellular heterogeneity within the tissue sample. In response to these difficulties, our laboratory has developed software capable of reconstructing the mammary ductal tree from serially sectioned glands and mapping proteins on that reconstruction. In this study, we have combined this software with immunohistological techniques to analyze estrogen receptor (ER)-a and progesterone receptor (PR) expression in wild-type murine mammary glands from 6-48 weeks of age. We have quantified the expression of the receptors in each of the mammary glands and shown the differences in number of receptor expressing cells between different morphological structures and developmental stages. These results stress the importance of examining cells within their three-dimensional histological context.

Three-Dimensional Histopathology of the Mammary Gland. *ABBEY HARTLAND (Shasta College, Redding, CA 96049) CARLOS ORTIZ DE SOLORZANO (Lawrence Berkeley National Laboratory, Berkley, CA 94720).* Breast cancer researchers today are faced with the extensive task of discovering and describing the mechanisms that drive the initiation and progression of mammary cancers. To correctly define these mechanisms, they must be studied within the context of the tissue where they appear and develop. Several techniques exist to detect or quantify proteins and genes involved in this neoplastic process, however none have been able to both identify and effectively preserve these chemicals within their histological context. In response to these difficulties, our laboratory has developed a computer-assisted microscopy system to transform serial sections of tissue into a three-dimensional (3D) image, thus allowing us freedom to both identify breast cancer markers and to visualize the context where these markers are found ex vivo. This system was utilized to reconstruct the mammary ductal trees of two peripubertal female mice: one transgenic c-neu overexpressing and one wild-type control. Combining this reconstruction with current immunohistochemical techniques, we mapped three major receptor proteins known to have a crucial role in the normal development of the gland: estrogen receptor (ER), progesterone receptor (PR), and the growth factor receptor neu. Numerical analyses indicate that the transgenic animal over-expresses HER2, resulting in an under-expression of ER and subsequent inhibition of ductal elongation. PR is expressed differentially in terminal end buds (TEBs), the lowest levels found in proliferating end buds of the wild-type animal, while the highest levels are found in the prematurely developed lobuloalveolar structures of the c-neu mouse, suggesting that PR expression in TEBs increases proportionately to the relative level of maturity. The data obtained from current and future analyses will enable us to determine changes in the morphology and the pattern of receptor expression associated with cancer initiation and development.

Primer Design for Singular Point Genomic Signature Tagging Using Alternative Phylogenetic Markers. *DIANE HEISER (Princeton University, Princeton, NJ 08544) NIELS VAN DER LELIE (Brookhaven National Laboratory, Upton, NY 11973).* Microbial organisms comprise an assembly of genetic and biochemical diversity rivalled by no other group on Earth and understanding their unique functions, roles, and complexity is a necessary step in capturing their vast capabilities. In order to expand such knowledge, a novel technology known as Singular Point Genomic Signature Tagging (SP-GST) has been developed at Brookhaven National Laboratory. By priming outward from a highly conserved area of a gene, unique 21 base-pair tags are generated in order to quantitatively analyse the composition and identify the species within a microbial community. To date, this technology has used universal primers designed for the phylogenetic marker ^{16}S rDNA. While this gene serves as a well-conserved priming point, its presence in multiple copies on bacterial genomes leads to an inaccurate representation of community composition. In order to resolve this problem alternative phylogenetic markers that occur only once in the genome (genes dnaK and recA) were investigated, as was the functional gene for dissimilatory sulfate-reductase (dsr). Through SP-GST technology rhizosphere soil samples from the Free-Air Carbon Dioxide and Ozone Enrichment (FACE) Project were used to analyze bacterial community composition under ambient and elevated CO_2. By doing so, changes in community structure and function were examined to determine the effects of a changing environment on this delicately balanced division of the ecosystem. DNA from both soil samples was extracted, purified and used for SP-GST analysis. SP-GST techniques were successful in compiling community composition profiles for both samples using the ^{16}S rDNA marker, and universal primers have been designed for alternative phylogenetic markers dnaK, recA, and dsrA. Future work will focus on the validation of the above mentioned genes as well as rpoC and uvrB in order to determine which gives the most accurate representation of community composition.

Small Angle Scattering Studies on Spinach Photosystem I. *KATIE HELTON (University of Tennessee, Knoxville, TN 37996) HUGH O'NEILL (Oak Ridge National Laboratory, Oak Ridge, TN 37831).* Oxygenic photosynthesis, the conversion of sunlight to chemical energy, is driven in series by Photosystems I (PSI) and II in the thylakoid membranes of higher plants and algae. PSI operates by a photo-induced activation of the special chlorophyll pair, P700, thereby translocating electrons from the lumenal side to the stromal side of the membrane to generate NADPH. This study seeks to use small angle scattering techniques to investigate the dynamic structural changes that occur in PSI after photon absorption and during intermolecular electron transfer via the electron relay proteins plastocyanin and ferredoxin. PSI was isolated from spinach thylakoids by solubilzation with 0.8% Triton X-100. A variety of detergents were tested to further purify the PSI preparation. These included 0.4% sodium dodecyl sulfate, 2.0% octyl-b-glucoside, and 0.15% dodecyl maltoside/ 0.2% Zwittergent. The purity of each preparation was analyzed based on Chl/P700 and Chl a/Chl b ratios obtained using visible absorption spectrophotometry. It is determined that solubilization with dodecyl maltoside/Zwittergent 16 yields the lowest Chl/P700 ratio. Small angle x-ray scattering (SAXS) studies were performed to determine the size and shape of PSI in a 0.5% Triton X-100 solution. An absolute size for the complex could not be determined but the initial data suggested that the PSI complexes had assembled into a lamellar sheet-like structure. Native Deriphat and lithium dodecyl sulfate (LDS) gel electrophoresis were used to compare the composition of PSI preparations solubilized with different detergents in order to further improve detergent optimization and verify the relative purity of each sample. It is concluded that dodecyl maltoside added to a Triton X-100 solubilized preparation at 0.5% yields complete solubilization when subjected to Deriphat-PAGE. In order to determine the subunit stoichiometry of each green band in the native gels, two dimensional gradient SDS-PAGE is currently being carried out.

Small Angle Scattering Studies on Spinach Photosystem I. *KATIE HELTON (University of Tennessee, Knoxville, TN 37996) ELIAS GREENBAUM (Oak Ridge National Laboratory, Oak Ridge, TN 37831).* Oxygenic photosynthesis is driven in series by Photosystems I (PSI) and II in the thylakoid membranes of higher plants and algae. PSI operates by a photo-induced activation of the special chlorophyll pair, P700, thereby translocating electrons from the lumen to the stroma generating NADPH. This study seeks to use small angle scattering techniques to investigate the dynamic structural changes that occur in PSI after photon absorption and during intermolecular electron transfer via the electron relay proteins plastocyanin and ferredoxin. PSI was initially isolated from spinach thylakoids by solubilization with 0.8% Triton X-100 followed by density gradient centrifugation. Further purification of this preparation was achieved by anion exchange chromatography on a HiTrapQ column using a Fast Performance Liquid Chromatography (FPLC) system. PSI was bound to the column under low ionic strength conditions and eluted with a linear salt gradient. The fractions with the highest PSI concentrations were pooled and further concentrated. The purity of the pooled fractions was analyzed spectrophotometrically based on a protein concentration of 1.15 mg/ml, Chl/P700 of 214 and a Chl a/Chl b ratio of 3.89. Native Deriphat gel electrophoresis was performed to determine the composition of the preparation in the concentrated PSI fractions. Small angle x-ray scattering (SAXS) studies were performed at the APS, Argonne to determine the size and shape of PSI in 0.1% and 0.5% Triton X-100 solutions using a range of PSI concentrations. The scattering data proved to be reproducible over the PSI concentration range employed and between the two detergent concentrations. The shape of PSI was an elongated cylinder with a radius of gyration of 63Å which is very similar to the radius of the published crystal structure. SAXS data from PSI prepared by gradient density centrifugation only revealed the formation of a lamellar sheet like structure with no measurable size; therefore, the implementation of anion exchange chromatography improved the quality of the sample. An enzymatic assay for determining the activity of PSI using the electron transfer from plastocyanin to ferredoxin via PSI will be used to determine binding properties of the electron carriers to PSI and overall efficiency of PSI in translocating electrons across the membrane. The data from this work will be used to design further SAXS experiments to investigate intermolecular electron transfer processes.

Generation of Phage Display Peptide Libraries and Target Protein Fusion Vectors. *JUSTIN HENRY (Grambling State University, Grambling, LA 71245) MICHAEL SCHOLLE (Argonne National Laboratory, Argonne, IL 60439).* The construction of phage display peptide libraries is very useful in analyzing protein-peptide interactions. The two main components in phage display are combinatorial peptide libraries and target proteins. The *E. coli* specific bacteriophage ssM13 (single-strand M13) DNA serves as a template for creating these libraries. Using peptide library construction protocol, an oligonucleotide coding for an 8-mer randomized NNK sequence is annealed to single-stranded M13 with a sequence fragment that contains an amber stop codon at the N-terminus of gene III. The second strand of DNA is generated in polymerase and ligase reactions. After the DNA is transformed into *E. coli* host cells, recombinants are screened using polymerase chain reactions. DNA sequences were translated revealing no bias in amino acid composition of the displayed peptides. The 8-mer NNK library was created with a diversity of 109 recombinant phage. With these libraries, affinity reagents for these target proteins can be identified. To aid in target protein expression and solubility, the chaperone fusion partners Glutathione-S-Transferase (GST) and Thioredoxin (Trx) were cloned

into the biotinylated vector, pMCSG16. Though the yield of recombinant yields were low in cloning Trx and GST (25% and ~8%, respectively), the clones may aid in the expression, solubility, and immobilization of currently insoluble proteins.

Comparative Analysis of the ApoE gene for humans and five primates. *MAYA HOVEY (City College of San Francisco, San Francisco, CA 94112) JAN-FANG CHENG (Lawrence Berkeley National Laboratory, Berkley, CA 94720).* Comparison of human sequences with the DNA of other primates is a means of identifying conserved functional elements in the human genome.The Comparative Genomics approach is the analysis and comparison of genomes from different species. The approach examines the counterparts of genes in different species by lining up multiple genomes and looking for conserved sequences. Conserved sequences represent regions of the genome that could serve common functions such as coding for proteins of similar function or regulatory sequences that control gene expression. The study of sequences in closely related species will determine conserved non-coding sequences in order to drive future research. This approach has been successfully used in comparing closely related species such as primates to identify functional domains of the DNA that are only present in the primate lineage. This approach will be used to detect potential regulatory sequences related to ApoE gene expression. The methods used in the finishing process were RCA, PCR and sequencing. The sequence for the Owl Monkey was completed. In multiple species comparison, known exons were shown to be conserved. Significant conservation in some non-coding regions suggests presence of regulatory elements. Humans and Old World monkeys share a duplication in the region of ApoC1, New World Monkeys do not.

Functional Survey of Conserved Noncoding Elements Near the PPARγ Gene. *NANCY HSU (University of California, Davis, Davis, CA 95616) JAN-FANG CHENG (Lawrence Berkeley National Laboratory, Berkley, CA 94720).* Cardiovascular patients commonly suffer from atherosclerosis, the narrowing of the coronary artery with low-density lipids. The human peroxisome proliferators-activated receptor gamma (PPARγ), a fatty acid receptor, regulates the formation of fat cells and their ability to function normally. Studying the regulatory mechanisms of the PPARγ gene may improve diagnosis and treatment of cardiovascular disease. One approach to understanding the functional content of the human DNA is comparative sequence analysis, also known as Comparative Genomics. By using various computational tools, such as VISTA (VISualization Tool for Alignment) and the University of California at Santa Cruz (UCSC) Genome Browser, conserved noncoding DNA sequences (CNS) surrounding the PPARγ gene can be detected and studied for regulatory function. In this study, three noncoding sequences upstream to the PPARγ, conserved among human, mouse, and chicken, were selected. They were subcloned from human genomic DNA into pWhsp68-lacZ reporter constructs, containing a minimal hsp68 promoter, and a lacZ reporter gene. Two insulators were also included to shield position effects. Accounting for both orientations of insertion, a total of six vectors were generated. In future work, the reporter constructs will be injected into mouse pronucleus zygotes for transient transgenic assay. If the conserved sequences can drive gene expression, then the lacZ gene, encoding β-galactosidase, will be expressed in a tissue-specific fashion. At 12.5 days, the embryos recovered will undergo X-gal staining and will be examined for lacZ expression.

Constructing the Protein-Protein Interaction Map for Human Mammary Epithelial Cells from Computationally Inferred Protein Domain Information. *DIANE HU (University of Washington, Seattle, WA 98195) HALUK RESAT (Pacific Northwest National Laboratory, Richland, WA 99352).* With recent developments in high-throughput technologies, proteins are being discovered and identified at an unprecedented rate. However, the large-scale detection of proteins provides little information about the actual biological processes in which they are involved in. Because proteins define the cellular constituents, they ultimately define the cellular networks, and knowing which protein-protein interactions occur in the cells is essential to understanding cellular behavior. Although the most reliable way to identify protein-protein interactions is through direct experimentation, the massive number of proteins found in a single cell makes this approach inefficient and impractical. Thus, there is a need to develop computational methods to predict the potential interactions between proteins. Because protein-protein interactions involve the physical binding of one protein domain to another, domain-domain interaction information can be useful in predicting protein interaction maps. Since large-scale domain interaction detection is very costly, we use computationally derived domain-domain interaction data instead from a protein domain interactions database called InterDom (http://interdom.i2r.a-star.edu.sg/). Based on this domain interaction information, we predict all possible pairs of interacting proteins using the domain information for each protein. This approach was implemented and applied to proteins from human mammary epithelial cells (HMEC) that were extracted and identified using mass spectroscopy. In doing so, a potential protein-protein interaction map could be derived for the epidermal growth factor, tumor necrosis factor, and G-protein coupled receptor pathways in the HMEC so that direct experimentation could be done to further validate the predicted interacting protein pairs with the highest possibilities of interaction.

Identification of the Cis-Acting Element within Promoter Arsa-43. *LAURA HUBBARD (Walla Walla College, College Place, WA 99362) ZIYU DAI (Pacific Northwest National Laboratory, Richland, WA 99352).* Arsa-43 is the promoter that regulates the Ubiquitin gene Ubi4 in the filamentous fungus Aspergillus niger. The Arsa-43 promoter is 900 bp but only a small part of this, the cis-acting element, produces the regulatory effect. Identification of the sequence of the cis-acting element can lead to the discovery of the associated trans-acting factors and ultimately allow genes to be regulated by the addition or withholding of these factors. The Arsa-43 promoter was subjected to sequential 5'-end deletion using restriction enzymes and PCR methods. The resulting four fragments (900 bp, 460 bp, 305 bp and 160 bp) were then inserted into plasmids containing the GUS reporter gene. A GUS assay was used to determine the activity of this gene and it showed a significant decrease in gene activity between 460 bp and 305 bp. This decrease suggests that the cis-acting element lies between these two boundaries. More research is needed to further target the cis-acting element and eventually determine its sequence.

The Roles of Tumor Necrosis Factor alpha and Inducible Nitric Oxide Synthase (iNOS) in the Response of RAW 264.7 Macrophages to Lipopolysaccharide. *LINDSEY JOSEPHSON (University of Washington, Seattle, WA 98105) BRIAN THRALL (Pacific Northwest National Laboratory, Richland, WA 99352).* Macrophages are the first line of defense against bacterial infections. These cells recognize invading pathogens and secrete pro-inflammatory mediators needed to clear infections. Among the pro-inflammatory mediators releases by activated macrophages are Tumor Necrosis Factor I (TNF) and Nitric Oxide ($NO^{\cdot}$). TNF and $NO^{\cdot}$ are thought to play a critical role in host pathogen interactions. Although low levels of TNF and NO- are necessary for proper immune function, high levels of either can be lethal to the cell. In this study we investigated the responses of macrophages to lipopolysaccharide (LPS), a component of gram-negative bacterial cell wall recognized by the macrophage. By exposing cells to LPS with and without inhibitors of TNF and iNOS, we found that while low levels of LPS stimulate growth, high levels result in cytotoxicity, which is mediated primarily through $NO^{\cdot}$.

Toxicity and Protection of Neuronal Precursor Cells Exposed to Ionizing Radiation. *RAHAL KAHANDA (Washington University in St. Louis, St Louis, MO 63105) MARCELO VAZQUEZ (Brookhaven National Laboratory, Upton, NY 11973).* Ionizing radiation is toxic to human cells. Prolonged space travel results in cellular degeneration due to exposure to heavy ions. Cellular toxicity is an important venue of study as the exploration into space broadens. Therefore, it is important to study and establish a mechanism in which we can identify cellular anomalies in response to radiation. Ntera 2 (NT2), neuronal precursor, cells were utilized to investigate radiation induced chromosomal abnormalities. To gain mechanistic insight into this process, specific drug candidates were tested for their potential abilities to protect cells from radiation-induced toxicity. Pifithrin-Alpha was chosen for its inhibition into the p53 mediated programmed cell death pathway, transformation growth factor (TGF-Beta) for its growth promotion effects, and melatonin and selenomethionine for their ability to scavenge and reduce toxic free radicals. Analysis by fluorescent imaging showed a significant decrease in radiation-induced abnormal chromosomal morphology by pretreatment with both selenomethionine ($p < 0.01$) and melatonin ($p < 0.05$). No significant effect was seen with TGF-Beta and PFT-Alpha. This strongly suggests that radiation induced nuclear toxicity in brain stem cells are at least partially mediated by the oxidative free radical species pathway. Although neurotoxicity induction by ionizing radiation has been demonstrated and linked with oxidative free radicals, there are still many questions that need to be answered. This study is an important part of the greater question as to how ionizing radiation adversely affects human neural stem cells.

Identification of a Critical Amino Acid Residue ofYiiP, a Zinc Transporter from Escherichia coli. *KATHERINE KAO (SUNY Stony Brook, Stony Brook, NY 11794) DAX FU (Brookhaven National Laboratory, Upton, NY 11973).* Homeostasis of metal cations in the cell is crucial to survival. YiiP is a metal transporter in E. *coli* which plays a central role in regulating cellular concentrations of Zn^{2+}. Transport of

these metals involves a coupled deprotonation mechanism, however, the structure and mechanism of function have not yet been revealed to atomic details. In this study, point mutations in wild type YiiP were made and the stability and secondary structure of YiiP mutants was studied with CD (circular dichroism). To perform CD analysis, His-YiiP was overexpressed using pET15b expression vector hosted in *E. coli*. BL21 (DE3)pLys cells. The protein was extracted from membrane vesicles and followed by purification with Ni-NTA metal affinity and size exclusion chromatography. CD analysis of the purified protein shows that the protein is mostly alpha helical and reveals one site, Asp 157, in particular that is critical to stability suggesting that it may have a role in the metal transport mechanism.

High Throughput Analysis of Stress Response in Metal and Radionuclide Reducing Bacteria. *NATALIE KATZ (Seattle Central Community College, Seattle, WA 98122) TERRY C. HAZEN (Lawrence Berkeley National Laboratory, Berkley, CA 94720).* The United States Department of Energy (DOE) has three million cubic meters of buried radioactive and hazardous waste, 75 million cubic meters of contaminated soil, 475 billion gallons of contaminated groundwater, and 120 nuclear weapons production facilities contaminated with radioactive materials, hazardous chemicals, asbestos, and lead. Bioremediation has proven to be a valuable and cost-effective way of eliminating and containing these hazardous substances through the use of microorganisms to reduce, eliminate, contain, or transform the contaminants to nonhazardous or less hazardous forms. The Center for Environmental Biotechnology at Lawrence Berkeley National Laboratory is conducting research as a part of the Virtual Institute for Microbial Stress and Survival (VIMSS). The VIMSS group aims to identify stress response pathways induced by various environmental factors, such as temperature, pH, oxygen, nitrate and nitrite concentration, and metal and radionuclide concentration. *Desulfovibrio vulgaris* is the model organism of choice because it is a known sulfate-reducing bacterium capable of reducing the metals of interest at these contaminated DOE sites, such as radioactive uranium (IV) and the heavy metal chromium(VI). *D. vulgaris* cultures were grown in LS4D defined media, and then used to inoculate media solutions containing different concentrations of nitrate, nitrite, or NaCl. These solutions were then used to inoculate a 96-well plate. The plates were placed in the Omnilog plate reader and allowed to incubate for 150 hours. VIMSS was looking for the minimum inhibitory concentration (MIC), defined as the amount of stressor needed to double the organism's generation time. The MIC determined for nitrate was 3500 ppm. The MIC determined for nitrite was 75 ppm. The MIC determined for NaCl was 250 mM. Hexavalent chromium and radioactive uranium (IV) will be added to the media solutions to see how the MIC's are affected in the presence of a heavy metal or radionuclide. These studies will be used to design time series experiments for the VIMSS project for rapid deduction of stress response pathways in metal and radionuclide reducing bacteria by simultaneous analyses using proteomics, metabolomics, lipidomics, transcriptomics, and phenomics.

Creating Functional Divalent Antibodies. *GABRIELA KIRK (University of Texas, Austin, TX 78705) STEPHEN J. KENNEL (Oak Ridge National Laboratory, Oak Ridge, TN 37831).* Antibodies to tumor antigens are used to deliver radioactive isotopes to tumor cells. Phage display, a new way of identifying antibodies, has been used to find a special antibody form called a single chain variable fragment antibody (scFv) that binds to laminin. This scFv, 15-9, homes to tumors in mice. ScFvs are composed of a single variable heavy chain sequence and a single variable light chain sequence which fold together to form a single binding site. To try to improve scFv 15-9 performance, attempts were made to produce divalent forms of the scFv in hopes that they would have a higher affinity for the target, laminin, and thus better binding to the tumor. Three methods were used to prepare divalent antibody in order to determine the validity of the theory. The first method uses molecular biology to shorten the linker between the two variable regions of each scFv allowing two different scFvs to crosslink. The next method is to produce a bivalent antibody chemically. Traut's reagent introduces a free sulfhydryl group into one batch of scFv and sulfosuccinimidyl 4-(N-maleimidomethyl) cyclohexane-1-carboxylate (sulfo-SMCC) introduces an active maleimide group into another batch of scFv. When these two scFvs are mixed, the maleimides react with the sulfhydryls forming thioether bonds and create bivalent products. Finally, non-covalent dimers were prepared using protein L or anti-myc, bivalent reagents that bind two scFvs together. Protein L binds to the VL regions of certain scFvs and anti-myc binds to the myc tags on the end of each scFv. By binding to two scFvs at their VL regions or myc tags, non-covalent dimers are produced. Results for the molecular biology approach are still pending. The results for the second approach show that a functional bivalent antibody can be produced only when certain amounts of Traut's and Sulfo-SMCC are added to the scFvs: adding more created a globular clutter and adding less meant not enough reaction to create a functional dimer. Thus the yield of dimer from this approach was low. The final approach showed that a functional dimer could be produced and was, in fact, more efficient at binding to the protein than a monovalent antibody. Through the various experiments using the three separate methods, it was shown that dimerized scFvs are more active than single valency forms at binding laminin in vitro. Further testing is necessary to determine if the dimer scFvs perform as better tumor targeting agents.

Introduction to the Technique of Phage Display as a Tool for Mapping Preotein-Peptide interactions. *APRIL KITTEL (Grambling State University, Grambling, LA 71245) BRIAN KAY (Argonne National Laboratory, Argonne, IL 60439).* Phage display has made significant contributions to the field of molecular biology. Its many applications have made it a very useful tool in mapping protein-peptide interactions. This paper outlines experiments on an appendage of AP-1(an adaptor protein), commonly known as ß-ear. Previous research has solved the structure of its sister appendage α-ear, therefore creating a push to improve understanding of this common protein. Our experiments show that ß- ear has very little in common with α-ear, as far as peptide ligands show. Using techniques such as, by biopanning and runing Enzyme Linked Immunosorbent Assays (ELISA), we were able to check ß-ear's specificity with cross-reactivity ELISAs. We were able to assay selective and specific peptide ligands to ß-ear, thereby creating a common motif that will help future research characterize ß- ear.

Purification and Crystallization Trials of C-Type Cytochromes from *Shewanella oneidensis* For Structure Characterization Using X-Ray Crystallography. *BRIANNA KLEIN (University of Oregon, Eugene, OR 97401) NANCY ISERN (Pacific Northwest National Laboratory, Richland, WA 99352).* Molecular machines are complex biomacromolecules which are able to utilize energy to complete specific actions. The electron transport system (ETS), an assembly of molecular machines, uses a proton gradient across a membrane to facilitate electron transfer, with concomitant energy production. C-type cytochromes (heme proteins) function in the ETS to reduce terminal electron receptors, which may be metals. Shewanella oneidensis is capable of reducing soluble metals such as uranium, iron and manganese to insoluble forms. Precipitation of uranium immobilizes the metal, which then does not migrate with groundwater, and can be used to effect removal of uranium from waste streams. Structural determination of c-type cytochromes will aid in elucidating function of these proteins and the mechanism by which they reduce metals. This in turn may lead to design of organisms which are capable of accelerated waste cleanup. This study focuses on the heme proteins MtrA, MtrB and MtrC from *Shewanella oneidensis*. MtrA passes electrons from the electron transport chain to soluble metals. MtrB is required for the correct positioning of other heme proteins to the outer membrane. MtrC is thought to function either as part of the terminal reductase, or to be involved in its stability or assembly. MtrA, MtrB, and MtrC were isolated and purified using metal-affinity columns, anion exchange columns, size exclusion columns, SDS page gels, and ammonium sulfate extractions. The purified proteins were concentrated for use in crystallization trials; however MtrA and MtrB were not pure enough to attempt crystallization. MtrC was prepared for crystallization at two different concentrations, 10.5mg/ml and 5 mg/ml. At the time of this paper, unfortunately, no useful crystals have been isolated. Further refinement of purification and crystallization protocols will be needed to obtain high quality crystals of MtrA, MtrB, and MtrC for three-dimensional structure determination.

The Synthesis of Anhydrotrypsin: A Trypsin Still Shot. *DONNA LEE (University of California, Berkeley, Berkeley, CA 94720) WALTER MANGEL (Brookhaven National Laboratory, Upton, NY 11973).* Trypsin is a classic model of a serine protease. Of the most prevalent proteolytic enzymes, serine proteases utilize a serine residue in their active site to cleave peptide and ester bonds. Previous studies have structurally characterized the later stages of hydrolysis, but the initial step of the reaction, substrate binding, remains elusive. Because of the tendency to rapidly progress beyond substrate binding, it is not feasible to obtain a static sample of trypsin bound to substrate pre-cleavage. However, it has been shown that conversion of the active site serine to alanine to form the trypsin derivative, anhydrotrypsin, renders the protein enzymically inert but retains the ability to form stoichiometeric complexes. In this study, we strived to synthesize this structurally intact yet inactive form of trypsin for the future purpose of crystallization of the anhydrotrypsin-substrate binding complex. With this end in mind, according modifications to the Ako et. al. method were followed. Treatment with 4-(2-aminoethyl) benzene sulfonyl fluoride (AEBSF) as measured by the rhodamine 110, bis-(N-CBZ-L-isoleucyl-L-prolyl-L-arginine amide) (BZIPAR) assay rendered trypsin < 0.001% active. Following base

treatment and the addition of tosyl lysyl chloromethyl ketone (TLCK), an irreversible inhibitor of active trypsin, separation was achieved by a soybean trypsin inhibitor (SBTI) affinity column. The separation profile revealed a relatively small non-specific flow thru peak and a large specific elution peak indicating that multiple non-binding species were separated from a unique species of binding intact trypsin. Mass spectroscopy was employed to verify the mutation of active site serine to alanine. Spectra of anhydrotrypsin compared to trypsin revealed a loss of 16 Da, the mass of an oxygen atom, suggesting conversion had occured. Non-reduced SDS-page gels produced a major band consistent with a trypsin standard, and size exclusion chromatography yielded consistent profiles between folded trypsin and anhydrotrypsin. In order to obtain the initial activity of trypsin, a delay time was sacrificed between dissolvation and addition of inhibitor allowing trypsin sufficient time to cleave itself. This cleavage may be the major contributor to the 11.1% yield obtained. In spite of this yield, the formation of enzymically inactive, binding apt, unfragmented, folded, and largely homogeneous anhydrotrypsin, leaves crystallization a promising prospect for further studies.

Preparation of Pseudomonas aeruginosa Proteins Potentially Involved in Quorum Sensing for Structure Characterization by Nuclear Magnetic Resonance (NMR). *ERIN LOCKERT (Central Washington University, Ellensburg, WA 98926) MICHAEL KENNEDY (Pacific Northwest National Laboratory, Richland, WA 99352).* Quorum sensing is an important mechanism bacteria employ to render themselves resistant to antibiotic action and remain established in their host. This phenomenon allows bacteria to detect their density in an environment and alter their metabolism through signal molecules. Pseudomonas aeruginosa bacteria readily colonize the lungs of individuals afflicted with cystic fibrosis in a biofilm formation, orchestrated through quorum sensing. Molecular biology techniques, including cloning, *E. coli* cell transformation and expression, SDS-PAGE and agarose gel analysis, protein purification, and ^{15}N-labeling were used to obtain target proteins PA1324 and PA5481 from this bacteria that may be involved in quorum sensing. Nuclear Magnetic Resonance (NMR) was conducted to provide a Heteronuclear Single Quantum Coherence Spectrum (HSQC) for each protein. These preliminary spectrums will provide the foundation for the complete structure characterization of proteins PA1324 and PA5481 through NMR analysis and a greater understanding of the role these proteins play in quorum sensing.

Crystallization of the Full-Length Nitrogenase Accessory Factor-Y (NafY) Protein. *MEHNAZ MALEK (Diablo Valley College, Pleasant Hill, CA 94523) GERRY MCDERMOTT (Lawrence Berkeley National Laboratory, Berkley, CA 94720).* Nitrogenase Accessory Factor-Y (NafY) is found in the bacteria *Azotobacter vinelandii* and is involved in nitrogen fixation. Understanding the structure and function of NafY may lead to better nitrogen harvesting techniques as well as improvement of crops in the agricultural industry. It can bind either to the iron molybdenum cofactor (FeMo-co) or to apodinitrogenase and may be involved in the transfer of FeMo-co into apodinitrogenase. The crystal structure of the NafY core domain has been solved; however, the entire protein has not been crystallized until recently. Initial screening of protein with the Hampton Peg Ion Screen resulted in large, multiple crystals. Lowering of protein concentration and MnC_{l2} additive yielded semi-singular crystals in various trays; silver stain gel tests proved them to be full length NafY protein crystals. As they did not diffract very well when tested in an x-ray source, it was not possible to solve their structure. Attempts to optimize the quality of the crystals through techniques such as seeding, and under-oil growth are in progress.

Isolation and Purification of Heme Proteins from *Shewanella oneidensis*. *GREGORY MARSING (Brigham Young University, Provo, UT 84602) NANCY G. ISERN (Pacific Northwest National Laboratory, Richland, WA 99352).* *Shewanella oneidensis*, as well as a number of other bacteria, have become of particular interest due to their ability to respire anaerobically reducing a variety of metal substrates. The ability of these bacteria to reduce metal substrates during respiration opens the possibility that they may be useful for bioremediation. Although these pathways of anaerobic respiration are not completely understood, a number of iron containing c type cytochromes have been shown to play an intergral role. Characterization of these c type cytochromes will provide information that will help us to understand the pathway of metal respiration better. We report a method for purification of one of the c type cytochromes found in *Shewanella frigidimarina*.

Root Engineering Innovation Technology Utilizing the Soil Depth Dimension for Gas. *SAMELLA MATSEY (Kennedy King college, Chicago, IL 60621) M. CRISTINA NEGRI (Argonne National Laboratory, Argonne, IL 60439).* Argonne National Laboratory is currently performing a comprehensive carbon management research program to sequester excess carbon which includes the maximization of the carbon sink potential of the terrestrial ecosystem. The vegetation on marginal, semi-arid, contaminated and/or damaged land is necessary for increasing the carbon inventory in the terrestrial ecosystem, i.e. by increasing rooting depth and enabling vegetative growth can soil carbon be increased. It is necessary that water is available to keep the trees growing and provide minerals at acceptable locations when or where the precipitation (rainfall or snow) is too scarce or unpredictable that may have a great affects on the growth of the trees depending on condition of their soil. An innovative technology was developed to render plantations independent of water supplies or irrigation by developing deep root systems that tap into deeper depths of groundwater. This technology was performed by the Applied Natural Sciences (ANS) that patented these technologies by using, TreeMediation® and TreeWell® Systems-Cartridges to overcome unfavorable soil conditions, which could include soil from marginal, semi-arid, contaminated and/or damaged land. Deep root are engineered to grow from phreatophytic trees that would root into soil with the expectation of the roots growing deep enough to reach groundwater levels. Deeper rooting depths can increase carbon sinks, and in turn will facilitate a trees water supply. Increase will especially aid in the growth of vegetation. The goal of this study focuses on first understanding gas levels in soil from pre-installed TreeMediation® and TreeWell® Systems-Cartridges installed by Applied Natural Sciences (ANS). These wells contain Willows: Salix alba var, tristis, Oak: quercus alba, Walnut: Juglans nigra, and controls which have no tree (only different soil types) cartridges. The most important gases influencing soil processes include carbon dioxide and nitrogen. The collection of soil gas is done by using a 60mL syringe to extract or pull gas soil samples from metal gas probes pre-installed at depths of 2ft, 4ft and 6ft. Soil gases are then analyzed using a gas chromatography to determine concentrations of CO_2, N_2, and O_2.

Periphyton and Water Quality. *DION MCCLURE (Washington State University, Vancouver, WA 98686) AMORET BUNN (Pacific Northwest National Laboratory, Richland, WA 99352).* Periphyton, the benthic primary producers in the Columbia River, is the bottom of the aquatic ecosystem food chain. The periphyton community consists primarily of algae and diatoms. It has the highest exposure to potentially contaminated groundwater entering the river. Understanding the uptake of potential contaminants by periphyton and the role it plays in our environment is just one aspect of the Biological Exposure Studies being conducted at PNNL. The objective of this study was twofold: determine growth rate of the periphyton on artificial substrate in the laboratory; and evaluate changes in water quality parameters by periphyton due to their response to light. Growth was determined by removing the material from the slides at intervals for dry weight analysis. Changes in water quality were evaluated for both static and flow-through conditions. Growth rate on the slides increased for the first 14 days then decreased. Water quality changed in response to light and water-flow conditions in the substrate set up. A side study with an algal mat was performed to quantify changes in water quality. The pH in the bin with the algal mat increased when the lights were off and decreased when on. It is concluded that growth rate is related to a balance between the primary producers and the consumers. Improved growth rate could have been achieved if the source of the periphyton had included fewer consumers and if the light intensity had been greater encouraging more production. The pH data collected was inconclusive, as the experiment could not be repeated. Further experiments are expected to indicate the role of periphyton on the quality of water.

Impacts of Offshore Wind Farms on Benthic Communities. *MICHAEL MCCORMACK (College of Charleston, Charleston, SC 29401) MIKE ROBINSON (National Renewable Energy Laboratory, Golden, CO 89401).* With improved technology and falling costs the wind industry is poised to begin a full-scale expansion into the offshore market. However, before this can be done safely, and with minimal impact to the surrounding environment, we must first understand the potential impacts that large offshore wind farms may produce. By narrowing the field of study to benthic communities we are able to better understand impacts on a small scale and then apply that knowledge to the larger environment. Two sites have been identified for this study: Horns Rev wind project, off the western coast of Denmark and Nysted wind project, offshore between Denmark and Sweden. Data taken from these projects suggest that offshore wind farms do not cause many significant lasting impacts to benthic communities and warrant no immediate corrective action. There will be some significant, but temporary impacts to the benthic community during dredging and construction as well as some lasting impacts caused by the presence of the turbine foundations acting as artificial reefs. However, the overall impact to the marine environment should not be great. Unfortunately, because the offshore

market is relatively new to expansion, the total data currently available is limited. It is therefore recommended that the findings in this paper be regarded only as preliminary reports until more sites are studied and analyzed for further support or rejection of conclusions herein.

Expression, Purification, and Crystallization Trials of the Enzymatically Active Light Chains of *Clostridium botulinum* neurotoxin type A and C (BoNT/A-LC and BoNT/C-LC). *ANN MEYER (Harvard Graduate School of Education, Cambridge, MA 02138) SUBRAMANYAM SWAMINATHAN (Brookhaven National Laboratory, Upton, NY 11973).* Botulinum neurotoxins (BoNTs) are amongst the most toxic substances known to humans. One gram of the toxin in crystalline form has the potential to kill one million people if it is dispersed properly. In order to design an effective inhibitor against all of the botulinum neurotoxins, the crystal structures of each must be determined. *Clostridium botulinum* produces seven serotypes of neurotoxins, each labeled by letter (A-G). The sequences and structures of these toxins are quite similar, however, the substrates and cleavage sites vary depending on the serotype. These neurotoxins are produced as a single inactive polypeptide chain of 150 kDa and cleaved into active dichains of heavy (HC, 100 kDa) and light (LC, 50 kDa). The catalytic activity resides in the light chain. Therefore, in order to solve the structure of the catalytic portion, the light chain of the toxin must be crystallized. Here, the light chain of type A (BoNT/A-LC) and type C (BoNT/C-LC) have been expressed *in E. coli* cells. BoNT/A-LC and BoNT/C-LC have each been purified using affinity chromatography on Ni-NTA agarose followed by size exclusion chromatography. BoNT/A-LC and BoNT/C-LC both show proteolytic activity on their substrates. Therefore, the structures of these proteins are useful in studying the mechanism of catalytic activity because their activity remains intact after expression and purification. The purified BoNT/A-LC and BoNT/C-LC protein are being used to get protein crystals in order to study their structures. Currently, various conditions are being tested to obtain useful crystals for X-ray data collection.

Characterization of Anuran Breeding Sites on the Hanford Reach. *BRIAN MILLER (Washington State University, Pullman, WA 99163) BRETT TILLER (Pacific Northwest National Laboratory, Richland, WA 99352).* Riparian zones along the Hanford Reach offer distinguished breeding sites for both endemic and introduced species of amphibians. Fluctuating water levels created by operations at Priest Rapids Dam upstream creates shoreline pools that allow various herpetofauna to successfully utilize these to reproduce. Fifteen pools within the Columbia River's riparian zone were located and characterized with three anuran species found utilizing these pools, the Great Basin Spadefoot (*Spea intermontana*), Woodhouse's Toad (*Bufo woodhousii*), and the Bullfrog (*Rana catesbeiana*). Visual Encounter Surveys (VES) and night-time call surveys were conducted between June and August in order to establish presence/absence of each species at corresponding sites. Surveys of anurans were conducted in three general geomorphic river classifications common along the Hanford Site shorelines. During the 2004 season, the Woodhouse's Toad comprised 79.5% of all night-time call surveys, followed by the Bullfrog at 16%, and the Spadefoot at 4.5%. All of the calls (100%) were heard in areas described as Backwater/Slough, as opposed to Riverine-Wide and Riverine-Narrow river classes. VES encounters with juvenile anurans indicated a preference to persistent pools with some aquatic vegetation, a wide range of substratum, and water temperatures greater than ambient river water proved to be important breeding site characteristics for anurans in the Hanford Reach of the Columbia River.

Elucidating Protein Structure through Wide Angle X-Ray Scattering (WAXS). *DAVID MINH (University of California, San Diego, La Jolla, CA 92093) LEE MAKOWSKI (Argonne National Laboratory, Argonne, IL 60439).* Theoretical and experimental wide angle x-ray scattering (WAXS) patterns were used to predict protein secondary structure content and detect fold similarity. Principal components analysis and multiple regression was used to predict secondary structure, yielding 19.48 and 12.97 percent error on theoretical patterns and 11.78 and 10.16 percent error on experimental patterns for alpha helical and beta sheet content, respectively. These errors are greater than those from circular dichroism predictions, but WAXS has greater potential for improvement. Pattern space distance was defined as the distance between vectors based on the principal components of a set of scattering patterns. Comparison of pattern space distance and DALI Z-scores shows that pattern space distance can be used as a measure of fold similarity. It is proposed that WAXS can complement structural genomics initiatives by gleaning information from proteins prior to crystallization, allowing for a wider sampling of protein fold space and contributing to the scientific understanding of protein folding.

1.6 Å Crystal Structure of YteR Protein from *Bacillus subtilis*, a Predicted Lyase. *TIMOTHY MINH (University of California, Berkeley, Berkeley, CA 94720) ANDRZEJ JOACHIMIAK (Argonne National Laboratory, Argonne, IL 60439).* The crystal structure of YteR, a 42.9 kDa cytosolic protein of unknown function from *B.* subtilis, has been determined at 1.60 Å by the multi-wavelength anomalous dispersion method. The protein, expressed with E. coli, was crystallized by vapor diffusion in hanging drops by mixing 1 µl of the protein solution (30 mg/ml) with 1 µl of 1.3 M sodium citrate, 0.1 M Tris, pH 7.5, and equilibrated at 295 K over 500 µl of this solution. These crystals belong to the hexagonal space group P6122 with cell dimension of a=b=91.86 Å, c=179.41 Å, a=ß=90° , γ=120°. YteR represents a new protein fold with an a/a double-toroid structure with its six a-hairpins arranged in a double a-helical barrel with diameter of 17 Å for inner and 30 Å for the outside barrel. The 71 known members of YteR family are found in bacteria and fungi. Sequence and structure analyses show a putative active site formed by six solvent exposed residues (Asp143, Leu145, Trp211, Arg213, Trp217, and Ser278). Further comparative studies between *B. subtilis* YteR and the homologous crystal structures of Bacillus sp. GL1 unsaturated glucuronyl hydrolase and *E. chrysanthemi* lyase suggest that *B. subtilis* YteR's possible role is to hydrolyze a specific glycosidic bond in unsaturated saccharides that are produced by polysaccharide lyases reactions and assist with the ultimate conversion of the released saccharide to an a-keto acid.

The Development of an Algorithm and Graphical User Interface for Wide Angle X-ray Scattering (WAXS) Background Subtraction and its Application the Macromolecular Crowding of Hemoglobin. *DAVID MINH (University of California, Berkeley, Berkeley, CA 94720) LEE MAKOWSKI (Argonne National Laboratory, Argonne, IL 60439).* Wide angle x-ray scattering (WAXS) is a promising technique for deriving structural information from proteins. However, use of the technique has been hindered by the lack of data analysis techniques and software. The Background Subtraction Suite (BSS) software package was developed in order to analyze WAXS patterns. The BSS performs two types of subtractions to calculate protein scattering: a direct subtraction and a subtraction calibrated for self-consistency with other subtracted scattering patterns of the same protein. Using WAXS patterns taken at the BIO-CAT beam line of the Advanced Photon Source at Argonne National Laboratory, the BSS was used to calculate a self-consistent concentration series for Hemoglobin. Differences in the WAXS patterns between the different Hemoglobin concentrations are proposed to be the result of signal to noise ratios, radiation damage, and macromolecular crowding. Macromolecular crowding is proposed to have a significant effect on protein folding and thermodynamics.

The Kinetics of BDE-47 Metabolism in Japanese Medaka (Oryzias latipes). *ELISABETH MUIRHEAD (University of Puget Sound, Tacoma, WA 98416) IRVIN R. SCHULTZ (Pacific Northwest National Laboratory, Richland, WA 99352).* Brominated diphenyl ethers (BDEs) are a class of flame retardants used in paints, plastics, textiles and electronics. They are also persistent organic polluters, because they build-up in the tissues of animals and humans that ingest them. Some of the toxic effects of these compounds include disruption of the thyroid system, neurobehavioral effects, and carcinogenicity. In this experiment, Japanese Medaka (*Oryzias latipes*) were orally dosed with 2,2',4,4' tetraBDE (BDE-47) and periodically terminated. The carcasses were analyzed using gas chromatography (GC) to determine the rate of absorption and elimination of BDE-47. We found that BDE-47 levels rose rapidly over the first 12 hours, then held steady until 36 hours, at which time levels rose slightly again before leveling off at 48 hours and beginning a slow elimination decline, which was not complete after 222.5 hours. The absorption rate (Ka) of BDE-47 was 0.02 ±0.01 hr-1. A single-compartment pharmacokinetic model showed that the behavior of BDE-47 can be predicted, which is an important finding considering the persistent nature of BDE-47.

Factors Influencing The Photosynthetic Response Of A Wetland Grass, *Phalaris arundinacea* L. *ALEXANDRA NAPIER (Washington State University, Pullman, WA 99163) JANELLE DOWNS (Pacific Northwest National Laboratory, Richland, WA 99352). Phalaris arundinacea* L., is an invasive, wetland grass species of Washington State, commonly found along the riparian zone of the Hanford Reach on the Columbia River. As part of ecological assessments focused on riparian species that may be potential contaminant receptors, we measured photosynthetic rates in selected *P. arundinacea* plants at locations near and away from Hanford areas. This work provides a baseline for understanding photosynthetic responses of a common receptor species to environmental variation along the Hanford Reach. Photosynthesis was measured at three locations along the shoreline of the reach to evaluate the variability in photosynthesis and fitness of the *P. arundinacea* under

differing conditions for soil moisture and substrate type. At each location samples were taken at two shoreline elevations that receive varying frequencies and levels of inundation depending on river fluctuation patterns and dam operations. All plants in the lower shoreline elevations were exposed to more frequent inundation than plants growing in the upper shoreline elevations. Plants receiving higher water levels also had higher rates of net photosynthesis. Our results indicate that shoreline elevation and substrate interact to affect mean photosynthetic rates. Photosynthetic rates of plants at lower versus upper shoreline elevations growing on cobble substrate were not significantly different (means=18.539 (μmol m^{-2} s^{-1}) and 18.587 (μmol m^{-2} s^{-1}) respectively) when gravimetric soil moisture was comparable. Plants growing in silty substrates showed significant differences in photosynthetic rates (means=7.888 μmol m^{-2} s^{-1}) and 12.349 μmol m^{-2} s^{-1}) respectively) between upper (drier) and lower (wetter) shoreline elevations. No significant difference in net photosynthesis was found between sites located downstream of contaminated seeps and reference sites located upstream of Hanford Site influence.

Use of 28S rRNA gene D1/D2 Domain Sequences for the Identification and Phylogenetic Analysis of Filamentous Fungi Isolated from Extreme Environments. *SUZANNE NITTA (California State University Fresno, Fresno, CA 93740) TAMAS TOROK (Lawrence Berkeley National Laboratory, Berkley, CA 94720).* Microorganisms have been found to thrive in some of the most extreme environments on earth, exposed to high radiation, chemical contamination, high salinity, acidic or alkaline pH conditions, or exceptionally low or high temperatures. Due to the vast diversity of extremophillic microorganisms, they have become a valuable bioprospecting target. An important aspect of bioprospecting is the taxonomic identification of these microorganisms, for this provides a greater understanding of their diversity, unique metabolism, and ecological function. An ongoing study in this laboratory focuses on the taxonomic characterization by molecular comparison of thousands of filamentous fungi isolated from sediments of Lake Baikal and geothermal sites in Kamchatka, Russia, and from the 30-km "exclusion zone" surrounding the failed nuclear power plant in Chernobyl, Ukraine. Pure cultures of the filamentous fungi were grown under standardized conditions. The genomic DNA was extracted using the BIO 101 FastDNA kit and protocol (Q-BIOgene, CA). The D1/D2 domain of the 28S rRNA gene was amplified by polymerase chain reaction (PCR). Amplicons were separated by gel electrophoresis in a 1.2 % agarose in a 1x TBE buffer. Prior to sequencing, PCR products were run through MicroSpin™ silica gel columns (Amersham Pharmacia, NJ) and ethanol precipitated. The University of California at Berkeley DNA Sequencing Facility sequenced the PCR products. Raw sequences were edited with EditView Ver. 1.0.1.1 (ABI, CA), aligned using the online site MultAlin (http://prodes.toulouse.inra.fr/multalin/multalin.html), and blasted against the National Center for Biotechnology Information database (http://www.ncbi.nlm.nih.gov/BLAST) to determine taxonomical relatedness of the filamentous fungi.

Brain Functional Change Using Fluorescence and Optical Imaging Reflected in Intracellular Calcium Information. *YINETTE PEREZ (Hostos Community College, Bronx, NY 10460) CONGWU DU (Brookhaven National Laboratory, Upton, NY 11973).* Calcium channel blockers interfere with the movement of calcium in and out of cells. During Ischemia, there is a massive invasion of calcium into neurons, which can lead to neuronal death. The L-type calcium channel blocker is used in various experiments and now, it is expected to reduce the metabolism in the ischemic brain tissue. Studies suggest alterations in calcium concentration in the brain, but a detailed understanding of these alterations is needed. A technique has been developed to identify the changes the L-type calcium channel blocker may cause in an ischemic brain. We tested the effect of an L-channel calcium blocker (Nimodipine) on ischemia-induced increases in intracellular calcium using this newly developed technique. This advance technique uses fluorescence and optical imaging to follow those changes. Primarily, calcium channel blocker is injected in the ischemic brain of a rat, rhodamine 2, the fluorescence dye, is also injected during this process. After dissection, the brain is frozen with liquid nitrogen. Sliced sections of the brain are observed under a fluorescence microscope and photographed. The photographs are taken to be analyzed using Image J, and the data was compiled in Exel's spreadsheets. There was a significant difference in intensity (reflecting difference in calcium load) between ischemic control brains and ischemic L-channel calcium blocker brains. Future research using this technique will allow us to acquire a better understanding of the pathophysiological changes of the ischemic brain under the influence of calcium blockers.

Design and Testing of a Ligase. *YURI POLUEKTOV (University of Illinois at Urbana-Champaign, Urbana-Champaign, IL 61801) PHILIP LAIBLE (Argonne National Laboratory, Argonne, IL 60439).* A ligase independent cloning reaction is a very efficient way of inserting specific genes into a plasmid for manipulation and cell expression. Just like its name implies the cloning reaction does not need to be ligated which saves at least an hour on the entire cloning procedure. In addition ligase independent cloning does not require unique restriction endonuclease sites to be present on the ends of the gene or inside the plasmid vector that the gene will be inserted in. This helpful attribute allows the process of cloning a gene to be automated so it can be performed in large numbers within a short period of time by a robotic instrument. The principle of a ligase independent cloning reaction is the generation of very large sticky ends on both the gene and the plasmid vector, so that when they are annealed the circular plasmid will not break while it is being transformed into a competent cell. Once the plasmid has been transformed the cell machinery can fix the tears within the plasmid. In order to generate those large sticky ends we must exploit the exonuclease activity of a DNA polymerase. First we make one cut in our cloning vector using a unique restriction site; the cut has to be such that a DNA polymerase can attach itself to the ends of the plasmid. Now instead of giving the DNA polymerase the four necessary nucleotide precursors: dTTP, dATP, dGTP, dCTP, we only give it one of the four. This results in the polymerase's inability to extend the DNA strand in the 5' to 3' direction, unless it can use the one nucleotide precursor that we gave it, however its exonuclease activity is still active and it will cut off nucleotides in the 3' to 5' direction until it reaches a spot where it can build the DNA strand using the nucleotide that we exposed it to. The gene insert is treated with a similar process after it is amplified using a PCR reaction. Both the plasmid and the gene insert DNA strands can be engineered in such a way that this exonuclease activity will eliminate around 15 nucleotides on the top and bottom strands of the plasmid giving us an extremely large sticky end and allowing us to conduct our ligase independent cloning reaction.

Heavy Metals and their Effects on Animal Tissues. *SEYMONE POWELL (Alcorn State University, Alcorn, MS 39096) JORG MASER (Argonne National Laboratory, Argonne, IL 60439).* The purpose of this project involved determining cadmium content in adult rat tissues previously exposed to cadmium chloride. The approach taken to investigate this initiative involved the use of inductively coupled plasma-mass spectrometry (ICP-MS) and X-ray microprobe fluorescence microscopy. Mean standard cadmium isotope concentrations demonstrated a direct linear relationship between increasing cadmium standard concentrations and increasing cadmium isotope masses (specifically, Cd^{110}, Cd^{111}, and Cd^{112}). Indium, a soft metal, used as an internal standard, was efficient in normalizing control and sample data. Elemental maps of (P, S, C, K, Mo, Fe, and Zn were generated from a single isolated rat hepatocyte previously treated with cadmium chloride. Representative relative values of intensities in linear and logarithmic scales were generated at 30 keV by x-ray fluorescence microscopy. The distribution of heavy metals such as cadmium L-lines at 30 keV was not detected in cyrosectioned frozen rat liver tissues during the X-ray probe microanalysis due to interference and high levels of potassium (K) k-alpha K-lines. This analysis would indicate that cadmium levels were much lower than that of potassium in this range at 30 keV. In order to effectively detect cadmium levels, 23 keV will be necessary to excite electrons to the cadmium L lines. Hard x-ray elemental mapping and spectroscopy may shed light on the roles of metals in pathogenesis and disease progression. Results from the X-ray probe microanalysis will be quantitated and expressed in mmol/kg dry wt to determine the elemental contents of P to Zn elements in isolated rat hepatocyte.

Using Balancer Chromosomes and Phenotypic Markers to Map the Locations of *Drosophila melanogaster* Genes. *JOSHUA PURVES (California State University Fresno, Fresno, CA 93740) SUSAN CELNIKER (Lawrence Berkeley National Laboratory, Berkley, CA 94720).* *Drosophila melanogaster* has a relatively small genome that is carried by three autosomal chromosomes (designated 2, 3, and 4) and two sex chromosomes (X and Y). The genome of D. *melanogaster* has two key features that simplify the creation of genetic crosses and facilitate the mapping of genes within it: (1) balancer chromosomes exist for each chromosome except the 4th, and (2) a plethora of phenotypic markers. Balancer chromosomes are lethal when homozygous and contain multiple inversions that prevent viable crossover products from forming between wild-type chromosomes and their balancers. Chromosome 4 does not have a balancer since its small size and high heterochromatin content virtually prohibit homologous recombination from occurring. Phenotypic markers associated with visible fruit fly characteristics such as the eye, body, wing, and bristles, are also plentiful within the

Drosophila genome. Balancer chromosomes are constructed to contain some of these visible markers and, as a result, they allow geneticists to follow the segregation of the balancer or its normal homolog by looking for the presence or absence of the marker itself. A number of genetic crosses were created to map the locations of transposons within the Drosophila genome. The transposons, called P-elements, were engineered to contain regulatory DNA sequences as well as a mini w+ gene. The mini w+ gene puts pigment in the eye of otherwise white-eyed mutants (which carry the mutation w1118). In the first mapping cross, males containing the transposon (and therefore having wild-type eye color) were mated to virgin, white-eyed (w1118) females. These crosses resulted in progeny where both male and female flies exhibited the wild-type (w+) or the white-eyed phenotype (w1118), indicating that the transposon in question could not be located on the X chromosome. If this transposon were on the X chromosome of the parental male fly, only the female progeny could have had the wild-type (w+) phenotype. Further crosses to map the location of this transposon are not yet complete. A second set of crosses has been established between w+ males and w1118 females that are also carrying a balancer (CyO) for the 2nd chromosome. It can be concluded that the eye color gene in question is on the 2nd chromosome if all of the CyO flies from this second cross are white-eyed (w1118) and all of the non-CyO flies are w+. If this is not the case, further crosses must be performed to complete the mapping process.

Development Of A Framework Map To Identify Canidate Genes Involved In Carbon Allocation And Partitioning In Populus. *KELLY RAMIG (Knox College, Galesburg, IL 61401) LEE GUNTER (Oak Ridge National Laboratory, Oak Ridge, TN 37831).* Carbon sequestration is the process by which a plant takes in CO_2 from the atmosphere and through photosynthesis converts it into carbohydrates that are stored in different parts of the plant such as the stem, roots, or leaves. The overall goal of this project is to enhance the quantity and longevity of carbon sequestered in long-lasting carbohydrate sinks, such as the trunk or root system, instead of short term sinks, such as leaves. If trees grown in plantation settings can be genetically improved to store additional amounts of carbon in long-term carbon sinks, our atmospheric CO_2 could be lowered by as much as 1.2 Gt per year globally. In order to better understand genetic control of carbon sequestration in trees, a genetic map of Populus can be used to identify candidate genes from the recently sequenced poplar genome. Genetic markers, specifically simple sequence repeats (SSR), are being used to identify framework loci in a subset of progeny from an interspecific mapping pedigree of > 1,000 progeny. Over the past three months, genomic DNA from two parents and 44 progeny has been extracted and quantified for amplification of SSR loci using touchdown PCR and fluorescent genotyping of alleles through capillary electrophoresis. To date, 62 out of roughly 250 loci needed for the framework map have been genotyped. Approximately 93% of these loci exhibit segregation consistent with that seen in a related pedigree. The fidelity of marker inheritance from one pedigree to another suggests that SSR markers represent the best choice for genetic mapping across pedigrees and implies a high degree of utility for fine scale mapping of genes involved in carbon sequestration.

Isolation and Growth of Hyperthermophilic Microorganisms. *AARON RAMIREZ (Austin Community College, Austin, TX 78613) TAMAS TOROK (Lawrence Berkeley National Laboratory, Berkley, CA 94720).* Recent improvements in the techniques to culture microorganisms in the laboratory have made the study of microorganisms from extreme environments possible. Extremophiles, thermophilic microorganisms among them, may possess novel and highly valuable genetic traits that agriculture, industry, and the biomedical field can benefit from. In this feasibility study fourteen environmental samples collected from Kamchatka, Russia, and four samples collected from Lake Baikal, Russia, were used to investigate the presence of microorganisms capable of growing at a temperature of 80ºC. These hyperthermophiles are of interest because they may contain an enzyme, a-galactosidase, capable of digesting raffinose series oligosaccharides (RSO). This activity has a potential application in plant biotechnology. Dietary supplementation with a-galactosidase is theorized to reduce viscosity and improve nutrient digestion by swine that are fed soybean meal (SBM) as their main food source. This project investigates the potential of using a high temperature a-galactosidase of microbial origin in transgenic soybeans activated by elevated temperature during a post-harvest processing. Preliminary results obtained during this internship provided evidence for the presence of hyperthermophiles in stored environmental samples. After approximately fourteen days growth was observed in six of the samples. Genomic DNA extraction was successful. PCR amplification was still pending at the time when the internship concluded. In follow up experiments the presence of thermostable a-galactosidase in these hyperthermophilic microorganisms will be elucidated. Enzyme activity will be tested using a p-nitrophenyl-a-D-galactopyranoside (pNP-a-gal) assay. Active enzymes will be tested for thermostability and substrate specificity with regard to soybean meal oligosaccharides. Then, with cloned PCR products plant transformation will be carried out to test the use of the heterologous microbial enzyme in post-harvest processing.

Fatty Acid Methy Ester Analysis by Gas Chromatography. *CRISTINA RAMIREZ (Austin Community College, Austin, TX 78730) TAMAS TOROK (Lawrence Berkeley National Laboratory, Berkley, CA 94720).* Cellular fatty acid compositions of 34 different filamentous fungi, including ascomycetes and deuteromycetes, were analyzed by the fatty acid methyl ester (FAME) method to determine if they can be differentiated from one another on this basis. The fungi were isolated from several geothermal sites in Kamchatka, Russia and the radiation contaminated soils in Chernobyl, Ukraine as part of an ongoing study of extremophiles and their potential for biotechnological applications. Many fungi were found to possess the same fatty acids but at different relative concentrations. Some fungi differed in both the fatty acids produced and their relative concentrations. Three cultures showed sufficient taxonomic differences to warrant further biochemical and genetic studies since taxonomic unrelatedness often signifies more interesting physiological attributes.

Structural Analysis of Nudix Hydrolases from *Deinococcus radiodurans*. *ALLEN RASSA (North Idaho College, Coeur D' Alene, ID 83815) STEPHEN R. HOLBROOK (Lawrence Berkeley National Laboratory, Berkley, CA 94720).* Nudix hydrolases, a family of proteins ubiquitous to all kingdoms of life are found in larege numbers in the bacterium *Deinococcus radiodurans* and are suspected to be a part of this organisms remarkable resistance to ionizing radiation. These proteins have been shown to specifically bind to toxic and mutagenic substrates and contribute extensively to DNA repair and genome maintenance. Structural studies of one of these proteins (DR1025) shows that it forms an intertwined homodimer, with each monomer containing the characteristic Nudix fold. Crystal structures of seven forms of the DR1025 protein were solved at high resolution (1.4-1.6 Angstroms) in the absences or presence of magnesium or samarium and either a non-hydrolyzable GTP analog or Ap4A, two putative substrates. Structural comparisons were conducted on the seven proteins and are presented here.

Oral Absorption of Dichloroacetic Acid in the Japanese Medaka (*Oryzias latipes*). *STACEY REED (University of Tampa, Tampa, FL 33606) IRV SCHULTZ (Pacific Northwest National Laboratory, Richland, WA 99352).* Dichloroacetic acid (DCA) is one of the many by-products found in drinking water. Chronic exposure is a possible cancer risk to humans; this concern has led to bioassays in rats and mice that had positive tumor responses. Japanese medaka have gained attention as an alternative animal model for cancer studies, yet doubt remains as to whether fish studies are applicable to human health concerns. Although consequently, a few studies have been conducted, the information is incomplete in many areas, most especially pharmacokinetics. Pharmacokinetics can give insight to the absorption, distribution, metabolism, and excretion (ADME) of DCA. My study used controlled oral doses to individual medaka to better understand the ADME of DCA in fish tissues. Three medaka were used per timepoint (0.5, 1, 2, 3, 4, 6, 8, 10, 12, and 24 h), at a dose of 10.75 ìg DCA/fish. They were euthanized with MS-222. Medaka were weighed, the gastro-intestinal tract was removed, and the fish carcass was frozen for future analysis. The fish were analyzed for DCA content, and the data were subjected to pharmacokinetic analysis using an iterative, nonlinear least-squares computer program. From 0-2 h, not much DCA is absorbed. From 2-6 h, the amount of DCA per gram of fish tissue increases. At 8 h, there is a significant drop in fish tissue levels. By 24 h, it has almost been completely eliminated. The absorption lag time was 2.84 h, whereas the time of occurrence of the predicted maximum concentration, 30.60 µg/g, was 5 h. The calculated elimination rate was 0.46. The elimination half-life was 1.5 h. The elimination rate and half-life values are similar to those from previous studies in rats, which gives credence to future use of medaka and other fish in cancer studies.

Screening of Phage-Display Outputs with an Enzyme-Linked Binding Assay (ELBA). *ASHLEY REED (Grambling State University, Grambling, LA 71235). BRIAN K. KAY (Argonne National Laboratory, Argonne, IL 60439).* Sortase, APC, and PTP1B are all proteins that are associated with a human infection or disorder. In order to treat these individual infections and disorders, the protein's function must be inhibited. An Enzyme-Linked Binding Assay, or ELBA, can be performed to see what affinity reagents will bind these proteins. The knowledge of the affinity reagents that will bind the proteins allows the possibility to develop medicines from the known motif of the reagent.

Feasibility of Using Fluorescence as an Accurate Measure of Algal Biomass. *SUSAN REPON (Merritt College, Oakland, CA 94601) WILLIAM STRINGFELLOW (Lawrence Berkeley National Laboratory, Berkley, CA 94720).* Algae were studied to determine the relationship between fluorescence and biomass. Scenedesmus sp. was isolated and cultured under laboratory conditions with a daily cycle of 14 hours light, 10 hours darkness. Fluorescence readings were taken every two minutes with an automated SCUFA unit, and manual cell counts were performed twice per day, during the light and dark conditions. The study found that fluorescence dropped significantly with increased light conditions, while cell counts remained statistically consistent.

Energy Production from Bovine Waste. *WHITNEY RIDENOUR (University of Tennessee, Knoxville, TN 37912) K. THOMAS KLASSON (Oak Ridge National Laboratory, Oak Ridge, TN 37831).* As energy is needed to overcome dependence on coal and oil, methane production from biomass has the potential to help limit the amount of fossil fuel used. This idea also supports the guidelines of the Clean Air and Energy Policy Act, since biomass represents a clean fuel source that can reduce SOX emissions, NOX emissions, and methane released into the atmosphere. In the past, studies have been completed on a small-scale at Oak Ridge National Laboratory to determine if bovine manure could be used as a clean method of energy production. Current studies are focusing on larger scale experiments in a 100 L anaerobic digester. The pilot-scale digester was operated for several months, and data were collected and compared with results from smaller-scale experiments. A gas chromatograph was used to measure the compositions of the produced gas, a wet gas test meter was employed to measure the amount of gas produced, and a high performance liquid chromatograph was used to determine the quantity of organic acids in the digester feed and effluent. Results showed the methane production depended on the rate at which volatile solids (the manure ingredient converted to methane) were fed into the digester. The performance of the pilot-scale digester was comparable to that of model predictions. Although more experiments need to be completed, this pilot-digester experiment was successful and the information could be used to design an industrial-scale digester to produce clean energy.

Design, Synthesis and Characterization of Cross-linkable Imidazolium Based Ionic Liquids. *MARIANGEL RUIZ (University of Puerto Rico, Mayaguez, PR 00680) MILLICENT FIRESTONE (Argonne National Laboratory, Argonne, IL 60439).* An ionic liquid is a material with interesting and useful physical properties. Some of them are: lack of vapor pressure, non-flammable, non-toxic, thermally stable, high conductivity, good electrochemical properties. These ionic liquids are capable to rearrange themselves when water is added. There were prepared three different ionic liquids. Two of them have the reactive group in the tail, C10 ene mim+Cl- and C8 Acy mim+Cl-, and the third one, C10 Vim+Cl- has the reactive group in the head. These reactive groups will allowed the molecule to do a cross-linkage. The synthesis of C10 ene mim+Cl- was done before but never published. For the purification of this material, it was needed to wash it with ethyl acetate in a separatory funnel. Then, the sample was passed through vacuum distillation in order to remove the remaining solvent. In order to isolate and purify C8 Acr mim+Cl- and C10 Vim+Cl- it was used silica gel column chromatography. These were gradient columns beginning with 100% ethyl acetate, and then using solutions of 90% EtOAc in MeOH to 50% EtOAc in MeOH, finishing with pure MeOH for washes. Thin layer chromatography was done to all the fractions to determine where the materials of interest were. Those fractions were passed through vacuum distillation. In order to verify that the materials correspond to the structure, ‘H NMR was done to the three compounds. The experiments of cross-linking are underway. There are three different ways to induce cross-linking in these ionic liquids: photo cross-linking, gamma irradiation, thermal cross-linking; all of them were performed.

Compositional Changes Observed in Subchondral Bone and Calcified Cartilage in Osteoarthritis. *MEGHAN RUPPEL (Stony Brook University, Stony Brook, NY 11794) LISA MILLER (Brookhaven National Laboratory, Upton, NY 11973).* An estimated 37 out of 100 Americans have an osteoarthritic condition, namely women and older persons. Osteoarthritis (OA) is characterized by a breakdown of articular cartilage and thickening of the subchondral bone within a joint. It has been suggested that mineralization of the joint cartilage leads to subchondral bone thickening. In this study, synchrotron-assisted infrared microspectroscopy (SIRMS) was used to determine the chemical composition of the calcified cartilage and subchondral bone plate as a function of OA severity. OA severity was determined through a principal components analysis of histomorphometric measures including articular cartilage damage and subchondral bone thickness and area. Knee joints from thirteen cynomolgus monkeys, ranging in age from 6 to 30 years old, and having normal to severe OA, were examined to determine levels of mineralization (phosphate/protein ratio), carbonate accumulation (carbonate/protein ratio), crystallinity and collagen structure. Composition was analyzed as a function of OA severity and animal age. Preliminary analysis revealed that the level of mineralization (phosphate/protein ratio) in the subchondral bone and calcified cartilage was linearly correlated with OA severity. There was no correlation between animal age and subchondral bone or calcified cartilage composition. These results suggest that mineralization levels increase in both the calcified cartilage region and subchondral bone region as OA progresses.

A Physical Map of the Heterochromatic Portion of the *Drosophila melanogaster* Genome. *ASHLEY RYLES (Howard University, Washington, DC 20001) ROGER HOSKINS (Lawrence Berkeley National Laboratory, Berkley, CA 94720).* With the reports of Celera Genomics Inc., the Berkeley Drosophila Genome Project, and others, approximately 70% of the genome has been sequenced. This portion is referred to as the euchromatin. However, the remaining 30% of the genome has yet to be mapped and sequenced due to its high repetitive sequence content. It was originally thought that this part of the Drosophila genome was “junk DNA,” though more recent studies have shown that the heterochromatin contains important molecular and genetic functions. Drosophila is an excellent model organism for understanding the structure and function of this part of the genome in other animals, including the human. A bacterial artificial chromosome (BAC)- based map was constructed of different chromosomes represented in Drosophila melanogaster. Sequence tagged site (STS) content, restriction fingerprinting, and in situ hybridization of radiolabelled DNA probes were all approaches used in order to produce these maps. The STS content map was used to divide the genome in segments and restriction fingerprints of BACs was used to assemble and edit the segment. Once the maps were compiled, a tiling path sequence was used to verify the results of the genome assembly. This project was designed to close gaps within the heterochromatic assembly. Mapping proceeded in an orderly manner across the 12Mb target. Data from approximately 192 probes was produced and analyzed. Of the probes used, 87% hybridized to BACs. The remaining 13% are not represented in the BAC library possibly due to high repeat content or restriction site distribution. In conclusion, a BAC-based physical map of 12Mb of Drosophila heterochromatin was successfully produced. The map will aid in positioning heterochromatin sequences on the chromosomes, and in finishing heterochromatin sequences to high accuracy. Most probes tested are represented in the BAC library, but some sequences are apparently absent from the library. Mapping these regions may requires a different approach. With this information, it should be possible to map and sequence a large fraction of the heterochromatin. This work was supported by the Director, Office of Science, of the U.S. Department of Energy under the Contract No. DE-AC03-76SF00098.

Ergonomic and Risk Analysis for Workplace Injury Reduction. *JEANNETTE SANTOS (University of Puerto Rico, Cayey Campus, Cayey, PR 00736) PATRICIA BENDER (Brookhaven National Laboratory, Upton, NY 11973).* In order to reduce occupational injuries, Environment, Safety & Health (ES&H) Professionals from Brookhaven National Laboratory (BNL) performed a research project to reduce injuries by proactively involving workers in risk identification and injury prevention training activities. This initiative had three different phases. After establishing focus groups (FG) from the highest injury experienced groups in Plant Engineering (EP) (Electricians, Site Maintenance’s workers, Refrigeration and A/C Engineers, and Riggers) each focus group attended meetings to identify work risks and prioritize the tasks for further analysis. Data submitted by the FG showing significant ergonomic risks as determined by all workers who perform similar tasks will be forwarded for subject matter expert ergonomic analysis. Focus group members along with the remaining employees for each group used the Washington Ergonomics Task Evaluation Booklets as the evaluative tool. This tool is actually a training exercise to involve and give them an awareness of extreme and neutral positions to prevent occupational injuries which is crucial to their safe work performance. Evaluation data collected from the custodians in 1998 and from custodians, electricians and site maintenance’s workers on 2002 showed that by identifying and assessing risks in the workplace and then training workers to be aware of extreme and neutral positions and postures to perform their tasks; it is possible to reduce the potential for certain types of occupational injuries. The data was summarized and conclusions drawn as presented in this research paper. BNL’s ES&H staff working with this new data will analyze and recommend task improvements to proactively address these risks, thereby minimizing the potential for future injuries.

Muon Magnetic Moment. *JEANNETTE SANTOS (University of Puerto Rico, Cayey, PR 00736) HELIO TAKAI (Brookhaven National Laboratory, Upton, NY 11973).* Muons produced in the atmosphere by cosmic rays can be used to measure their magnetic moment. The precision of the measurement is not near to those obtained in accelerator environment but explain the first principles of how intrinsic properties of particles can be measured. The first experiment of its kind ever was setup by Claude Amsler in 1974. Amsler's apparatus is a "classic" setup where low energy muons are stopped in a copper target located inside a solenoid electromagnet. Most recently (2002), David Richard Ely reproduced the experiment taking extremely high quality data. However his analysis results in a value of the muon magnetic moment far from the accepted value. We have built an apparatus to measure the muon magnetic moment based on Amsler's experiment. Our setup as opposed to previously published is very compact and maximizes the magnetic field uniformity. A narrow cross section air core magnet was built for this. Also, to have a reasonable counting rate the detector is long. Although the experiment is fairly simple a number of technical challenges needed to be addressed. The coil overheating was one of the main problems and drives the stability of the magnetic field. Data was taken over 6 weeks for 0 field, 30 Gauss and 50 Gauss. Analysis tools were developed in Excel. Results will be presented and an overall comparison with previous results will be made. The experiment can also be used to measure negative muon lifetime. We have not explored this feature. The setup is now complete and considered ready for use by others that would like to pursue other measurements.

Effects of Local Precipitation and Temperature on the Emergence of *Ambystoma tigrinum tigrinum*, Eastern Tiger Salamander, From Vernal Pools at Brookhaven National Laboratory. *JENNIFER SEARS (University of Hull, Kingston-Upon-Hull, UK) TIM GREEN (Brookhaven National Laboratory, Upton, NY 11973).* The emergence times of larval eastern tiger salamanders, *Ambystoma tigrinum tigrinum*, in two vernal in Brookhaven National Laboratory, Upton, NY, was investigated as related to the local precipitation and temperature. The study was conducted in July and August of 2001, 2003 and 2004 using drift-fence arrays and coverboard-capture techniques. Salamanders were weighed, measured and released after capture. The correlation between tiger salamander migration, temperature and weather was measured using the Pearson's Product Moment Coefficient. It was found that there was a statistically significant relationship between salamander emergence times and precipitation. There was no significant relationship between temperature and emergence. In 2003 and 2004 it was also concluded that the precipitation levels, and thus pool-drying rate, influenced population sizes and length and weight on emergence.

Environmental Factors in Artificial Seeding of Wyoming Big Sagebrush and Sandberg's Bluegrass. *PRABU SEGARAN (Pacific University, Forest Grove, OR 97116) MICHAEL SACKSCHEWSKY (Pacific Northwest National Laboratory, Richland, WA 99352).* Developing cost-effective methods for restoring late-successional sagebrush-steppe habitat requires an understanding of the complex interactions among biotic and abiotic components that comprise the community. Seeding of Wyoming big sagebrush (Artemisia tridentata ssp. *wyomingensis*) and Sandberg's bluegrass (*Poa secunda*) was examined considering effects of surrounding vegetation, cheatgrass (*Bromus tectorum*) competition, and soil texture on establishment. Sagebrush seedling density and percent cover of Sandberg's bluegrass were used as measurements of establishment, and particle size analysis was performed on collected soil samples. Proximity of natural seed source and higher proportions of finer-sized soil fractions resulted in greater establishment. Although these factors may be difficult to control in practical restoration projects, further research of their influences may lead to more efficient restoration efforts.

Distribution and Localization of the Eastern Tiger Salamander. *RAFAEL SIERRA (Universidad Metropolitana, San Juan, PR 00908) TIMOTHY GREEN (Brookhaven National Laboratory, Upton, NY 11973).* The tiger salamander, a New York State endangered species, is locally abundant in parts of eastern Long Island. Eastern Long Island is composed of sandy Pine Barrens areas with ideal vernal pools for breeding and life activities for amphibians. These areas are found in abundance at Brookhaven National Laboratory where the eastern tiger salamander population is conserved in natural ponds and man-made depressions filled with water. During winter-spring 2004 egg masses were found at several vernal pools. To confirm use of vernal pools by salamanders, egg mass data was recollected during the months of February through April 2004 in 18 different vernal pools around the laboratory; considering the relationship between the kind of pond, amount of egg masses, height of egg mass deposited above pond bottom on twig or weed stems, and water temperature. For the purpose of improving breeding season success in some ponds, artificial deposition sites were installed, which resulted in positive use in some ponds. This study quantifies the distribution and localization of egg masses and the amount of eggs found in each pond showing a range between the bioconcentration in each pond and ideal conditions for tiger salamander breeding activity.

Predicting Fertility: Determination of Holes Made by Sperm in the Perivitelline Membrane of Japanese Quail Eggs. *PRACHI SINGH (Illinois Institute of Technology, Chicago, IL 60616) CRYSTAL J. DRIVER (Pacific Northwest National Laboratory, Richland, WA 99352).* Many chemicals are released into the environment and they may have harmful effects on humans as well as wildlife. Some of these chemicals may have an adverse affect on the endocrine system; such chemicals are known as "endocrine disruptors". Endocrine disruptors may have an adverse affect on the fertility of endangered wildlife species. This study focuses on the applicability of determining the effect of a certain endocrine disruptor on the fertility of male Japanese quail by determining the number of holes created by sperm in the perivitelline layer of the egg during fertilization. The procedure developed by Howarth and Donaghue for testing flock fertility was altered and followed and then applied to this toxicity study. It is possible to determine how many sperm were able to penetrate the perivitelline layer by counting the holes that the sperm create in the layer during the acrosome reaction. The perivitelline membrane has to be carefully separated from the albumen and the yolk without disturbing the germinal disc. The perivitelline membrane around the germinal disc is removed and after it has been prepared and stained, it is examined under the microscope for the number of holes. By determining the approximate number of holes that are present, it is then possible to compare the results of each group of male quail that were exposed to different concentrations of the endocrine disruptor and to determine if the endocrine disruptor has had any effect on the fertility of the males.

Innovative Root Technology Self - Irrigation that Exploits the Soil Depth. *GAYETTA SLEDGE (Kennedy King College, Chicago, IL 60617) M. CRISTINA NEGRI (Argonne National Laboratory, Argonne, IL 60439).* Phytoremediation and Phytoengineering were implemented at Argonne National Laboratory in 1999. This technology like others such, as bioremediation and natural attenuation has drawn criticism because biological or natural systems are generally unpredictable. Applied Natural Sciences (ANS) patented technologies (TreeMediation® and TreeWell® systems) have been applied in order to manage carbon. Carbon management program are developed to sequester excess CO_2 that includes the maximization of the carbon sink potential of a terrestrial ecosystem. These types of programs enable the growth of phreatophytic (moisture seeking plants) tree roots to extend their root system down to a depth of 30 feet (9 m) to reach ground water at these depths. This method is expected to enhance several things such as; increase depths of soil carbon, increase density of soil carbon (organic / and or inorganic) in the soil, increase mass and / or depth of roots and finally decrease the decomposition rate of soil carbon. Carbon, Oxygen, and Nitrogen gases in soil air are being tested and monitored at different stages for root growth, soil moisture levels, and carbon levels. The primary focus of this study is to measure soil moisture levels using the KS-D1 Digital Delm-hurst Moisture Tester on pre-installed 5201F1 Soilmoisture Gypsum Blocks at 2ft, 4ft and 6ft on pre-installed ANS-TreeMediation® and TreeWell® systems. These pre-installed ANS-(TreeMediation® and TreeWell® systems) Cartridges which contains Willows (*Salix alba var.tristis*), Walnuts (*Juglans nigra*) Oaks (*Quercus alba*) and as controls, a set of cartridges with no trees (just different soil types), are prototype installations of new planting techniques to vegetate damaged land. Overall, the goal is to develop a model cartridge with a selected tree type to be used to establishing or reestablishing vegetation of marginal, semi-arid or damaged land. According to Dr. M. Cristina Negri, Argonne National Laboratory, Energy System Division (2002) this method may be considered a necessary approach in order to increase both below and above ground carbon inventory in terrestrial ecosystems.

Amphibian Species Richness and Abundance at Brookhaven National Lab. *FRANK SMITH (Community College of Rhode Island, Warwick, RI 02886) JEREMY A. FEINBERG (Brookhaven National Laboratory, Upton, NY 11973).* Brookhaven National Laboratory (BNL) is located in the Central Pine Barrens on Long Island. The Central Pine Barrens offer a unique environment that is inhabited by many species of amphibians. Because amphibians are excellent indicators of the health of an ecosystem, measurements of species richness and abundance can provide vital information regarding ecosystem stability. In order to obtain this information, drift fences were placed at three distinct vernal pools on BNL property: a human made pool (DF-3), a

natural pool (DF-2), and a human altered pool (DF-1). *Rana clamitans melanota* metamorphs, *Rana catesbeiana* metamorphs, *Rana sylvatica* adults, *Ambystoma tigrinum* metamorphs and adults, *Bufo woodhousei fowleri* metamorphs and adults, and *Pseudacris crucifer* adults were captured at DF-1. *Rana clamitans melanota* metamorphs, *Rana sylvatica* metamorphs and adults, *Ambystoma opacum* metamorphs and adults, *Ambystoma tigrinum* metamorphs and adults, *Notophthalmus viridescens* metamorphs and adults, and *Scaphiopus holbrooki holbrooki* metamorphs were captured at DF-2. *Rana clamitan melanota* metamorphs and adults, *Ambystoma tigrinum* metamorphs and adults, a *Bufo woodhousei fowleri* adult, a *Hyla versicolor* adult, *Notophthalmus viridescens* adults, *Plethodon cinereus* adults, *Pseudacris crucifer* adults, *Rana sylvatica* metamorphs and adults, and a *Scaphiopus holbrooki holbrooki* metamorph were captured at DF-2. Data collected implementing drift fences at BNL suggests that there are viable populations of many species of amphibians on site. There seems to be a viable population of *Ambystoma tigrinum* on site, although the species is considered endangered in New York State. The success of amphibians at BNL contrasts with the dwindling numbers of amphibians globally. While many amphibian habitats in the country have been destroyed due to development, a large portion of BNL property remains undeveloped and safe from commercial development.

Benchmarking Best Practices Of Diversity In The Workplace. *KATRINA SMITH (University of Alabama in Huntsville, Huntsville, AL 35899) MYLISSA BUTTRAM (Oak Ridge National Laboratory, Oak Ridge, TN 37831).* Companies in America that embrace workforce diversity as a bottom-line business imperative priority, have implemented various strategies to promote the concept of "inclusion" in the workplace. Inclusion in the workplace is a management approach that fully utilizes all people in the workforce that enables them to achieve their full potential, and maximizes their contributions toward the mission of the company or organization. The goal of this research project is to find the best in class companies focusing on diversity and improving inclusion in the workplace. Diversity studies acknowledge that different approaches have extensive value to the organizational success of companies by supporting and utilizing the distinctive knowledge base and capabilities of every individual. Best practices for inclusion and addressing underutilizations for underrepresented women and minorities are to be evaluated in the survey as well. Supportive data used to sustain the fundamental goals of this project will explore the mainstream views of diversity by defining: (1) Affirmative Action (2) Equal Employment Opportunity and their implications for inclusion in the workplace. The tool of measurement was a survey constructed for easy online submission. The construction of the survey included questions derived from a booklet entitled, "Best practices In Achieving Workforce Diversity," it was based on similar research conducted through telephone interviews and contact persons from national laboratories operated by the Department of Energy. The result of this survey may be used to influence management strategies to strengthen the Oak Ridge National Laboratory workplace diversity initiatives. The final results of this project are fourth coming. However, there are some projected items that may impact the outcome of the research and they are the incompatibility between the electronic survey data base, designated spreadsheet, and functionality of personal computers, a short response and turn around time request, lack of time to complete the survey, and low priority by participants. ORNL Diversity representatives will have an opportunity to review the research and contribute to the final research.

Development of a Novel AC Calorimeter for Nanogram Samples to Investigate the Vortex Lattice Melting in Bi-2212. *SARAH SMITH (Truman State University, Kirksville, MO 63501) ANDREAS RYDH (Argonne National Laboratory, Argonne, IL 60439).* The nature of the melting transition from vortex lattice to vortex liquid in the high temperature superconducting oxides has been a subject of major interest since their discovery. Measurement of a latent heat from the vortex lattice melting in $Bi_2Sr_2CaCu_2O^{8+}$d (Bi-2212) would provide clear evidence of a first order transition, but small samples and weak signals place requirements on instrumentation and technique that have not yet been satisfied. In this work, we develop and characterize a differential, steady-state AC microcalorimeter based on a Si3N4-membrane with thin film heaters and thermocouples for studies of nanogram samples. Our preliminary measurements give evidence of a good, linear response in both AC and DC signals to heater power. The frequency response is well-behaved over a wide range of frequencies, but shows an upturn at low frequency, caused by a transformer impedance mismatch due to a too-high resistance load of the film thermocouples. Preliminary measurements of the heat capacity of Bi-2212 at room temperature were made on a ~150 ng crystal, and found to be 2.09 x 10-7 J/K, more than twenty times larger than expected. This discrepancy is suggested to be due to a lower-than-expected Seebeck coefficient of the thermocouple.

Sample Optimization in ^{67}Zinc Solid State NMR Spectroscopy. *GREG STAEHELI (Creighton University, Omaha, NE 68178) ROBERT W. HECK (Pacific Northwest National Laboratory, Richland, WA 99352).* Solid-state Nuclear Magnetic Resonance (ssNMR) spectroscopy of half-integer quadrupolar nuclides has received a lot of interest recently with the advent of new methodologies and higher magnetic fields. The only spectroscopic method available to probe the electronic environment surrounding zinc is NMR. This spectroscopy is providing a unique perspective on the nature of metal binding sites in several classes of metalloproteins. This information is furthering our understanding of the enzymatic mechanisms. Recent work has shown that increased sensitivity and resolution in ^{13}C spectroscopy can be achieved by preparing ssNMR samples in crystalline form. Also, "cryoprotected" preparations have shown an increase in sensitivity in ^{13}C and ^{31}P spectroscopy. In this study we investigated whether the same preparation methods increase the resolution and reduce the disorder in ^{67}Zinc ssNMR spectroscopy. Using carboxypeptidase we removed the natural abundance zinc and added ^{67}Zn to the enzyme. Different sample preparations were then used to reduce the linewidth and increase sensitivity. These included PEG-8000 and Trehalose additions as well as polycrystalline samples. The NMR was done using a Varian Infinity Plus console with a widebore Oxford magnet operating at 9.4 T with a home-built double resonance probe (^{1}H and ^{67}Zn) and an Oxford Instruments continuous flow cryostat for 10K temperatures. At the time of the paper samples are being studied and the results will show how sample preparation affects ^{67}Zn ssNMR spectroscopy. Future work will focus on new preparation methods including rapid freezing, precipitation, and variations of the work done here.

The Henslow's Sparrow: Activity and Location at Fermi National Accelerator Laboratory. *SARAH STARKS (Middle Tennessee State University, Murfreesboro, TN 37218) ROD WALTON (Fermi National Accelerator Laboratory, Batavia, IL 60510).* The Henslow's sparrow is a rare and endangered bird in the state of Illinois. Until 2000, the Henslow's sparrow had not been sighted at Fermi National Accelerator Laboratory since 1978. Our study's objectives were to discover where on the Fermilab site this bird is most abundant, to track the type of vegetation that the male Henslow's sparrow prefers to perch on, and to confirm breeding of the Henslow's sparrow on the Fermiloab site. A Global Positioning System (GPS) was used to collect the points where a Henslow's sparrow was seen or heard. Notes on vegetation were taken when we saw a male Henslow's sparrow perched. Also, any notes on possible breeding confirmation at a site were taken. Results showed that 50% of sightings of the Henslow's sparrows were recorded in the South Eola grasslands of the Fermilab site. Results also showed that male Henslow's sparrows do not prefer a certain type of vegetation to perch on. Further achievements in this study were that two breeding confrmations occurred, one in the Dusaf Pond area of Fermilab and another in the North Eola grasslands. It can be inferred from these results that the abundance of Henslow's sparrows at Fermi National Accelerator Laboratoy is in the South Eola grasslands. It can also be inferred that male Henslow's sparrows perch on vegetation that is the most abundant or tallest. The breeding confirmations prove that Henslow's sparrows are thriving on site. Further research could be done to prove if vegetation height or abundance correlates to the abundance of Henslow's sparrows at each site.

Defining the Minimum Energy Requirement of Methane Cycling Organisms using Methane Consumption and Production Rates. *JESSICA STEPHENSON (University of Virginia, Charlottesville, VA 22903) RICK COLWELL (Idaho National Engineering & Environmental Laboratory, Idaho Falls, ID 83415).* Most environmental organisms exhibit very low metabolic activities in nature. These activities are lower than normally observed in the lab and are important parameters in models that describe natural microbial processes. The objectives of this research were to provide improved estimates of microbial methane consumption and production rates that occur in the environment. Multiple methods were used to measure the activity of a well-characterized methane-consuming organism (methanotroph) Methylosinus trichosporium strain OB3b, and a methane-producing organism (methanogen) Methanoculleus submarinus. Acridine orange direct counts (AODC) were used to enumerate the total cells of both strains. Most probable number (MPN) statistical culture method was used to determine the number of viable cells of methanotrophs and methanogens. Methane production/consumption rates in active cultures were quantified using gas chromatography (GC). An ultra violet (UV) spectrophotometer was used to quantify the methane monooxygenase activity through metabolism of coumarin, a fluorescent substrate analog of methane.

Methane production in the Nankai 1 strain was estimated at 6.4 x 10^{-16} moles per cell, per day. The better rate estimates are intended to improve methane cycle modeling that supports DOE missions related to methane as a fuel source, methane as a greenhouse gas, and methane as a cometabolite of environmental contaminants, such as trichloroethylene (TCE).

Molecular Dynamics Simulations of Adenovirus Proteinase Activation. *JULIE STERN (Stony Brook University, Stony Brook, NY 11794) WALTER F. MANGEL (Brookhaven National Laboratory, Upton, NY 11973).* The adenovirus proteinase (AVP) is a relatively inactive enzyme that can be activated by an 11-amino-acid peptide cofactor, pVIc. The binding of pVIc increases the activity of AVP more than 3500-fold. The cofactor binding site is relatively far from the active site, over 30 angstroms away. Thus, a signal must be transduced from the pVIc binding site to the active site of AVP; this signal must involve a sequence of molecular structural changes. The aim of this study is to determine the activation mechanism at atomic resolution, i.e. the sequence of structural changes that occurs along the signal transduction pathway. Molecular dynamics (MD) simulations were used to determine atomic level structural changes. Removal of the peptide represents the reverse of binding. The peptide is removed from AVP, leaving it in a high energy state. The system then undergoes a series of conformational changes as it lowers its energy state until it reaches a stable structure or equilibrium. Biologically significant events were observed that may play a role in the signal transduction pathway. These observed events include: loss of an induced pocket, loss of beta-strand character in a portion of a beta-strand, helix-coil transitional changes, an amino acid residue flip transformation, and parallel stacking of amino acid residue rings. In addition to these events, MD was also used to determine ranges of motion of portions of the molecule. These motions include: highly flexible loop regions, confirmation that rigid regions stay rigid, amino acid side chain flexing due to hydrophobic or hydrophilic character, rotations of amino acids about carbon bonds, forming and breaking of bonds, and the spring-like motion of helices. These significant atomic movements and structural changes are being used to build a model of the signal transduction pathway that activates AVP. Sites along the pathway will ultimately be used as targets for drugs that will act as anti-viral agents.

Characterization of Xylanases to Improve Distillers Dried Grain (DDG) Processing. *JESSICA STRATTON (Washington State University, Pullman, WA 99164) JON MAGNUSON (Pacific Northwest National Laboratory, Richland, WA 99352).* Distillers Dried Grain with Solubles (DDGS) is a byproduct of fuel ethanol production and is currently being sold as animal feed. By developing the enzyme technology to hydrolyze hemicellulose (arabinoxylan), which is one of the three main components of DDGS, to the substituent sugars, greater value can be extracted from each bushel of corn and the production of ethanol from cornstarch can become more profitable. For this experiment eight thermophilic fungi were grown on a DDG media and assayed for ß-xylosidase and a- arabinofuranosidase enzyme activity. If one or both of these enzyme activities were identified, the fungus was harvested and ground using liquid nitrogen to break the cell wall, exposing the genomic DNA. Samples of this DNA were mixed with degenerate primers to amplify a portion of the gene encoding for the enzyme. PCR products from positive reactions were inserted into E. coli. Colonies were tested for TOPO vector containing an insert, and then sent to Iowa State Sequencing Facility. The resulting DNA sequences were analyzed for homology to sequences of genes for the respective enzymes. Four of the eight thermophilic fungi gave positive assay results for both a-arabinofuranosidase and ß-xylosidase. Two of these four fungi gave positive sequence results for ß- xylosidase. Sequence results for a-arabinofuranosidase were negative, showing sequences of the vector DNA without insert.

Nesting Success of Horned Larks in 60-Year-Old Abandoned Farmland. *MARYLEE STRUB (University of Idaho, Moscow, ID 83843) AMORET BUNN AND BILL RICKARD (Pacific Northwest National Laboratory, Richland, WA 99352).* The nesting success of horned larks (*Eremorphila alpestris*) on the U.S. Department of Energy's (DOE) Hanford Site is unknown; particularly in those areas that pose a potential risk to wildlife from Hanford-derived contaminants. From February through May 2004, a preliminary field study was undertaken to provide information on abundance and nesting success of horned larks in 60-year-old abandoned irrigated farmland habitat on the Hanford Site. A total of 214 individual birds representing 12 species in 12 families were recorded within 12, 100-m fixed-radius survey points. A total of 160 horned larks were tallied overall. Of the 17 horned lark nests located 41 eggs were laid, however14 eggs (34%) hatched. Of the hatchlings 32% fledged. The major cause of nest failure was predation (35%). Eighteen percent of the nests failed to hatch and 18% of the located nests did not contain eggs. Nests were placed predominantly (59%) at the base of a large perennial bunchgrass, sand dropseed (*Sporobolus cryptandrus*). The dominant plant cover overall in the vicinity of the nests was the dead stems of cheatgrass (*Bromus tectorum*) produced in years prior to the 2004 growing season.

ErbB Clone Characterization for Specificity and Affinity Using a Yeast Fab Antibody Display System. *JULIE SWEDBERG (Washington State University, Pullman, WA 99163) JAMES R. COLEMAN (Pacific Northwest National Laboratory, Richland, WA 99352).* Cancer is the second leading cause of death in the United States. In 2003, an estimated 1,334,100 new cases of cancer were diagnosed and 556,500 people died from cancer in the United States. Research indicates that there can be a 95 percent survival rate for cancer if it is detected in its earliest stages. ErbB1, ErbB2 and ErbB3 are members of the Epidermal Growth Factor Receptor family which act as oncogenes. These ErbB proteins trigger abnormal cell growth resulting in cancer. Our laboratory has developed yeast (*Saccharomyces cerevisae*) display system in which genetically engineered yeast display Fab antibodies on their cell surface. Using this system several clones were identified and isolated which produced Fab antibodies that bound to ErbB peptides. The purpose of this investigation was to characterize these antibody clones for specificity and affinity to five different ErbB peptides. By using the yeast display system and affinity binding assays we were able to determine the KD for several of the ErbB clones. Clone A5 showed significant binding to several antigens and clones D4, A10 and #9 all had binding to a specific antigen. Clones D4 and D9 were found to be identical by DNA sequence analysis. In addition, two clones (A10 and #9) were tested to determine whether or not they were variable heavy (VH) only binders. The VH only A10 clone was shown to bind antigen, while the data for clone #9 was less convincing. Our research found two potential candidates (A5 and D4) that can possibly be used in detection of ErbB proteins in a clinical setting. These two clones have the potential to be made into higher affinity binders which may be useful in the early detection and treatment of cancer.

XPG Protein Levels and Protein Interactions After Exposure to Various DNA Damaging Agents. *ANI TEJIRIAN (Diablo Valley College, Pleasant Hill, CA 94523) BRETT MAHER HALTIWANGER (Lawrence Berkeley National Laboratory, Berkley, CA 94720).* Exposure to ionizing radiation (IR) and hydrogen peroxide (H_2O_2) cause several types of DNA damage: DSBs, SSBs, and base damage, some of which can lead to stalled replications forks. Different proteins are known to be involved in each of the various repair pathways which occur. Preliminary evidence suggests that XPG interacts with other proteins know to be involved in the repair of replication forks, and may have role in base excision repair (BER), a process important in repairing base damage due to IR H_2O_2. There is evidence that BER is inducible and may be important to the same process as the adaptive response. The adaptive response is induced in cells which are treated with a priming dose of low IR or H_2O_2 and allowed to repair before treated with a challenge dose of higher IR or H_2O_2. These cells exhibit less damage then cells treated with a high dose of IR or H_2O_2 alone. The study was done to determine (A) the degree of colocalization of H2AX and XPG, and (B) whether XPG levels increase with increasing doses of H_2O_2 in cell lines known to induce an adaptive response. Colocalization between XPG and H2AX was determined by immunofluorescence. U_2OS XPG/V5 tagged osteosarcoma cells were treated with 0, 40, 100 µM of H_2O_2 or 0, 1, 4 Gy of IR. Lymphoblastoid cell lines +/- for an adaptive response were treated with 0, 40, 100 µM of H_2O_2 and analyzed by both western and IF. Our results revealed the number, brightness, and size of H2AX and XPG foci seemed to increase for both IR and H_2O_2 doses. In the U_2OS cells exposed to IR the degree of colocalization seemed to increase with increasing dose. In lymphocyte, the XPG staining seemed concentrated in the cytoplasm of the cells. The summary of western results revealed XPG levels to increase in one adaptive cell line (10), and remained the same in the other two lines. The increase of colocalization and XPG supports some interaction occurring at the site of damage. However, further research must be done to solidify these conclusions.

The Effects of Pressure on Bone Mineral and Applications to Understanding Osteoporosis. *JYOTI TIBREWALA (Massachusetts Institute of Technology, Cambridge, MA 02139) LISA MILLER (Brookhaven National Laboratory, Upton, NY 11973).* Bone mineral density is a widely used measure of bone strength. Loss of bone density is characteristically found not only in elderly osteoporotic and bedridden patients, but also in astronauts after long periods of space travel and weightlessness. In both cases, the pressure exerted on bone is scant. However, gravity and routine activities (such as walking or stair climbing) exert great amounts of pressure on bone. Studies of disuse and microgravity-exposed patients indicate the importance of pressure

for bone growth. The present work studies the effects of pressure on human dentin and a series of five model mineral compounds. Fourier-transform infrared (FTIR) spectroscopy was used to examine the effects of increasing pressure on the n4 phosphate band in the infrared spectra of these samples. Samples were mounted in a diamond-anvil cell and raised to pressures of up to 120 kbar; pressures were measured by ruby fluorescence spectroscopy, using a 488 nm excitation laser. In all samples, the application of pressure induced upward shifts in peak frequencies, as well as changes in peak ratios. All changes were reversed upon the release of pressure. The shifts in frequency are expected and indicate a compression of the crystal lattice structure of the mineral. The observed changes in peak integration values suggest that chemical changes may be occurring. Further work involving x-ray diffraction may help elucidate specific pressure-induced chemical transitions. Additionally, in the short period of time each sample was pressurized, both trends were reversible for both the dentin and mineral samples. This may not be the case if samples are studied after being left under pressure for longer periods of time.

Siloxane-based Electrolyte for Rechargeable Lithium Ion Batteries. *STEPHANIE TRAN (Michigan State University, East Lansing, MI 48825) KHALIL AMINE (Argonne National Laboratory, Argonne, IL 60439).* Rechargeable lithium ion batteries are currently using carbonate based electrolytes that have shown many problems regarding their safety. To address this issue, several nonvolatile, flame retardant siloxane based electrolytes have been examined. To determine their effects on the rechargeable lithium ion battery system we used differential scanning calorimeter techniques, ionic conductivity tests, cyclic voltammetry test cycles, and charge-discharge performance tests. We were able to determine the siloxane based electrolytes' thermal and performance properties in comparison to the commercial carbonate electrolyte properties. All the siloxane electrolytes showed good ionic conductivity. They were also very electrochemically stable and displayed excellent performance capabilities. These promising siloxane based electrolytes could enhance the lithium ion battery system, while at the same time making the batteries safer to use.

Methods Development for Analysis of Chemical Warfare Simulants in Blood and Saliva. *CYNTHIA TURPIN (University of California, Berkeley, Berkeley, CA 94720) ERIC HOPPE (Pacific Northwest National Laboratory, Richland, WA 99352).* Currently, chemical warfare exposure determination is dependant upon blood or urine analysis. These methods can be slow since there is a lag time to detect exposure in the urine, invasive when obtaining blood samples, and expensive due to the preparation time and analysis. A simplified method, using a quickly respond and readily available matrix (e.g., saliva), is necessary to reduce cost and make exposure testing more available on a real time or near-real time basis. The objective of this project was to develop analytical techniques to analyze dibutylphosphate (DBP), a model compound similar to the chemical warfare simulant diisopropyl-fluorophosphate (DFP), from spiked plasma and saliva. The techniques developed for DBP will be applied to the analysis of DFP. The methods were developed by first spiking rat plasma with DBP. The plasma was extracted using dichloromethane and the resulting residue was treated with N-methyl-N-(t-butyldimethylsilyl)-trifluoroacetamide (MTBSTFA) to derivatize the DBP. The derivatized DBP was analyzed using gas chromatography/mass spectrometry (GC/MS). Due to successful recovery of DBP from the spiked rat plasma, a similar analysis protocol was developed for the analysis of spiked saliva. Future work will include spiking rat plasma with DFP and studying possible hydrolysis products using the derivatization procedures developed for the analysis of DBP. Once analytical procedures for DFP are verified, rats will be exposed to DFP after which blood and saliva samples will be humanely collected and analyzed for the presence of the chemical warfare simulant, DFP. Results from this work show that the model compound, DBP, can be satisfactorily recovered from both spiked rat plasma and spiked saliva samples. These initial results show that saliva may have the potential to be utilized as a readily available fluid for noninvasive biomonitoring of chemical warfare agent exposure. Further research will make use of this procedure when testing for other various chemical compound exposures.

Searching for Androgen Pollutant Biomarkers in Female Trout Using Isoelectric Focusing and Reverse Phase High Performance Liquid Chromatography. *DAVID VILLENEUVE (Linn Benton Community College, Albany, OR 97321) DAVID WUNSCHEL (Pacific Northwest National Laboratory, Richland, WA 99352).* Factors such as dilution, adsorption and degradation make chemical pollutants difficult to directly measure in aquatic systems. Furthermore, direct detection does not allow us to evaluate the biological effects of chemicals with endocrine disrupting activity. Therefore biomarkers produced in aquatic organisms, such as teleost fish, have been used to measure the effects of exposure to compounds (such as estrogen) and its analogues. In particular, the egg laying protein vitellogenin has been widely used as a marker for estrogenic exposure in either sex of several species; however no equivalent biomarkers for androgens have been found. A single example has been described in androgens for the three spined stickleback (*G. aculeatus*), where the protein spiggin is produced, however the marker is isolated to this species. This study's objective is to develop a method to identify protein biomarkers via fish plasma. Using isoelectric focusing (IEF) and Reverse Phase High Performance Chromatography (RP-HPLC) we attempt to obtain high resolution between protein peaks in order to understand what changes occur when we expose female trout (*O. mykiss*) to trenbolone, an androgen pollutant. The coupling of liquid phase IEF to RP-HPLC eliminates any size limitations (common to gel electrophoresis) in the first dimension separation, and it also provides for highly reproducible retention times and an easy transition to additional analytical techniques like mass spectrometry. The data collected from this study allows us to create a 3-D representation of the trout plasma; the first dimension is created using the Bio-Rad Rotofor which, using Isoelectric focusing, separates the proteins based on their pI value. The second dimension, retention time, and the third, the level of absorbance are created by means of RP-HPLC. Surface plots were created within the software package Matlab for data visualization. This was used to illustrate the relative abundance of proteins appearing at a particular pH and retention time. These plots allowed us to create virtual 2-D gel data to easily identify changes in protein expression related to androgen exposure, and isolate the biomarker for our eventual goal, identification by mass spectrometry. In this way potential biomarkers of androgen exposure in female trout can be visualized as differences between control and treated samples prior to purification and identification.

The Use of Fluorescence Techniques to Quantify Hydrogen Peroxide in Cigarette Smoke. *SERENE WILLIAMS (Knoxville College, Knoxville, TN 37921) GUY GRIFFIN (Oak Ridge National Laboratory, Oak Ridge, TN 37831).* This work describes the application of fluorescence measurement techniques for the analysis of hydrogen peroxide (H_2O_2) production in cigarette smoke. It is currently unknown which of the many reactive oxygen species (ROS) present in, or produced by, cigarette smoke are responsible for most of the oxidation damage in vivo. Thus, procedures for measuring and quantifying ROS in cigarette smoke must be developed. The end goal of this project is to develop a biosensor device for measuring H_2O_2 within extra-cellular fluid of vital body organs such as the lungs. Cigarette smoke produces ROS, including H_2O_2. The interaction of H_2O_2 and other ROS can lead to oxidative damage to the lungs and other body organs, possibly resulting in cancer. The biosensor device will enable the monitoring of extra-cellular fluid in the lungs of individuals exposed to cigarette smoke; therefore enabling the quick, sensitive detection and quantification of H_2O_2. In this study, the amplex red reagent assay was used for fluorometric detection of H_2O_2. Amplex red reagent (non fluorescent compound) in the presence of horse radish peroxidase (HRP) enzyme, reacts with H_2O_2 to produce the red fluorescent compound resorufin. Resorufin has excitation and fluorescence emission maxima of approximately 563nm and 587nm respectively. Using a standard stabilized solution of H_2O_2, calibration plots of fluorescence intensity versus H_2O_2 concentration were constructed. H_2O_2 concentrations in aqueous solutions resulting from bubbling 5 puffs of cigarette smoke samples were also determined from calibration plots. Micro molar levels of H_2O_2 were detected in aqueous solution of cigarette smoke samples. In addition, measurements over time of H_2O_2 production in cigarette smoke samples bubbled through phosphate buffer saline (PBS) showed an increase of H_2O_2 up to 120 minutes reaching a plateau thereafter. Other analytical techniques can also be used to detect H_2O_2 production from cigarette smoke, but these require a prior separation step (e.g., HPLC). This work demonstrated the feasibility of measuring H_2O_2 production in cigarette smoke without prior separation from total particle matter. Further studies to investigate H_2O_2 concentration in a single puff of cigarette smoke bubbled through aqueous solution, are under way. This work will lead to safer manufacturing processes of cigarettes, which will decrease the level of ROS injuries to lungs.

Mutational Screening of Mouse Genes to Better Understand Human Gene Function. *JAMES WILLIAMS (Bethune-Cookman College, Daytona Beach, FL 32114) MITCHELL KLEBIG (Oak Ridge National Laboratory, Oak Ridge, TN 37831).* Identifying and studying mutated genes in mice allows for better comprehension of human gene functions, which may lead to a greater understanding of diseases and disorders associated with those genes. ORNL's Mammalian Genetics group has generated a mutation screening resource called the Cryopreserved Mutant Mouse Bank (CMMB). The CMMB samples consist of DNA, tis-

sues and sperm from 4,000 C57BL/6JRn male mice, that are heterozygous for a large number of N-ethyl-N-nitrosourea (ENU) induced point mutations throughout the genome. The 4,000 DNAs from these mice are being used to screen for possible mutations at the genomic DNA level. DNA fragments of genes of interest are rapidly generated from the CMMB DNA archive by Polymerase Chain Reaction (PCR) amplification. Subsequent heteroduplex analysis of the PCR products, performed with Temperature Gradient Capillary Electrophoresis (TGCE), identifies those that contain single base changes, which are then sequenced to determine the precise nucleotide change. The primary genes studied in this project are Ap2s1, which is involved in endocytosis, and Myd88, involved in the immunological reaction to viral and possibly other lethal infections such as anthrax. A heteroduplex was identified by TGCE in a PCR product containing exons 3 and 4 of the Myd88 gene. This PCR product was sequenced and found to contain a G to A nucleotide change in exon 3, which changes the open reading frame of the gene from a valine (V) to a methionine (M) codon for amino-acid residue #175 of the encoded protein. Since this V amino acid is highly conserved in vertebrates, mice containing this mutation can be rederived by intra cytoplasmic sperm injection (ICSI) from the frozen sperm of the mouse whose DNA carries the mutation. Mice homozygouos for the mutation can then be studied for phenotypic effects of the mutation.

A Reagent-less Fluorescent Sol-gel Biosensor for the Detection of Hydrogen Peroxide. *SERENE WILLIAMS (Knoxville College, Knoxville, TN 37921) GUY GRIFFIN (Oak Ridge National Laboratory, Oak Ridge, TN 37831).* This work describes the development of a reagent-less fluorescent sol-gel biosensor for the analysis of hydrogen peroxide (H_2O_2), and its potential application in near-real-time monitoring of H_2O_2 generated from aqueous extracts of cigarette smoke. H_2O_2 occupies a central role in oxygen metabolism, is produced by various reactions in several subcellular compartments and is the precursor to other reactive oxygen species (ROS). It is currently unknown which of the many ROS present in, or produced by, cigarette smoke are responsible for most of the oxidation damage in vivo. Thus, procedures for measuring and quantifying ROS in cigarette smoke must be developed. Cigarette smoke produces ROS, including H_2O_2. The interaction of H_2O_2 and other ROS can lead to oxidative damage to the lungs and other vital body organs, possibly resulting in cancer. The development of a biosensor device will enable the monitoring of extra-cellular fluid in the lungs of individuals exposed to cigarette smoke; therefore enabling the quick, sensitive detection and quantification of H_2O_2. The primary goal of this summer research project is to investigate the applicability of the sol-gel encapsulation technique for the immobilization of both a fluorescent indicator and an enzyme catalyst for the detection of H_2O_2. Sol-gel encapsulation has opened up an interesting new way to immobilize biological materials, which include proteins, enzymes, antibodies and even whole cells. Carefully prepared silica-based sol-gels are able to retain the bioactivities of embedded biomaterials and remain accessible to external reagents by diffusion through the porous silica. The Amplex Red assay was used for fluorometric detection of H_2O_2. Amplex Red reagent (a non fluorescent compound) in the presence of horse radish peroxidase (HRP) enzyme reacts with H_2O_2 to produce the red fluorescent compound resorufin. Sol-gel encapsulation of both Amplex Red reagent and HRP was carried out by mixing an Amplex Red reagent working solution with a sol stock solution containing tetramethyl orthosilicate (TMOS) and acid water. Glass slides were spin-coated with the liquid sol solution to form sol-gel thin films. These films were kept in the dark, allowing for gelation, aging, and drying before use. Calibration curves were constructed to determine the fluorescence intensity versus different H_2O_2 concentrations.

Genetic Polymorphisms in Glutathione S-Transferase Genes and Implications in Breast Cancer. *SARAH WILSON (City College of San Francisco, San Francisco, CA 94102) REGINE GOTH-GOLDSTEIN (Lawrence Berkeley National Laboratory, Berkley, CA 94720).* The role of the glutathione S-transferase (GST) enzyme family is to detoxify environmental toxins and carcinogens and to protect organisms from their adverse effects, including cancer. The genes GSTM1 and GSTT1 code for two GSTs involved in the detoxification of carcinogens, such as polycyclic aromatic hydrocarbons (PAHs) and benzene. Epidemiological studies indicate that GST polymorphisms increase the level of carcinogen-induced DNA damage and several studies have found a correlation of polymorphisms in one of the GST genes and an increased risk for certain cancers. We examined the role of polymorphisms in genes coding for these two GST enzymes in breast cancer. A breast tissue collection consisting of specimens of breast cancer patients and non-cancer controls was analyzed by polymerase chain reaction (PCR) for the presence or absence of the GSTM1 and GSTT1 genes. We found that GSTT1 deletions occurred more frequently in cases than in controls, but found no relation between GSTM1 deletions in our raw data. The superior detoxifier (putative low-risk) genotype (defined as presence of both GSTM1 and GSTT1 genes) was less frequent in cases than controls (28% vs. 37% respectively). However, the sample size of this study was too small to provide conclusive result

Creating Manageable Databases for the Structural Biology Center. *SETH WYNCOTT (Indiana Wesleyan University, Marion, IN 46953) FRANK ROTELLA (Argonne National Laboratory, Argonne, IL 60439).* The research project assigned to me here at Argonne National Laboratory is to take Word or text-based documents and convert them to a web-based form through the use of Hyper Text Markup Language (HTML) and the assistance of Common Gateway Interface (CGI) scripts. This provides the scientists of the Structural Biology Center (SBC) with the ability to access and interact with these documents from a web browser on any computer supporting web browsing. Through the use of HTML and the development of CGI (Common Gateway Interface) scripts, I am able to create manageable documents that can quickly and easily be placed on the World Wide Web. With this opportunity, I am able to provide the scientists with a common medium for accessing information. As of now, quite a few of the instructional procedures for beamline operations throughout the Structural Biology Center are not in an Internet form and therefore, they are not as readily accessible as they could be. Since many of these documents have not yet been placed on the web, the scientists can quickly become involved in the lengthy process of finding the proper instruction, all before they are able to continue in their research. Through the help of my supervisor, and an HTML compiler, I am able to further develop these documents into a form, which is readily accessible, and can then easily be placed on the homepage for the Structural Biology Center.

Mussel Feeding Study: Will Mussels Capture And Ingest 1-Micron Particles?. *SARA WYNVEEN (Oregon State University, Corvallis, OR 97330) MEG R. PINZA (Pacific Northwest National Laboratory, Richland, WA 99352).* Mussels, as filter-feeders, are capable of accumulation of hazardous materials from the water system. Due to selective feeding behaviors exhibited by mussels, whether or not a specific material will be ingested and subsequently concentrated within the mussel is influenced by many factors, including particle size. In this study, the possible use of mussels as biomarkers for the presence of hazardous bacteria and bacterial spores is explored by examining the mussels' uptake and concentration of particles roughly the size of bacterial spores; about 1 µm. Mussels were exposed to a concentration of fluorescent polystyrene beads, 1 µm in diameter, in a static system, and then removed from the beads for varying periods of depuration. Concentration of beads in the water as well as presence of beads within the mussel tissue were monitored to determine whether the beads were being captured and ingested by the mussels. A trend of decrease in bead numbers was noted over the 4 hour exposure period, and beads were found in the tissues and hemolymph of all mussels. The findings of this study have shown that mussels do capture particles of this size. These findings will contribute to the design of future experiments involving the concentration and retention of bacterial spores by mussels.

A Study of Reliability of Sequential Neighbor Analysis in Protein Classification with Support Vector Machines. *KELLY YACKOVICH (Clarion University of Pennsylvania, Clarion, PA 16214) NELA ZAVALJEVSKI (Argonne National Laboratory, Argonne, IL 60439).* An abundance of data characterizing protein sequence and structure has been discovered in recent years, however, in order to find useful ways to apply this new data, automated techniques such as machine learning need to be used to extract and interpret the relevant information from this data. The focus of this project is finding a way to classify immunoglobulin light chains, specifically the λ family of light chains, into amyloidogenic and benign categories. This could lead to the discovery of ways to predict and treat amyloidoses, examples of which are type II diabetes, Alzheimer's and Parkinson' s diseases. The support vector machine (SVM) algorithm was chosen for this problem because it has good generalization capacity even with small data sets such as ours. We performed SVM classification with both individual amino acid sequence encoding and amino acid neighborhood (window) sequence encoding to evaluate whether the window approach gave improved results for the classification of the λ family of immunoglobulin light chains. We used random resampling of the data sets and repeated runs of the SVM program to establish the significance of the study with the limited data sets. In all cases, the average classification error significantly decreased and the ability of the SVM to detect amyloid light chains significantly increased, indicating that the window approach is superior for classifying λ light chains. However, attempts to determine which specific positions or windows were important in determining the classification outcome were unsuccessful.

Use of A Virtual Reality Wall in Biomass Refinement. *REBECCA YULE (Brigham Young University - Idaho, Rexburg, ID 83440) THOMAS FOUST (Idaho National Engineering & Environmental Laboratory, Idaho Falls, ID 83415).* Alternative energy sources have been researched to lower the use of fossil fuels, a nonrenewable resource that contributes to pollution. Energy, in the form of cellulose found in the biomass of wheat and corn, can be extracted and fermented into ethanol to be used in place of gasoline. Genetically altered wheat and corn that yield a higher concentration of cellulose sugar is being tested which will enable ethanol to be used as an affordable alternative fuel. Modifications of harvesting combines, to ensure that harvest of biomass is efficient, continue to be made allowing the replacement of essential nutrients back into the soil and a higher yield of biomass. To aid in this research, a virtual reality wall was constructed that will transform computational data that has been gathered from lasers and camera systems in a two-dimensional format to a three-dimensional model. These images will aid in tracking the flow of biomass in a combine and support the designing of combine attachments that will allow for an efficient collection of corn and wheat. There were two aspects to the building of this wall: the physical construction and the implementation of software. Physical construction of a tower and placement of a screen, projectors, monitors and computers in a specific arrangement to create a three-dimensional effect was completed. Software, contributed by Iowa State University, was implemented and results will begin to be gathered within the next two months. In the future, the Idaho National Engineering and Environmental Laboratory (INEEL) plan to build a six-walled cave, which will aid in model validation of the inner workings of a combine. This research is in the forefront of fluid dynamics and has implications in automobile research, meteorology, and many other fields of study.

1.70 Å Crystal Structure of Hypothetical Protein yqjY From *Bacillus subtilis*. *FATIMA ZAPATA (University of Texas Pan-American, Edinburg, TX 78541) ANDRZEJ JOACHIMIAK (Argonne National Laboratory, Argonne, IL 60439).* The crystal structure of yqjY, a 17.85 kDa hypothetical protein from *Bacillus subtilis*, has been determined and refined to 1.70 Å by the multiple-wavelength anomalous dispersion (MAD) method. The Se-Met derivative of yqjY crystallized in the P 31 2 1 space group with unit cell dimensions of a=b=103.61 Å, c = 72.06 Å, α = β =90.00º , γ =120.00º. The crystal structure of yqjY is the only member of the Hypothetical protein N-acetyl transferase (NAT) family in the four-hairpin Acyl-CoA N-acyltransferases superfamily in the SCOP 1.65 database. Other members of this SCOP superfamily include N-myristoyl transferase, NMT (55748), Acyl-homoserinelactone synthase EsaI (75508), and FemXAB nonribosomal peptidyltransferases (82749). When doing a BLAST search against SWISS-PROT/TrEMBL, it found 6 sequences in its genome and genomic neighbors of yqjY which are hypothetical protein Q7P0N4, hypothetical conserved protein Q8ETH4, acetyltransferase, GNAT Family AAT32174, AAS42000, and Q81NW4. Although there are currently no homologous structures released in the Protein Data Bank (PDB), it found a related entry with the crystal structure of yeast gna1 bound to coa and glnac-6p also known as Transferase.

Role of XPG in Global Repair of Oxidative Damaged DNA. *SAM ZENHARI (Contra Costa College, San Pablo, CA 94806) BRETT HALTIWANGER (Lawrence Berkeley National Laboratory, Berkley, CA 94720).* Oxidative DNA damage is removed by the base excision repair pathway(BER). In this experiment we look at the specific repair of DNA containing Thymine glycol damage, in human cells. We are investigating the role of XPG which is a protein that has both essential role in nucleotide excision repair and a role in BER to see if there is a significant difference in repair between the cells that have XPG compared to ones that lack XPG. In previous experiments it was shown that XPG stimulates the DNA repair activity of some specific BER enzymes in vitro, notably hNTH1. We are hoped to see in support of this idea by introducing a plasmid containing Thymine glycol damage into cells. This experiment was done by treating plasmid DNA with OsO_4 and tranfecting the damaged plasmid into VA13 a cell line that contains XPG and 94RD27 a cell line that is XPG deficient.

Analytical Methodologies for Detection of Gamma-valerolacone, Delta-valerolactone, Acephate, and Azinphos methyl and Their Associated Metabolites in Complex Biological Matrices. *ERIKA ZINK (Columbia Basin College, Pasco, WA 99301) JAMES A. CAMPBELL (Pacific Northwest National Laboratory, Richland, WA 99352).* Non-invasive biomonitoring for chemicals of interest in law enforcement and similar monitoring of pesticides together with their metabolites can not only save money but can lead to faster medical attention for individuals exposed to these chemicals. This study describes methods developed for the analysis of gamma-valerolactone (GVL), delta-valerolactone (DVL), acephate, and azinphos methyl in saliva and serum. Liquid chromatography/mass spectrometry (LC/MS) operated in the negative ion mode and in the positive ion mode and gas chromatography/mass spectrometry (GC/MS) were used to analyze GVL and DVL. Although both analytical techniques worked well, lower detection limits were obtained with GC/MS. The lactones and their corresponding sodium salts were spiked into both saliva and serum. The lactones were isolated from saliva or serum using newly developed extraction techniques and then subsequently analyzed using GC/MS. The sodium salts of the lactones are nonvolatile and require derivatization prior to analysis by this method. N-methyl-N-(t-butyldimethylsilyl)-trifluoroacetamide (MTBSTFA) was ultimately selected as the reagent for derivatization because the acidic conditions required for reactions with diazomethane caused the salts to undergo intramolecular cyclization to the corresponding lactones. In vitro studies were conducted using rat liver microsomes to determine other metabolites associated with these compounds. Azinphos methyl and acephate are classified as organophosphate pesticides, and are known to be cholinesterase inhibitors in humans and insects, causing neurotoxicity. For this reason they have both exposure and environmental impact implications. These compounds were spiked into serum and saliva and prepared for analysis by GC/MS. Continuation of this research would include analysis by GC/MS under positive ion mode to determine the parent ions of the unknown metabolites. Further research is planned through an in vivo analysis of the lactones and pesticides. These methodologies could be extended for further analysis of other similar compounds as well as chemical and biological warfare agents.

CHEMISTRY

Comb Polymer Electrolytes for Lithium-ion Batteries. *ADEWUNMI ADEYEMO (Chicago State University, Chicago, IL 60628) JOHN B. KERR (Lawrence Berkeley National Laboratory, Berkley, CA 94720).* Lithium ion batteries are been studied extensively for their use as rechargeable batteries in consumer appliances such as cell phones and portable computers. This is because they provide long range performance and are safer than other batteries such as the Nickel-Cadmium batteries which has toxic metals. One of the main factors that is considered when developing lithium ion batteries is the polymer electrolyte. Our goal is to synthesize and characterize polymer electrolytes that have low glass transitions and have a conductivity of around 10^{-3} S/cm at ambient temperature. To reach this goal, we have synthesized and characterized comb polymer electrolytes that have a polypropylene oxide (PPO) backbone and have side chains containing ethylene oxide (EO) or trimethylene oxide (TMO) repeating units. This provided different polymer architectures that were mixed with four different salts, lithium bis(fluoromethanesulfonyl) imide(LiTFSI), lithium bis(perfluoroethylsulfonyl) imide (LiBETI), lithium trifluoromethane sulfonate (LiTF) and lithium methide. The glass transition temperature and ionic conductivity were measured using a differential scanning calorimeter and an alternating current impedance analyzer respectively. Our results show that LiTf has the lowest conductivity when compared to the remaining salts and that increasing the number of ethylene oxides units on a side chain increases conductivity. In addition, comb polymer electrolytes containing only ethylene oxide units on the side chain differ in conductivity when compared to electrolytes with some trimethylene oxide units.

FM LASER ABSORPTION OF THE ˜A (000) ←Ã (010) AND ˜A (010) ←Ã (011). *RYAN BIRD (Southampton College, Southampton, NY 11968) TREVOR SEARS (Brookhaven National Laboratory, Upton, NY 11973).* The 000←010 and 000←011 bands of the Ã←˜X system of HCCl lying at approximately 11 100cm-1 and 10 300cm-1, respectively, were recorded and analyzed. HCCl was formed by the photolysis of a continuous flow of a 1% mixture of $HCClBr_2$ in nitrogen buffer gas at a total pressure of 1 Torr using an ArF excimer laser at 193nm. The spectrum was recorded in absorption using a continuous wave, frequency-modulated, Ti:Sapphire laser and a Herriot-type absorption cell. In the, stronger, 000←010 transition, four subbands, K= 0←1, 1←0, 1←2, 2←1, of $HC_{35}Cl$ and two subbands, K= 0←1, 1←0 of $HC_{37}Cl$ were identified. In additions, the K= 0←1 band of the 010←011 transition was identified and assigned. Since the upper states in the transitions are known from previous work, the analysis characterizes these ground electronic state levels of HCCl for the first time.

Did Obsidian Found on Two Adjacent Ecuadorian Mountain Peaks Originate From a Source Closer to the Ancient Volcano Antisana? *JAMES BRADFORD (Mississippi State University, Mississippi State, MS 39762) FRANK ASARO (Lawrence Berkeley National Laboratory, Berkley, CA 94720).* In 1994, Dr. Asaro and his research group published data on obsidian artifacts from Ecuador. They found Ecuadorian obsidian from two sources. One of these, called the Yanaurco - Quis-

catola source, was located at the top of two adjacent mountains called the Yanaurco and Quiscatola peaks. It appeared obsidian had landed on the mountaintops because of a volcanic eruption elsewhere. Later, it was found that obsidian rock from a source much closer to a huge ancient volcano, called Antisana, had almost the same chemical abundance profile as the obsidian from the Yanaurco and Quiscatola peaks. The only difference was in the abundance of the element Samarium (Sm). As the measurement on the source close to the volcano Antisana had been made by a different laboratory, it was desirable to measure a source sample of that here at Lawrence Berkeley National Laboratory (LBNL). Although Sm abundances had been measured in the past by Dr. Asaro's group, unfortunately they no longer do so because the necessary equipment is no longer operable. The purpose of my study is to assist in attempting to develop a technique for measuring Sm and a few additional other abundances with the existing equipment. We anticipate results within a month.

Synthesis, Spectroscopic Characterization, and Binding Studies of Lanthanide and Actinide Complexes Containing Anionic Tripodal Kläui-Type Ligands. *YAKINI BRANDY (University of the Virgin Islands, St. Thomas, VI 00802) GREGG LUMETTA (Pacific Northwest National Laboratory, Richland, WA 99352).* The use of anionic Kläui-type tripodal ligands in the selective binding and separation of lanthanides and actinides is an area of active research at the Pacific Northwest National Laboratory. In an attempt to better understand the structural and binding characteristics of these ligands, a series of lanthanide (M= La, Nd, Pr) and actinide (M = Th, U) complexes were prepared in 1:1 and 2:1 (L:M) stoichiometry by reacting MXn (X = NO3- or Cl-) with the required stoichiometric amount of (C5Me5)Co(P(=O)(OR)2)3Na (R= Me or Et). The complexes were characterized by IR spectroscopy and NMR spectroscopy. Attempts were made to crystallize the materials and obtain crystals suitable for x-ray crystallographic studies. The neodymium and lanthanum chloride complexes were successfully crystallized. Binding studies, with Nd^{+3}, U^{+4}, Am^{+3}, and $PuO2^{+2}$ using the (C5Me5)Co(P(=O)(OR)2)3Na (R= Me) ligand were initiated. UV-Vis spectroscopy was the spectroscopic tool used for these measurements. The metal ions were chosen because of their unique absorption bands in the visible spectral range and they represent the wide range of oxidations states encountered for the actinide elements. The computer program SQUAD (Stability Quotients using Absorbance Data) was used to evaluate the spectral data and calculate the binding constants.

Poly (ethylene oxide) Clay Based Nanocomposites for Lithium Batteries. *APRIL BUCKLEY (Olive - Harvey College, Chicago, IL 60617) GISELLE SANDI (Argonne National Laboratory, Argonne, IL 60439).* The development of a lithium polymer battery would alleviate many limitations that are currently inhibiting a suitable cycle life for electronics of higher energy applications. The goal of our research is to develop a solid membrane that would replace the liquid electrolyte and be able to efficiently transfer lithium ions between the anode and cathode. This would improve the battery's cycle life and its overall performance. When the batteries are used under proper conditions, a solid membrane would decrease the chances of leakage and exposure to hazardous chemicals. The two synthetic clays that were used to make our membranes are Synthetic Lithium Hectorite clay (SLH) and Tetraethylorthosilicate clay (TEOS). Once these clays were produced in a powdered form they were mixed with different ratios of Poly (ethylene oxide) (PEO) which is a polymer, to enhance the transfer of lithium ions therefore enhancing conductivity. There were five different membranes made. Two types of catalytic membranes were made with platinum and palladium. One membrane was made with zirconia and the other types were made with PEO / SLH or PEO / TEOS ratios. When a viable membrane was produced it was ran through a series of characterization analysis including thermogravemetric analysis to measure the weight, x-ray diffraction analysis to analyze the structure and electrochemical impedance spectroscopy to measure the conductivity. Of all the membranes that were made, the one that had the best characteristics was a 1.2 PEO / TEOS membrane. X-ray diffraction analysis shows that the polymer (PEO) was successfully intercalated within the layers of the clay but there was also excess polymer around the layers. Thermogravemetric analysis shows that of the total weight of the sample, 2% is H_2O and the other 47% is polymer. Electrochemical impedance spectroscopy confirms that our membrane has a conductivity of 10^{-5} but the conductivity that is feasible for a lithium battery is 10^{-3}.

Comparison of Ozone Instrumentation and Ambient Ozone Levels in Rural and Urban Locations. *MARK CARLOS (Columbia Community College, Sonora, CA 95370) TOM JOBSON (Pacific Northwest National Laboratory, Richland, WA 99352).* Fossil fuel energy emissions affect the distribution of ozone (O_3) in the troposphere which influences climate change on the regional and global scale, and impacts human health in urban environments. Understanding the distribution of O_3 and its relationship to energy related emissions is an active area of atmospheric research. We describe both chemiluminescence and UV absorption methods for O_3 analysis and focus on our efforts to establish a baseline methodology using the UV absorption method. This project compares the performance of two commercially available O3 monitors that use UV absorption spectrometry to measure O_3 at the parts-per-billion (ppb) level. These instruments are being evaluated for future use on the Department of Energy (DOE) Research Aviation Facility G-1 aircraft and for calibration of a next-generation chemiluminescence O_3 analyzer. Tests were performed in the laboratory to measure instrument precision, stability and dynamic range. The instruments were then operated in the field, collecting ambient O3 level data in the rural Richland, Washington area for two weeks, prior to rebuilding and calibration of one of the analyzers. Both analyzers were then returned to the field where measurements were collected for a third week. The pre- and post- rebuild/calibration data were compared and it was determined that the rebuilt analyzer was operating within statistical parameters prior to the rebuild and calibration. The Richland data, acquired at Pacific Northwest National Laboratory (PNNL), were then compared to O_3 levels measured at Nashville, TN., Houston, TX., and Mexico City, Mexico., to identify differences in diel trends due to energy emissions. The data show that the Richland area is relatively free of O_3 precursors with O_3 levels building modestly throughout the day due to ground level heating and resultant inversion layer breakup. Future research will center on completing construction of a chemiluminescence O_3 analyzer that will be calibrated against an accurate UV-absorption O_3 analyzer. Both instruments will then be used on the DOE G-1 aircraft in an experiment designed to compare chemiluminescence to UV-absorption methodologies at high air speed.

Differentiating the Gas Chromatograph and the Mass Spectrometer for High School Students. *CAROLYN CARTER (University of Northern Iowa, Cedar Falls, IA 50613) DEON ETTINGER (Argonne National Laboratory, Argonne, IL 60439).* A more effective means of instruction was needed to teach high school students about the gas chromatograph-mass spectrometer (GCMS). This was evident from research presentations given by high school students in the 2003 summer program sponsored by the Division of Educational Programs at Argonne National Laboratory. The students were unable to explain either the GCMS technique or properly interpret their data. While the GCMS is a complex instrument, its ubiquitous presence in scientific investigation merits attention even at the high school level. Therefore, a new approach was developed to demystify the GCMS. After a brief verbal instruction, the students were divided into three smaller groups to complete two contrasting lab activities. It was the objective that one lab activity focused on the GC function of the instrument and one lab focused on the MS function of the instrument, would allow the students to be able to delineate the techniques and more confidently interpret their research data. To test the effectiveness of this new approach, the students were given a set of six questions as both a pre-test and post-test. A significant improvement on the test was measured as the mean score increased from 1.81 to 5.55 on a six point scale. It was concluded that the comprehension of the GCMS by high school students was enhanced by a brief verbal instruction coupled with two distinct lab experiences carried out in small groups.

The Long and Winding Road to Understanding Uranium Binding to *Deinococcus radiodurans*. *JULIA CHAMBERLAIN (Reed College, Portland, OR 97202) HEINO NITSCHE (Lawrence Berkeley National Laboratory, Berkley, CA 94720).* Microbial activity in soils and sediments can significantly affect transport of radionuclides in the environment. A molecular-level mechanistic understanding of actinide-bacterial interactions, including surface complexation and redox chemistry, is necessary for designing bioremediation methods for hazardous nuclear waste. Actinide complexation in aqueous solutions has been studied using time-resolved laser fluorescence spectroscopy (TRLFS) to determine stability constants for many actinide complexes. These stability constants quantify the overall thermodynamic stability of a given species. To study the surface complexation of U(VI) binding to *Deinococcus radiodurans*, a TRLFS experiment requires an aqueous system that will maintain intact bacterial cells, but that does not affect the U(VI) oxidation state, nor contain ions which quench the emitted fluorescence. In this study, we consider solution constraints and examine the viability and intactness of *D. radiodurans* cells over time in solutions of varying pH, ionic strength, and ion species. *D. radiodurans* were cultured to stationary phase and stained with Hoechst Stain solution, a fluorescent DNA stain commonly used to identify intact cells. Results indicate intact bacterial cells for 0.10 M solutions of NaCl, $NaNO_3$, and $NaClO_4$ at ambient pH, as well as $NaNO_3$ with an initial pH of 4.5. Further studies

will focus on the effects of these solutions on cell life, as we proceed with our TRLFS study of U(VI) binding to D. radiodurans.

Metallic Coatings on Intermetallic Anodes: A Study in Low Temperature Deposition. *JESSICA CLEVENGER (Ball State University, Muncie, IN 47306) JOHN VAUGHEY (Argonne National Laboratory, Argonne, IL 60439).* A lithium ion battery is an important component of many devices that require portable power - be it a CD player, implanted medical device, or hybrid-electric automobile. The battery has three main parts - a cathode (usually a highly oxidized metal oxide), an organic electrolyte to conduct ions, and an anode (usually lithium metal or graphite). In many of these devices the anode is the limiting factor in either device performance or device cost. Present anodes work but have many safety issues - notably overcharge problems or lifetime problems related to lithium's unique electrochemistry. Alternative materials, typically Sn- or Sb-based alloys, have several problems, notably high irreversible capacity, the amount of lithium inserted on the first charge that doesn't come out on discharge. We sought to lower this amount by adding silver to the electrode surface, thereby altering the interface between the electrode and the electrolyte. Silver coatings were deposited using four different methods: (1) a variation of the Tollens test for aldehydes was used to coat a natural (Chinese) graphite, a synthetic (GDR) graphite, and the alloy Cu6Sn5; (2) in-situ coatings were attempted by using 0.5 wt % $AgNO_3$ in LP40 electrolyte - a 50/50 wt mixture of EC (ethylene carbonate) / DEC (diethyl carbonate) with 1.0 M LiPF6 - and 4.6 wt % $AgClO_4$ in the DOE's ATD program Gen 3 electrolyte - 40% DEC / 30% PC (propylene carbonate) / 30% EC, 1.0 M $LiPF_6$; (3) a physical ball-milled mixture of silver metal and Cu_6Sn_5; and (4) a surface coating of an insoluble silver salt: we coated the electrode materials with silver succinate, silver fumarate, silver ascorbate, and silver oxalate. Each method was found to produce different results. The silver coatings via the aldehyde reduction (Tollens test) improved the performance of the C-GDR cells, but the results with the other graphite or the alloys was less pronounced and requires more work to draw a conclusion, whereas the in-situ deposition method significantly decreased the irreversible capacity for Cu_6Sn_5. The ball-milled physical mixture actually made the irreversible capacity worse, probably due to the probable oxidation of the underlying electrode materials. Overall, silver coatings look very promising, but more work needs to be done yet.

Voltammetric Detection of Lead and Heavy Metals on a Carbon Paste Electrode Modified with Glycinylurea Self-Assembled Monolayer on Mesoporous Silica Supports. *MARIANNE CONNER (Eastern Washington University, Cheney, WA 99004) YUEHE LIN (Pacific Northwest National Laboratory, Richland, WA 99352).* Current technologies for detecting trace metals in aqueous solution has relied on the use of expensive, non-field deployable, spectroscopic techniques such as Inductively Coupled Plasma-Mass Spectroscopy (ICP-MS) and Atomic Absorption Spectrometry (AAS). To minimize governmental and industrial expenses for testing groundwater and waste water, in addition to maintaining a sensitive and selective method for determining metal ion concentrations in solution, researchers are seeking to develop more efficient, low cost, compact and field-deployable electrochemical sensors. The following study investigates the likelihood of a new electrochemical sensor based on a carbon paste electrode (CPE) modified with Glycinylurea Self-Assembled Monolayers on Mesoporous Silica Supports (Gly-UR SAMMS) for the detection of Pb^{2+} in the presence of other heavy metals. The Gly-UR SAMMS CPE was activated by presoaking it in a stirred metal ion aqueous solution, followed by anodic stripping voltammetry steps including electrolysis, stripping, and regeneration in a 0.3M nitric acid solution at quiescent condition. Data was acquired for current response vs. potential using square-wave voltammetry. Current response vs. concentration (ranging from 2.5 to 50 ppb Pb^{2+}) at 2.0 minutes preconcentration was collected to calibrate the electrode. The dependence of current response on preconcentration time (ranging from 1 to 15 minutes) for a 25 ppb Pb^{2+} was also evaluated. Results show reproducibility of measurements up to N = 6, with a relative standard deviation (RSD) of less than 5% on the individual electrode for a tested 50 ppb Pb^{2+} solution, and less than 10% RSD between separately prepared electrodes. For interference studies, the presence of Cu^{2+}, Hg^{2+}, Mn^{2+}, Cd^{2+}, and Zn^{2+} did not affect the detection of Pb^{2+}. The detection limit for Pb^{2+} with Gly-UR SAMMS is as low as 2.5 ppb for 2.0 minutes preconcentration. Overall, the Gly-UR SAMMS CPE is a sensitive and selective method for detecting lead ions in the presence of other heavy metal ions in aqueous solution and compensates the need for a low cost, compact, and field deployable electrochemical sensor.

Plutonium Metal Sample Exchange. *PATRICK DEARMOND (Indiana Wesleyan University, Marion, IN 46711) JACQUELINE FONNESBECK (Argonne National Laboratory, Argonne, IL 60439).* Rocky Flats began producing weapons grade plutonium in 1952 as part of the nation's weapons program. The plutonium was expected to meet strict requirements regarding isotopes of plutonium and content of impurities. The Plutonium Metal Sample Exchange Program was developed to meet this need, which led to the present program operated by Los Alamos National Laboratory (LANL). Within this program, samples of weapons grade plutonium were shipped from LANL to Argonne National Laboratory-West for destructive measurements of elemental concentration, isotopic abundance, and metallic and nonmetallic impurities. Methods of preparation of the samples included electropolishing to remove the residual external oxide layer and anion-exchange chromatography to chemically separate plutonium and uranium. Methods of analysis included thermal ionization mass spectrometry, inductively coupled plasma-atomic emission spectroscopy, inductively coupled plasma-mass spectrometry, colorimetry, and gamma-ray spectroscopy. The samples consisted of about 94% ^{239}Pu, almost 6% ^{240}Pu, and minute concentrations of uranium, neptunium, americium, carbon, nitrogen, oxygen, and trace metals.

Seasonal Flux and Gas-Particle Partitioning of Semi-Volatile and Particulate Polycyclic Aromatic Hydrocarbons in Seattle Air. *COLE DOVEY (Middlebury College, Middlebury, VT 05753) LARA GUNDEL (Lawrence Berkeley National Laboratory, Berkley, CA 94720).* The definition of clean air, and hence the air quality standards that aim to preserve it, may be skewed by seasonal changes in polycyclic aromatic hydrocarbon (PAH) concentrations and their gas-particle partitioning. This study investigates the seasonal flux and partitioning of a group of PAHs, focusing on retene ($C_{18}H_{18}$), a wood smoke marker and possible carcinogen. Winter and Spring PAH samples were collected using the Integrated Organic Gas and Particle Sampler (IOGAPS) and analyzed via reverse-phase HPLC. The data suggest that particulate PAH concentrations are higher in colder months. They also indicate that retene is present only in colder months and partitions toward the gas phase. Because of retene's gas-particle partitioning, sampling instruments and detection methods that are applicable for gases and particles must be used in order for retene to be an accurate wood smoke marker. Future research should examine these issues across a longer period and more seasons, and develop our understanding of the source apportionment of wood smoke.

A Novel Method Utilizing Nanocomposites for the Elimination of Carbon Monoxide from a Hydrogen Gas Mixture. *MATTHEW EIBLING (County College of Morris, Randolph, NJ 07869) GISELLE SANDÍ (Argonne National Laboratory, Argonne, IL 60439).* The sequestration of CO in a gas mixture has become necessary for the purification of H_2 for use in fuel cells. Our method improves upon a preceding attempt. Previously, the separation of CO from H_2 was endeavored by using a polymer nanocomposite (PNC) membrane as a molecular sieve. It achieved a 500 H_2/CO flux. This is far below the 10ppm required for use in a fuel cell. We improved this by adding reduced Pt to the membrane. This caused an oxidation of the small amount of CO entering the PNC membrane so that it would exit as CO_2. Pure synthetic lithium hectorite (SLH) pellets were also produced and tested for selectivity of H_2 over CO. We discovered the temperature at which an oxidation of CO would take place in a poly(ethylene oxide) (PEO)/[Pt/SLH] catalytic PNC membrane and if a pure SLH clay pellet could, due to its gallery size of 3.1 Å, serve as a barrier for all gasses except H_2. For the Pt membrane, Pt^{+2} was added in a 2.4 wt% ratio to SLH clay through ion exchange, then PEO was added in the desired ratio. Solution was puddle casted on a Teflon surface yielding a yellowish, flexible, semi-transparent membrane about 0.063mm in thickness. It was reduced in an oven at 140°C for two hours under a N_2 and H_2 environment. The resulting membrane, now black in color, was tested in a reactor. This determined the oxidation of CO through our membrane to occur at temperatures above 260°C. This is far above the temperature at which PEO decomposed. The pure SLH pellet was produced by pressing powdered SLH clay under ten tons of force in a die. It was tested for H_2 flux and H_2/CO selectivity in the above used reactor. Results revealed H_2 flux to be excellent, but upon addition of CO the pellet maintained a selectivity of only 2.5 H_2/CO.

Spectroscopic Investigations of Catalytic Hydrogen Production from Dimethylamine Borane. *JULIA FERRIS (Western Washington University, Bellingham, WA 98225) S THOMAS AUTREY (Pacific Northwest National Laboratory, Richland, WA 99352).* Currently research is being performed in the area of increasing the efficiency of on board hydrogen storage for fuel cell powered vehicles. This is a key factor that will be necessary in the twenty first century. With the idea of changing the energy economy there have been many different ideas on what type of hydrogen storage takes the least amount of energy and produces the greatest amount of products, H_2 per unit weight and volume. Currently scientists at PNNL are studying the release of H_2 in dimethylamine

borane (DMAB) using a rhodium catalyst to measure rates and to learn about the reaction which takes place. Using the IR spectrometer we were able to monitor the loss of the solvents MeOH, THF, diglyme, glyme, and toluene. We tried to optimize the concentration of catalyst and DMAB to determine the optimum conditions to study the reaction kinetics. Monitoring the vibrational stretches and bends of the molecule for about 5 minutes we are able to study the whole reaction. We made dilution measurements of the DMAB in toluene to look for intermolecular hydrogen bonding in toluene. However, after making 4 dilutions with the change in concentrations, we were not able to detect any changes in the vibrational peaks. Using the disappearance of the N-H band in the DMAB starting material we attempted to monitor the kinetics of H_2 loss in the presence of Rh catalyst. There were experiments done changing the concentrations of DMAB and changing the solvents which enabled us to monitor these losses. In the presence of the catalyst, hydrogen gas seemed noticeable after 1.5 minutes by the bubbles forming into the external wet cell. The goal of our work is to find the optimal experimental conditions to measure the loss of H_2 from DMAB.

Electrical and Morphological Properties of Inkjet Printed PEDOT/PSS films. *ERIK GARNETT (University of California, Berkeley, Berkeley, CA 94704) DAVID GINLEY (National Renewable Energy Laboratory, Golden, CO 89401).* Organic solar cells and LEDs are becoming more popular because their low cost materials, potential manufacturability, and recent gains in efficiency make them feasible for widespread commercialization in the near future. One significant manufacturing problem, especially for OLEDs, is the cost associated with creating patterned devices with spatially non-specific deposition methods such as spincoating. Inkjet printing can remove this problem. In recent years, inkjet printed polyethylene(3,4-dioxythiophene)/ polystyrene sulfonate (PEDOT/PSS) has been incorporated into many organic devices to help charge transfer, but there has not been much research regarding the effect of different printing parameters on the electrical and morphological film properties. In this work, an atomic force microscope, four point probe, and Kelvin probe were used to study the effects of printing parameters on roughness, conductivity and workfunction. Inkjet printed PEDOT films were also compared to spincoated films to determine how the polymer deposition method affects the above properties. Generally, inkjet printing created rougher but more conductive films with a smaller workfunction. Additionally, it was demonstrated that the workfunction of PEDOT films could be tuned over a range of about 0.5 V by changing the solvent mixture or substrate surface pretreatment. All additives to the as received PEDOT/PSS suspension caused the workfunction to decrease. It was discovered that workfunction decreases as printing voltage increases, but the trend reverses after annealing the films. This phenomenon suggests that when DMSO interacts with PEDOT, the workfunction changes. Finally, the results support previous publications suggesting that DMSO increases conductivity through a screening effect and also by changing the distribution of PEDOT and PSS in the film.

Characterization of Neptunium - Zirconium Alloys. *JACKLYN GATES (Westminster College, New Wilmington, PA 16335) J. RORY KENNEDY (Argonne National Laboratory, Argonne, IL 60439).* As part of the Advanced Fuel Cycle Initiative, Argonne National Laboratory is preparing low and non-fertile zirconium based alloys with additions of uranium, plutonium, americium and neptunium. However, the neptunium-zirconium system has not been well studied and concerns have arisen over the formation of low melting neptunium phases. In this report, three neptunium-zirconium alloys were characterized in order to determine temperatures of transitions, heats of transitions and heat capacity. The results presented here are most in line with the phase diagram put forth by R. Julián Rodríguez et. al., of the European Institute for Transuranium Elements (EITE). In addition, the heat capacity of solid neptunium, and its contribution above its melting point up to 1000°C, was determined using the heat capacities of the three neptunium-zirconium alloys. The neptunium heat capacity values were found to be in agreement with literature values to 200°C.

Develop Ab Initio Quantum Continuum Solution Theory to Predict Aqueous Thermochemistry of Radicals and Ions. *QUINN GILCREASE (Western Washington University, Bellingham, WA 98225) DON CAMAIONI (Pacific Northwest National Laboratory, Richland, WA 99352).* The purpose of the project is to develop models for predicting the chemistry of nuclear waste stored in underground tanks, such as those at the Hanford site in Richland, WA. The substances stored in these tanks are a mixture of solids, and aqueous ionic solutions. Predictive models of the chemistry of these tanks are needed to support the resolution of issues concerning storage and treatment of the wastes and closure of the waste tanks. Electronic structure calculations were performed using Gaussian 98 to optimize the molecular structure of molecules and ions in vacuum. Solvation free energies of the optimized structures were computed using the COSMO continuum solvation model as implemented in the Gaussian 98. Data analysis was performed using a Macintosh (Mac OS X) computer. Software tools were developed to prepare input files for Gaussian 98, Scripts to extract data and Visual Basic macros to import data. These were used to create the data to supply to an analysis program that would help develop the predictive models, given a large test set. The work on the program then began. The early results from the program look promising. Work should continue on the program to provide the predictive protocols. The program will make it easy to add more molecules and new atoms to improve accuracy and add more definitions.

Preparation of a Software Package to Measure the Thermal Dependence of Viscosity for Ionic Liquids. *ANDRE GRANGE (Brooklyn College, Brooklyn, NY 11210) MARK N. KOBRAK (Brookhaven National Laboratory, Upton, NY 11973).* Ionic liquids, salt that are molten at room temperature, have been heavily studied. The choice of the cations and anions used to make these liquids affect the overall properties of the liquid such as the liquid's viscosity. Currently theories for ionic liquid systems predict certain relationships between viscosity and electrical conductivity for an "ideal" ionic liquid, requiring knowledge of viscosity as a function of temperature. Such measurements involve time- consuming equilibration at each temperature, and it therefore useful to automate the process. In this work, a computer program was designed to integrate a viscometer and a temperature bath using the Lab View software suit. This program reduces the time required to characterize novel ionic liquids and eliminates some of the errors associated with the manual operation of the experiment.

Synthesis, Spectroscopic Characterization, and Binding Studies of Lanthanide and Actinide Complexes Containing Anionic Tripodal Kläui-Type Ligands. *JENNIFER GREAUX (The University of the Virgin Islands, St. Thomas, VI 802) GREGG LUMETTA (Pacific Northwest National Laboratory, Richland, WA 99352).* The use of anionic Kläui-type tripodal ligands in the selective binding and separation of lanthanides and actinides is an area of active research at the Pacific Northwest National Laboratory. In an attempt to better understand the structural and binding characteristics of these ligands, a series of lanthanide (M= La, Nd, Pr) and actinide (M = Th, U) complexes were prepared in 1:1 and 2:1 (L:M) stoichiometry by reacting MXn (X = $NO3^-$ or Cl^-) with the required stoichiometric amount of (C5Me5)Co(P(=O)(OR)2)3Na (R= Me or Et). The complexes were characterized by IR spectroscopy and NMR spectroscopy. Attempts were made to crystallize the materials and obtain crystals suitable for x-ray crystallographic studies. The neodymium and lanthanum chloride complexes were successfully crystallized. Binding studies, with Nd^{+3}, U^{+4}, Am^{+3}, and PuO_2^{+2} using the (C5Me5)Co(P(=O)(OR)2)3Na (R= Me) ligand were initiated. UV-Vis spectroscopy was the spectroscopic tool used for these measurements. The metal ions were chosen because of their unique absorption bands in the visible spectral range and they represent the wide range of oxidations states encountered for the actinide elements. The computer program SQUAD (Stability Quotients using Absorbance Data) was used to evaluate the spectral data and calculate the binding constants.

A Survey of Oxidation Reactions of Propylene Glycol with Hydrogen Peroxide and Metal Catalysts. *BENJAMIN HARRIS (University of Minnesota - Twin Cities, Minneapolis, MN 55414) ROB DISSELKAMP (Pacific Northwest National Laboratory, Richland, WA 99352).* Polyols derived from biological feedstocks and polyols formed in secondary reactions in industrial processes may be used as low cost starting materials for higher commodity reagents. The conversion of polyols to higher commodity compounds can involve the oxidation of at least one of the polyol's alcohol groups to carbonyl groups. These experiments employed propylene glycol as the substrate with the metal catalysts copper (II) oxide, copper (I) oxide, palladium black, and ruthenium on carbon or alumina supports, or as a pure metal. The reactions involved the use of hydrogen peroxide as the oxidant and were conducted under reflux conditions. pH buffering salts were used to control hydrogen peroxide oxidizing capacity. GC/MS spectra were taken to test for product formation and to determine conversions for each experiment. Over-oxidation in the reaction occurred when acetic acid and formic acid were formed. The partially oxidized intermediate, hydroxy acetone, was observed with the use of copper (II) oxide and palladium black, and the partially oxidized product, lactic acid, was observed with the use of palladium black. The unexpected compound, propionaldehyde, was also formed using ruthenium at mildly basic conditions (pH of 8.5). The formation of an aldehyde from a 1,2 diol is the most promising reaction that was observed in this survey of reactions, and it could potentially be a reaction that has commercial applications.

Self-organized Nanostructures for Device Applications. *EMIL HERNANDEZ (University of Puerto Rico-Mayaguez, Mayaguez, PR 00681) SAMUEL MAO (Lawrence Berkeley National Laboratory, Berkley, CA 94720).* Since the early 1950's anodization of aluminum has been studied. This process results in the formation of self-organized porous with diameters in the order of nanometers, and it is know as Anodic Aluminum Oxide (AAO). This phenomena is been used as a template to grow nanotubes, which are of great interest due to their physical properties and potential applications. In this work AAO templates were develop in Oxalic Acid. Further, the samples were coated with Cobalt, to catalyze the nanotubes growth. Carbon nanotubes were synthesized by heating the sample in a tube furnace with flowing methane. To characterize the samples Scanning Electron Microscopy (SEM) was employed. The nanoporous developed had an average diameter of 45 nanometer, and well vertically aligned carbon nanotubes were grown. On going work will focus on measuring the field emitting properties of the nanotubes and use these nanostructures for light emitting devices (LED) development.

Electrochemical Hydrogen Storage: Materials and Methods. *SARA HOBBS (Bethel College, North Newton, KS 67117) JOHN VAUGHEY (Argonne National Laboratory, Argonne, IL 60439).* Hydrogen storage has been designated by the Department of Energy one of the most challenging science and engineering problems of the hydrogen economy. In practice there are only 3 ways it has been demonstrated: 1) metal hydrides, 2) liquid or compressed gas, or 3) as a hydride salt. All of these methods have advantages and disadvantages that must be addressed before a technology is chosen. A problem all of the chemical methods face is temperature and kinetics. The hydrogen is stored and released at high temperature slowly. This summer we evaluated a low temperature method of hydrogen storage based on the principles of the lithium-ion battery. In our work we evaluated a method to insert hydrogen into a lithium metal salt (Zintl) matrix electrochemically. We were able to determine the voltage of insertion (0.4-0.5V vs. Li), optimize the conductivity of the materials used as electrodes as well as the amounts of active materials, determine the voltage and temperature stability range of PEO-based electrolytes, and evaluate the hydrogen response versus applied current. In another set of experiments, we examined the system Ag-M-PO_4 (M=Co, Fe, Ni) by two different methods to evaluate these materials as possible cathodes for mid-rate medical batteries. In this work we found that there was only one ternary compound in, $Ag_3Ni_6(PO_4)_5$. We evaluated it, as well as $AgMO_2$ (M=Co, Fe), in a lithium battery configuration. The silver nickel phosphate showed some activity (200 mAh/g) down to 1.0V with an average voltage of 2.0V.

Sulfate Extraction Using Dioctylguanidinium. *CHRISTIAN HOYDIC (Clarion University, Clarion, PA 16214) LATETITA DELMAU (Oak Ridge National Laboratory, Oak Ridge, TN 37831).* This study focuses on sulfate extraction using dioctylguanidinium. Sulfate is in low-activity waste after the wastes have been treated and deteriorates the low-activity waste glass required for storage due to the high concentration levels. An effective extraction of sulfate is therefore very attractive both economically and environmentally. Based on other solvent extraction applications using this extractant, it was theorized that guanidinium-based molecules could be used in the extraction of the sulfate anion. Guanidinium seems to be favored because it is an organophilic cation that can extract anions from the aqueous layer. Extraction of sulfate is challenging due to its ionic double charge, rendering its transfer into the organic phase very unfavorable. The weak acid characteristics of dioctylguanidinium make it sensitive to pH variations. It was also determined in preliminary experiments in which the concentrations of nitrate, sulfate, and guanidinium were varied that sulfate was extracted according to a reaction involving the exchange of one sulfate ion with two nitrate ions. Also, when the pH was previously varied from 2 to 12, the sulfate distribution ratios decreased as expected but, surprisingly, there was evidence of two decreases rather than one, as would be expected based on the monoacidity of dioctylguanidinium. The presence of carbon dioxide in the system, forming bicarbonate in mildly basic conditions, could explain this unexpected behavior. An inert gas, argon, is now used to prevent bicarbonate contamination. To determine the number of acidic sites in dioctylguanidinium, the compound was washed with concentrated caustic solutions to form the neutral guanidine form and then titrated in glacial acetic acid using triflic acid. It was proven that the compound is indeed a monoacid. In order to see the efficiency of dioctylguanidinium as an extractant, solvent extraction methods will be used including employing radioactive sulfur as a radiotracer to follow the extraction of sulfate. Since it was demonstrated that dioctylguanidinium can be deprotonated only once, it is expected that, under carefully monitored conditions, the system will show only one decrease of distribution ratio values rather than two when pH is varied.

Synthesis of Cobalt Nanoparticles From New Cobalt Complex. *KYLEE HYZER HYZER (University of Missouri at Rolla, Rolla, MO 65409) JOHN SCHLUETER (Argonne National Laboratory, Argonne, IL 60439).* The new cobalt complex, consisting of three carbon atoms at the center surrounded by oleic acid is formed under argon atmosphere by adding an excess of oleic acid in octyl ether to octacarbonyldicobalt ($Co_2(CO)_8$) in octyl ether. If less oleic acid is added to the cobalt, nanoparticles are formed. The nanoparticles, once made, can be transformed back into the complex by adding more oleic acid. In the present study, the complex is fully understood, by forming nanoparticles from the complex. Several methods were attempted to convert the complex to nanoparticles such as simply heating the complex, and using various solvents and reducing agents. The technique of adding super-hydride dissolved in octyl ether to the complex produced nanoparticles. This control of the complex and formation of these nanoparticles will greatly help in creating a monodisperse size among the particles. This is an important property of magnetic nanoparticles and will be useful in their many applications.

Bis(oxalato) Borate (BOB) Anion Based Ionic Liquids and Their Properties. *NEEL KHANNA (Brooklyn College, New York, NY 11210) JAMES WISHART (Brookhaven National Laboratory, Upton, NY 11973).* Ionic Liquids, salts that are molten at room temperature, have demanded greater attention in recent research because of their potential applications as environment-friendly solvents in chemical reactions, particularly in nuclear chemistry. Production of these salts involves the combination of unique cations and anions to form novel ionic liquids. These liquids are therefore tailored to fit given purposes based on the physical properties imparted to them by their respective cations and anions. The bis(oxalato) borate (BOB) anion synthesized in this study is particularly interesting because of the presence of the element boron in the compound. Boron is a thermal neutron scavenger, meaning it can absorb neutrons that may have otherwise been available to cause further nuclear reactions. The BOB anion can therefore potentially make these liquids useful in the recovery and handling of nuclear fuels. In this study, the aforementioned BOB anion was synthesized and combined with a series of cyclic pyrrolidinium cations, through metathesis reactions to produce novel ionic liquids. After cleaning and purification, these ionic liquids were characterized physically. The ionic liquids appeared viscous and were sometimes solid at room temperature probably due to the strong van der waals forces between the large BOB anions, making the liquids possibly useful as solvents for high molecular weight organic substances. Future work will involve pulse radiolysis studies of these compounds to test their potential as solvents in nuclear chemistry.

Water Gas Shift Catalyst Development. *ADAM KUESTER (Lawrence University, Appleton, WI 54911) THEODORE KRAUSE (Argonne National Laboratory, Argonne, IL 60439).* A hydrogen rich gas can be produced by reforming gasoline, natural gas and other hydrocarbon fuels, for use with fuel cell systems. The gas, termed reformate, contains a mixture of hydrogen, carbon dioxide, and carbon monoxide plus nitrogen, if air is used as the source of oxygen in the reforming process. Carbon dioxide and nitrogen do not affect the performance of anode catalyst used in proton exchange membrane fuel cells (PEFC), while carbon monoxide poisons the catalyst. To maintain an acceptable level of performance, the concentration of carbon monoxide in reformate must be reduced to <10 ppm. The water gas shift (WGS) reaction is used to reduce the bulk of the carbon monoxide to carbon dioxide. This research project supports the effort to develop new WGS shift catalysts for use in fuel processors designed for fuel cell applications. Catalysts compositions consisting of bimetallic Pd/Co and monometallic Ni were investigated. For the Pd/Co catalysts, the effect of weight loading of each metal was investigated by measuring the WGS reaction rate as a function of temperature. The reaction order for carbon monoxide was also determined. Pd/Co catalysts exhibit high activity for the WGS reaction; however, they do form methane and deactivate rapidly. Further work is needed to reduce methanation and to better understand the deactivation mechanisms. The WGS activity and the selectivity for methanation were measured for the Ni catalysts.

Determination of Relative Sensitivity Factors (RSFs) for the Actinide Elements by Inductively Coupled Plasma Mass Spectrometry (ICP-MS). *MICHAEL LAZAR (Utica College, Utica, NY 13502) JEFF GIGLIO (Argonne National Laboratory, Argonne, IL 60439).* Uranium can be used to find relative sensitivity factors for other actinide elements in an ICP-MS analysis because of similar chemical properties. Experiments are done to compare the sensitivity slopes of uranium and bismuth to the sensitivity slopes of neptunium, plutonium, and americium. Relative sensitivity factors were calculated as a ratio of the sensitivity slopes of the actinides over the sensitivity slope of uranium or

bismuth. Errors reported to be ~5% or less for a uranium standard and ~7% or less for the bismuth standard.

HDO: A Possible Effluent from Heavy Water Reactors. *LACY LEDBETER (Central Washington University, Ellensburg, WA 98926) RICHARD WILLIAMS (Pacific Northwest National Laboratory, Richland, WA 99352).* Deuterated water is of potential interest to treaty monitoring organizations tracking the technology in nuclear proliferation. D_2O, called heavy water, has deuterium atoms in place of hydrogen atoms. Deuterium is a heavy isotope of hydrogen; it has one neutron in addition to the one proton in the nucleus. Heavy water, nuclear reactors use D_2O as the neutron moderator, a more efficient moderator than light water for its low cross section for neutron capture. Its efficiency eliminates the need for the expensive Uranium-235 enrichment process. Upon release from a heavy water reactor, D_2O would undergo isotopic exchange with the H_2O in the environment to produce HDO. Thus, the objective of this study was to investigate the suitability of HDO as a signature for heavy water reactors. This entailed using a laser-based near-infrared spectrometer to analyze HDO and D_2O from a 2.5 to a 0.3 nanometer region to find the line strengths of HDO, that are needed to calculate quantitative concentrations of ambient samples where HDO is detected. Through Beer's law, the line strength of HDO at 6545.94 cm^{-1} was found to be 2 $x10^{-23}$ cm/molecule. Using current instrumentation in the lab, this absorption peak could be detected at about 500 ppb; a reasonable level to detect in the field.

The Anodic Electrodeposition of Cerium Oxide. *JENNIFER LEE (Kennedy-King College, Chicago, IL 60608) JONG-HEE PARK (Argonne National Laboratory, Argonne, IL 60439).* My experimental goal was to investigate on the formation of cerium oxide deposits through the electrochemical deposition (called as "electrodeposition"). We have performed the cyclic voltammetry to obtain the proper conditions for the cerium oxide deposition using the cerium ion bearing electrolyte solutions. We prepared the zirconium-working electrode by cutting the commercial zirconium alloy, zircaloy-4. As the counter electrode foil platinum was employed. An rt-saturated calomel electrode was used as a reference electrode. The used electrolyte solution was 0.1M cerium acetate, and the solution pH values were 8.0 and 10.2, these were adjust by adding the KOH in the aerated condition at the various test temperatures of 25, 45, 60, and 97 C. The results obtained at various temperatures with cerium ion bearing solutions were compared with the ACR-700 water condition. As a conclusion, we have found possibility of the cerium oxide film deposition on the surface of the zircaloy-4 nuclear cladding tube by means of electrodeposition technique

Hydrological and Geochemical Processes Governing the Transport and Fate of Sr^{2+} and Chelated Sr. *QIAN LIU (Northwestern University, Evanston, IL 60201) MELANIE MAYES, MOLLY PACE, XIANGPING YIN, PHILIP JARDINE (Oak Ridge National Laboratory, Oak Ridge, TN 37831).* Accelerated migration of ^{90}Sr has been observed in the unsaturated vadose zone beneath the tank farms at the DOE Hanford Reservation, located near Richland, WA. Studies have shown that metal organic chelate complexes such as $SrEDTA^{2-}$ may contribute to ^{90}Sr mobility. Furthermore, the tank farm environment is unsaturated and has implications for the restriction of flow to finer-grained soil. The goal of this research is to examine the geochemistry of Sr^{2+} and $SrEDTA^{2-}$ when they are in contact with sediments from Hanford tank farms. Two laboratory-based techniques, batch isotherm experiments and saturated packed column experiments, will be conducted to quantify geochemical and hydrological processes controlling Sr^{2+} and $SrEDTA^{2-}$ sorption in Hanford sediments. The batch experiments will mix varying concentrations of Sr^{2+} and $SrEDTA^{2-}$ with soil sediments of different grain sizes (bulk, and separations of sand, silt, and clay). The different grain sizes may strongly affect adsorption. Also, the batch experiments are conducted under a 2:1 and 1:1 solid: solution ratio. This aspect of the experiments will show how sorption changes with the amount of sediments added. In the column experiments, solutions of Sr^{2+} and $SrEDTA^{2-}$ pass through 2 columns of different lengths (4.5 and 2 cm). This type of study is more relevant to the tank farms as it measures the transport of cations (Sr^{2+}) and anions ($SrEDTA^{2-}$) under flowing conditions. Even though the research is still in its initial stages, results from kinetic batch experiments show a similar absorption K_d (distribution coefficients) for $SrEDTA^{2-}$ and Sr^{2+} samples. Since cationic and anionic absorption differs for each pH, this must indicate that, under soil conditions (pH ~8), $SrEDTA^{2-}$ dissociated into $EDTA^{4-}$ and Sr^{2+}. This suggests that in both experiments the Sr^{2+} was sorbed by the soil. The 1:2 solid to solution ratios have higher K_d than their 1:1 counterparts, suggesting that the increased ionic exchanges due to more soil had a greater effect than the increased sites for sorption. Also, the column data show that $SrEDTA^{2-}$ dissociates upon contacting soil (by comparing the breakthrough curves of Sr^{2+} and $SrEDTA^{2-}$). In conclusion, the batch studies show that Sr sorption is sensitive to solid: solution ratios., the results of the experiments so far imply that $SrEDTA^{2-}$ probably does not contribute to ^{90}Sr mobility under tanks, which will reduce the spread of contamination near Hanford farms more than expected.

Controlling Sampling Artifacts for Semi-Volatile Species in Seattle, WA. *RACHELLE MAJESKE (Crafton Hills Community College, Yucaipa, CA 92399) LARA GUNDEL (Lawrence Berkeley National Laboratory, Berkley, CA 94720).* In response to the national push to learn more about air pollution and its health effects, the EPA funded five particulate matter (PM) research centers in 1999, one of which is the Northwest Research Center for Particulate Matter and Health. The Beacon Hill (BH) area of Seattle, WA, has an air quality monitoring station that makes the area a prime location for collecting samples of PM. These particles come from vehicle exhaust, as well as seasonal wood burning and other sources. Air samples were collected at Beacon Hill as well as indoors and outdoors at private residences using Lawrence Berkeley National Laboratory's (LBNL) Integrated Organic Gas and Particle Sampler (IOGAPS). These samples were then analyzed for gas and particulate polycyclic aromatic hydrocarbons that are known carcinogens. Our objective was to find correlation between organic carbon (OC) and elemental carbon (EC) data for denuded and non-denuded PM.

Adsorption And Reaction of Hydrogen Sulfide and Methanethiol on Reduced and Oxidized Ceria Surfaces. *TOM MCDONALD (Kalamazoo College, Kalamazoo, MI 49006) DAVID MULLINS (Oak Ridge National Laboratory, Oak Ridge, TN 37831).* The interaction of hydrogen sulfide (H_2S) and methanethiol (CH_3SH) with thin films of highly oriented $CeO_2(111)$ was studied in an effort to characterize this surface¡¦s desulfurization capacity. Desorption energies of both compounds were determined over a variety of ceria oxidation states, and the products of their chemical reactions were studied via thermal desorption spectroscopy. On completely oxidized films (cerium present almost exclusively in its +4 oxidation state), CH_3SH demonstrated no significant chemical reactivity, and desorbed from the surface under 200 K intact. As the degree of ceria oxidation was decreased ($Ce^{4+/3}Ce^{3+}$), its chemical activity increased substantially, wholly in the 500-700K temperature range. CH_3SH was seen to chemisorb to the surface, where it is proposed to occupy an oxygen vacancy and then protonate an adjacent oxygen atom to create a hydroxyl group. This hydroxyl group, along with the chemisorbed CH_3S^-, makes subsequent reactions possible, including the creation of water, hydrogen, and methane, as well as methanethiol (presumed to occur through a recombination pathway). Increasing surface reduction appears to favor the pathway for the creation of methane and water. With regard to H_2S, it also has a very small amount of chemical reactivity on highly oxidized ceria, with only a small amount of water desorbing at low temperatures. When chemisorbed to surfaces of lower oxidation, it appears to proceed through two different pathways: one in the 20-55% Ce^{3+} range, and the other in the >60% Ce^{3+} range. In the former, thermal desorption appears to favor the production of water. Progression to the latter oxidation state increasingly favors the production of hydrogen. Several factors (both kinetic and thermodynamic) appear to direct this behavior, but the primary notion at work is the increasingly difficult task of removing oxygen from a surface that is becoming more reduced. Additionally, the low temperature desorption energy of H_2S decreases as the degree of surface oxidation decreases. With regard to the overall study of ceria as a desulfurization catalyst, it has shown effectiveness in the total decomposition of H_2S (into H_2 and H_2O), but less success in the decomposition of CH_3SH, primarily due to the presence of the high temperature recombination pathway.

Ultrasound Techniques Used to Measure the Viscosity and Density of Fluids. *ELLIS MIMMS (Tuskegee University, Tuskegee, AL 36088) BILL ELLINGSON (Argonne National Laboratory, Argonne, IL 60439).* Our main goal during this research program is to use ultrasound techniques to measure the density and viscosity of different fluids. Also another goal in our research efforts is to analyze the flow rate's effect on the viscosity of different liquids. We will also analyze different liquids and substances in a static state and a dynamic state of motion to see if a change in motion will affect the viscosity or density of a fluid. Using the data that we collect from the oscilloscope to analyze wavelengths we will use several equations to compute the viscosity and density of the fluids.

BEARS ^{15}O Production and the Application of a Piston Syringe Drive. *REBECCA MINER (Montana State University, Bozeman, MT 59715) JAMES P. O'NEIL (Lawrence Berkeley National Laboratory, Berkley, CA 94720).* Berkeley Experiments with Accelerated Radioactive Species (BEARS) is an ongoing project that provides the 88-inch Cyclotron at Lawrence Berkeley National Laboratory with a light-ion radioactive beam. This radioactive beam has been used to conduct ex-

periments with ^{14}O and ^{11}C examining astrophysical concepts to further the understanding of star formation and destruction in the universe. Researchers are also looking to conduct experiments with ^{15}O formed by the reaction $^{15}N(p,n)^{15}O$ allowing them to better model the formation of stars and to better understand novae. The high cost of the isotopically enriched ^{15}N needed for the reaction requires the implementation of a piston syringe drive to recycle the target gases. The syringe drive was tested with air to ensure the integrity of the system and the drive's ability to pressurize a target to 200 psi. At the conclusion of these tests the system was then used in ^{14}O production to ensure that the target gases were uncontaminated and that the syringe did not lose pressure overtime. The results from these tests demonstrated a consistent ^{14}O activity yield both with and without the syringe drive at 5μA. The yield was also stable over a period of 26 minutes with the syringe drive in use. The stability of the yield with and without the syringe drive in use signifies a lack of significant target gas contamination and demonstrates the syringe's ability to hold pressure with repeated actuation of the plunger. The syringe drive also worked for a short test of ^{15}O production. The ^{15}O yield found in the test was greater than that of the ^{14}O yield found in earlier tests, as is expected due to the longer half life of ^{15}O ($t_{1/2}$= 122 s) and higher cross section.

CO_2 Capture Using Ethylenediamine-modified SBA-15. *DEREK MOSER (Texas A&M University, College Station, TX 77844) DONNY MENDOZA (Pacific Northwest National Laboratory, Richland, WA 99352).* Excessive CO_2 emissions are one of the causes of global warming, and CO_2 emissions need to be reduced in the future in order to stabilize the earth's climate. A step in accomplishing CO_2 reduction is the capture of carbon dioxide from major emission sources such as fossil fuel power plants. At Pacific Northwest National Laboratory (PNNL), solid materials functionalized with amine groups are being tested for the capture of CO_2. Carbon dioxide adsorption capacity of ethylenediamine-modified mesoporous silica, EDA-SBA-15, was measured using a fixed bed flow system. The effect of different concentrations of CO_2 and the effect of adsorption temperature were studied. The capacity for this sorbent is 22 mg/g for CO_2 with a feed stream of 15% CO_2 and balance N_2. EDA-SBA-15 is fully regenerable using thermal swings past 110ºC (the temperature of desorption) during cyclic adsorption/desorption. The capacity is optimized at a base temperature of 95ºC.

Partial Oxidation of Polyols Using Precious Metal Catalysts and Hydrogen Peroxide. *JAYSHREE PATEL (County College of Morris, Randolph, NJ 07869) ROBERT DISSELKAMP (Pacific Northwest National Laboratory, Richland, WA 99352).* Oxidizing primary alcohols to acids, while either dehydrating or reducing secondary and tertiary alcohols using catalysis, is a possible first theoretical step in the manufacture/synthesis of healthier food oils. To form lactic acid from propylene glycol as a model reaction, this work attempts to oxidize primary alcohol to an acid and leave the secondary alcohol intact. The research team worked to identify the basic chemical transformations of polyols into substituted acids. Oxidation of aqueous propylene glycol and similar compounds were carried out under reflux conditions at temperatures between 90-100 ºC, using precious metals rhodium on carbon and platinum on carbon, and hydrogen peroxide. Oxidation of propylene glycol towards pyruvic acid was performed under both acidic and basic conditions using pH buffers such as NaH_2PO_4 (pH= 4.5), H_2SO_4 (pH= .79), NaOH (pH= 12.9), Na_3PO_4 (pH 12.5) and $Mg(OH)_2$ (pH= 7). Our results have shown that over-oxidation of propylene glycol produced undesirable products such as acetic acid, formic acid, and hydroxyacetone. The desirable target compounds were lactic acid and pyruvic acid. The products were identified using GC/MS. Hydroxyacetone and lactic acid were identified as two separate pathways toward pyruvic acid formation. Additional experiments employing dioxygen as an oxidizer were briefly performed as a more cost effective oxidation process.

The Products of Manganese (II) Oxidation. *ALANA PERKINS (Philander Smith College, Little Rock, AR 72202) JOHN BARGAR (Stanford Linear Accelerator Center, Stanford, CA 94025).* Manganese, the second most abundant transition metal in the earth's crust, exists in a number of oxidation states, among which the II, III, and IV oxidation states are of greatest environmental importance. Produced through microbial activity, manganese oxides help to mediate redox reactions with organic and inorganic compounds and help to sequester a variety of metals. The mechanism by which Manganese (II) is oxidized to Manganese (IV) is a biologically catalyzed process. There are at least three different pathways by which Mn(II) can be bacterially oxidized to Mn(IV); the first in which states that Mn(II) can be oxidized to mixed Mn(III, IV), and Mn(IV) oxides and oxyhydroxides. The second of these pathways is that Mn(II) can be directly oxidized to Mn(IV) and the last of these pathways is that Mn(II) follows an enzymatic bond with a Mn(III) intermediate in which Mn(II) oxidizes to Mn(III) and then to Mn(IV). The pathways of focus for this research are the latter two pathways.

Variability in Environmental Tobacco Smoke Exposure. *MAURA PERRY (Allegheny College, Meadville, PA 16335) BRUCE TOMKINS (Oak Ridge National Laboratory, Oak Ridge, TN 37831).* Previous studies have determined breathing zone exposure to environmental tobacco smoke (ETS) both in and away from the workplace. These studies showed that individuals who live and/or work with smokers receive more exposure than those who do not. However, these studies have been generally limited to single day exposure measurements. The current study is designed to examine the degree to which the exposure of nonsmokers, who live and/or work with smokers, varies daily. Also, it has made the first known measurements of ETS exposure on a weekend day. The breathing zones of sixty nonsmoking subjects have been sampled using a modified version of a personal monitoring system described in the open literature. The vapor phase of nicotine and 3-ethenylpyridine (3-EP), ETS specific markers in the gas phase, are determined by ASTM method D 5075-01. Respirable suspended particulate (RSP) matter is calculated by pre and post exposure weighings of the particle filters on a microbalance. Ultra-violet absorbing particulate matter (UVPM) and fluorescing particulate matter (FPM), combustion specific components of RSP, and solanesol particulate matter (Sol-PM), an ETS specific component of RSP, are determined by ASTM methods D 5955 and D 6271-04, respectively. Research is ongoing, but preliminary data is available for nicotine and 3-EP. Nicotine shows a bimodal distribution of variation with the two curves centered approximately at 30% and 60%. Additionally, there are many subjects whose nicotine exposure varied over 100%. About half of the variation in 3-EP exposure is less than 40%. For both nicotine and 3-EP there is more variation in exposure at work than away from work. A majority of the time weighted average (TWA) nicotine concentrations for a subject's weekday mean and the weekend sample agree within standard deviation. About 2/3 of weekend 3-EP TWAs did not agree with the subject's weekday mean. The wide range of variation observed for all parameters, both at work and away from work, among all subjects, indicates that ETS exposure cannot be assumed as a constant from day to day. Additionally, a weekday away from work sample may not be indicative of ETS exposure on a weekend. Completion of the study will provide more confident estimates of ETS exposure variability, useful for determining organ dose distribution of a variety of indoor air contaminants.

Determination of Preferred Cesium Complexation Site in an Asymmetrical Calix[4]arene Bis-crown-6. *ALICIA POWERS (Georgia Institute of Technology, Atlanta, GA 30332) LÆTITIA H. DELMAU (Oak Ridge National Laboratory, Oak Ridge, TN 37831).* A solvent extraction process using calixarenes is being developed to extract cesium-137 from nuclear waste. One calixarene that has been studied in this process is calix[4]arene bis[4-(2-ethylhexyl)benzocrown-6] (BEHB), which extracts cesium well and shows good selectivity for cesium over sodium. To improve stripping, an amino group was added to BEHB (AMBEHB). The goal of this project is to determine in which crown of AMBEHB the cesium resides, which will determine whether the position of the amino group in the molecule is important or whether it can be placed in the easiest place for synthesis of AMBEHB. Using radiotracers and varying the concentration of first BEHB and AMBEHB and then the concentration of cesium in both Isopar L and chloroform, the stoichiometry of BEHB, AMBEHB, and cesium in the solvent extraction process was determined. The proton and carbon Nuclear Magnetic Resonance (NMR) spectra of BEHB and AMBEHB alone were compared as well as the proton, carbon, and cesium NMR spectra of BEHB and AMBEHB with cesium and the cesium NMR spectrum of cesium alone. The experiments using radiotracers produced a slope of one for the graph of the log of the BEHB concentration versus the log of the distribution coefficient of cesium in both Isopar L and chloroform. Similar results were also obtained for AMBEHB in Isopar L and chloroform. In the experiments varying the concentration of cesium, the graph of the log of the cesium concentration versus the log of the distribution coefficient of cesium showed a slope of negative one for the higher concentrations of cesium and a slope near zero for lower concentrations of cesium with both BEHB and AMBEHB in both Isopar L and chloroform. The NMR spectra showed a splitting of peaks for AMBEHB alone compared to the spectra of BEHB alone. BEHB with one cesium for each calix also showed a splitting of peaks, and a chemical shift in cesium was observed from when the cesium was alone, when it was complexed with BEHB and when it was complexed with AMBEHB. The experiments with radiotracers show a one to one stoichiometry between cesium and the calixarenes so the comparisons of the NMR spectra for organic phases containing equal amounts of calixarene and cesium will reveal which crown contains the cesium.

Preparation and Characterization of the Rutile TiO_2 (110) Surface with Atomic Resolution by Scanning Tunneling Microscopy. *DARREN PUIGH (University of Washington, Seattle, WA 98105) IGOR LYUBINETSKY (Pacific Northwest National Laboratory, Richland, WA 99352).* In order to better understand and improve catalytic reactions involving rutile TiO_2 (110), there must first exist a means to efficiently and reproducibly acquire a surface that is free of any contamination on the atomic level. Ion bombardment with argon, annealing at high temperatures, and oxygen plasma were all used as cleaning tools. Use of O_2 plasma produced long filaments extending from the terraces, perpendicular to the typical step edge. Annealing at 950º C in O_2 (PO_2 = 3.0×10^{-5} Torr) produced an unrecoverable surface with no visible steps. Auger electron spectroscopy (AES) was used to determine quantity and nature of contamination. Our largest contaminating element was carbon, and it was removed after only a few sputtering and annealing cycles. Curiously, there was never any signal from calcium, a commonly reported segregation impurity in TiO_2. It was found that annealing temperature played a more important role than annealing time. Higher temperatures led to a much faster regrowth of terraces and steps than longer annealing times. Temperatures of 1340º C and above produce a (1×2) reconstruction of the surface. Most interesting was acquisition of an image with a scanning tunneling microscope (STM) using a negative sample bias voltage. Clusters on the image, thought to be electronic effects caused by oxygen vacancies, appear similar in size, shape, and number to those on an STM image taken with a positive sample bias voltage. Future work will focus on STM studies of the adsorption of NO and CuO molecules on the surface of TiO_2.

Effects of pH and Saturation State on the Dissolution Kinetics of a Nepheline Glass Formulation, $Na_3Al_4Si_4O_{16}$. *LUNDE REED (Sacramento City College, Sacramento, CA 95823) ERIC M. PIERCE (Pacific Northwest National Laboratory, Richland, WA 99352).* Borosilicate glass has been proposed as a primary waste form candidate for the immobilization of high and low activity waste left over from nuclear material production by the Department of Energy. Achieving the near permanent, safe containment and disposal of these materials requires an understanding of the environmental factors which affect the reaction kinetics of glass. Three key environmental factors that affect glass dissolution are pH, temperature, and the solution composition in contact with the glass. The effect of these factors on alkali-ion exchange (IEX) and matrix dissolution, two processes which govern glass dissolution, were investigated using the single-pass-flow-through (SPFT) apparatus. The SPFT apparatus allows the transfer of fresh influent solution from a reservoir bottle into a Teflon reactor, where the influent solution contacts the mineral or glass of interest (e.g., nepheline glass), and finally into a sample collection vial. To investigate the effects of specific conditions on nepheline glass dissolution, several experiments were conducted as a function of pH, from 7 to 12, and at 40°C. Results show typical glass behavior where the dissolution rate increases with an increase in the solution pH from neutral to alkaline. Although this trend is typical for glasses, results from geochemical modeling suggest the solution saturation state may have altered the measured dissolution rates. These results highlight the importance of pH and solution saturation state on glass dissolution.

The Partial Oxidation of Isobutene on TiO_2(110). *MATTHEW ROBBINS (The University of Texas, Austin, TX 78712) MICHAEL HENDERSON (Pacific Northwest National Laboratory, Richland, WA 99352).* General techniques for the direct partial oxidation of alkenes by molecular oxygen are a goal for surface science and catalysis research as they may lead to more efficient and environmentally-friendly industrial processes. In order to better understand the thermal and photoactivated surface chemistry of metal oxides toward alkene partial oxidation, the interactions of isobutene on TiO_2 (110) were studied using temperature programmed desorption mass spectrometry (TPD). Isobutene was found to adsorb and desorb molecularly below 200 K on the clean titania surface. With exposure to oxygen (> 1000 L) and unknown quanitities of water (< 10 L), isobutene monolayers were found to react on TiO_2 to form partial oxidation products which may include methacrolein, isobutyraldehyde and dimethylketene. This family of products points to a common 2,2 dimethyloxirane surface intermediate. This same oxirane intermediate has been proposed in theoretical studies of gas phase isobutene oxidation. This work supports the usefulness of the TiO_2 (110) substrate for further studies of alkene partial oxidation both independently and as a support material for transition metals or metal oxides more active towards alkene oxidation.

Measuring the Specific Activity of ^{18}F-Fluoride Ion Used for Radiopharmaceuticals In Positron Emission Tomography (PET) Scans. *ROBERT SALAZAR (California State University Fresno, Fresno, CA 93740) JIM P. O'NEIL (Lawrence Berkeley National Laboratory, Berkley, CA 94720).* High specific activity (radioactivity of an isotope per unit mass of the stable isotope of a stated element) of radioactive ^{18}F-Fluoride ion (^{18}F-, t½=110min.) is desired to produce radiotracers for PET scans. However, the amount of naturally occurring ^{19}F- that is contained in the ^{18}F- "target water" lowers the specific activity of the 18F- solution. A method designed to measure the amount of ^{19}F- in a decayed ^{18}F- solution is necessary to determine the initial specific activity. In a decayed ^{18}F- solution, ^{19}F- can be measured by using a Fluoride ion selective electrode (ISE). A calibration curve, ranging from 1ppm to 0.1ppm, was made by measuring the electric potential (in mV) versus the log of known ^{19}F- concentrations. An expanded range of concentrations, from 0.1ppm to 0.04ppm, was made to test the lower limits of the Fluoride ISE. The concentration of ^{19}F- in any solution may be determined by measuring the electric potential using the Fluoride ISE and the standard calibration curve. Establishing a process to determine the specific activity of ^{18}F-, will help future procedures aimed at finding sources of unwanted of ^{19}F-.

Comparison of Heavy-Duty Diesel Engine Emissions Testing at High and Low Altitudes. *MATTHEW SCHMITT (Central Washington University, Ellensburg, WA 98926) CHRIS TENNANT (National Renewable Energy Laboratory, Golden, CO 89401).* The ability to measure heavy-duty engine emissions at both high- and low-altitude conditions in one location is a primary goal for the National Renewable Energy Laboratory's ReFUEL laboratory in Denver, Colorado. Engine testing is accomplished using a DC-electric dynamometer with electronic controls and a sophisticated emissions measurement system. The air-to-fuel ratio is one of the major factors affecting emissions formation, and altitude can affect that ratio because of lower air density at higher altitudes. Previously, an engine would have to be tested at a high-altitude lab and at a lab at sea level to quantify the effect of significantly different atmospheric conditions due to altitude. By supplying pressurized air at the engine intake and increasing the back-pressure on the exhaust accordingly, we can accurately simulate lower altitudes from a mile-high location. This was accomplished using an altitude simulation system developed during this project that features a centrifugal blower (30 hp, 1000 cfm), a heat exchanger to maintain cool air intake conditions, and butterfly valves for pressure control. The emissions of a 2002 Cummins ISB 5.9 L engine were measured at both 5280 ft in altitude and simulated sea level conditions. The two types of regulated emissions of greatest interest for diesel engines are oxides of nitrogen (NOx) and particulate matter (PM) because they are the leading components of air pollution. Emissions data were collected at three different engine settings at each altitude to evaluate levels of PM and NOx using low-sulfur diesel fuel. A tendency for PM to increase and NOx to decrease was noted at higher altitude under full load conditions.

Electrochemical Investigation of Zirconium 4 Nuclear Cladding in ACR-700 Water Between 25° - 94° Celsius. *BRYAN SMITH (Salt Lake Community College, West Valley City, UT 84118) J H PARK (Argonne National Laboratory, Argonne, IL 60439).* Current electrochemical studies of Zirconium 4 alloy are taking place to be used in the CANDU (CANada Deuterium Uranium) reactor. The water used in these reactors is known as ACR-700 water, which has specific properties. Due to the high temperatures and pressure found in nuclear reactors the properties of Zirconium need to be studied so that the Zirconium cladding around the Uranium can keep it from containing the water which is used to create energy from steam. By using electrochemistry to coat and strengthen the Zirconium cladding we can prolong the life and efficiency of the CANDU reactors. Future work involving other scientists and more time to gather data will look at higher temperatures and pressures of this Zirconium cladding.

Studies of Solution Deposited Cerium Oxide Films on Textured Ni-Alloy Substrates for YBCO Superconductor. *ERIN STEWART (Indiana University of Pennsylvania, Indiana, PA 15701) M. P. PARANTHAMAN (Oak Ridge National Laboratory, Oak Ridge, TN 37831).* Cerium oxide, (CeO_2), buffer layers play an important role for the development of $YBa_2Cu_3O_{7-x}$, (YBCO) based superconducting tapes through the RABiTS (Rolling Assisted Biaxially Textured Substrates) approach developed at ORNL. Metal organic decomposition (MOD) approach has been used to grow epitaxial CeO_2 films on the textured Ni-W alloy substrates using various starting precursors of Cerium. Precursors such as Cerium acetate, Cerium acetylacetonate, Cerium 2-ethylhexanoate, Cerium nitrate, and Cerium trifluoroacetate were prepared in suitable solvents. The optimum synthesis conditions for these Cerium precursors were an Ar-4%H_2 atmosphere, concentration levels of 0.2-0.5M, a dwell time of 15 minutes, and a process temperature range of 1050-1150°C. X-ray diffraction, texture measurements, SEM (scanning electron microscopy), and optical microscope were used to characterize the CeO_2 films. This study has successfully demonstrated the growth of

textured CeO_2 layers on Ni-W substrates using Cerium acetate, Cerium acetylacetonate and Cerium nitrate as starting precursors. Results obtained on these textured CeO_2 layers will be presented.

Development of Passive Samplers for Automated Nicotine Measurement. *ELIZABETH STEWART (University of California, Los Angeles, Los Angeles, CA 90024) LARA GUNDEL (Lawrence Berkeley National Laboratory, Berkley, CA 94720).* A passive sampling device for Environmental Tabacco Smoke (ETS) was developed and tested for retention of nicotine and 3-ethenylpyridine vapor. Passive sampling is preferred because it requires no energy and is small. The devices will be placed into the households of participants in a smoking intervention program. Correlation will be made between the level of ETS exposure and the severity of the participants' children's asthma. Due to the complex nature of ETS and high basicity of nicotine, measurement of urine cotinine (a metabolic byproduct of nicotine) levels may not be an accurate measure of ETS exposure. The passive sampler will provide a more accurate measure of ETS exposure and prevent misclassification of the study participants. Several passive sampling approaches were tested. These included acid-coated quartz fiberglass filters, tenax-coated quartz fiberglass filters and tenax-filled thermal tubes. Passive samplers were exposed for 300 minutes in an environmental chamber while two cigarettes were smoked. The validated, standard method of active sampling using a tenax-filled thermal tube was employed concurrently for comparison. The passive tenax-filled thermal tubes most closely replicated the results of the standard method. Additional retention tests were performed to evaluate loss of semi volatile compounds. A significant amount of nicotine was lost when exposed to clean air for 28 hours meaning that shorter sampling intervals may need to be used. Loss was minimal when tubes were capped.

Comparative Study of Flat and Notched Barriers on a Langmuir Trough in Detecting Dipalmitoylphosphatidycholine Monolayers. *KRYSTYNA TATE (Alcorn State University, Alcorn State, MS 39096) BINHUA LIN (Argonne National Laboratory, Argonne, IL 60439).* Langmuir troughs are used to study compressed molecules that form monolayers which sit on the surface of water. The better the compression, the tighter the molecules will move closer together and make a smooth monolayer. The barrier is moved by a motor which makes the compression. The barrier's task is also to make sure as few molecules escape as possible and this is monitored by the pressure reading. With the use of a Langmuir trough and NIMA software version 5.16, this study compared a flat barrier that moved across the top of the surface of the trough and notched barrier that moved across and along the inside walls of the trough. The barriers were moved to compress molecules of dipalmitoylphosphatidycholine three times with three different amounts of water. After each trial the results were read from the software, recorded and recorded again after thirty minutes. Although the notched barrier was designed to help catch escaping molecules, the flat barrier showed better performance at keeping the molecules compressed. The trough can now perform more accurate tests with other materials such as diluted gold and can be used in performing x-ray beam tests of the compressed films.

Rapid Moisture Determination Method for Corn Stover Using Near Infrared Spectroscopy and Projection to Latent Structures Quantitative Analysis. *NGOC DUNG THANH (University of Colorado at Boulder, Boulder, CO 80309) BONNIE HAMES (National Renewable Energy Laboratory, Golden, CO 89401).* Moisture determination in corn stover feedstock is essential for identifying feedstock samples that require additional drying before analyzing with compositional Rapid Biomass Analysis (RA). RA is a method using a combination of near infrared (NIR) spectroscopy techniques and projection to latent structures (PLS) multivariate analysis to quantify the chemical composition of biomass. A rapid moisture determination method allows monitoring of the moisture content in biomass and detection of interference of water with the NIR/PLS analysis of the chemical composition. This equation was built with calibration corn stover samples taken at varying moisture levels. Validation tests reveal the equation predicts moisture values with a standard error of prediction of 2.4% relative to the measured values and has an excellent correlation. The capabilities of the equation may be expanded with different types or lots of corn stover feedstock.

Synthesis of Clays and Organo-Clays for Catalytic Applications. *ASHLEIGH THEBERGE (Williams College, Williamstown, MA 01267) KATHLEEN A. CARRADO (Argonne National Laboratory, Argonne, IL 60439).* Synthetic hectorite clays and organo-grafted hectorite clays offer a wide range of opportunities for the incorporation of chemical catalysts such as metal nanoclusters and organometallic compounds. Metal nanoclusters may be incorporated into interlayers or on clay surfaces. Catalytic activity of nanoclusters is dependent upon both size and location within the clay. Organometallic compounds may be covalently bonded to the interlayer of organo-clays grafted with functional groups that are spaced to accommodate the catalytic compound. This research focused on developing and evaluating methods for Pt loading and reduction in synthetic clays, with emphasis on determining the impact of varying the Pt salt and reduction method on nanocluster formation. In addition, procedures for the synthesis of inorganic-organic hybrid clays with varied degrees of interlayer functionalization were investigated. Pt was incorporated into synthetic hectorite clays via the incipient wetness (IW) method or during hydrothermal crystallization (HC) of the clay. Three different Pt salts were used with varying levels of success (cis-$Pt(NH_3)2Cl_2$, $Pt(NH_3)4(NO_3)2$, and $Pt(NH_3)4Cl_2$). In some cases, HC caused in situ reduction of the metal concurrent with clay crystallization. The products of IW were subsequently exposed to a reducing atmosphere (H_2 in N_2 at 80-95ºC) to reduce the Pt(II) salt to Pt(0). Products were characterized by X-ray diffraction (XRD) to determine crystallinity of the clay as well as the Pt(0) particle size via the Scherrer equation. In some cases, the latter values were confirmed by transmission electron microscopy. For example, one cis-Pt-clay reduced in H2 showed both rafts (primarily 1.5-2 nm in width and 10 nm in length) and spherical particles (approximately 2.5 nm in diameter) with some polydispersity. Metal loadings were in the 1-2.4 wt% range. Regarding the organo-grafted clays, various ratios of phenyltriethoxysilane and tetraethylorthosilicate were employed to create clays with different levels of organic (in this case, phenyl) loading. XRD was used to confirm crystallinity and thermal gravimetric analysis was used to determine the level of organic incorporation (8.4-29.6 wt%). Major contributions of this research include the development of a novel Pt(II) reduction method involving in situ reduction during clay HC, evaluation of various techniques for Pt loading, and successful variation of organic grafting levels in the organo-clays.

Odor Sample Concentration to Enhance Electronic Nose Performance. *CARRIE THOMAS (Michigan State University, East Lansing, MI 48864) JOHN F. SCHNEIDER (Argonne National Laboratory, Argonne, IL 60439).* In many cases, electronic nose technology is not sufficiently sensitive to characterize odors in the environment. In order to enhance detection, a novel and highly versatile analytical system featuring the Cyranose electronic nose and Airsense EDU has been utilized to detect and identify diverse analytes, ranging from pure solvents to simple organics to common grocery products. The Cyranose has already proven extremely effective in identifying the smell prints of many such analytes; coupling this instrument to the Airsense EDU greatly increases overall sensitivity and, therefore, its detecting abilities and possible real-world applications. Important considerations for this system such as proper methodizing and parameters, as well as sensitivity and detection limits, have been explored and will be presented. It is expected that the ability of the coupled Cyranose and Airsense EDU to identify and catalogue unique "smell prints" of analytes will dictate many practical and pertinent future applications for this emerging characterization technique.

Adsorption of the Perrhenate Analog Perchlorate on Activated Carbon at Different pHs. *QUYEN TRUONG (Contra Costa College, San Pablo, CA 94806) WAYNE LUKENS (Lawrence Berkeley National Laboratory, Berkley, CA 94720).* Perchlorate (ClO^{4-}) contamination of ground and surface waters has placed drinking water supplies at risk in communities throughout the US. Several major assessment studies of that risk in terms of health were released by the U.S. Environmental Protection Agency in early 2004. This contamination results from perchlorate salts that are primarily from the manufacture of rocket motor. Due to the perchlorate anion's fundamental physical and chemical nature, the contamination is difficult to treat or remediate. Activated carbon has some properties that can be used to address perchlorate contamination. Many studies have shown that activated can adsorb pertechnetate ion (TcO^{4-}) in HNO_3 solution. Since TcO^{4-} and ClO^{4-} have similar sizes and the same charge, they can be expected to behave similar with regards to ion exchange. Perrhenate (ReO^{4-}) is an analog for perchlorate. Cationic functional groups on activated carbon were identified for adsorption of anions. With respect to anion exchange, the major nitrogen functional group in AC is pyridinic and the important oxygen functional group is pyridonic. When the surface of activated carbon was examined by NEXAFS at different pHs, the spectra show that oxygen functional groups do not appear to be responsible for anionic exchange. This also was supported by the studied of pH-metric titration and the distribution coefficient of perrhenate absorption. The perrhenate adsorption isotherm at pH 2 of activated carbon shows that the number of exchange sites is 0.25 meq per g with a high affinity for perrhenate.

Analytical Technique Development for Determination of Chemical Warfare Exposure. *ELSBETH WICHERN (Colorado State University, Ft. Collins, CO 80523) JAMES A. CAMPBELL (Pacific Northwest Na-*

tional Laboratory, Richland, WA 99352). In the modern world, the threat of exposure to chemical warfare agents is growing. Along with this emerging threat, there are many new varieties of exposure testing devices being explored. Currently, the best way to test for exposure is by acquiring a blood sample from an exposed subject. Analysis of a blood sample takes days and many lab materials are needed to analyze the sample. The testing of blood is also expensive and results take days. If it were possible to test exposure through a person's saliva, results would be quick, inexpensive and few lab supplies would be needed. This research aims to develop a technique using saliva as a non-invasive matrix to test for exposure to chemical warfare agents. By using dibutylphosphate (DBP), a chemical similar in structure to the chemical warfare simulant diisopropylflurophosphate (DFP), which is similar in structure to sarin. A technique is being developed using saliva to test for exposure to DBP, DFP, and eventually sarin. Samples of blood and saliva were spiked with DBP. DBP was then isolated, derivatized, and subsequently analyzed by gas chromatography/mass spectrometry (GC/MS). Preliminary results indicate that DBP can be recovered from both blood and saliva. These developed procedures for DBP will then be applied to DFP in blood and saliva. If DFP is also quantatively recovered from these biological matrices, saliva may have the potential for being used as a non-invasive biomonitoring matrix to indicate exposure to chemical warfare agents. Future research will hopefully develop a device allowing people in the field to simply spit on a hand-held detector and determine, quickly and inexpensively, if they have been exposed to a chemical warfare agent, pesticide, or other chemical.

Study of Ion Mobility Spectrometry with Resistive Glass Channel. *SHUO YU (Vanderbilt University, Nashville, TN 37235) JUN XU (Oak Ridge National Laboratory, Oak Ridge, TN 37831).* As the world becomes increasingly more aware of the severity of global terrorism, ion mobility spectrometry (IMS) has become a useful tool for detecting explosives, drugs, and chemical weapons. An IMS instrument generates ions from a sample using pulse discharge ionization and separates ions in a drift channel. The identity of the sample, such as TNT explosive, can be determined by measuring the mobility of the ions through the drift tube. Profound progress has been made in recent years in the miniaturization of such instruments, compacting the IMS device for ease of mobility. In a conventional ion mobility spectrometer, a drift channel consists of electrodes separated by insulating spacers and connected with resistors. In order to miniaturize such an instrument, it is desirable to combine all electrodes, spacers, and resistors as one piece. The objective of this project is to use a resistive glass channel to achieve exactly this. Resistive glass with open channels was used as ion drift channels. The initial procedures include: designing an instrument with a pulse discharge ion source, housing the resistive glass tube, and implementing a Faraday-cup detector. The dimensions for the finished results are 2.5 in. x 1.0 in. x 0.5 in., showcasing a sleek pocket-sized instrument. The design of the housing, tube mounts, insulators, and spacers was accomplished using the computer program AutoCAD©. Simulations to calculate ion trajectories and contour lines of potentials were performed using codes from the computer simulation program SIMION. The simulations, in absence of a buffer gas, show that the drift tube exhibits a linear decreasing potential with a sufficient amount of ions reaching the detector within milliseconds. Simulation suggests that the detector is feasible for detecting ions. Preliminary tests show that discharge ionization occurred when a pulsed potential that is above the discharge threshold was applied between the tip and the target electrode. The new detector will continue to be tested by measuring mobility spectra of reactant ion peaks (RIP) as a function of drift field and by characterizing time resolution. Future work for the project includes testing resistive glass for accuracy and reliability as a drift channel for miniature IMS. During the course of the project, participation at the 13th International Conference on IMS allowed for great opportunities to learn from and discuss with scientists from around the world.

Study of Charge Transfer Across TiO_2/Dopamine/DNA Triad System Through Silver Metal Deposition-Probing DNA Recognition. *LIU ZHAO (Pasadena City College, Pasadena, CA 91106) TIJANA RAJH (Argonne National Laboratory, Argonne, IL 60439).* Bioinorganic hybrid nanocomposites that bind TiO_2 nanoparticles with DNA oligonucleotides through bridging chemical enediol, such as dopamine, were developed. Upon illumination, ground state electrons of dopamine were excited directly into the conduction band of TiO_2 semiconductors, achieving extended electron/hole charge separation. Light-induced charge separation across the nanocrytalline-DNA interface can be manipulated to fingerprint DNA oligonucleotide hybridization and sequence. The characteristics (hybridization, sequence, and mismatch) of DNA linked with nanoparticles determine the charge separation and determine the behavior of the triad system. The triad system can be coupled with a redox chemical reaction, e.g. $Ag^+ + e^- \rightarrow Ag^0$, at the nanoparticle surface or incorporated into a circuit. By measuring the amount of silver deposition or the magnitude of electric current, we can obtain the information about the hybridization or/and the sequence of the DNA oligonuleotide linked to the system. This triad system (TiO_2-dopamine-DNA) is a promising route for rational design of electrochemical devices that sensor DNA hybridization and/or sequence DNA oligonucleotides. In this paper, we reported the study of the effects of charge transfer and hole transport across the TiO_2-dopamine-DNA triad system through silver metal deposition. The immobilization of TiO_2 on conductive support and the technique to calculate the thickness of the nanoparticle films were discussed as well.

COMPUTER SCIENCE

Software Development in Visual Basic 6.0 to Interface with a Low Cost Control System for an Ion Mass Spectrometer. *LUIS ACEVES (University of California Los Angeles, Los Angeles, CA 90025) MICHAEL ALEXANDER (Pacific Northwest National Laboratory, Richland, WA 99352).* Commercial ion mass spectrometers (IMS) range from $60,000 to $200,000 and typically built for a single application. With National Instruments (NI) off-the-shelf component cards and software developed using Microsoft's Visual Basic 6.0, we have been designing a control system platform that can be easily modified and tailored to do various types of research. This control system would be fairly low cost ($15,000 - $20,000) in comparison to commercially developed systems. The control system will be communicating with a Teledyne (IMS) that provides real-time data acquisition and analysis tools, to assist researchers in the areas of chemical ionization techniques, atmospheric chemistry, materials science, biology and many more. Our teams' project focused on the development of the software modules, programming several algorithms that aid in the data acquisition, data storage, data viewing and instrument calibration for the new control system.

An Implementation of the BLMVM Algorithm for General Use. *JIM ADDUCI (Illinois Institute of Technology, Chicago, IL 60616) STEVEN BENSON (Argonne National Laboratory, Argonne, IL 60439).* Bound constrained optimization problems have long been studied and a variety of efficient algorithms have been developed for their solution. Many of these algorithms, however, depend on second derivative information which is not always available. Because it does not require evaluation of the Hessian matrix, the BLMVM algorithm has found particular use in the solution of bound constrained optimization problems in which the Hessian matrix is too large, or computationally difficult to evaluate. In implementing the BLMVM algorithm for general use, a variety of interfaces for the solver were explored. Support was implemented for the input of function, gradient, and convergence information as C functions, Fortran routines, and Python scripts. Also, the use of automatic differentiation for the generation of gradient information was implemented using Adifor 2.0. Drivers were written to test BLMVM on several well known sets of test problems. Specifically, the Minpack-2 test suite and the CUTE problems were solved and the corresponding performance data was recorded. For demonstrative purposes, several sample problems were implemented for each interface developed.

Evaluating Geospatial Datasets and Geocoding Error. *STEVE AHRENS (University of Tennessee, Knoxville, TN 37996) BUDHENDRA BHADURI (Oak Ridge National Laboratory, Oak Ridge, TN 37831).* The Geographic Information Science and Technology Group at Oak Ridge National Laboratory is currently producing LandScan USA, which models the actual spatial distribution of both daytime and nighttime populations. Analysis of the LandScan USA daytime distribution along with comparison between the daytime and nighttime population allows a host of statistical and planning analyses to be made, including exposure/health risk assessment, urban sprawl estimation, and estimating populations at risk from natural and anthropogenic disasters. A time-dependant occupancy probability coefficient derived for each spatial unit is combined with an occupancy estimate for that area to arrive at a population for that area for a given time. High-resolution aerial photography, land cover/land use data, and data from or derived from various census, transportation, or housing datasets are the primary input data sources. Of particular usefulness are the locations of buildings with predictable usage patterns such as prisons, schools, or hotels. For hotels in the Boston, MA area, a list was generated from searches of online hotel portals and the resultant addresses located on a road network dataset produced by Geographic Data Technology (GDT) through a process known as geocoding. Ease of list generation and the accuracy of the geocoded locations were assessed by comparing the digital model generated to aerial photography of the area. It was shown possible to construct a list of properties from public sources, and the geocoded

locations of these properties in the digital model produced indicated an average disparity of 405 ft. from the actual ground-truth verified for 27 of the 121 Boston area hotels. Two of the hotels exhibited error in excess of 1000ft.; both were due to limitations of the road network data used. The other 25 properties exhibited an average error of a mere 131ft. Errors introduced by the assumptions made by the geocoding process are dwarfed by those that result from limitations in the road network. As no single dataset is perfect, each much be evaluated in the context of the needs of a particular application. It may be necessary to supplement the best spatial dataset for project with a non-spatial data source as well, such as the hotel databases searched.

Parallelization of an N-body Simulator Code Using the Message Passing Interface (MPI). *BASSAM ALDHAFARI (Contra Costa Community College, San Pablo, CA 94806) CHARLES VERBOOM (Lawrence Berkeley National Laboratory, Berkley, CA 94720).* The project pursued is a computer programming effort, completed with a C++ code that simulates the N-body problem. A starter code of the N-body problem written by Pict Hut and Jun Makino is changed in such a way that it can be compiled and executed on a cluster of Pentium 4 processors. After a series of code transformations the code was parallelized using the Message Passing Interface (MPI) and then run on a cluster containing up to seven processors. The processing time of running the original code on a single processor and that running the parallelized code on the cluster is recorded and compared for performance.

Toolkit for the Analysis of Gridded Data in Curvilinear Coordinates and Spatial Statistics. *ROBERT ALTMILLER (California State University Bakersfield, Bakersfield, CA 93311) JAY LARSON (Argonne National Laboratory, Argonne, IL 60439).* We have been developing a parallel toolkit in Fortran 90/95 that performs two-dimensional spatial data statistical polishing. The statistical polishing methods being used are mean and median polishing on a two-dimensional logically Cartesian grid. Sea level pressure fields and global temperature is used to test the product and effectiveness of the module. The data being used to test the product is a twenty year sea level pressure climatology (1979-1998) from the NCEP/DOE AMIP-II Reanalysis data (http://wesley.wwb.noaa.gov/reanalysis2). The toolkit now has the capability to do spatially-weighted statistical polishing, with the spatial weights proportional to the cell area surrounding a grid point. This is done to avoid bias resulting from the large density of grid points at high latitudes. This weighted polishing technique is important because it allows us to separate spatial scales: the large scale effects as embodied by the row (longitude), column (latitude), and all (global) effects, and small scale effects in the two-dimensional residue field. This data is collected in the form of an augmented M x N matrix with M+1 rows and N+1 columns where M and N are integers. Missing spatial data is also accounted for using an estimation equation. The large scale effect is graphed using four dimensional graphing utilities called Grid Analysis and Display System (GRADS) and the Graphing, Advanced Computation and Exploration of Data (GRACE). From these graphs we interpret how the structure of the sea level pressure field is affected by large scale effects versus local surface topography effects. We also compare this technique with the standard technique of Zonal Eddy Statistics.

A LaTeX Driver for the FreeHEP VectorGraphics Framework. *ANDRE BACH (Reed College, Portland, OR 97202) MARK DONSZELMANN (Stanford Linear Accelerator Center, Stanford, CA 94025).* The FreeHEP library is the ongoing project of an open source collaboration to create and share Java code in high energy physics and other fields. One component of FreeHEP is the VectorGraphics framework, which enables the export of graphics to a wide variety of formats beyond Java's basic capabilities. This paper describes an addition to VectorGraphics, a driver for the LaTeX PSTricks package. LaTeX is a markup language in wide use by physicists and others for producing academic papers for publication. PSTricks is an extension of LaTeX that provides PostScript macros allowing complicated vector graphics to be written directly into LaTeX code. The ability to export graphics directly to a LaTeX native format will ease their inclusion into such documents. The context of FreeHEP and VectorGraphics into which this driver fits is described. All the main functionality of the driver is in place, but some limitations remain. Some details of its construction, as well as outstanding problems, are addressed.

Upgrading the Graphical User Interface and Computer Hardware for the Digital Radiation Monitoring System (DRMS) in the Advanced Test Reactor Using LabVIEW Programming Language. *CHRIS BALMFORTH (Brigham Young University - Idaho, Rexburg, ID 83440) RUSS GOLD (Idaho National Engineering & Environmental Laboratory, Idaho Falls, ID 83415).* The DRMS system provides Radiation Control Technicians and Reactor Operators with real-time data to monitor radiation, particulate, iodine and noble gas levels in the building that contains the reactor. This data is critical as it serves to ensure that the work environment is safe for all employees. The DRMS system receives data from as many as 26 Data Control Modules (DCM) that contain Continuous Air Monitors (CAM) and Radiation Area Monitors (RAM). The DCM acquires continuous data from the CAMs and RAMs, which must be gathered by the Radiation Control Unit (RCU). The graphical user interface (GUI) must be in constant communication with all active DCMs to be able to monitor radiation levels throughout the plant and present current information. Part of the difficulty in creating the program is that the system must be able to handle all of the communications with the DCMs and keep the GUI current at the same time that the system operators access the system to display reports and adjust settings at the DCMs. The current system utilizes two specialized independent computers that pass data back and forth to perform its required tasks. These computers will be replaced with a single standard workstation PC that will perform all of the current functions but will do so with much greater speed. This will enhance the effectiveness of the DRMS system.

Runnning the Linpack Benchmark on a Commodity Cluster. *ADAM BARLEV (Contra Costa College, San Pablo, CA 94806) CHARLES VERBOOM (Lawrence Berkeley National Laboratory, Berkley, CA 94720).* The primary goal of the project was to achieve as high a rating as possible on the Highly Parallel LINPACK (HPL) Benchmark on a Linux cluster. The secondary goal was to look at some of the factors that affected the performance of Linux clusters. The HPL is the test that determines placement on the top 500 supercomputers list. I hypothesized that the network bandwidth would be the limiting factor as we added more nodes. The FlashMobComputing bootable cluster CD was used as a platform to perform the test. The highest rating achieved was 9.233 gflop/s on 12 nodes. This is a successful application of the same methods used on computers on the top 500 list. The network bandwidth proved to have little effect at the number of processors used. The results of these tests will give users of commodity Linux clusters a rough estimate of the performance of highly parallel applications.

Development of Interactive Physics Analysis Tools for Atlas in Python. *JEROME BARNES (Borough of Manhattan Community College, New York, NY 10007) KÉTÉVI A. ASSAMAGAN (Brookhaven National Laboratory, Upton, NY 11973).* Atlas is a project that is a worldwide initiative to build a sub atomic particle detector, which will try to track and detect new particles, such as the Higgs Boson and other super symmetric particles. Python is an interpreted, interactive, object-oriented computer programming language often compared to Perl, or Java. The main focus of my research is to develop interactive analysis tools to analyze and translate the data produced by the atlas detector. Python program code closely resembles the program code used in other languages like C and C++ and Root but does not require the high level of syntax of these languages. This allows us to produce an environment that easy to interact with. Python also has the ability to accept data from other languages like C++ and Root using extensions to the environment called PYLCGDICT and PYROOT. The Physics Interface (PI) is a group of algorithms that claim to add greater functionality to the Python environment. The PI claim's to be able to aid python in analyzing data collected by the particle detector. PI accepts data from other languages for example Root and translates it into a graphic representation, a histogram in Python. The goal of utilizing the Physics Interface is to produce an unbinned histogram. An unbinned histogram is a histogram where the ranges (or intervals on the X axis aren't set) and the number of bins are not predefined. PI's promised ability to do these things is very important to us and Atlas because it allows us to take the data from the Atlas detector and look for specific periods or occurrences of decay and to produce graphical representation of data collected by the atlas detector.

Improving Data Maintenance with Computer Software. *JUSTIN BECKER (University of New Mexico, Albuquerque, NM 87131) NANCY STEWART (Argonne National Laboratory, Argonne, IL 60439).* Data entry is a major issue in many scientific facilities because it involves a great deal of time and effort if the proper tools are not employed. This is the problem the TSD (Treatment, Storage, and Disposal) department at Argonne National Lab West (ANL-W) encountered when one of its major facilities (the Radioactive Scrap and Waste Facility) accumulated too much data to manage without computerized aid. In order to reconcile this problem a data entry application was designed and created using Microsoft's Visual Basic .NET development tools. Using Visual Basic's RAD (Rapid Application Development) approach to computer programming, the project was off the ground in a few weeks and usable in a few more. Among the methods used to ease the burden of computer programming was the object oriented model, which greatly enhanced

the ease of modifying computer code to fix certain problems. Ultimately the application was brought to a usable and error-free point and then distributed to a few individuals for continued testing. My project manager will continue to refine this application and will eventually distribute it to numerous departments across Argonne National Lab West.

CrySis: Fusing Neural Network Intelligence with the LoMAD Peak Finding. *ALEC BERNTSON (Cornell University, Ithaca, NY 14853) VIVIAN STOJANOFF (Brookhaven National Laboratory, Upton, NY 11973).* High-throughput protein crystallography requires the automation of multiple steps used in the protein structure determination. The first step involves locating and refining the centroids of the Bragg Peaks from a given diffraction pattern. Simple as this task may seem to the human eye, automatic peak finding is a highly non-trivial task for a computer. Difficulties arise due to varying degrees of exposure, contrast differences and background noise. The LoMAD (Local Maxima Analysis of Diffractions) algorithm was developed to offer robust performance over a wide variety of diffraction images and is completely automatic. LoMAD refines peaks and accurately locates and removes ice rings and double peaks from data. LoMAD's performance is comparable with commercial peak finding applications such as DENZO and will be included in the CrySis software package.

Security Log Analysis to Reduce False Positives and Increase True Positives. *WESLEY BLAND (Tennessee Technological University, Cookeville, TN 38505) WALTER DYKAS (Oak Ridge National Laboratory, Oak Ridge, TN 37831).* The log files generated by a secure shell server are large and contain seemingly useless and confusing data. The programs currently in use to process this data have become outdated, causing the reports to be less useful and cumbersome for an administrator to review. In order to reduce the amount of information being presented and make it easier to quickly read and understand by an administrator, the reports must be efficient and concise. An analysis of the user's sessions was implemented that looked for the use of certain suspicious, common, and new commands for each user. Attempting to find commands individual users would always execute proved not to be useful because they would not remain constant enough to create a true list. The same problem occurred with the analysis of new commands. Searching for suspicious commands was more successful when tested against known hacks, but still generated some false positives because some users occasionally used these commands. These programs would be useful as a reference for someone who already suspects a user ID has been compromised, but due to the large number of false positives, it is not feasible to alert anyone of suspicious activity. Another method of searching for suspicious activity was profiling the source Internet Protocol (IP) address for each user by building a list of valid source IPs for each user and comparing new connections to that list. The program adapted to users who had dynamic IP addresses and could quickly add new IPs to a user's profile. It seemed to be very successful at removing false positives because of these features. To help present the newly generated data, a program called GraphViz was used to create visual representations. By automating this program, these reports can be more useful in allowing the administrators to quickly pinpoint suspicious activity. This method is especially helpful when analyzing source IP addresses. As a way to increase the success of the programs in the future, a method called Google Hacking was explored. Through this type of "hacking," vulnerabilities can be found on a website that expose important data such as login names, passwords, operating systems, and other sensitive information. The data discovered from this can be used to protect against future attacks as well as working towards removal from public view.

Tracking Potential Cyber Threats Through Pattern Recognition. *JANELLE BLOUNT (Borough of Manhattan Community College, New York, NY 10007) RICHARD CASELLA (Brookhaven National Laboratory, Upton, NY 11973).* The Cyber Security department protects against the access to classified data, unauthorized user resources, viruses, and personal data from being lost. One of the ways in which they protect their company is they collect log files from all of the machines especially the machines that allow communications from off-site. The volume of logs collected daily which makes it very difficult to manage log filters to search for interesting events that occur on the network. The purpose of my research is to develop a dynamic log-filtering program that does not depend on specific patterns of interesting events. This program will develop unique signatures of all log entries to aid in identifying interesting events without knowing ahead of time what they are.

Designing and Configuring a Database Driven Intranet Web Page for Network Authentication and Security. *CHERYL BROWN (Borough of Manhattan Community College, New York, NY 10007) PATRICIA WILLIAMS (Brookhaven National Laboratory, Upton, NY 11973).* The objective of this research paper is to apply practical theory of transitioning Microsoft (MS) Access Database forms to an Intranet Webpage. The program that was used to design BNL's EPSAFETYNET database website was Microsoft FrontPage 2000. There are many products for web design programs that can produce web pages without the user having to understand HTML. As a result of utilizing Microsoft FrontPage, the challenge was to create a professional full-featured web site, which required hand coding, design know-how, graphics experience, and in-depth knowledge of how the Internet works. In conjunction with developing a Microsoft FrontPage design, the procedures for configuring the webpage for Network Authentication and Security to these forms will be developed. The configuration for Network Authentication and Security is a method that is used to prevent unauthorized access to Brookhaven National Lab webpage. There are two ways to configure a Database Authentication: Access Database or an SQL Server Database as the back end for the network administrator's data access page. In this case, the Access Database was chosen for the encryption. For the greatest flexibility when using an Access database, the database should be secured by using user-level security. User-level security allows the network administrator to define different roles (called "groups" in the product documentation) with different levels of permissions. If this level of flexibility is not required, then a single database password is required to open the database.

NEESgrid Data Acquisition Tester and Labview Plugin. *JOSE CALDERON (University of California, Berkeley, Berkeley, CA 95632) PAUL HUBBARD (Argonne National Laboratory, Argonne, IL 60439).* Software needs to be tested so bugs can be found before is released and not after. Currently, under development there is a program writing in Java to test the reliability, correctness and usability of three NEESgrid software components, data acquisition (DAQ) system, a NEESgrid Streaming Data Server, and a NEESgrid Streaming Data Server driver. This paper explains to some extent what the DAQ tester does and how it works. The DAQ tester is only one of the components that will be implemented. So the current test suite only tests the data acquisition system. The DAQ tester has been completed in this term. This software was developed using Java. Two reasons for choosing Java is its portability and the Swing components to create graphic user interfaces (GUI). The DAQ tester tests all possible commands that the data acquisition understands and checks that it meets the protocols such as data format and time stamps. Because of its GUI one goal is to be very user friendly. Efforts have been made to accomplish this goal, such error handling and error recovery. The DAQ tester should not freeze because of bad design. A second project was the implementation of a Labview plugin. The Labview plugin (aka lvplugin) is a code plugin for the NEESGrid Teleoperations Control Program (NTCP) (PDF)4 server. The purpose and the applications of the plugin will be explained.

Visual Basic: The Past, Present, Future and its Potential Impact on the Economic Community. *KYLIE CANADAY (Indiana University, Bloomington, IN 60527) CRAIG HUBER (Argonne National Laboratory, Argonne, IL 60439).* Visual Basic is a programming language that enables the user to create endless applications within the Microsoft Windows package. This tool has been essential to numerous companies throughout various industries, allowing for the convergence of the Windows suite and a customized application instrument. While the language has been essential to growth in these industries, through the progression and demand for web-based programs, a new VB was born: Visual Basic .NET. This program allows for the development of applications for Windows along with the web. This latest tool has created a much more resourceful and practical programming tool for its users. In addition to its many uses, I plan on someday incorporating my visual basic knowledge to create a variety of economic tools. I believe that Visual Basic along with Visual Basic.NET will make the financing world more efficient and accurate by adapting to specific needs and requirements among financial institutions.

Creation of Geometric Calculator to Ease Computation of Thermal Heat Flux and Thermal Resistance of Whole Wall Areas. *BRETT CARMICHAEL (Pellissippi State Technical Community College, Knoxville, TN 37921) JAN KOSNY (Oak Ridge National Laboratory, Oak Ridge, TN 37831).* Thermal resistance of a wall area is used to calculate the flow of heat from one wall surface to another. Decreasing the flow of heat (either containing the heat in cold weather conditions, or keeping it out in warm weather conditions), becomes the main focus of a more energy efficient home. Vast amounts of research have been done within this area, but accurately accessing the proper information remains difficult. This is due to the widely varying composition of different details of wall technologies. Examples of these details include the construction material of the wall, the interior fill of the wall, and even the general shape of the wall foundation. Due to the lack of

commercial software which can adequately handle this task, creation of a user friendly computer application has become the focus of the research. Formation of this application began with an investigation into the compendium of programming languages available. The program requires a visually pleasing yet effective language, the ability to handle complicated engineering computations, the ability to communicate with a database, and also to be able to fully function over the internet. J# (pronounced J sharp), operating within the Microsoft .NET framework, was chosen for its ability to adhere to these requirements. The calculator begins by taking user input as to the type of wall system being used. This includes properties such as the structural material and the exterior lining of the wall. The program continues on to gather information about the building structure. Once all information about the particular building has been gathered, the calculations are made. All calculations are based on experiments done at Oak Ridge National Laboratory which have found the R Values for each detail in a particular wall technology. There are currently eighty five different wall technologies which have been logged and are available for use. These detail R Values reside in a database located on an ORNL server and will be continually updated as new research becomes available. The flexibility of the calculator to be updated and dynamically change with time makes it an invaluable tool to help calculate the energy efficiency of a building.

Collaborative Tools for Computational Biology. *RICO CARRELL (Governors State University, University Park, IL 60466) SOON-OK PARK (Argonne National Laboratory, Argonne, IL 60439).* Research in genomic and biological science has the promise of benefiting society. One goal of bioinformatics is to mine biological databases to identify genes and their encoded products that govern biological reactions. Systems biology research uses computer models to help understand the behavior of the biological processes. This summer there were two main objectives in the project; 1. Add the ability to connect to multiple databases simultaneously. 2. Add the ability to use multiple database technologies. We have achieved these goals during our research at Argonne National Laboratory. Previous ongoing research at Argonne National Laboratory has produced prototype tools to help build models. Kah is a framework for writing systems biology programs and the Model Editor is a graphical user interface (GUI), written in terms of Kah, that a scientist can use to build biochemical models. The previous KahDB was built with Oracle. This summer we have worked on extending Kah to easily utilize any database such as Oracle, Postgres and MySQL. We have engaged in creation and modification of programming code to actually load the biological data into multiple databases. Our project focused on developing a collaborative tool which would allow scientists the ability to connect multiple databases of same or different type simultaneously. We developed software to provided simultaneous access to multiple databases. Our research with building and collaboration of the project has created a foundation for the collaborative tools for computational biology.

The PHP and XML Web Compatible Batch DQR (Batch Data Quality Reports) Checking and Parsing of Text Formatted Data. *LONMAE CHU (SUNY-Suffolk County Community College, Brentwood, NY 11717) RICHARD WAGENER (Brookhaven National Laboratory, Upton, NY 11973).* There currently exists on the DOE-ARM (Department of Energy-Atmospheric Radiation Measurement) website, an application that users manually insert data for uploads. This existing program has virtually little checking in its algorithm. These DQRs are important for maintaining the data quality of the ARM GIS (Geographical Information System). There has been a need for multiple DQR submittals, or BatchDQRs, (composed of related or unrelated individual DQRs) to be checked and uploaded and when acceptable sent to a SYBASE database. The uploaded batch text file will be formatted and this is to be checked. There are proposals for a format similar to XML so it is to our advantage to migrate to XML. Two scripting languages, XML and PHP, are highly compatible with HTML, and will provide the tools for uploading, formatting, parsing, and checking the incoming BatchDQR text data to a Sybase Database and to an HTML screen. Either the formatting failures are determined and then listed or the acceptable formatted batch data is sent to the database and a note is displayed to the screen in HTML. Although the dataflow seems straightforward, designing without all the initial specifications intact invoked problems. The research was always trying to be one step ahead of the design part. We found an intact implementation of a hard core program was more important than the lure of researching more information to invoke more design changes. In this way we would have some programming substance to actually show and work on. The choices for this project had not been properly determined before the design was in place. Time was a determining factor proving that a practical approach was preferred over a theoretical approach. Whether the XML and PHP testing and parsing program will be proven as a valid beginning for the continuation of this project, will be seen as the future unfolds.

Dynamic Web Content System. *JONTHAN CHUGG (Idaho State University, Pocatello, ID 83209) SERA ERIN WHITE (Idaho National Engineering & Environmental Laboratory, Idaho Falls, ID 83415).* The Dynamic Web Content System (DWCS) was created for the Geospatial Science and Engineering Group (GeoSE) at the Idaho National Engineering and Environmental Laboratory (INEEL). The primary purpose for creating the DWCS was to decrease the cost and time involved in website management. The DWCS dynamically generates website content using Microsoft Access, Active Server Pages, HTML, and JavaScript. DWCS features include adding and changing menus, adding and changing images, and managing page text. The DWCS allows the user to modify existing content, add new content, as well as change the look and feel of the web page by editing the website's Cascading Style Sheets properties. The particular goals of the project included producing an easy-to-use web management tool that does not require the user to possess web programming skills and building the website dynamically every time it is accessed.

The Goals of System Remediation. *NICK CLEMENTE (Farmingdale State University, Farmingdale, NY 11735) FRANK QUARANT (Brookhaven National Laboratory, Upton, NY 11973).* In my short time here at Brookhaven National Laboratory, I have been working on the Windows system remediation project. This is perfect for me since my major is security systems and remediation primarily involves making computers secure. In order for a computer to be considered "remediated," the system must be completely current with system updates, be running all necessary anti-virus programs, and most importantly to have no high risk vulnerabilities. A high risk vulnerability is usually a result of an unnecessary service running on the system, such as FTP or Telnet, that creates an open port which an outside attacker can exploit. To evaluate high risk vulnerabilities, we at ITD use a program called Nessus. This is a security scanner that does a very thorough scan of a specified system by the IP address and produces detailed explanations as to what the vulnerability is and how to correct it. If there is no patch available then it is up to us to find an alternative solution to correct the problem, i.e., disabling the share on a folder or setting a password on a user account that doesn't have one. The good part is that some of these vulnerabilities can be avoided. It's really up to the user but it is nonetheless simple. All that needs to be done by the user is to install all necessary security updates provided by Microsoft. If you're running Windows 2000 or XP and have Microsoft Software Update Service installed a window will pop up on your icon tray in the lower right hand corner alerting you of updates and they will be installed automatically. This is the key to keeping your computer secure. Once all patches are applied and updates are installed then your machine has been remediated and will fall off of the "high risk" list.

Development of Efficient and Flexible Subroutines for an Ion Trap Mass Spectrometer Control System. *BRADLEY COFFMAN (University of Washington, Seattle, WA 98105) MICHAEL ALEXANDER (Pacific Northwest National Laboratory, Richland, WA 99352).* The focus of this paper is the development and implementation of algorithms used in an Ion Trap Mass Spectrometer (ITMS) control system. The system was recently developed by Dr. Michael Alexander, Kenneth Swanson, Derek Hopkins, and Michael Buschbach1, but lacked certain key functions including mass calibration, efficient data storage, and data analysis. Mass calibration was implemented using a graphical, user-friendly approach using moveable mass cursors. Data saving efficiency was increased by buffering input data in local memory before writing to the hard drive. Data analysis abilities added to the program include an algorithm for finding the baseline in a dynamic mass spectrum, and generating an accurate stick spectrum. These enhancements should increase the efficiency, functionality, and user-friendliness of the control system.

Documenting the Functionality of a Geographic Information System Based Dust Dispersion Modeling System. *DUARD CRANDALL (Brigham Young University - Idaho, Rexburg, ID 83440) FREDERICK RUTZ (Pacific Northwest National Laboratory, Richland, WA 99352).* Dust dispersion is an issue that affects both humans and the environment. As residential areas continue to develop around military testing sites, the effects military generated dust dispersion will have on civilians and the environment has become a growing concern. The effects that dust dispersion generated by military maneuvers may have on particulate air quality has become of particular concern. Civilians and military personal needed a possible solution that would enable the military to minimize the effects of dust dispersion and create dust mitigation strategies. It was under this pretense that a project supported by the Strategic Environmental Research and Development Program

(SERDP) of the Department of Defense was initiated to develop a dust dispersion modeling system for use by government sites. This modeling system would be integrated with a geographic information system (GIS) application to ensure usability. In doing so, the modeling system developed under the name DUSTRAN, would allow military personnel to generate near real time dust dispersion models by inputting data for a scenario into a user friendly interface for display on maps within a GIS application. This paper discusses the usability and functionality of the DUSTRAN user interface.

Normalizing the Data for the Advanced Photon Source/Experiment Facilities Division. *AUDREY DANCE (Elizabeth City State University, Elizabeth City, NC 27909) FRANCESCO DE CARLO (Argonne National Laboratory, Argonne, IL 60439).* Normalizing the data of the Experiment Facilities Division has helped to attain knowledge of the internal structures of materials. The tomographic experiments were conducted at the XOR Sector-2 beam line at Argonne National Laboratory (ANL). The experiments involve objects of study from the material science point of view. In each experiment, a parallel beam of x-rays are sent through experimental objects. As these rays pass through, the object absorbs the rays at varying degrees. These rays are received by the detector camera which records the intensity of received rays. The initial intensity is 4095, which represents no absorption. Zero represents complete absorption of the x-rays. The absorption is recorded in a computer file in Hierarchical Data Format (HDF). The data in the HDF file is used to form a grey scale image showing the absorption of the experimental object. We found that there is absorption in the non-image portion. To get absorption of the object alone, the absorption due to experimental conditions is to be removed. This process is known as normalization of the data. A C++ program was written to perform the normalization.

From Chaos to Content: An Integrated Approach to Government Web Sites. *NORA DEMUTH (El Camino College, Torrance, CA 90505) CHRISTA KNUDSON (Pacific Northwest National Laboratory, Richland, WA 99352).* The web development team of the Environmental Technology Directorate (ETD) at the U.S. Department of Energy's Pacific Northwest National Laboratory (PNNL) redesigned the ETD website as a database-driven system, powered by the newly designed ETD Common Information System (ETD-CIS). The ETD website was redesigned in response to an analysis that showed the previous ETD websites were inefficient, costly, and lacking in a consistent focus. Redesigned and newly created websites based on a new ETD template provide a consistent image, meet or exceed accessibility standards, and are linked through a common database. The protocols used in developing the ETD website support integration of further organizational sites and facilitate internal use by staff and training on ETD website development and maintenance. Other PNNL organizations have approached the ETD web development team with an interest in applying the methods established by the ETD system. The ETD system protocol could potentially be used by other DOE laboratories to improve their website efficiency and content focus.

Pricing Optimization for Social Welfare: Algorithms and NP-Completeness. *ANDREW DRUCKER (Swarthmore College, Swarthmore, PA 19081) ROBERT VAN BUSKIRK (Lawrence Berkeley National Laboratory, Berkley, CA 94720).* This paper studies variations on the problem of pricing a set of substitute goods so as to maximize 'social welfare' defined by an additive utility function, subject to the constraint that net profits be nonnegative. The problem, which has applications in public policy and development, is found to vary in computational complexity depending on the model of consumer decision-making used. For a budget-based model of decision-making, an efficient algorithm is given; for a model in which consumers maximize the subjective 'surplus' or profit from their purchase, we show NP-completeness; finally, we outline an approach to solving the problem in its continuous limit, using calculus-based optimization.

Model and Simulation of Critical National Infrastructures Project. *JULIE DURTSCHI (Brigham Young University, Provo, UT 84602) DON DUDENHOEFFER (Idaho National Engineering & Environmental Laboratory, Idaho Falls, ID 83415).* The attacks of September 11, 2001, have focused concern upon the security and reliability of the nation's critical infrastructures, and their vulnerability to terrorist attacks, natural disasters, and cascading events. The Northeast Blackout of August 2003 further heightened concern in these areas. The focus of this project has been to develop a modeling and simulation tool which will provide end users the ability to identify an electrical network's critical nodes, predict the response of the system to events, map electrical components affected by outages, and visualize outage areas and affected systems. The Idaho National Engineering and Environmental Laboratory (INEEL) tool developed for this is called Critical Infrastructure Modeling System (CIMS). As a point of validation and in support of a Department of Energy (DOE) project, the power grid of the Idaho Nuclear Technology and Engineering Center (INTEC) was modeled. Data collection and design was the first phase of this project. Some of this data included coordinates, inputs, outputs, total capacity, and flow patterns. The second phase was application development and testing. The various modules for CIMS were written using C++, Visual Basic, VTK, FLTK, and Microsoft Access. Access was used to enter the data, then to create input files. 3D StudioMax was used to create 3D icons or infrastructure elements. The final and ongoing phase includes testing, debugging, code review, and data validation. There are different types of Modeling and Simulation (M&S) software tools that exist to model the critical and vulnerable pieces of the power infrastructure system. As a further point of validation, CIMS was compared to another M&S application, Smallworld-Interdependent Energy Infrastructure Simulation System (IEISS), developed by General Electric and Los Alamos National Laboratory. New technologies, such as CIMS, can help assure the long-term reliability and stability of the energy infrastructure, by providing decision makers and designers with insight into the complex interdependencies that exist between different infrastructures. On August 11, CIMS will be shown in St. Louis, Missouri. Representatives from DOE, Department of Homeland Security, and other state and federal agencies will be present to evaluate this tool.

Development of Customized Websites Utilizing ASP. *JEFFREY EASLEY (Norfolk State University, Norfolk, VA 23504) JESSICA WILKE (Brookhaven National Laboratory, Upton, NY 11973).* ASP, or Active Server Pages, is a Microsoft-based language found embedded in web pages. It was created out of the need for sites to produce dynamic content, including the need for database-driven websites. It can also be used to create templates, such as the ones used all over Brookhaven's websites. By creating templates, website design for anyone becomes faster and efficient, regardless of skill level. Using an asp include function, we can easily make sites with templates already created beforehand.

Collective Error Detection for MPI Collective Operations. *CHRISTOPHER FALZONE (Edinboro University of Pennsylvania, Edinboro, PA 16504) EWING LUSK (Argonne National Laboratory, Argonne, IL 60439).* An MPI profiling library is a standard mechanism for intercepting MPI calls by applications. Profiling libraries are so named because they are commonly used to gather performance data on MPI programs. Here we present a profiling library whose purpose is to detect user errors in the use of MPI's collective operations. While some errors can be detected locally (by a single process) other errors involving the consistency of arguments passed to MPI collective functions must be tested for in a collective fashion. While the idea of using such a profiling library does not originate here, we take the idea further than it has been taken before (we detect more errors) and offer an open-source library that can be used with any MPI implementation. We describe the tests carried out, some details of the implementation, illustrate the usage of the library, and present some performance tests.

Assessing the Current Residential Markets for a Water Heating Dehumidifier. *MATTHEW FIELDS (Trevecca Nazarene University, Nashville, TN 37210) MELISSA LAPSA (Oak Ridge National Laboratory, Oak Ridge, TN 37831).* A new a dual-service "water heating dehumidifier" (WHD) appliance is being developed at ORNL in collaboration with Western Carolina University, Asheville-Buncombe Technical Community College, American Carolina Stamping Company, and Clemson University. To understand the potential market for this technology a market assessment is being conducted. The purpose of this assessment is to study the extent to which the WHD will penetrate the residential market. The secondary purpose is to gather important feedback from potential supply chain partners and incorporate these findings into the design of the WHD technology. This collection of data will be used to judge market readiness as well as evaluate preferred consumer attributes into the design that will drive end-user demand for this product. In collaboration with a graduate student from Clemson University, research was conducted and discussions were held with eight representative supply chain sectors, including Builders, Contractors, End-Users, Manufacturers, Retailers, Advocates, Utilities, and Distributors. The data was then organized into a shared database and then evaluated. Research also included an analysis of the costs, benefits, and energy consumption of existing water heaters and dehumidifiers. After the evaluation, the data was summarized and incorporated into a draft market assessment report. The analysis showed that there is a potential need for this new technology in regions with high humidity, mainly in the Northwest, the Southwest, and some coastal areas. The technology should be marketed as a water heater with dehumidifying capability. Utilities and organizations that advocate energy-efficient technologies would benefit

most from energy savings and Energy Star ratings. The WHD technology should be inexpensive and priced in the range of existing technology. According to the analysis, the new technology should be easily understood, pay for itself after a short time, save energy, and produce cool dry air in the homes. Future evaluation will focus on the potential supply chain and consumer response to demonstrated reliability, ease of installation, low energy cost and dual-service capabilities.

Implementation of Constant Folding within xaifBooster for Open Automatic Differentiation. *PETER FINE (Rose-Hulman Institute of Technology, Terre Haute, IN 47803) JEAN UTKE (Argonne National Laboratory, Argonne, IL 60439).* Within the automatic differentiation (AD) community, there are very few people that employ constant folding as a way to reduce the size of the directed acyclic graphs that are used to compute the Jacobians of the program that the automatic differentiation is being applied. So since performing such an action will save run-time of AD. Performing Constant Folding is very useful, because runtimes can be several times the runtime of the function itself. On large codes that runtime might takes hours or days by itself, so anything that can reduce the total cost is beneficial.

Histograms and You: A Java Program for the Viewing of Ambient Data. *ANDREW FISHER (California State University Chico, Chico, CA 95929) VICTOR SERBO (Stanford Linear Accelerator Center, Stanford, CA 94025).* The BaBar detector system has a large number of sensors and data feeds, called ambient feeds. These feeds are vital to the operation and monitoring of the Pep rings and the BaBar system. In order to more easily monitor these systems a simple web interface to display graphical representations of the data is needed. Towards this end it was decided that using a Java Web Servlet (Sun Microsystems) would be an effective and simple way to achieve this effect. By combining Web Servlets with the Corba Technology (OMG) this provides a way for many people to access data from anywhere in the world. Using this type of program in conjunction with the HEP AIDA systems for graphing makes a powerful tool for the monitoring of the BaBar system. An overview of the BaBar system, and how the Ambient data is given. The uses and limitations of this method for viewing the data as well as examples of other ways to access the data and potential other uses for the servlet are also discussed.

Improving Output Readability and Functionality of the SCALE Software System Through the Use of Browser Supported Languages and Scripts. *AARON FLECKENSTEIN (Western Michigan University, Kalamazoo, MI 49093) BRADLEY REARDEN (Oak Ridge National Laboratory, Oak Ridge, TN 37831).* The Standardized Computer Analysis for Licensing Evaluation (SCALE) software system is used for nuclear safety analysis. KENO V.a is part of the SCALE software system and is a widely used Monte Carlo neutron transport program for nuclear criticality safety. Traditionally, SCALE produced a plain text output report of considerable length. This output had very limited plotting and formatting capabilities. All of the text was the same size and color, impairing the highlighting of important data. Tables were restricted to text forced to line up by using spaces, and precisely plotted output had to be created with special plotting software. Searching the document was tedious and time-consuming, and error and warning messages were scattered throughout the output. An interface was needed that would display the information in a convenient format for the user. The chosen solution was to display the code output in a web browser such that the user could browse though the data in a familiar web-type interface. The interface is the basic three-pane approach that is common to the Internet community. A scrollable, simplistic navigation system consisting of sorted, headed sections of links is located on the left edge of the screen, across from the main display area where the code output is presented in a colorful well-formatted manner. Above both is the title section that is updated to reflect the current information being displayed. Information is formatted to the user preferences such as link color, heading color, and data color. A descriptive table caption is centered below each table and is distinguished from the table data by border, font size, and italics. Precise plots are displayed in the documents through browser plug-ins, removing the need to open other software. An improved message system collects the messages and displays them together in one place. The interface creation is a dynamic process that adds or removes features dependent on the input passed to the SCALE software. The creation occurs inside of the normal progression of the SCALE software without the need for user interaction. This interface was chosen for its ease of use, its familiarity to a common Internet user, and because the need for additional software has been kept to a minimum. Future work on the interface will include combining the menu and title bar into a floating bar located at the top of the browser. This will allow a larger area to display data.

Architecture and Deployment of a Secure Computer Systems Administration Network. *BRYANT FORTSON (Richard J. Daley College, Chicago, IL 60652) PAUL DOMAGALA (Argonne National Laboratory, Argonne, IL 60439).* The primary goal of this project is to design, construct and implement a private administration network which will be separate and distinct from the network resources available to users. This will essentially give us a “backdoor” into our current building networks, keeping our administration network unseen from information thieves and attackers. This will provide us with a separate logical and physical network from our primary networks, thereby increasing security and reliability. Finally it will provide greater flexibility of our networking infrastructure. The primary, in fact only users of this new network will be the system administration staff. With the implementation of this system, a multitude of functionality is acquired. Better monitoring of our system will provide greater problem analysis/solution, capacity planning and projection of future architecture needs. We will also be able to utilize monitoring features such as Simple Network Management Protocol (SNMP) safely and more extensively. Under ordinary circumstances, use of such protocols might present a serious security concern. Our network will be constructed using an array of standard networking devices and protocols, including but not limited to; VLANS, Network Interface Cards (NIC), network switches and Unix, Linux, Macintosh and Windows servers.

Implementation of a Java Channel Access Application and Development of a Model to Create Java Applications Utilizing JCA. *DANIEL FUNKEN (University of Kentucky, Lexington, KY 40506) MICHELE JOYCE (Thomas Jefferson National Accelerator Facility, Newport News, VA 23606).* Throughout the Thomas Jefferson National Accelerator Facility, input/output controllers (IOCs) control every physical property of ongoing experiments and give constant feedback. This information is communicated through EPICS (Experimental Physics and Industrial Control system) Channel Access (CA), written in C++. Since java is cross-platform compatible, it has become the preferred language, requiring an interface between CA and the java application. Currently, the client application accesses the IOCs through a Common DEVice (CDEV) gateway, a C++ and Java framework utilizing a server. This server provides slow connection speeds and creates a bottleneck. This project implemented a Java Interface for Channel Access (JCA) to establish a direct link between the client program, CTableUtility, and the IOCs, and provided a model to simplify the creation of JCA-based java applications. The existing CDEV hierarchy was recorded, creating a list of CDEV functions and objects. These existing functions and objects were then mimicked implementing JCA code. Also the java application code was checked for statements executing the CDEV code, and these statements were replaced with JCA statements and objects. JCA code possesses many features, which were used to create a few enhancements to show its versatility. A series of website tutorials were created to teach JCA Basics. This project also tested the feasibility of java control system applications helped decide on a superior CA interface. The program successfully compiled and ran faster and more reliably then its CDEV counterpart, as it cuts out the CDEV gateway server bottleneck. The CDEV and JCA applications were timed, and the use of JCA showed a significant decrease in update times averaging around 0.745 seconds for each channel. The website tutorial, allowed others to learn how to use JCA and create a JCA program in a fraction of the initial time. These results lead to the conclusion that JCA is the better choice for Java applications and greatly increases connection speeds. This project has produced a practical display tool that can be used in the control room, and provides a model for others to use in their creation of applications that utilize java and JCA, for greater portability and speed.

Implementing an Automated Clear Sky Detection Method in C Using LabWindows. *CHRIS GONZALES (Fort Valley State University, Fort Valley, GA 31030) STEVE WILCOX (National Renewable Energy Laboratory, Golden, CO 89401).* Understanding the local clear sky climatology can help in many areas of work at the National Renewable Energy Laboratory, including photovoltaic cell research, atmospheric studies, and changes in solar irradiance reaching earth over time. Clear-sky detection of plotted solar irradiance data is fairly easy for the human eye to distinguish from that of cloudy data. However, instructing a computer to automatically accomplish this distinction of clear-sky detection is more difficult. Based on the work of Long and Ackerman I accomplished this automation by evaluating 1 to 5 minute diffuse and global solar irradiance data collected at the Solar Radiation Research Laboratory in Golden, Colorado. The data from 1985-2003 were scrutinized through a specialized mathematical model developed to isolate and identify clear-sky minutes from those of cloudy-sky minutes. Once the data pass initial testing, they are reevaluated multiple times using tighter constraints. A collection of possible clear-sky minutes from an

entire day is then fit to model parameters. After finding the best fit to the clear-sky minutes, the coefficients of the fit are saved. Once all the data have been examined and values saved they are processed for modeling. The program then presents the modeled data to the user in an interactive graphical display. This interface allows the user to examine modeled clear-sky climatology of a region over the span of the input data. The user then has multiple output options of the modeled and measured data for analysis, including clear-sky diurnal profiles by week for multiple years or by month for multiple years. Data provided by the Solar Radiation Research Laboratory was examined by the software. The effect of volcanic eruption and radiometer calibration on clear-sky irradiance, seasonal effects upon global irradiance and average percent of clear-sky days by week of years are presented.

Contributions to a Paper Discussing Systems Management. *JOSEPH HAGEDORN (University of Illinois at Urbana-Champaign, Urbana, IL 61801) CRAIG STACEY (Argonne National Laboratory, Argonne, IL 60439).* Systems Administrators are faced everyday with the problem of managing the configuration of computer systems across various operating systems and computing architectures. It is difficult and time consuming to manage a large number of diverse systems without a configuration tool that is able to effectively upgrade and configure settings across all of them without any trouble. We have designed and implemented BCFG, and system management tool intended to provide abstracted access to configuration constructs on multiple architectures. For reasons of usability, it is desirable that BCFG use vendor-provided system management tools where possible. As the capabilities of these tools vary widely from system to system, the extent to which BCFG can support different platforms varies as well. The experience of porting BCFG to Mac OSX has provided valuable insights into the suitability of automated vendor tool usage. We will discuss the high-level capabilities required for automated usage, common pitfalls, and desirable features which could be added to these vendor tools.

Extracting Dynamic Imagery Features From Disparate Imagery Sources. *JARED HESS (Columbia Basin College, Pasco, WA 99301) GEORGE HE (Pacific Northwest National Laboratory, Richland, WA 99352).* The benefits of imagery analysis are well known in terms of environmental management, resource production, national security, as well as other interests. Automatically extracting dynamic information with disparities is becoming increasingly important to scientists and practitioners in the field of imagery analysis. State-of-the-art methods of imagery analysis tend to extract spectral and spatial information frame by frame individually. This research investigates the feasibility of using the disparities among adjacent frames to characterize dynamic information embedded among a sequence of image frames. A theoretical model is constructed and examined, then a practical application of the dynamic information extraction process. In this process, first, a set of linear span of neighborhood intensity values from adjacent images is used to construct the data cube with the necessary and required dimensionality for subsequent classification. Second, the newly formed data cube is classified to locate pixels with dynamic information using classification algorithms; e.g., FDA, and LCDA. Third, the pixel values from the original image frame set in the neighborhood of the extracted pixel location is used to find the conjugate (indexing). Fourth, the location vectors of the conjugate pairs are used to characterize the dynamic information from the imaging sequence. Future work includes improvements in the extraction process and process automation.

Grid Portals for Scientific Visualization: Experiences Developing a Volumetric Rendering Portlet for OGCE. *BRIAN HLUBOCKY (University of Illinois at Urbana-Champaign, Urbana/Champaign, IL 61820) MIKE PAPKA (Argonne National Laboratory, Argonne, IL 60439).* Recently, there has been increased interest in grid computing for use in research and corporate systems. More companies are looking at decreasing costs through the use of “thin clients,” or low-end computers connected to powerful servers. One form of “thin client” technology is the portal, a collection of web applications accessible by a web browser. Grid portals, a combination of the portal and grid computing paradigms, give scientists a method for conducting their research through a simple and ubiquitous interface. As the importance of grid computing in the scientific community grows, so too does the value of grid portals. In this paper, we present our work toward creating a grid portal designed for scientific visualization. The Open Grid Computing Environment (OGCE) is composed of many open source applications and is the grid portal used as a test bed for our research. Using OGCE, we created a portlet that performs volumetric rendering of scientific data sets. With this portlet, scientists are able to obtain complex visualizations of their data using only a web browser.

Integrating FRAMES 1.X Models into FRAMES 2.X. *RUSSELL HOWELL (Utah Valley State College, Orem, UT 84058) MITCHEL PELTON (Pacific Northwest National Laboratory, Richland, WA 99352).* Framework for Risk Analysis in Multimedia Environmental Systems (FRAMES) is a software platform that manages data flow between multiple models, where each model represents a physical process or entity. FRAMES, developed at Pacific Northwest National Laboratory (PNNL), allows a user to dynamically add and connect models into the data flow. The user then follows the flow of data through the various models encountered. In FRAMES Version 1.X, data was stored in formatted, sequence dependant ASCII files that each developer was required to write. PNNL is currently developing FRAMES Version 2.X. One of the primary differences between the two versions is the manner in which the data is stored and accessed. In FRAMES 2.X, data is stored using an Application Programming Interface (API) and upgraded file specifications, where the developer doesn’t have to be concerned about the format or sequence of the data. The API also supports multiple programming languages and allows for developers to integrate their own models. This paradigm shift to an API and updated specifications meant that FRAMES 1.X models would no longer work in FRAMES 2.X. To address the problem, it was decided that the migration should be universal and written once for all models in the system. For each of the known file types and formats, pre and post processors were written, using the API. These processors would then be used based on individual model needs allowing them to work within FRAMES 2.X. By developing the FRAMES API, the functionality of FRAMES is increased dramatically, making it a useful and valuable tool for process model simulation. The paradigm shift is import because it provides for more QA/QC to be done on data while allowing access to the data more readily.

Constructing a New Visitor Notification Form Using Microsoft Active Server Page Language. *AKEEM JACKSON (Bronx Community College, Bronx, NY 10453) JOHN FLANNIGAN (Brookhaven National Laboratory, Upton, NY 11973).* The Visitor Notification Form is a web page designed for the use of short-term visits into the Brookhaven National Laboratory (BNL). This Visitor Form will require various programming languages that will include VB Script- a smaller section of Visual Basic; Java Script-which is somewhat similar to C++; and most of the form will be done in Hyper Text Markup Language (HTML). These languages will be used in editors such as Microsoft Visual InterDev 6.0 and Microsoft FrontPage. Another program that must be used is Structured Query Language (SQL) Navigator. SQL Navigator is a very important tool used for project development, which enables you to view and test the database. SQL provides us the opportunity to enter, delete, or review data in a database and also construct tables, queries, and indexes. There are necessary field names that this form must also have to achieve its purpose of retrieving date. These field names are broken down into three sections. First is the Submitter’s Information; this includes the Submitter’s Name, Life Number and Email address. The second section is the Visitor Information- First Name, Last Name, Company Name, Visitor/Vendor Type, Expected Time of Arrival, Start Date, End Date, Is Visitor Housed on Site, Is Visitor a US citizen, Reason for coming (Event), and Visitor’s Destination. The final section is the Point of Contact, the field names here are: Name, Organization, Building, Room, Work Phone, Pager, Home or Alternate Phone, Fax, Visitor’s Email address and Comments. This form is for the use of the Main Gate Security and can only be requested by BNL Employees or Guests who have a current BNL domain account. Our ultimate goal is to have the visitor’s information as well as BNL Employees, Guests, and Faculty Members in a program called People Soft. So, instead of scurrying from database to database, this would make it much easier to locate and retrieve data on an individual or group. Constructing a new Visitor’s Notification Form provided us the vision to generate a new appearance and offer easier access.

Software for IceCube: Object-Oriented Programming. *TANNUS JOUBERT (Southern University A&M College, Baton Rouge, LA 70813) SPENCER KLEIN (Lawrence Berkeley National Laboratory, Berkley, CA 94720).* IceCube is a high-energy neutrino detector, which will search for astrophysical sources of neutrinos at the South Pole by using ice as the detection medium. These neutrinos collide with ice producing showers of charged particles, which generate Cerenkov radiation. The neutrino energy is determined by reconstructing events from the arrival times and locations of Cerenkov photons. The purpose of this project was to use object-oriented programming in creating or developing a software module. The software module was used to make the geometry for the detector by reading in the IceCube geometry from a file. The geometry can be used by various simulations to determine the efficiency and accuracy of neutrino event reconstruction.

Single Axioms for Weak Orthomodular Lattices and Weak Boolean Algebras. *KENNETH KEEFE (Southern Illinois University - Carbondale, Carbondale, IL 62901) WILLIAM MCCUNE (Argonne National Laboratory, Argonne, IL 60439).* A single axiom for an algebras refer to a single equation that can be used to prove all know laws of that algebra. The search for these single axioms have traditionally been done by hand, usually yielding very large axioms. This paper discusses the methods used to search for single axioms with the aid of computers and reasoning programs. Now, not only can single axioms be found, but they can be concretely proven to be the shortest or simplest possible single axiom. The progress of the search for single axioms for Weak Boolean Algebras and Weak Orthomodular Lattices, is discussed within.

Migration of Web-Based Applications and Databases to Open Source Systems. *JOHN KELLY (North Carolina State University, Raleigh, NC 27607) VINCE BISHOP (Oak Ridge National Laboratory, Oak Ridge, TN 37831).* Over the past few years, the amount of open source software has increased dramatically, partly due to the growing popularity of Linux. Since open source software is free, the prospect of migrating to open source is intriguing to many businesses. One of the main problems that seems to stop many companies from making this move is compatibility. In the case of web-based applications, changing to an open source operating system is easy, but changing the software that is used to deploy the application can be a problem. The Operational Safety Services Division at ORNL has a web-based application called WebSurvey that is used for numerous tasks within the division. Currently WebSurvey is running off of a Windows server, with Macromedia ColdFusion MX to serve CFML pages, and an Oracle server to serve up databases. In an attempt to reduce costs, and possibly set up a server with WebSurvey locally at HFIR or PNNL, WebSurvey was transferred to an open source system running Red Hat Enterprise Linux ES. Almost all of the applications that were used to deploy WebSurvey are open source and free. The main software needed was an Apache web server, New Atlanta's BlueDragon server (not open source, but free) to serve up CFML, and a MySQL server to serve up databases. The overall cost of hardware and software for the server was less than $1000. Migrating to open source software for the new server caused some problems, but it actually forced some things to be improved and saved thousands of dollars. Most of the problems arose from differences between the CFML servers and differences between the MySQL and Oracle databases. There were a few other problems involving smaller applications that run within WebSurvey, but most of these were fixed with Java programs or custom JavaScript. WebSurvey was successfully set up on the open source machine with even a few improvements made as far as versatility goes. As with any new system there are still a few glitches, but with a little more time and testing these glitches should be worked out. Once this happens, the server will be set up locally at HFIR, which would act as a back-up in case a connection to the main WebSurvey server is lost. The server at HFIR would be synchronized with the main server once the connection to the main server is restored. Now that WebSurvey is on one open source machine, it can easily be set up on many more servers and implemented at many more sites.

Adaptive Optimization Framework. *ADRIAN KENNEDY (Norfolk State University, Norfolk, VA 23504) THOMAS PELAIA (Oak Ridge National Laboratory, Oak Ridge, TN 37831).* Multi-variable, multi-objective optimization problems commonly arise when dealing with complex systems. These problems may be linear, non-linear, continuous, discontinuous, or have many local extrema. For example here at the Spallation Neutron Source (SNS) a few of these problems are orbit correction, controls based software feedback systems and fitting data to models. Traditionally when solving optimization problems the user would first choose the best algorithm, then cast the problem to fit the chosen algorithm. This process resulted in much time spent looking for the best algorithm and figuring out how to best solve the problem, which limited these problem solvers in their efficiency. Our approach to problem solving is the adaptive optimization framework which automatically learns how to best schedule algorithms as the problem is being solved. Our adaptive optimization framework makes use of an algorithm pool, that contains several algorithms that are each suited to a different class of problem. The types of algorithms it will contain include: algorithms that are fast at finding local extrema; algorithms that are slower, but more robust at finding global extrema; algorithms that are designed for linear problems; algorithms that are designed for non-linear problems. The adaptive optimization framework's intelligence is in the form of a market that dynamically and in real time schedules algorithms while solving the problem. Our optimization framework is highly customizable in that it accepts multiple variables, objectives, hints and constraints for problems. The user provides the model that can score a solution for each objective. At every iteration the framework generates a new trial solution to be scored by the model and keeps track of the best solutions. Our framework is open source, extensible, component based and implemented in pure Java. Thus far the foundation for our framework has been designed and implemented. We are currently implementing the market and adding additional algorithms.

HP to Sun Script Conversions, Crystal Report Migration, Gatepass and Training by Design Testing, Software Application Testing On Multiple Platforms. *PAUL KETO (Lewis University, Romeoville, IL 60446) RONALD J. FIERRO (Argonne National Laboratory, Argonne, IL 60439).* The purpose of the internship was to provide me with real world applications and workings of computer technologies. Materials for study included Windows 2000 Professional, Internet Explorer, Mozilla, Macintosh OSX, Microsoft Office 2003, Opera, Netscape, and Windows. Problems were studied on an issue to issue basis depending on the scale and severity of the issue. Problems were solved using logic, a good sense of the people around me, immediate and clear communication with a basic view of what was wrong and what needed to be fixed. Resulting from all of this was a decrease in production time, in increase in product development, increases in reliability, and an enhanced understanding of developing and new technologies. Training by Design (TBD), Gatepass, Opera, Crystal Reports, Microsoft Office 2003, and the HP to Sun conversion have all benefited due to the my participation and help in all categories.

Design and Development of Web-Based Applications Using the Lotus Notes Domino Development Platform. *TRACY KISSIRE (Columbia Basin College, Pasco, WA 99301) MARK D. BAYLESS (Pacific Northwest National Laboratory, Richland, WA 99352).* The proliferation of computers in the work environment has fueled the demand for web-based applications facilitating the daily managerial processes. Managers are striving to utilize web-based applications capable of increasing workflow efficiency while ensuring the accuracy and integrity of data being processed. There is a demonstrated need for the Limited Term Employee (LTE) Request form to be transitioned into a web-based application from the current Microsoft Word document format. The LTE Request form was previously processed by editing the document and submitting it using e-mail. This method posed two primary problems. First, the lack of a centralized repository for the form led to multiple versions of the form being edited and submitted. This introduced varying degrees of inconsistent and erroneous submissions. Second, the submission method was e-mail and each corrected submission produced duplicates. These situations led to redundant processing efforts because of the additional verification required to determine the accuracy of the form and data. To solve these situations, the form was transitioned into a database-driven web-form, designed in Lotus Domino Designer 6.5.1. The resultant form is generated upon access from a secure, centralized server environment. The form fields editable by the user are controlled in both content and location. The data is retained in a database on the server and can be saved, retrieved, and edited at a later date. This transition from an e-mail based document to that of a server-generated form is an example of the continued effort of managers to facilitate the increase of daily workflow efficiency.

Developing Full Size Models of Industrial Facilities for Agent Based Simulations in a Computer Environment. *JOSEPH LAKE (University of Tennessee, Knoxville, TN 37996) ROBERT SANDERS AND DAVID SULFREDGE (Oak Ridge National Laboratory, Oak Ridge, TN 37831).* After September 11th, 2001, our nation has gained a heightened awareness of the need for greater national security. In order to protect our nation, we must not only protect the public, but also the facilities and infrastructure that permit normal day-to-day life for the population. These facilities include, but are not limited to: power plants, factories, military bases, and government buildings. Determining the best course of action for guarding these facilities and the security analysis of such structures is a daunting task. Due to the uniqueness of each facility, creating a general model is not always possible for real world scenarios. What is required is the ability to create separate models for each critical facility. These models need to be used many times over to generate a variety of different scenarios, and then the data from those scenarios needs to be assessed in a timely manner. Using the Unreal Tournament 2004 (UT2004) Engine, it is possible to make such models that will provide real-time data analysis for agent-based simulations. To create a representative model requires the software packages UnrealEd3.0 and Alias Wavefront's Maya 5.0 PLE, both included with the UT2004 distribution, and Discreet's 3D Studio Max. Employing these packages and detailed engineering drawings, a model of an industrial facility in the United States has been created. This model contains key systems (i.e. turbines, cooling stations, generators, etc) that will be linked to ORNL's VISAC fault tree analysis code to assess the result of damage to those systems from a variety of terrorist attack scenarios.

These simulations will be run using the UT2004 Engine. Areas of interest in the simulations include, but are not limited to: possibility of meltdown, zones of reduced security, and the likelihood of disabling the plant. The ultimate objective of this methodology is to help identify and increase security in vulnerable areas, determine the vulnerability of key system components from internal and external attacks, visualize what subsystems are affected if an attack is successful, and estimate the probabilities of catastrophic events. In the future, we hope to be able to manipulate the Unreal Engine's code to allow for artificial intelligence capabilities that will mimic the behavior of known terrorist groups in an effort to create force-on-force simulations for training purposes.

Normalizing the Data for Advanced Photon Source/Experiment Facilities Division Tomographic Experiment. *TONETTE LATHAM (Elizabeth City State University, Elizabeth City, NC 27909) FRANCESCO DE CARLO (Argonne National Laboratory, Argonne, IL 60439).* X-ray tomography has been very helpful to scientists and others who decide to use it. At ANL's APS/XFD x-ray tomography experiments are conducted. Each experiment consists of passing a parallel beam of x-rays through an experimental object. Of this beam of x-rays, a part of it passes through the object. The x-rays that pass through the object are attenuated depending upon the composition of the object's material. Ideally, the x-rays that do not pass through the object should not be attenuated. But it is found that these x-rays are attenuated to some extent due to conditions in the experiments. In order to get the real absorption of x-rays by the experimental object, the attenuation of x-rays due to experimental conditions is to be removed. Removing this attenuation is normalizing the data. In my summer internship in the FaST Program at ANL, I worked on the study of x-ray tomographic image formation. This includes showing the attenuation of x-rays by experimental objects and attenuation inherent in experimental conditions. The data of these experiments are recorded in computer files. These computer data files are in Hierarchical Data Format (HDF). Our faculty wrote a C++ program to normalize the data. The program normalizes the data to a fair extent. Perfect normalization is hard to achieve at this stage.

Simplification of the Calculation of Thermal Resistance of Whole Wall Areas for Building Envelopes. *NATHANIEL LAWS (County College of Morris, Randolph, NJ 07869) JAN KOSNY (Oak Ridge National Laboratory, Oak Ridge, TN 37831).* The thermal resistance of a wall area, measured in R-Values ($h \cdot ft^2 \cdot °F/Btu$), is used to calculate the flow of heat from one wall surface to another. These R-Values are used in describing the amount of heat energy that is transferred through a wall area. The higher the R-Value the longer it takes for thermal energy to move through the exterior wall of a building envelope from a hotter area to a colder area. The general method for measuring the overall R-Value for a building envelope was to test the thermal resistance for a section of clear wall and then to apply its R-Value to the entire opaque wall area. However, this has been found to be extremely inaccurate. It has been discovered that the R-Value for a section of clear wall can vary greatly from the true R-Value for the whole wall area. This is because the R-Values for interfaces such as the wall/roof intersections, corner intersections, and wall/window intersections can vary from as much as double to half the clear wall R-Value. Large amounts of research have been allocated for the testing of different wall systems to discover the respective R-values for each detail dimensions of a building envelope. Recently, focus of the research has evolved to include the development of a new geometric calculator, along with a massive database of wall system R-Values, to simplify the calculation of the whole wall R-Value. The calculator takes geometric information for up to fourteen different detail dimensions to calculate the whole wall R-Value. It also calculates a simulated area, thermal heat flux, and influence factor, for each dimensions detail. All calculated values are then displayed using simple pie and bar charts as well as a printable text description. This calculator gives developers and builders the ability to easily discover the whole wall R-Value for any house they are designing, simply by entering basic geometric dimensions and selecting from a list of tested wall systems. Included is the ability to compare the R-Values of different wall systems based upon the entered geometric dimensions. This tool significantly simplifies the development and design of more cost effective and energy efficient building envelopes.

Open Grid Computing Environment (OGCE) Interface: Developing and Integrating Portlets Using JAVA Programming Language. *ANDREW LOBBAN (Harold Washington College, Chicago, IL 60601) DOUGLAS OLSON (Lawrence Berkeley National Laboratory, Berkley, CA 94720).* Portlet is a JAVA program associated with a Portal website. The portal website manages how each portlet is executed and oriented on screen. A program was created in Bash, a shell script language, that executes and gathers data from several .crl files that sit on a Linux Server. The .crl files contain certificates of authority that are electronic signatures. Its purpose is for user authentication. The script reads each certificate and outputs user specific data to a log file on the same server. The data gathered from the .crl files are the expiration date and user information-name, division, etc. A JAVA file is created to read the log file on the server and alert the owner of the time left on his/her certificate when logged into the OGCE website.

Collaborative Tools for Computational Biology. *FREDDRICK LOGAN (Governors State University, University Park, IL 60466) SOON-OK PARK (Argonne National Laboratory, Argonne, IL 60439).* Research in genomic and biological science has the promise of benefiting society. One goal of bioinformatics is to mine biological databases to identify genes and their encoded products that govern biological reactions. Systems biology research uses computer models to help understand the behavior of the biological processes. This summer there were two main objectives in the project; 1. Add the ability to connect to multiple databases simultaneously. 2. Add the ability to use multiple database technologies. We have achieved these goals during our research at Argonne National Laboratory. Previous ongoing research at Argonne National Laboratory has produced prototype tools to help build models. Kah is a framework for writing systems biology programs and the Model Editor is a graphical user interface (GUI), written in terms of Kah, that a scientist can use to build biochemical models. The previous KahDB was built with Oracle. This summer we have worked on extending Kah to easily utilize any database such as Oracle, Postgres and MySQL. We have engaged in creation and modification of programming code to actually load the biological data into multiple databases. Our project focused on developing a collaborative tool which would allow scientists the ability to connect multiple databases of same or different type simultaneously. We developed software to provided simultaneous access to multiple databases. Our research with building and collaboration of the project has created a foundation for the collaborative tools for computational biology.

Elimination Techniques on Linearized Computational Graphs and Dual Graphs with an Emphasis on Data Locality. *ANDREW LYONS (Vanderbilt University, Nashville, TN 37235) PAUL HOVLAND (Argonne National Laboratory, Argonne, IL 60439).* Use of the chain rule in the preaccumulation of jacobian matrices yields a computationally complex search space of elimination sequences. Current techniques attempt to minimize arithmetic operations in the generated code, which is generally considered to be an NP-hard problem, though no proof currently exists. The heuristics described in this paper focus on generating code that makes use of cache and other fast memory to speed execution. We describe heuristics that focus on data locality for vertex and edge elimination on linearized computational graphs, as well as heuristics for face elimination on dual graphs. The runtime of the generated accumulation code is then compared to that of ops minimizing heuristics such as Markowitz.

Cyber Security. *LINDSEY MARCUM (Bevill State Community College, Fayette, AL 35555) TERRY HEATHERLY (Oak Ridge National Laboratory, Oak Ridge, TN 37831).* Cyber security is of vital importance for the majority of business organizations that use the Internet. The main goal of this project is to monitor, assess, and research numerous methods required to resolve cyber security vulnerabilities. Cyber security viruses, Trojan horses, and malware are developed and propagated with the capabilities to exploit systems and networks, intending to cause significant downtime. Thus, the cost of business operations extensively increases. Several software tools and techniques are used to protect the security of networked systems. For example, the Engineering Science and Technology Division (ESTD) at Oak Ridge National Laboratory (ORNL) utilizes an automated software application known as the Vulnerability Scan Web System (VSWeb) to identify and address known vulnerabilities of computing systems in ORNL's network that may be vulnerable or exploited. VSWeb was developed to identify and record known security flaws, test systems for these flaws, and generate a report of the results. An employee or system administrator can use the VSWeb report to resolve the problem, thus improving ORNL'S network security. The primary duties of this project include focusing on cyber security vulnerabilities that are reported by the VSWeb application. In addition, other tasks consist of assisting ESTD staff in their offices and laboratories to research and apply the appropriate method to correct the vulnerability. The ESTD staff employs more than a thousand data network connections to support their ongoing research activities, which makes the VSWeb application crucial to the management of the ORNL infrastructure. Identifying and eliminating vulnerabilities is necessary to maintain a safe and secure network and to support important research activities.

Summary of Internship in Science Writing. *DANIEL MARGETICH (Richard J. Daley College, Chicago, IL 60652) FLOYD BENNETT (Argonne National Laboratory, Argonne, IL 60439).* This is a summary of what I did and learned during my Community College Institute (CCI) internship in science writing. My internship was as a technical writer in the Technical Communication Services (TCS) department of the Information and Publishing Division (IPD) at Argonne National Laboratory. TCS provides a number of communication services (primarily writing and editing) to the Argonne community. TCS also provides web-related services. The writers and editors function as consultants who work on a project-to-project basis. The work varies from creating exhibitions, posters, and web sites to publishing full-fledged glossy volumes explaining and promoting the work done by researchers at the Advanced Photon Source (APS). I had three projects during my internship: proofing a feasibility study, copyediting a journal article, and developing a website.

Development of a Laboratory Information System Based on 3-Tiered Client/Server Architecture. *MAGEN MARTIN (Brigham Young University - Idaho, Rexburg, ID 83440) MICHAEL SAYER (Argonne National Laboratory, Argonne, IL 60439).* The Analytical Laboratory at Argonne National Laboratory - West (ANL-W) utilizes a Laboratory Information Management System (LIMS) consisting of a Database Management System (DBMS) and Database Application (DBA) to record, track, and report analytical information for samples received and analyzed by the laboratory. The DBMS currently consists of a Microsoft Access 97 database which resides on a Windows 2000 network server. The DBA known as ALSTAR (Analytical Laboratory Sample Tracking and Reporting System) was created in Visual Basic and is a distributed system which can be used in the Analytical Laboratory to interface with the database. This system is out of date and in need of revision. My project modernized the Laboratory Information Management software (LIMS) program. I did this by creating a new database application in ASP.NET using VB.NET and converting the data from an Access Database to a Microsoft SQL Database and Server.

Extracting Dynamic Imagery Features From Disparate Imagery Sources. *GLEN MCNABB (Columbia Basin College, Pasco, WA 99301) GEORGE HE (Pacific Northwest National Laboratory, Richland, WA 99352).* The benefits of imagery analysis are well known in terms of environmental management, resource production, national security, as well as other interests. Automatically extracting dynamic information with disparities is becoming increasingly important to scientists and practitioners in the field of imagery analysis. State-of-the-art methods of imagery analysis tend to extract spectral and spatial information frame by frame individually. This research investigates the feasibility of using the disparities among adjacent frames to characterize dynamic information embedded among a sequence of image frames. A theoretical model is constructed and examined, then a practical application of the dynamic information extraction process. In this process, first, a set of linear span of neighborhood intensity values from adjacent images is used to construct the data cube with the necessary and required dimensionality for subsequent classification. Second, the newly formed data cube is classified to locate pixels with dynamic information using classification algorithms; e.g., FDA, and LCDA. Third, the pixel values from the original image frame set in the neighborhood of the extracted pixel location is used to find the conjugate (indexing). Fourth, the location vectors of the conjugate pairs are used to characterize the dynamic information from the imaging sequence. Future work includes improvements in the extraction process and process automation.

Development of Biometrics. *VIRAJ MEHTA (Suffolk Community College, Selden, NY 11784) U.S. ROHATGI (Brookhaven National Laboratory, Upton, NY 11973).* Biometric Identification methods are the next level of security in a digital world because they are easy to use but are extremely difficult to compromise. In fact, email passwords and ATM pin numbers can be easily hacked, stolen or misused while biometrics is unique to every human being and uses fingerprints, hand scans, voice samples and iris scans, to identify the person. This technology helps to reduce identity theft and is also used to protect valuable resources of a company or individual. The results obtained from the integrated hardware with the software were good. The software was able to identify authorized users / personnel 95% of the times. Out of the remaining percentage, 2% went towards giving permissions to unauthorized users, and 3% produced “Invalid Image” errors. An integrated biometric system was developed that combined fingerprints, face scans and scan to identify a person. This was done is simply to make it more secure and more flexible so it could meet the requirements of the end user. The functionality of the software application was tested with the use of “generic” fingerprint scanners, WebCam(s) and digital cameras as described below. A literature search has been done to select the best-suited scanner for our project. Similar software solutions have the same function, come bundled with their own proprietary hardware, making them expensive. The software application we developed can use any “off the shelf” scanner to achieve the same goal. A comparison between the scanners indicated that, results varied on scanner to scanner. More complex scanners exist but Digital Persona’s U.are.U 4000S sensor was chosen, as it was easier to use, cost effective and efficient. For face scans, any WebCam could be used for identification purposes, as WebCam’s are very cost effective compared to other security cameras. The digital camera was used to create a replica of hand scans. Upon obtaining all the necessary hardware, the software was tested to find any bugs or errors within it. There were problems during the integration, but were resolved with the constant feedback with developers and other beta testers who had access to the software.

Efficient Research Exposure Via XML. *JANE MEYERS (East Tennessee State University, Johnson City, TN 0) T.A. BODEN (Oak Ridge National Laboratory, Oak Ridge, TN 37831).* Even in the most widely published journals, the lead time between manuscript submission and final publication often exceeds a year. For many researchers, it is important to efficiently and effectively communicate findings in a timely manner. The inefficiency of scientific paper publication entails not only the comprehension of the material but the unnecessary downtime between research disclosure and the biannual journal publication. In efforts to adapt to the new era of technology, we are creating a virtual newsletter in replacement of our annual publication. The clear advantage of an electronic interface for searching, reading, and efficiently publishing and updating research, is obvious. It is important that even electronic articles have a standard format. A relatively new language that includes the capabilities for creating archetypes for a web based documents is xml. Since browsers currently do not support xml we chose to use the Xmlspy editor for this project. Because Xml is object oriented, the first step involves developing a schema with appropriate elements and attributes. Logistically creating a form in which the input fields serve as empty elements is a simple method for the general user to create an xml document. Stylevision, a separate Xmlspy program allows the creation of article templates, including conditional statements, graphics, and placement of inputted data. Pulling the project together was the program Authentic, where a form is completed and an html is file created via the xslt translator. The resulting html article is automatically saved on the server where it will later be parsed and sorted into the appropriate newsletter subsection. Future work with new versions of Xmlspy will hopefully allow manipulation of meta-tags and facilitate the addition of dynamic graphics.

A Cubic Hermite Boundary Integral Approximation for the Solution of Moving Boundary Problems. *MATTHEW MOORE (University of Tennessee, Knoxville, TN 37916) LENNY GRAY (Oak Ridge National Laboratory, Oak Ridge, TN 37831).* In many problems in science and engineering, the goal is to track the time evolution of a “moving boundary”, e.g., modeling the breaking of a water wave or the dripping of a faucet. Obtaining the boundary velocity generally requires solving a partial differential equation, and in many instances, it is convenient to recast this differential equation as an integral equation on the boundary. This transformation is based upon the singular Green’s function - an exact solution to the differential equation. The primary advantage of the integral formulation is that it is only necessary to re-discretize the evolving boundary, a much simpler task than re-meshing the entire volume. The goal of this project is to develop a highly accurate boundary integral equation method suitable for solving moving boundary problems. The approach was developed in the context of the two-dimensional Laplace equation, but it will be generally applicable. The numerical solution of the integral equation requires approximations of the boundary, the primary boundary function, and the normal derivative of the function. For the Laplace equation the primary boundary function is the potential, and the normal derivative of this function is the surface flux. In previous work, it was shown that the standard linear (first order) approximations could be significantly improved by employing a cubic (Hermite) polynomial interpolation. However, this higher order approximation was only applied to the boundary and the potential, while the flux remained linear. In this project, it is shown that a cubic interpolation can also be developed for the normal derivative function (the flux). The key difficulty is that the Hermite approximation requires computing tangential derivatives of the flux, and these integral expressions involve highly singular third order derivatives of the Green’s function. However, by defining the integrals as a limit to the boundary, the divergent terms have been explicitly computed and shown to cancel. The resulting limiting value of the integral is therefore a finite quantity. Based upon this analysis, it is now possible to have a complete cubic boundary integral approximation. It is expected that the higher accuracy of this approximation will

be important for a wide range of applications involving simulations of moving boundaries.

Development of the Historical Data Entry (HDE) Module of the Foreign Ownership Control or Influence(FOCI) Electronic Submission and Processing System (ESPS) using SQL, ASP, HTML, JavaScript and VBScript. *MICHAEL NOWAK (Bradley University, Peoria, IL 61606) JUDITH GROSS (Argonne National Laboratory, Argonne, IL 60439).* The Foreign Ownership Control or Influence (FOCI) Electronic Submission and Processing System (ESPS) is a web based system that utilizes Active Server Pages, HTML, JavaScript, VBScript and the Microsoft SQL Server database. The system keeps track of information relating to contracting companies that require access to Department of Energy (DOE)/National Nuclear Security Administration (NNSA) facilities where sensitive information or nuclear materials are present. The system is important for the national security and includes all types of contractor clearance packages a user can fill out. Historical Data Entry is an important part in the Foreign Ownership Control or Influence system. Historical information is important to include for analyzing threats and security issues. A sophisticated set of tools will be developed that will utilize the Historical Data Entry (HDE) Module along with the current information that users can submit through the website to the DOE or NNSA via the database.

Computational Analysis for the Support of Biologists. *JOHN PETERSON (Southern Utah University, Cedar City, UT 84720) NATALIA MALTSEV (Argonne National Laboratory, Argonne, IL 60439).* Over the Spring 2004 semester, my internship involved providing computational support to biologists. I worked on two projects, the Microbial Informatics Core user interface for genetic sequence analysis of pathogenic prokaryotes, and the TARGET database and analytical workflows for protein structural analysis.The field of computer science merges beautifully with the life sciences. Pathos and Target show how computational methods have provided solutions and predictions for wet lab researchers, by focusing there energy and resources on targets that will, with greater probability, result in positive results. This has been successfully shown by the superior results that our collaborators have achieved, from the support such systems and scientific workflows provide.

Computational Assistance of Biological Research. *JOHN PETERSON (Southern Utah University, Cedar City, UT 84720) NATALIA MALTSEV (Argonne National Laboratory, Argonne, IL 60439).* Over the Summer 2004 semester, my internship involved providing computational support to biologists. I continued work on two projects from my previous the Spring 2004 internship which included the Microbial Informatics Core user interface for genetic sequence analysis of pathogenic prokaryotes, and the TARGET database and analytical workflows for protein structural analysis. The field of computer science works well with the life sciences. Pathos and Target show how computational methods have provided solutions and predictions for wet lab researchers, by focusing there energy and resources on targets that will, with greater probability, result in positive results. This has successfully been shown by the superior results that our collaborators have achieved, from the support such systems and scientific workflows provide.

Development of the ARM Data Dependency Database. *ELSA QUIJADA (South Mountain Community College, Phoenix, AZ 85040) KAREN CREEL (Pacific Northwest National Laboratory, Richland, WA 99352).* Atmospheric Radiation Measurement (ARM) sites collect data such as, sunlight, radiated energy and cloud coverage. This information is used by scientists to improve climate research and prediction. National Oceanic and Atmospheric Administration (NOAA), Navel Research Laboratory, NASA, and many universities are just a few of the agencies that use this information. Currently the data is being managed by the technical database (TDB) and run on an UNIX system, which was developed over 10 years ago. Some of the data is run manually. The Data Dependency Application (DDA) development will improve the quality, automation, and simplification of the system architecture. This will be a database that treats ingest data and Value Added Products (VAP) interchangeably, making it manageable for new equipment to be added and the ability to track VAP dependencies. Implementing this will start with populating the DDA using Structured Query Language (SQL) and Practical Extraction Report Language (PERL). SQL is the most common database language.

New Smarts from Off-the-Shelf Parts: Modifying a Photon Simulation to Run on a Linux Cluster. *MARTIN ROBEL (Contra Costa College, San Pablo, CA 94806) CHARLIE VERBOOM (Lawrence Berkeley National Laboratory, Berkley, CA 94720).* Cluster computing with commodity components and the Linux operating system offers a relatively low cost and readily accessible alternative to supercomputers and has the potential to significantly broaden the availability of high performance computing. To use a cluster to run an existing modeling program, the code must be modified for parallelization. Message Passing Interface (MPI) is a popular parallelizing protocol which was used for this project. The modeling code selected for parallelization simulates heat distribution using a Monte Carlo simulation. Changes were made to the code to incorporate MPI and make it run efficiently on a cluster. The best and easiest applications for parallelization are so called “embarrassingly parallel” problems. This Monte Carlo simulation is such an application, since the “photons” into which the total heat from the source is divided do not interact with each other. Consequently, the calculation can be simply divided up and passed out to multiple computers. Performance testing of the parallelized version of the program illustrated the importance of both the total number of calculations and the cluster communication latency in selecting an appropriate sized cluster for a given problem. Specifying a photon count of 10,000 (the number specified in the original program) was fastest when two nodes shared the job, but increasing the number of nodes slowed the program execution. To capitalize on the expected speed improvement, a graphical user interface which immediately updates changes to simulation parameters was designed. Visualization was intended to be extended into a fourth dimension by rapidly recalculating and redisplaying the heat distribution upon changes to parameters. However, the effects of latency were too large to realize the anticipated speed improvement; the fastest execution times for the original number of photons run on the cluster were nearly twice as long as for the unmodified program. Hence total number of operations, amount of data transfer, cluster size, target application, and network hardware should all be considered when deciding which programs are well suited to parallelization.

Design and Development of the RPS/HS Material Control Database System. *KEVIN SCHAFER (University of Idaho, Moscow, ID 83843) ROBIN STEWART (Argonne National Laboratory, Argonne, IL 60439).* The Radioisotope Power System and Heat Source (RPS/HS) Program operating at ANL-W has put strict measures in place to identify and control all non-special nuclear materials, tools, and components under control of the program. The current system of tracking materials is a paper system of logs, and transfer and receipt inspection forms. The RPS/HS Material Control Database (MCDB) application is being developed to provide an easy way to track materials, get an inventory of RPS/HS related material on the ANL-W site, and generate the complete pedigree history of a material. The MCDB application is a dynamic Web based application accessible to Web browsers located on the ANL-W Intranet. The application’s Web pages are generated by the server using a system of Java Server Pages (JSP), Java Servlets, Java Beans, HTML, and XML. When completed authorized users will be able to add, transfer, and update materials as well as add, list, and update user information and pull-down selection field items.

Analysis of Luminosity Data in BaBar. *REBEKAH SCHILLER (Oglethorpe University, Atlanta, GA 30319) STEFFEN LUITZ (Stanford Linear Accelerator Center, Stanford, CA 94025).* Luminosity is a value describing the number of interactions between particles when their respective beams collide. The BaBar (B and B-bar) ambient database and the Oracle server contain archived measurements of instantaneous luminosity from two separate detectors. It is important to understand these data to describe the performance of the B-Factory. Extracting these data, the more reliable PEP-II (Positron Electron Two) luminosity detector can be calibrated to the data collected by the more accurate BaBar L3 (Level 3) detector. Using the ROOT programming language and standard BaBar tools for data extraction, graphs and statistics are generated. Some logistical errors contained in the logbook are also corrected. These programs help aid in understanding both what is happening within the B-Factory, as well as the correlations between the interrelationship of detector data and the information recorded in the logbook.

Creation of a Remote Configuration Utility for the RSS-131. *MICHAEL SCHMIT (Gustavus, St. Peter, MN 56082) ROBIN STEWART (Argonne National Laboratory, Argonne, IL 60439).* Currently there are four Solar Powered Area Monitors (SPAM) deployed around the outer perimeter of Argonne National Laboratory West (ANL-W) to provide gamma radiation level detection for the facility. Each of these SPAM units has a solar panel, radio, battery, and RSS-131 device. The current Configuration and Validation Utility, version 3.8.0, for the RSS-131 units forces ANL-W employees to connect to the devices serially in order to configure its various parameters. This is rather inconvenient due to the distance, terrain, and a lack of roads where the SPAM devices are located. Because of this inconvenience it was proposed that a new Configuration Utility be created to mimic the functionality of the old Configuration Utility with the added ability to remotely connect to the devices. Although further testing is required before the new Configuration

Utility can be issued for use, preliminary testing shows the application is working properly and that it should satisfy the design and functionally requirements outlined by the clients.

Developing and Benchmarking a Comprehensive Set of Tutorials for High Performance Computing. *PETER SCHMITT (DePaul University, Chicago, IL 60604) MIKE DVORAK (Argonne National Laboratory, Argonne, IL 60439).* High performance computing via super computers or large clusters of networked computers is becoming increasingly in high-demand to help scientists make new discoveries. Traditional serial (one computer) programming techniques are inadequate to develop software for high performance parallel computing. A comprehensive set of parallel programming tutorial software was developed and analyzed in this paper. The tutorials include four different input/output implementations, runtime and post visualization in serial and parallel, and a strong focus on good software engineering practices. An analysis of the tutorials provide evidence of why good software engineering techniques are necessary for high performance computing.

Building an IDE for Multi-Language Components Using the Scientific Interface Definition Language and Babel. *EDDY SFEIR (Chapman University, Orange, CA 92866) BOYANA NORRIS (Argonne National Laboratory, Argonne, IL 60439).* Language interoperability is a concept in computer science that has been intriguing many scientists recently. The goal is to have different users implementing the same set of interfaces, each in their own preferred language, or possibly the same user using more than one language in an application. Though the project did not directly involve the use of components yet, they are units of software development that play a big role in language interoperability. We used the Scientific Interface Definition Language (SIDL) and the compiler Babel to attack our problem. Once a SIDL file is created, Babel can be called to compile the file and generate language-specific output where the language is chosen by the user, among a choice of six languages: C, C++, Java, F77, F90 and Python. The programming language being used is Python, along with the wxWindows Graphical User Interface (GUI) framework that is crucial to the reach of our goal. Our ultimate goal is to develop a full fledged Integrated Development Environment (IDE) where users can create, compile, use, connect and experiment with components and SIDL files. The IDE is aimed to be very user-friendly and equipped with good graphical representations of SIDL files and components. This is currently being achieved through the extensive use of wxPython graphical toolkit.

MetaMind: A Meta-data Extraction Tool for Classifying Web Content Using Domain-Specific Context and Content Heuristics. *STEVE SILVA (Washington State University, Pullman, WA 99163) SCOTT BUTNER (Pacific Northwest National Laboratory, Richland, WA 99352).* Developing software agents which can reliably classify web documents is an important prerequisite to widespread adoption of semantic web technologies. Effective agents must be able to process large numbers of web documents in a timely and cost effective manner, while providing for classification accuracy that is comparable to that of a human reader. This research paper discusses the design and implementation of the MetaMind tool, along with preliminary results obtained from the web-based classification of environmental compliance assistance documents. MetaMind is a meta-data extraction tool designed to (1) extract domain-specific meta-data attributes from web documents; and (2) use these meta-data attributes (along with additional context clues) to aid in classifying these documents against predefined, hierarchical subject taxonomy. MetaMind's classification and meta-data extraction rules are based on both document content (analysis of word frequency and word/phrase position) and context cues (including web domain and path structure, analysis of inbound and outbound hyperlinks, etc). In order to facilitate integration with other applications, MetaMind is being implemented as a web service using a combination of Java Servlet technology and JESS, a Java-based Expert System Shell developed by Sandia National Laboratory. An extended form of the Rich Site Summary standard (RSS) is being used to present the resulting meta-data information to the user. MetaMind is being developed to support the US EPA's Compliance Assistance Clearinghouse, an online meta-data repository focusing on documents providing regulatory interpretation and assistance to the business community. While MetaMind is being developed for application to a specific and relatively narrow domain, we believe that many classification tasks are similarly constrained within narrow subject domains. In such applications, classification heuristics encoded as production rules can be used very effectively without suffering the problems of scaling and maintainability that often occur when such approaches are applied to broader subject areas.

Development of a Data Acquisition Program for the Purpose of Monitoring Processing Statistics. *PAUL STONAHA (Alfred University, Alfred, NY 14802) MATTHIAS WITTGEN (Stanford Linear Accelerator Center, Stanford, CA 94025).* A current shortcoming of the BaBar monitoring system is the lack of systematic gathering, archiving, and access to the running statistics of the BaBar Online Computing Infrastructure's farm machines. Using C, a program has been written to gather the raw data of each machine's running statistics and compute various rates and percentages that can be used for system monitoring. These rates and percentages then can be stored in an EPICS database for graphing, archiving, and future access. Graphical outputs show the reception of the data into the EPICS database. The C program can read if the data are 32- or 64-bit and correct for overflows. This program is not exclusive to BaBar and can be easily modified for any system.

Adding Remote I/O Capabilities to ROMIO, Using FOBS. *THERON VORAN (Illinois Institute of Technology, Chicago, IL 60616) RAJEEV THAKUR (Argonne National Laboratory, Argonne, IL 60439).* This paper is about the integration of ROMIO and the FOBS protocol to provide remote I/O capabilities to ROMIO. ROMIO is the implementation of the MPI-I/O specification developed at Argonne National Laboratory. FOBS is a protocol developed by Dr. Phillip Dickens at the Illinois Institute of Technology, with the goal of utilizing the maximum amount of available bandwidth in a given connection. Remote I/O is the concept of performing file I/O on data at a remote site, instead of having to transfer the data to a parallel system, like a cluster, before computation.

Fortran vs. C/C++. *DAVID WAGNER (Benedictine University, Lisle, IL 60532) ROB JACOB (Argonne National Laboratory, Argonne, IL 60439).* Throughout the history of programming languages there has been several views of different people on which of the languages is better. Although mostly opinionated, the views in which programming languages are compared up depend solely on the purpose in which the languages are used. In this case FORTRAN will be compared with the C language. Each language has their differences in which make them unique, giving them each a strong point into why they should be used. The differences will depict the versatility of the two languages and thus depict which of the languages is better.

Normalizing the Data for the Advance Photon Source/Experiment Facilities Division Tomographic Experiments. *TRACEY WARD (Elizabeth City State University, Elizabeth City, NC 27909) FRANCESCO DE CARLO (Argonne National Laboratory, Argonne, IL 60439).* The tomographic experiments at APS/XFD involve the study of absorption of x-rays by the experimental objects. In each experiment a parallel beam of x-rays is sent through the experimental object. After the rays pass through the object, these rays are received at a detector camera. The camera in term is connected to a computer. The intensity of the detected x-rays is recorded in a computer file. The data of each experiment is a table of numbers with about 1024 rows and 1024 columns. Each data item is a number between 0 and 4095. The data item 0 represents complete absorption of the x-rays and the data item 4095 shows no absorption of the x-rays. The data in each computer file can be used to form a gray scale image showing the absorption in the experiment. In the gray scale image formation, perfect absorption intensity 0 is represented by black color and no absorption intensity 4095 is represented by white color. Intensities between 0 and 4095 will be represented accordingly in a gray scale. At the beginning of each experiment, the first file of data recorded is with no experimental object. The gray scale image of this has to be white as there is no experimental object present and hence no absorption. In reality, this image is not white, showing that there is absorption present in the experimental conditions. The absorption shown in the data file with an image has two components. One being absorption due to the experimental object and the other is due to experimental conditions. Removing the absorption due to experimental conditions is normalizing the data. Our faculty wrote a C++ program which makes use of the data file with no image and the data file with an image to produce a new file, which is normalized data of the image file. While normalization by this program is not perfect, it normalizes the data to a fair extent. Perfect normalization is hard to achieve at this stage.

Interactive Visualization of Output from Eulerian Chemical Transport and Transformation Model (CTM) for Atmospheric Sulfur. *MATTHEW WEBER (New Jersey Citu University, Jersey City, NJ 07305) CARMEN BENKOVITZ (Brookhaven National Laboratory, Upton, NY 11973).* Simulation models describe worldwide phenomena such as the transport and transformation of trace species in the Earth's atmosphere. Computer visualization plays an important role in the evaluation of model results with observations and in detailed studies of the physical and chemical processes represented in the model. The goal of this

project is to develop software that will provide interactive visualization of five-dimensional (longitude, latitude, altitude, physical species variable and time) environmental data on an irregular 3D grid. The main functionality, accessible through a menu-driven interface provided by the OpenGL-based software, will include: volume rendering, isosurface generation, plane slicing, animation, and interactive operations, such as rotations, translations, and zooming. Volume rendering is done using a view-aligned 2D slicing algorithm adopted from Vis5D, and the generation of iso-surfaces is done with the Marching Cubes algorithm. The software's functionality will allow users to perform interactive, multidirectional visualization of data, potentially giving scientists the ability to gain greater insight and understanding into the flow patterns, distributions, and mechanisms of atmospheric species. The visualization software also provides flexible data-handling facilities so that both binary formatted data without further conversion or a Vis5D formatted file can be used. The modular design of this code, similar to Vis5D or VisAD, allows it to be extended for future development. The available detailed documentation will assure the continuity of this research work.

The Development of Sophisticated Cardiac Models for Use in the Virtual Soldier Project. *SARAH WING (Davidson College, Davidson, NC 28036) RICHARD WARD (Oak Ridge National Laboratory, Oak Ridge, TN 37831).* As the United States continues to send troops abroad into the war zone, the demand increases for better heath care on the battlefield. The goal of the Defense Advanced Research Projects Agency (DARPA) Virtual Soldier Project is to maximize the efficiency of health services to soldiers. The "Virtual Soldier" would be a complete computerized model of the human body. With such a model, doctors could see the effect that a specific injury would have on the soldier, allowing for faster diagnosis and treatment. At this stage in the project, computerized models of blood circulation in the heart and in the remainder of the body are being made. These models are becoming more sophisticated as factors such as baroreceptor control and gas exchange are included. The goal of this stage of the project is to create an ICU-type monitor that scrolls the graphical results from the models across the screen. The original cardiac models are written in a program called JSim. The models, created at the University of Washington, may be downloaded from the internet and manipulated in JSim. Once the tuned parameters are entered into the JSim input (or ".mod") file, the file is sent to a Web Service at the University of South Carolina, where the model is run using the batch processing engine of JSim and results sent back. This is a necessary logistical component of the project because it means that doctors would be able to manipulate certain parameters of the model, using the command line for input for the Web Service. Once the data is received, it may be plotted in such a way that the display resembles an ICU monitor. This part of the project is still under way, however, as it has been difficult to get the results of specified variables to scroll as a function of time. Work is also being done to create visual circuit representations of the models, in order to assist in interpreting the models. When this portion of the project is complete, the most sophisticated of the models will be useful to doctors in the hospital as well as on the battlefield. Doctors will have information about what specific graphical patterns correspond to certain injuries, allowing for more efficient diagnosis and treatment.

Web-Based User Interface and Database Design for Experiments on Cell Signaling Pathways. *STEVEN WRIGHT (Southern Utah University, Cedar City, UT 84720) RONALD TAYLOR (Pacific Northwest National Laboratory, Richland, WA 99352).* Understanding cell signaling is key to effectively treating such diseases as cancer, autoimmunity, and diabetes. Pacific Northwest National Laboratory (PNNL) scientists are studying cell signaling under the Integrated Data Structures for Mapping Cellular Networks project. Because this project generates data from many sources, researchers needed a database and web server that could store diverse data types. I created a biological database and web server that could store data from flow cytometry and Western Blot experiments. The database management system uses Oracle 9i, on a Dell Windows server. The schema used, with some modifications, comes from the ExperiBase project. The web server software for handling the distribution of web pages is Tomcat. The web pages are serviced by Java programs that communicate with the Oracle database through the JDBC (Java DataBase Connectivity) Library. The database will be expanded when mass spectroscopy and microarray experiments are conducted. Creation of the database and the associated web interface fulfill Fiscal Year 2004 project goals for lab data storage requirements.

ENGINEERING

High Gradient Magnetic Filtration of Paramagnetic Particles from Suspension Using Permanent Magnets. *DOUGLAS AARON (Universitiy of Tennessee, Knoxville, TN 37996) COSTAS TSOURIS (Oak Ridge National Laboratory, Oak Ridge, TN 37831).* Separation of paramagnetic particles from a suspension is economically desirable, but difficult to achieve. Paramagnetic particles are weakly attracted to a high gradient, high intensity magnetic field. Of specific interest in these experiments is the filtration of fine mineral particles, such as the ferrite in iron ores, from suspension. When processing, the valuable magnetic components much be separated from the gangue. The waste streams must be treated to recover those valuable minerals. As an alternative to conventional wet chemistry or other physical treatments, magnetic filtration is being investigated. In these experiments, iron oxide (Fe_2O_3) nanoparticles were suspended in a water/propylene glycol mixture to simulate paramagnetic particles suspended in a machine coolant stream. To ensure particle size consistency, the feed suspension was sonicated prior to and during the experiments. Two rare earth (FeNdB) magnets were used with an aluminum spacer in between to hold the filter in place. The Fe_2O_3 suspension was pumped through a filter packed with stainless steel 430 wool. The stainless steel wool was in place to generate a high gradient magnetic field, effecting greater attraction and filtration of the paramagnetic Fe_2O_3 particles. This high gradient magnetic field is necessary to attract the paramagnetic particles, due to their low magnetic susceptibility. Each filter was tested with and without a magnetic field present, to observe the effect of the filter's mechanical filtration (as opposed to magnetic filtration). The relative concentration between the effluent and feed was used to measure separation effectiveness. Initial results were obtained using a spectrophotometer and then compared with atomic emission spectroscopic analysis. The effect of flow rate, packing density, magnetic shielding, magnet orientation, and different filter treatments was investigated. Filter treatments observed included normal stainless steel wool, sintered stainless steel wool, nickel treated sintered stainless steel wool, and acid etched stainless steel wool. Greater filtration was achieved using higher packing densities, slower flow rate, and an acid-etching treatment.

Sensing and Detecting Trace Explosives Using Microwave and Millimeter-Wave Technologies. *MARK ADKINS (The College of New Jersey, Ewing, NJ 08628) NACHAPPA GOPALSAMI (Argonne National Laboratory, Argonne, IL 60439).* With national security at an all time high effective passenger screening at airports is essential to deterring terrorists from using aircrafts as potential weapons. Terahertz radiation mass spectroscopy provides an efficient and cost effective method of detecting trace levels of explosive materials on travelers and their luggage. Utilizing the polar characteristics of chemical explosives a mass spectroscopy system was developed focusing on the spectral range of 220-380 GHz. Four explosives were tested in the experiment (PETN, DNT, TNT, RDX) to provide a range of spectral absorption lines. A Backward Wave Oscillator was used to provide a terahertz radiation source in this region and a heat cell was used to heat and store the sample being investigated. The chemicals were identified using their unique spectral absorption lines and all tests were found to be repeatable verifying the accuracy and precision of the mass spectroscopy system.

Resin Wafer Characterization as part of Separative Bioreactor. *ADRIANA ALDANA (Universitiy of Missouri-Rolla, Rolla, MO 65401) YUPO LIN (Argonne National Laboratory, Argonne, IL 60439).* Electrodeionization is a process that involves ion permeable membranes and ion exchange resins and requires the application of an electrical current. Electrodeionization allows the transfer of ions from a dilute solution by passing it through the ion exchange resin membrane and brings the ions, absorbed by the resins, across the ion-exchange membrane for separation. In this study, ion exchange resin ratios were varied to create different resin wafers and determined their efficiency in the transfer of sodium chloride ions from a sodium chloride solution by performing conductivity and porosity tests. The ratios tested were 51.2% cation-48.8% anion which is 1:0.95, 48.7% cation-51.3% anion which is 1:1.05 and 25% cation-75% anion that is 1:3.00 utilizing anion resin Purolite PFA444 and cation resin Purolite PFC100E. We also utilized a different cation resin named Amberlyte 120H, at a ratio of 51.2% cation-48.8% anion which also is 1:0.95 (061104-D). It was found that increasing porosity would have an impact on the conductivities shown by the resin wafers, but it also showed that if porosity gets too high we loose conductivity by the resin wafers. These tests will allow the future work to be done, to be more accurate and, finally to utilize such tests in the Separative Bioreactor, as our main goal.

Effects of Temperature on Structure and Tribological Behavior of Near Frictionless Carbon Coatings. *BRANDON ALDRIDGE (Tuskegee University, Tuskegee, AL 36088) GEORGE FENSKE (Argonne National Laboratory, Argonne, IL 60439).* Near-Frictionless Carbon's advent brought with it improvements in reducing friction and increasing wear resistance. This study was to investigate the temperature effects on the structure of the coating and its friction and wear characteristics. The test sample used had a coating thickness of NFC-2 approximately 1 micron. Upon exposure to high temperature at 400°C, Raman spectrometer revealed that NFC-2 coating had pronounced graphite and disordered graphite components. On tribometer test, results also indicated that the NFC-2 failed with high friction at a corresponding high temperature. Wear volume analysis demonstrated that NFC-2 has small amount of wear until the critical temperature had been reached.

Mechanical Engineering Design Group: Seven Summer Projects. *JUSTIN BAKER (Brigham Young University, Provo, UT 84602) MAX HOWELL (Argonne National Laboratory, Argonne, IL 60439).* The mechanical engineering section of the Engineering and Technology Division (ENT) at Argonne National Laboratory-West does a wide variety of engineering tasks ranging from operational support on glove boxes to facility improvements. As a member of the mechanical engineering section of ENT during the summer of 2004, my projects were many and varied. Starting with writing the testing procedures for HEPA (high efficiency particulate air) filters and ending with determining the necessary ventilator size for a new sand blast structure, this paper describes my efforts on the seven major engineering projects that occupied my time. The majority of the projects required that I define the design criteria, propose a solution to the specific problem, and create a budgetary cost estimate. Thereafter, detailed design documents were created with budget approval. Several of the projects required some type of formal analysis. The seven projects described in order in this paper are 1) HEPA Filter Test Procedure, 2) Shielded Survey Cart Design, 3) Compressed Air Extension for SEM (Scanning Electron Microscope), 4) Drum Crusher & Contamination Tent Installation, 5) IAAC (Inert Atmosphere Assembly Chamber) Crane Analysis, 6) Replacement of Building 713 Stairs & Entry Ramp, and 7) Replacement of Sand Blast Structure.

Optimization and Regional Cost Analysis for Wind/Diesel Hybrid Systems in Remote Alaskan Villages Overview. *JENNIFER BAKISAE (John Carroll University, University Heights, OH 44118) IAN BARING-GOULD (National Renewable Energy Laboratory, Golden, CO 89401).* The cost to deliver diesel fuel to remote native Alaskan villages for power generation is high because of this region's severe weather and challenging terrain. The Hybrid Optimization Model for Electric Renewables (HOMER) was used to study the feasibility and cost effectiveness of using wind turbines there for power generation. Villages were chosen based on the availability of wind resource data and accurate electrical load information for a range of village sizes. Loads ranged from tens of kilowatts to hundreds of kilowatts of average load. Data for the electrical load demand and wind resource for several villages were obtained and combined with wind turbine and diesel cost and performance data in order to model system configurations and cost of energy (COE) in HOMER. The COE was further analyzed to study how it was affected by loads, regional wind, penetration of renewable power, and diesel costs. We validated the use of a regional load and wind resource model and found cost-effective hybrid solutions for regions with class 4 and better wind regimes. This work is part of a larger initiative by the U.S. Department of Energy (DOE) and the Alaskan state government to improve the quality of life of those living in remote villages. The data will be the basis for recommendations at a user conference of decision makers on wind and hybrid systems in September of 2004 in Alaska.

Centralized Laser Energy Monitoring System (CLEMS) with Network Capabilities and Remote Triggering. *DMITRIY BEKKER (Rochester Institute of Technology, Rochester, NY 14623) KARL KUSCHE (Brookhaven National Laboratory, Upton, NY 11973).* The Accelerator Test Facility (ATF) at the Brookhaven National Laboratory has a number of interconnected laser laboratories where laser energy is measured with various types of joulemeters. To increase convenience and improve efficiency of operating the laser system from multiple locations, a centralized laser energy monitoring system has been developed that allows for: (1) data acquisition from up to eight wired laser energy probes, (2) the ability to read all eight channels from any networked computer in the facility, and (3) the ability to trigger, by remote control, a single laser pulse synchronized to ATF' s electron linear accelerator (LINAC). CLEMS has been designed using National Instrument's (NI) LabView 5.1.1. The program interacts with NI's MIO-16E-1 data acquisition board and the BNC-2090 accessory. Optoacoustic laser probes used to measure laser energy have been studied and calibrated to work with the BNC-2090 accessory. The remote synchronous triggering capability of the system has been developed using Rayming's transmitter and receiver boards along with Reynolds Electronics' RX-6 relay module and a synchronization circuit. CLEMS has been verified to work on the network with optoacoustic laser probes and remote synchronous triggering capability in a high electro-magnetic noise environment associated with operation of ATF's laser system. More electro-magnetic noise will be generated once ATF's terawatt laser amplifier system is powered on. The functionality of CLEMS in the presence of the terawatt amplifier system is currently under investigation. Future work will include setting up CLEMS to work with a variety of joulemeter probes, making improvement to the server/client interface, and studying the effects of noise on remote synchronous triggering and data acquisition.

Health Monitoring for Space Power Systems Using a Phosphor-Based Sensor Suite. *NOAH BERGERON (University of Louisiana at Lafayette, Lafayette, LA 70504) STEPHEN ALLISON, SHAWN GEODEKE, WILLIAM A. HOLLERMAN (Oak Ridge National Laboratory, Oak Ridge, TN 37831).* Phosphors are fine powders created by doping inorganic materials with rare earth or other elements. For many years, phosphors have been used for non-contact temperature measurements in hostile environments, including large blackbody radiation backgrounds, vibration, rotation, fire/flame, or pressure. Often these environments restrict the use of more common thermocouples or infrared thermometric techniques. Phosphors like $Y_3Al_5O_{12}$ (YAG) doped with Eu, Dy, or Tm, Y_2O_3 doped with Eu, or similar compounds, will survive high temperatures and can be configured to emit light that changes rapidly in lifetime and intensity. Recently, research has also shown that triboluminescent (TL) phosphors show promise for use as the active element in impact sensors. Preliminary testing shows that TL emission can be detected for impact velocities from 0.2 m/s to about 6 km/s. A TL detection system could determine if a particle had hit, and record the relative intensity of the impact. To be used in a nuclear propulsion system, any phosphor must also be resistant to ionizing radiation that is present in the natural space environment and produced during operation of the fission engine. For example, research over the last decade has shown that proton irradiation reduces the intensity of fluorescence. This presentation will discuss our efforts to utilize phosphors as health-monitoring tools for an operational nuclear spacecraft. The goal of this research is to try to invent an integrated "suite" of sensors to simultaneously measure temperature, impact, and radiation fluence for components in a future nuclear engine.

Electrical Engineering Support for Plant Projects. *RICHARD BINGHAM (University of Idaho, Moscow, ID 83843) DARREL BEEBE (Argonne National Laboratory, Argonne, IL 60439).* Electrical engineering at Argonne National Laboratory - West involves little research. What it does involve is an extensive amount of application of electrical engineering concepts to ensure equipment functions properly and safely. Projects cover a broad spectrum of topics from power system design to control systems both digital and analog. The projects focused on in this paper are more basic in nature involving primarily power distribution to equipment and analog control system analysis. Projects include installation packages for a split-system air conditioning unit, a 55-gallon drum compactor and a 10,000 pound capacity platform scale. Each project is discussed individually from start to finish to avoid confusing topics and to demonstrate the engineering process.

Robot Design And Refurbishment Using The Creative Design Process. *HELEN BONDS (University of Tennessee, Knoxville, TN 37916) BRADLEY WEIL (Oak Ridge National Laboratory, Oak Ridge, TN 37831).* In order to develop the most efficient and innovative solution to meet a set of problem requirements, engineering teams use a process called the creative problem solving process, or the creative design process. This process was demonstrated and observed in two projects. The first was a creative design workshop conducted for teams of high school students and the second was a team project to propose upgrades for a commercial robot. For the workshop, students received a brief presentation introducing the creative problem solving process and then used LEGO® Mindstorms Robotic Invention Systems to create an autonomous robot that would perform certain table top missions. This required building and programming the robot with minimal instruction. The high school students used the creative design process unconsciously, as a way of thinking, as they built and modified their robots in unique ways. The process was apparent while students discussed with teammates how to modify the robot in more creative and efficient ways to accomplish an objective. For the robot upgrade proposal project, research was conducted and ideas were developed to repair and upgrade a used Andros Mark V robot for use in emergency response situations. The creative design process was used to evaluate new requirements, organize ideas to upgrade the robot, and direct the development of the proposal. Requirements for the robot system were provided by the

Emergency Preparedness Group (EPG) at Oak Ridge National Laboratory (ORNL). The creative design process helped the proposal team organize the vendor information researched for upgrading the Andros robot. The process also allowed for effective presentation of ideas by the proposal team for the Andros upgrade within the desired parameters for the proposal. In these ways, the creative design process served as an outline for proposal's development. The creative design process can be a thinking style used in an unconscious manner, as shown in the student workshop, but the process can also aid in idea organization, as seen in the Andros proposal construction. Both uses of the process can result in a more efficient and productive design development.

Transfer and Storage of a Refrigeration Plant's Components. *TERESA BONK (Binghamton University, Binghamton, NY 13902) DANA ARENIUS (Thomas Jefferson National Accelerator Facility, Newport News, VA 23606).* In preparation for the 12 GeV Upgrade of the Continuous Electron Beam Accelerator Facility (CEBAF), the Cryogenic Systems Group at JLab is planning the construction of a new End Station Refrigerator (ESR), a refrigeration plant. The majority of the equipment for this new cryogenics plant is being transferred from Brookhaven National Laboratory (BNL). The implementation of this new cryogenics plant can be summarized in four stages. First, a transportation plan was devised, taking safety and condition of the equipment into consideration. Second, upon the arrival of the items at JLab, a storage plan with exact locations was established. Next, an inventory record was kept of all crated parts arriving from BNL. Finally, a plan for the new ESR building operational layout was devised. A storage layout was formulated for all items. A Microsoft Access database was developed and implemented which includes identification numbers, descriptions, and pictures of the corresponding parts. This storage layout will assist in maintaining the usability of the parts, prevent any further deterioration, and create an orderly environment. The database will provide information to determine what additional equipment is required during the new ESR design and assembly.

Increasing Productivity and Communication Among Users in a Product Development Environment. *SPENCER BONNER (Brigham Young University - Idaho, Rexburg, ID 83440) PAUL CHOI (Argonne National Laboratory, Argonne, IL 60439).* A concurrent environment exists at Argon National Laboratory, with multiple Users updating, changing, and modifying designs - which unattended to can lead to many problems. Productivity and communication are essential; Pro/Intralink solves many of these problems. This product development environment allows attributes to be saved to drawings in an organized manner, as well as regulate the changes occurring to them. We have been updating old drawings, many of which are still in use, so that they may be placed in Pro/Intralink, allowing users to search for, find, and change these drawings as needed. This is accomplished by inserting new Titleblocks, Revisionlines, and Bills of Materials (B.O.M.) into the drawings and placing them in Pro/Intralink. Also to increase productivity, we have developed many "Blocks" (Revisionlines, B.O.M. and Symbols). These Blocks, capable of being inserted into any drawing, provide a common standard and save time. The results of implementing these have provided a timesaving standard and made more information accessible to Users.

Thermal Analysis of Non-Fertile Uranium Metal Alloy Transmutation Test Fuels and Kinetic Analysis of Oxidation of Uranium Hydride. *ALLISON BOURKE (University of Arizona, Tucson, AZ 85719) J. RORY KENNEDY (Argonne National Laboratory, Argonne, IL 60439).* The research completed this summer at Argonne National Laboratory aided in two investigations. The first study is part of the Advanced Fuel Cycle Initiative (AFCI) and is designed to dispose of the long lived minor actinides in spent fuel. Specifically, a portion of Argonne's goals are centered on transmutation of minor actinide isotopes in metal alloy fuels. The first project was thermal analysis of a non-fertile metal alloy transmutation test fuel (Pu-^{12}Am-^{40}Zr), and the ceramic ZrN fuel baseline material. Using a Differential Scanning Calorimeter/Thermogravimetric Analyzer (DSC/TGA), the heat capacity was determined. Both of these heat capacity measurements assisted in determining the thermal conductivity of the fuel which helps model the fuel in the reactor. The second project was analysis of kinetic data that was produced from the oxidation of uranium hydride (UH_3). The goal was to fit the kinetics of the reaction to one of four basic kinetic equations: linear, parabolic, paralinear, and logarithmic. The focus of the research reported here is toward understanding the properties and reaction of metal and ceramic fuels.

Proposal for The Department of Energy to Modify and Maintain the Andros Mark V Robot. *CHADWICK BRANHAM (Roane State Community College, Harriman, TN 37748) BRADLEY SCOTT WEIL (Oak Ridge National Laboratory, Oak Ridge, TN 37831).* The Emergency Preparedness Group (EPG), in the Laboratory Protection Division of ORNL, needs a robotic system to assess damages and hazards in emergency situations, caused by accidents, terrorism, or natural disasters. It could be used when personnel access is limited due to the presence of biological, chemical, or radiological agents. The Remote Systems Group (RPG), of the Nuclear Science and Technologies Division, has an Andros Mark V robot which may be applicable in this situation. Parts of the robot are contaminated from previous environmental cleanup, and it is not readily equipped to handle the assessment of a hazardous environments. There exist several options which might be pursued to augment the capabilities of the Andros robot. A number of meetings have been held with different companies who may be beneficial in providing new technologies for this project. Remotec, the company that built the robot, has offered several solutions. A tether is currently used for the control link; however, Remotec has suggested the use of fiber optics or wireless connections. Remotec also offers sensors which have mounts already designed for the Mark V: the APD 2000 chemical detector, ADM 300 radiation detector, and MultiRae gas monitor. The IPIX Corporation has presented their 360° view camera system. A digital x-ray system is also available from Golden Engineering which could be valuable for inspecting unkown objects. For any of these modifications rewiring of the internal components of the robot must be done. A proposal is being prepared for the Department of Energy to give a cost estimate of these modifications and of personel training in the robot's operation. Some of these options meet the requirements of the EPG more than others, and each option will be weighed. The goal is to complete the proposal and submit it to DOE to be funded.

Large-scale Spatial Data Segmentation. *TIGE BROWN (Southern University A&M College, Baton Rouge, LA 70128) KENNETH TOBIN JR. (Oak Ridge National Laboratory, Oak Ridge, TN 37831).* Large-scale spatial data segmentation focuses on aerial images using region segmentation to train imaging programs for automatically locating important structures of interest such as buildings, vehicles, or land resources. The goal of this work is to evaluate three different segmentation approaches. To accomplish this goal, two commercially available software packages (ERDAS IMAGINE 8.5 and Adobe Photoshop Elements 1.0) and one custom algorithm written in MATLAB (a high-level technical computing language) were used to segment the image background from the region of interest. There are two pixel classification methods available for defining region segmentation: supervised and unsupervised. Histogram classification is the process used in both the ERDAS and Adobe software. However, ERDAS allows for user input in defining the quantity of histogram classes (unsupervised) or automatic histogram processing of classes (supervised). Adobe only allows for the latter, which requires a simple single-threshold value to eliminate the background image. All applications require the user to manually select the region of interest for training images. Only ERDAS and Matlab allows for automatic selection after the training process. The effectiveness of algorithms is determined after visually inspecting several printed samples. Preliminary results using Matlab, the histogram min/max-threshold for the ERDAS, and simple-threshold for Adobe illustrate the usefulness of each program. Each program required user visual decision making in determining when the process is complete. This method tends to lead to minor error, as each user will visualize an image differently. After visual examination, ERDAS IMAGINE 8.5 and Adobe PSE 1.0 appear to reproduce the best-segmented regions. Matlab produced relatively similar segmented regions based on a neighborhood-based Euclidean-distance method. Adobe and Matlab are easier to use with few processes required by the user. However, Matlab's automated segmentation resulted in a faster completion time, unlike Adobe's manual processing throughout. Further testing is required in order to get a complete visual analysis of each application. Once the selection of the training tools is complete, Matlab or another programming language such as MS Visual C++ will utilize the training examples to automate image segmentation. This tool will greatly assist in many areas of business, military field operations, or National Security.

The Tuff Cell. *JEFF BROWN (Brigham Young University - Idaho, Rexburg, ID 83440) DAVID CARTER (Argonne National Laboratory, Argonne, IL 60439).* We have been working for a long time on the SOFC to create less internal resistance, and to make it more resilient to physical abuse and less expensive. The new TUFF CELL is the modified design of the SOFC that meets these criteria. The expensive support layers in the SOFC (nickel and zirconia) are made thinner in the Tuff Cell and are reinforced with stainless steel. This gives even better support than the brittle ceramics of the SOFC model. Also, with a one step sintering process, one less interface is required between the cell and interconnect, which decreases the internal resistance of the cell.

We have not actually succeeded in completing a satisfactory sample Tuff Cell, but future work will surely complete and perfect what we have begun.

Analysis of Fuels Effects on Autothermal Reforming. *TAMIKA BROWN (Lewis University, Romeoville, IL 60446) JOHN KOPASZ (Argonne National Laboratory, Argonne, IL 60439).* Autothermal reforming is the production of hydrogen for fuel cells through the combined processes of oxidation and steam reforming. In order to learn more about this process and the effects that fuel composition will have on this process we are performing tests with the use of our Short Term Test Reactor. The reforming process is accomplished by combining a hydrocarbon fuel with steam and oxygen with the use of a catalyst and recording data at reactor temperatures ranging from 650-800°C in increments of 50°C. Study was done on the effects of 1% hydrogen peroxide (H_2O_2) on the reforming of isooctane. The results indicate that hydrogen peroxide has a positive effect on the reforming process. Future testing will focus on what outcomes a 10% hydrogen peroxide solution has on the reforming process as well as other additives.

Separation and Recovery of Plastics from Auto-Shredder Residue. *FELICIA BURKES (Georgia State University, Atlanta, GA 30303) BASSAM JODY (Argonne National Laboratory, Argonne, IL 60439).* The separation of polystyrene (PS) and acrylonitrile butadiene stryene (ABS) from auto-shredder residue (ASR) will be discussed. The product of these two thermoplastics yielded above 95% using a method referred to as froth flotation. Froth flotation has proved to be an effective method for separating these two plastics which have overlapping densities. The thermoplastics were analyzed using FT-IR and wet chemistry techniques. Keywords: polystyrene, acrylonitrile butadiene styrene, auto-shredder residue.

3-Phase Inverter Control with PC-Generated Pulse Width Modulation. *TIMOTHY BURRESS (University of Tennessee, Knoxville, TN 37916) CURT AYERS (Oak Ridge National Laboratory, Oak Ridge, TN 37831).* Most controller implementation methods require a vast amount of controller development time to be spent on programming microprocessor(s) for their specific application. A primary goal of this project was to implement an automated process that quickly accommodates to design changes. This is possible by directly controlling systems through a computer interface. The controller was modeled in Simulink on a console PC and then compiled and simulated with RT-LAB software on a PC-cluster consisting of 3 processors running at 1 GHz. Two of these processors are in a dual-CPU configuration on one motherboard which is connected by FireWire to another motherboard and processor. A National Instruments NI6602 card was used to generate the PWM signals based on a duty cycle command from one of the computational nodes (computers) each sampling period. Output signals were monitored to test the controller's capabilities while using various switching frequencies and time sampling steps of 100 µs and 50 µs. Compilation and distribution of the controller model to the PC-cluster was achieved in under a minute. Initially, tests were performed with parts of the controller distributed to separate computers and the results contained unacceptable modulation error. When using only the Dual-CPU computer, the controller performed properly until the carrier frequency surpassed the sampling rate, which is expected. Distributing the model on the PC-cluster requires communication between the computers by the FireWire connection, which limits the time step to just below 100 µs. If closed loop control is needed, more intensive calculations may require another CPU. Hence, the switching frequency will be limited to about 10 kHz due to FireWire communication. The IEEE-1394b FireWire standard is faster and will permit higher sampling rates and switching frequencies to be used. If the closed loop controller uses techniques such triangular wave comparison, RT-Events blocks need to be used to account for precise intra-step events. By modeling the controller in Simulink, it can be tested on an inverter modeled in Simulink before connecting it to an actual inverter. This also creates a possibility to save a large amount of development cost and time.

Design and Operation of a Cryogenic Radiation-Effects Apparatus. *KIMBERLY BUTCHER (University at Buffalo, Amherst, NY 14261) GEORGE ALANSON GREENE (Brookhaven National Laboratory, Upton, NY 11973).* The evaluation of radiation effects is crucial in the design and operation of facilities which would be subjected to long periods of high-intensity, high-energy particle irradiation. Such effects can be encountered in diverse applications such as space exploration, nuclear physics studies and nuclear reactor facilities. Our objectives were to design, construct and operate a portable and versatile vacuum-cryostat apparatus that would be capable of performing measurements on the effects of various forms of ionizing radiation on matter, with a precision not previously achievable. The apparatus would use novel cryogenic techniques recently developed at Brookhaven National Laboratory to perform precision measurements of radiation effects, including energy deposition due to nuclear spallation radiation of protons and heavy ions in structural materials and radiation damage in metals, oxides and superconductors by protons and neutrons. The apparatus consists of a vacuum chamber into which a liquid helium cryostat is inserted; instrumented targets are mounted to the cold-head. Resistance measurements are taken of the targets with high precision at liquid helium temperature in a hard vacuum. Radiation effects are evaluated by correlating these electrical resistance measurements with physical parameters in, such as specific energy deposition (J/gm/particle) or radiation damage displacement cross sections (barns), order to quantify the effects. Initial shakedown testing of the apparatus indicates reliable operation at 10-9 Torr and 5K for up to 24 hours, with a precision of 0.01 K in controlling temperature. Our experimental plans are to measure radiation damage displacement cross sections by neutrons and protons, and eventually heavy ions, over an energy range of several MeV to several GeV.

Mapping Antireflection Coating Thickness Using GT-FabScan 6000: Experimental Implementation. *BRIAN BUTTERFIELD (California Polytechnic State University, San Luis Obispo, CA 92117) BHUSHAN SOPORI (National Renewable Energy Laboratory, Golden, CO 89401).* Typically, AR (antireflection) coating of a Si (silicon) solar cell should have a uniform distribution of about 750 Å of thickness. Commercial AR coatings in the PV industry exhibit variation of ± 100 Å in film thickness, which is about 3-4% loss in cell photocurrent density. However, in the current Si solar cell fabrication technology, AR coating is also used as a buffer for fire-through screenprinted contact. The characteristics of AR coating on Si wafers can critically influence the electronic yield of completed solar cells. Thus, there is a need for the development of a method for rapid measurement of AR coating on Si solar cells. Using the GT-FabScan 6000™ (previously known by other names i.e., Sopori Reflectometer or PV Reflectometer), AR coating may be rapidly mapped into an image representing the thickness distribution. To accomplish this rapid mapping capability, the GT-FabScan 6000™ uses a camera fitted with a bandpass filter to record an image of an AR coated Si solar cell sample. Using an algorithm, the recorded intensity-image is processed and the resulting image is a mapped thickness distribution. The converted image is then assigned a false-color scheme to identify thickness distribution. These maps provide valuable information for monitoring the behavior of the AR coating deposition machine and control subsequent Si solar cell manufacturing processes.

Friction and Wear of NFC-6 and Super Hard Coatings in Dry Nitrogen. *JEAN SCOTTY CADE (Illinois Institute of Technology, Chicago, IL 60616) GEORGE FENSKE (Argonne National Laboratory, Argonne, IL 60439).* The purpose of the project is to assess the tribological parameters of Near Frictionless Carbon (NFC-6) and Super Hard Coating (SHC) on steel under dry nitrogen sliding. The speed, load, and environment, were kept constant while considering the coated and uncoated surfaces as the independent parameters. Numerous analytical and numerical data were collected using a number of instruments. A High Frequency Reciprocating Rig (HFRR) records the friction coefficient between the sliding surfaces. An Optical Profilometer was used to estimate the amount of material removed. An optical microscope was used to for visual identification and measurement of coating thickness. Raman Spectroscopy was used to assist in determining whether the surfaces become more amorphous or crystalline as shown on Graph 2. Importantly, although friction and wear both arise from sliding surface contact, high friction does not necessarily mean high wear. Results indicate overall that Bare-ball-NFC-6 plate has the lowest coefficient friction; however, Bare ball-SHC plate has the highest wear resistance. Future work will include revalidating some of the experiments for reliable results but most importantly testing in isobutane and hydrogen varying the speed, load, temperature, etc.

Examining Rhodium Catalyst Complexes for Use with Conducting Polymers Designed for Fuel Cells in Preparing Biosensors. *MELISA CARPIO (University of California, Berkeley, Berkeley, CA 94720) JOHN B. KERR (Lawrence Berkeley National Laboratory, Berkley, CA 94720).* Biosensing devices are important because they can detect, record, and transmit information regarding the presence of, or physiological changes in, different chemical or biological materials in the environment. The goal of this research is to prepare a biosensing device that is effective, quick, and low cost. This is done by examining which chemicals will work best when placed in a biosensor. The first study involved experimenting on the rhodium catalyst complexed with ligands such as bipyridine and imidazole. The rhodium catalyst is important because it reduces from RhIII to RhI, releasing hydrides that can react with nictotinamide adenine dinucleotide (NAD+) to selectively

produce 1,4-NADH, the reduced form of NAD+. The second study looked at different types of ketones and enzymes for the enzyme-substrate reaction converting a ketone into an alcohol. This is the final of a three step process that is common to biosensing devices. Prelimary results show that the rhodium complexed with bipyridine was able to carry out all the reactions, while the rhodium complexed with imidazole was not able to reduce and release hydrides. In addition, the most effective ketone to use is benzylacetone with the enzyme alcohol dehydrogenase from baker's yeast. Future work includes experimenting with bis-imidazole, which mimics the structure of bipyridine to see it if has the capability to reduce and if the reduction rate is comparable to the bipyridine complex. Once all testing is completed, the fastest of the catalysts will be combined with polymer membranes designed for fuel cells to prepare a biosensor.

Ultrasonic Viscometer. *JENNY CHIN (Onondaga Community College, Syracuse, NY 13207) S.* SHEEN (Argonne National Laboratory, Argonne, IL 60439). The Argonne National Laboratory's Ultrasonic Viscometer is a device that measures both density and viscosity, by using ultrasonic technique. This is based on a technique that measures acoustics and shear impedance. The reflection of incident ultrasonic shear and longitudinal waves launch toward the surface of the two-transducer wedges that are in contact with fluid are than measured. This means it can be reflected off very small surfaces, which generates a hearing range above human hearing called ultrasound. For both solid /liquid and solid/gas flows ultrasonic techniques or instruments that have been developed to measure average velocities of particles and fluids. Two basic qualities are measured in ultrasonic: the time of flight or the amount of time for the sound to travel through the sample and amplitude of received signal. Longitudinal waves measures fluid density and the shear wave measures the viscosity. Current research on the following substances has been tested, which are air, water, glycerol with different concentrations, corn oil, condensed sugar, and motor oil.

Digital Lock-In Amplifier Based Ground Loop Monitoring System for Magnetically Confined Plasma Devices. *TIMOTHY CONNELLY (Villanova University, Villanova, PA 19085) HANS SCHNEIDER (Princeton Plasma Physics Laboratory, Princeton, NJ 08543).* The National Spherical Torus Experiment (NSTX) at the Princeton Plasma Physics Lab currently uses an analog lock-in amplifier in its Ground Fault Monitor (GFM) system for ground loop detection. For the forthcoming National Compact Stellerator Experiment, a new GFM is under development. The GFM for NSTX is a heritage system originally designed for the Tokamak Fusion Test Reactor and has since had significant enhancements of increased Loop Fault Sensitivity, improved operator interface, and data archiving. Although the analog GFM is highly effective, a digital GFM may further increase operational performance while adding new features using Digital Signal Processing techniques. The digital system runs on a Personal Computer with National Instruments NI-4472 data acquisition hardware along with the tightly integrated LabVIEW software. LabVIEW's Lock-In Amplifier and Digital Signal Processing building blocks saved a significant amount of development time. The primary goal of the research was to determine the feasibility of a LabVIEW based GFM on a bench test setup. The LabVIEW Lock-In Amplifier returns measurements in volts. However, for the GFM, resistance measurements are needed. The system was tested over a range of resistances with a transmit frequency of 140 Hz, drive amplitude of 15.9 volts, and Lock-In FIR filter settings of 8 (s) time constant and 60 decibel rolloff. The data was plotted in Microsoft Excel and the trendline feature was used to obtain an equation to convert the voltage returned by the Lock-In Amplifier to resistance. A second filter and spectral measurements have been implemented successfully using LabVIEW functions. The tasks to be accomplished in the future are data-archiving, in-situ testing on NSTX, test for capacitive loop fault detection, and creating a dynamically variable transmit signal. The LabVIEW Lock-In Amplifier was shown to function at least as well as the previous system detecting faults of 15 kilohms and with some adjustments to filter settings and conversion equations the performance of the digital Lock-In Amplifier should exceed the performance of the analog system.

Development of Electronic Logic for the Brookhaven Atmospheric Tracer Sampler. *JOHN CORNWELL (Duke University, Durham, NC 27708) JOHN HEISER (Brookhaven National Laboratory, Upton, NY 11973).* The Brookhaven Atmospheric Tracer Sampler (BATS) is designed to collect air samples by pumping air though adsorbent tubes. Manmade tracers, which are released into the atmosphere at various locations, pass though the tubes and become trapped on the adsorbent material inside. The tubes are then brought back to the lab for analysis. Although the pumping and pneumatic valve systems are still state of the art, the electronic logic within the BATS has become outdated over the past 20 years. It lacks programmability and is prone to failure in the field. The main goal of this internship was to examine possible means of improving or replacing these electronics. Options ranged from simply redesigning the digital logic to imbedding a ruggedized laptop within the machine to control it. The option mainly explored was to use a Personal Digital Assistant (PDA) to control the pump and valves. The PDA was programmed using Embedded Visual C++ to have the functionality of the BATS logic through a graphical user interface. To activate the pump and valve assembly, the PDA was connected to a simple circuit board through a nine-pin serial cable. This circuit board was developed with a PIC18F1320 microcontroller to read serial input signals and provide motor controllers to activate the pump and valves on the BATS. The benefits of using a PDA are its programmability and it's ability to change sample periods on the fly using 802.11b wireless internet. Although this solution still requires circuitry, it was simple and inexpensive to develop a working prototype. The circuitry needed was uncomplicated because all of the behavior of the unit was stored in memory on the PDA.

Automation of Spallation Neutron Source Diagnostics Instruments: Laser-Wire Magnet Mapping Test Stand. *SCOTT CRAWFORD (Colorado College, Colorado Springs, CO 80903) SAEED ASSADI (Oak Ridge National Laboratory, Oak Ridge, TN 37831).* The Spallation Neutron Source particle accelerator being constructed at the Oak Ridge National Laboratory requires testing equipment for beam components that allow for fast measurements with high repeatability, high accuracy, and that are easy to use. The laser-wire magnet mapping device is a four axis stepper motor control stage. A graphical user interface has been designed using the LabVIEW programming language. The purpose of this project is to automate the magnet field mapping, through the space between two annular magnetic plates with incremented input control current, to allow systematic and consistent measurement of the 3D field collector profile. This will reduce the needed human labor to perform the measurements, document the measurements, and setup time. Spatial position, electrical current, and magnetic field values between the magnetic plates are tabulated by the program. These values are stored in a data file for future reference or graphing. The field readings can be used to determine if changes have occurred in the magnet over time, or initially to discover if there are any manufacturing defects in the magnet. The automation program has been written, tested working, and is thoroughly documented.

Fine Temporal and Spatial Scale Remote Sensing. *KATHLEEN CUMMINGS (Franklin W. Olin College of Engineering, Needham, MA 02492) EARL MATTSON (Idaho National Engineering & Environmental Laboratory, Idaho Falls, ID 83415).* Most existing multispectral remote sensing systems are satellites. NASA's Landsat 7 Enhanced Thematic Mapper Plus (ETM+) looks at a patch of ground 185km wide and revisits an area every 16 days. Cloud cover can prevent meaningful data from being obtained. A higher temporal and spatial resolution sensor will allow data to be collected during times of high precipitation and cloud cover, which coincide with times of high plant growth. To get higher resolution data, a remote sensing system was designed that is capable of capturing aerial images from a height of 35 feet at short time intervals. The system collects data from both a thermal and a multispectral camera in the red, green, near infrared, and thermal infrared bands. The cameras and a single-board computer run off of solar power and can be left in remote locations for extended periods of time. The initial application for this system will be studying percolation ponds in the Vadose Zone Research Park (VZRP), an instrumented region near the Idaho Nuclear Technology and Engineering Center (INTEC). The ponds appear to shrink and grow, and an attempt will be made to correlate the surface area of the pond to the flow rate of water into the pond. Possible future applications for this image capturing system include studying vegetation stress and recharge, thermally identifying exothermic reactions in landfills, and identifying groundwater runoff in streams. The cameras will eventually move from a tower platform to small, unmanned aircraft, allowing for easier mobility and image capture over a larger area.

Development of a Lithium Thin Film for Electron Stripping. *MICHAEL DALY (University of Illinois, Champaign, IL 61820) VINCENT J. NOVICK (Argonne National Laboratory, Argonne, IL 60439).* A flowing liquid lithium thin film is a novel approach to electron stripping. Rather than a solid material which would be vaporized by a high energy beam, a flowing liquid is necessary to be able to dissipate the power of the Rare Isotope Accelerator (RIA) particle beam. The goal of this development effort is to demonstrate the capability of producing a lithium thin film that flows at at least 50 m/s and is 4 microns thick. Initial tests have been conducted with water to assess the stability of a thin film with various nozzles and pressures. Using dimensionless Weber and Reynolds numbers, it has been postulated that the thickness and velocity of water and lithium are linearly related based on the physical properties of the liquids. It was found that all water films were convectively stable if their

Weber number was above 27.7 and some were stable with Weber numbers as low as 21.6. This range suggests that the lithium film desired for electron stripping would be convectively stable also. It is also suggested from the water data that the collision between the nozzle jet and the deflector is virtually elastic.

Autothermal Reforming Catalysts for Fuel Processing for Fuel Cell Systems. *WESLEY DARIN (University of Illinois at Urbana-Champaign, Urbana, IL 61801) THEODORE KRAUSE (Argonne National Laboratory, Argonne, IL 60439).* Autothermal reforming of fossil fuels is being studied in order to develop an onboard reforming system that would produce hydrogen for use in a fuel cell powered automobile. Autothermal reforming (ATR) is the process where fuel, water, and air react in appropriate ratios in the presence of a catalyst in order to produce hydrogen. An effective catalyst is one that will enhance the production of hydrogen, limit hydrocarbon production, and resist coke formation. The catalyst must be able to perform at both high and low temperatures, and also have a high sulfur tolerance. The ideal catalyst must also be cost effective and readily available, so that it may be used commercially. ATR tests were performed in a microreactor using both rhodium (Rh-Re, Rh-Pd), and platinum (Pt-Pd) based catalysts. All catalysts tested were on a lanthanum alumina ($La\text{-}Al_2O_3$) support. Tests were performed on gasoline and isooctane, both with and without sulfur. Sulfur containing fuels were tested to investigate the sulfur tolerance of the catalyst. Tests were performed at 700°C and 800°C to observe the effect of temperature on the catalyst. A gas chromatograph was used to sample and analyze the product gas. The goal was to find the best possible catalyst for ATR. Tests showed that rhodium is a better catalyst than platinum. However, the rhodium catalysts that were tested fail to meet all of the criteria, as they not only have a problem with coke formation (due to sulfur), but also are far too expensive and rare to be a viable solution for commercial use. Future tests will continue experimenting with different metal combinations as catalysts, perhaps trying to use non-precious metals that would be more cost effective.

Devices and Methods for Synthesis and Investigation of Porous Aluminum Oxide. *ROCIO DIAZ (Richard J. Daley College, Chicago, IL 60653) REX E. GERALD II (Argonne National Laboratory, Argonne, IL 60439).* Solid-state lithium ion batteries are one of the most promising battery technologies for future hybrid and electric cars. However, because these solid-state batteries present low ion conductivities of 10-5 S/cm, they need to be improved. We propose a novel solid-state separator/electrolyte that will provide the high power and energy densities demanded for good acceleration and driving range. Anodized aluminum oxide (AA0) has been identified as an ideal material for studying fundamental solid-state ion-transport mechanisms. Synthesis and characterization of AAO membranes is conducted for basic understanding of structure and composition. AAO synthesis is performed using the Single Sided Anodizer (SSA) device by electrosynthesis of aluminum metal plates in 0.3 M aqueous oxalic acid. Following the electrosynthesis process, the backside residual aluminum metal was removed by chemical oxidation using a solution of $CuCl_2$ in 2 M HCl. We report our investigations of AAO membranes by characterization using AFM, FTIR, TGA and NMR. AFM gives information on the AAO pore structure, for example AAO pore diameter in the range of 50 to 120 nm. FTIR is used for studying functional groups of molecules trapped in the AAO membranes. We observed a broad OH band in the 3700-3200 cm^{-1} region and CO_2 formation via a sharp band in the 2300-2200 cm^{-1} region. Removal and monitoring of OH, assigned to bulk water, was performed in-situ by employing an FTIR heater device. TGA was used for investigation of pore density; we found a 20 wt. % reduction in AAO membranes. NMR shows nearly 100% highly mobile ionic lithium cations in a LiI/Al_2O_3 solid-state electrolyte system. Future work will focus on a more detailed AAO synthesis, measuring lithium ion conductivity in AAO membranes, and assembling and cycling of lithium-ion batteries.

Fundamentals of Programmable Logic Controllers (PLCs) and designing a PLC Controlled Accelerator Experimental Beamline Access Security System. *WILLIAM DINAPOLI (Bronx Community College, Bronx, NY 10462) VINCENT CASTILLO (Brookhaven National Laboratory, Upton, NY 11973).* Allen-Bradley (A-B) has 2 Programmable logic Controllers (PLC) application software packages: RS Logix generates logic codes for reading data from sensing modules and writing commands to controlling modules and RS View allows for the formulation of human-machine (H-M) interfaces, on computer screens, that interact with operating systems in real time using the information from the RS Logix program. Simple RS Logix programs are written and tested on hardware in a laboratory setting to get an understanding of how these programs function, along with the RS View H-M interfaces. This knowledge and skill with RS Logix and RS View is used to build a Controlling system for access security to a typical Experimental Beamline on the Experimental floor of the Alternating Gradient Syncrotron (AGS).

Thermal Effects On Structural and Tribological Properties/Behavior of NFC-7 Coatings. *STEVEN ELMORE (Tuskegee University, Tuskegee, AL 36088) GEORGE FENSKE (Argonne National Laboratory, Argonne, IL 60439).* Near Frictionless Carbon (NFC) is an astonishing new coating developed by the Energy Technology's Tribology section. It is used on different materials as a lubricant that helps minimize the friction and wear between two sliding surfaces. There are three different types of NFC coatings. There is NFC-2, NFC-6, and NFC-7. The NFC-7 coating was used in all the tested materials for this project. The overall goal of these experiments was to study the high temperatures properties of the coating on various substrates. There were three main tests that were performed. The first two tests were done using circular disk samples that were made from steel. That last test was done using a silicon substrate. In each test the samples were coated with NFC-7. From the test results we found that there is a critical temperature at which the NFC-7 starts to fail. This temperature was said to be somewhere between 200 and 300 degrees Celsius. When this temperature is reached the coating completely comes off the silicon substrate however it remains on the steel substrate. Also above the critical temperature we discovered that NFC-7 has a significant increase in the wear volume. Future work would consist of focusing on the exact temperature at which the coating fails and why it fails at that temperature. It would also be beneficial to explore ways to make the coating last at higher temperatures.

Shutdown and Maintenance of Central Helium Liquefier. *OLGA EPSHTEYN (The Cooper Union for the Advancement of Art and Science, New York, NY 10306) DANA ARENIUS (Thomas Jefferson National Accelerator Facility, Newport News, VA 23606).* At Jefferson Lab, cryogenics is one of the major utilities of the accelerator, providing the essential liquid helium required for the operation of the superconducting cavities. Between July 26 and August 25, shutdown and partial maintenance for the Central Helium Liquefier (CHL) is planned, leaving the accelerators in a stand-by mode. In order to prevent the loss of helium, during the shutdown, the Stand-By Refrigerator (SBR) will be used to maintain the two superconducting accelerators, the Continuous Electron Beam Accelerator Facility (CEBAF) and the Free Electron Laser (FEL), at cryogenic temperatures. Since the SBR is used on a very limited basis, preparation is required to properly operate the system and to maintain liquid helium within it. An adequate procedure and schedule must be made in preparation for the shutdown. The SBR must be checked and purified before it is connected to the accelerator system. It is important to note that the SBR only has limited operational power. Unlike the CHL, which services the Linear Accelerators (LINACs) at 2.1K, the SBR operates at 4.5K with limited refrigeration capacity. This temperature is just low enough to maintain helium in its liquid state, but it is not enough to keep the accelerators operating. Once the SBR is ready and operational refrigeration, the maintenance will begin with repair of the CHL compressor system, which includes the compressors and piping. After the compressors are serviced, the main cold-box will be shutdown and temporarily replaced with the SBR cold-box. During maintenance, the charcoal adsorbers and the damaged valves will be replaced, the CHL cooling tower basin will be repaired, along with any other necessary maintenance. After the scheduled maintenance, the CHL will be cleaned and purified before startup for any contaminants such as air or water. Because of the limited refrigeration capacity provided by the SBR, it is important to prepare an organized schedule for the shutdown and to complete the maintenance in the allotted period to minimize the accelerator down time. The requirements for maintenance, safety, the clean-up time, other customer demands, and general deadlines must be taken into account in preparation for the CHL shutdown. With the completion of the shutdown, the CHL will be able to return to standard operations, providing customers with 2.1K operational liquid helium for the accelerator and various experiments.

Practicality of Biomass Energy Production. *DANIEL FEINAUER (Brigham Young University - Idaho, Rexburg, ID 83440) CHUCK SOLBRIG (Argonne National Laboratory, Argonne, IL 60439).* This report is an evaluation of biomass energy. The report describes biomass as electricity produced from biological material. The report is focused on four types of biomass power plants: direct-fired combustion, co-firing, gasification, and small modular biopower. Direct fired combustion plants burn biomass fuel in a boiler. The boiler causes stream that rotates turbine blades connected to an electric generator and produces electricity. Co-firing plants are coal plants that replace a portion of coal with biomass. Gasification turns solid biomass into a liquid flammable gas a more efficient source of energy. Small modular biopower is smaller biopower plants that are used to provide energy to rural areas. This

report also discusses the sources or fuels used to produce biomass energy namely: urban residues, mill residues, forest residues, agricultural residues, and energy crops. Urban residues consist of wood chips and wood grindings. Mill residues include sawdust, bark, and wood scraps from paper, lumber, and furniture manufacturers. Forest residues include underutilized logging residues, imperfect commercial trees, dead wood, and other non-commercial trees. Agricultural residues are the biomass materials remaining after harvesting agricultural crops. For example, corn stalks can be used to produce ethanol and when mixed with gas creates gasohol. Energy crops are crops developed and grown specifically for biomass fuel. The pros and cons of biopower are discussed. The main purpose of this report is to help the reader make an educated stand on whether they should be for or against biomass energy. The possible future expansion of biomass energy is discussed. The results of previous studies of biomass are discussed to determine the amount of biomass power that can be used in the US. This report should give the reader a basic knowledge of the biomass energy role in the US energy picture.

Hybrid Geothermal Heat Pump System Simulation. *ANTHONY FLORITA (University of Wyoming, Laramie, WY 82071) JOHN SHONDER (Oak Ridge National Laboratory, Oak Ridge, TN 37831).* Geothermal or ground source heat pumps exchange heat with the earth through a network of buried vertical or horizontal heat exchangers. The earth has a number of advantages as a thermal source and sink for heat pumps. Deep earth temperatures remain near constant throughout the year which allows more efficient heat pump operation compared with traditional air-source equipment. However, if the building is cooling-dominated, more heat is rejected to the soil than is absorbed, and the temperature of the soil near the heat exchangers will rise over time. This reduces the capacity and efficiency of the heat pumps. Installing additional ground heat exchangers is one solution, but because heat exchangers are costly - accounting for one third to one half of the cost of the system increasing their size is not usually cost-effective. A better solution is to offset the imbalance in heat rejection with a supplemental heat rejecter such as a cooling tower. Systems with ground heat exchangers and supplemental heat rejecters are called hybrid geothermal systems. The objective of this project was to develop a dynamic simulation of a hybrid geothermal system, and optimize the size of the heat exchanger and cooling tower so as to minimize life cycle cost over a twenty year period. The simulation model contains individual system components that interact with each other by overcoming a building thermal load for a given time step. The results show that heat exchanger length can be reduced and heat pump performance maintained with the hybrid system implementation. It can be concluded that hybrid geothermal heat pumps are a viable option, but further research must be performed in order to understand the sizing and control relationship between the ground heat exchanger and the supplemental unit.

Design and Integration of a Robotic Driver for Chassis Dynamometer Vehicle Testing. *PAUL FRASER (University of Wisconsin-Madison, Madison, WI 53711) MICHAEL DUOBA (Argonne National Laboratory, Argonne, IL 60439).* A robotic driver has the potential to maximize the repeatability of research conducted. Previous driving cycles were performed by a person to simulate on-road driving conditions during performance benchmarking and emissions testing. This can lead to test inconsistencies, which necessitated the use of a robotic driver to remove human error and improve the consistency of generated data. A design was produced using solenoid valves and pneumatic actuators to control the acceleration and braking in research vehicles. Feedback control will be implemented to more precisely trace programmed driving conditions using National Instrument's Labview as the command software. Preliminary findings demonstrated the actuators, electronic signals, and safety features are functional. Positive results are expected for an improvement in the robotic driver's testing repeatability, but conclusive tests are forthcoming. Future plans are in progress to improve the robotic driver design by implementing more accurate signals using PID (proportional-integral-differential) control and to develop signal conditioning.

Incorporating a Fast Fourier Transform into an Analysis Tool. *ANTHONY FRAZER (Madisonville Community College, Madisonville, KY 42431) JAMES SKORPIK (Pacific Northwest National Laboratory, Richland, WA 99352).* This task involves transformation of a time-domain to a frequency-domain by computing the FFT, Fast Fourier transform, of a discrete set of data values. The time domain function being transformed to the frequency-domain is x(t), and the frequency-domain result is given as Re(f)+ jIm(f). Re(f) is referred to as the real part of the frequency, and Im(f) is referred to as the imaginary part. Together, these two parts are referred to as a complex-valued function in rectangular form. In this case, windowing and sampling of a simple sine wave is sampled with a sampling frequency of 60Hz and the windowed DFT, Discrete Fourier transform, is computed with N = 3 at every 0.01 second over the interval from 0.00 second through 0.02 second. The FFT algorithm is written in assembly language due to its speed and convenience. The Fast Fourier coefficients are in exponential format: the real parts equalled 2.52E-05, -1.75E-05, and -1.75E-05 and the imaginary parts equalled 0, 2.25E-05, and -4.46E-05. Fourier coefficients have a dramatic impact on the power grid system and are aimed at energy metering conservation. Electricity generation stations throughout the United States are interconnected in a system called power grids. Fast Fourier coefficients are used to look at real-time frequencies to control output devices through a microcontroller. Prototypes like these will eliminate grid power failures and "brown outs". Metering data must be available to forecast daily energy use. Today, advances in energy metering devices perform waveform sampling for monitoring power grid parameters.

Spark Plug Erosion In Natural Gas Engines. *SARAH GALYON (Virginia Polytechnic Institute and State University, Blacksburg, VA 24060) TIM THEISS (Oak Ridge National Laboratory, Oak Ridge, TN 37831).* As the nation's energy demands increase, alternative methods of producing power will be used. Among the options being investigated, is the use of natural gas engines during times of peak energy consumption. The main maintenance issue with natural gas engines is spark plug failure. The spark plugs in natural gas engines fail by erosion, in which the tips of the spark plugs wear away until the gap distance is too large for the plugs to fire. The purpose of this project is to determine the cause of spark plug erosion, so that spark plug life may be increased. Optical spectroscopy, the analysis of the visible electromagnetic radiation emitted as electrons change energy states, is used to determine what elements are coming off a running spark plug. Because each element emits unique wavelengths and intensities of electromagnetic radiation, an unknown element can be determined from measured wavelengths and intensities, by comparison to the known parameters for each element. The optical spectroscopy measurements of the spark plugs are completed in a chamber pressurized to 200 psig. While the spark plug is firing a computer records the wavelengths and intensities from the spectrometer. Once the testing is completed, the spectroscopy data is run through a computer program to determine the elements eroding off of the spark plug. The elements most commonly seen by optical spectroscopy are nitrogen, nickel, platinum, and calcium. The calcium present comes from a lubricant used in the engines, while the platinum and nickel are from the spark plugs tips, and the nitrogen is from the air in the chamber. The current results are that spark plugs with around 200 hours of engine run time show more platinum and nickel coming off during firing, than spark plugs with longer run times, several thousand hours, which show very little to no platinum or nickel coming off, but mainly calcium. The reason that the metals may be seen at lower running times may be due to the build of a calcium oxide on the spark plug tips over longer running times. While the oxide may at first be protective, over time the oxide may cause the platinum to erode away, increasing the spark gap to the point that the plug no longer sparks. To fully determine if the oxide is the cause of the spark plug failure, more optical spectroscopy needs to be completed on spark plugs with around 100 to 200 hours of engine run time.

The Bimetallic Monolith Catalyst and The Kerosine. *PALOMA GARCIA (ITESM, Monterrey, NL 66220) JOHN KOPASZ (Argonne National Laboratory, Argonne, IL 60439).* Fuel cells generate energy through a chemical reaction between two abundant elements in the Earth, hydrogen and oxygen. The application for fuel cells is vast, ranging from power stations to transportation (automobiles). The main problem regarding the use of fuel cells is the weak hydrogen infrastructure present today. Scientists have been researching the conversion of existing sources of hydrogen such as natural gas, gasoline and diesel to hydrogen-rich gas. At Argonne, a device that can do this has been developed and tested. This method is known as auto thermal reforming in the presence of a catalyst. The catalysts developed at Argonne consist of selected metals as well as oxygen-conducting ceramic materials. Several catalysts and fuels were analyzed, in order to determine the hydrogen yield, using the two Long Term Test Reactors (LTTR) and the Short Term Test Reactor (STTR). A detailed description of both can be found in the Reactors and Methods section of the report. The LTTR #1 used a bimetallic monolith catalyst and Benchmark fuel (BMF) (a mixture of paraffin, olefin, aromatic and napthtenic components that simulate gasoline) with sulfur was tested. The LTTR #1 ran with BMF for 400 hours without any sulfur being added. Around the 400 to 500 hour range sulfur was added. The experiments showed that the performance was poor, while using sulfur. The LTTR #2 ran with BMF with a detergent surrogate (sec-butyl amine) and the Argonne's Benchmark catalyst. The system ran about 140 hrs using BMF without detergent but started having problems with the

pressure when detergent was added. The experiments concluded that the hydrogen yield decreased when detergent was present. The Short Term Test Reactor (STTR) experiments, using Kerosine, showed that the best conditions to reform this fuel is at 800 C temperature and low space velocities. It is recommended that more tests be made in order to have a full and better understanding of the catalysts used in order to determine the optimum catalyst. Currently, the fuel cell team is working in developing new catalysts that will have a better performance than those used in these tests.

Understanding the Furnace Modeling of the Mobile Melt-Dilute System. *EDITH GARCIA (University of California, Berkeley, Berkeley, CA 94709) KENNETH BATEMAN (Argonne National Laboratory, Argonne, IL 60439).* The purpose of this project is to model the Mobile Melt-Dilute (MMD) process. This MMD process will melt highly enriched uranium fuel assemblies with depleted uranium in order to decrease its composition. The advantage of this technology is that these spent fuel assemblies will be treated at the reactor site storage locations. It will be compact and staged on a transportable vehicle and will be capable to process many of the Former Soviet Union spent fuel assemblies at their storage site. It will provide an immediate proliferation solution for the processing of this spent fuel assemblies, which pose a potential terrorist threat. These spent fuel assemblies contain 90% uranium 235, which will be melted and diluted into a low enriched Uranium (LEU) ingot, which will contain less than 20% of Uranium. This LEU will be used as fuel in commercial nuclear reactors or it will be placed in interim storage. The design of the furnace is one of the most important keys of this technology since that will be the place where the melting and dilution will occur. In order to analyze this furnace, experiments have been performed and results have been analyzed. Also, a computer model is implemented in order to simulate the physical conditions used in the experiment to calculate the melting process of these fuel assemblies. Gambit and FIDAP are the two computational tools used in this case. The mesh of the canister inside the furnace will be created using Gambit a preprocessor software that creates high quality meshing to complicated geometries. Then, this mesh will be exported into FIDAP, which will solve the melting process of the spent fuel assemblies and depleted Uranium. Some of the benefits of modeling this process are that it will reduce the number of experimental runs, it will help to define processing time, and it will give us a better understanding of the melting and blending of the spent fuel assemblies and depleted Uranium. These studies will contribute to the nonproliferation of nuclear weapons.

A New Optical Sensor for the Simultaneous Measurement. *DUSTIN GARVEY (University of Tennessee, Knoxville, TN 37909) STEVE ALLISON (Oak Ridge National Laboratory, Oak Ridge, TN 37831).* The recent arrival and growth of fuel cell technology has necessitated the development of a wide range of specially designed sensors. Two such sensor types desired are temperature and relative humidity. Initial research focused on relative humidity (RH) exclusively and resulted in several sensor designs that did not exhibit requisite sensitivity. Progressive innovations eventually led to a unique sensor that, not only, has the capacity to measure RH, but can also measure temperature. This sensor design is currently the focus of a pending patent disclosure. Because specific details of the sensor's design and testing are deemed patentable, they will not be discussed. The general character of the sensor and its results will, however, be presented. The thermal-humidity sensitive material of the sensor was created by mixing various constituent chemicals and resulted in a mixture that optimized the effects of the addition of water. Two characteristics of the sensor were found to vary with the environmental conditions: 1) Material response time (MRT) and 2) Material response magnitude (MRM). The MRT is used to determine parameters used in determining the RH and depends only on temperature. The MRM was found to depend on both temperature and RH. The percent change for the MRM was found to be -33% at 132 degrees Celsius (0% RH) and 25% at 100% RH (21 degrees Celsius). The equations resulting from these calibration tests allow for the temperature and RH to be calculated, given a specific material response. Following these calibrations, the response time of the sensor was compared to that of a standard, type K, thermocouple for the insertion and removal from a hot-humid environment (approx. 90 degrees Celsius and 100% RH). It was found that the two parameters of interest for the sensor performed better then the thermocouple (3 min insertion and 2 min removal) in all but one case. The exception was the slowing of the response of the MRM for its removal (3 min), which is due to latent water located on the sensor. It must be noted that this lengthening of response time is representative of a 100% RH change which is not a likely shift in most systems. Overall, the sensor has a very promising future and work is now being conducted on the effects of changing the topology of the sensor and its associated system in order to improve the certainty in temperature and RH measurements.

Formulating Methods and Procedures to Calibrate a Computer Model of the Drift Tube Linear Accelerator Module Three Cooling System. *SHAUN GILLIAM (Tennessee Technological University, Cookeville, TN 37830) JIM SCHUBERT (Oak Ridge National Laboratory, Oak Ridge, TN 37831).* The Spallation Neutron Source uses a linear accelerator (LINAC) to accelerate hydrogen ions towards a target at upwards of 80 percent the speed of light. The LINAC is comprised of several modules that accelerate hydrogen ions in different manners. The Drift Tube LINAC, or DTL, uses Radio Frequency (RF) as a "power source" for this acceleration. The structure is energized with RF energy and the electric field pushes the particle faster. The term "drift tube" is drawn from the physical mechanism which achieves this acceleration. The particle accelerates through a large cavity of copper as the RF signal's sine wave area is positive. While the RF sine wave "resets," the ion passes through a drift tube where the RF energy does not penetrate and decelerate the ions. Only 20 percent of the RF energy is converted into the ions increase in kinetic energy, the remaining 80 percent must be removed from the system as waste heat. The DTL Resonance Control System (RCCS) re-circulates de-ionized water from the DTL through a heat exchanger to remove this excess heat and maintains a constant temperature (± 0.1°F) throughout the DTL. This is important because the temperature of the copper determines the frequency properties needed to accelerate the particle. Too much or too little and the particle will not synchronize with the RF frequency. Because of several technical problems this has been hard to maintain. To help understand and propose changes to the RCCS system a computer model has been generated using the AFT Fathom 6.0 flow and heat transfer software that predicts the errors noted during current operation. This will enable changes to be made on the computer and obtain confident results, which will save time and materials compared to testing various changes on the RCCS system. The model has been built based on the RCCS-DTL3 system and existing system data is being used to calibrate and validate the model. This preliminary work will allow future progress to be made at a much faster pace with proven methods and procedures already in place. Once the changes have been implemented on the RCCS-DTL3 system additional models will be generated for the other 10 DTL and Closed Coupled Linac (CCL) systems.

A New Standard in Quality Assurance: Nondestructive Evaluation of Automotive Welds. *JOHN GLOVER (San Jose State University, San Jose, CA 95192) DEBORAH HOPKINS (Lawrence Berkeley National Laboratory, Berkley, CA 94720).* The LBNL Engineering Division is working on a project funded by the Department of Energy to develop an ultrasonic phased-array inspection system in collaboration with General Motors, Ford, and Daimler Chrysler. Nondestructive evaluation (NDE) could save the automotive industry millions of dollars a year and more importantly, is more efficient in detecting structural flaws than current methods. The criterion currently used in industry to determine if a weld is acceptable is the diameter of the weld button left after separation of the spot-welded joint. Inspected parts often require rework after pry checks, and are discarded after teardown. Our ultrasonic NDE inspection system includes a multi-element phased-array probe that gives full dynamic control over the acoustic beam, allowing electronic scanning for high-resolution images and reliable weld classification. NDE allows more samples to be inspected in a shorter time interval than conventional methods. For each weld, the probe is electronically scanned in one direction and mechanically scanned in the perpendicular direction to obtain two-dimensional images of the welds. Each image consists of just over 3000 acoustic signals. Once the acoustic data is collected and verified, it is transferred to our weld analysis program. The acoustic energy transmitted through the welded region is analyzed to determine weld quality. Since we are acquiring and analyzing data for hundreds of samples, physical analysis of all welds is nearly impossible. Therefore, when choosing the weld samples for further physical analysis, we pick a few that we feel represent four general types of spot welds encountered in practice. The metallographic process allows us to verify weld quality and validate our NDE results. The samples are cross-sectioned through welds then polished and etched to reveal grain structure. Based on these results, we find that our data collection methods and signal analysis program are sound. The next stage of this project will be to design and build a prototype to be tested by our industry partners under realistic manufacturing conditions. The refined prototype will be the model for a new robotic system. The ultimate goal of the project is to automate the inspection system for use on the assembly line. This will allow companies to collect inspection data, identify trends or other potential problems, and will help them to detect flaws quickly and efficiently setting a new standard in quality assurance.

Initial Design of the Neutralized Drift Compression Experiment. *GUSTAVO GONZALEZ (University of California, Berkeley, Berkeley, CA 94720) ENRIQUE HENESTROZA (Lawrence Berkeley National Laboratory, Berkley, CA 94720).* Fusion promises a clean and efficient method for creating energy. We focus on the inertial fusion approach and the use ion beams to compress and fuse together a deuterium-tritium target. The Neutralized Drift Compression Experiment (NDCX-I) will seek to test the feasibility of a neutralized drift compression system, neutralized transport of a beam through a solenoid magnet, and the feasibility of accel-decel-load-and-fire solenoid bunching injectors. The accel-decel-load-and-fire solenoid bunching injector system is composed of flat plates that will accelerate, decelerate, match and load the beam into a solenoid magnet that will then be injected into a system of solenoid magnets where the neutralized drift will occur. To place the plates to their positions a mechanical design was formulated where the main issue was that of mechanically aligning them during future assembly. The other concerns of heating and electrostatic fields were also taken into account, but they were at a smaller scale, specific to the insulators and the extraction plate not the whole system. Continuing work will focus on the heat transfer and electrostatic fields of the complete accel-decel-load-and-fire solenoid bunching injector system.

The Construction of a Novel Apparatus for the Study of Natural Gas Hydrates. *BRYAN GRABIAS (Columbia University, New York, NY 10027) DEVINDER MAHAJAN (Brookhaven National Laboratory, Upton, NY 11973).* This work describes the setup and operation of a high-pressure cell used in natural gas hydrate kinetic studies. Due to their thermodynamic stability requirements (pressures in excess of 1000 psi and temperatures below 277K), laboratory hydrates are typically formed in one of two ways, depending on analysis requirements. For large volumes of hydrate (greater than 1-2 cm^3), a sealed vessel is used - not allowing for the visual inspection of in situ hydrates. To alleviate such a problem, a small vessel fitted with a high-pressure window (usually of single-crystal sapphire) is constructed. However, such a small cell is not useful for studying hydrate behavior on a large and industrially applicable scale. Additionally, while it is possible to construct a voluminous cell made entirely of the high-strength single crystal sapphire, the cost for most laboratories would be excessive, making such a construction economically impractical. In order to solve both problems simultaneously, those of in situ inspection and macroscopic applicability, a large (500 cm^3) stainless steel cell fitted with two borosilicate windows was constructed. The cell is pressure rated to 5000 psi and has temperature capabilities (limited currently by a water bath) from 273 - 313K, making it an ideal vessel in which to study hydrates at oceanic conditions. Additionally, the cell is highly configurable, and can support a host of hydrate forming environments, from crude oils to sediments, with very little modification on the part of the researcher. We have obtained preliminary methane hydrate formation data and found that the cell can adequately conform to predictions made by theory. With the viability of our novel cell now validated, we plan to examine the potential for hydrate deposits to serve as sites of carbon dioxide sequestration as well as study current dissociation models.

Friction and Wear of NFC-6 and Super Hard Coatings in Dry Nitrogen. *FRANCISCO GUTIERREZ (Illinois Institute of Technology, Chicago, IL 60629) GEORGE FENSKE (Argonne National Laboratory, Argonne, IL 60439).* The purpose of the project is to assess the tribological parameters of Near Frictionless Carbon (NFC-6) and Super Hard Coating (SHC) on steel under dry nitrogen sliding. The speed, load, and environment, were kept constant while considering the coated and uncoated surfaces as the independent parameters. Numerous analytical and numerical data were collected using a number of instruments. A High Frequency Reciprocating Rig (HFRR) records the friction coefficient between the sliding surfaces. An Optical Profilometer was used to estimate the amount of material removed. An optical microscope was used to for visual identification and measurement of coating thickness. Raman Spectroscopy was used to assist in determining whether the surfaces become more amorphous or crystalline as shown on Graph 2. Importantly, although friction and wear both arise from sliding surface contact, high friction does not necessarily mean high wear. Results indicate overall that Bare-ball-NFC-6 plate has the lowest coefficient friction; however, Bare ball-SHC plate has the highest wear resistance. Future work will include revalidating some of the experiments for reliable results but most importantly testing in isobutane and hydrogen varying the speed, load, temperature, etc.…

A Study of the Managerial Efficiency and Styles of the Operations Department. *AARON HADLEY (Vanderbilt University, Nashville, TN 37235) JOHN CZACHOWSKI (Oak Ridge National Laboratory, Oak Ridge, TN 37831).* Often times, in the researcher's zeal and haste to start a new endeavor, the issue of safety can be neglected or brushed aside. This is where the Operations Department of the Engineering Science and Technology Division enters to assist the researcher in doing his job. Through studying the staff of the Operations Department a fresh look and analysis of the processes and styles of management used can be produced, allowing the staff to better provide for the safety of the employees of the division which will keep the Lab's researchers producing new research and developments. The researcher at Oak Ridge National Lab does not spend all his time in the laboratory or at the drawing board. Instead he is often required to promote his ideas, search for investors, and spend hours and days at tasks that merely lead up to the actual work. The Operations department assists the researcher fulfilling training requirements required for the project and obtaining and clearing necessary lab space. Lab Space Managers watch over each laboratory, maintaining their condition, keeping them stocked with necessary equipment and resources, and ensuring hazards are minimized. Operations personnel ensure that appropriate assistance visits, inspections, and audits of office and lab spaces for safety, environmental health, cleanliness, and efficiency are conducted periodically and when requested. This is to allow work to be conducted in a manner that ensures the safety of the researchers, protection of the environment, and compliance with applicable State, Federal, DOE and ORNL Standards Based Management Systems rules and regulations. Through this study of the Operations Department of the Engineering Science and Technology Division conclusions will be sought regarding the efficiency of the group, leading to recommendations on how to best improve its value to the researcher.

Ultrasonic Technique for Measuring Density and Viscosity of Liquids. *TRAVIS HARPER (Tuskegee University, Tuskegee Institute, AL 36088) S. SHEEN, A. CHIEN AND C. CHEN (Argonne National Laboratory, Argonne, IL 60439).* Fluid particles are generally engaged in a continuous variation of relative position and form. The motion of a particle at the center of mass of a fluid body seldom represents the mean motion of the fluid as a whole. It therefore becomes essential to determine the forces producing motion at each point in a given flow. For this reason, the mass per unit volume or density, ρ, is of interest more than the total mass of a fluid. Another important fluid property is the viscosity which describes a fluid's resistance to flow. The purpose of this research was to measure the viscosity and density of several liquids and oils through ultrasonic nondestructive evaluation (NDE). This project has been accomplished by using two different ways of moving the liquids and oils. The first way was done by using a static flow and the second way by using a dynamic flow. Current research up to this point has been focused on these liquids: water, glycerol/water (different concentrations), mineral oil, poly (1-butene), corn oil and sugar water. Results of this experimental research have similar data to actual data. Future research should eventually lead to the capability of other flow rate methods.

Database Architecture for the Resonance-Coupled Photoconductive Decay in Solar Cells Using the FileMaker Pro 7.0 Suite. *MATTHEW HARRIS (Colorado State University, Fort Collins, CO 80521) PAT DIPPO (National Renewable Energy Laboratory, Golden, CO 89401).* The domestic application of photovoltaic cells to garner energy from the sun's light is certain to further a trend toward a clean, renewable, and efficient means of generating electricity. Consequently, a comprehensive research program has been elemental to the evolution of semiconductor photovoltaic devices. Particular to this research is the study of the recombination of minority carriers in crystalline semiconductor compounds. Empirically determining, with optical luminescence, the photoconductive decay observed in such materials establishes a profile between the flux of voltage potential as electron-hole pairs recombine and time, which defines the electrical stimulus and thus, in part, the efficiency of a photovoltaic cell. The results of this extended research were compiled into a disordered array of file extensions particularly inaccessible for reference and unfit for the professional presentation of data. In order to mitigate the entropy encountered in this development, a comprehensive database architecture was designed using the FileMaker Pro 7.0 suite with the intention of electronically exchanging records documented for the resonance-coupled photoconductive decay of solar cells by the LabVIEW data acquisition module directly into a database management system through an open database connectivity interface between the two otherwise incompatible applications. However, we found upon development that FileMaker Pro does not support open database connectivity for other software packages on the latest Macintosh operating system and thus elimination of a third-party application for data transmission was not obtainable. The desire to integrate an operational simplicity into the database management system as requested by researchers was therefore unfulfilled, Nevertheless, installment of the FileMaker Pro database management

system enforced a majority of the aspirations sought in its conception: to condense a litany of empirical data into a single operating platform, to improve the accessibility of data, and to establish a presentational format for record keeping.

Reaching Net Zero Energy in the Most Economical Manner. *ADAM HAYES (Brigham Young University - Idaho, Rexburg, ID 83440) JEFF CHRISTIAN (Oak Ridge National Laboratory, Oak Ridge, TN 37831).* Engineering a house that uses as much energy as it produces on site during a year is intriguing to home owners across the globe. The cost of producing a zero energy house is expensive due to the need for energy efficient technologies and solar collection systems. Four houses have been constructed within the last two years and are being monitored for energy efficiency and solar power generation. Each house is equipped with a different hot water heater, air handling system, and building materials package so comparisons can be made. Sensors and meters have been installed to measure thermal activity and energy efficiency, gathering data every 15 minutes. Thermal couples read ambient, interior, crawlspace, solar collector, air duct, and hot water temperatures. Meters measure the flow of electricity to the air handler unit, water heater, refrigerator, compressor, inverter, and incoming and outgoing electricity to the whole house. Water flow is also measured to collect hot water usage. Data is downloaded daily from the data logger system through the telephone line. Comparisons are made between houses as the data is interpreted by use of spreadsheets. Data provides detailed energy efficiency of various parts of the homes. These results include information on efficiency of the water heater, space heat pump which provides heating, cooling and dehumidification, and shows the whole house energy efficiency. Using this data, conclusions are drawn about the average daily cost of energy; these houses are 50 to 70 percent more efficient than today's minimum code compliant housing. With the electric utility green power generation partnership program buying the solar power the average daily cost of all energy needs from off site is less than 80 cents per day. Typical houses in this area average six to nine dollars per day. The cost of these houses is available and will be used to draw conclusions about the most cost efficient method of saving energy and reaching the ultimate goal of creating affordable zero energy houses in the future. The analysis of these four near zero energy house data bases will be used to make recommendations for a fifth prototype house to be built in the fall of 2004.

Analysis and Optimization of Current Leads Associated with Superconducting Undulator Phase Error Corrections Methods. *JORGE HERNANDEZ (University of California, Berkeley, Berkeley, CA 94704) STEVE MARKS (Lawrence Berkeley National Laboratory, Berkley, CA 94720).* An evaluation of the thermal issues associated with three different phase error-correcting methods (shimming) is conducted for the development of a short-period superconducting undulator (SCU) at Lawrence Berkeley National Laboratory (LBNL). Evaluation of the three methods is accomplished by a thermal budget of all the sources of heat leaking into the SCU. The key criterion for the selection process is heat flux through wires via conduction entering from an ambient 300[K] to a cryogenically cooled 4.2 [K] environment and the heat generated by the P.S.'s. A one-dimensional model of a wire broken into two segments is used to determine the heat flux entering the cold end. Conduction heat transfer through the wire is governed by the heat equation. The temperature dependence of and and the associated (non-linearity of this heat equation) makes an analytical solution for the heat flux unlikely, and has to be solved numerically. The equation was solved numerically by developing a Matlab 6.5 code that uses built in function ode45 to solve the differential equation. Two checks were used to ensure the validity of the solution. The heat flux through the wire for the three operational conditions of I=0 [A] ,35 [mA], 200 [A] at each end of the two segments is determined. A minimum heat flux can be found for the segment with a temperature range 300 [K] -80 [K]. A comparison of the different amounts of conduction heat transfer among the three methods will help identify the best method to proceed with for the project.

Engineering Calculations for ALS Insertion Devices. *JORGE HERNANDEZ (University of California, Berkeley, Berkeley, CA 94704) STEVE MARKS (Lawrence Berkeley National Laboratory, Berkley, CA 94720).* A 5cm period Elliptically Polarizing Undulator (EPU 5.0), the third device of its kind built at Lawrence Berkeley National Laboratory (LBL), generates four polarization modes of intense synchrotron radiation for use in scientific experiments at the Advanced Light Source (ALS). The magnetic structure consists of four separate beams that are designed to move parallel to the axis relative to each other. Magnetic forces are a function of the beam position, thus a change in position, results in a change in sign through the range of motion. Measurements show that significant deflection occurs transverse to the axis of mechanical motion. The design of a new EPU with a longer period and stronger forces will be underway soon, therefore it is important to understand why there is deflection/mechanical motion on previous models and correct for it. This paper will present measurements and several analytical methods for calculating deflection. One approach involves performing a finite element analysis (FEA) on the structural beams for deflection and comparing the results to a simplified analytical model. The results indicate calculated deflection is small compared to measured motion, signifying that the structural rigidity of the device is not the source of the problem. Future work involves further investigation and design modification.

Conceptual Analysis of a Persistent-current Switching Network for Active Phase-error Correction of Superconducting Undulators. *SHANTELL HINTON (Vanderbilt University, Nashville, TN 37235) STEVE MARKS (Lawrence Berkeley National Laboratory, Berkley, CA 94720).* Considerations in the application of persistent current switches and the formulation of a series of small switching logic networks that will allow current to be directed into different trim coils in a Superconducting Undulator are the focus of this project. The network will need to allow current to go through, around, or bypass the coil. For each directed current, one or more persistent switches will be triggered and activated as mentioned previously. Essentially, the network will set the persistent switches as binary operators, on or off, that will control the flow and direction of current at user specified positions within the array of superconducting magnets. As a result, these networks will become an active type of "shimming" that will provide an accurate and convenient method for phase error control of electrons passing through the array of the Superconducting Undulator.

Laser Personnel Safety System Design Required for Ultraviolet Free Electron Laser and Terahertz Radiation. *LAUREN HUIE (Binghamton University, Binghamton, NY 13902) KEVIN JORDAN (Thomas Jefferson National Accelerator Facility, Newport News, VA 23606).* The Thomas Jefferson National Accelerator Facility (TJNAF) Free Election Laser (FEL) facility houses various class four lasers, as classified by the American National Standards Institute (ANSI). These class four lasers require both engineering and administrative controls to protect laser users. Currently, the Laser Safety System (LSS), an interlocking system, provides personnel protection against the hazards of the class four infrared (IR) FEL beam and table top lasers. The FEL machine will undergo a major upgrade thereby producing both infrared and ultraviolet (UV) FEL beam. The terahertz (THz) radiation will be channeled from the FEL into a user lab. The existing LSS does not meet safety requirements for these multiple laser hazards. LSS system level analysis has identified areas requiring improvement. Firstly, the modicon programmable logic controllers (PLC), which now control the LSS, have insufficient resources to support the FEL upgrade and must therefore be replaced. Next, a more efficient system of access control is necessary, as each user lab is an access point to multiple laser hazards. Lastly, tedious hard wiring of communication requires an upgrade of both efficiency and aesthetics. These improvements will form a strong foundation for the new Laser Personnel Safety System (LPSS) design. The LPSS will not only offer protection against the IR FEL beam and table top lasers, but will now interlock the new hazards of the UV FEL beam and the THz radiation. The UV transport line requires duplication of IR beam blocking mechanisms. Master and slave PLC resources will double and triple respectively. Upgrades to access control will be expanded to include additional user information. In addition, indication of proper safety goggles will minimize human error associated with multiple laser hazards. Communication from the master to the slave PLCs will exist in a ring configuration to form a self-healing network. Each location on this network must be stand alone to ensure communication will not be destroyed. Fail-safe communication will allow users to continue safe operation of table top lasers should FEL operation cease due to power failure. Sufficient system resource flexibility is necessary as the installation of the UV FEL beam and additional user labs may not be completed at the time of LPSS installation. Diligent design of PLC software and fail-safe interlocks of the LPSS will save the lives of scientists using the facilities at the Jefferson Lab.

Design, Development, and Implementation of an Energy Code Web Application. *TRACY HUMMER (Washington State University, Pullman, WA 99163) HEATHER DILLON (Pacific Northwest National Laboratory, Richland, WA 99352).* With so much information available on the internet in such a variety of topics, it is time consuming to sort high quality information from other materials. The Building Energy Codes Program (BECP) Resource Center has been created to reduce this time consuming process of sorting through millions of search results to find the desired information. The Resource Center is expected to be the central web application containing up-to-date information about energy codes and above code materials. It was created using open-source tools such

as Cocoon and Lucene, along with extensible markup language (XML), an internet programming language used to transfer data that is growing in popularity. The Resource Center web application was designed to be easy to navigate, user friendly, and provide a variety of searchable media types. It is expected to be available by October 2004 and can be accessed through the BECP website.

Are You Centered? Computer-controlled Crystal Centering Using Cryscenter. *ANUBHAV JAIN (Cornell University, Ithaca, NY 14853) VIVIAN STOJANOFF (Brookhaven National Laboratory, Upton, NY 11973).* True high-throughput protein crystallography requires an automatic crystal centering system. Automated centering greatly improves the efficiency of the data collection process, allowing more samples to be tested and making the beamline more user-friendly. A fully computer-controlled centering software, Cryscenter, is introduced. Cryscenter analyzes images from a camera using image processing techniques, locating the loop's position. The location of the x-ray beam is determined via a set of crosshairs imprinted on the image, which have been calibrated to the beam position. Cryscenter uses this information to automatically move the goniometer head such that the loop is centered in the beam, ready for diffraction. Crystal centering is achieved simply by double-clicking the crystal in the Cryscenter frame. This software currently allows researchers to center crystals in less time, without needing to go inside the hutch and press motor switches. Future work will concentrate on no-click crystal centering, opening up the possibility of fully automated beamlines.

Recovery, Separation, and Identification of Plastics in Automobile Shredder Residue Using Froth Flotation and FTIR Analysis. *QUOVAUNDA JEFFERSON (University of Illinois at Chicago, Chicago, IL 60612) SAM JODY (Argonne National Laboratory, Argonne, IL 60439).* While recovery of metals from end-of-life automobiles has become a standard operational procedure in automobile recycling, the technology to recycle other materials from automobiles shredder residue (ASR), including plastics, did not exist due mainly to the lack of cost effective technology. Yet, in recent times, the need for post-consumer plastics has created the demand to recycle plastics. In addition, concerns about landfill space and cost have increased the need for technology to recycle ASR. One such feasible solution is a process that is being developed at Argonne National Laboratory. This process uses a froth flotation technique that not only separates different types of ASR material; it can also separate different types of plastics that have similar densities. The process is being tested in a 1000 lb/hr pilot plant. A series of bench scale flotation experiments, using solutions of several different criteria, has been conducted in support of the pilot plant work. The separated plastics are identified on a Fourier Transform Infrared Spectroscopy (FTIR). The results of separation experiments show that recovered plastics have properties that are useful for making quality products.

Combined Heating and Power: A Feasible Way to Save Energy, Money, and Emissions. *BARRY KALDENBACH (Clemson University, Clemson, SC 29632) KIRBY WILCHER (Oak Ridge National Laboratory, Oak Ridge, TN 37831).* Combined Heating and Power (CHP) is a relatively new technology in the energy world. The main principle behind this system is to capture and reuse exhaust heat of an electric generator, thus reducing emissions and conserving energy and money. This exhaust heat, which is usually released into the environment, can be used for many applications such as heating a building or chilling water through an absorption chiller. Currently there are many CHP projects underway in federal facilities. Collecting information from these sites can be important for future implementation of CHP applications. Acquiring data on current performance allows improvements to be made and specific problems to be addressed. This data from federal CHP sites was stored in a database (Excel format). It was 74 columns wide and 68 pages when printed (size 4 text). A more user-friendly database was created using Microsoft Access. This new database stores information in a series of organized and manageable tables and queries. It also includes forms for quick and easy input of updated information and automatically generates reports that are commonly needed by users. The data in this database has begun to be updated and confirmed accurate via email and telephone. Updated information has been input into the new database. This information will continue to be updated and be forwarded to the Federal Energy Management Program (FEMP) annually. In addition to the existing CHP sites, many other federal sites are assessing the possibility of implementing CHP technology for upcoming projects. Four initial screenings for such sites were performed using annual electricity and fuel consumption data. Many CHP possibilities were assessed and the best possibility was recommended to the site in a written report. These reports address factors such as energy and dollar savings, as well as simple payback. They also advised on potential "next steps" for the project. Also, the annual Mid Atlantic Application Center for CHP conference was attended in Washington D.C. Promotion of CHP in the Mid Atlantic Region was discussed. Results from data collection suggest that fuel cell technology might need more work in the drawing board before it can feasibly be implemented at sites. All known federal CHP sites with fuel cells have been shut down. Otherwise, results show that CHP seems to be a viable and practical means of saving energy, money, and emissions. DOE should continue to push application of CHP for federal sites.

NuSTAR: Vibro-Acoustic Tests. *KAWTHAR KASIM (University of California, Berkeley, Berkeley, CA 94720) WILLIAM CRAIG (Stanford Linear Accelerator Center, Stanford, CA 94025).* NuSTAR is a satellite that will be carrying X-ray optics that consist of many nested glass cylinders. Due to different acoustic environments, the glass may react such that cracks and/or fractures may form. Cracks and/or fractures in the glass would not allow the optic to work properly. Therefore, it is necessary to test the glass and optic prototypes to determine if they will be able to withhold when experiencing certain acoustic environments. The vibro-acoustic testing conducted at the Jet Propulsion Laboratory (JPL) in Pasadena determined that under the minimum workmanship acoustic environments, the glass on the optics will not fail. Overall, the results of the test were successful which gives confidence that when the satellite is launched into the air and then dropped into space, the glass in the optics will not fail.

Commissioning a Helium II Test Facility at Stanford Linear Accelerator Center. *ANDREW KATZ (Duke University, Durham, NC 27708) JOHN WEISEND (Stanford Linear Accelerator Center, Stanford, CA 94025).* Liquid helium is the only fluid that exhibits the unique properties characteristic of a superfluid when cooled to temperatures near absolute zero. This superfluid helium state is commonly referred to as He II. Among the many odd properties are a vanishingly small viscosity and a high effective thermal conductivity. A He II test facility will provide researchers in the Experimental Facilities Department at SLAC with the opportunity to do research in the superfluid range with relative ease. The nature of this project is to test the functionality of the existing helium components in the cryogenics lab and recommend improvements. The basic experimental setup consisted of a helium dewar, a vacuum pump system, and a network of sensors. After adding liquid helium into the dewar and turning on the vacuum pump, we observed that the pump was able to reduce the pressure down comfortably into the superfluid state. Furthermore, by adding heat to the fluid in set increments we learned what amount of heat could be added while still keeping the helium in the superfluid range. Our final test was to see if we had the ability to change the pressure via the MKS exhaust valve controller. The controller failed miserably and was found to be inadequate for the type of experiments to be done. Among the other recommended improvements were: adding isolation valves to the vacuum pump line, erecting a supply line for clean helium gas, incorporating a relief valve in the helium recovery line, and documenting the existing vent and vacuum lines. Once these improvements are made, the He II test facility should be up and running, allowing researchers to dive as deep as they please into the superfluid state.

Chromium Contamination in Cathodes for Solid Oxide Fuel Cells. *JULIE KIDD (Iowa State University, Ames, IA 50010) MARK HASH (Argonne National Laboratory, Argonne, IL 60439).* Solid oxide fuel cells (SOFCs) are currently being developed at Argonne National Lab. The development of a SOFC would allow for a cleaner more efficient energy generation by using hydrogen and air for a diverse array of energy applications. SOFCs are dependent on cathodes and interconnects for successful operation. Chromium contamination of cathodes is believed to be happening due to the chromium content of selected interconnect materials. The levels of contamination of the cathode by various interconnect materials are being tested in argon and in air. Chromium contamination is believed to shorten cell life and pose an environmental risk. Initial investigations into this problem utilize scanning electron microscopy (SEM) and energy dispersive spectroscopy (EDS) to evaluate the levels of contamination in cathode materials are underway. Preliminary analysis shows that Lanthanum Strontium Manganate (LSM) and Lanthanum Strontium Ferrate sub-stoichiometric (LSFss) are less susceptible to chromium contamination than Lanthanum Strontium Ferrate (LSF). Material testing continues to learn about which interconnect materials pose the least threat of chromium contamination and which cathodes are least affected by it.

Evaluation of Reverse Osmosis System for Tar Removal From the Thermochemical Process Development Unit Scrubber Water. *ZACHARY KIMBALL (Colorado School of Mines, Golden, CO 80401) CALVIN FEIK (National Renewable Energy Laboratory, Golden, CO*

89401). The Thermochemical Process Development Unit (TCPDU) at the National Renewable Energy Laboratory specializes in the production of energy via the gasification or pyrolysis of biomass. The liquid produced in this process must be disposed of as hazardous waste according to the government's Resource Conservation and Recovery Act (RCRA) because a number of the components of the scrubber water exceed the regulated concentration limits. A reverse osmosis water-purifying unit was used to investigate its effectiveness for filtering benzene from wastewater. Benzene was chosen because its concentration leaving a packed-bed stripper was one order of magnitude too high. The reverse osmosis system implemented was a four-step process consisting of a pre-filter, two granular activated carbon filters, and a cellulose acetate membrane. Initially, the unit was tested with 5 ppm by weight benzene in water, but the scope of the research expanded to include the aqueous effluent directly from the scrubbers, which includes acetone, benzene, cresols, and phenols. The experimental results show that the reverse osmosis unit was extremely successful in removing benzene in water to below the RCRA limit of 0.5 ppm. Moreover, it was the two granular activated carbon filters that removed most of the benzene. The membrane was not required to achieve the desired levels. However, after completely purifying ½ gallon of scrubber water, the reverse osmosis system failed allowing acetone, phenol and cresols to bypass the filters. This degradation of the membrane was a result of feeding chemicals incompatible with the membrane. If a membrane is used, cellulose acetate must be replaced with a material compatible with phenolic ketone compounds. We feel that using 4 activated carbon filters in series would clean more scrubber water at a faster rate than a system including a membrane.

Interactive Virtual Modeling of Robotic and Automated Equipment of a Nuclear Fuel Cycle Facility. *BRIAN KOHLSAAT (Western Michigan University, Kalamazoo, MI 49008) YOUNG SOO PARK (Argonne National Laboratory, Argonne, IL 60439).* With the nation's stockpile of spent nuclear fuel accumulating, it has become evident that a process must be devised to control the growth. The method proposed, which consists of a batch of processes, requires advanced robotic equipment. This equipment is fabricated to provide the discrete material handling that is required for spent nuclear fuel. Furthermore the creation of these robotic devices consists of the advanced integration of Computer Aided Drafting (CAD) programs. Every aspect of the recycling facility is constructed in the virtual world using CAD. First, individual components are assembled into a device, and then multiple devices are combined into a workcell for the final product. This virtual world of design is then enhanced with unique programming known as Graphic Simulation Language (GSL). The individual devices are programmed to function as an entire process in order to allow for an accurate simulation of the final routine. With the advantage of CAD's ability to improve an existing layout of devices with easy, the design of the recycling facility will continuously be streamlined. Human interaction with the computer programs is necessary to allow for accurate usage of the robotic mechanisms. Not only will human integration help, but it will also lower the risk of accidents due to naturally occurring abnormalities in a system. Overall future work will focus on the compliance of human and computer interaction.

Hydraulic Modeling Analysis of Brookhaven National Laboratory's Potable Water Supply System. *ALAN KOUCHINSKY (University of Maryland, College Park, MD 20742) MICHEAL KRETSCHMANN (Brookhaven National Laboratory, Upton, NY 11973).* The potable water supply distribution network at Brookhaven National Laboratory consists of 26 miles of mains, 253 hydrants, and 477 valves. A majority of the network is between 40 and 60 years old. The piping supplies water for experimental cooling, domestic consumption, fire suppression systems and Fire Department use. It has been determined by annual flow tests that the flow capacity of the aging network is diminishing over time. For example, one of the 23 annual flow test sites showed a flow capacity decrease of 15 percent in the last decade. A quantitative analysis of the potable water supply distribution network, by building a hydraulic model based on the Hazen-Williams formula, is necessary to understand and mitigate the diminishing flow capacity in the BNL network. In order to create a realistic hydraulic model, two major data sets are needed to accurately portray the present hydraulic dynamics of any water supply network. The two data sets are: establish the "C" factor (roughness) for sampled categories of pipe groups, and determine the distribution of experimental cooling, and domestic water usage throughout the network. To establish the "C" factor, nine pressure gradient tests were selected to represent the different categories of pipe based on pipe material, sizes, and age groups in the network. Factors that influence the results were: type of pipe material, pipe size, average water velocity from daily water usage, and proximity to water supply sources. Determining the true distribution of experimental cooling, and domestic water usage throughout the network requires the use of both documented information and estimation methods. BNL consumed an average of 1.43 million gallons per day over the last 12 month period. Dividing the average daily demand between experimental cooling and domestic water usage is based on hypotheses because of the limited use of water meters on the piping network. Domestic consumption was determined based on industry averages for daily consumption by total number of employees in each building or structures at BNL. Assigning experimental cooling usage for each building will require determining consumption of equipment/processes. The preliminary work to create the hydraulic model is vital to determining how to maintain flow capacities to fight fires at BNL. This work is a continuous process, and further analysis needs to be complete to mimic actual flow rates.

Creating a Statistical Bone Atlas for 3D Registration of Normal Bone Models to Biplaner Fluoroscopic Images. *MICHAEL KUHN (Colorado School of Mines, Golden, CO 80401) KARA KRUSE (Oak Ridge National Laboratory, Oak Ridge, TN 37831).* Common surgical navigation techniques require a number of preoperative and intraoperative steps in order to function. The preoperative steps include computed tomography (CT) scans, while the main intraoperative step is monitoring the absolute 3D position of bones and surgical equipment using an optical tracking system (e.g., Optotrack systems, Northern Digital). This requires placing markers on all of the surgical equipment and the bones so that they can be tracked by the optical system. The process proposed here will eliminate the need for performing a CT scan and will simplify the intraoperative overhead. Instead of using CT scans to get a model of the bone, an existing statistical atlas for all of the bones in question (for example one for the femur and one for the tibia) will be used. These atlases will allow each bone to be represented by a few key modes of variation. The bones for that individual patient will then be constructed by taking two X-ray images using a fluoroscope machine. This will be done by placing two fluoroscope machines orthogonal to each other. A 3D optical tracking system will be used to monitor the positions of the fluoroscope machines. This will allow camera calibrations to be done so that the 3D fluoroscope scenes can be recreated. The images will be orthogonal to one another, one in the sagittal plane and one in the coronal plane. An iterative optimization algorithm will then be used in conjunction with an atlas for each bone to register a 3D model of each bone to the biplaner X-ray images. First the simulated annealing algorithm will be used to rigidly align a base model to the two X-ray images (12 degrees of freedom (DOF) - 3 translation and 3 rotation for each image). Once the base model is rigidly aligned, the genetic algorithm will be used to vary the shape of the bone through the modes of variation, which for the femur constitutes between 7-9 DOF. This is the only preoperative step. The intraoperative technique, which will use the models created in the preoperative step, is much less invasive than the 3D optical tracking system described above. It is the same basic setup with biplaner images except that the genetic algorithm does not need to be used to vary the shape of the bone, so the bones only need to be rigidly aligned to the X-ray images. Although this project cannot be completed over one summer, it has been beneficial in the sense that it has tied together many disparate biomedical imaging concepts.

Computational Fluid Dynamics in Abdominal Aortic Aneurysms Using Automatic Dynamic Incremental Nonlinear Analysis (ADINA). *MITCHELL LADD (University of Tennessee, Knoxville, TN 37916) KARA KRUSE (Oak Ridge National Laboratory, Oak Ridge, TN 37831).* An abdominal aortic aneurysm (AAA) is the abnormal dilation of the abdominal aorta caused by the weakening of the aortic wall. AAAs are the 13th leading cause of death in America resulting in nearly 15,000 deaths per year. AAAs are particularly threatening because they generally are asymptomatic which can cause unforeseen death upon sudden rupture. In fact, a ruptured aneurysm is fatal in 90% of all cases. Traditionally, the risk of AAA rupture is determined by the overall diameter, i.e. if the diameter is larger than 5 cm, the AAA is at a high risk of rupture and is repaired surgically. This method of predicting rupture risk is insufficient because often AAAs with diameter smaller than 5 cm have a higher stress and thus risk of rupture than larger AAAs. Past studies have used computer generated models to investigate the wall stresses of AAA's in hopes of developing a better method for predicting rupture. Currently, most studies neglect the effect of shear stress on the wall and the fluid-wall interaction caused by the blood flow in the aorta. Hence, the addition of shear stresses and fluid-wall interactions to computational models will more accurately locate regions of high stress and determine the relative risk of rupture. Ideal cylindrical models of the aorta and ideal AAA geometries were created as shells and fluid volumes using the ADINATM. ADINA was chosen for its fluid structure interaction (FSI) capability of simultaneously solving both fluid flow and

mechanical stress simulations using the finite elements method (FEM). The idealized models were tested, using FEM in ADINA, to reproduce results from prior studies in the literature, thus validating the solutions computed by ADINA. Different boundary conditions and element types were used in order to find the most realistic solution. The preliminary results did match prior publications where the highest stress occurred at the inflection points. Initial FSI models were successful, but still need to be improved in order to arrive at more realistic solutions. The initial ideal models verify the accuracy of ADINA's solutions, thus demonstrating ADINA's potential to take AAA modeling to the next level by accurately interfacing fluids and solids. The ideal models need to be further optimized and tested after which AAA models generated from patient CT scans can be evaluated. This work would be a great step towards a better method for determining the risk of AAA rupture and need for surgery.

Strontium-90 BGRR/ WCF/ PFS Groundwater Treatment System. *BRENT LEE SHUE LING (City College of New York (CUNY), New York, NY 10031) ALAN RAPHAEL (Brookhaven National Laboratory, Upton, NY 11973).* This project addresses the removal and treatment of contaminated groundwater emanating from the central portion of the Brookhaven National Laboratory (BNL) site. The groundwater in this area has been impacted by concentrations of Strontium-90 (Sr-90) above the drinking water standard (DWS) of 8 pico curies/liter, which originated from the Brookhaven Graphite Research Reactor (BGRR), its associated Pile Fan Sump (PFS) area, and the Waste Concentration Facility (WCF). Volatile Organic Compounds (VOCs) are also present in the groundwater above the dinking water standard of 5 ppb and are being treated as well. A plume distribution map was created from geoprobes samples that were collected at multiple depth intervals at a total of 60 locations within the areas of contaminant sources. Groundwater characterization has shown a maximum level of Sr-90 concentration at 3,150 pCi/L from a geoprobe located south of BGRR Building 701 at a depth of 44 feet below land surface Corrective action has included plans to install a Groundwater Remediation System on the BNL campus in Upton, New York at Building 855 located to the east of the WCF and to the northeast of the BGRR and PFS. The system will incorporate groundwater extraction, treatment using ion exchange and on-site discharge of treated water. A column study that was conducted as part of the Sr-90 Pilot Study has shown clinoptilolite a naturally occurring zeolite would be the most efficient ion exchange media. Groundwater modeling simulations were used to refine and optimize the groundwater extraction (different number of extraction wells and locations). The groundwater modeling also was used to predict the time needed to reach the cleanup goal (8 pCi/l) in the aquifer. This resulted in a proposed system which will include 5 extraction wells placed at the "hot spots" for optimal contaminant removal with a combined pumping rate of 25 gallons/minute (gpm). The lower concentration portions of the Sr-90 plumes will be allowed to naturally attenuate through radioactive decay as they travel south with the regional groundwater flow, while remaining within the BNL campus. This process is projected to return the groundwater to a DWS state in approximately 65 years. This project is currently in the construction stage and is anticipated to be completed in the Fall of 2004.

In Vivo Determination of the Effectiveness of Wearing an Anterior Cruciate Ligament Knee Brace. *JENNIFER LILLY (University of Tennessee, Knoxville, TN 37996) KARA KRUSE (Oak Ridge National Laboratory, Oak Ridge, TN 37831).* Many physicians feel that knee braces designed to aid patients with anterior cruciate ligament (ACL) injuries are ineffective. The knee joint is comprised of the distal end of the femur, the patella, and the proximal ends of the tibia and fibula bones. In addition, various ligaments stabilize the knee during movement. The ACL is located in the middle of the knee and aids in preventing the tibia from sliding out in front of the femur, as well as provides rotational stability to the knee. A study was designed to analyze the knee joint of six subjects, three with a non-repaired ACL deficient knee and three with an ACL replacement of a patellar tendon graft. Computed tomography (CT) scans were performed on all six subjects. Amira was utilized to visualize, segment, and create 3D models of bones from the original CT data of the ACL (deficient or replaced) knee joint. Segmentation invovled both automatic and manual segmenting. Thresholding, an automatic segmentation method, identifies the various pixel intensity levels of each object in the CT scan. A sensitivity analysis was executed to identify the correct intensity of the bones. Manual segmentation was then performed to remove any excess material that did not correspond to bones of the knee. A 3D surface model was generated from the segmented data and its accuracy was verified by comparison with anatomical books and the Virtual Human Project. In the future, the 3D models obtained from the segmentation will be used by Simulated Algorithmic Anatomical Modeling (SAAM), an in-house software package developed by the biomedical engineering department at the University of Tennessee. Fluoroscopic images will be made of the subject's knee during gait and down-hill walking. All patients will perform these activities without a brace and then while wearing two custom ACL knee braces and one off-the shelf knee brace. SAAM will reproduce the 3D scene viewed by the fluoroscope machine, which allows the 3D models to be registered to the 2D x-rays by an optimization algorithm that automatically adjusts the pose of the model at various flexion/extension angles; thus allowing various analysis to be performed. Examination of the data will include evaluation of axial rotation, screw axis calculations, and relative motions of the femoral condyles and tibial plateau. Upon completion of the investigation, the quantitative results will aid in determination of the effectiveness of wearing an ACL knee brace.

Proposal to The Department of Energy for Upgrading an Andros Mark V Robot. *WILLIAM LISA (Roane State Community College, Harriman, TN 37748) BRADLEY S. WEIL (Oak Ridge National Laboratory, Oak Ridge, TN 37831).* The Emergency Preparedness Group (EPG), in the Laboratory Protection Division of Oak Ridge National Laboratory, is interested in having a robot available to be used in emergency situations and highly radioactive areas. At the moment, the EPG has nothing readily available for a possible natural disaster or reconnaissance mission. The Remote Systems Group, of the Nuclear Science and Technology Division, has a Remotec Andros Mark V robot that is suitable for this type of situation. However, several parts of the robot are being decontaminated from a previous job in which it was used in an environmental cleanup project. Although the Andros will eventually be fully functional, the EPG desires several options that can be implemented onto the robot to meet certain expressed standards. Several meetings have been held with companies, such as Remotec and IPIX, to identify certain options that can be employed. Fiber optics, X-Ray technology, and 360 viewing capabilities are just a few upgrades that can be applied to the robot. There are several different conclusions that have been developed, each including various upgrades. A proposal to the Department of Energy (DOE) is being developed to receive funding for the upgrading, maintenance, and training of personnel for the robot. Once the proposal is developed and issued, the EPG and DOE will explore every option and decide what would best suit Oak Ridge National Laboratory.

A Study of Pit Growth and Metal Dusting of Ni-based Alloys. *DAVID LOPEZ (University of Texas at El Paso, El Paso, TX 79936) KEN NATESAN (Argonne National Laboratory, Argonne, IL 60439).* Recently, there has been a great deal of focus on the effects of metal dusting corrosion on commercial alloy surfaces. This phenomenon attacks alloy surfaces at intermediate temperature ranges, usually between 400 C and 700 C inside carbon rich atmospheres. This study focuses on Ni-based alloys, which suffer from a graphite corrosion layer on its surface. Continued exposure to the effects of metal dusting corrosion will eventually lead to the alloy's failure or it will cease to be effective in its use. For experimentation, the Ni-based alloy samples' dimensions were 12 x 20 x 1 - 2 mm and were acquired from various commercial sources. They were placed in quartz specimen trees that were then inserted in horizontal furnaces. The furnaces were sealed from the outside environment while a carbon-rich atmosphere was fed through the holding tubes. The samples were removed every 400 hours for optical and SEM metallography as well as for XRD studies. Using SEM micrographs it was possible to track the growth of the pits that were eventually created on the alloy's surface. Some alloys were clearly able to resist metal dusting for about 5000 hours while others were able to resist metal dusting for 8000 hours. One alloy in particular, Alloy 203 exhibited little resistance to metal dusting. Further studies will focus on the relationship between alloy chemistry and an alloy's ability to resist metal dusting.

Mechanical Design Study of a Five-Meter Superconducting Undulator. *PATRICK LYNCH (Bucknell University, Lewisburg, PA 17837) JOHN SKARITKA (Brookhaven National Laboratory, Upton, NY 11973).* In an effort for brighter, shorter pulse radiation, engineers around the world are looking to improve upon synchrotron light sources through updated insertion device technology and specifically, the superconducting undulator. This study aims to develop a mechanical design for a superconducting undulator, five meters in length, including cryogenic cooling and vacuum containment systems, as well as a variable gap mechanism. A simple wedged bearing system connecting the magnet cores with a thick steel plate set on rails will allow for vertical separation between the magnets through horizontal movement of the plate. In addition, a specially designed beam tube will eliminate the need for the magnet cores to be located within ultra-high vacuum and thus allows for maintenance and insertion without breaking into the ultra-high ring

vacuum. Finally, recent advancements in Pulse Tube cryocoolers have enabled sufficient cooling to reach the 4.2 K temperatures necessary for superconductivity. While this study has provided several solutions to the engineering design issues associated with a superconducting undulator, more in depth studies are necessary. These include finite element analysis to evaluate thermal properties, as well as strength, flexure, and cryogenic heat transfer studies. The results of this study will be used in the future design of a working superconducting undulator, which may initially be used within the Nation Synchrotron Light Source.

Cost Study of a Deep Water Floating Wind Turbine Platform. *JUNE MARIE MALTA (University of Texas at Austin, Austin, TX 78712) WALT MUSIAL (National Renewable Energy Laboratory, Golden, CO 89401).* The implementing of offshore wind turbines in the Eastern United States requires research on different types of platforms in order to address the deeper waters found along the eastern coastline of the United States. In this study, a deep water floating wind turbine platform is being analyzed. The concept for this floating platform is a tension leg platform (TLP) with three tendons. This platform is assumed to be static, neglecting any dynamic effects and is supporting a 5 MW wind turbine that is in a water depth of 200 meters. It is also assumed that two tendons have unloaded due to the overturning moment on the tower and platform, because this is the worst-case loading scenario. In this cost model, concrete dead weight anchors are assumed to be at a cost of $.05/lb and steel costs are $1.50/lb. Using these assumptions it is concluded that the cost of all three anchors is approximately $1 M when the cost of the entire platform (including anchors) reaches its lowest cost at approximately $2.7 M. This occurs at a tank diameter of 12 meters with a tank height to diameter ratio of 0.9.

Adventures in Database and Structural Management. *JOE MANIER (Taylor University, Upland, IN 46989) PAUL CHOI (Argonne National Laboratory, Argonne, IL 60439).* As requirements for successful management of large amounts of data increase, databases have become more important to businesses and industry in today's world. Although we did not develop new techniques for managing information, we did learn current techniques in one of today's prominent research facilities - Argonne National Laboratory. The information in the database consisted of roughly two-hundred thousand engineering drawings used in the designing and building of the Advanced Photon Source (APS) during the late '80s to mid '90s. The database currently provides support for maintaining and continuing the design and construction of the APS.

Editing Geographic Data Files Along The U.S.-Mexico Border. *KENNY MARTIN (Roane State Community College, Harriman, TN 37748) DEMIN XIONG (Oak Ridge National Laboratory, Oak Ridge, TN 37831).* Currently the U.S. Department of Housing and Urban Development (HUD) and the National Transportation Research Center (NTRC) are working together to develop data on housing and infrastructure conditions in poor communities, called Colonias, along the U.S.-Mexico Border. One of the data development efforts is to adjust Colonias boundaries in coordination with existing Census 2000 boundaries so that population and social economic data collected by Census can be effectively utilized for Colonias. The current project makes use of the Geographic Information System (GIS), ArcView, as a primary tool to check, refine, and modify Colonias boundaries that come from external sources. To ensure the quality of the boundary adjustment, Census population data and remotely sensed imagery are overlaid with Colonias boundaries to support adjustment decisions. Census population data map out where people are located in a given area. With the data, Colonias boundaries can be drawn upon where population is found. Imagery can provide evidence on human activities on the ground. Therefore imagery can be referenced when Colonias boundaries are identified. During the project, all three states that are required by HUD, which include Arizona, California, and New Mexico, were completed. The adjusted boundaries provide improved correspondence to the Census boundary files, which means that these adjusted boundaries will help improve the accuracy when Census statistic data are to be transferred to Colonias. There is a couple of cases where Colonias boundaries are not yet identified. In these cases, additional field work will be necessary in order to make the Colonias boundaries available.

Motivation for a Nuclear Power-based Methanol Energy Economy. *HOPE MATIS (Clarkson University, Potsdam, NY 13699) MICHAEL SIMPSON (Argonne National Laboratory, Argonne, IL 60439).* The current energy consumption of the world and especially the United States is higher than ever before and continues to grow, seriously depleting the world's fuel resources and causing heavy environmental impact. This sort of expenditure is not sustainable, and alternative fuel sources must be found before the supply of fossil fuels runs out. Hydrogen is the fuel of choice for current research due to its high energy content and "clean" combustion. This study was performed in order to assess two different types of hydrogen production, conventional and high-temperature (steam) electrolysis, and to choose the "best" technology based on energy concerns and efficiency. Issues facing the use of gaseous hydrogen and the feasibility of the use of a synthetic liquid hydrocarbon fuel as an alternative to hydrogen were examined. Finally, a method of capturing carbon dioxide from the atmosphere was investigated as a source of carbon for methanol production, and the energy concerns of a conceptual methanol plant were assessed. An extensive literature search as well as calculations and preliminary design were performed. Steam electrolysis was determined to be the more efficient process for hydrogen production, linked to a clean and renewable nuclear power source. The use of hydrogen gas is neither energy- nor cost-effective, so the use of methanol was shown to be a feasible alternative. The capture of atmospheric carbon dioxide using a selectively sorbent substance such as calcium oxide or magnesium oxide can potentially provide a source of environmental carbon and create a closed loop system. Finally, the energy provided by a high-temperature stream of hydrogen from an electrolysis unit could provide a considerable amount of the energy needed to run processes in a conceptual methanol plant. Nuclear energy has the potential to provide a low-emissions, high-efficiency source of power to produce the fuel for the next generation of vehicles.

Development of Computer Code for the Selection of a Working Fluid for a Rankine Cycle Power Conversion System for Space Applications. *JUSTIN MCBREARTY (Texas A&M University-Kingsville, Kingsville, TX 78363) GRAYDON YODER (Oak Ridge National Laboratory, Oak Ridge, TN 37831).* Most commercial and all nuclear reactor based power conversion systems utilize the Rankine cycle for power production. The Rankine cycle uses boiling and condensing processes to extract heat from the energy source to superheat a fluid that is expanded in the turbine to develop power. Space based Rankine cycle systems are very similar to those on Earth except that they use liquid metals as the working fluid. A potassium Rankine cycle is ideal because of its high power output per unit mass, it requires compact components, has high efficiency up to thirty percent, and operates at high temperatures and low system pressure. One of the main issues to be resolved before a potassium Rankine power conversion cycle can be used in space is the characterization of two-phase behavior under low gravity conditions. However, testing two-phase potassium systems in manned space vehicles such as the shuttle or International Space Station (ISS) will be difficult because of safety concerns, and testing in unmanned launch systems will be cost prohibitive at this stage in the development process. Developing appropriate dimensionless groups for the different processes of the Rankine cycle will allow other, more benign fluids to be used and simulate the behavior of the potassium system. This work utilizes the appropriate dimensionless groups and the Chempak Add-in software to develop a Microsoft Excel computer code to determine cycle parameters such as boiler tube length, tube diameter, power requirements, exit velocity, and other properties. This computer code can be used to simulate the behavior of different candidate fluids to evaluate their appropriateness for a space based experiment. A limited number of fluids and experiment geometries will be identified for further analysis and more detailed experimental design.

Testing to Support the Calcium-Bromine Hydrogen Production: Calcium Oxide Solubility in Molten Calcium Bromide. *CHRISTOPHER MCGRADY (University of Pennsylvania, Philadelphia, PA 19104) MICHAEL SIMPSON (Argonne National Laboratory, Argonne, IL 60439).* Nuclear power provides an outlet for processes to create hydrogen without emitting greenhouse gases. The Calcium-Bromide cycle is considered one of the top two or three processes for creating nuclear power produced hydrogen. In order to overcome particle fractioning in the thermochemical steps, Dr. Michael Simpson and Dr. Richard Doctor have proposed a molten salt reactor to run the thermochemical reactions in molten form. Since calcium oxide melts at a temperature (2570°C) well above the proposed reactor temperature of 800°C, calcium oxide will have to be dissolved into calcium bromine. Excess calcium oxide was loaded into a ¼ fritted tantalum tube, and allowed to dissolve into 5-10g samples of calcium bromide at 800°C for varying lengths of time. It was found for the maximum time length tested (10.5 days), 1.175% by weight calcium oxide existed in the molten solution. The definite presence of the calcium oxide residing in calcium oxide shows merit in the molten reactor design, and encourages further study.

Using Statistical Bone Atlas for Automatic Segmentation and 3D Registration to Biplanar Fluoroscopic Images. *BRANDON MERKL (Colorado School of Mines, Golden, CO 80401) MOHAMED MAHFOUZ (Oak Ridge National Laboratory, Oak Ridge, TN 37831).* With rising healthcare costs, it becomes increasingly important to develop methods

of surgery that minimize expensive procedures such as Computed Tomography (CT) scans. Many surgical techniques such as Total Knee Arthroplasty (TKA) require such high resolution scans only for the preservation of the bone' s 3D orientation and structure. This study proposes to capture the same 3D data contained in the CT using biplanar fluoroscopic images to retrieve bone orientation and a deformable bone atlas to retrieve bone scale and shape. Statistical bone atlases have previously been created to capture the variation of small sections of bones. In studies of TKA it remains necessary to complete the atlas for entire bones of the knee (tibia, femur, and patella) so the true 3D orientation can be captured from biplanar images. To create the atlas of entire bones, the Matlab™ programming environment has been used to properly format bone models segmented from CT data for correct insertion into the statistical atlas. Once the atlas has been created, using CT data, digitally reconstructed radiographic (DRR) images will be generated to simulate fluoroscopic images for testing. Initially the images will be perpendicular, with one image representing the knee joint's coronal view and another the sagittal view. Using existing 3D to 2D registration techniques, first the base atlas model will be rigidly aligned with the biplanar images using a Simulated Annealing (SA) algorithm. At this point the bone is aligned to the dataset, but not the correct scale or shape. An evolution-based Genetic Algorithm (GA) will then be used to deform the base model to the correct shape. Progress on the project has been quite rapid, as many existing components of the overall algorithm have been pieced together. The current difficultly is creating the atlas of full femurs. The shape of the bone varies uniquely from person to person which is difficult to capture with statistics. Future work is necessary to ensure that critical features are not lost in the formatting process. When the method is perfected, TKA surgeons can then use inexpensive fluoroscopic images both in preoperative planning and eventually for intraoperative surgical navigation. The future is promising for an intraoperative surgical navigation system because surgeons using optical trackers on instruments with real-time feedback could perform surgeries using minimally invasive surgical techniques.

Spark Plug Erosion in Natural Gas Engines. *WILLIAM MICHIE (University of Maryland, College Park, MD 20742) TIM THEISS (Oak Ridge National Laboratory, Oak Ridge, TN 37831).* Internal combustion natural gas engines have gained popularity in the fields of distributive and emergency power generation. One of major maintenance issues with these systems is spark plug failure. The spark plug in a natural gas engine is similar to those in automobiles, but because the plug uses expensive components, platinum and iridium, it makes them considerably more costly. An even greater concern is the engine down time during spark plug servicing. The failure, it appears, is due to an increase in the gap distance between electrodes as surface material is eroded away. One of the ways to determine what elements are eroding off the spark plug is to use optical spectroscopy. Using this method the visible spectrum of the electromagnetic radiation emitted during a spark event is analyzed. Each element emits specific wavelengths of light when the electrons, within the atoms, changes energy states. By analyzing the intensity and wavelengths of several 'peaks' the unknown elements can be determined through comparison to known parameters for given elements. This is performed at 200 psig to simulate the pressures at time of ignition. Several different plugs have been and will be tested from engines that have run for various lengths of time. The primary elements that are being seen have been nickel, platinum, nitrogen, calcium, and oxygen. The platinum and nickel are results of the spark plug electrodes being ionized during the spark event. Nitrogen and oxygen are from the air inside the test chamber. The calcium is a result of the engine lubricants and is not present in plugs that have not been run in the engines. The intensity of the nickel decreases while the intensity of the calcium increases with use. Preliminary results show that as the spark plugs are run they first emit strong nickel lines, probably coming off the spark plug cathode, an increase in calcium due to longer exposure to the engine lubricants, and an initial decrease in intensity followed by increasing intensities. The decrease then increase in intensity is postulated to be the result of a calcium-oxide layer forming on the electrodes. The oxide layer then reduces the voltage required to bridge the spark gap resulting in a lower intensity photonic emission. Future areas for examination will be to first see if plugs run for x amount of hours on either side of the trough will support or refute the hypothesis.

Database Managment. *ANDREW MIKLOS (University of Illinois at Chicago, Chicago, IL 60607) PAUL CHOI (Argonne National Laboratory, Argonne, IL 60439).* Database management included many different tasks. First, the drawing was located on the H drive, which is the local drive that contains individual's drawings. These drawings were then imported into a workspace in Intralink, a software program which holds drawings. Intralink reads AutoCAD drawings using a software package called Legend by I-Cubed. Unfortunately, many of the drawings have misprints, so corrections had to be made. The newly introduced drawings were linked to previous drawings. The drawings were then checked into the commonspace in Intralink where anyone can view them. The drawings were plotted as a full and 11x17 size. The drawings had to be checked and signed before taking them to the Document Control Center to be filed. A copy was also filed in the Design and Drafting Group's office where it was made. I also created a drawing showing the floor anchor locations for a new beam line in the Advanced Photon Source. The drawing was created using drawings of the individual parts and placing one after another in a line to form the entire assembly. This drawing will be one the first things used when construction begins during the next shutdown because it shows where everything goes.

The Four Point-Probe Technique for Determining Matrix Resistivity and Contact Resistance in Cathode Compounds as Used in Li-Ion Batteries. *BRENDEN MILLSTEIN (Harvard University, Cambridge, MA 02138) KATHRYN STRIEBEL (Lawrence Berkeley National Laboratory, Berkley, CA 94720).* The effectiveness of hybrid-electric and electric vehicles is greatly limited by the cost of their batteries. The use of lower-cost and higher capacity Li-ion batteries for this application is limited by their safety and power characteristics. Recent research has shown the most resistive part, and hence largest factor limiting the power of a Li-ion battery, is the cathode. Various methods are being developed to lower the resistivity of cathodes, resulting in multilayered cathodes. One of the power losses in a Li-ion battery comes from the contact resistance between the current collector and active material layers in cathode compounds. In order to measure this contact resistance, a four point-probe technique is used. A known current is passed through the outer two probes, and the voltage difference between the inner two probes is measured. The mathematical solution to the conduction problem in a porous and multi-layer system has recently been completed at the U. of Michigan and delivered as a computer program to LBNL in a collaborative effort. In order to accurately measure the matrix and contact resistances, extremely accurate probe positioning is required and the probes must not penetrate the active mass on the current collector. Two probes, with two different probe spacings as required for the calculation, were constructed with gently spring-loaded gold-plated contact pins, mounted into Lexan blocks. The blocks were drilled to an accuracy of one one-thousandth of an inch. The pins protrude from the block 20 microns and withdraw to flush with the surface when the block is rested on the substrate. Only trifling compression effects were found in the substrates. Spring loading the contact pins ensures good electrical connection, while the gold plating reduces the contact resistance between pin and substrate to a negligible level, further reducing the error bar on measurements. The probes have been used successfully on various anode constructions. However, the high resistivity of the cathodes tested so far suggest that even smaller probe spacing and higher accuracy voltage measurements will be required for accurate measurements of the contact resistance in the cathodes. Alternatively, a new geometry has been suggested whereby all of the current must flow across the cathode construction. This is the subject of future work.

Fundamentals of Programmable Logic Controllers (PLCs) and Designing a PLC Controlled Accelerator Experimental Beamline Access Security System. *MWESIGWA MUSISI-NKAMBWE (Stony Brook University, Stony Brook, NY 11972) VINCENT J. CASTILLO (Brookhaven National Laboratory, Upton, NY 11973).* Allen-Bradley (A-B) has 2 Programmable logic Controllers (PLC) application software packages: RS Logix generates logic codes for reading data from sensing modules and writing commands to controlling modules and RS View allows for the formulation of human-machine (H-M) interfaces, on computer screens, that interact with operating systems in real time using the information from the RS Logix program. Simple RS Logix programs are written and tested on hardware in a laboratory setting to get an understanding of how these programs function, along with the RS View H-M interfaces. This knowledge and skill with RS Logix and RS View is used to build a Controlling system for access security to a typical Experimental Beamline on the Experimental floor of the Alternating Gradient Syncrotron (AGS).

The Study of Cascading Failures in Complex System. *BERTRAND NKEI (Virginia Polytechnic Institute and State University, Blacksburg, VA 24060) BENJAMEN CARRERAS (Oak Ridge National Laboratory, Oak Ridge, TN 37831).* The disturbance of large interconnected infrastructure is very often caused by cascading failures of loaded system components. For instance, large blackouts of electric power system are caused by cascading failures of overloaded components. The CASCADE model of cascading failures of a system with many identical components randomly loaded is used to study the propagation of failures in both a single system and in coupled systems. Considering

a single system (electric power grid for instance), an initial disturbance causes some components to fail by surpassing their loading limit. Failed components interact with other components by transferring a fixed amount of load to them that increases the probability of further failures. As components fail, failure of other components becomes probable. This model has been implemented in a C++ cellular automaton code. The original CASCADE model studied in a single system gave results similar to the more detailed ORNL-Pserc-Alaska (OPA) model for blackouts dynamics, but it shows some clear discrepancies. It captured only few of the features of the OPA model. By adding truncation and randomization of outages to the model, it gives results more similar to that of the OPA model. After comparing the features of the CASCADE model to that of the OPA model in a single system, we have extended the model to coupled systems. Even though many infrastructures can be modeled individually, in reality they interact with each other in more complex ways. These interactions can lead to a decrease or increase of the risk of failures in those individual systems when coupled, depending on the sign of the coupling coefficient κ. The CASCADE model is modified to study the impact and to investigate on the interdependencies between those complex infrastructures, in particular a coupled system.

The Study of Cascading Failures Using the Cascade Model with Truncation and Randomization of Outages. *BERTRAND NKEI (Northern Virginia Community College, Annandale, VA 22003) VICKIE LYNCH (Oak Ridge National Laboratory, Oak Ridge, TN 37831).* The disturbance of large interconnected infrastructure is very often caused by cascading failures of loaded system components. For instance large blackouts of electric power system are caused by cascading failures of overloaded system components. The CASCADE model of cascading failures of a system with many identical components randomly loaded is used to study the propagation of failures in an electric power grid. An initial disturbance causes some components to fail by surpassing their loading limit. Failed components interact with other components by transferring a fixed amount of load to them that increases the probability of further failures. As components fail, failure of other components becomes probable. This model has been implemented in a C++ cellular automaton code. The original CASCADE model gives results similar to the more detailed ORNL-Pserc-Alaska (OPA) model, but it shows some clear discrepancies. It captured only few of the features of the OPA model. By adding truncation and randomization of outages to the model, it gives results more similar to that of the OPA model and there is some progress in understanding the relationship between the CASCADE and the OPA models. In these two modifications of the CASCADE model, failing components interact by transferring loads to a random sample of components. With truncation the cascading failures stops after an arbitrary number of failures in the system while with the randomization of outages, overloaded components fail with a given probability P1. The CASCADE model is characterized by some parameters (θ and λ) that control the propagation of failures and the goal of this research is to find if they can be applied to a real-world power system.

Image Segmentation of Natural Scenes in the Support of Content-Based Image Retrieval. *MASHAMA OSBORNE (Southern University, Baton Rouge, LA 70813) KEN TOBIN (Oak Ridge National Laboratory, Oak Ridge, TN 37831).* Content-based image retrieval is the retrieval of images from a database using information within the image data. The analysis may involve manual intervention, or it may be entirely automated. Manual analysis involves human interpretations to identify properties within an image. Automated analysis extracts image features that describe the properties of the image. There is a need for organizing extremely large images into a database searchable platform categorized by image characteristics. An automated segmentation technique can be used to help organize image data and assist research in defining image characteristics best suited for searching the contents of the database. The evaluation and comparison of the performance of the manual segmentation techniques versus the automated routines implemented in Matlab are the main focus of this research. To evaluate the segmentation results from two different methods a routine in Matlab was provided to compare the performance of the segmentation techniques. Synthetic images were created to verify the correct implementation of the Matlab routines for comparison. Verifying the Matlab routines consisted of synthetic images being processed and a 100% performance produced for all the evaluation measures. The synthetic images are used to verify the % correct; % coverage, % misclass, and % uncertain. The % correct corresponds to the correct number of pixels that match both the ground truth and the result of the automated techniques, % coverage is proportional to the number of pixels that are covered in the image, % misclass is proportional to the number of pixels that don't match the ground truth data and the % uncertain is proportional to the pixels that are undefined areas in the ground truth. To validate the performance of the automated segmentation routines, ground truth data was generated from 6 example images. The ground truth data was manually generated from these 6 images using visual characteristics that differentiated areas of interest such as water, heavy trees, mixed vegetation and buildings. The areas of interest are then filed into a searchable database for automated retrieval applications. In this area of research the automated and the manual techniques both have their advantages and disadvantages. These techniques go hand in hand to perform ideal evaluations for image processing.

Cryogenic Cycle for a High Temperature Superconducting Magnet. *JENNIFER PAI (Cornell University, Ithaca, NY 14853) KUO-CHEN WU (Brookhaven National Laboratory, Upton, NY 11973).* With current advances in high temperature superconductivity, new superconductors can be run at temperatures higher than 4K. These new materials require cooling and refrigerating to temperatures between 5 and 80K while still producing similar results as those of previous superconductors. Currently at Brookhaven National Laboratory, a fragment separator is studied that operates at 20-30K. Several process cycles were developed and studied with parameters specific to this magnet. The parameters included a 5,000 watt heat load based on previous studies on the magnet. Thermodynamic calculations were performed using Excel with helium properties provided by a Hepak program. Process cycles were adapted from existing 4K refrigerators with a modified cold end configuration. Each process cycle was evaluated with Carnot efficiencies ranging from 11 to 23%. The most efficient process design happened to contain the fewest components. This resulting process cycle will serve as the baseline and later be refined for cooling the high temperature superconducting magnet at Brookhaven National Laboratory.

Helping The Environment With Zero Energy Houses. *CHARITY PATE (Bevill State Community College, Fayette, AL 35555) JEFFERY CHRISITAN (Oak Ridge National Laboratory, Oak Ridge, TN 37831).* Is it possible for people to buy an affordable home, in a Mixed Humid Climate, where they will have a net zero energy bill? This possibility is becoming more of a reality with the research of attempts at zero energy housing. Construction on this project began in 2002 and now in 2004 there are four near zero energy houses that have been researched. These houses have many unique features; most of these houses have structural insulated panels, mechanical whole house ventilation, insulated unvented crawl spaces, high efficiency windows with a low U-Factor and Solar Heat Gain Coefficient, space integrated heat pump water heater, and (1.98kWp-2.2kWp) grid-connect solar photovoltaic system along with many more energy efficient technologies. These features together create an air tight envelope, the ability to use as little energy as possible, and give the house the capability to produce on site energy. Sensors were installed in the house to monitor these energy efficient technologies and the roof top photovoltaic solar electric system. These sensors retrieve the data from the houses and store it in a data base for research. These houses are at least six times more air tight, and use 40% to 70% less energy than similar houses with 2x4 frames. Throughout this project the data from each existing house was compared and analyzed in order to make the next house or houses more energy efficient. Comparing the data will make it easier to accomplish net zero energy. The long term goal of this project is to build 6 houses, getting closer each time to a net zero energy house and then make similar housing available to the housing market. With well executed research plans and prototype construction, zero energy friendly occupants and maybe even a little luck these houses will contribute to solutions to excessive ozone, smog, and particulate concentrations.

Statistical Analysis of Parameter Variations in an Integrated Circuit Amplifier for the ATLAS Cathode Strip Chamber. *JOSE PEREZ (The City College of New York, New York, NY 10031) PAUL O'CONNOR (Brookhaven National Laboratory, Upton, NY 11973).* The ATLAS (A Toroidal LHC ApparatuS) experiment is one the most ambitious projects in modern physics. One of the objectives of the project is the discovery and study of elementary particles obtained in the head-on collisions of protons of extraordinarily high energy. This research consisted in the testing, data collection and analysis of the monolithic pre-amplifier shaper ICs to be used in the ATLAS Cathode Strip Chamber (CSC). The function of the pre-amp is to generate a pulse signal based on the energy, trajectory, and time of occurrence of particles passing through the CSC. For this research, this event was simulated with the Automated Test Motherboard (ATM), which measured the amplitude, width, base-line, and other parameters of the pulse generated by the pre-amp and stored this information into a database. Using a hybrid pre-amp, the values of the injection capacitors in the test board were measured and the gain of all pre-amp channels were calculated. C scripts were written and used with ROOT to generate plots of the data collected. An analysis

of these plots showed a correlation between the value of the injection capacitors and the pre-amp's measured gain. This information, as well as other data analysis, will be used in the future to select the pre-amps that will make the final cut to the assembly phase and into ATLAS.

Low-Power Hydropower Water Energy Resources and Technology Assessment. *JOSHUA PETERSON (Idaho State University, Pocatello, ID 83201) CHERYL O'BRIEN (Idaho National Engineering & Environmental Laboratory, Idaho Falls, ID 83415).* Hydropower currently supplies about ten percent of the current United States electricity production. Undeveloped U.S. water energy resources that are not restricted from development by federal statutes and policies are estimated to be about 170 GW of annual mean power. However, hydropower facilities can have harmful environmental effects upon aquatic and terrestrial ecosystems. Because of these effects, development of new hydroelectric plants has slowed significantly. Low-impact hydropower facilities may be the answer to future hydroelectric power production as they do not require dams and reservoirs, but do provide low impact power generation. A recent report published by the U.S. Department of Energy (DOE) entitled Water Energy Resources of the United States With Emphasis on Low Head/Low Power Resources estimated low-power (< 1 MW) water energy resources of about 50 GW. It also estimated that an additional 120 GW of available high power (> 1 MW) water energy resources exist that could partially be used for low impact hydropower generation. Currently, there is not a comprehensive reference informing private organizations, utilities companies, and government officials of the availability or abundance of low-power hydropower technologies. Collecting data on current, low-power hydropower technologies is the first step in creating such a reference. A request for information regarding low-power technologies was sent to over 100 vendors and designers. This data will be available on-line in a user-friendly, searchable catalog planned for release via the Hydropower Program website in the fall of 2004. Additionally, an onsite survey of five low-power hydropower facilities was conducted around the area of Twin Falls, Idaho to obtain information about operating, licensed, low-power hydropower facilities. This information will help emphasize that while hydropower is one of the first energy sources of mankind, new technologies help make it feasible today as a method of generating needed electrical energy with low environmental impacts. The recently published DOE report estimating significant water energy resources available in the United States combined with the new online, searchable catalog of existing low-power technologies, will provide private organizations, utility companies, and government agencies with needed information to make informed decisions regarding low-impact hydropower, a renewable energy resource helping meet increasing demands for electricity.

Increasing Efficiency of Argonne Wakefield Accelerator Klystron and Linear Accelerator. *TONG QUAN (Purdue University, West Lafayette, IN 47906) WEI GAI (Argonne National Laboratory, Argonne, IL 60439).* The current low level radio frequency synthesizer and amplifier used to power the klystron for the main gun at the Argonne Wakefield Accelerator uses much outdated technology that is increasingly becoming an impedance against the efforts to condition the linear accelerator. One major concern to updating the current RF system is to gain more output power. Accompanying this goal are other performance enhancing factors such as less EMI interference, equipment conglomeration and other stability issues. After purchasing the parts of the RF system, a slew of tests were conducted and documented both with test bench equipment and in conjunction with the klystron before an aluminum chassis is built. The new RF system was able to map out the entire operating spectrum of the klystron and at the same time delivering power with decreased phase noise and other interferences. Although further testing is still needed, current analyses on the new RF system has met or exceeded all user expectations and is currently ready for operation.

Increasing Accuracy in Western Power Grid Models Through Intense Grid Data Analysis. *ENRIQUE RAMIREZ (South Mountain Community College, Phoenix, AZ 85042) CODY RAY (Walla Walla Community College, Walla Walla, WA 99362) CANDEE HASSLER (South Mountain Community College, Phoenix, AZ 85040) MATT DONNELLY (Pacific Northwest National Laboratory, Richland, WA 99352)DAVID CHASSIN (Pacific Northwest National Laboratory, Richland, WA 99352).* As the population of users of the western power grid grows, the demand upon the aging grid increases. Computer models, based on complex mathematical relationships are being developed to assist in the forecasting of grid dynamics. This project utilized gigabytes of data collected by computer over the last few years, consisting of the frequency versus time of an AC line source. This data was stored in a database, enabling easy access from Matrix Laboratory (MATLAB). Event information was obtained from sources such as Western Systems Coordination Council (WSCC) to determine the supply drop, the change in power recorded into a new table and calculations were performed upon these specific events. MATLAB was programmed to perform necessary calculations to approximate the average slope of the frequency deviation in the data. This quantity represents the proportion of frequency drop with a given amount of time. Utilizing the theoretical relationship between change of power and frequency deviation (Where M is an inertial property of the Grid, and □P is the difference between Supply and Load), we were able to calculate many values for M. We found that M has an extremely small value, suggesting that the Western Grid has a high inertial value. This means that the Grid itself resists change strongly. Upon plotting m as a function of system wide load taken at the time of the events, there existed minimal correlation. Plots utilizing other data entries also yielded little if no relationship. Application of MATLAB noise filtering algorithms yielded much lower slopes, and did not change the lack of correlation. Future studies need to focus on more accurate and more available data. Successful computational models are dependent on real world data analysis for accuracy. Studies such as this are imperative in the success of such models.

Building a Statistical Database of 3D Patient-Specific Models. *EMILY REAGAN (University of Tennessee, Knoxville, TN 37996) KARA KRUSE (Oak Ridge National Laboratory, Oak Ridge, TN 37831).* Non-invasive techniques such as computed tomography (CT) can be expanded through image processing to give more information about the shape, movement, and interaction of muscles, bones, or arteries. Segmentation is the process of building a unique 3D model from patient CT data by interpolating between images to generate a surface of the desired anatomical structure. An automatic algorithm for segmentation would greatly reduce the time and error associated with manual segmentation. However, blurry images, noise, and dataset irregularities hinder the accuracy of both manual and automatic segmentations. Automatic approaches include "thresholds", where data is selected based on pixel intensity levels, "snakes" in which a simple contour expands to contrast boundaries in the image, and "deformable models", where an existing 3D model expands to fit a data volume. Currently, each technique has difficulty accurately identifying the tissue or bone to be modeled. In this study, Amira™ software is used to transform raw data into corresponding models through a combination of thresholds and manual segmentation. Each model, represented by a mesh, is then formatted for input into a custom database through a Matlab™ script that re-meshes the models based on rigid alignment and affine warping to a base model. As more models are added, more statistical knowledge will be developed to determine how anatomic structures vary from person to person. With current available patient CT data, segmentation is underway for 30 scans of the leg and 4 of the lumbar spine for bone analysis. The database is being constructed for use with the current data and investigation is ongoing to determine the most efficient way to build and remesh bone models without data loss. The database promises a variety of applications. It will allow a statistical analysis to be performed for use in creating a normal base mesh for a deformable-model automatic segmentation. Also, the availability of 3D bone structures will be a tool in the future for building a surgical navigation system to simulate patient-specific surgery scenarios. Hypothetical models can be created from the statistical database for stress analysis of joints, and vascular models can be used for fluid dynamics studies. In addition, registration of bone models onto fluoroscopy can be used to calculate in vivo kinematics.

Laser Electron Facility Sample Changer. *ALEXANDER REBEN (Florida Institute of Technology, Melbourne, FL 32901) JAMES WISHART (Brookhaven National Laboratory, Upton, NY 11973).* The Laser Electron Accelerator Facility (LEAF) contains an apparatus that is used to investigate fast reaction radiation chemistry. Since the facility puts out high radiation levels it is not possible to be in its protected vault while operating. If an experimenter wanted to test several solutions, they would need to shut down the accelerator to manually switch samples. Implementing an automatic sample changer can overcome this problem. Multiple solutions were investigated, including an expensive but precise system using motorized stages, but ultimately the decision was to make a simple "carousel" system using a microcontroller interface to LabView instrumentation control software. The system consists of a round aluminum plate with four square sample holder holes in it. The sample holders are of a standard size as to facilitate interoperability between sample holder systems and the ability to accommodate different sample containers. This disk is then attached to a low speed motor that in turn connects to relays that are connected to the microcontroller. The plate has four optical switches to read position and three limit switches to report the stop command to the microcontroller. This whole assembly is then connected to a custom "block" that contains the mirrors to guide the pulse laser and proper hardware to attach itself to the beam lines. It

was important to keep the device together as a module so that it could be removed and attached with minimal recalibration. The “block” inside the vault is then fed its control through cables from the control box outside the vault, which contains the microprocessor. This control box provides audio/visual feedback and allows complete manual control of the changer if so desired. The control box then provides rudimentary control signals in the form of TTL binary logic to the LabView interface board. It is at this point where the signals are opto-isolated for safety. The LabView then has a custom “Virtual Instrument” to control the sample changer and read its position, ensuring proper operation. This system will enable scientists to continue their research with minimal interruption and downtime due to the shutdown and warm up time required to perform sample changes.

Conductivity Analysis of Membranes for High-Temperature Proton Exchange Membrane Fuel Cell Applications. *RYAN REED (University of Washington, Seattle, WA 98195) JOHN TURNER (National Renewable Energy Laboratory, Golden, CO 89401).* Low-temperature operation requirements for per-fluorinated membranes are one factor that limits the viability of current fuel cell technology for transportation and other uses. Because of this, high-temperature membrane materials are being researched. The protonic conductivity of organic/inorganic hybrid composites membranes, a per-fluorinated membrane from Russia, and heteropoly acid doped Nafion membranes was studied using the BekkTech® conductivity test cell. The goal was to find a high-temperature membrane with sufficient conductive properties to replace the currently implemented low-temperature membranes, such as Nafion. Organic/inorganic hybrid membranes were prepared at the National Renewable Energy Laboratory (Golden, CO) using a sol-gel method. Plastpolymer (St. Petersburg, Russia) supplied the Russian membrane material. Heteropoly acid doped Nafion membranes were produced at the Colorado School of Mines (Golden, CO) using a method previously discussed. Four-point conductivity measurements were taken using cyclic voltammetry. For the duration of our tests, most membranes were quasi-stable at +100°C. Results showed that the organic/inorganic membrane, SFA/BSPPO, has similar protonic conductivity to Nafion of similar thickness. The Russian membranes were shown to have similar to slightly better conductivity than Nafion at high-temperatures. However, like Nafion, performance dropped upon dehydration of the membrane at higher temperatures. Of the heteropoly acid doped Nafion membranes studied, silicotungstic acid was found to be, overall, the most promising for use as a dopant.

Effectiveness of an Enthalphy Recovery Ventilator at Climate Control Cost Reduction. *KEVIN RHODES (University of Tennessee, Knoxville, TN 37996) JAN BERRY (Oak Ridge National Laboratory, Oak Ridge, TN 37831).* An enthalpy recovery ventilator (ERV) works to transfer both latent and sensible heat between building supply and exhaust air. This recycling of energy already expended by a buildings’ heating and cooling system, potentially increases climate control efficiency and reduces operating costs. An analysis of the Semco FV7500H installed at the National Transportation Research Center (NTRC) in Oak Ridge, TN was performed to determine if and to what extent this unit is saving energy. A pair of standardized HOBO data loggers were placed inside the Semco ERV in order to calibrate the readings given by permanent sensors already installed in the unit. These permanent sensors transmitted data via the SuperVision data acquisition program and these data were corrected as needed for calibration to the standardized values.The electrical current drawn by the heat exchange wheel and two blower fans was measured and used to find the power consumed by the ERV--resulting in an accurate estimate of parasitic losses. A spreadsheet was developed for calculating savings based upon common indoor heat and humidity requirements and energy costs in the Tennessee River Valley. Data collected thoughout July 2004 showed a daily average savings of 156.2 kWh, valued at approximatly $6.41 in the Tennessee valley power region. Of note is that the amount of latent heat recovery expressed in Btu/h consistently overwhelmed that of sensible heat recovery by one or two orders of magnitude. It is clear that notable energy savings result from the ERV equipment at NTRC during summer conditions. If the averages for July were taken as an estimate of the daily average for the entire year, the ERV would pay for itself in roughly seven years. However, since each season exposes the system to different operating conditions, the systems performance must be carefully monitored over an entire year before the actual effectiveness of the ERV in reducing the cost of climate control can be accurately determined.

Regional Distribution of Arachidonoyl Ethanolamide (anandamide) in Relation to the Location of Fatty Acid Amide Hydrolase (FAAH) in Mouse Brain. *ELIZABETH RICHARDSON (Salt Lake Community College, Salt Lake City, UT 84116) ANDREW GIFFORD (Brookhaven National Laboratory, Upton, NY 11973).* Past studies have demonstrated that fatty acid amide hydrolase (FAAH), plays a crucial role in the degradation of the neurotransmitter anandamide. Anandamide, when administered to FAAH knockout mice, has similar localized effects as D 9-tetrahydrocannabinol or (D 9-THC), the psychoactive component in marijuana (Cravatt, 2001). In this project, we hope to establish a concrete link between the regional accumulation of anandamide and its metabolites and the rate of regional degradation in vivo. In order to find this connection, four wild type mice were injected along a time course with radiolabeled anandamide. After which, the amount of radioactivity was quantified in the collected blood samples and different portions of the brain including the anterior cortex, posterior cortex, hippocampus, caudate putamen, and cerebellum. A higher accumulation of anandamide and its metabolites was observed in the anterior cortex, posterior cortex, and cerebellum when normalized over the caudate putamen. These findings corroborate recent imaging data that also observed differential accumulation of AEA and its metabolites in wild type mouse brains, but not the brains of FAAH knockout mice. Together, these data suggest that FAAH activity is driving the observed differential accumulation. It is our hope that this recently developed protocol can be used as a screening method for FAAH inhibitors with the goal of using inhibitors of anandamide metabolism as a pharmaceutical drug with only localized activity.

Analyzing Petroleum Displacement Impact of Medium- and Heavy-Duty Natural Gas Engine Research and Development. *CHRISTINE RIKER (Albion College, Albion, MI 49224) MIKE FRAILEY (National Renewable Energy Laboratory, Golden, CO 89401).* The United States imports more than 50% of the petroleum it consumes, much of it from politically unstable countries. The use of natural gas fueled vehicles can help decrease this petroleum need, reduce emissions, and facilitate the transition to a transportation network based on hydrogen fuel. The National Renewable Energy Laboratory (NREL) and the Department of Energy conducts research and development (R&D) on natural gas engines for use in medium- and heavy-duty vehicles because of these vehicles’ high fuel consumption and emissions. One goal of this project was to develop methods for determining the amount of petroleum displaced by natural gas engines that NREL R&D helped to bring to commercial viability. Another goal was to determine the amount of petroleum that could be displaced by using natural gas engines in refuse trucks, transit buses, demand response vehicles (shuttle buses not operating on a fixed route), and school buses. This information will aid in selecting future natural gas engine and vehicle projects with the highest potential impact. Data used to calculate fuel consumption were collected from national statistical databases, NREL evaluation studies, expert opinions, and fleet data. It was assumed that one natural gas vehicle would replace one diesel vehicle of the same type. The results indicated that replacing diesel vehicles with natural gas vehicles could displace the following quantities of petroleum per year: 430 million gallons from refuse trucks, 590 million gallons from transit buses, 55 million gallons from demand response vehicles, and 520 million gallons from school buses. Results of this study, based on preliminary engine sales data, have shown that 313 million gallons of petroleum have been displaced since 1994 due to DOE/NREL natural gas engine projects. This study uncovered several important data sources as well as limitations of current data needed for calculating detailed petroleum displacement for the target vehicles. The data identified and methods used created a solid base upon which NREL can build to revise and expand its understanding of the impact of its natural gas engine and vehicle projects. Future work may include evaluating the petroleum consumption of additional vehicle types (e.g., pick-up and delivery vehicles) and enhancing project selection by predicting the amount of petroleum that will be displaced by prospective projects.

Model and Simulation of DOD Battlefield Communications Based on a Markov Process Tied to Varying Network Topology. *MICHAELA ROBERTS (Prairie View A&M University, Prairie View, TX 77446) GLENN O. ALLGOOD (Oak Ridge National Laboratory, Oak Ridge, TN 37831).* Oak Ridge National Laboratory is currently working on developing a communication model, for the Army’s Future Combat Systems (FCS), that will provide insight into information and data transfer across the battlefield communication network. These communication models will be designed to analyze latency and assess combat effectiveness. Work is being done to develop a “next generation” Speed of Service (SOS) model that can be related to Combat Identification (CID). At the core of this work is the development of a Markov Chain and associated conditional probabilities in MATLAB. MATLAB is a high level technical computing language and interactive enironment and can be used for doing numerical computations with matrices and vectors. The Markov Model consists of five nodes with five states within each

one.The conditional probabilities calculated determine, with the use of probabilty transistion matrices, which state or node the program transitions to, and are calculated in consideration of a number of elements, to include: latency, data integrity, Quality of Service, throughput, network configuration, network tropology, and commander confidence. With these elements used to determine the probabilties, and the probabilites fueling the Markov Model, the abiltiy to produce varying times across the network has been established. The program is now at the stage inwhere the time varying variable and the function for the calcuated probablilites are to be added. Expectations remain high that this step will be completed before the end of the appointment and be ready to be used for a presentation within the next few upcoming months.The product from the research will be integrated into the Combat ID System of Systems Application and be used to assess the information flow and data integrity across a real time varying network.

High-Performance, Small Commercial Building Case Study: National Wind Technology Center (NWTC) Security Post Energy Performance and Trombe Wall Benefit Analysis. *MATTHEW ROOKE (Messiah College, Grantham, PA 17027) PAUL TORCELLINI (National Renewable Energy Laboratory, Golden, CO 89401).* A small security building built in late 2002 at the entrance of the National Wind Technology Center near Boulder, Colorado provides a platform for research into the energy performance of small commercial buildings. The 160-ft^2 building has many features designed to reduce energy consumption. In addition, a hybrid uninterruptible power supply (UPS) produces electricity with the ultimate goal of energy self-sufficiency, a net-zero building. Building temperature and electrical data collected from June 2003 to May 2004 is used in this performance analysis. The annual net energy use is 785 kWh; on-site renewables provided 63% of the building's energy needs. A specific point of interest is the un-vented Trombe wall, a feature designed to provide passive solar gains during the winter months. The wall is 4-inches thick, much thinner than most Trombe walls. A two-week experiment, verified by a simulation with the SUNREL building energy program, established that 0.5 kWh/day could be saved by covering the wall during the summer. A year-long simulation predicted that, on a yearly scale, the Trombe wall was un-beneficial for the building unless it was covered during the summer months.

Beam Loss Monitor Test and Calibration Station. *LUKE ROSEBERRY (Virginia Polytechnic Institute and State University, Blacksburg, VA 24060) SAEED ASSADI (Oak Ridge National Laboratory, Oak Ridge, TN 37831).* The Beam Loss Monitor detectors at the Oak Ridge National Laboratory's Spallation Neutron Source are used to document the distribution of beam losses, aide in reducing the losses and radioactivation of accelerator equipment and, in the case of an excessive loss, inhibit the beam through the Machine Protection System (MPS). In order for these detectors to be useful they must be tested and calibrated inside of a radiation field. The Beam Loss Monitor Test Station (BLMTS) performs this task. The Beam Loss Monitors are composed of several different types of detectors designed by Brookhaven National Laboratory. These detectors are 400 ion chambers, 30 neutron detectors, 18 fast PMTs, and 12 x-ray detectors (ORNL designed). The BLMTS is an automated system comprised of a Cs-137 source with automated holder, a three dimensional stage, environment monitoring detectors, Stanford Research Systems, Inc PS350 5000V power supply, a Keithley 6517A pico-ammeter, three computers, and a personal protection system. The project involved coupling all of these devices together to create programs that performed the necessary actions. The programs were written in LabVIEW utilizing state machine architecture. There are two separate computer systems running their own programs. The first system controls the testing of the detectors and the second system continually takes environment radiation readings. Not only can the BLMTS perform a detector calibration, but the station can use a detector to create a map of the radiation field. The environment radiation readings are automatically saved to the local system and to an Oracle database. The result of this project was an operating test station with the safety features and protections expected in a radiation environment.

Determination of Diesel Fuel in Oil. *ALYSSA ROSENQUIST (University of Tennessee, Knoxville, TN 37916) SAMUEL LEWIS (Oak Ridge National Laboratory, Oak Ridge, TN 37831).Several components, which operate a diesel engine can cause engine wear over a period of time.* One area of concern is that of increased friction occurring between the surface areas of a piston and cylinder. The problem stems from the presence of diesel fuel found in the oil, which used to lubricate the operation, thus diluting it. Initially, the method for calculating the amount of fuel in the oil was done through a difference in weight measurement. The weight of the oil added to the engine was recorded, then after operating for approximately 2400 hours, the oil was drained completely from the engine and its weight was recorded and then subtracted from the initial weight of the oil to obtain the amount of fuel which was present. Although it was determined that there was fuel present in the oil, this required too much time and was based more on an estimated value, rather than an accurate calculation. An alternative to this procedure was developed on the basis that oil was composed mostly of hydrocarbons and that diesel fuel consisted mostly of aromatic compounds. This allowed for an analytical technique to be used for analyzing a used oil sample taken directly from a diesel engine and measuring its aromatic content. Once the aromatic content is known, the concentration of the fuel in the oil can then be accurately determined and recorded. In order to monitor the aromatic content, however, the hydrocarbons from the oil must be removed before analysis. For sample preparation, Elution Chromatography was chosen to separate the nonaromatic compounds from the aromatic ones prior to each analysis. Once the preparation process is complete, each sample is then analyzed using GC/MS while select ion monitoring thus identifies and measures the area count of the aromatic compounds present in the diesel fuel added to each sample of oil. Standards using a range of concentrations will be the basis for a calibration curve and further used for the determination of the actual concentration of the fuel in each sample. An equation calculated from this graph can then determine the concentration of fuel in an actual oil sample taken from a diesel engine that has been in operation over varied amounts of time. Once this is proven, future steps can be taken to prevent this dilution by eliminating the addition of fuel in the oil itself, or a more resistant type of oil made to reduce this increase of friction that is caused and thus aid in reducing engine wear.

The Impact of Complex Inorganic Color Pigments on the Thermal Performance of Residential Roof Systems. *BENJAMIN RUDOLPH (Virginia Western Community College, Roanoke, VA 24012) WILLIAM A. MILLER (Oak Ridge National Laboratory, Oak Ridge, TN 37831).* Escalating energy costs and heightened environmental concerns are rapidly changing the energy design and materials selection for roofing. Costs can be reduced by increasing ceiling insulation; however, where annual cooling loads dominate, a highly reflective and highly emissive roof can significantly reduce the energy consumption. Complex inorganic color pigments (CICPs) applied to the roof paint exhibit dark color in the visible spectrum and high reflectance in the near-infrared portion of the electromagnetic spectrum. Simulations show that roofs coated with CICPs pigments can reduce the surface temperature of the roof and in turn lead to energy savings of ~30% of the heat flow through an attic having recommended ceiling insulation and the same color roof. To validate these simulations a field study was set up to expose clay and concrete tile roofs on the Envelope Systems Research Apparatus (ESRA). Thermocouples and heat flux transducers were embedded in the roof deck and in the attic cavities to measure heat flow, and relative humidity probes were placed in the attic to monitor moisture gradients. Data acquisition programming was completed for recording data and electronically filing results. The data shows that the reflectance of the tile roofs is important and is not obscured by the thermal mass of the tile or by the venting designed into the tile's construction. Data now coming online shows the clay tile with solar reflectance of 0.51 had surface temperatures 30°F cooler and attic air temperatures 20°F cooler than an asphalt shingle roof. Trends show that heat flow is roughly proportional to roof reflectance. Heat flow trends within the enclosed air gap under the clay S-tile indicate the presence of natural convection. In addition, venting appears to have little impact in the roofs with counter battens, suggesting that an obstructed air channel is not conducive to convection cooling. Further data acquisition of air channels under stone coated metal roofing is hoped to clarify the role of natural convection and help quantify the energy savings of CICPs.

Development of a Modular Automation Scheme for a Liquid Helium Cryofurnace. *MARIANO RUIZ (University of Texas, Brownsville, TX 78520) LOUIS SANTODONATO (Oak Ridge National Laboratory, Oak Ridge, TN 37831).* The Spallation Neutron Source (SNS) is an accelerator-based neutron source. Neutron scattering is a great tool used by scientists in the fields of material science and nanotechnology. The basic setup consists of placing a sample in a neutron beam. The scattered neutrons are collected and interpreted by observing the diffraction or inelastic scattering pattern. To properly use neutron scattering, the sample requires the use of devices to regulate many factors such as temperature, pressure, magnetic field, etc. Many of these sample environment devices are manually controlled. The SNS sample environment team is striving for full automation of the equipment. One of these devices uses liquid helium to control the temperature. It is a cryofurnace. By using this device, the sample temperature can be set to any temperature within 2 to 600 Kelvin by carefully balancing its heating and cooling mechanisms. Its heating mechanism consists of a resistor powered by a temperature controller. Its cooling mechanism is based

on the flow of liquid helium. The flow of helium has been manually controlled with a needle valve. Presently, flow regulation is in the process of being tested with a motor driven valve and a computer running Labview. Labview is a graphical programming language based on data flow execution. The stepper motor valve is controlled with an EAD-404 drive. The pulses and direction are sent from a Galil DMC 2143 multi-axis controller with an interconnected module. The Galil controller receives commands via Ethernet from the computer running the program. The program receives a voltage reading representing pressure by using the Keithley 2700 Data Acquisition System (DAS) connected to a pressure gage located near the needle valve. The new motorized valve is installed and in the process of being tuned. Once the new automated valve is adjusted, it will allow computer-controlled feedback loop regulation from the immediate computer or from any computer connected to the instrument control private network. This new control system will decrease the cooling and heating response time of the cryofurnace and will not require manual control.

Production of Hydrogen Gas from Hydrogen Sulfide. *GREGORY RYBKA (Pennsylvania State University, University Park, PA 16802) GREG KRUMDICK (Argonne National Laboratory, Argonne, IL 60439).* Hydrogen sulfide, H_2S, is released during oil and natural gas drilling. There are great health and environmental concerns associated with it, and for that reason emissions are regulated on international, federal and state levels. The gas has little industrial use, so it is traditionally converted to sulfur dioxide using the well known Claus process. In this procedure the hydrogen is oxygenized and is converted to water, thus the H_2 goes unutilized. As the country begins to reduce its dependency on fossil fuels and converts to a Hydrogen Economy it is crucial to have economic sources of hydrogen. There are a few different methods of recovering hydrogen from H_2S. The method project involves molten copper used as an intermediary step. The H_2S is sent into an alumina crucible containing the copper which is placed in an environmentally closed alumina reactor tube. The reaction is heated to 1200°C in a high temperature furnace (maximum 1700°C) by $MoSi_2$ heating elements. H_2S is sent through an alumina lance and bubbled through the liquid copper. The copper is converted it into Cu_2S and associative desorption occurs to the hydrogen forming hydrogen gas, which then flows out of the reactor tube. The copper sulfide is then oxidized forming sulfur dioxide gas (SO_2) and liquid copper, which is an industrial technique used for over 100 years. The results of these experiments could provide a cost-effective hydrogen fuel source for a swifter transformation to the Hydrogen Economy. Additionally, there would be a reduction in pollution production in comparison to fossil fuels and current hydrogen production processes.

Phase Noise Measurements in Stanford Linear Accelerator Center (SLAC) Linac. *KATIE SCHAFFOLD (Temple University, Philadelphia, PA 19122) RON AKRE (Stanford Linear Accelerator Center, Stanford, CA 94025).* The Linac Coherent Light Source (LCLS) that is under development at SLAC will become the world's first x-ray free electron laser. This laser will enable revolutionary studies in many different areas of science. Before the laser goes into operation at SLAC, phase noise measurements need to be taken to determine whether the existing linac structure will be able to run the LCLS. The phase noise of a system is translated into timing jitter, and the LCLS can only tolerate a certain amount of jitter. The measurements taken on the linac were higher than expected and we hypothesized that our measuring devices might have been the source of high-noise readings. After designing new low-noise amplifiers to amplify the signal, the phase noise and timing jitter levels went down. We were able to target the PEP phase shifter as the component of the linac system that was adding a lot of noise. More work needs to be done to further reduce the phase noise and timing jitter levels.

Model Analysis of Homogeneous Charge Compression Ignition (HCCI) Engine Using GT-Power. *SARA SCHMIDT (University of Missouri-Columbia, Columbia, MO 65201) PAULA MOON (Argonne National Laboratory, Argonne, IL 60439).* The struggle for greater fuel efficiency with lower emissions has initiated the development of the Homogeneous Charge Compression Ignition (HCCI) engines. The HCCI is a controlled auto ignition engine that uses a homogeneous lean air-fuel mixture. Models of a Volkswagen TDI engine and a HCCI engine were made using GT-Power. The analysis of the HCCI looked at various conditions such as air-fuel ratios, intake and exhaust tuning affects, nitrogen-enriched air composition, and variation in compression ratio. GT-Power was used to graph the pressure and temperature traces as well as several other graphs for the conditions listed above. The stoichiometric air-fuel ratio, 8.16, proved to have higher IMEP, volumetric efficiency, and NOx concentration. Tests were done on lambda 1 (stoich) through lambda 3 (lean). The optimal volumetric efficiency for the intake and exhaust tuning affects was 0.875 for an intake runner length of 54.09 cm and an exhaust runner length of 73.14 cm. The optimal engine speed found for these runner lengths was 1500 rpm. The nitrogen-enriched air composition proved to lower the amount of NOx. As the air-fuel ratio increased, the amount of NOx decreased. When the compression ratio was varied the brake torque and power increased as the compression ratio increased. The volumetric efficiency and the NOx decreased when the compression ratio increased. The results from model in GT-Power will allow the HCCI engine to be tested more efficiently.

Superconducting Magnets: Designing a Build-up Stand. *LUCAS SCHRAB (Milwaukee School of Engineering, Milwaukee, WI 53202) AURELIO HAFALIA JR (Lawrence Berkeley National Laboratory, Berkley, CA 94720).* The Superconducting Magnet Group at Berkeley National Lab consists of 23 engineers, physicists, and technicians whose primary goal is to push the limits of high-field accelerator superconducting magnet technology. These magnets are needed for experiments that are on the leading edge of science and technology. The group holds the world record for the strongest dipole magnet, HD-1. HD-1 produces a magnetic field of 16 Tesla developing 15 to 17 million pounds of Lorentz force. The group uses a build-up stand to hold the magnets while they are preparing them for testing. The previously used stand was not designed for the 6,000 lb + weights of world-record-breaking magnets like HD-1. The stand that is currently in use allows engineers and technicians to install instrumentation and to set-up the magnet, but decidedly without a proper level of safety for both the people and the equipment. To properly design such a stand, one must understand all of the procedures which are currently expedited with the use of such a stand. The new stand design fulfills the previous requirements along with enhancements in versatility and capacity. The project involved extensive use of Pro/Engineer CAD and Design Space/ANSYS FEA programs.

Dehydrogenation of Decalin. *JAMEEL SHIHADEH (University of Illinois, Champaign, IL 61820) DI-JIA LIU (Argonne National Laboratory, Argonne, IL 60439).* Unlike other hydrogen storage techniques, organic hydride dehydrogenation have a very fast startup, are easy to handle, and existing distribution networks can be modified to accommodate them. The objective of our group is to formulate a hydride that offers large hydrogen storage density while maintaining the safety and ease of distribution that DOE targets. The dehydrogenation of decalin to naphthalene was analyzed for hydrogen production capacity and catalyst efficiency in a semi-bath reactor under 210°C boiling and 7°C refluxing conditions. The catalysts used were 5 wt% Pt/C and 5 wt% Pd/C. The Pt/C catalyst showed outperformed the Pd/C catalyst in all aspects. The ratio of decalin to catalyst was also varied from 3ml/0.75g catalyst to 6ml/0.75g catalyst. It was found that a ratio of 3 ml/0.75 g catalyst had the highest production and catalytic activity. Temperature variations from 220°C to 250°C were performed on the 6ml/0.75 g catalyst to compare hydrogen production rates. The higher temperatures gave a noticeably higher reaction rate. More tests will be done to better describe the decalin/naphthalene system.

Thermal Effects on Structural and Tribological Properties/Behavior of NFC-7 Coatings. *IAN SMITH (Tuskegee University, Tuskegee, AL 36088) GEORGE FENSKE (Argonne National Laboratory, Argonne, IL 60439).* The near frictionless carbon (NFC) coatings are used on different materials as a lubricant that helps reduce the friction and wear between two surfaces in relative motion. The NFC-7 coating was used in all the tested materials for this project. The goal of these experiments was to study the properties of the coating after being exposed to various temperatures on various substrates. We ran three main tests each having individual tests inside of them. The first two tests were done using a circular disk samples made from steel. The last test was done using a silicon substrate. In each test the sample were coated with a layer of NFC-7 on the substrate material. We learned from these tests the there is a critical temperature at which the NFC-7 starts to fail. This temperature lays somewhere between 200 and 300°C. Between these temperatures the NFC-7 coating on the silicon substrate does not exist, however it remains visible on the steel substrate. The NFC-7 also has a significant increase in the wear volume after it has reached its critical temperature. Future work would include focusing on the exact temperature at which the coating fails and why it fails at that temperature. It would also be interesting to find ways to make the coating last well beyond the critical temperature. However, to make these experiments consistent, there needs to be a development on how to keep the coatings evenly distributed on the surface of the substrates. This would allow us to make a more precise hypothesis.

Analytical and Experimental Preparation for Testing of Spallation Neutron Source (SNS) Liquid Mercury In Beam Bubble Test Loop. *MARK SNYDER (Pellissippi State Technical Community College,*

Knoxville, TN 037933) MARK WENDEL (Oak Ridge National Laboratory, Oak Ridge, TN 37831). The Spallation Neutron Source (SNS) is an accelerator-based neutron source being constructed at Oak Ridge National Laboratory (ORNL). The SNS is a DOE facility that will provide scientists a place to perform experiments in fields including material science and nanotechnology. ORNL is responsible for the design of the SNS target. Methods to mitigate large-amplitude pressure waves that are expected during operation of the liquid mercury target are being investigated by SNS staff. Preliminary experiments on test targets have shown that cavitation (pitting) damage to the target structure may limit the target lifetime. The damage would be induced by pressure waves within the mercury target immediately following a proton beam pulse. The In-Beam Bubble Test Loop (IBBTL) could provide answers to questions about one of these mitigation techniques. This experiment involves adding helium bubbles to mercury flow to see if this reduces pitting damage. The strain on the stainless steel wall that contains the mercury will also be measured. In-beam testing will be conducted at Los Alamos National Laboratory (Los Alamos, NM) during Spring 2005. Bubble count and size distribution will be measured with hydrophones that are part of a new instrument called an Acoustic Bubbler Spectrometer (ABS). Before in-beam testing at Los Alamos, extensive preparations must take place at ORNL. During the summer of 2004 initial calculations and testing for IBBTL were performed including: (1) Preliminary hydrodynamic and thermal analysis of the loop operation using Microsoft Excel and Visual Basic; (2) Development of procedures for each step of the loop operation; and (3) Execution of procedures that can be preformed at ORNL (out-of-beam). Based on engineering calculations the mercury loop meets safety and design criteria for operation. Also revision of the test plan was completed. Preliminary tests with the loop were successful.

Miniature Sensor for the Detection of Environmental Tobacco Smoke. *MICHAEL SPEARS (Laney College, Oakland, CA 94607) MICHAEL G. APTE (Lawrence Berkeley National Laboratory, Berkley, CA 94720).* New cost-effective population-based environmental tobacco smoke (ETS) exposure assessment tools are currently being developed in order to better understand the health effects related to ETS exposure. Determining a method for accurate ETS identification is vital in the development of these devices. We are currently testing the feasibility of using transmission measurements to identify ETS particles collected on a Silicon Nitride (SiN) membrane. Experiments were conducted in an 24 m^3 environmental chamber during either a five-hour period during the day or overnight. A range of one to three cigarettes was smoked separately at one-hour intervals by an automatic smoking machine during each experiment. The SiN was placed on a mount approximately 0.5 mm from a nickel alloy wire, and two optical probes connected to an ultraviolet light source and a spectrophotometer were positioned on the mount to take spectral measurements of the SiN membrane. When current was run through the wire, a temperature gradient was established between the wire and the SiN. Thermophoretic forces then pushed particles flowing between the wire and the SiN onto the SiN membrane. Analysis of the spectral data for each experiment did not conclusively confirm that transmission spectroscopy is an accurate method for ETS identification. Although our results show an increase in absorbance throughout each experiment, which we believe is partially due to the presence of ETS, there is a considerable amount of noise in our data that we need to control in order to obtain concrete results.

Fiber Testing and Cleaning for Use in Hybrid Lighting System. *SCOTT STELLERN (Clemson University, Clemson, SC 29634) DAVE BESHEARS (Oak Ridge National Laboratory, Oak Ridge, TN 37831).* Hybrid Lighting is a new concept which uses sunlight, in conjunction with electrical light, to light a room. The Hybrid Lighting system uses a reflective dish, made of either glass or plastic, placed on the roof of a building to collect sunlight. The collected sunlight is focused into a fiber bundle which transports the light indoors to provide day lighting to interior space. The entry face of the fiber bundle is exposed to a large flux density of sunlight. A number of fiber bundles have failed at the entry face due to over heating. The overheating appears to be a function of the level of contaminants which become trapped in the voids between the fibers due to manufacturing and polishing procedures. It is desirable to develop techniques for certifying fibers for “on-sun” performance in hybrid lighting systems. A technique being evaluated for pre “on sun” screening of the entry face of the fiber bundles uses a thermal imaging camera and a light engine. A fiber to be tested is secured in the lab; the light engine is used to focus light onto the fiber for a specified amount of time. The thermal imaging camera then observes the end of the fiber, noting temperature changes and hot spots. Using this technique, researchers hope to be able to identify excessive heating and hot spots that might cause the fiber to fail if put “on sun.” This has the potential to save time and money. Through the use of this technique differences in fiber bundle performance can be identified. Techniques for cleaning the fiber bundle entry face are also being evaluated. Once a fiber is received, it is submitted to the light engine test. After the first test, the fiber is sent through a cleaning process and tested again. Through this testing process, researchers can evaluate how effective the cleaning process is and if there are any contaminants remaining on the fiber face. The cleaning process for the fiber starts with a four hour sonic cleaning in a sonic washer. Next the fiber is removed and observed using magnifying equipment to search for any abnormalities or contaminants that the cleaning may have missed. If any impurities are spotted, a thin metal wire is used to try and remove the remaining impurities. The fiber cleaning has typically reduced the heating by up to 40%. This study has shown the potential for using the thermal imaging camera and light engine to certify a fiber bundle prior to “on sun” use.

Hardware and Software Design of an Environmental Tobacco Smoke and Nicotine Sampler. *GEORGE STERN (Gonzaga University, Spokane, WA 99258) MICHAEL APTE (Lawrence Berkeley National Laboratory, Berkley, CA 94720).* Environmental tobacco smoke (ETS) has been proven to be a significant health risk for asthmatic children. In previous health studies on ETS exposure in asthmatic children, ETS particles, a suspected trigger of asthma, were not measured due to the invasive and prohibitive cost of monitoring them. In order to conduct an ETS exposure study that directly assesses ETS exposure rates, new measuring equipment had to be developed. The equipment had to be quiet, cheap, small, and noninvasive, necessitating a deploy-and-forget model. After creating an initial prototype, the hardware was reassessed for product availability, cost, and compatibility to maximize ease of implementation and reliability while minimizing cost. The final design implements a real time clock, an analog temperature sensor, 128Kbits of electronically programmable read only memory, an rs232 chip for communication, photointerupters and an h-bridge for precise motor control of an ETS gas passive sampler and photovoltaic relays to control wires for thermophoretic collection of ETS particles onto a plate. The hardware was packaged onto a printed circuit board in preparation for mass production. The software, written in mbasic and used to test the prototype, was not stable enough for deployment in the field due to errors in the compiler. The software was rewritten around the compiler’s flaws and new features were added to make it more suitable for gathering the desired data. After finalizing software and hardware design, the team has created a device that is now ready for mass production and deployment in the field.

Comparison of Isobutane and Ammonia for Use as Working Fluids in Low-Temperature Geothermal Power Cycles. *LAUREL SWIFT (University of Colorado, Boulder, CO 80309) CHUCK KUTSCHER (National Renewable Energy Laboratory, Golden, CO 89401).* Current production of electricity from low-temperature geothermal resources relies on a binary Rankine cycle utilizing an organic working fluid such as isobutane. The use of this type of plant to develop low-temperature geothermal resources is limited by its low thermal efficiency and high equipment cost. In this study, we compared the performance and cost of a representative binary Rankine cycle using isobutane as the working fluid and an alternative binary Rankine cycle using ammonia as the working fluid. Models of the two power cycles were created using ASPEN Plus chemical process modeling software and Engineering Equation Solver software. Plant performance was examined at resource temperatures of 230°F, 280°F and 330°F. Models were optimized for each set of working conditions by adjusting the working fluid flow rate, turbine inlet pressure and temperature, condenser pressure, and heat exchanger area. Ammonia offers some advantages as a working fluid. Lower working fluid mass flow rates are needed because ammonia has superior thermal transport properties such as greater thermal conductivity and heat of vaporization, and lower molar mass. This reduces the necessary piping diameters, parasitic pump power, and heat exchange area of the plant. Effective measures of proposed plant performance are thermal efficiency and capital costs represented in dollars per kilowatt of net power production. For a 330°F resource, the large equipment cost for an isobutane Rankine cycle plant is $629/kW. Previous studies have shown that a plant with a water-cooled condenser using ammonia as the working fluid can reduce equipment costs by $245/kW. We show that in the case of an air-cooled plant, using ammonia as the working fluid decreases heat exchanger costs by $53 to $86/kW depending on the resource temperature. Additional work is necessary in order to optimize the performance of the ammonia Rankine cycle. More detailed cost analysis is also necessary in order to determine changes in costs of other large equipment. Further analysis may show that ammonia can perform as a superior working fluid in binary Rankine cycle power plants.

Friction and Wear of NFC-6 and Super Hard Coatings in Dry Nitrogen. *LASHAWNA TAYLOR (Illinois Institute of Technology, Chicago, IL 60616) GEORGE FENSKE (Argonne National Laboratory, Argonne, IL 60439).* The purpose of the project is to assess the tribological parameters of Near Frictionless Carbon (NFC-6) and Super Hard Coating (SHC) on steel under dry nitrogen sliding. The speed, load, and environment, were kept constant while considering the coated and uncoated surfaces as the independent parameters. Numerous analytical and numerical data were collected using a number of instruments. A High Frequency Reciprocating Rig (HFRR) records the friction coefficient between the sliding surfaces. An optical profilometer was used to estimate the amount of material removed. An optical microscope was used to for visual identification and measurement of coating thickness. Raman Spectroscopy was used to assist in determining whether the surfaces become more amorphous or crystalline. Although friction and wear both arise from sliding surface contact, high friction does not necessarily mean high wear. Results indicate overall that Bare-ball-NFC-6 plate has the lowest coefficient friction; however, Bare ball-SHC plate has the highest wear resistance. Future work will include revalidating some of the experiments for reliable results but most importantly testing in isobutane and hydrogen varying the speed, load, temperature, etc.…

The Effects of Heat Treatment on Recovery and Recrystallization of Nb-1%Zr. *DAVID VERMILLION (Roane State Community College, Harriman, TN 37748) STEVE J. ZINKLE (Oak Ridge National Laboratory, Oak Ridge, TN 37831).* The research and development of Nb-1%Zr in space reactor applications is studied, with particular emphasis on the recovery and recrystallization behavior. Annealing and microstructural characterization tests will be conducted on sample deformations of 20%, 50%, 80%, and 95% in order to provide optimum heat treatment conditions for high temperature thermal creep testing. Microhardness testing is conducted on the as-deformed samples as well as the annealed specimens to determine annealing effects on the grain structure and strength. X-ray orientation distribution function (ODF) testing is also conducted on both as-deformed Nb-1%Zr specimens and post-annealed samples to determine if the recovery and recrystallization behavior is a function of the grain structure texture of grain structure. The annealing temperatures on specimens of Nb-1%Zr will be between 1200° - 1600°C. The initial annealing will be 1500°C for 1 hour, paying close attention to the heating rate. The degree of recrystallization that occurs for the initial annealing condition will determine the next stage of annealing temperature and rate at which the specimens are heated. Further work which includes electrical resistivity, orientation imaging microscopy, and transmission electron microscopy is needed to be performed before verifiable recovery and recrystallization data of Nb-1%Zr can be obtained.

Design of Equal Channel Angular Extrusion Die. *ADAM WATTERSON (South Dakota School of Mines and Technology, Rapid City, SD 57701) GLENN GRANT (Pacific Northwest National Laboratory, Richland, WA 99352).* Equal Channel Angular Extrusion (ECAE) is a type of extrusion process that shows a promising future in producing bulk material containing ultra-fine grain size. Recent advancements have produced successful designs of the die that is used in this process. Unfortunately, die designs producing a ¾”x ¾” cross sectional billet are not adequate for larger sizes of billets that are passed through the ECAE die. In order to achieve even larger bulk material for larger applications, a die assembly was scaled and redesigned to produce a 2”x 2” cross sectional billet. In order to create a safe and efficient die, many areas of concern were explored. The subject of safety was investigated using finite element analysis and other calculations. The issues of friction and wear were addressed and measures were taken to reduce these problems. The design of a backpressure system was also created.

Radio Frequency (RF) Characterization of a Variable High Power Coaxial Phase Shifter. *ALFRED WECHSELBERGER (Stanford University, Stanford, CA 94309) YOON KANG (Oak Ridge National Laboratory, Oak Ridge, TN 37831).* In many charged particle accelerator radio frequency (RF) system designs, for cost reasons, it is desired to use one klystron to power several cavities through a power splitter which depends on the independent control of RF power outputs that operates efficiently at specific frequencies. A high power fast ferrite phase shifter is being developed for use in such a system, allowing amplitude and phase control of (RF) power at 402.5 MHz. The phase shifter employs a square coaxial structure with microwave ferrite slabs between the center and the outer conductors. The coaxial structure is set inside a solenoid that can produce a variable strength axial magnetic field to cause variable phase shifting of the RF power transmitted through the device. For fine tuning of the structure, some RF computer simulations were performed. The prototype phase shifter was characterized through bench measurement using an RF vector network analyzer (VNA). The RF properties measured include insertion loss, impedance matching, and phase shift range.

Stabilizing Radiation Boundary Monitoring System Data Fluctuations Caused by Thermal Effects. *ELAYNE WESLEY (University of Rochester, Rochester, NY 14627) ERIK ABKEMEIER (Thomas Jefferson National Accelerator Facility, Newport News, VA 23606).* Six electronic radiation boundary monitoring devices (RBMs) are installed along the accelerator site boundary of Thomas Jefferson National Accelerator Facility (JLab). RBMs monitor the offsite radiation dose due to JLab’s operations in order to ensure the public’s protection from radiation exposure. Over the past two years, the Radiation Control Group (RCG) expressed particular concern for the sporadic erroneous data generated by the RBM system. Since electrical components in the RBM system are intolerant to extreme environmental temperatures, the majority of the inaccuracies produced by the RBMs can be attributed to severe environmental conditions. To eliminate the errors, environmental chambers for the RBMs were modified by fabricating economically efficient temperature-controlled enclosure. A NEMA four-rated outdoor enclosure with a 110 cfm muffin fan and 100 W strip heater was obtained. To maximize internal airflow, an additional 110 cfm muffin fan was installed. A temperature process-controller with a relay and analog output was obtained to relay the thermal devices’ electrical circuitry around the set point value of 89°F and interface them with the RBM system. A temperature data logger acquired the enclosure’s internal temperature hourly for four days under environmental conditions. Given that only 126.4 cfm was required to keep the enclosure’s temperature one degree above ambient temperature, internal temperatures were still able ascend up to five degrees. Due to the fact that the RBM system is located in a shaded area, and not in direct sunlight as tested, it can be presumed that the internal temperature will not reach the operational maximum temperature. Hence, given that the test configuration unit with the muffin fans was a successful solution, the RCG is investigating implementing this configuration for all RBM units.

The Development of Finite Element Based Models to Predict the Microscopic Performance of Proposed Gas-cooled Fast Reactor Fuels. *JARED WIGHT (Brigham Young University - Idaho, Rexburg, ID 83460) MITCHELL MEYER (Argonne National Laboratory, Argonne, IL 60439).* Thermal and mechanical performance of proposed Generation IV Gas-cooled fast reactor (GFR) fuel was assessed using CAD and finite element analysis (FEA) software. The reference fuel being analyzed consisted of a (U, Pu, Am)C spherical particle with a low density silicon carbide buffer layer uniformly dispersed in a silicon carbide (SiC) matrix. Models were created using Alibre and ProEngineer software. Mesh generation was then performed using Algor software with which the analyses were then performed. The models were created on a microscopic scale to establish stresses due to particle interaction. Results were extrapolated from the web between four adjacent fuel particles. Maximum principle stress was set as the limiting factor because tensile stress is the leading cause of failure in a ceramic such as SiC. Stress limits were set at approximately 150 MPa. Thermal gradients proved negligible. Modeling of static stress included pressure build-up from fission gases, He production from americium (^{241}Am), and fuel particle swelling. The fission gas release rate is also accounted for. Parametric studies including increasing temperature, content of ^{241}Am, and percent burnup are discussed. Results show that as percent burnup increases stress increases exponentially. Stress also increases linearly as temperature and content of ^{241}Am increased.

Microstructure Gas Electron Multiplier. *SHAYLA WILKINSON (Southern University, Baton Rouge, LA 70813), CLIFFORD WILLIAMS (Southern University A&M College, Baton Rouge, LA 70813) PETER SIDDONS (Brookhaven National Laboratory, Upton, NY 11973).* A unique feature about a Gas Electron Multiplier (GEM) detector is that it can be easily adapted to the experimental needs with pads or strips avoiding any accidental discharges. Using a GEM will allow the electrons to be collected directly onto a collector electrode, limiting their traveling distance, thus decreasing electron loss. Our team will be testing a new prototype 1-D x-ray detector located at Brookhaven National Laboratory (BNL). The microstructure gas electron multiplier consists of a GEM which is a theoretically simple technique for producing a large gas avalanche gain by focusing the drift field over a very short distance, to the point that avalanching occurring increasing the number of drifting electrons. The GEM consists of a thin polymer sheet (Kapton) covered on each side with a thin metal layer (Cu); with tiny holes approximately 100μm in diameter through its entirety and with a pitch of typically 200μm on each side of a square matrix. The microstructure also includes a metal cathode plate. Below the GEM and cathode plate are collecting metal strips that direct the charge to amplifiers. These components will be enclosed in a 38x33mm rectangular airtight plexi-

glass structure. $ArCO_2$ will enter the structure via one inlet while exiting out another. Then an x-ray beamline, located at National Synchrotron Light Source, BNL, will pass through the microstructure interacting with $ArCO_2$ creating an avalanche affect of electrons.

Comparison of Three Common Methods Used to Sample Tars in Biomass Gasification. *KRISTIN WILLIAMS (University of Colorado at Boulder, Boulder, CO 80309) STEVEN PHILLIPS (National Renewable Energy Laboratory, Golden, CO 89401).* Biomass gasification will play an important role in future energy production, because it creates limited air pollution and will diminish reliance on foreign oil. The first step to reducing the undesirable higher molecular weight hydrocarbons, or tars, that are produced as a by-product is identifying specific molecules through accurate sampling. The impinger method of tar sampling captures both gravimetric tars and volatile organic tars. In this method, process gas flows through a heated filter that collects particulate solids, then to a series of six solvent-containing impingers to cool and collect the remaining organics. Three impinger samples were taken at filter heater temperatures of 450°C, 350°C, and 250°C under similar process operating conditions. The Gas Chromatograph Mass Spectrometer (GCMS) results from these samples indicated that the amount of material collected by the impingers was a direct function of the filter temperature. As the temperature decreased, the concentration of organics also decreased, because a greater percentage of organics condensed onto the filter at lower temperatures. Solid-phase absorption (SPA) and gravimetric tar (GT) are two simpler sampling methods. SPA, which is a modified OSHA 032 method, measures volatile organic tars, which can be compared to the gas chromatography (GC) tars in the impinger method. The GT method uses a filter to selectively trap high-boiling-point organics, comparable to the gravimetric tars from the impinger sample. In the SPA and GT method setup, process gas was diluted to a 1:14 ratio of process gas to helium, and then was diverted to either a set of impingers or a sampling port. The first type of SPA tube, containing Tenax®, showed an overload for all sample sizes, revealing that they are inadequate for this purpose. The second type of sorbent tube, containing activated charcoal, showed a direct correlation between volume and material collected. GT method results indicated that the concentration of GT increased in proportion to the sample size on both paper filters and glass fiber filters. Results for SPA and GT sampling determined that a combination of the two could achieve the effectiveness of impinger sampling. Future research will develop a method using a circulating solvent to condense the organics of interest, and establish a stable dilution system for SPA and GT sampling.

High Voltage Ramp Generator for Electro-Optically Tunable Filter for the Motional Stark Effect-Collsionally Induced Fluorescence Diagnostics on National Spherical Torus Experiment. *YING WU (University of Illinois at Urbana-Champaign, Urbana, IL 61801) FRED M. LEVINTON (Princeton Plasma Physics Laboratory, Princeton, NJ 08543).* The Motional Stark Effect (MSE) diagnostic is routinely used to determine the safety factor, or q-profile in large fusion devices. To apply the MSE diagnostic to experiments with low magnetic fields such as the National Spherical Torus Experiment (NSTX), a tunable birefringent Lyot filter can be used. A high voltage ramp generator circuit is under development to produce a 5 kilo-volt signal using a simple design involving metal-oxide-semiconductor field effect transistor (MOSFET) ladders. The goal is to design the circuit so that it can ramp ±5000 volts at a frequency of around 1 kilohertz. This would allow the filter to sweep over a range of ~ 1 nanometer. The filter is made from lithium-niobate crystals, which are coated with a layer of indium tin-oxide (ITO) to make it electro-optically active. This means that by applying an electric field across the crystal the index of refraction is varied. This allows tunability of the filter. Putting multiple crystals together and tuning them individually, it is possible to pass certain wavelengths of light and reject others. The first prototype high voltage ramp circuit involves a chain of n-type enhancement and n-type depletion MOSFETs which act as a push-pull system for current. A capacitor is charged and discharged by the MOSFET ladders to simulate the behavior of the lithium-niobate crystal. Finally, resistors are also used in the circuit as current limiters and voltage dividers as not to overload the MOSFETs. This circuit can successfully drive a 2.5 kV ramp at a frequency of 5 Hz. This is a major accomplishment in that the original design was only supposed to drive 500 volts. To improve the circuit so that it can swing ±5 kV with a DC offset, a second circuit was developed. This new circuit used 2 MOSFET ladders, but also employed 2 operational-amplifiers as class-A pull-up amplifiers with a constant-current source. The MOSFET ladder provided the constant current source to the two op-amps driven as an anti-phase bridge. This yielded a voltage gain of 350, allowing for a ±3500 volt ramp. Tests on the actual filters with an active laser showed that this concept indeed can work; the only problem was that there was a lot of noise but those can be taken out with other filters. A ±5 kV ramp is easily within reach with the addition of a few more MOSFETs. This circuit's performance is very comparable to commercial high voltage amplifiers which cost thousands of dollars.

Studies of the Solubility of Alumina in Molten Potassium Fluoride and Aluminum Fluoride Mixtures at Low Temperatures. *CATHERINE WUNSCH (University of California, San Diego, La Jolla, CA 92586) GREG KRUMDICK (Argonne National Laboratory, Argonne, IL 60439).* To combat the problems currently faced in the primary production of aluminum in industry, researchers are developing inert anodes for use in the electrolytic cells. The problems associated with the use of traditional, carbon-based, consumable anodes are that it requires a high capital investment, is labor intensive, consumes a large amount of energy, is less than fifty percent energy efficient, and has high greenhouse gas emissions. The use of inert anodes will eliminate these problems. This study of the solubility of alumina (Al_2O_3) in molten potassium fluoride (KF) and aluminum fluoride (AlF_3) mixtures will aid in the development of inert anodes. The necessary information about the composition of the electrolyte and the characteristics of the melt will be available. With the information gathered from this study, informed decisions can be made about the electrolyte that will optimize the cell. To determine this information the salts were melted together in a graphite crucible at relatively low temperatures around 700°C. An alumina disc was rotated at 340 rpm in the molten salts, until they were saturated with alumina. Both the change in weight of the alumina disc and the oxygen content of the samples taken were used to determine the amount of dissolved alumina. The solubility of alumina in molten KF and AlF_3 salts was shown to vary with changing cryolite ratio (CR), amount of sodium fluoride (NaF) added, and temperature. The weight percent of alumina dissolved in the salt bath increases with increasing CR. There is a slight increase in the solubility of alumina when NaF is added to the salt bath. The average increase of the dissolved alumina is 0.72 wt%, when the content of NaF is 4 mol%. The average increase in the solubility is 1.1 ± 0.7 wt%, with a 50°C increase in temperature. Because only one trial was conducted for each data point in the effect of NaF and effect of temperature experiments, repetitions of those trials will be conducted. Also, future experiments are planned to investigate the effects of LiF and CaF_2. This data will be used to make informed decisions about the electrolyte used in the primary production of aluminum with inert anodes. Knowing the different solubilities of alumina under different conditions will allow the researcher to choose which combination of salts, at which temperatures is most desirable for the composition of the electrolyte to be used. Thus the electrolytic cells can be optimized.

High-Gradient Magnetic Separations of Paramagnetic Colloidal Particles. *DANIEL YATES (Columbia Basin College, Pasco, WA 99301) COSTAS TSOURIS (Oak Ridge National Laboratory, Oak Ridge, TN 37831).* Paramagnetic colloidal particles are separated from a liquid suspension using high-gradient magnetic fields across ferromagnetic wire packed in a filter. The goal is to improve upon the method, termed high-gradient magnetic filtration, for use in wastewater treatment and recovery of valuable materials. In the experimental setup, a pair of rare-earth permanent magnets provides a magnetic field perpendicular to the liquid suspension flow, up to 0.5 Tesla. In the case of similar poles of the magnets facing each other, the field strength near the edge is 0.8 Tesla. The former arrangement creates an attractive force between the two magnets, while the latter causes the magnets to repel each other. The liquid suspension consists of particles of ferric oxide in water or in solutions of 50/50 by volume water/propylene glycol, which was used to simulate wastewater and machine coolant, respectively. For consistency, the suspension that was passed through the magnetic filter was sonicated prior and during filtration to maintain uniform concentration and size distribution. A water-cooled jacketed beaker was used to contain the feed solution and to control the temperature. Filters were made from stainless steel 430 wool that was packed randomly and uniformly into glass tubes. Methods to generate a high surface area and a high-gradient magnetic field included (i) creating sharp edges on the surface of the wire by depositing a layer of micron-size particles of nickel and (ii) etching the wire with concentrated hydrochloric acid. Other filter designs incorporated highly compacted discs of extruded stainless steel wool stacked perpendicular to flow and a filter with increasing packing density. Initial experiments with the different magnet setups, as well as the filter design with increasing packing density, showed little change in removal efficiency. However, both cases of treated material indicated an improvement over the untreated wool. Furthermore, experiments with the extruded discs performed better than a random uniform packing of same length, diameter, and density. However, the fluid pressure drop between the input and output of the extruded filter design increased more rapidly than the uniform randomly packed design. Future experi-

ments will incorporate the extruded discs in a design that will create less pressure drop. In addition there will be further research using both treated materials and improving upon the setup utilizing the repelling magnets.

Comparative Analysis of Subatmospheric Flash Geothermal Power Plant. *TONY YU (Columbia University, New York, NY 10027) CHUCK KUTSCHER (National Renewable Energy Laboratory, Golden, CO 89401).* In order for geothermal energy to become a viable alternative to fossil fuels, geothermal power plants must become more economically competitive with conventional power plants. Previous studies have suggested the subatmospheric flash cycle as a cheap alternative to binary cycles for low temperature geothermal resources. However, the effect of noncondensable gases (NCGs) on the performance and cost of the subatmospheric flash cycle have largely been ignored. A subatmospheric flash cycle, along with a baseline binary cycle, was modeled. A 2.55 million lb/hr geothermal source was assumed with brine temperatures of 330°F, 280°F, and 230°F and NCG content varying between 0.3% and 0.01%. ASPEN Questimate was used to estimate the cost of a baseline power plant of 280°F and 0.1% NCG content. At these conditions, the binary plant had a specific cost (capital cost per kilowatt of power plant capacity, $/kW) of $1,746/kW, while the subatmospheric flash plant had a specific cost of $1,323, suggesting that the subatmospheric flash could produce power at a lower cost. Scaling factors were then used to estimate the plant costs for different brine temperatures and NCG contents. Although NCG content had only a small effect on the net power output of the subatmospheric flash cycle, it had a significant impact on the specific cost of the plant. For geothermal resources of 330°F, 280°F, and 230°F, it was estimated that a subatmospheric flash power plant would be more cost effective than a binary power plant if the NCG fraction were lower than about 0.13%.

Environmental Science

Implementation of Quantitative Real-Time Polymerase Chain Reaction (PCR) to Analyze Belowground Abundance of Roots in a Climatically-Controlled Environment. *JESSICA ADAMS (University of Tennessee, Knoxville, TN 37916) LEE GUNTER (Oak Ridge National Laboratory, Oak Ridge, TN 37831).* Although ecologists have concluded that the below-ground activity of plants and microbes is crucial to understanding the growth, competition, and adaptation to environment of different plant species, studies of plant ecosystems have been limited to observations of above-ground interactions because there existed no clear methodology with which to examine complex belowground microcosms. However, the synthesis of biology and ecology into the science of ecosystem genomics promises new techniques of studying below-ground activity that could revolutionize the world of plant ecology. In this project, quantitative real-time PCR (QRT-PCR) was used to measure the abundance of seven different species of plants typical of an old field in a controlled environment under different climatic conditions. Core soil samples were taken from 15 experimental plots representing three blocks that differed in their temperature, carbon dioxide, and moisture treatments. Coarse and fine roots were removed, lyophilized, and DNA was extracted using the DNeasy Plant Mini kit. Samples from one complete block were quantified and evaluated by QRT-PCR using species-specific primers to determine the relative abundance of each plant species within the sample based on threshold cycle (TC) values. QRT-PCR operates by the addition of a fluorescent dye, SYBR green, to the PCR mixture. The dye adheres to double-stranded DNA and the resulting complex exhibits a fluorescence that is measured at the end of every cycle. Samples have been successfully amplified both with standard PCR and QRT-PCR. Standard PCR amplification with species-specific primers was useful in determining presence or absence of species. Species-specific standard curves based on known dilutions of pure species DNA were made with QRT-PCR that associate template quantity with a particular TC value, showing that as template increases, TC decreases. Comparison of these standard curves with experimental samples suggests abundance of particular species within a treatment. For example, Plantago was abundant in nearly every sample, while other species were only present in one or two samples. This indicates that Plantago is an invasive species belowground, and that it is dominant in many interspecific competitions. However, these results are inconclusive since only one repetition has been performed. Further experiments will be necessary to draw conclusions about the below-ground activity of field plants in different climatic conditions.

On-Road Measurement of Diesel and Gasoline Vehicle Emission Factors. *ZACHARY APTE (Hampshire College, Amherst, MA 01002) THOMAS KIRCHSTETTER (Lawrence Berkeley National Laboratory, Berkley, CA 94720).* This paper reports the measurement of gas and particle phase emissions from vehicles in a northern California roadway tunnel during summer 2004. Separate measurements were made of uphill traffic in two tunnel bores: one bore carried both light-duty vehicles and heavy-duty diesel trucks, and the second bore was reserved for light-duty vehicles. The removal of methyl tertiary-butyl ether from gasoline, its replacement with ethanol and fleet turnover, are expected to have affected vehicle emissions since they were last measured in 1997. In the tunnel, heavy-duty diesel trucks emitted 11 and 17 times more fine particles and black carbon mass per unit mass of fuel burned than light-duty gasoline vehicles, down more than 50% from the 1997 ratios of 24 and 37. This study suggests that vehicle particulate emission factors in California have dropped significantly from previous years. This study also indicates the need for a follow-up study on the wavelength dependence of light-absorbance of particulate pollution, an important component of carbon particulate speciation measurements. Initial results indicate a much lower optical saturation concentration than previously thought.

Local Mercury Deposition from Coal Fired Power Plants, Case Study: Kincaid, Illinois. *AKINI BANDO (New York City College of Technology, Brooklyn, NY 11213) TERRY SULLIVAN (Brookhaven National Laboratory, Upton, NY 11973).* Mercury emitted to the atmosphere comes from two main sources, natural and anthropogenic emission. Emissions from coal-fired power plants may be a past and present source of soil and vegetation contamination of mercury. In this study, we evaluated if the emissions from the stacks at the Kincaid Power Plant are a source of excess mercury within the neighboring vicinity. Computer generated deposition models were used to aid in predicting potential Hg concentration areas. To determine the impact of the plant's emission, soil and vegetation samples were collected at approximately 140 sites within a 10-mile radius of the power plant. Samples were then shipped back to Brookhaven National Laboratory (BNL) to be analyzed for mercury concentration by the Direct Mercury Analyzer. Although the deposition models gave us an idea of where high and low concentration areas of Hg were located, sampled data presented us with a different conclusion. The study was inconclusive as to whether or not the Kincaid Power Plant is a source of excess mercury.

Characterization of Basalt Formations and the Potential for CO_2 Sequestration. *RACHEL BERKOWITZ (Yale University, New Haven, CT 06520) STEPHEN REIDEL (Pacific Northwest National Laboratory, Richland, WA 99352).* Geologic sequestration of CO_2 in flood basalt formations is a technology currently being developed at Pacific Northwest National Laboratory (PNNL) as a way of permanently storing anthropogenic CO_2. As proposed, supercritical CO_2 is injected into wells positioned in the porous flow top of basalt formations. After a period of time, the supercritical CO_2 would react with the basalt resulting in the precipitation of carbonate minerals. Current high-pressure supercritical CO_2 studies being conducted on samples collected from the Columbia River Basalt Group (CRBG), located in the Pacific Northwest, show a carbonate mineral (calcite) forms as the reaction product. To assess the implications of this technology on global carbon management scale, other basalt formations from around the world were characterized and compared to the CRBG. If the properties of other basalts are similar to those of the CRBG, there exists a high probability that CO_2 could be stored as calcite in these formations as well. Mineralogical analysis of samples representing basalts from India (Deccan Traps), Africa (Karoo Igneous Province), and eastern United States (Central Atlantic Magmatic Province, CAMP) were conducted. The Deccan basalts contained the albite, anorthite, and augite. The Karoo basalts contained augite and andesine. The CAMP basalts contained anorthite and pigeonite. Quartz was a secondary mineral in all of the basalts. Chemical data along with site descriptions and physical properties of each basalt formation were retrieved from the literature if available and compared to the CRBG. The mineralogical and chemical similarity between these formations and CRBG samples suggests that they could be used in CO_2 sequestration.

Climate Change: Using a Model with Interactive Tracers to Visualize Climate Impacts. *NICHOLAS BURNS (California Polytechnic State University, San Luis Obispo, CA 93407) SURABI MENON (Lawrence Berkeley National Laboratory, Berkley, CA 94720).* Climate data such as radiation budgets, cloud micro and macro physical properties, aerosol optical depths, etc., are typically provided by satellites and as such is in a 2D form. Numerous programs like Grads and Panoply analyze and visualize 2D climate data. Climate simulations, from a model, are typically in 3D format but have to be condensed to 2D to be analyzed by the above mentioned programs. This condensation process may hide important information. ModelE is a global climate model that is used by the NASA Goddard Institute for Space Studies (GISS) to predict climate change due to natural and anthropogenic causes. The goal of this research was to write a language to statistically analyze and visual-

ize multi-dimensional data, provided by ModelE, in an easy reusable way. The end product is mapCalculator, a powerful functional scripting language. MapCalculator can list, analyze and visualize data produced by ModelE or any other generic climate model. 3D Animations would also be possible with mapCalculator.

Environmental Assessment: Data Development for the Interagency Steering Committee on Radiation Standards (ISCORS) Parameter Source Catalog Web-Site. *JOEY CHENG (Vanderbilt University, Nashville, TN 37235) BRUCE BIWER (Argonne National Laboratory, Argonne, IL 60439).* Due to the necessity of environmental cleanup actions, federal regulatory agencies have assigned different projects to several separate departments. Before these departments carry out the actual actions, they have developed their own computer models in order to estimate any possible risks which will affect human health. As programmers designed these computer models based on specific needs of their projects, different results may be concluded for the same site. As a result, the Interagency Steering Committee on Radiation Standards (ISCORS) has developed a web-based catalog in order to provide the most updated information for the common parameters to minimize the inconsistencies. In order to promote the utility of the catalog, we need to provide a definition for each of the common parameters found among the codes, and also search for supporting references. Therefore, we have searched and entered some more recent sources into the database. Future work will focus on searching the most up-to-date sources in order to keep the catalog useful to the users.

Spread Sheet Based Simulation of Furnace Operation and Annual Energy Consumption. *JEREMY COLEMAN (University of Rochester, Rochester, NY 14611) JIM LUTZ (Lawrence Berkeley National Laboratory, Berkley, CA 94720).* While gas consumption in two stage residential furnaces has been regulated to minimum efficiencies for over a decade, little consideration has been given to the furnace's corresponding electricity consumption. That seems rather inconsistent considering the average furnace blower can easily draw the same amount of power as a large refrigerators, and it rarely operates above 30% mechanical efficiency. The purpose of this research was twofold: the first was to provide a better understanding of the factors affecting the operation and annual energy consumption of two stage residential gas furnaces, the second was to supply data necessary to conduct performance evaluations for Permanent Split Capacitor (PSC) and Electronically Commutated Motor (ECM) type airhandlers. To accomplish this task, a spreadsheet simulation was written to integrate airhandler test data with modeled duct conditions and furnace operating characteristics; thus simulating the field operation of furnaces tested under laboratory conditions. This model accounts for the electricity use of the blower motor, auxiliary components (draft inducer and ignitor), startup/shutdown procedures (system purges), the central A/C system, and standby power, with consumption calculations based both on burner on-time time and total number of cycles. This simulation was capable of derating air conditioning capacity in cases of insufficient airflow, as well as accounting for the heat energy inputted to the living space from blower motor waste heat. Findings from this analysis showed significant electricity savings for the ECM over the PSC, with dramatic savings in occurring in cases of efficient duct conditions and year round mechanical ventilation.

Distribution and Species Richness of Odonate at Brookhaven National Laboratory. *SUSAN COSTA (Community College of Rhode Island, Warwick, RI 02889) TIMOTHY M. GREEN (Brookhaven National Laboratory, Upton, NY 11973).* Odonate research was conducted at Brookhaven National Laboratory (BNL) during the summer of 2004. The purpose for the research was to continue the Odonata research that began in the summer of 2003, which consisted of identifying and cataloging the specimens found at BNL. Identification was to species level whenever possible. In addition the 2004 goal was to survey the bodies of water at BNL primarily for adult odonates, to observe species richness, and catalog and preserve the specimens collected in support of the New York Odonate Atlas. To date a total of forty-six species have been identified at BNL between the two summers of research. Twenty-five adults and twelve larvae were identified during the summer of 2003 and fifteen different adults species were found and identified during the summer of 2004. Future research may continue at the ponds in order to expand cataloging of Odonates; to possibly look at a link between species richness and pH of ponds; and to continue the larger on going biotic inventory of BNL.

Assessing the Safety Impacts of Decontamination & Decommissioning Wastes. *FRANCISCO CRESPO (Stony Brook University, Stony Brook, NY 11794) TERRY SULLIVAN (Brookhaven National Laboratory, Upton, NY 11973).* Nuclear reactors produce radioactive waste. Extensive research has been already done on the radionuclide behavior of this operational waste. Inevitably, the nuclear reactor components and piping become radioactive and after shut down the reactor must be disposed of properly. The main initiative is to use the Disposal Unit Source Term (DUST) computer program to assess the impacts of the decontamination and decommissioning (D&D) wastes on the safety of disposal. The DUST code was developed in Brookhaven National Laboratories in the mid-1990s to model the release and transport of radionuclides from nuclear wastes. Before this code could be used, the graphing capabilities of the software needed to be updated. Modern operating systems no longer support the necessary system calls for this program's graphing function to work. The graphing program has now been updated and improved. The user can plot multiple graphs without having to restart the program every time. Its original capability of plotting only a linear graph has been extended to do semi-log and log-log graphs as well. The archaic textual interface has been redesigned to an easy-to-use graphical user interface. The next phase is to model the transport and release of radionuclides from D&D wastes in order compare and contrast these concentration with that of drinking water standards.

The Products of Mn(II) Oxidation. *JUANA DOMINGUEZ (Merced Community College, Merced, CA 95363) JOHN BARGAR (Stanford Linear Accelerator Center, Stanford, CA 94025).* Manganese, the second most abundant transition metal in the earth's crust, exists in a number of oxidation states, among which the II, III, and IV oxidation states are of greatest environmental importance. Produced through microbial activity, manganese oxides help to mediate redox reactions with organic and inorganic compounds and help to sequester a variety of metals. The mechanism by which Manganese (II) is oxidized to Manganese (IV) is a biologically catalyzed process. There are at least three different pathways by which Mn(II) can be bacterially oxidized to Mn(IV); the first in which states that Mn(II) can be oxidized to mixed Mn(III, IV), and Mn(IV) oxides and oxyhydroxides. The second of these pathways is that Mn(II) can be directly oxidized to Mn(IV) and the last of these pathways is that Mn(II) follows an enzymatic bond with a Mn(III) intermediate in which Mn(II) oxidizes to Mn(III) and then to Mn(IV). The pathways of focus for this research are the latter two pathways.

Effects of Deer Control on Forest Vegetation in the Big Woods of Fermi National Accelerator Laboratory. *AMY FEHRMAN (University of Illinois at Chicago, Chicago, IL 60607) RODNEY WALTON (Fermi National Accelerator Laboratory, Batavia, IL 60510).* Fermi National Accelerator Laboratory has made efforts to stabilize its ecology by controlling deer populations over the last ten years. Changes in vegetation conditions have been monitored since the start of deer population control in the Big Woods on Fermilab campus. The purpose of this study is to determine if efforts of deer population control have been effective upon vegetation conditions. Two different areas within the Big Woods were studied consisting of four plots, two of which are deer exclosures and the other two being control areas. The concentrated areas of study were one-meter squared quadrants, twenty-five of which were located within each area of study. One hundred quadrants were used in this study to observe, collect, and analyze data for this study. Conditions of vegetation that were measured were percent vegetation coverage, average plant height, maximum plant height, and plant species diversity. Estimates were taken of the percent cover, average plant height, and a ranking system was used to decipher the differences in presence of plant species. A meter stick was used to measure the maximum plant height within each quadrant. Results showed that there were significant differences between vegetation conditions between the exclosures and control areas as well as between the north and south plots. Average and maximum vegetation heights were higher in the exclosures than the control areas, and both vegetation heights were higher in the south plots than in the north plots. Species diversity was also higher in the exclosures than in the control area, and the south plots were found to be more diverse than the north plots. It can be inferred from these results that the efforts of deer control at Fermilab have been helpful towards the growth of vegetation conditions. The number of deer consistently being removed over the past few years has created equilibrium in the ecological environment at Fermilab.

Uranium Release From Contaminated Sediments as a Function of Water Content Through Water-unsaturated Sediments. *STEVEN FORRESTER (Washington State University, Pullman, WA 99164) DAWN WELLMAN (Pacific Northwest National Laboratory, Richland, WA 99352).* The Hanford site is a desert that is abundant with contaminated soil, which may be hazardous to the water supply. The objective of this investigation is to evaluate the hydraulic conductivity and moisture retention of three similar, although unique sediments found on the Hanford site, as it relates to the migration of uranium through the sediments at varying degrees of hydraulic unsaturation.

Hydraulic conductivity, moisture retention, and uranium transport curves were created for three sediment types with water contents above 85% saturated, using an adapted centrifuge method. These experiments were accomplished using centrifugation techniques to achieve steady-state hydraulical unsaturated conditions. Using an ultracentrifuge, the sediments were run at varying times and speeds after fully saturating each sediment overnight. Like a desert, the sand sediments used did not retain much of the water during the moisture retention experiments. The hydraulic conductivity results are completely opposite those of the moisture retention curve. For the uranium transport experiments the results are mixed, but for any two sediments that are alike, the results would be about the same. Since a sandy sediment does not retain much water, it would be a great sediment for retaining uranium, since it has such large pores. This is only a portion of the completed work, and in the future more work will be done testing the hydraulic conductivity, moisture retention, and uranium transport capabilities of other sediments from the Hanford site.

Sounds of Rapids as an Attractant for Migratory Fish. *ALLISON FORTNER (University of Tennessee, Knoxville, TN 37996) CHARLES C. COUTANT (Oak Ridge National Laboratory, Oak Ridge, TN 37831).* Wild populations of migratory fishes have been declining due to many factors including climate change, overfishing, and hydropower dams. These factors leading to high mortality rates are dangerous to salmonid populations because the population declines can lead to species endangerment and ultimately decreased genetic diversity. Hydropower dams are a danger to migratory fish because they can inhibit upstream migration and also injure fishes migrating downstream which are caught in turbines. Reservoirs associated with hydropower dams do not have the natural features of streams, and therefore no natural cues such as areas of rapids. Because of this loss of natural cues, there is a need to direct fish to downstream bypasses. Sound has been used to frighten fish away from turbine intake areas, but recent research indicates that fishes may, in fact, be attracted to natural sounds, such as rapids. To investigate whether fish are attracted to natural sounds, preference-avoidance experiments were conducted in which a sound (natural rapids, flowing water recorded in the lab, or sounds of dams) was played from a speaker at one end of a U-shaped tank. A rainbow trout (*Onchorhynchus mykiss*, *Salmonidae*) was placed in the tank at the base of the "U," so that it had a choice between the arm with sound and the arm without sound, in an adaptation of the classical "Y-maze" behavioral test. A digital video system above the experimental tank observed the behavior of the fish for 30 minutes. The instantaneous position of the fish every 30 seconds of the 30-minute experiment was recorded, and the average position and average activity level of the fish were calculated. If the fish spent a greater amount of the time near the speaker, it was determined that the fish was attracted to that sound, and vice versa. Results of this ongoing study indicate that in 173 trials with 32 fish, there was a large individual variation in fish responses, such that, overall, fish did not show a general attraction to natural sounds or a repulsion from sounds of dams. Explanations for this could be that sounds played thus far may not be in the range of hearing of the rainbow trout, or that fish do not respond to these cues in the laboratory. In future studies, if fish exhibit attraction to a certain sound, the results may be used to develop a system which can be used to guide migratory fish around hydropower dam intake areas, and therefore decrease mortality rates of these species.

Linking Microbial Diversity with Functional Stability of a Fluidized Bed Reactor During Remediation of Nitrate- and Uranium-Contaminated Groundwater. *RACHEL GOLDSTON (Cedarville University, Cedarville, OH 45314) JIZHONG ZHOU (Oak Ridge National Laboratory, Oak Ridge, TN 37831).* The Field Research Center (FRC) located at Y12 is a site for research on bioremediation of metals and radionuclides. Along with other contaminants, this site is heavily contaminated with uranium and nitrate. The goal is to reduce soluble U(VI) to insoluble U(IV) in order to decrease the dispersal of uranium with groundwater flow, but this process is inhibited by the high nitrate levels. This project investigates nitrate removal thorough an aboveground fluidized bed reactor (FBR) which contains bacteria on a granular activated carbon matrix and uses ethanol as an electron donor. To determine if there is a correlation between the microbial diversity and process stability of the FBR, clone libraries of denitrification genes were developed. Three samples were collected from the FBR when groundwater feed was beginning (9/4/03), during a bulking sludge problem (10/31/03), and when groundwater feed was decreasing (12/19/03). Genomic DNA was extracted from the samples, and genes for nitrite reduction (nirS and nirK) were separately amplified by Polymerase Chain Reaction (PCR). The products were separated by size on an agarose gel, and the bands of expected size were excised and purified. These nirS products were cloned into competent *E. coli*. Approximately 200 colonies were selected from each sample and cultured. Of these, 95 colonies were screened for inserts using vector-specific primers, purified, and sequenced. The forward sequences were edited using Sequencher and compared to published sequences using BLAST. The cloned sequences were aligned with reference sequences using Clustal, and a phylogenetic tree was constructed using MEGA. Results show that there were five major groups of organisms, four of which show less than 87% similarity to published nirS sequences. All samples were dominated by the same group. The 10/31/03 sample had less diversity than the others and an increase in the dominance of one group, which corresponded to the bulking sludge problem that interrupted FBR function. This suggests a correlation between process stability and microbial diversity in the FBR. For future study, the reverse sequences will be aligned with the forward sequences and re-edited to confirm the nirS clone sequences. The unique nirS sequences described in this study will be published in GenBank. In order to have a more compete picture of the diversity of denitrifying bacteria in the FBR, nirK clone libraries will also be developed.

Home Range and Activity Patterns of the Eastern Hognose Snake, *Heterodon platyrhinos*, in Upton Ecological Reserve at Brookhaven National Lab. *STEPHEN GOODYEAR (University of Texas, Austin, TX 78712) JEREMY FEINBERG (Brookhaven National Laboratory, Upton, NY 11973).* Once thought to have been extirpated from Long Island, viable populations of eastern hognose snakes, *Heterodon platyrhinos*, were rediscovered at Brookhaven Nation Lab (BNL) in 2001. Since their recent discovery at BNL, intense surveys have extrapolated many valuable data on population size estimates, home ranges, and densities. In this study we used radio telemetry to track and record movements of 12 snakes during two years, movements were mapped using GPS and GIS. In addition to tracing movements, we recorded weekly measurements of weight, snout-vent length, and total length for each snake. Our results confirm that home ranges of individual hognose snakes are extensive and that movement patterns show trends regarding daily and yearly cycles. Estimates of home range sizes are needed to determine the amount of land and types of landscapes necessary to manage viable populations of *H. platyrhinos*. As destructive development continues, intense conservation techniques will be needed to protect *H. platyrhinos* in Pine Barrens habitats of the Northeast USA.

The Effect of Elevated Carbon Dioxide and Water Stress on Carbon and Nitrogen Metabolism in Field Grown Soybean. *CHESSA GOSS (University of Rhode Island, Kingston, RI 02813) ALISTAIR ROGERS (Brookhaven National Laboratory, Upton, NY 11973).* Nitrogen fixation has been shown to be very sensitive to drought. There is evidence that the sensitivity of N-fixation to drought is due to (a) a reduced supply of carbon for N-fixation, (b) feedback inhibition of ureides on N-fixation and (c) a direct effect of reduced soil moisture content on N-fixation. We hypothesized that growth at elevated CO_2 will provide additional carbon for exchange with Rhizobia, and reduce the potential for ureide feedback on N-fixation through the provision of additional carbon skeletons for ureide catabolism and subsequent production of amino acids. We found that hexose levels were significantly higher ($P< 0.05$) with the highest levels of amino acids in the elevated CO_2 leaves. We speculate that an increased availability of carbon skeletons in drought conditions may have allowed a greater degradation of ureides and subsequent formation of amino acids. The marked increase in the availability of carbon at elevated CO_2 suggests that the supply of carbohydrate to N-fixing bacteria in the root nodules is unlikely to limit N-fixation. The reduction in ureide content and increase in amino acid content suggest that the greater availability of carbon skeletons in drought stressed plants may have facilitated increased catabolism of foliar ureides, increasing the plants tolerance to feedback inhibition.

A Comparative Study of Three Soil Salinity Determination Protocols. *HEATHER GRAHAM (Santa Monica College, Santa Monica, CA 90405) NIGEL WT QUINN (Lawrence Berkeley National Laboratory, Berkley, CA 94720).* Salinity, the amount of inorganic soluble salts, is an important soil property to monitor, as an excess of salts in the soil will decrease the variety and quality of vegetation that the land can support. Increased salinization of arable land is a major concern for agriculturalists. Several laboratory protocols exist for analyzing soil salinity. These methods measure the electrical conductivity (EC) of an aqueous soil extract and differ primarily by the water content of the soil at the time of extraction. Most plant salt tolerance data has been published using the Saturation Paste Extract method (ECse). This technique saturates a soil to field capacity before extraction and can be a time-consuming, subjective process for some soil types. Alternative methods have been developed using specific soil-to-water ratios, 1:2

and 1:5 (EC1:2 and EC1:5) being the most common. Because these soils extracts are far more dilute than field conditions, fixed volume tests are not appropriate for soils high in sparingly soluble salts, such as sulfates and carbonates. This study compares the ECse, EC1:2 and EC1:5 measurements of 48 soil samples from managed wetlands in the San Joaquin Valley of California and finds relatively comparable results. This study also suggests conversion factors for obtaining ECse measurements from EC1:2 and EC1:5 data for certain wetland soil types.

Determining Successful Planting Areas by Characterizing a Previously Mitigated Sagebrush Site. *SARA HAINES (Oregon State University, Corvallis, OR 97331) MIKE SACKSCHEWSKY (Pacific Northwest National Laboratory, Richland, WA 99352).* Significant loss of shrub-steppe habitat in the Columbia Basin, caused by human activities, has occurred over the past 100 years. To minimize further negative impacts, it is often necessary to perform mitigation. Currently, there is no preferred cost-effective method of mitigation on the Hanford Site at Pacific Northwest National Laboratory. Therefore, it is useful to consider site characteristics of previously mitigated areas when selecting future sites to increase planting success. Canopy coverage, slope, aspect, soil type and particle size distribution are factors that may be key to the survival of Wyoming big sagebrush (*Artemisia tridentata ssp. wyomingensis*) seedlings. To determine what factors may impact long-term sagebrush growth and survival, data were collected along four 100-m transect lines that traverse a planting site established in December 2000. Canopy coverage was determined following a cover class method, using a 0.5-m x 0.5-m sampling frame. Soil was collected using a soil auger at five points along each transect, and soil particle size distribution was determined using the dry-sieve method. Slope and aspect were determined using a clinometer and compass. It was found that the presence of cryptogamic crust and shrubs may improve sagebrush survival. Sandy soil possessing both coarse (>1.0mm) and very fine particles (<0.106mm) may also enable seedlings to access more moisture. However, due to the limited number of transects available for monitoring, it is difficult to reach a conclusion. Slope and aspect provided the main differences observed within the site, and it is recommended that further research be done regarding these factors. Overall sagebrush survival is due to a combination of factors that most likely include some not examined in this study. Further research will enhance the success of shrub-steppe mitigation plantings and allow for a greater understanding of environmental interactions as they relate to sagebrush habitat.

The Effectiveness of Various Modeling Programs as Tools for First Responders in New York City's Urban Canopies. *TALESHA HALL (North Carolina A&T State University, Greensboro, NC 27411) R.M. REYNOLDS (Brookhaven National Laboratory, Upton, NY 11973).* There are many models used to predict dispersion of gases. However, not all of these models do a good job at predicting how gases are going to disperse in deep urban canyons such as those found in New York City. This problem was studied by running three different models under the same conditions to determine which one gave the best output while also considering the time needed to run the program and ease of using the program. The chosen models were Hazard Prediction and Assessment Capability Urban (HPAC-Urban), Hysplit 4.0, and Areal Locations of Hazardous Atmospheres (ALOHA). It was discovered that HPAC-Urban, the only model capable of making predictions in the urban environment, was the most useful as a tool for first responders, and it also was able to run quickly while having a easy user-interface that requires little scientific knowledge. One can conclude form this study that the techniques employed in HPAC-Urban need to be incorporated in all emergency response models for urban environments, so that a model can be available for first responders in the near future.

Environmental Building Controls. *CARLOS HERNANDES (Laney College, Oakland, CA 94607) PHILIP HAVES (Lawrence Berkeley National Laboratory, Berkley, CA 94720).* Control system is a control loop that consists of a network of DDC controller and a web-based operator interface. Operators perform all normal functions setting up schedules, set points, trends and alarms through the web browser. The control loop has three elements. The first is sensors measuring data, such as temperature, pressure, relative humidity and airflow. The second is controller processing the data from the sensors. The third is a control device responding to signals from the controllers. The system uses the BACnet (Building Automation Control Network) protocol for communication between operator workstation and control modules. BACnet control devices include M-line (multi-equipment controller unit), S-line (single-equipment controller unit) and U-line (unitary-equipment controller unit). The system is tested with a real-time simulation of a building and HVAC system is using a hardware interface. A prototype has been constructed and tested.

Optical Absorption Spectroscopy for Air Pollution Measurements. *ULISES HERNANDEZ (Richard J. Daley College, Chicago, IL 60652) JEFFREY S. GAFFNEY (Argonne National Laboratory, Argonne, IL 60439).* Urban air quality and their connections are being examined at Argonne National Laboratory. Black carbon (soot) is monitored using an aethalometer that has seven wavelength outputs in the solar spectral visible region. The instrument's manufacturer supplied the optical attenuation factor for black carbon. The combustion of diesel-powered engines is believed to be a major contributor of particulate matter released into the atmosphere that poses a potential health risk to urban populations. By comparing data from a holiday period and normal work days, the contributions from normal traffic and construction activities that use diesel engines can be examined. Data from before the 4th of July, 2004 and during the holiday period clearly show that the traffic and construction activities are contributing to higher levels of black carbon in Chicago by as much as a factor of two.

Long-term Effects of Grout Immobilization: pH and Solubility of Transuranics. *JONATHAN HILL (Brigham Young University - Idaho, Rexburg, ID 83460) MARK FUHRMANN (Brookhaven National Laboratory, Upton, NY 11973).* High-level nuclear waste at West Valley, NY has been removed from tanks and solidified in glass waste forms. The portion that could not be effectively removed remains adhering to internal structures in 600,000 gallon tanks. To keep the remaining radionuclides, especially the transuranics, from leaching into the soil or water table, a method of encapsulating the waste within the tanks is necessary. One approach is to fill the tanks with a grout containing blast furnace slag, fly ash, portland cement, and either zeolite or apatite. As long as the grout's pH remains high, the transuranics will not be able to leach out of the tank. Testing must be performed to determine the rate at which the pH changes as the grout comes in contact with groundwater over long periods of time. This testing includes grout/water mixtures that had potassium bicarbonate ($KHCO_3$), in set increments, added to them through titration, neutralizing hydroxyls (OH^-) that leached from the grout and thus lowering the solution's pH. We started by adding 1 mL increments of 1 M $KHCO_3$. This reagent was chosen because it provides reactions with the grout that are reasonable analogs to exposure to West Valley groundwater and atmospheric CO_2. When this was unable to further lower the pH, 0.4 mL increments of 2 M hydrochloric acid (HCl) were used. The results were then graphed to evaluate pH reduction over the amount of reagent titration. By using a model of estimated groundwater flow in the burial area of the tanks, the pH data gathered can be used to predict future pH levels of the grout over long times. These data also will be utilized to conduct further experiments to determine the rate at which specific transuranics leach out as the cement pH declines.

Optimization of Temperature and Substrate Availability Parameters of Survivability Tests of Chironomids (*Chironomus tentans*) for Use in Designing Future Toxicity Studies. *AMANDA HODGMAN (Grinnell College, Grinnell, IA 50112) AMORET BUNN (Pacific Northwest National Laboratory, Richland, WA 99352).* Accurately testing the toxicity of a given contaminant to an organism depends on the successful simplification of the test system. In order to determine the toxicity of strontium-90 on chironomids (Chironomus tentans), the survivability of the testing environment must first be determined. Survivability was determined by adding chironomid larvae to 400 mL jars containing various amounts of substrate (75, 100, or 150mL) under two different feeding conditions (fed every weekday or only fed at initiation of the experiment) and at two different water temperatures (8°C or 20°C). Larvae in jars exposed to 20°C experienced lower mortality and a faster rate of growth than those exposed to 8°C water temperature. The amount of substrate present also influenced the mortality rates; at 8°C there was a slight decrease in mortality as the amount of substrate increased, and at 20°C the decrease in mortality was much greater with an increase in substrate. The results indicate that temperature was a more important factor in survival than substrate availability. This also indicates that at 8°C, metabolic rates were very low and the amount of food present in the smaller amounts of substrate was sufficient for survival of the larvae. Feeding did not clearly influence survival, although larvae in jars that were fed grew to be larger than those in jars that were not. For toxicity testing, it is suggested that larvae are kept at 20°C water temperature and with 150mL of substrate.

An Analysis of the Success of Head Started Hatchling Spotted Turtles (*Clemmys guttata*) at Brookhaven National Laboratory. *KRISTINE HOFFMANN (University of Massachusetts, Amherst, MA 01003) JEREMY FEINBERG (Brookhaven National Laboratory, Upton, NY 11973).* As turtle species worldwide continue to decline, headstarting has become one of the more popular techniques of ex situ conservation. However, the focus and funding for these projects is usually

limited to the raising of the hatchlings, and little evaluation of this costly technique has been performed after their release. At Brookhaven National Laboratory, twenty headstarted spotted turtle (*Clemmys guttata*) donated from Cold Spring Harbor Fish Hatchery and Aquarium were introduced into two wetlands to supplement an existing population. Ten of these turtles were released with radio transmitters glued to their shells in hopes of analyzing their transition from captive to wild turtles.

Interactive Visualization of Output from Eulerian Chemical Transport and Transformation Model (CTM) for Atmospheric Sulfur. *THOMAS HRONOPOULOS (New Jersey City University, Jersey City, NJ 07305) STEPHEN SCHWARTZ (Brookhaven National Laboratory, Upton, NY 11973).* Simulation models describe worldwide phenomena such as the transport and transformation of trace species in the Earth's atmosphere. Computer visualization plays an important role in the evaluation of model results with observations and in detailed studies of the physical and chemical processes represented in the model. The goal of this project is to develop software that will provide interactive visualization of five-dimensional (longitude, latitude, altitude, physical species variable and time) environmental data on an irregular 3D grid. The main functionality, accessible through a menu-driven interface provided by the OpenGL-based software, will include: volume rendering, isosurface generation, plane slicing, animation, and interactive operations, such as rotations, translations, and zooming. Volume rendering is done using a view-aligned 2D slicing algorithm adopted from Vis5D, and the generation of iso-surfaces is done with the Marching Cubes algorithm. The software's functionality will allow users to perform interactive, multidirectional visualization of data, potentially giving scientists the ability to gain greater insight and understanding into the flow patterns, distributions, and mechanisms of atmospheric species. The visualization software also provides flexible data-handling facilities so that both binary formatted data without further conversion or a Vis5D formatted file can be used. The modular design of this code, similar to Vis5D or VisAD, allows it to be extended for future development. The available detailed documentation will assure the continuity of this research work.

Uncovering the Sources of Low Dissolved Oxygen Levels in the San Joaquin River. *KATHLEEN HUTCHISON (University of Rochester, Rochester, NY 14627) WILLIAM STRINGFELLOW (Lawrence Berkeley National Laboratory, Berkley, CA 94720).* During the fall and summer, dissolved oxygen (DO) levels in the San Joaquin River (SJR) drop below the national water quality level limit (5 mg/L) and inhibit migration of salmon. The DO levels become low (sag) at the Deep Water Ship Channel in Stockton where the river depth increases significantly. The DO sag is due in part to the mass of algae that enter the Channel from upstream sources and consume oxygen when they sink to the deeper benthic waters (as opposed to producing oxygen as occurs in the photic zone). To remediate this problem, it is necessary to discover why such large amounts of algae are in the river. Current remediation and management strategies assume that that the growth of the algae in the SJR is limited by light. The objective in this study was to determine algal growth kinetics along the length of a tributary to the SJR in relation to levels of nutrients, light and related variables. Water samples were collected at 20 sites along the San Luis Drain (an important tributary of the SJR), put on ice and stored at 4°C in the dark until various analyses were performed. The results of these analyses were combined with data concerning site location, flow rate, temperature and pH, and analyzed to give a clearer picture of how and why algae grows in the SJR and its tributaries. Results from this study indicate that nutrients associated with sediments may be more important than light for algal growth. If nutrient limited growth occurs in the SJR, currently proposed remediation strategies will be ineffective.

Chlorform and Phenol Degradation Using Biotic and Abiotic Methods. *COURTNEY ITA (University of Northern Iowa, Cedar Falls, IA 52613) LI-YANG CHANG (Lawrence Berkeley National Laboratory, Berkley, CA 94720).* The future of wastewater treatment does not lie in the use of powerful chemicals, such as strong oxidants, to clean and purify water. This type of treatment will only contribute to the already growing problem of harmful byproducts in the water. More natural ways of decontaminating the wastewater using bacteria and iron, are proving to be effective and environmentally safe. According to theory and other observations, iron and bacteria are able to efficiently break down chlorinated organic chemicals, such as chloroform, which are common contaminants in groundwater or drinking water, and change them into a harmless state. However, several components might interfere with that process, including the toxic chemicals, such as phenol and dichloromethane. During the reaction between chloroform and iron another toxic byproduct, dichloromethane, is released in which iron cannot break down. In theory, since bacteria has been proven to decompose both chloroform and dichloromethane, if iron and bacteria are used together, purified water would be produced without using other hazardous chemicals in the process. Our results demonstrated that when water samples contain chloroform (40 to 50 mg/liter) and iron shavings (1 to 2 mm size) the contaminant can be completely degraded in 7 days, but a mixed bacteria culture will only degrade 70% in 9 days. In our study, we also found phenol is a resilient chemical that is not easily broken down into a harmless state. Iron shavings have no effect on phenol degradation, but bacteria degradation has shown encouraging results when phenol concentration is low. Our test results of several water samples containing both chloroform (90 to 100 mg/liter) and phenol (10 to 15 mg/liter) showed that although phenol was degraded totally in 8 days, chloroform degradation was delayed (70% in 20 days). Long term research will focus on (i) cultivating the bacteria that can degrade chloroform/phenol, (ii) developing degradation processes using both iron shavings and bacteria, and (iii) encouraging engineers and industries to use innovative and environmental-friendly processes to treat their wastes containing hazardous chemicals.

Leaf Absorption and Extraction of Trichloroethylene (TCE). *EMILY KAY (University of Chicago, Chicago, IL 60637) CRISTINA NEGRI (Argonne National Laboratory, Argonne, IL 60439).* Phytoremediation is the technology in which trees can be used to absorb and transpire volatile organic compounds (VOCs) from soil and groundwater sources. Coring is a traditional method used to test VOC uptake by trees but is often damaging to them and cannot be performed more often than once every two months. By contrast, sampling leaves and branches to measure VOC content, if proven to be an accurate method for quantifying a tree's chemical uptake, can provide a biomonitoring alternative to core sampling that can be repeated more frequently and is less injurious to trees. To address the question of leaf chemical quantification we have used an equilibration method to introduce trichloroethylene (TCE) into leaves. Equilibrations were set up with crab apple (*Malus spp*.) leaves, known amounts of TCE, and approximately 450ml of high purity water in glass jars with Teflon septa. From these equilibration set-ups, leaves and 1ml samples of the solutions (post-leaf) were extracted and analyzed by headspace gas chromatography for TCE. Using this method for TCE introduction into leaves, we executed a series of experiments to test concentration, freezing, and heating and on TCE mass recovery from leaf samples. Though we were only able to recover 50% of the initial mass of TCE added to our equilibration systems, we can still compare our data from the leaves and their concentrations on a relative scale. We think a purge and trap gas chromatograph will give a better mass reading from the water solutions and correct the error in our total mass balance for TCE. Comparing our data, we were able to create a basic procedure to best extract VOCs from leaves. We found that increasing concentration increased the amount of TCE recovered from samples and freezing samples for 7 days and heating them for 2.5 hours at 90°C is optimal preparation to fully extract the TCE from samples.

Development of Multi-Agency Radiological Laboratory Analytical Protocols Training Manual. *JAMES KEDVESH (Eastern Illinois University, Charleston, IL 61920) DAVID S. MILLER (Argonne National Laboratory, Argonne, IL 60439).* Since the development and application of radioactive materials in sites such as hospitals, federal-weapons facilities, and industrial mines, concern has been growing regarding the contamination and remediation of these sites. The U.S. Department of Defense (DOD), U.S. Department of Energy (DOE), U.S. Environmental Protection Agency (EPA), and U.S. Nuclear Regulatory Commission (NRC) had come together to develop a manual called the Multi-Agency Radiation Survey and Site Investigation Manual (MARSSIM) which had the objective of demonstrating the successful completion of a cleanup effort, and establishing a standard for remediation. However, this manual did not address the topics of site planning or instrumentation; therefore, the DOD, DOE, EPA, and NRC worked together with representatives from the National Institute of Standards and Technology, U.S. Geological Survey, and the U.S. Food and Drug Administration to create a set of protocols which can be used as a guideline in site cleanup. This set of protocols is called the Multi-Agency Radiological Laboratory Analytical Protocols (MARLAP). It is the objective of this project to develop a working training manual which can be used to effectively instruct groups of all ability levels who need to be informed of the protocols presented in MARLAP. The manual is currently in progress and will be refined and edited for implementation beginning spring 2005.

Enhancement of Stratigraphic Representations for Site Specific Tank Locations. *JOSEPH KEPHART (Central Washington University, Ellensburg, WA 98926) SIGNE K. WURSTNER (Pacific Northwest National Laboratory, Richland, WA 99352).* The System Assessment Capability (SAC) is a computer modeling assessment tool designed by scientists at Pacific Northwest National Laboratory to assess the cumu-

lative impacts of radioactive and chemical wastes at the Hanford Site. The tool is divided into two main components. The first is the Inventory and Transport component which performs calculations simulating the transport of contaminants through the atmosphere, vadose zone, groundwater, and the river. This produces estimates of radioactive and chemical waste concentrations in each of these media. The second component assesses risks and impacts from contaminated media upon the environment, the economy, humans, and social and cultural resources. Part of the first component, the Vadose Zone Flow and Transport Module uses a computer code known as STOMP (Subsurface Transport Over Multiple Phases) to simulate contaminant flow and transport in the vadose zone. The unconsolidated sedimentary layers representing the vadose zone and located beneath the Tank Farms of the Hanford Site are represented in SAC by templates. These templates also provide SAC with hydraulic and geochemical parameters for each sedimentary unit in the vadose zone. SAC currently uses four generalized templates to describe the geology beneath the Hanford Site Tank Farms. These four templates represent the geology for all eighteen tank farm locations. In order to improve the capability of SAC, more templates, providing more site-specific representation, are needed for the SAC database. Interpretation of site-specific borehole data provides the means to construct more representative templates for each tank farm area. By using unique templates, the STOMP code will produce a better depiction of the localized geology beneath the individual tank farms, creating a more accurate conceptualization of contaminant migration.

Design and Analysis of an Integrated Sustainable Development Model for Rural Eritrea. *ELENA KRIEGER (Harvard University, Cambridge, MA 02138) ROBERT VAN BUSKIRK (Lawrence Berkeley National Laboratory, Berkley, CA 94720).* Inhabitants of rural Eritrea, East Africa, struggle with lack of fuel, poor access to safe water, low electrification rates, and health problems associated with indoor air pollution among other challenges. We analyzed the costs and benefits of a project that would integrate clean water, energy-efficient stove and solar energy technologies to help alleviate some of these problems. The proposed model would use donor-granted money to offer loans at 2% interest to rural villagers in an effort to create a market for solar-powered lights, energy-efficient stoves, and clean water. As the seed money is paid back it will be returned to a revolving fund from which money would then be taken to introduce the project to a new set of villages. Costs were calculated in terms of initial fixed costs and monthly maintenance and upkeep fees, while benefits took the form of money saved, CO_2 emissions reduced, hours saved and lowered losses of Disability-Adjusted Life Years (DALYs). The stoves were worth their purchase price in carbon credits in a matter of two years, while both the stove and water projects were found to save significant numbers of DALYs. The integrated model proved much more cost-effective than if the components were sold individually because of the reduced overhead. Given a ten-year loan, and assuming that willingness-to-pay is additive, we found that more than half of the rural population would be able to afford the improvements, yielding a positive result as a sustainable development model.

Analysis of Measurement Techniques for Intrinsic Permeability of Soils. *MARK MACHACEK (University of Minnesota Duluth, Duluth, MN 55812) MARK WHITE (Pacific Northwest National Laboratory, Richland, WA 99352).* The industry standard for determining the intrinsic permeability of soils has long been applied without detailed consideration of internal flow patterns. A fundamental premise of this experimental methodology is that the experimental apparatus will yield uniform flow across the diameter of the test cylinder for homogeneous soils; as, nonuniform flow generated by the apparatus will result in determination errors. To investigate the extent of possible errors in the current experimental methodology, experimental trials and numerical simulations were conducted. To isolate errors due to the experimental apparatus, homogenous soils (i.e., within the soil packing capabilities) were used. An array of experiments were conducted using five uniform sands and three test cylinder diameters. Experimental error was quantified using trial repetition. The experimental trials showed a dependence between intrinsic permeability and test column diameter (i.e., increasing permeability with decreasing diameter). Numerical simulations yielded similar results. Moreover, both experimental trials and numerical simulation demonstrated increasing measurement error in intrinsic permeability with increasing test column diameter. A modification to the conventional test apparatus is proposed that reduces measurement error.

Monitoring of Vegetation Changes in Created Mitigation Wetland R at Argonne National Laboratory. *JULIE MARGALUS (Benedictine University, Lisle, IL 60532) KIRK E. LAGORY (Argonne National Laboratory, Argonne, IL 60439).* The construction of the Advance Photon Source building in 1991 led to the destruction of three existing wetlands on the site of Argonne National Laboratory (ANL). In accordance with the United States "no net loss" wetland policy of 1990, ANL constructed another wetland, designated Wetland R. Initially, a five-year management and monitoring program was required by the U.S. Army Corps of Engineers to examine vegetation and water levels in the wetland from 1992 through 1996, but more recently the wetland has been monitored annually since 2002. The purpose of this year's project is to create a more consistent method of testing the delineated area, along with recording and comparing vegetation changes and water cover area. This was first done by designating a stable baseline and point of origin. Next, ten transect lines were randomly chosen with five randomly selected quadrat points along each line. Vegetation was sampled at each of the sites using a $0.25m^2$ quadrat frame. Both an ocular estimation of percent cover and a cover abundance coefficient were recorded for each plant species. The nativity, coefficient of conservatism (C), and wetland status for all the species present were also documented. Through observation and sampling, a total of 66 vascular plant species were found in Wetland R and 41 were identified in the quadrats. Forty-four of those species are considered native to the Chicago area. Using calculations of percent cover averages, 11 most abundant species were established. *Spirodela polyrhiza* and *Andropogon gerardii* were observed for the first time and were among the most abundant species in the wetland. The percent cover of *Lindernia dubia* and *Sagittaria graminea*, two species with high C values, increased greatly. Unfortunately, the percent cover of *Cirsium arvense* and *Coronilla varia* increased as well, and both are invasive species. This study demonstrates that Wetland R continues to perform typical and necessary wetland functions. It would be advantageous to continue conducting controlled burns and herbicide treatments to manage adventive species populations. Annual monitoring of Wetland R should continue in order to ensure future success and functioning of the wetland.

GeoPowering the West. *MICHELLE MARTIN (Lewis-Clark State College, Lewiston, ID 83501) PATRICK LANEY (Idaho National Engineering & Environmental Laboratory, Idaho Falls, ID 83415).* Geothermal energy represents a major economic opportunity for the American West, an area characterized by a steadily increasing population requiring reliable sources of heat and power. The U.S. Department of Energy (DOE) GeoPowering the West (GPW) program is a commitment to increase the use of geothermal energy in the western United States. GPW works with private citizens, local, state and federal officials, and industry to provide information on geothermal energy and resources. GPW increases state and regional awareness of opportunities to enhance local economies and strengthen our nation's energy security while minimizing environmental impact. DOE has tasked the Idaho National Engineering and Environmental Laboratory to prepare various types of geothermal resource maps. The goal of this effort is to produce a map of geothermal "Direct Use" for the U.S. Geothermal Direct Use is the use of warm or hot water in applications such as food processing, resorts and spas, green houses, fish production (aquaculture), heating buildings and other processes that require heat. This project required updating the information on geothermal direct use in the U.S. and preparation of a map using Geographical Information Systems (GIS) mapping technology. The next step in the process will be to create an interactive website where individuals can select a state, and then through an on-screen map interface, zero-in on a specific area of interest to view geothermal potential and applications. The information from this website will provide potential energy developers with information necessary to make informed decisions.

Monitoring Long-Term Soil and Vegetation Changes on Walker Branch Watershed. *ALLEN MCBRIDE (Swarthmore College, Swarthmore, PA 19081) PAT MULHOLLAND (Oak Ridge National Laboratory, Oak Ridge, TN 37831).* Although the balance between forest net primary productivity and soil respiration is a key component in the global carbon budget, little is understood about how temporal changes in forest soils and vegetation over a scale of decades may alter that balance within a forest ecosystem. In the winter of 2004, soil, forest floor, and vegetation were resampled on 24 undisturbed sites in Walker Branch Watershed. Soil samples had not been collected on 16 of these 24 sites since 1972. Soil and forest floor samples are currently being dried and ground into powder. Concentrations of H^+, C, N, base-forming cations and heavy metals will be measured in the soils and forest floor samples. Correlations between these data and each site's vegetation, geomorphic setting, and soil parent material will be analyzed to compare the relative importance of these factors in controlling soil property changes. Allometric equations will be used to estimate changes in the watershed's aboveground biomass, and the species-specific data that has been collected will be used to determine which species are responsible for biomass changes that are found. Past studies of this watershed

have revealed greater than expected temporal change in carbon pools and soil chemistry. Mostly, however, past studies have revealed wide variability among sites in both vegetation and soil properties, making it difficult to find patterns with a small sample size. It is expected that the larger sample size used in the present study will allow for a more robust description of patterns in soil and vegetation changes on the watershed.

Changes in the Structure and Composition of Plant Communities of the Wetland R Restoration Project at Argonne National Laboratory, Illinois. *AUBREY MCGAUGHY (University of Illinois at Chicago, Chicago, IL 60647) KIRK LAGORY (Argonne National Laboratory, Argonne, IL 60439).* Destruction of wetlands has increased at an exponential rate creating extensive problems of flooding, a decline in water quality, destruction of wildlife habitats, and a threat to vegetation. The Environmental Protection Agency and the U.S. Army Corps of Engineers are two agencies responsible for the preservation of natural wetlands and the creation of mitigation wetlands. Due to the construction of the Advanced Photon Source at Argonne National Laboratory, three natural wetlands were destroyed and replaced by a mitigation wetland, Wetland R, located on-site. In compliance with federal wetland policies, a five-year monitoring plan of Wetland R was executed, during the years of 1992-1996. The monitoring plan was completed in 1996, and a follow-up project was initiated in 2002. The objective of the 2004 project is to quantify and categorize native and non-native plant species within Wetland R. Random transects and quadrat points were placed allow for a consistent comparative analysis. One of the non-native invasive plant species found, *Phalaris arundinacea* (Reed Canary Grass) has dramatically dropped in percent cover due to herbicides used in previous years. *Sagittaria graminea* (Grass Leaved Arrowhead) a native plant species has noticeably increased; demonstrating high quality plant species are increasing and surviving in Wetland R. Herbicides are recommended to control other non-native low quality threatening species, to facilitate the growth of native high quality plant species. For this trend to continue, active management of Wetland R must be maintained.

Using Satellite Remote Sensing to Determine the Cause of Whiting Events in Lake Michigan. *ADAM MILEWSKI (State University of New York at Buffalo, Buffalo, NY 14226) BARRY LESHT (Argonne National Laboratory, Argonne, IL 60439).* Whitings are responsible for most of the fine-grained carbonate sediments held in suspension in both alkaline and marine carbonate environments. It is believed that Lake Michigan experiences these whiting events, which is caused by calcite ($CaC0_3$) precipitation into the water column. These whiting events can have significant detrimental effects on Lake Michigan's ecological systems. Remote sensing offers a synoptic view of Lake Michigan. Using Moderate Resolution Imaging Spectrometer (MODIS) data made available through National Aeronautics and Space Administration (NASA) and coupling that with raw data from moored buoys to determine the factors governing the precipitation of calcite in the open water column and understanding when, where, why, and how these events occur using remote sensing is the goal of this study. Remote sensing images [from 07/01/03-10/15/03] support the hypothesis that calcite precipitation is caused by both; inorganic precipitation of calcite due to seasonal climatic changes causing temperature fluxes, and bioinduced precipitation due to the removal of CO_2 by photosynthesis from phytoplankton. Thus, Sea Surface Temperature (SST) and chlorophyll-a concentration are directly linked to the precipitation of calcite.

Quantifying Material Surface Areas in Residences. *KATHERINE MING (Sacramento City College, Sacramento, CA 95822) BRETT C. SINGER (Lawrence Berkeley National Laboratory, Berkley, CA 94720).* Average Americans spend the majority of their time indoors, so much of their exposure to air pollution occurs while they are in buildings. Pollutants can enter buildings from outside or be emitted from indoor sources. Pollutant concentrations depend on the rates of emission and other factors including sorption of gases to indoor surfaces. Sorption is the process involving a gas phase molecule binding to a surface, the sorbent. The amount of surface area of the sorbent is a main factor affecting sorption rates, where larger exposure areas contribute to more sorbed gas phase molecules. Experiments have been conducted to quantify sorption onto common materials. Yet the amount of such materials in occupied residences is not known. A method was developed to efficiently catalog material surface areas in residences. All objects were treated as a combination of two dimensional surfaces. The dimensions and materials of each surface were entered into a database designed to calculate total surface area by material, object or room type. Materials were grouped according to their sorptive potential for volatile organic compounds, a common class of indoor air pollutants. A pilot study of four residences, including a dormitory room, a two bedroom one bath house lodging a family of four, a four bedroom one and a half bath house occupied by four single adults, and a three bedroom two bath house lodging two single adults. We found that the surface to volume ratios depended on room type and size. Bathrooms had very high surface to volume ratios ranging from 4.6 to 5.2 due to their small size and high object amounts, where as common areas such as living rooms, bathrooms, and dining rooms had low surface to volume ratios ranging from 2.3 to 3.0 due to their larger size. The floor, ceiling, and walls accounted for roughly half of the surface area in all rooms therefore the materials that were most prevalent in the houses were wallboard, painted plaster, and wood and vinyl flooring. In all residences, more moderate and lightly sorbing materials were present than heavily or non-sorbing materials. This data along with sorption rates will be used to develop mathematical models to describe changing concentration levels of indoor air pollutants.

Reconfiguration and Characterization of the Mini Raman Lidar System. *KENT MURRAY (University of Nevada, Reno, Reno, NV 89557) ARTHUR SEDLACEK (Brookhaven National Laboratory, Upton, NY 11973).* The Min Raman Lidar System (MRLS) is a standoff chemical detector designed at Brookhaven National Lab. Created primarily for first responders, the MRLS can potentially enhance situational awareness by providing emergency personnel with a new tool that can identify a spill of unknown material at a distance. Since terrorists have repeatedly attacked the United States (and its interests) and since they are able to obtain increasingly more dangerous materials, it is very likely that first responders will have to deal with more dangerous agents. Currently, the only methods for determining the identity of unknown spills are to either to take a sample or place a probe into the chemical. Either method requires a first responder to approach the spill and to safeguard against the "worst possible scenario" (i.e., a nerve agent spill), emergency personnel must don a chemical protection suit. The MRLS can potentially accomplish the same task without the need for expensive and bulky chemical protection equipment. In order to conduct further characterization tests on the device, the MRLS was reconfigured from a MIE scattering lidar platform back to its original Raman scattering detection scheme. In addition to the hardware changes, the MRLS's controlling program was also revised to address slight problems with program flow and dynamics. Finally, data was collected to demonstrate that the MRLS was working properly.

Argonne National Laboratory-West Groundwater Monitoring Assessment. *ROBERT NEWBRY (University of Idaho, Moscow, ID 83843) SCOTT LEE (Argonne National Laboratory, Argonne, IL 60439).* Argon National Laboratories West currently has four monitoring wells and one production well being used to monitor their four main potential ground water pollutants. In the past four years the groundwater has dropped around ten feet. There were some discrepancies that the ground water flow direction may have shifted due to this drop. This could cause the monitoring wells to not be in the aquifer down gradient of these waste sites. My summer project was to take groundwater level measurements and create ground water flow maps to make sure the monitoring wells are still in the correct spots. I also preformed single well pump tests to determine certain variances between the monitoring wells. The maps I created showed the wells were still in the correct spots.

Communicating Scientific/Technical Information via the Internet. *CANDACE NEWSON (Claflin University, Orangeburg, SC 29115) MARILYN BROWN (Oak Ridge National Laboratory, Oak Ridge, TN 37831).* Developing effective ways to communicate technical information has always been an important research topic. Society today wants information that is up-to-date and easily found and consumed. There are several mechanisms used to convey information such as newspapers, television, radio or the Internet. The Internet is increasingly important because it provides a large amount of information and is easily accessible. Although the Internet is very useful, many websites fail at effectively communicating information. Most sites fail in the basic design and organization. Therefore, how to improve the design of a website and effectively communicate information is of extreme importance. Many methods were used to determine exactly how to improve a website containing scientific and technical information. These findings were compared to Oak Ridge National Laboratory's (ORNL) Energy Efficiency and Renewable Energy website. Many websites with a similar focus were evaluated i.e., ("benchmarked") for organization, design, graphics, and content. Lawrence Berkeley National Laboratory's Environmental Energy Technologies Division site was a good example of a well-designed site. The site organized all of its technical publications on one page and there was a well-organized links page. Literature written on improving website design was also a source. ORNL's Energy Efficiency and Renewable Energy website was reviewed and its design and content were evaluated carefully to determine if it is communicating information in an effective manner. ORNL's site compared favorably

to most of the sites reviewed, however certain effective characteristics from other sites were noted.

Modulation of Poly(3-Hydroxybutyric) Acid in *Halomonas sp.* in the Presence of Toxic Metals and Radionuclides. *MICHAEL OKRENTOWICH (Housatonic Community College, Bridgeport, CT 06604) GUSTAVO VAZQUEZ (Brookhaven National Laboratory, Upton, NY 11973).* Poly(3-hydroxybutryric) acid (PHB), a natural biopolymer synthesized by bacteria, plays an important role in carbon storage and energy regulation. We studied the accumulation of PHB in Halomonas sp., immediately following exposure to Cr, Ni, Pb, and U at their early exponential and early stationary phases. Under this stress conditions, in both growth phases, the accumulation of PHB was less, comparatively, to those bacteria that were not subjected to the toxic metal and actinide incubational period. This is the first report showing that perturbations to growth conditions, such as exposure to toxic elements, have an immediate impact upon PHB degradation. Polyphosphate (polyP) was also monitored as an indicator of physiological stress of the bacteria, and, as suspected, the accumulation of this biopolymer was affected by the presence of these stress factors in both stages of growth. Therefore, the modulation of accumulation of PHB can be used as a physiological stress factor indicator for bacteria with the same reliability as polyP.

Generation of Poplar Aux/IAA Antisense Constructs. *MEGAN O'SHAUGHNESSEY (Purdue University, West Lafayette, IN 47906) UDAYA C. KALLURI (Oak Ridge National Laboratory, Oak Ridge, TN 37831).* Over the past centuries CO_2 levels have been increasing, resulting in increased global warming. Plants play an important role in terrestrial carbon sequestration owing to their natural ability to fix atmospheric CO_2 through photosynthesis. This study concentrates on identifying and characterizing genes that control the fate of belowground carbon in plants. *Populus* is an excellent model for this study because it is a fast growing model tree, has its genome sequenced, and its the molecular biology and transformation tools are well established. Auxin is a hormone that plays a major role in plant bioprocesses such as cell division, cell elongation, vascular development and root formation. Cell walls are a long-term sink for carbon from photosynthates and thus auxin helps to indirectly control carbon storage levels. AUX/IAAs are a family of plant genes that are involved in auxin signaling and response. Therefore, in this project, Populus AUX/IAA RNAi constructs are created for the end use in creation of transgenic plants. When properly manipulated a gene fragment can be inserted into the flanking region upstream from a hairpin loop (sense-antisense) construct, thus creating an RNAi construct. Upon expression of the construct in transgenic plants, the hairpin loop is degraded and the action carries over upstream to the AUX/IAA gene-fragment. This in turn leads to targeted gene down-regulation of the endogenous AUX/IAA gene. Upon down-regulation of a specific AUX/IAA gene, its functional role can be elucidated through observation of phenotypic changes in the plants. Hence, RNAi constructs for specific genes will ultimately help in understanding the possible functional roles they play in carbon sequestration. To this end, gene-specific fragments were amplified from *Populu*s genomic DNA though PCR techniques and then directionally cloned using a D-TOPO pENTR reaction, resulting in an entry clone that is subsequently used to create an expression clone using pCAPT vector in a gateway technology-based recombination reaction. Upon sequence confirmation, the expression clone was introduced into *Agrobacterium* C58 cells for use in Populus transgenesis. To date, five AUX/IAA RNAi constructs have been generated and eight other genes are at various stages of the process.

Local Mercury Deposition from Coal Fired Power Plants. *RAFAEL PENA (New York City College of Technology, Brooklyn, NY 11201) TERRY SULLIVAN (Brookhaven National Laboratory, Upton, NY 11973).* Mercury emitted to the atmosphere comes from two main sources, natural and anthropogenic emission. Emissions from coal-fired power plants may be a past and present source of soil and vegetation contamination of mercury. In this study, we evaluated if the emissions from the stacks at the Kincaid Power Plant are a source of excess mercury within the neighboring vicinity. Computer generated deposition models were used to aid in predicting potential Hg concentration areas. To determine the impact of the plant's emission, soil and vegetation samples were collected at approximately 140 sites within a 10 mile radius of the power plant. Samples were then shipped back to Brookhaven National Laboratory to be analyzed for mercury concentration by the Direct Mercury Analyzer. Although the deposition models gave us an idea of where high and low concentration areas of Hg were located, sampled data presented us with a different conclusion. The study was inconclusive as to whether or not the Kincaid Power Plant is a source of excess mercury.

The Oral Absorption of Dibromoacetic Acid in Japanese Medaka. *AMANDA PRATT (Trinity Western University, Langley, BC 098231) IRVINE R. SCHULTZ (Pacific Northwest National Laboratory, Richland, WA 99352).* Water treatment by chlorination has saved many lives from diseases caused by a number of microorganisms. Although chlorination was believed to have no human health risks when instituted, scientists have determined that chlorination produces harmful disinfection by-products (DBP) that could be carcinogenic after chronic exposure. One important class of DBPs is halogenated acetic acids (HAA), which include dibromoacetic acid (DBA), dichloroacetic acid (DCA), and trichloroacetic acid (TCA). Concern for these compounds has emerged, because rodent studies have found these compounds to cause liver cancer. A small aquarium fish, the Japanese Medaka (*Oryzis latipes*), has been proposed as a fish model for the determination of this risk. It is easily manipulated, maintained, and has a short tumor response time. The purpose of this study was to observe the bioaccumulation of DBA in both naïve and DCA-pretreated Medaka. DCA-pretreated fish were dosed over a month with DCA and were expected to metabolize DBA at slower rates compared with naïve fish that had not been pretreated. These Medaka were observed in two separate studies for the kinetics of DBA metabolism during a 24-hour period. It was determined that DBA is metabolized faster in naïve fish, and that the DCA pretreatment reduces the metabolism ability of the fish, thereby implying an increased human cancer risk with the mixture of DBPs found in drinking water. These data may facilitate further studies that will determine more specifically the human cancer risk, which can support regulations on DBP concentrations generated during water treatment.

Compilation and Data Management of Underway and Bottle Metadata of Ocean Carbon Related Measurements. *KRISTEN REEVES (Southeastern Louisiana University, Hammond, LA 70402) ALEXANDER KOZYR (Oak Ridge National Laboratory, Oak Ridge, TN 37831).* The Carbon Dioxide Information Analysis Center (CDIAC) has served as the primary information and integration component for the U.S. Department of Energy's (DOE) Global Change Research Program (GCRP). This program will facilitate data acquisition and data management activities necessary for basic research on global change, promote the enhancement of modeling designed to improve representation of Earth system interactions, and develop advanced analytic methods to facilitate fundamental research. CDIAC maintains hundreds of data sets that are related to climate change. These data have been submitted to CDIAC by scientists, programs, and data centers around the world. CDIAC has provided the data management for carbon related data in the ocean since 1992. The focus of CDIAC's ocean data activity has been to compile an oceanographic collection for quantifying the amount of carbon stored in the oceans and understanding changes in the ocean carbon pool. DOE funded ocean measurements of pH, total alkalinity, pCO_2, and total carbon dioxide as contributions to the larger oceanographic programs (WOCE) and (JGOFS). Major computing resources have been invested to improve access, visualization, and retrieval of CDIAC ocean holdings. CDIAC has developed and is now implementing the Ocean OME (ORNL Metadata Editor) and the Oceans instance of Mercury, which is a Web-base search engine used to inventory and document the world's collection of ocean carbon measurements. The OME was used to collect and edit all 'Underway' and 'Bottle' metadata gathered from cruise documents found on CDIAC's Oceans website. The metadata consist of PI information, graphical coverage, dates of a specific cruise, location of data sets, and description of methods. All metadata has been collected from the readily available sources and XML files have been created in a development area. Each primary PI responsible for a specific cruise, then received an email with an attached file for that cruise. Ideally, the PI will respond to the email by supplying the metadata needed and/or make corrections to the metadata that was collected before. The OME was then be used to modify the existing XML file. Finally, those files were moved to the CDIAC development server, where they were used by the Oceans instance of Mercury to build the oceans index nightly. Anyone who chooses to use Mercury will be able to search and view the contents of XML files that were created before. This will eventually help aid scientists in modeling design and research.

Solidification Treatment for Mixed Waste. *MATTHEW RODRIQUEZ (University of Idaho, Moscow, ID 83843) ROY GRANT (Argonne National Laboratory, Argonne, IL 60439).* Treatment and the disposal of mixed waste is a process that is very crucial to the environment because improper disposal could can be a threat to humans, animals, and plants. Something can be categorized as mixed waste if it is radioactive and hazardous (chemically). Argonne National Laboratory (ANL) operates Treatment, Storage, and Disposal facilities used to treat mixed waste. To guarantee the mixed waste be treated and

disposed of properly the Resource Conservation Recovery Act (RCRA) has regulations that are mandatory for this to happen. RCRA provides the list of characteristics identifying whether something is a hazardous waste. RCRA also states the regulated levels for disposal of a mixed waste. However, radioactivity is regulated by the U.S. Department of Energy (DOE). Material Profile 3463P was a waste stream generated at Test Area North on the Idaho National Laboratory that was stored at the Sodium Components Maintenance Shop (SCMS). This mixed waste contains metals that are considered to be hazardous under the RCRA regulations. The hazardous waste codes used for these metals are D008 for mercury and D009 for lead. There were three drums of mercury sludge that contained a different concentration for each drum. The drums were ANL020297, ANL020298, and ANL020299. Treatment and disposal was the goal for these three drums. In order to properly treat the drums, the lead and mercury had to be bound in the treatment matrix so they would not leach and be below the Universal Treatment Standard (UTS). The Universal Treatment Standard for the lead is .75 mg/l Toxic Characteristic Leaching Procedure (TCLP) and the UTS for mercury is .025 mg/L TCLP. The method used to treat the drums was to separate the less concentrated water into new drums and mix the concentrated sludge into a new drum as well and solidify all three drums. This method worked very well in treating the drums to the land disposal regulations (LDR) so the drums can de disposed of.

Microbial Degradation of Cellulose and Isosaccharinic Acid in Radioactive Waste. *UDAI ROHATGI (Bucknell University, Lewisburg, PA 17837) JEFF GILLOW (Brookhaven National Laboratory, Upton, NY 11973).* Transuranic (TRU) waste is radioactive waste contaminated (>100 nCi/g) with radioactive elements from nuclear weapons development and testing and includes a significant amount of contaminated biodegradable material (cellulosics, lab coats, and sludges). Currently TRU waste is disposed at the Waste Isolation Pilot Plant (WIPP) in Carlsbad, New Mexico, an underground site. The high levels of cellulose and alkaline conditions can cause the formation of compounds that do not naturally occur. One such compound is isosaccharinic acid (ISA). ISA is a potential danger for radioactive waste disposal sites because of the tendency for radioactive properties to change in its presence: ISA forms stable soluble complexes with radioactive elements. The biodegradation of cellulose can change its properties and its interaction with radionuclides, likewise, it is possible that the biodegradation of ISA can decrease the solubility of radionuclides. Initially, ISA was synthesized, its purity determined, and its biodegradability assessed under anaerobic and aerobic conditions. In addition, the products of cellulose biodegradation under conditions relevant to WIPP were examined and their contribution to radionuclide mobility was considered. These studies will provide information to help understand the role of microorganisms in the chemical transformation of TRU wastes in a repository environment.

Potential for Metals Leaching in High Ammonia Fly Ashes. *ROSE RUTHER (New College, Sarasota, FL 34243) TONY PALUMBO (Oak Ridge National Laboratory, Oak Ridge, TN 37831).* Concern over global climate change has raised interest in terrestrial carbon sequestration as one means of reducing or stabilizing atmospheric levels of CO_2. It has been shown that certain types of fly ash (a byproduct of coal combustion) greatly increase the rate at which organic carbon is sequestered by soils (humification). Thus, while fly ash amendments could potentially be used to treat degraded lands, concern still exits over the potential for toxic metals to leach from the ash. Past investigations have evaluated the potential for metal leaching from predominantly alkaline fly ashes. These studies showed that while metals were leached, their concentrations were low. The current research focuses on acidic fly ashes with very high ammonia concentrations. Relatively mild extraction procedures, designed to mimic environmental applications, were used to leach any metals from the fly ash material. The leachate is to be analyzed on an Inductively Coupled Plasma Mass Spectrometer for the presence of B, Al, Cr, Ni, Cu, Zn, As, and Cd. The leachate will be further tested for toxicity using the Microtox system. Data from these investigations will provide evidence for the feasibility of large-scale applications of fly ash amendments.

Ice-Rafted Erratics: A Study of Boulder Distribution on Rattlesnake Mountain, Hanford Reach National Monument. *BRONWYN RYAN (Harvard University, Cambridge, MA 02138) BRUCE BJORNSTAD (Pacific Northwest National Laboratory, Richland, WA 99352).* Due to copious amounts of cataclysmic flooding during glacial periods as early as 1.5 to 2.5 million years ago and probably periodically throughout the Pleistocene Epoch there are large boulders distributed throughout the Southeastern portion of Washington State. Some (or many) of these boulders could be from glaciations older than 18,000 years ago. Along with the native dark basalt are thousands of light colored rocks, called erratics that were brought in during flooding periods, brought in on icebergs from as far away as British Columbia. The purpose of this study is to determine the nature and time of ice age flooding. Three types of ice-rafted debris are: isolated erratics, erratic clusters, and bergmounds. These are recorded as found according to geologic descriptions such as lithology, shape, weathering, and type of erratic. Data is collected with a GPS unit, a tape measure on to data sheets. By recording locations and aforementioned data we can analyze the data and identify trends in the erratic distribution that will give clues about flooding activity in the past. The area of study is located within the ALE (Fitzner- Eberhart Arid Land Ecology) now under the jurisdiction of the U.S. Fish and Wildlife Service. Due to the size, lithology, and elevation of the erratics their arrival is thought to have occurred during Ice Age floods as they were rafted in on ice bergs. The flooding that took place here is an important part of how the landscape came to exist as it does today. The more we can understand about the glacial and geologic forces through the study of the erratics, the more we can understand the history and dynamics of flooding. Ongoing research is important as it addresses the question of the relative ages of floods, the relative size of floods, and it fosters the proposal for an Ice-Age Floods National Trail that will recognize a part of the area's rich geologic history.

The Regional Carbon Cycle: Predicting the Carbon Cycle in Oklahoma to Prevent, Delay, and or Retard Global Warming by Testing Wheat and Soil Samples. *BRAULIA SAPIEN (California State University Fresno, Fresno, CA 93740) MARGARET TORN (Lawrence Berkeley National Laboratory, Berkley, CA 94720).* Global warming has been a topic of great concern over the past few decades due to the increase of CO_2 in the atmosphere. The Department of Energy ARM (Atmospheric Radiation Measurement) Program was created in order to model photosynthesis and the carbon cycle to predict climate changes, especially in the state of Oklahoma. This research is being done in Kansas and Oklahoma crop fields, mainly wheat, which can be tested for moisture and carbon-nitrogen ratios. The goal is to be able to predict the carbon cycle by predicting the carbon flux in the entire state of Oklahoma. Both wheat and soil are dried at the Lab, weighed, and tested for moisture, carbon, and nitrogen content. The leaf C: N ratio was determined separately in the green and brown leaves. Nitrogen is mostly present in green leaves since brown leaves have senesced. The amount of nitrogen found in wheat is of great importance to the research. Knowing the amount of nitrogen is necessary to model photosynthesis. The rubisco enzyme is an important enzyme in the photosynthetic process and it uses nitrogen in order to fix atmospheric CO_2 into sucrose and starch in the plant. Photosynthesis is also measured with the Eddy flux technique. The information gathered can then serve to predict atmospheric CO_2 concentration which is the main driver for climate changes such as global warming.

Diversity of Monooxygenase Genes in Microbial Communities at Two Forested CO_2 Enrichment Sites in the Southeastern United States. *MELISSA SCHUYLER (Eastern Michigan University, Ypsilanti, MI 48197) CHRISTOPHER W. SCHADT (Oak Ridge National Laboratory, Oak Ridge, TN 37831).* Nitrifying bacteria (ammonium oxidizers) and Methanotroph bacteria (methane oxidizers) perform important ecosystem processes that potentially could cause feedbacks in global warming scenarios caused by increases in greenhouse gases such as carbon dioxide (CO_2) and methane (CH_4). As a result of these concerns a large study is being conducted of the effects of elevated CO_2 on ecosystems at a number of Free Air CO_2 Enrichment (FACE) sites. Using DNA extracted from samples taken of soils at ambient and elevated CO_2 levels at two of these sites, Oak Ridge National Laboratory and Duke University, ammonium monooxygenase (AMO) and methane monooxygenase (PMO) genes were amplified using polymerase chain reaction (PCR). The DNA was then cloned in *E. coli*, the DNA was amplified using vector specific primers, purified and sequenced. Analysis of the resulting DNA and inferred protein sequences was performed using BLAST searches and phylogenetic techniques. Results show low diversity in the genes sequenced from the Duke samples and a predominance of PMO genes from one type of organism. A more even distribution of AMO and PMO genes was observed in the samples from ORNL. Using this bulk sampling method from one spring time point there was little evidence of differentiation between ambient CO_2 levels and elevated CO_2 levels at these sites. However further analysis at multiple time points may be necessary to observe such phenomena. The results of this study will be used to design microarrays to aid in such an assessment.

Development of Building Sustainability Metrics. *KATHLEEN SPEES (Iowa State University, Ames, IA 50010) KIMBERLY FOWLER (Pacific Northwest National Laboratory, Richland, WA 99352).* The Federal Energy Management Program (FEMP) Building Cost and Performance Data Project (CPDP) has developed a set of high-level whole-building

performance metrics. These metrics were developed to rely on in-practice measurements as opposed to modeling or projection to compare the relative performance of traditionally and sustainably designed buildings. Straightforward dollar metrics and relative productivity metrics represent cost evaluation. Environmental and social metrics complete the set for a holistic evaluation. Data collection and analysis remain difficult due to normalizing concerns, regional variation, and interdependent systems, but general performance implications will be discerned. Conclusions drawn from data collection may guide federal agency market transformation efforts toward sustainability.

Landsat Thematic Mapper Band Ratio Mixture Tuned Matched Filter Analysis of Basalt Outcroppings. *JOHN SPRITZER (University of Montana, Missoula, MT 59812) JERRY TAGESTAD (Pacific Northwest National Laboratory, Richland, WA 99352).* To inform our vegetation classification for the Central Snake River Plain of Idaho, we need to know the amount of basalt exposed in each 30 meter x 30 meter Landsat TM pixel. This is a problem in that many of the lava outcroppings are much smaller than the pixel itself and the basalt spectra obfuscate the spectral return of the vegetation, reducing the apparent Landsat TM pixel value, making the classification of shrub-steppe vegetation difficult. This problem can be addressed by using an algorithm (IR-MTMF) for preprocessing Landsat TM imagery that has shown to be effective in enhancing basalt signal, reducing noise, and false positives. Statistical and qualitative analysis of the algorithm also demonstrate that the IR-MTMF out-performed both Linear Unmixing and Mixture Tuned Matched Filtering in estimating percentages of basalt in the pixels.

Detection of Perchlorate Anion on Functionalized Silver Colloids Using Surface-Enhanced Raman Scattering. *JACQUELINE TIO (Massachusetts Institute of Technology, Cambridge, MA 02139) BAOHUA GU (Oak Ridge National Laboratory, Oak Ridge, TN 37831).* Perchlorate anion interferes with the uptake of iodide by the human thyroid gland and consequently disrupts the regulation of metabolism. Chronic exposure to high levels of perchlorate anion may lead to the formation of thyroid gland tumors. Although the Environmental Protection Agency (EPA) has not set a maximum contaminant level (MCL) for perchlorate, a draft drinking water range of 4-18 ppb based on a 2 liter daily consumption of water has been established. The current EPA approved method for detecting perchlorate uses ion chromatography which has a detection limit of ~4 ppb and involves lengthy analytical time in the laboratory. A unique combination of the surface-enhanced Raman scattering (SERS) effect and bifunctional anion exchange resin bead selectivity may provide an alternative way to detect perchlorate at even lower concentrations and with higher selectivity. SERS, which uses near-infrared laser excitation of adsorbed perchlorate anions on silver nanoparticles, has been shown to detect perchlorate anions at concentrations as low as 50 ppb and has shown enhancement factors ranging from 10^2 to 10^{14}. Raman analysis of perchlorate adsorbed onto resin beads has detected even lower concentrations at 10 ppb. In an effort to integrate these two effects, silver nanoparticles were coated with N-trimethoxysilylpropyl-N,N,N-trimethylammonium chloride, a functional group similar to that found on the resin bead, and subsequently inserted into different perchlorate concentration environments. This method has resulted in perchlorate detection down to ~10 ppb and a more consistent detection of perchlorate anion at ~50 ppb than that of earlier methods. As suggested by the direct insertion of functionalized silver colloids into perchlorate samples, this technique may also allow for the development of a probe using on-site Raman spectrometry to detect significantly low concentrations of perchlorate in situ rather than in the laboratory.

On Developing Models of Airflow and Gas Dispersion in Complex Multi-Floor Commercial Buildings. *STEFFENIE TOMLIN (Millsaps College, Jackson, MS 39210) MICHEAL D. SOHN (Lawrence Berkeley National Laboratory, Berkley, CA 94720).* Many researchers have developed multi-zone models of pollutant dispersion and airflows in residences and simple office buildings. However, for larger, more complex, commercial buildings, the availability of relevant studies and data is limited and the modeling of such structures has not been studied extensively. The process of developing a computational model of a complex building requires an analysis of the physical building, a mathematical formulation of the system (i.e., a model design), and the implementation of the model. Field studies and data are required not only to provide details about the system, but also to serve as a standard by which to judge the quality of the model. We have a large quantity of data, obtained from an intensive study of several buildings, conducted in July 2003. With data taken from one experiment of this study, we characterized and modeled a multi-floor, multi-HVAC commercial building using a first-order, linear mass-balance approach. We calibrated the model using Bayesian updating with Markov Chain Monte Carlo Integration. Our model produces results that agree well with the data, and therefore may provide a framework for more complex models in the future.

Missouri-Madison Hydroelectric Project (No. 2188). *TIFFANY TOY (Middle Tennessee State University, Murfreesboro, TN 37132) MARTI SALK (Oak Ridge National Laboratory, Oak Ridge, TN 37831).* The Missouri-Madison Hydroelectric Project (No. 2188) is a series of nine dams constructed between 1891 and 1958 along the Madison and Missouri rivers in southwestern Montana. In an effort to continue electrical generation to meet power demands, in 1993 Montana Power Company (MPC) applied to the Federal Energy Regulatory Commission (FERC) for a new license for the project. Because issuing a new license would constitute a major federal action that could significantly affect the quality of the human environment, FERC prepared an environmental impact statement in compliance with the National Environmental Policy Act. The new FERC license, which was issued in 1999, contains numerous license conditions to protect the environment. This research was conducted to determine the status of MPC's compliance with these license conditions. Compliance is determined by MPC's submittal of various reports, plans, and other documents required by the license conditions. Although many of these documents are available to the public through FERC's on-line library, some are not due to security precautions enacted after September 11, 2001.

Water Absorption Levels of Willows (*Salix alba var. tristis*), Walnuts (*Juglans nigra*) and Oaks (*Quercus alba*), in Determination of Self –Irrigation that Exploits the Soil Depth Dimension for Carbon Sequestration. *FELICE WATSON (Kennedy King College, Chicago, IL 60621) M. CRISTINA NEGRI (Argonne National Laboratory, Argonne, IL 60439).* Presently, Argonne National Laboratory (ANL) is studying an innovative root engineering system designed to utilize a specialized self-irrigation method of tree root growth, allowing for carbon dioxide evolution at depth; thus exploiting soil depth dimension for carbon sequestration. Applied Natural Sciences (ANS) patented technologies (TreeMediation® and TreeWell® systems)-Cartridges were designed as an instrument to manage carbon levels in soil, with the prospect to develop an exceptional method usable in instituting or reinstituting vegetation on damaged land soil. One major component in designing an unsurpassed ANS cartridge system is to determine the premium tree/plant type that could be used for optimum water absorption. Our study was accomplished by monitoring water absorption levels of phreatophytic trees, placed inside an ANS cartridge system. This experimental carbon management program is implemented at the Southwest Area-Green House, Building 485, where phreatophytic/moisture seeking and crop trees (commercial hardwood) with elongated root systems in a semi-arid environment, is being tested in a 20-month field study that will examine planting method, root growth, soil moisture and carbon dioxide evolution at various depth. In order to determine the type of tree suitable for the ANS cartridge system to be used for future phytoremediation techniques, this study will primarily concentrate on observing and measuring water absorption levels of different tree species, which includes Willows (*Salix alba var. tristis*), Walnuts (*Juglans nigra*) and Oaks (*Quercus alba*), and as controls, cartridges where no trees were installed. Water absorption levels will be measured using the Fisher M-Scope-Water Level Indicator, which is inserted into pre-installed piezometer tubing in each the ANS-Cartridges. Results strongly suggest that the Willows (*Salix alba var. tristis*) absorb the most water.

Effects of Acoustic Transmitters on Juvenile Sockeye Salmon. *KELLY WELLES (University of Maine at Machias, Machias, ME 04654) DAVID GEIST (Pacific Northwest National Laboratory, Richland, WA 99352).* Salmon are anadromous fish spawning in fresh water, and living most of their lives in salt water. At about a year old, in the smolt stage, salmon prepare for their journey to the ocean. Many salmon are tagged in order to track their journey and their return back to the river. The purpose of this research was to test the effects of the tags and how well the salmon will be able to compensate for their extra weight as they swim through hydroelectric dams. Juvenile sockeye salmon, *Oncorhynchus nerka*, were tested on the effects of acoustic tags on swimming performance and overall survival. The salmon were surgically tagged with a 0.7 gram acoustic transmitter (about 6% of the fish's body weight) and placed in a tank to recover. The control group received no tag and the sham-tagged group underwent the surgery, but received no tag. Swimming performance was tested in a large swim tube set at varying current speeds. Since the sham-tagged fish swam at a similar rate as the control fish, it was found that the surgeries and anesthesia had no ill effect on their swimming performance. While not statistically significant, the tagged fish swam at a slightly lesser rate than the control. It was concluded that the tags must have had a minor negative effect. The tags were found to have no adverse effects on survival. Only 2 of the 75 fish were lost during the tests, both of which were lost when they

jumped out of their tanks. Further research will focus on improvements to these tests and the transmitters in order to reduce fatalities in salmon traveling through hydroelectric dams.

Developing and Monitoring a Project Related Wesite for the Hydrology Group. *APRIL WICKERSHAM (Columbia Basin College, Pasco, WA 99352) LANCE W. VAIL (Pacific Northwest National Laboratory, Richland, WA 99352).* Numerical models used to support environmental management decision making often requires large amounts of data. Often the required data involves a long sequence of values measured at a single location for a long period of time. Such data is generally called 'time series' data. Conventional relational database software is generally poorly suited to manage such data sets. Often the data is so large, used so infrequently and constantly being added to with new data that storing and keeping time series databases up to date in local computers is both costly and unnecessary. Accessing the data over the Internet just in time (JIT) to its use minimizes the storage required while keeping the data up to date. By combining an efficient time series storage protocol with a metadata base that provides JIT widgets for accessing data from its primary server via the Internet, environmental modeling can be improved. To achieve more efficient time series data storage, we have adopted a protocol called NetCDF (Network Common Data Form). A metadata database is being developed that identifies the location of the database on the Internet and the widget used to access the data. The widgets are being developed in Java. Java is preferred for these applications because of its multiple platform and web-access features.

The Modifications of the Automated Sampling System of the Relaxed Eddy Accumulation For Accurate Flux Measurements. *RONNIE WOODALL (Richard J. Daley College, Chicago, IL 60617) PAUL V. DOSKEY (Argonne National Laboratory, Argonne, IL 60439).* The Relaxed Eddy Accumulation (REA) System is used for flux measurements of vertical air currents. Within the air currents are eddies, which contain organic compounds that are being deposited to the biomass and the atmosphere. The eddies are both absorbed in the biomass from the atmosphere and absorbed in the atmosphere from the biomass. By analyzing this transfer process we can better understand the effects modern society is having on the environment: what we distribute in the soil may also pollute the atmosphere and vice-versa. Specifically we are analyzing oxygenated hydrocarbons, CH_4, and N_2O emissions; however the modifications that were made to the Automated Sampler caused problems in our REA system that resulted in a delay of our experiments. The discrepancy was caused by the increase number of stainless steel canisters, which resulted in leakage and an incorrect flow rate distribution.

Heating and Cooling Residential Energy Consumption Using DOE-2 and Energy Plus Models. *WEIHUA ZHANG (Laney College, Oakland, CA 94607) ALEX LEKOV (Lawrence Berkeley National Laboratory, Berkley, CA 94720).* Building energy simulation programs have illustrated their usefulness in accurately predicting the building's energy consumption and its subsequent economical impact. DOE-2 and EnergyPlus are two such powerful programs. Given hourly weather profile, description of the building and its space-conditioning equipments, DOE-2 and EnergyPlus are able to calculate hourly energy consumption utilizing method of heat flow and heat and mass balance, respectively. In this study, the two programs are used to model a single-family, 1980-vintage, two-story, detached residential house in Washington DC. Taking advantage of EnergyPlus' translation utility, DOE-2 model is converted to EnergyPlus. DOE-2 model reported that in the end use report, 90.7 MBtu of heating energy and 2700 kWh of cooling energy are consumed by the house during a typical year. Compared with EnergyPlus, 92.9 MBtu of heating energy and 3750 kWh of cooling energy are consumed by the house during a typical year. Detailed monthly, typical peak day, weekday and weekend comparisons between the two program's results are also presented in the paper. Overall, results of DOE-2 and EnergyPlus are within 10% of each other in heating energy consumption; however, cooling energy consumptions differ by a wide margin.

Functional Analysis of a dps Mutant Strain of *Shewanella oneidensis* Using DNA Microarray Technology. *EIZABETH ZHOU (Washington University, St. Louis, MO 63105) DOROTHEA K. THOMPSON (Oak Ridge National Laboratory, Oak Ridge, TN 37831).* The groundwater and sediments of numerous U.S. Department of Energy (DOE) field sites are contaminated with mixtures of metals and radionuclides as well as nitrate, chlorinated solvents, and hydrocarbons. Chromium(VI), for example, is one of several risk-driving contaminants at DOE sites and in the discharged effluents from various industries. The remediation of such mixed wastes constitutes an immediate and complex waste management challenge for DOE, particularly in light of the costliness and limited efficacy of current physical and chemical strategies for treating mixed wastes. In situ bioremediation exploiting the intrinsic respiratory processes of dissimilatory metal ion-reducing bacteria remains a potent, potentially cost-effective approach to the reductive immobilization or detoxification of environmental contaminants. The bacterium *Shewanella oneidensis* strain MR-1 is able to grow both aerobically and anaerobically by utilizing a variety of terminal electron acceptors such as oxygen, iron, nitrate, chromium, and uranium. *S. oneidensis* can grow naturally almost anywhere and is harmless to humans and other organisms. These characteristics make it an ideal organism for bioremediation of contaminated areas while reducing the risk of harmful side effects often associated with site clean-up. The dps gene in *Escherichia coli* codes for Dps, a nucleoid protein that sequesters iron and protects DNA from damage. Dps homologs are encoded in the genomes of numerous bacteria, including *S. oneidensis*. In this study, we used a dps deletion (Δdps) strain of *S. oneidensis* derived from the parental strain DSP-10, which differs from the wild type strain in a point mutation that enables rifampicin resistance. We exposed the Δdps mutant and DSP-10 to 2M chromium and monitored the growth rates by measuring absorbance using a spectrometer at a wavelength of 600 nm. Global transcriptional differences in the Δdps mutant and wild-type reference in response to Cr exposure were then compared using high-throughput, miniaturized DNA microarray technology. Total cellular RNA from DSP-10 and Δdps was isolated, labeled with fluorescent dyes, and then hybridized to microarray slides covering ~99% of the total predicted protein-encoding open reading frames in *S. oneidensis*. Analysis showed a great number of genes in Ddps were repressed as opposed to induced in response to chromium shock. In addition, the Dps family protein was over 62-fold induced in DSP-10 relative to Δdps.

General Sciences

Utilizing Guided Inquiry Techniques at the Lawrence Hall of Science and Exploring Japanese Lesson Study with Growing Learning Communities. *EVELYN ANDRADE-MOLINA (California State University, Dominguez Hills, Carson, CA 90747, RENEE BAZANT (California State University at Long Beach, Long Beach, CA 90840)) KATHY BARRET (Lawrence Berkeley National Laboratory, Berkley, CA 94720).* At the Lawrence Hall of Science, students enjoy hands-on activities designed to engage and educate learners of all ages. The Hall of Science is unique in its philosophy that students learn best through guided inquiry. Guided inquiry techniques involve experimenting, creativity, role-playing, and investigation. Guided inquiry techniques help students to build concrete ideas as a foundation for future learning. It also fosters cooperative reasoning abilities in students of all ages and enables students to construct essential concepts through hands-on experiments. At the Hall of Science, we studied educational research and curriculum development. Our goal this summer was to observe how educators at the Hall of Science use these guided inquiry techniques to teach interactive science and math lessons to students of varying grade levels. The second component of our research consisted of the observation and participation in the Growing Learning Communities Summer Institute. This institute was created out of the collaborative efforts of the UC Botanical Gardens in conjunction with the Lawrence Hall of Science. Growing Learning Communities was designed to promote math, science, and lesson study in school gardens. Based on research that compares the educational success in math and science of students in Japan versus those in the United States, actively participating in the Japanese Lesson Study process enabled us to research how lesson study aided the collegial aspects of teaching as well as promoting a better understanding of student learning and student work.

A Preliminary Coupled Model of Electricity Markets and Cascading Line Failures in Power Transmission Systems. *DAVID BERRY (Rice University, Houston, TX 77005) BEN CARRERAS (Oak Ridge National Laboratory, Oak Ridge, TN 37831).* Most research on the reliability of electrical service has tended to treat market and network factors in isolation. This paper posits, however, that it is most likely the interaction between markets and networks which is responsible for causing blackouts. A simple representation of a uniform price auction electricity market driven by an agent-based learning algorithm is proposed. This market model is coupled to an existing simulation of power transmission which has been used to study cascading line failures (i.e., blackouts). Agents are found to behave plausibly in an idealized market without transmission constraints. Preliminary results of experiments about how market demand affects the probability and size distributions of blackouts are presented. Finally, an agenda for future research is suggested.

Science Writing: Finding the Human Face Within Scientific Discovery. *MARGRET CHANG (State University of West Georgia, Carrollton, GA 30736) DAVID BAURAC (Argonne National Laboratory, Argonne, IL 60439).* "Taken as a story of human achievement, and human blindness, the discoveries in the sciences are among the great epics." Such were the words of physicist J. Robert Oppenheimer, who headed the controversial Manhattan Project during World War Two. His comments, which speak to the need for recording the stories behind scientific discoveries, are an apt characterization of the unique role of the science writer. As transcribers of tales involving atoms, molecules, and Petri dishes, science writers face a continuous challenge in that their subject matter may seem incomprehensible or even trivial to the average reader. These obstacles, however, may be overcome by keeping in mind the human aspect of the scientist's work. This writing selection is a tribute to that aspect, focusing on themes such as science education and the impact of science on public affairs. News articles about scientific visions, tools, and experiments are also included--all written with the intent to present complex ideas in ways that can be appreciated by the general public. Through a multi-disciplinary, multifaceted look at some of the events at Argonne National Laboratory, it is hoped that these documents will provide a snapshot into Oppenheimer's conception of the "epic" story of science.

Documenting the Pacific Northwest National Laboratory (PNNL) Grid Monitor Screensaver. *ROBERT GELSTON (Heritage College, Toppenish, WA 98948) MIA BOSQUET (Pacific Northwest National Laboratory, Richland, WA 99352).* Without a major shift in the way the energy system is planned, built, and operated, the United States will invest nearly $500 billion in the electric infrastructure over the next 20 years. This study documents the Pacific Northwest National Laboratory (PNNL) Grid Monitor Screensaver, developed under the Department of Energy GridWise™ program, one small technological building block in the immense task of building the future electrical infrastructure. GridWise™ seeks to modernize the nation's electric system and to create a collaborative network filled with information and abundant market-based opportunities. Documentation focused on three key components of the screensaver: the scientific development and design, the usefulness of the information to related industries, and the possibility of enhancing the communication of electrical grid information to consumers. The screensaver has five graphical sections, each contributing to a picture of the stability of the power grid at a point in time. Major changes in these graphs can indicate a possible grid event that has occurred or is likely to occur. In order to understand the descriptions and purpose of each graph, a series of focused research questions was developed. Interviews with technical staff, technical journals, and textbooks helped bring together background information on the screensaver. Public sources of information such as the Web gave a picture of the readily available energy literature. Existing written sources of information proved limiting in providing insight for a straightforward, relatively non-technical understanding of the graphs in the Grid Monitor Screensaver. The limited availability of written information oriented toward the educated public is an indicator of the nature of this tool: interdisciplinary and at the forefront of technological research. As this screensaver indicates, the electrical power grid has many variables, and making meaningful changes to it must involve clear communication within all aspects of society. Recommendations for potential areas of improvement include enhanced cross-disciplinary communication throughout the electrical power structure.

Meta-Analysis of Available Data to Determine Sites of Significant Geothermal Potential in Colorado. *BRANDON GILLETTE (University of Kansas, Lawrence, KS 66045) GERALD NIX (National Renewable Energy Laboratory, Golden, CO 89401).* Geothermal electric power generation is a potential source of clean, renewable energy, especially in the western United States. In order to determine the geothermal potential of a particular site, a number of factors must be considered. Geologic factors include the heat content, fluid content, and permeability of subsurface rock. Data on these factors were gathered from a number of experts, universities, and organizations such as the Colorado Geological Survey (CGS) and the United States Geological Survey (USGS). These data were analyzed using the ArcMap Geographic Information System (GIS). This program overlays different spatially referenced data sets onto one map for analysis purposes. ArcMap GIS was used to interpolate data and create contour maps for some of these data sets. Based on criteria developed by the Geothermal Technologies Group at the National Renewable Energy Laboratory (including 120°C at depth, 400 to 600 gpm/MW flow rate, and accessibility), the site with the most significant potential for a geothermal power plant in Colorado was found to be the Mt. Princeton/Chalk Creek vicinity. Other factors to consider before development are the environmental, economic, and cultural impacts of a geothermal power plant on the surrounding ecosystems and community. There is little development in the area but concerns exist among local residents and businesses about possible impacts on the ecosystem and tourist-based economy. Future analysis should include hydrologic, geochemical and geophysical surveys, more precise geologic and structural mapping.

Integrating the Sciences. *KARA HARTMANN (University of Wisconsin-Oshkosh, Oshkosh, WI 54901) CLARISSA BERKMAN (Pacific Northwest National Laboratory, Richland, WA 99352).* Advances in science and the communication of scientific information have revolutionized the world and have enhanced how societies exist today. History shows how scientific and technological advances have greatly accelerated the dissemination of information about science and the sharing of novel ideas. However, the increasing specialization of science education and widening communication barriers between science-related fields have led to the loss of a comprehensive scientific worldview. Moreover, these barriers have made collaboration among multidisciplinary scientists and the integration of scientific knowledge difficult. To successfully integrate scientific knowledge across disciplines, changes in the way that scientists are educated and an increased awareness of the role of science and scientific communication by scientists will be essential.

Gas Composition Measurements from a Fluidized-Bed Biomass Gasifier. *MELISSA HIGHFILL (University of Colorado, Boulder, CO 80302) STEVEN PHILLIPS (National Renewable Energy Laboratory, Golden, CO 89401).* Biomass is plant matter or other biological material of non-fossil origin such as wood chips, corn stover and manure. Biomass can be converted into gaseous forms (syngas) or liquid forms (pyrolysis oils), depending on the reaction conditions. Each of these reactions produces a number of byproducts. A goal of research is to eliminate, reduce or find ways to utilize these byproducts. Scientists at the Thermochemical Process Development Unit (TCPDU) at the National Renewable Energy Laboratory (NREL) have characterized the byproducts produced at the end of the gasification process; however, no sampling has been done at the beginning of the process. The goals of this research are to demonstrate the feasibility of sampling at the beginning of the gasification process and to collect data regarding the composition of the gas produced in the fluidized-bed reactor. The data will then be compared with data obtained from samples collected after thermal cracking using the same methods. It is necessary to know the components of the gas stream throughout the process in order to reduce or eliminate unwanted organic tars. This research used a newly constructed probe to sample gases above the bed of the reactor. Analysis of the tar samples by Gas Chromatography-Mass Spectrometry (GC-MS) showed that a mixture of secondary and tertiary products formed in the bed of the reactor. These products were different from the expected primary products. Gravimetric analysis showed that the tars produced in the fluidized bed were approximately ten times as concentrated as the tars present after cracking. Future work on this project will involve modification of the sampling system, collection of data at various times after the start-up of the reactor and sampling at various heights in the bed. The data will determine if the level of char in the bed influences the composition of the gas stream.

A Method for Improving Global Pyranometer Measurements by Modeling Responsivity Functions. *ALISHA LESTER (Smith College, Northampton, MA 01063) DARYL MYERS (National Renewable Energy Laboratory, Golden, CO 89401).* Accurate global solar radiation measurements are crucial to climate change research and the development of solar energy technologies. Pyranometers are instruments that measure solar radiation. They produce an electrical signal proportional to global irradiance. The relationship of this signal to irradiance is defined as the responsivity (RS) of the instrument (RS = signal/irradiance = microvolts/(W/m2)). Most measurements are made using a constant RS; research shows, however, that RS varies with day of year, zenith angle, and net infrared radiation. This study proposes a method to find an RS function that better models the instrument's changing RS. Using a reference irradiance calculated from direct and diffuse instruments, instantaneous RS for two global pyranometers over 31 sunny days in a two-year period were found. We performed successive independent regressions of the error with respect to zenith angle, day of year, and net infrared in order to obtain a function characterizing RS. An alternative method replaced the infrared regression with an independently developed technique to account for thermal offset. Results show improved uncertainties with the function method than with the single calibration value. Lower uncertainties also occur using a black and white (8-48) rather than all black (PSP) shaded pyranometer as the diffuse reference instrument. We conclude that the function method is extremely effective in reducing uncertainty in the irradiance measurements for global PSP

pyranometers if they are calibrated at the deployment site. Furthermore, it was found that the function method accounts for the pyranometers' thermal offset, rendering further corrections unnecessary. The improvements in irradiance data achieved in this study will serve to increase the accuracy of solar energy assessments and atmospheric research.

Baseline Landcover and Invasive Species Mapping in the Lower Elwha Watershed. *KARITA MALTOS (Heritage University, Toppenish, WA 98948, JASON NAVARRETE (Heritage University, Toppenish, WA 98948)) KAREN STEINMAUS (Pacific Northwest National Laboratory, Richland, WA 99352).* Heritage University students working under a NASA PAIR (Partnerships for the Integration of Research into Undergraduate Education) program, in conjunction with a Pacific Northwest National Laboratory internship, used remote sensing technologies to develop landcover and invasive species maps in the Elwha River watershed. Two invasive species, Blackberry and Scotch Broom, were cited as species of interest. Landcover classes include water, deciduous and conifer species, impervious surfaces, and bare ground. Both maps will assist restoration efforts as well as create baseline information for comparisons during and after the removal of two dams. The upper Glines Canyon and the Lower Elwha dams will be removed by the Bureau of Reclamation beginning in 2007, as endorsed by the 1992 Elwha River Ecosystem and Fisheries Restoration Act. Since construction on the Lower Elwha dam began in 1908, the Elwha's historical salmon runs have been severely depleted. A 4-meter resolution, multispectral IKONOS satellite image was obtained for the 132 square kilometer study area. A 20-class unsupervised classification of the imagery was used as a preliminary guide for collecting field data. GPS coordinates and digital photographs of landcover and invasive species types were collected and a field laptop was used to perform on-site analysis. Twelve classes were derived from training areas using commercial-off-the-shelf GIS and image processing software. A supervised classification was completed using GPS derived field study points and a geographically linked red/near infrared scatterplot. A post-classification error-assessment study provides confidence intervals for the resultant maps and the twelve classes.

High School Student Research Participation Program at Lawrence Berkeley National Laboratory. *MICHELLE SHAVER (California State University Fresno, Fresno, CA 93740) ROLLIE OTTO (Lawrence Berkeley National Laboratory, Berkley, CA 94720).* As part of a continued effort to promote science education and give students access to further opportunities in the scientific field the Center for Science and Engineering Education (CSEE) department at Lawrence Berkeley Labs provides a High School Student Participation Program (HSSRPP) each summer. The program seeks to provide students with a real world experience towards careers in science and encourage their continued education in science and engineering. This six-week program provides selected high school students from the San Francisco Bay Area with summer work experiences in science, computing sciences, technology and related areas. As participants in this program students are given the opportunity to work as paid interns at a variety of locations (biosciences, earth sciences, life sciences, physics, material sciences, engineering, etc.) with an assigned mentor scientist being involved with their research and given roles within these research teams to reinforce classroom learning and promote their pursuit of a career in science and engineering. They are assigned a project designed by their mentor scientist to complete that may encompass a wide range of laboratory tasks. As a pre-service teacher having the role of teacher supervisor in this program was rewarding and informative. I was given the opportunity to observe these young scientists grow in their interest and understanding of the field. As a teacher supervisor I provided support for these students along with getting the opportunity to experience the research being done through their eyes. This experience helped to demonstrate what students would like to see in the classroom. Also co-authoring a paper compiling answers from high school students on how they would design their high school science department if given the chance and analyzing the responses further solidified the desire by students to see a change from the traditional teacher centered lecture style learning based on the textbook to a more student centered learning style where activities and experiments would allow the students to experience the curriculum for themselves with the teacher acting as a facilitator for their learning experience.

Technology in the Classroom. *ESTE WHITEHEAD (Chicago State University, Chicago, IL 60628) DEON ETTINGER (Argonne National Laboratory, Argonne, IL 60439).* Calculator Based Laboratories (CBL) allow teachers to use technology in science classrooms to motivate and help students' learning because students can focus on the exploring, understanding, and construction of scientific concepts without spending much time on the process of collecting data. A CBL is a device designed to collect and store data received from sensors as a function of time. The CBL collects data using detachable sensors or probes. Data can be collected with over 40 different probes such as: pH probe, colorimeter, flow rate and many more. I tested several experiments using the CBL. The experiment that I think students will like the most is the Energy Content of Foods. In this experiment I had to determine the energy released (in kJ/g) as various foods such as cashews, marshmallows, peanuts, and popcorn burn. The result for this first experiment was a success. My hypothesis was that the cashew and the peanut would have the highest energy content. For the popcorn and marshmallow my hypothesis was that they would have the lowest energy content. These skill development activities will introduce you to some of the many ways CBL can be used in the classroom to enhance the learning process. The first skill development activity will provide a sample of movies, experiments, and pictures that could be used for teaching purposes.

Materials Sciences

Oxidation Behavior of Nb and Ta Silicides. *MICAH BAQUERA (University of Texas at El Paso, El Paso, TX 79968) K.NATESAN (Argonne National Laboratory, Argonne, IL 60439).* Advancement in the field of high-temperature materials has given engineers a tool to increase the efficiency of their designs. An interest in the use of intermetallics and a high-temperature material has developed and become a research focus within the last fifty years. Intermetallics show promise for use as high-temperature materials due to high melting points good creep, oxidation, and corrosion resistance. Nb and Ta silicides were chosen to study their oxidation behavior. Samples were then oxidized at temperatures ranging from 500°C-1200°C. Characterization of these samples in the as cast and oxidized condition was critical due to little or no research having been previously preformed on these alloys. Characterization was completed by using a JEOL JSM-6400 Scanning Electron Microscope (SEM). Samples were weighed periodically during the oxidation and the weight change per unit surface area was plotted. It can be seen that the oxides forming at higher temperatures, above 1090°C, protect the specimen, while those below this temperature reduce it to powder. It is not yet understood what oxides are forming and at what temperatures, that is why further experimentation must be completed to characterize the oxides and analyze at what temperatures they form to optimize operating temperatures for these materials. These materials must either be alloyed to form a protective oxide at temperatures below 1000°C or implement a thermal coating in order to be considered as a useful high-temperature material.

Environmental Degradation on Arsenic Trisulfide (As40S60) Glass. *RICHARD BARAN (Clarkson University, Potsdam, NY 13699) NORMAN ANHEIER (Pacific Northwest National Laboratory, Richland, WA 99352).* The formation of a cloudy haze has been observed on thermally evaporated arsenic trisulfide (As40S60) thin films. These glass films are a critical component of the photonic devices under development. Identifying the chemical make up and understanding both the underlying causes of the cloudy haze and determining the steps needed to mitigate this problem are the topic of this research paper. Raman Spectroscopy, Fourier Transform Infrared Spectroscopy (FTIR), and X-ray Photoelectron Spectroscopy (XPS) were all used in the analyses. An experimental matrix, which accounted for the most probable causes of the degradation (light, H_2O, O_2, and temperature), was developed and implemented. The experimental results showed that the combination of light and H_2O is both necessary and sufficient to promote the cloudy haze formation. XPS has been conclusive in identifying the presence of arsenic oxide As-O and sulfur oxide S-O in the degraded samples. The results of this study show that the combination of light and H_2O is critical to the formation of As-O and S-O on the surface of $As_{40}S_{60}$. The formation of these oxides contribute to the observed detrimental degradation.

Magnetic Field Modification of Microstructures in a 52100 Steel. *NICHOLAS BEMBRIDGE (Florida A&M University, Tallahassee, FL 32307) GERARD LUDTKA (Oak Ridge National Laboratory, Oak Ridge, TN 37831).* Magnetic fields have been known to drastically alter the transformation kinetics traditionally associated with steels. Ongoing research seeks to explore the extent of this phenomenon and to ideally put it to use in optimizing processes already employed by the steel industry. In this particular experiment the application of high magnetic field processing to influence the phase equilibria and transformation kinetics during continuous cooling of an SAE 52100 low alloy hypereutectoid steel was investigated. Specifically the effects on the quenching of austenitized steel in a magnetic field exceeding 10 T were investigated. At the onset of the experiment, a continuous cooling rate that allows 52100 steel to undergo martensitic transformation was determined through dilatometry. This optimum cooling rate needed to yield a typical

microstructure of martensite and retained austenite and was found to be about 40°C/s. A number of samples were then continuously cooled at this rate from different austenitizing temperatures with varying field conditions. Optical and electron microscopy, chemical analyses, and microhardness hardness tests were also carried out on the material in its as received and magnetically processed states. In addition, intrinsic Type S (Pt-PtRh) thermocouples were used to plot the changing temperature and also detect any recalescence heat given off during transformation. Significant recalecence occurred in instances where the starting temperature was below 850°C and the field strength was at least 10 T. This investigation clearly demonstrated that high magnetic fields applied during continuous cooling, under the correct conditions, will not only expedite the onset of equilibrium phase transformation but also accelerate the rate at which it occurs. The implications of these results on potential new material thermal processing methodologies will be presented and discussed.

Where Physics Meets Rendering: The Construction of Computer Graphics For High-Temperature Superconductivity. *JOSHUA BIETZ (Georgia Institute of Technology, Atlanta, GA 30309) THOMAS SCHULTHESS (Oak Ridge National Laboratory, Oak Ridge, TN 37831).* As the world of physics evolves, the complexity and abstract nature of the problems, as well as the competition between different groups, grows rapidly. This competition extends to funding. Because an expertise in these fields is rare, eliminating syntax in explaining the physics is desirable. As a result, a set of tools designed to convey the ideas and methods intrinsic to the investigation process has significant value. The toolbox is comprised of the utmost complexity. Thusly, enough foresight to anticipate its dynamics is difficult, if not impossible, to obtain. An ad hoc approach has been employed to both create a desired rendering and to investigate the dynamics associated with the process in hopes of further developing the bank of information necessary for the tool box. The Hubbard model has been selected as the candidate as it contains the complexity and abstract nature that veil it to the lay person, and is the current workhorse of High-Temperature Superconductivity studies – a highly competitive topic of great interest. A Graphical User Interface has been employed to utilize the infrastructure of OpenGL, which involves on the fly graphics construction allowing the rendering itself to cater to any platform. This particular software enhances both the complexity and the malleability of the rendering process. As a direct result, the rendering lies in the initial stages, but when complete, any representation platform can be utilized to its maximum resolution. Such a characteristic is necessary to make use of the power wall facility. A movie wherein the three-dimensional superconducting crystal, for which a graphical representation has been designed, will be cleaved down to the two dimensional plane of interest will be built. This shall be followed by a folding of the multiple orbitals and interactions into a square lattice of single orbitals – the essential two-dimensional Hubbard model describing itinerant electrons interacting locally. Electrons will then be visualized, and the model shown in action. The next step consists of visualization of the doping process to demonstrate one hypothesized mechanism of High-Temperature Superconductivity. Due to recently acquired evidence, it appears that a three-dimensional crystalline structure may be necessary to accurately model the system. It is probable that future work will involve the manifestation of a three-dimensional model involving electronic tunneling between the planes.

Evaluating Quartz Crystal Microbalance Experimental Techniques In Ion Bombardment Erosion Studies. *CHRISTOPHER CHROBAK (University of Wisconsin - Madison, Madison, WI 56706) AHMED HASSANEIN (Argonne National Laboratory, Argonne, IL 60439).* A quartz crystal microbalance (QCM) dual crystal unit is a powerful tool used in interpreting the sputtering rate of materials exposed to irradiations of energetic ions. The QCM sensor consists of a 0.550” diameter pure quartz crystal disc coated with a thin film of gold that oscillates near 6 MHz inside the QCM detector. The sensitivity of these crystals is sufficient to detect a noticeable change in frequency from just a single angstrom of deposited material. However, the crystals also respond sensitively to many unwanted background factors, such as temperature transients and oxidation reactions. We have found methods to minimize the effects of these backgrounds and make use of the signal in low yield cases. Methods include measuring sufficient background signal before and after sputtering, understanding the effects of temperature transients on frequency, minimizing crystal exposure to unwanted background effects, and manipulation of incident beam flux and current. The IMPACT facility is designed for modeling and diagnosing ion material interactions pertaining to semiconductor manufacturing, plasma produced Extreme Ultra-Violet (EUV) light sources, and first-wall fusion reactor materials. This work focused on understanding the effects that these simulated environments have on the sputtering measurement tools and finding methods to minimize those effects.

Synthesis of Metallic Mesoporous Materials. *ANTHONY CRISCI (University of Illinois, Champaign, IL 61820) MILLIE FIRESTONE (Argonne National Laboratory, Argonne, IL 60439).* Mesoporous silicas are structured materials that possess an ordered 2D hexagonal array of parallel cylindrical channels with tunable pore diameters (e.g., 30-70 Å). Mesoporous silicas, such as MCM-41 and SBA-15 have been used primarily as passive frameworks in which active guests (e.g., catalysts) are housed. Considerably less work has been directed at preparing active mesoporous materials that could be used to control the functionality of the intercalated guest. In this report, we describe several synthetic approaches used to develop an electrochemically active ordered mesoporous structure of gold. Briefly, an aqueous gold salt is mixed with a surfactant-based template, which is ordered by thermal treatment. Photochemical or chemical reduction is applied to reduce the gold ions (Au^{3+}) to Au0 which initiates the formation of interconnecting gold bonds encompassing the template. The surfactant-based template is removed by washing with water. Analysis of a surfactant-free sample by small angle x-ray scattering (SAXS) indicated a highly ordered, autonomous structure remained after washing. A nitrogen adsorption study is scheduled to determine the surface area and aperture diameters of the gold mesopore product. Currently, we wish to develop an efficient standard synthesis protocol for metallic mesoporous materials (e.g. gold); to enable the production of functionalized mesopores.

Fuel Liner Compatibility Studies of Advanced Cladding Materials for the Generation IV Reactor Systems. *DAVID CULLEN (Brigham Young University, Provo, UT 84602) JAMES COLE (Argonne National Laboratory, Argonne, IL 60439).* The addition of a fuel liner between the cladding material and metallic fuel of the Generation IV Sodium Fast Reactor (SFR) has been proposed in response to concerns about possible development of brittle or low-melting phases. Diffusion couple studies using vanadium, zirconium, T122 stainless steel, and oxide dispersion strengthened steel (ODS) are designed to study the extent of the diffusion zone formed between the proposed liner and cladding materials. Initial diffusion couple experiments were carried out at 700°C in an argon-purged atmosphere for 50 hours. Annealed diffusion couple samples were prepared for analysis with a transmission electron microscope (TEM) and scanning electron microscope (SEM). Images taken with a SEM show the development of a multi-phase diffusion zone between 2 and 5 μm thick at each interface. These zones will be studied using energy-dispersive x-ray spectroscopy (EDS) on both a SEM and TEM to determine the exact composition. Further diffusion studies will be carried out to better understand the kinetics of the diffusion behavior.

Friction Stir Experiments: Surface Modification of Magnesium Alloy AM60 and Welding of 304 Stainless Steel. *CASSANDRA DEGEN (South Dakota School of Mines and Technology, Rapid City, SD 57702) STAN DAVID (Oak Ridge National Laboratory, Oak Ridge, TN 37831).* Friction stir welding (FSW), developed and patented in 1991 by TWI, is a process of joining two solid state materials. Friction stir processing (FSP), a variation of FSW, is a process involving the stirring of material to modify microstructure and mechanical properties. FSP differs from FSW only in that the objective is to modify microstructures rather than to weld parts together. The current project involves two parts. The first part is FSP of a magnesium alloy, AM60, and the properties related with the FSP area compared with the properties of the as-cast metal. In recent years, it has been recognized that FSP can be used to improve the surface properties of alloys. Die-cast bars of AM60, provided by Ford Motor Company, were friction stir processed to modify the surface microstructure using a FSW pin tool. Overlapping passes were made to ensure that the material was evenly stirred. Hardness was measured across the FSP area, and tensile specimens were machined from the FSP area as well as the as-cast area for comparison. Cross-section specimens of the FSP area were also prepared for metallography. It was found that the alloy experienced grain refinement in the FSP area and porosities were greatly reduced or eliminated. Tensile tests are currently underway, and are expected to show increased properties as well. These results show that FSP could lead to strengthening select fatigue-prone areas in cast magnesium alloy parts. The second part of the project is FSW of 304 stainless steel, and the change in microstructure that takes place. FSW research over the past 13 years has dealt mainly with low-temperature materials. Because of the lack of pin tool choices, FSW of high-temperature materials is limited. Using a tungsten based pin tool developed at Oak Ridge National Laboratory, 304 stainless steel was friction stir welded. A sample was prepared to determine the ferrite content. The mean ferrite content in the base metal was 1.57%, where the mean ferrite content in the weld metal was 3.37%. This sample was then investigated in metallography to determine ferrite

to sigma phase transformation. Optical metallography examination showed some evidence of ferrite to sigma phase transformation. Future work using transmission electron microscopy is underway to confirm this result. The results of this investigation show that microstructure and properties of metals and alloys can be modified drastically through friction stir processing and friction stir welding.

Development, Growth and Characterization of Gd-Ceria Films as Electrolytes for Solid Oxide Fuel Cell. *ADAM DIRKES (Washington State University, Pullman, WA 99163) LAXMIKANT SARAF (Pacific Northwest National Laboratory, Richland, WA 99352).* We report the development and modification of an experimental system which is used to grow cerium oxide thin films using DC magnetron sputering in a mixture of argon and oxygen ambient. The development part includes, set-up of 2" and 4" magnetron sputter sources in a high vacuum chamber. We have also installed the substrate heater used to grow thin films at higher temperature. After the set-up, we have successfully grown highly oriented Gd-doped cerium oxide thin films on single crystal Al_2O_3 substrate. Oxygen transport characterization of these films were carried out using AC impedence conductivity measurements. The structural properties were studied using x-ray diffraction technique and the films were observed to be highly oriented in direction. Initial conductivity results show the activation energy of 1.14 eV in case of cerium oxide film grown at 650°C. These results are discussed in details from the point of view of application in the area of solid oxide fuel cells.

Atomic Layer Deposition. *DAVID DOTZAUER (University of Wisconsin-Platteville, Platteville, WI 53818) GREG KRUMDICK (Argonne National Laboratory, Argonne, IL 60439).* The task of this project has been to build an atomic layer deposition (ALD) reaction chamber. It will be used to grow thin films for use in different applications in the industrial areas including microelectronics, semiconductors, superconductors, and many others. Following the ALD reactor design that is used by Jeff Elam in the Materials Science Division, we have built a reactor that will have the same capabilities of film growth. However, we have not yet begun growing films in this reactor. The primary goal was to develop a reactor that is easy to use, and can be easily modified to use different precursors in film growth. When the system is complete and properly checked for leaks, it will be able to contain eight separate precursors at one time. This will provide an advantage of being able to produce more advanced films without stopping the growth cycle. Although there are no experimental results to refer to, this paper will discuss the process of ALD, some of its possible uses, ways of studying film growth, and past experiments that have been performed.

Thermal and Mechanical Properties of $LaCoO_3$. *LAURA FEGELY (Drexel University, Philadelphia, PA 19104) EDGAR LARA-CURZIO (Oak Ridge National Laboratory, Oak Ridge, TN 37831).* Structural Characterization of Ion Conducting Perovskites by X-Ray Diffraction Ion conducting perovskite ceramics are of great importance for advanced energy systems, such as Solid Oxide Fuel Cells (SOFCs). They can be used in the design of cathodes, electrolytes, and anodes in lower temperature SOFCs. Due to the harsh environments found in SOFCs, it is necessary for the structural properties of these materials to be rigorously examined. This study reports on the structural characterization of ion conducting perovskites by X-ray diffraction for use in advanced energy applications. Work was completed on the verification of phase compositions and for $LaCoO_3$ after it had been heated and reduced in an isothermal $4\%H_2/96\%Ar$ environment. Samples of $LaCoO_3$ were then evaluated after being reduced for various amounts of time. The amount of time for each sample was based on the minimums and maximums of the graph of the thermal expansion of $LaCoO_3$ versus time, in which a $LaCoO_3$ sample was heated to 850ºC in air, then switched to a $4\%H_2/96\%Ar$ mixture and kept isothermal at 850°C. After a maximum of 88 minutes in the reducing atmosphere, followed by a minimum after 172 minutes, another maximum after 325 minutes, and finally, a continuous contraction curve until the gas mixture ran out at 2211 minutes. After identifying these transition points, fresh samples of LaCoO3 were heated and reduced to each point, cooled, ground, and X-ray powder diffraction was performed. A Scintag PADV Room Temperature X-Ray Diffractometer, and associated software, was used to perform phase verification scans from 10-140 degrees, on 6-8 sec. steps of 0.02 deg. Phase compositions were verified through use of the MDI Jade 6.5 Program. These results show the phase composition of $LaCoO_3$ after reduction in hydrogen (H_2;4%:Ar;96%), during which significant structural changes were observed and new compounds were formed, including $La_3Co_3O_8$, La_2CoO_4, $La_4Co_3O_{10}$, La_2O_4, $Co3O_4$, CoO, and Co .

Synthesis of Open-Cage Fullerene Derivatives for Application to Quantum Computing. *RUSSELL FUNK (The University of Chicago, Chicago, IL 60637) JOHN SCHLUETER (Argonne National Laboratory, Argonne, IL 60439).* In recent years, quantum computing (QC) has attracted the interest of physicists, chemists, computer scientists, and even the United States Department of Defense. Quantum computers offer tremendous advantages over "classical" bit based computers by using quantum bits, or "qubits." One way for these qubits to be created is by using endohedral nitrogen encased in C_{60} ($N@C_{60}$). In order for the endohedral nitrogen to be created however, fullerene molecules with large open-ring orifices must be synthesized, so that the nitrogen can be readily inserted into C_{60}. Our goal was to find a procedure for creating large amounts of open-cage fullerenes with high yields. We did this using a previously reported method for the synthesis of several open-cage fullerene derivatives, and then attempted to create greater amounts of an 8-membered-ring fullerene ($C_{80}H_{14}N_2$) by increasing the amounts of the reagents used. We also tried to obtain higher yields of $C_{80}H_{14}N_2$ by doubling the chemical amount of 3-(2-pyridal)-5, 6-diphenyl-1, 2, 4 triazine used in the initial reaction. Finally, we tried to expand the 8-membered-ring orifice into a 12-membered-ring by subjecting the $C_{80}H_{14}N_2$ to ultraviolet (UV) radiation. We found that our attempts to scale up the synthesis of $C_{80}H_{14}N_2$, and increase the yield were successful based upon the UV-vis results that we ran on our sample compared with those in previously reported literature. The 12-membered-ring will be examined further for purity, hopefully using nuclear magnetic resonance (NMR) and infrared spectroscopy (IR). While this quantum computing project is still in its infancy, it is crucial to have large amounts of open-cage fullerenes for later phases of this project.

Design, Synthesis and Characterization of Cross-linkable Imidazolium Based Ionic Liquids. *CRISTIAN GONZALEZ (University of Puerto Rico, Mayaguez, PR 00681) MILLIE FIRESTONE (Argonne National Laboratory, Argonne, IL 60439).* An ionic liquid is a material with interesting and useful physical properties. Some of them are: lack of vapor pressure, non-flammable, non-toxic, thermally stable, high conductivity, good electrochemical properties. These ionic liquids are able to rearrange themselves when water is added. Three different ionic liquids were prepared. Two of them have the reactive group in the tail, C_{10} ene mim^+Cl^- and C_8 Acy mim^+Cl^-, and the third one, C_{10} Vim^+Cl^- has the reactive group in the head. These reactive groups will allowed the molecule to do a cross-linkage. The synthesis of C_{10} ene mim^+Cl^- was done before but never published. For the purification of this material, it was necessary to wash it with ethyl acetate in a separatory funnel. Then, the sample passed through vacuum distillation in order to remove the remaining solvent. In order to isolate and purify C_8 Acr mim^+Cl^- and C_{10} Vim^+Cl^- it was used silica gel column chromatography. These were gradient columns beginning with 100% ethyl acetate, and then using solutions of 90% EtOAc in MeOH to 50% EtOAc in MeOH, finishing with pure MeOH for washes. Thin layer chromatography was done to all the fractions to determine where the materials of interest are. Those fractions passed through vacuum distillation. In order to verify that the materials correspond to the structure, 'H NMR was done to the three molecules. The experiments of cross-linking are underway. There are three different ways to induce cross-linking in these molecules: photo cross-linking, gamma irradiation, thermal cross-linking all of them were performed.

Effect of Reinforcing Carbon Fiber Morphology on Tribological Behavior of Polyether Ether Ketone (PEEK) Polymers. *AARON GRECO (Iowa State University, Ames, IA 50011) LAYO AJAYI (Argonne National Laboratory, Argonne, IL 60439).* Polymer and composite polymer materials are being used in an increasing number of engineering applications. In some applications the tribological performance of these materials is crucial to the operation of the device. Many polymeric materials take advantage of additives and reinforcement to improve their performance in certain severe conditions. However, depending on the conditions that this operation occurs there is limited understanding of how these composite materials will behave. This study focuses on testing the tribological influences of additives in a commonly used polymer matrix (polyether ether ketone) PEEK under relatively sever contact conditions (up to 70 m/s sliding speed and 600 MPa contact pressure). To conduct these high speed tests a custom built bench top test rig was used to simulate a unidirectional sliding contact condition. There were three forms of PEEK tested: base PEEK material, 450FC30 a composite of short carbon fiber reinforcement and solid lubricant, and CPK53 a composite using a fabric of woven carbon fiber. These materials were tested against a spherical stainless steel counter face and in two different humidity environments. The results of these tests consisted of friction profiles across varying sliding speed and calculated specific wear rates. It was easily determined that there is a frictional dependence to sliding speed for most of the tested materials, and that the additives in the composite materials have an influence on both the frictional response as well as the respective wear rate. It was also

determined that the composite's additives do not improve the tribological performance of the polymer under certain tested conditions.

High Speed Tribological Testing of Candidate Materials for Toroidal Intersecting Vane Machine (TIVM) Air Compressor. *AARON GRECO (Iowa State University, Ames, IA 50011) OYELAYO AJAYI (Argonne National Laboratory, Argonne, IL 60439).* There have been many exciting advancements in fuel cell technology, specifically in the automobile application. However, as with any technological advancement there are typically many hurdles that accompany their development. The development of fuel cell powered automobiles is no exception to this trend. There are many technological issues that have slowed the advancement of this evolving energy alternative. One such issue involves the pressurization of the fuel cell stack. The air compressor used for this application must meet several strict performance restrictions. This project outlines the performance evaluation of several possible materials to be used in a toroidal intersecting vane machine (TIVM) compressor. The materials were tested with respect to two main tribological properties: frictional stability over a range of high sliding speeds (40-70 m/s), and the resulting wear of the material. These tests were also conducted under two separate atmospheric conditions: ambient humidity (30-40% RH) and saturation humidity (99.9% RH). The tests used a three ball on disk setup, with a contact pressure around 100 psi. The test matrix included three separate ball materials which were tested against six different disk materials. The balls material included: 440C steel, 2017 aluminum, and steel coated with a Near Frictionless Carbon (NFC) coating. The disk material included: three types of polyetherimides (PEI) (Ultem 1000, Ultem 4000, Ultem 4001), Poly(ether ether ketone) (PEEK), a composite of woven carbon fibers with a PEEK matrix (CPK), and steel coated with NFC. The frictional response was tested with respect to a continuously varying sliding speed (0-70 m/s). It was determined that there was little frictional dependence on sliding speed for each material combination tested. The average coefficient of friction was compared for each material combination, here it was determined that the CPK and NFC coatings gave the lowest values around 0.1-0.15. The total resulting wear was then calculated by measuring the volume of material removed from both the ball and disk during the test. These results showed that CPK and NFC coatings showed the least amount of wear by a considerable amount. This combined with the fact that they exhibited the lowest frictional coefficients, makes these materials, CPK and NFC coated steel, good candidates for the TIVM compressor.

High Speed Tribological Evaluation of Polymer Composite Materials. *AARON GRECO (Iowa State University, Ames, IA 50011) OYELAYO AJAYI (Argonne National Laboratory, Argonne, IL 60439).* Polymer and composite polymer materials are being used in an increasing number of engineering applications. In some applications the tribological performance of these materials is crucial to the operation of the device. However, depending on the conditions that this operation occurs there is limited understanding of how these composite materials will behave. This study focuses on testing the influences of additives in polymer composites to tribological behavior in high speed (80 m/s) sliding conditions. To conduct these high speed tests a custom built bench top test rig was used to simulate a unidirectional sliding contact condition. There were two series of polymers tested: Polyetheretherkeytone (PEEK) and Polyetherimide PEI; under each series there where three different materials tested which consisted of both composites and base resin. These materials were tested against three different metal counter faces and in two different humidity environments. The results of these tests consisted of friction profiles across varying sliding speed and calculated specific wear rates. It was easily determined that there is a frictional dependence to sliding speed for most of the tested materials, and that the additives in the composite materials have an influence on both the frictional response as well as the respective wear rate. From these results it was determined that CPK53, a carbon fiber reinforced composite of the PEEK series, exhibited the most preferred tribological performance by having the lowest friction coefficient with the high wear resistance. Furthermore, this study presents the possible implication too develop a mode for predicting the tribological behavior of polymer materials given conditions and certain material properties.

Corrosion Behavior of Iron and Nickel Base Alloys. *PRISCILLA GUERRERO (University of Texas at El Paso, El Paso, TX 79968) K. NATESAN (Argonne National Laboratory, Argonne, IL 60439).* Designs of advanced combustion systems that exploit coal as a feedstock must improve thermal efficiency and considerable decrease in release of sulfur oxides, nitrogen oxides, and carbon oxides. In order to create reliability and long term trouble free conditions for these materials, simulated coal combustion environments were developed. Iron and nickel base alloys utilized in industry to evaluate corrosion behavior of each material when exposed to two coal ash mixtures and temperatures ranging from 650°- 800°C. The Fe base alloys include HCM12A, Super 304H, 347HFG, NF709, HR3C. 310TaN, and SAVE 25. The Ni base alloys include 600, 601, 690, 617, 625, 602CA, 214, 230, 45TM, HR 160, and 693. The experiments were conducted in a horizontal heated furnace covered in an ash and sulfate mixture or ash, sulfate, and NaCl mixture. Samples were analyzed on a JOEL JSM-6400 scanning electron microscope (SEM) to measure internal penetration. Results showed Fe base alloys experienced catastrophic corrosion with the ash, sulfate and NaCl mixture at 725°C. Ni base alloys generally experienced less corrosion at 725°C.

Developing $LiMn_2O_4$ Cathodes Using a LT-$LiCoO_2$ Coating. *BRETT ISSELHARDT (Westmont College, Santa Barbara, CA 93108) CHRISTOPHER JOHNSON (Argonne National Laboratory, Argonne, IL 60439).* $LiMn_2O_4$ has been proposed as a safer and more cost effective alternative to HT-$LiCoO_2$ for use as a cathode in Lithium-ion batteries. Although $LiMn_2O_4$ works well at room temperature it is prone to rapid capacity fade and cell failure in rechargeable Lithium batteries because of unstable surface chemistry at elevated temperatures due to dissolution of the electrode. Preliminary studies have suggested that coating $LiMn_2O_4$ with a LT-$LiCoO_2$ may be able to overcome the faults of the $LiMn_2O_4$ and provide a stable cathode material. Two simple methods were developed for coating the $LiMn_2O_4$, which were studied using electrochemical analysis, thermo-gravimetric analysis, and x-ray diffraction to characterize the coating properties and its interaction with $LiMn_2O_4$. An ideal coating thickness was identified between 2-4 wt.% that allowed for the optimization of both capacity per gram and fade rate per cycle, the fade rate was reduced by an order of magnitude from .22% to .035% creating a stable cathode. A cubic $LiCoO_2$ phase was matched to cubic $LiMn_2O_4$ to provide a uniform material which preserves the physical structure of the uncoated $LiMn_2O_4$. The temperature and time required to achieve this phase match were also identified. This research has created and characterized a simple method for coating $LiMn_2O_4$ with $LiCoO_2$ that allows for its use within Lithium ion batteries.

Structural Analysis of RuPt Samples Using Grazing Incidence X-ray Diffraction. *LINDSAY JONES (Northeastern University, Boston, MA 02115) MICHAEL F. TONEY (Stanford Linear Accelerator Center, Stanford, CA 94025).* Ruthenium (Ru, Z = 44) is a Platinum Group Metal that has a standard hexagonal close packed (HCP) crystalline structure. Platinum (Pt, Z = 78) has a face-centered cubic (FCC) crystalline structure. When these metals are co-sputtered onto a silicon substrate, creating a few nm-thin film, they form an alloy with a combination of HCP and FCC structure. Direct methanol fuel cells rely on an anode catalyst to draw hydrogen from liquid methanol. Highly efficient fuel cells based on polymer electrolyte catalysts, known as proton-exchange membrane fuel cells, have been developed, but require large amounts of a costly platinum catalyst. Thin-film nanostructure bimetallic alloys have been produced to reduce the amount of expensive Platinum needed for catalysis, and also to improve the electrochemical properties of the catalyst. Supported RuPt particles have been shown to have superior activity as anode catalysts for methanol electro-oxidation and demonstrate an improvement in resistance to poisoning in comparison to unalloyed Pt. The percentage of Ruthenium in a RuPt thin film and the process by which the alloy is produced will dictate the crystalline structure, and thus the electrochemical properties of the film. Pure Ruthenium, Pure Platinum, and eight intermediate samples at differing percent composition of Ruthenium were characterized by their X-ray diffraction patterns. The incident beam is from the Stanford Synchrotron Radiation Laboratory beam and operates at approximately a 1.4 Angstrom wavelength. The results show that 0% Ru through 46.17% Ru exhibit a majority FCC structure, 56.07% Ru and 60.61% Ru are mixed phase, and from 67.03% Ru through 100% Ru, the samples exhibit a HCP structure.

Synthesis, Structural Characterization and Transport Measurement of High Temperature Superconducting Thin Film. *TONY DAVIS (NC Agricultural & Technical State University, Greensboro, NC 27401) JEFFERY JORDAN (NC Agricultural & Technical State University, Greensboro, NC 27411) JULIUS STEAD (NC Agricultural & Technical State University, Greensboro, NC 27401) DAVE CHRISTEN (Oak Ridge National Laboratory, Oak Ridge, TN 37831).* The conduction of energy-loss-free electric currents needed for practical applications of superconductors poses unique requirements, a delicate balance between material perfection and disorder. An optimal array of defect nanostructures is needed to immobilize the quantized magnet flux structures (vortices) against dissipative motion. These material defects play an important role for both large-scale power devices requiring large energy-loss-free current conduction, and in superconducting electronic devices for the minimization of voltage noise. In principle, the ideal pinning nanostructure is an ordered array of optimally-sized normal material dispersed

in a crystalline superconducting matrix. In practice, pinning defects are randomly distributed in both size and configuration, resulting in reduced efficiency for pinning of a regular vortex lattice. In light of practical need, the goal of our studies was to develop a fabrication technique and a fundamental understanding for dispersing ordered array of normal materials in superconducting matrix. To realize this goal we had divided our studies into three tasks: (i) creation of nano-sized dot of barium zirconate ($BaZrO_3$) with optimum spacing and size distribution on single crystal $LaAlO_3$ and polycrystalline Ni-W alloy substrates using a solution technique, (ii) pulsed laser deposition of $YBa_2Cu_3O_{7-x}$ superconducting thin films on uncoated (controlled) and $BaZrO_3$ nanodots-coated substrates, and (iii) structural and superconducting measurements and analysis of YBCO thin films on controlled and $BaZrO_3$ nanodots-coated substrates. The findings from our investigation are expected to lead to novel approaches in the pursuit of superconducting devices that fully exploit the higher operating temperatures of the cuprate superconductors.

Characterization of Superhydrophobic Materials. *WENSING KUO (The University of Texas at Austin, Austin, TX 78705) JOHN T. SIMPSON (Oak Ridge National Laboratory, Oak Ridge, TN 37831).* A hydrophobic material is a material in which water droplets prefer to cling to themselves more than the material. There are a few materials in which this self-clinging preference becomes so large that tiny water droplets tend to bead up into nearly perfect spheres. These materials are known as superhydrophobic materials. Surface roughness and uniformity at the nano-scale play an important role in enhancing the inherent hydrophobic qualities of a material, which cause a surface to become superhydrophobic. Naturally occurring in nature, this kind of water-repellant surface can be observed on the leaves of lotus plants. As opposed to the many hydrophilic surfaces that are conducive to the flattening of water droplets, the ability of superhydrophobic materials to make water bead up lies partly in the trapped air pockets that result from the coarse surface structure. A recent discovery has been made to easily and cost-effectively engineer and fabricate such a surface. In order to characterize the superhydrophobicity of this material, Python, a high-level programming language, was used to interface to a device driver for a Mikrotron Inspecta frame-grabber. This camera is used to capture high-speed images and will be instrumental in characterizing the interaction of water droplets with the superhydrophobic material. Also important to the characterization of the material is the measurement of the contact angle of a drop of water. The contact angle, which serves as a measure of how water-repellant the surface is, can be found from the intersection of the tangent lines to the droplet surface and the substrate surface. With the use of Python, a program was written to capture an image of a water drop and subsequently calculate the contact angle of that drop on the superhydrophobic surface. What shall be shown is that the more superhydrophobic a surface, the closer the contact angle will approach 180 degrees. This work is a small portion of a larger study to characterize the behavior of this superhydrophobic material. As more is learned about this material's interaction with water and water based solutions, the more widespread the applications are expected to become such as for its use in drag reduction or for the purpose of water-proofing various surfaces like lenses and windshields.

Mixed Conducting Ceramics Based on $Ca_2Fe_2O_5$. *RICHARD LAWSON (Tennessee Technological University, Cookeville, TN 38505) ANDREW PAYZANT (Oak Ridge National Laboratory, Oak Ridge, TN 37831).* Ceramics that exhibit both ionic and electronic conduction (mixed conduction) have a variety of uses, including fuel cells, sensors, and separation membranes. A series of ceramics of the structure $Ca_2Fe_{(2-x)}B_xO_5$, where B = Al and Ga and x = 0, 0.4, and 0.8 was investigated using direct current (dc) conductivity measurements and x-ray diffraction (XRD) to determine viability of their use as mixed conductors. Glycine-nitrate synthesis was used to create powders of the ceramics in the desired compositions. XRD was used for phase analysis of both powder and pellet samples. The dc conductivity measurements were made using a four-point van der Pauw technique in air, dry argon, and dry argon - 4 wt% hydrogen atmospheres over a range of temperatures from 300°C to 900°C. The samples where x = 0 and 0.4 undergo a phase transformation from srebrodolskite to brownmillerite. The samples where x = 0.8 maintained a single phase even at elevated temperatures, but they each were a different phase; $Ca_2Fe_{1.2}Ga_{0.8}O_5$ was srebrodolskite and $Ca_2Fe_{1.2}Al_{0.8}O_5$ was brownmillerite. All doped samples were stable in both reducing and oxidizing atmospheres, whereas $Ca_2Fe_2O_5$ decomposed when heated in air after exposure to a reducing environment. All doped samples gave indication of being mixed oxygen/electronic conductors, with further work to be done to prove oxygen conduction.

The Analysis and Modeling of Irradiation Induced Creep Strain in Graphite. *SARAH LESESNE (University of Richmond, Richmond, VA 23173) TIMOTHY BURCHELL (Oak Ridge National Laboratory, Oak Ridge, TN 37831).* Much is known about the physics of neutron damage and how the structure and properties of graphite alter upon irradiation. One of the most interesting phenomena is that of irradiation induced creep strain. Creep can be described as the slow, continuous process by which a material deforms when a load is placed on it. However, graphite does not creep at temperatures below 2800°C except during neutron irradiation. Previously collected irradiation data was analyzed. These data showed changes in volume, diameter, density, coefficients of thermal expansion and creep strain with varying levels of neutron dose. The raw data were placed in spreadsheets and graphed in order to visualize the graphite's varying behavior. The first step in analyzing the graphs was to validate previous elementary models describing the creep behavior of the graphite at low neutron dose levels. Further analysis of this data involved using those previous models to design more appropriate ones that would not only be able to predict the behavior where data might be missing but be more applicable at greater doses. The data were evaluated to determine the magnitude and nature of the correction that should be applied to account for irradiation induced structure changes in the graphite. Significant progress was made, however further work must be performed to extend the irradiation creep data and model.

Application of Glass Beads as a Shear Vane Reference Material. *NATHAN LESTER (Heartland Community College, Normal, IL 61761) ADAM POLOSKI (Pacific Northwest National Laboratory, Richland, WA 99352).* Development and use of a shear strength reference material is important for assuring adequate quality control for shear vane experiments. In this publication, glass beads are proposed as a shear strength reference material because they exhibit reproducible shear strength results, are easy to prepare, are reused without degradation to the material, and are stable under normal laboratory conditions. Understanding the mechanics of glass beads during shear vane measurements is integral to their development as a standard reference material. Two equations describing a frictional based mechanistic model of granular materials are derived. A hydrostatic pressure profile as a function of vane depth and a pressure profile for granular materials described by the Janssen equation are the basis for the two equations. These equations can be used to predict torque values during shear vane measurements. To test these equations, shear vanes of various dimensions are attached to a Haake M5 viscometer. The shear vanes are immersed to a known depth, rotated at a constant rate, and a resulting torque versus time profile is obtained. This procedure is repeated at multiple vane submergence depths. Peak and equilibrium values are determined from the torque/time profiles and correspond to the static and kinetic frictional cases respectively from the mechanistic equations. A least squares regression is performed on the experimental data to calculate two fitting parameters in the mechanistic equations. These fitting parameters represent 1) the number of contact points in a differential element on the surface area of the cylinder formed by rotating the vane 2) the ratio of the lithostatic axial stress to radial stress that Janssen demonstrated as significant to granular materials. Good agreement is observed between the measured and predicted kinetic values using these techniques. This agreement demonstrates an initial understanding of granular material mechanics during shear vane measurements and provides a basis for a potential shear strength reference material.

Thermal and Mechanical Properties of $LaXO_3$ (X= Co, Fe, Ga) Based Perovskites. *JOHN LLOYD (Drexel University, Philadelphia, PA 19104) EDGAR LARA-CURZIO (Oak Ridge National Laboratory, Oak Ridge, TN 37831).* Ion conducting perovskite ceramics hold importance for their potential application in advanced energy systems, particularly Solid Oxide Fuel Cells (SOFCs). They have the potential to make good cathodes, electrolytes, or anodes in low temperature SOFCs. In order to successfully design SOFCs using La based perovskites, it is critical to understand how their thermal and mechanical properties change in different environments, such as reducing or oxidizing atmospheres and at elevated temperatures. This study reports on the Coefficients of Thermal Expansion (CTEs) and mechanical properties of the $LaXO_3$ (X= Co, Fe, Ga) based perovskites in both reducing and oxidizing environments and at elevated temperatures, up to 1000°C. The CTEs were determined using a Thermal Analysis® Q400 Thermal Mechanical Analyzer (TMA), mechanical properties including shear modulus, Young's modulus, and Poisson's ratio were determined by Resonant Ultrasound Spectroscopy and a Thermal Analysis® Q800 Dynamic Mechanical Analyzer (DMA). Stress vs. Strain curves were collected in both air and hydrogen (5% H_2, 95% Ar) using an Instron® 1380 Low Cycle Creep Fatigue Machine. A deviation from linear expansion at

230°C found in $LaCoO_3$ when heated and cooled in air was explained by a transition from an intermediate spin state to a high-spin state. However, expansion anomalies were not detected during heating/cooling $La_{0.8}Sr_{0.2}Ga_{0.8}Mg_{0.2}O_3$ and $LaFeO_3$ perovskites in air. The calculated average values of coefficients of thermal expansion of $LaFeO_3$, $La_{0.8}Sr_{0.2}Ga_{0.8}Mg_{0.2}O_3$, and $LaCoO_3$ perovskites in air were found to be 10.8, 11.7 and 22.9 10-6 K-1, respectively.

Low Energy Ion Scattering Spectroscopy in IMPACT. *WAYNE LYTLE (University of Illinois at Urbana-Champaign, Urbana, IL 61801) AHMED HASSANEIN (Argonne National Laboratory, Argonne, IL 60439).* Ion Scattering Spectroscopy (ISS) is a surface analysis method that uses the scattered energy of the incident ion to determine the composition of the surface of a sample. It is a very valuable method to compliment erosion studies of thin films, to gather surface composition information of liquid metals, determine concentration of multi-component materials versus depth and estimate thin-film thicknesses with calibrated markers. This paper discusses three specific areas: calibration of the PHOIBOS hemispherical energy analyzer, the surface analysis of a melting/liquid indium surface, and a depth profile of a single layer ruthenium sample. Of the four pure metal samples studied, gold, palladium, ruthenium, and silver, we observed between a 1.73% and 3.35% error in the location of our measured intensity peak to the theoretical intensity peaks. When heating the indium metal sample, we saw a general decrease in intensity of the peak, and at the melting temperature (157°C), the indium peak disappeared. After bombardment by 12μA 5keV Xe^+ for thirty to forty-five minutes, impurities that had diffused to the surface after melting were removed off the sample. The indium intensity returned to what it had been before heating began. The depth profile of a single layer ruthenium sample yielded predicted results in that it approached a steady state surface composition of 66% oxygen, 15% titanium, and 15% silicon after 120 minutes of constant irradiating. We concluded that the PHOIBOS hemispherical energy analyzer was operating adequately, and that our ISS system could be used to analyze the surface of pure elements, single layers, multi-component materials, and liquid metal samples.

Morphological Evolution of Epitaxial $SrRuO_3$ Thin Films as a Function of Thickness and Substrate Offcut. *MATTHEW MCKEON (Mohawk Valley Community College, Utica, NY 13501) HANS CHRISTEN (Oak Ridge National Laboratory, Oak Ridge, TN 37831).* The evolution of the surface morphology of crystalline metal-oxide thin films during growth must be understood in order to address problems at the interface with other thin films in multilayers. An example of particular interest is the interfacing of electrical contacts which often must be integrated (at the top and the bottom in a capacitor geometry) in a way to preserve the crystal structure of all layers in an epitaxial heterostructure. This is vital as electrodes are necessary to measure particular electrical properties of materials. Previous research indicates that films of the perovskite $SrRuO_3$ are suitable for use as an electrode for other perovskites because of the relatively low lattice mismatches with the most commonly used oxide single crystals. To use $SrRuO_3$ as the bottom electrode, however, its surface must remain atomically flat after growth, such as to assure the abruptness of the interface with a subsequently deposited layer. The goal of this study is to determine the critical thickness to which this material can be grown without deterioration of the surface quality. Growth mechanisms are known to depend on both the substrate offcut angle and the thickness; therefore, the critical thickness of $SrRuO_3$ to sustain the single terrace steps on the surface will be determined as a function of this offcut. Pulsed-laser deposition is employed to grow $SrRuO_3$ at various thicknesses. Atomic-force microscopy is then used to analyze the surface morphology at atomic-scale resolution. Results indicate that as the offcut angle increases and the thickness increases, the chance that step bunching will occur increases. The deterioration due to step bunching appears to be somewhat linear with thickness. This linearity however is not absolute as there are other unknown factors which also contribute to the deterioration of the surface quality. Another outcome of increased thickness is that more spirals are produced due to terrace step bunching originated from step flow of instable $SrRuO_3$ where its thickness reaches a critical point.

Micromagnetism in Isolated Submicron Quasi-Spherical Nickel Dots. *PATRICK MCNEFF (University of San Francisco, San Francisco, CA 94118) GORAN KARAPETROV (Argonne National Laboratory, Argonne, IL 60439).* The possibilities of higher density magnetic storage for technological applications have made the study of micromagnetic properties a current field of interest in material science. A specific direction of this research is the studying of discreet patterned magnetic structures. Structures in highly organized arrays, which can be created on submicron scales through means of self assembled templates, hold great potential in this search for high density storage. In order for these structures to become feasible for magnetic storage, the bulk properties of these arrays as well as the individual components must be understood in detail. Our work focused on the properties of single isolated quasi-spherical magnetic nickel dots. Using micromagnetic simulations we were able to model magnetization and external field nickel dots with different aspect ratios, then using the Magnetic Force Microscope, were able to observe actual magnetic properties of dots remanent state. Hysteresis loops were also both simulated and found experimentally for nickel dots. It was found that different aspect ratios are an important influence in remanent magnetic state. This dimensional dependence on magnetic characteristics demonstrates the need for better means of sample patterning if data storage is ever to become a practical application. Hysteresis loops also show minimal energy required to flip magnetization of nickel dots, making the sample of investigation a poor candidate for data storage.

Dissipation of Heat with Two-phase Cooling. *RICHARD MICHELHAUGH (University of Tennessee, Knoxville, TN 37922) CURY W. AYERS (Oak Ridge National Laboratory, Oak Ridge, TN 37831).* As automotive companies demand more efficient and compact hybrid vehicle electrical systems, more efficient cooling systems are required to handle the increase in heat flux. Engineers in the Power Electronics and Electric Machinery Research Center (PEEMRC) are developing a process to remove excess generated heat without adding a totally new cooling system. The PEEMRC is researching the effects of using a vehicle's existing 1, 1, 1, 2 -Tetrafluoroethane (R-134a) based air conditioning system. This solution would eliminate the need for a separate cooling system, and would also be able to effectively cool electronics. In order to simulate one of these electronic silicon chip/substrate systems, four 22-Ohm resistors were bonded to two kinds of copper, one being smooth, and the other having an enhanced surface of 200 fins per inch, while both were insulated with foam, so that only the apparatus' s face was exposed. A thermistor was installed to record internal temperature. To simulate the effects of R-134a cooling, a chemical with similar properties, FC-72 (Fluorinert by 3M) was employed. First, these two systems were submerged vertically in the Fluorinert. A current was run through the system and the temperature began reaching 150°C, a limiting temperature. Secondly, the systems were immersed horizontally into the Fluorinert, to see if orientation played a role in the dissipation of heat. The heat flux generated was approximately 2.9 Watts/cm^2. This low heat flux is not high enough to see a difference in the different surface types. A thin-film resistor with small surface area was then employed to generate a higher heat flux, and to hopefully achieve a goal of 100 W/cm^2. A heat flux of 50 W/cm^2 was generated before the resistors failed. Since the goal was not reached, experiments will continue, possibly employing a different type of thin film resistor and smaller copper substrate. When the 100 W/cm^2 heat flux is reached, temperature data will be gathered and will be able to support a conclusion on whether orientation or surface type affects two-phase cooling.

Binder Synthesis in the Development of Titanium Injection Molding. *MEGAN MILLER (University of Alabama at Birmingham, Birmingham, AL 35205) KEVIN SIMMONS (Pacific Northwest National Laboratory, Richland, WA 99352).* The powder injection molding process was employed for the production of titanium specimens from the feedstock/binder mixes of Titanium-6Aluminum-4Vanadium (Ti-6-4) or Titanium Hydride (TiH_2)/naphthalene, stearic acid, and EVA. Several titanium specimens were produced from these feedstock/binder mixes. These specimens were tensile tested and the ultimate tensile strength for the Ti-6-4 sample was 51.2 ksi, while the ultimate tensile strength for the six TiH_2 samples ranged from 62.7 ksi to 99.2 ksi. Initially, the tensile strengths of the titanium specimens tested in the 14.0 ksi to 20 ksi range, so the recent values obtained are very much improved. The fracture surfaces of all of the specimens were flat, which was indicative of brittle behavior; as a result, the samples showed very little elongation under tension. The microstructures of the titanium specimens were analyzed in order to gain a better understanding of the failure modes. All of the microstructures showed porosity and grain boundaries throughout the sample. Also, cracks and voids were evident within the Ti-6-4 microstructure; these flaws were caused by the inadequate removal of naphthalene during debinding. A second phase, ß-vanadium was also seen throughout the Ti-6-4 microstructure; this phase resulted from heating the parts to 1100°C during sintering. All of these inherent flaws acted as stress-raisers in the specimen; therefore, premature failure under tension resulted. Further steps need to be taken in improving the microstructural properties of the titanium specimens. For instance, sintering time and temperature could be evaluated in order to insure a more thorough densification process.

Magnetic Field Cycling Of 1045 Steel. *PAMELA MILLS (Florida A&M University, Tallahassee, FL 32310) GERARD LUDTKA (Oak Ridge National Laboratory, Oak Ridge, TN 37831).* This study focuses on the influence of cyclic, high magnetic field (B=10T) processing on the cellular decomposition and reaustenitization phase transformations for SAE 1045 hypoeutectoid steel under isothermal conditions. SAE 1045 steel samples were tested to yield considerable grain refinement capabilities by cycling about the eutectoid temperature in high magnetic fields. To accurately define the phase decomposition kinetics and isothermal hold temperature, a thorough dilatometry analysis was conducted. After the experiments were conducted, Scanning Electron Microscope (SEM) techniques in conjunction with microhardness measurements were used to further resolve grain boundaries and strength characteristics of the SAE 1045 steel samples. The results of this investigation will be discussed and the implications of these research findings for potential industrial applications in the U.S. steel industry.

Oxidation Behaviors of Stainless Steel Foils. *JEREMY MOSER (Pellissippi State Technical Community College, Knoxville, TN 37933) BRUCE PINT (Oak Ridge National Laboratory, Oak Ridge, TN 37831).* One goal of the Department of Energy's Distributed Energy Resources program is to improve the efficiency of small (30-300 kW) gas turbine engines or "microturbines." Increasing the engine temperature is the most effective strategy to increase efficiency. However, at temperatures exceeding 600°C, type 347 stainless steel (Fe-18Cr-11Ni foil, all compositions in wt%), used in the heat exchanger or recuperator, can experience accelerated corrosion due to the presence of water vapor in the exhaust gas. Therefore, new corrosion-resistant alloys are needed for this application. Experiments are being conducted on specimens of commercial alloys 120 (Fe-25Cr-35Ni) and 840 (Fe-20Cr-20Ni) and model alloys Fe-20Cr-20Ni+0.2Si and Fe-20Cr-20Ni+1.7Mn+0.2Si at temperatures of 650°-800°C in air and 10% water vapor to simulate the environment. Specimen mass changes are measured at room temperature after every 100h cycle, and the water vapor content of the gas is checked. After 5, 100h cycles, the commercial alloy 120 foil specimens (80μm) showed small mass gains at 650° and 800°C, while at 700°C a small decrease was observed. Small mass losses are believed to be caused by formation of volatile $CrO_2(OH)_2$. Mechanical properties of alloy 120 foil after 500h at 700°C and 800°C were conducted to compare to results from an engine test. These tensile test results showed a similar loss in ultimate tensile strength as previous test of foils exposed in engine test. Sheet specimens of alloy 840 have initially shown similar low mass changes as alloy 120, except at 800°C where mass losses indicate scale spallation. The oxidation behavior of the model alloys indicated some effects of Mn and Si in this environment. Foil specimens of Fe-20Cr-20Ni+0.2Si showed low mass changes at 700° and 800°C. However, at 650°C all four specimens showed accelerated oxidation attack in less than 500h. The model alloy with Mn and Si did not show accelerated attack at 650°C suggesting a beneficial effect of Mn. However, all of the specimens of Fe-20Cr-20Ni+Mn+0.2Si showed large mass gains after the first cycle followed by low mass changes. This suggests possible defects in the foil. Although data collected so far are only preliminary, the findings after >1,000h testing will result in more accurate conclusions about the best replacement alloys for type 347 stainless steel in this application.

Microstructural Investigation of Bonding Processes for Monolithic Fuel Development. *CORTNEY MOTHERSHEAD (Colorado School of Mines, Golden, CO 80401) CURTIS CLARK (Argonne National Laboratory, Argonne, IL 60439).* The Reduced Enrichment for Research and Test Reactors (RERTR) Program has been tasked with a project to convert remaining high enriched uranium (HEU) fueled research and test reactors to low enriched uranium (LEU) fuel. These remaining reactors are unable to use existing LEU dispersion fuel because of high fuel density requirements. Currently, RERTR is looking at meeting the high fuel density requirement with a monolithic fuel. The monolithic fuel consists of a fuel foil inside the fuel plate unlike the standard dispersion fuel where the fuel is in the form of a powder dispensed in an aluminum matrix. The monolithic fuel type has proved impossible to fabricate by the roll bonding method used for dispersion fuel and requires the development of a new fuel production method. Processes being looked at include friction stir welding (FSW), transient liquid phase bonding (TLPB), and hot isostatic pressing (HIP). Research was on the effects of these processes on the microstructure of the fuel plate in the aluminum-to-aluminum bonding interface. The study used a control of Al 6061 and a roll-bonded sample as a reference for desirable grain structure. FSW and TLPB samples made using various parameters were examined. The HIP samples supplied by BWX Technologies were examined as fabricated. FSW, TLPB, and HIP produced grain structures and interfaces that warrant further investigation in irradiation tests.

Vacuum Technology and Target Holder Design in Particle Radiation Interactions with Matter Experiments (IMPACT). *HUSSAIN NOMANBHAI (University of Illinois at Urbana-Champaign, Urbana, IL 61801) JEAN PAUL ALLAIN, AHMED HASSANIEN (Argonne National Laboratory, Argonne, IL 60439).* The Computational Physics and Hydrodynamics group at Argonne National Laboratory has performed all the computational aspect of particle/radiation interaction with matter with the use of High Energy interaction with General Heterogeneous Target Systems software. To complement the computational work a Particle/Radiation Interaction with Experiments facility was created to carry out the real world experiments. Interaction of Materials with charged-Particle and Component Testing (IMPACT) is one of the first experiments in PRIME. IMPACT has a custom designed vacuum chamber, a unique target holder, and a high intensity ion gun to conduct experiments in the field of liquid-metals, plasma facing components, and extreme ultra-violet lithography. Preparing the system for experiments by achieving ultra high vacuum conditions and the calibrations of the equipment mentioned above was an challenging task, and now it is ready for experiments.

Arsenic Trisulfide Nanowire Formation on Acid-Etched and Baked Quartz Surfaces. *JULIANA OLMSTEAD (Massachusetts Institute of Technology, Cambridge, MA 02139) S. K. SUNDARAM (Pacific Northwest National Laboratory, Richland, WA 99352).* Arsenic trisulfide (As_2S_3) nanowires have been successfully synthesized by a sublimation-condensation process in an evacuated quartz ampoule. The present study shows both the surface substrate conditions and the molar volume of glass used in this process have significant effects on the formation of these nanowires. Two experiments have been conducted using acid-etched and baked (AEB) quartz substrates, which were etched with 5% HNO_3: 5% HF for 20 min, rinsed with deionized water, and baked at 1000°C for 1 hour. The first experiment used 4.14 x 10^{-3} moles of As_2S_3 and the second used 8.41 x 10^{-3} moles of As_2S_3, while the volume of the ampoule was held approximately constant. After the sublimation-condensation process, a thin film of As_2S_3 coated the upper walls of the ampoule. Portions from this deposition region were sectioned from the ampoule and analyzed via scanning electron microscopy (SEM). Micrographs were taken of nanowires and microdroplets, and these features were semi-quantitatively measured using Adobe Photoshop CS. The first AEB experiment produced only droplets, with diameters ranging from 175 ± 25 nm to 2.35 ± 0.61 μm. The second AEB experiment produced both droplets and nanowires. Wire diameters ranged from 31 ± 6.1 nm to 86 ± 7.6 nm, and droplet diameter ranged from 2.0 ± 0.3 μm to 5.5 ± 0.3 μm. The differences between the results of the two AEB experiments were likely caused by both differences in internal vapor pressure and in moles per unit volume and per unit surface area. Additionally, the wires produced in the second AEB experiment were qualitatively compared to those produced on a water-washed surface in a previous study. Differences between wires formed on the water-washed and AEB surfaces were likely cause by differences in surface roughness and hydrocarbon content. Further examination will be required to determine the roles of these factors. This study marks the first time that nanowires have been successfully formed on an AEB surface. As acid-etching and baking is a well-defined process that can be replicated consistently and accurately, this result should lead to a more standardized nanowire production process, which is a major step toward commercial As_2S_3 nanowire production.

Specimen Preparation Techniques for the Study of Copper Contamination in Low-k Dielectric Thin Film Stacks. *BRIAN PULTZ (San Joaquin Delta College, Stockton, CA 95207) A. SCOTT LEA (Pacific Northwest National Laboratory, Richland, WA 99352).* Determining the amount of copper (Cu) contamination in semiconductor devices at high spatial resolution due to processing poses a significant challenge. Transmission electron microscopy (TEM) was chosen because of the resolution and analytical capabilities needed to evaluate processed thin film stacks. Sample preparation methods that minimize cross-contamination while maintaining the integrity of the brittle materials, however, remain to be developed. To this end, a preparation protocol was evaluated. Samples were sandwiched with epoxy, polished and then placed in a precision ion mill. After milling, the samples were viewed with the TEM and the copper contamination levels measured by energy dispersive X-ray analysis (EDX); the results were similar to samples that were just cleaved and evaluated with Auger electron spectroscopy (AES). In order to determine how much of the copper contamination was from the specimen preparation, samples were evaluated using AES after each preparation step. Polishing the sample spread copper across the surface. Subsequent treatment with precision ion milling removed

the resulting contamination from the polished surface. Although TEM appears to be the best method for evaluation of Cu contamination in the thin film stack, other methods are required to check for specimen contamination during preparation. In the future, focused ion beam (FIB) sample preparation may need to be explored for comparison with the method developed here.

Temperature Dependence of the Thermal Conductivity of Partially Graphitized Carbon-Bonded Carbon Fiber. *AUSTIN REID (Davidson College, Davidson, NC 28035) T.D. BURCHELL (Oak Ridge National Laboratory, Oak Ridge, TN 37831).* Specimens of Carbon Bonded Carbon Fiber (CBCF) were partially graphitized to varying degrees of crystalline perfection in an Argon atmosphere in a high-temperature, short duration furnace. The thermal conductivity of these samples was measured through a range of temperatures, exhibiting a general increase in conductivity as annealing temperature, time, and temperature of measurement increased. The subsequent data were compared to the existing model, with the explicit goal of improving the existing model for thermal conductivity as a function of annealing temperature and time, and the temperature of measurement, notably for measurement temperatures less than 700 K. The existing model is limited by its approximations, restricting it to short duration annealing, and high measurement temperatures. The improved model is more accurate for longer annealing times and a wider spectrum of measurement temperatures, due to a more accurate approach to the crystallinity of carbon fiber.

Theoretical Model for the Oxidation of Propene by Vanadium Oxide Catalysts. *TIMOTHY ROGERS (Valparaiso University, Valparaiso, IN 46383) LARRY CURTISS (Argonne National Laboratory, Argonne, IL 60439).* Supported vanadium oxide catalysts are used industrially for the conversion of alkanes to alkenes, but the chemical structure of these catalysts as well as the mechanism by which they catalyze reactions is not yet well known and is the topic of much recent study. An important side reaction in this process is the subsequent catalyzed combustion of alkenes by the same vanadia catalysts. Computer models for the chemical adsorption of propene onto vanadia catalysts (VO_5H_5 and $V_2O_9H_8$) were optimized using the Hartree Fock and B3LYP methods to determine the thermodynamic energy of reaction (ΔE) in the first step of the catalyzed combustion of propene. All possible surface adsorbed product species on the vanadyl oxygen of the VO_5H_5 cluster were analyzed along with a selection of products on the $V_2O_9H_8$ cluster. Of those products analyzed, the ketone (propanone) was found to be the most thermodynamically favorable on both vanadia clusters. Calculated ΔE's varied based on the catalyst cluster model and the model chemistry. $V_2O_9H_8$ adsorbed species were 10-20 kcal/mol more stable than VO_5H_5 adsorbed species. B3LYP results are consistently 90-100 kcal/mol higher than Hartree Fock.

Erosion Studies of Extreme-ultraviolet Lithography (EUVL) Candidate Mirror Materials in the IMPACT Experiment. *DANIEL ROKUSEK (University of Illinois at Urbana-Champaign, Urbana, IL 61801) AHMED HASSANEIN (Argonne National Laboratory, Argonne, IL 60439).* As deep-ultraviolet lithography (DUVL) reaches its limits, there exists a need for a new technology to manufacture smaller microprocessors. Extreme-ultraviolet lithography (EUVL) uses 13.5nm light to etch circuit paths, a wavelength far more desirable than the minimum 153nm that DUVL offers. EUVL is an intense area of research. The IMPACT (Interaction of Materials with charged Particles And Components Testing) experiment is fit to study various candidate mirror materials for EUVL. IMPACT features a robust ion source and system that facilitates energy, angle-of-incidence, and temperature dependent studies. Various samples can be bombarded with noble gases, including Xe, He, Ne, and Ar. Candidate mirror materials studied in IMPACT include Pd, Ru, and Re. These samples are loaded into the IMPACT vacuum chamber via a transfer-lock system. Once inside, IMPACT uses a quartz crystal microbalance - dual crystal unit (QCM-DCU) diagnostic system for in-situ real-time erosion measurements as samples are exposed to the ion beam. Another feature of IMPACT is the capability of performing low-energy ion scattering spectroscopy (LEISS) to facilitate the characterization of multi-component surfaces as they erode. Studies have shown a direct relationship between energy and sputtering yields for Pd and Ru thin-film mirrors. Sample characterization by LEISS has been successfully implemented and tested in IMPACT allowing to compliment erosion measurements to create depth profiles of multi-component samples.

The Electrical and Optical Properties of Indium-Zinc Oxide Thins Films Prepared Using the Sol-Gel Method. *VELISSA SANDOVAL (University of Denver, Denver, CO 80210) TANYA KAYDANOVA (National Renewable Energy Laboratory, Golden, CO 89401).* Sputtered films of $In_xZn_{1-x}O_y$ (IZO) previously have been shown to demonstrate the best conductivity along with good optical properties at x of ~0.7. Thin transparent conducting films of $In_{0.5}Zn_{0.5}O_x$ and of $In_{0.7}Zn_{0.3}O_x$ were prepared using sol-gel method from the solution of indium nitrate hydrate and zinc acetate dihydrate in 2-methoxyethanol and ethanolomine. Films of 1,3 and 5 layers corresponding to 1200 Å ±200 Å, 2400 Å ±200 Å and 3600 Å ±200 Å thick were spin-coated on to 1737 Corning glass substrates with the intermediate baking steps at 300°C in air for 10 minutes after each layer. The conductivity and the transmission of the as-deposited IZO films was ~ 0.0051 $S \cdot cm^{-1}$ and 80% respectively. Consequent annealing in argon and forming gases at 300-700°C lead to the desired increase in conductivity reaching values of 84.27 $S \cdot cm^{-1}$ with a corresponding transmission coefficient of over 80% in the visible light region. The film with the highest conductivity was the 50:50 In to Zn 5-layer film. X-ray diffraction (XRD) measurements showed that the films were amorphous both as-deposited and after annealing below 600°C. Atomic Force Microscopy (AFM) has revealed dense and smooth surface with RMS roughness on the order of 3Å as expected for amorphous films. The composition of the films and chemical purity were tested using X-ray Photoelectron Spectroscopy (XPS) and Electron Probe Microanalysis (EPMA) techniques. The XPS and EPMA determined that films had a composition of 50:50 In to Zn ratio, and a decrease in carbon content after air baking at 500°C & 600°C. Overall, the films conductivity improved by four magnitudes when compared to as-deposited with optimal optical properties while remaining in the amorphous phase.

Spin Density Wave Antiferromagnetism in Cr/CrV Superlattices. *KAYA SHAH (Massachusetts Institute of Technology, Boston, MA 02139) J. LEE ROBERTSON (Oak Ridge National Laboratory, Oak Ridge, TN 37831).* The magnetic properties of thin films is a topic of current interest because of the large range of applicability to technologies such as magnetic storage. In this study, the magnetic properties of an epitaxial (001) superlattice of $[Cr(10nm)/Cr_{98}V_2(10nm)]x75$ on an MgO substrate will be investigated. This material is an artificial single crystal that consists of alternating layers of 10 nm of pure chromium and 10 nm of $Cr_{98}V_2$ repeated 75 times. The pure chromium layer is antiferromagnetic with a Néel temperature of 310 K. Additionally, a spin density wave (SDW) forms with the modulation of the magnetic moments along the (001) direction, which is normal to the plane of the substrate. The period of the SDW in this layer is ~79 Å. In general, when chromium is doped with vanadium, the Néel temperature is lowered and the period of the SDW decreases. In the case of $Cr_{98}V_2$, the Néel temperature decreases to 150 K, and the SDW period is reduced to ~40 Å, or about half the SDW period of chromium. Due to the epitaxial relationship between the layers, the antiferromagnetic order is coherent. Neutron scattering experiments will be carried out in order to probe the interaction between the spin density wave periods of the pure chromium and the chromium vanadium alloy as a function of temperature, and results are forthcoming.

Examining Single Walled Carbon Nanotubes in a Conductive Polymer Using Electron Microscopy. *AMANDA SIMENS (Lehigh University, Bethlehem, PA 18015) ANDY MINOR (Lawrence Berkeley National Laboratory, Berkley, CA 94720).* Due to their high conductivity and unique electrical properties, single-walled carbon nanotubes (SWNT) are an ideal candidate for improving the efficiency of organic light emitting diodes (OLED). The charge transport properties of light emitting polymers can easily be tuned by adding small amounts of SWNT. The dispersion of SWNT in the light emitting polymer matrix is a crucial factor affecting OLED performance. This study uses electron microscopy techniques to study the dispersion properties of SWNT in the conductive polymer at the nanometer scale. The SWNT is dispersed in a new amphiphilic light emitting polymer, poly(2,7-9,9(di(oxy-2,5,8-trioxacdecane))fluorine) (PFO). PFO has a rigid backbone and oligoethyleneoxide polar side chains. The polar side chains enable the PFO to wrap around the SWNT to facilitate the nanotube dispersion. Electron microscopy, both Transmission Electron Microscopy (TEM) and Scanning Electron Microscopy (SEM) are used to image the PFO and nanotube composite. The images indicate different levels of dispersion of SWNT in the PFO coexist, with a significant amount of single tube dispersion. The images show a smooth coating of PFO on the SWNT. To compare the interaction between the polymers and the SWNT, the PFO nanotube composite was compared with a similar conductive polymer, poly(2,7-9,9 didecly fluorine) (PF) and nanotube composite. PF possesses regular alkyl side chains and is hydrophobic, therefore the interaction between the PF and SWNT is small. The TEM images demonstrated that the PF aggregates in clumps on the nanotubes and does not coat the tubes uniformly as the PFO does.

Synthesis and Structural Elucidation of $CsAlSiO_4$-ANA. *STACEY STANDRIDGE (Univeristy of Oregon, Eugene, OR 97401) MARSHA LAMBREGTS (Argonne National Laboratory, Argonne, IL 60439).* Radioactive Cs-137 is a fission product of uranium. Cesium aluminosilicates have been identified as a waste form for the storage and immobilization of radioactive cesium. The intent of this project was to synthesize the novel phase $CsAlSiO_4$-ANA, and to determine its crystal structure. The samples were synthesized by first performing an ion exchange on zeolite A to get cesium ions in the aluminosilicates framework. Next, the samples were heated to 1100°C for three hours, 1250°C for four hours, and 1350°C for three hours. X-ray diffraction was used to analyze and characterize the samples. The rietveld refinement program GSAS was used to investigate the crystal structure. The low form of $CaAlSiO_4$-ANA was successfully and consistently synthesized. The proposed crystal structure for this phase, which is the cesium analog of the mineral analcite, does not match the experimental data. In the future a hydrothermal treatment will be employed to synthesize the high form of $CsAlSiO_4$-ANA. Further x-ray diffraction and refinement will be used to identify the crystal structure of both polymorphs of $CsAlSiO_4$-ANA.

Effects of Annealing and Buffer Layer on Magnetic Structure in $Ga_{1-x}Mn_xAs$. *ZACHARY WEBER (Kenyon College, Gambier, OH 43022) ULRICH WELP (Argonne National Laboratory, Argonne, IL 60439).* $Ga_{1-x}Mn_xAs$ films are being considered as possible materials for use in a variety of new spintronics devices. Electron spin is responsible for creating magnetization, so the magnetic structure of $Ga_{1-x}Mn_xAs$ must be understood in order to design more effective spintronics devices. Here the effects of annealing and three buffer layers (low-temperature GaAs, $In_xGa_{1-x}As$, and ZnSe) on the magnetic structure of epitixial $Ga_{1-x}Mn_xAs$ are explored. We observed the propagation of magnetic domains through the magneto-optical Faraday Effect technique. Results were complimented with superconducting quantum interferometer device (SQUID) magnetization measurements. We found that $In_xGa_{1-x}As$ buffers created micro scale magnetic disorder in the $Ga_{1-x}Mn_xAs$ films. As-grown $Ga_{1-x}Mn_xAs$ with a ZnSe buffer displayed well defined, large scale domains. At low temperatures, the as-grown sample showed biaxial easy magnetization along the [100] and [010] directions. As temperature increased, the easy magnetization axis turned to the [110] direction and became uniaxial. The rotation of the easy magnetization axis orientation is due to the competing, temperature dependent anisotropy energies from the tetragonal structure of $Ga_{1-x}Mn_xAs$ (biaxial easy magnetization) and layer-by-layer surface reconstruction (uniaxial easy magnetization). The annealed $Ga_{1-x}Mn_xAs$ sample also contained biaxial to uniaxial transitions similar to the uniaxial sample. However the magneto-optic images revealed a disordered magnetic structure and rough domain boundaries. This phenomenon may be due to the precipitation of Mn clusters subsequent to annealing.

Developing an Inert Anode for Aluminum Electrolysis. *RICHARD WIESE (University of Missouri-Columbia, Columbia, MO 65201) GREG KRUMDICK (Argonne National Laboratory, Argonne, IL 60439).* An inert anode for Aluminum electrolysis has great potential for reducing the production and environmental costs of the process. An Aluminum Copper Bronze alloy anode material has been settled upon as a material to test with as it has proved to be stable enough to survive in the harsh, corrosive environment of liquid Aluminum while still conducting the necessary current to promote the electrolysis of Al_2O_3, into Aluminum liquid and Oxygen gas. In conjunction with a low-temperature molten salt bath, the Aluminum Copper Bronze alloy anode has proven to lead to low contamination of the product aluminum on laboratory scale tests at various levels of current density on the anode. Future investigation will focus on scale-up of the process and experimentation with further optimizing the material of the anodes along with refining the process methods.

Development of LabVIEW Software to Replace Current X-Ray Diffractometer Control Software. *DAVID WIESNER (University of Tennessee, Knoxville, TN 37996) THOMAS R. WATKINS (Oak Ridge National Laboratory, Oak Ridge, TN 37831).* The current software package, DMSNT, provided by Thermo ARL for operation of the Scintag, Inc. 4-axis x-ray diffractometer will have no future upgrades beyond the current version, v1.39beta - build 125. Continued problems with axis control coupled with the desire to re-implement the use of a position sensitive detector (PSD), not supported by DMSNT, have led to the need for "specialized" software. DMSNT operates via serial communication with a 256k microprocessor to operate the x-ray diffractometer. With its built-in serial communication virtual instruments, LabVIEW is an ideal platform for the replacement software. The current objective of this project is to replace the basic scanning and data collection functions of DMSNT, as it currently operates with a point detector to ensure operational stability. Prior use of the PSD was achieved with VAX code written in FORTRAN 77 code on a VMS operating system. To re-integrate the PSD for operation on a PC the FORTRAN code is being converted initially to Visual C++ and compiled into generic software for preliminary debugging purposes before the code is written in LabVIEW, which will allow for future software control to be retained and modified locally.

Aluminum Casting: How the Composition of Aluminum Alloys Affect Grain Size. *LING XU (Georgia Institute of Technology, Atlanta, GA 30332) QINGYOU HAN (Oak Ridge National Laboratory, Oak Ridge, TN 37831).* The grain size of an aluminum alloy can be controlled by the composition of elements within the alloy. Grains develop as the alloy cools from its liquid state, the presence of other elements in the alloy change the cooling properties and therefore the grain size. The experiment will test the effect of adding the elements copper and zinc to aluminum in relation to the grain size of the alloy. Adding small amounts of Cu to make an aluminum alloy will decrease the grain size because the Cu will break up Al dendrites. However, when larger amounts of Cu are added, grain sizes will begin to increase because of separation between areas of concentrated Al and areas of Cu. Procedure of the experiment will involve the use of a master alloy which is a composition at the multiphase point. Subsequent alloys of lower concentrations of Cu and Zn will be produced by adding aluminum to the master alloy. All samples will then be cut and etched in order to reveal grain boundaries, which will be measured using an optical microscope and image-pro plus. Special attention will be paid to the cooling of the melts as they are poured into molds. The molds consist of metal mold with a small hole drilled into it for a thermocouple to measure the cooling rate. The results show that adding amounts of copper and zinc will decrease their alloys' grain size up to 5.5% and 9.5%, respectively. Beyond that point the grains become larger as more copper and zinc are added. The grain sizes of the different alloys are directly related to the composition of elements within the material. Grain sizes decrease with the introduction of small amounts of copper and zinc, however when larger amount of the two elements are added grain sizes increase and return to the natural size of pure aluminum. However the shapes of the grains are dramatically different from the two high points. The dendrite structure for pure aluminum is mainly a centralized nucleation whereas the grain size when high amounts of copper and zinc are added, many dendrite arms appear.

Medical and Health Sciences

Radiation Induced Genomic Instability and Bystander Effects in Human RKO Cells Exposed to Low-Linear Energy Transfer (LET) Electrons. *BENJAMIN ARTHURS (Washington State University, Pullman, WA 99163) BRIAN ESTES (Gonzaga University, Spokane, WA 99258) GARY HOLTOM (Pacific Northwest National Laboratory, Richland, WA 99352).* Traditional models of radiobiology assume that only ionizing events occurring within the nucleus are capable of inducing biological effect. According to this, unrepaired damage resulting from deposition of energy in DNA will result in either phenotypical change, passed on to cellular progeny, or cell death. However, recent evidence for radiation induced genomic instability and bystander effects have challenged the definitions of these conventional paradigms. These delayed and non-targeted phenomena produce similar endpoints as seen in direct genomic irradiation, but they prevail at low doses of low-LET radiation. At these low levels where ionizing events are few and far between, the likelihood of radiation traversing the DNA is slim, yet significant effects still occur. This apparent discrepancy regarding assumed exposure risks demands reevaluation. In order to test these effects for low-LET radiation, we have used a charged particle microbeam to irradiate human-RKO derived cells with varying doses of electrons. Using a specially fabricated aluminum as a shield, we irradiated 100, 10, and 1% subpopulations of cells in order to analyze bystander effects. In addition, we utilized a green fluorescing protein (GFP)-based assay to determine whether cellular colonies express radiation induced genomic instability. Data suggests that instability was induced above background levels of 1%, however no conclusive trend was apparent. The difficulties in determing bystander effects and induced genomic instability were primarily due to low plating efficiency and in consistencies in plating. Future applications of the microbeam and GFP-based assay will further research the mechanisms producing bystander effects and induced genomic instability. In the end this data will be vital to determing how these phenomena relate to carcinogenesis and what impact they have on our understanding of radiation exposure risks.

Development of a Highly Sensitive Technique to Quantitatively Measure Hydrogen Peroxide in Cigarette Smoke. *CE'ZONNE BROWN (University of Tennnesee, Knoxville, TN 37916) GUY GRIFFIN (Oak Ridge National Laboratory, Oak Ridge, TN 37831).* The multitude

of injurious health effects which may be caused by increased levels of reactive oxygen species (ROS) within the body has only recently begun to receive attention. The lungs may be particularly susceptible to ROS injury, since they are exposed to airborne oxidants arising from pollutants. In addition, the alveolar white blood cells may contribute to an ROS-mediated inflammatory response, as they respond to microbial or fiber (e.g., asbestos) infiltration within the lung. Although cigarette smoke has been shown to have a very large number of chemical constituents, it is still unclear what the most hazardous constituents might be. This study has been undertaken to attempt to develop a reliable, sensitive procedure to measure the amount of hydrogen peroxide, which is produced when the cigarette is smoked on a five-port smoking machine and the smoke is bubbled through an aqueous solution. Preliminary evidence from other laboratories has suggested that total hydrogen peroxide formation, as cigarette smoke is collected into an aqueous solution (such as might occur in alveolar fluid), might be quite high. In this study fluorescent detection techniques have been investigated, since they can be very sensitive, as well as amenable to development into a stand-alone sensor. After trials involving several possible fluorophores, it was found that the Amplex Red reagent (10-acetyl-3, 7-dihydroxyphenoxazine, Molecular Probes, Inc.) provides high sensitivity plus selectivity to detect hydrogen peroxide in a chemically complex sample matrix (such as cigarette smoke). The reaction involves the reaction of hydrogen peroxide with Amplex Red reagent, catalyzed by horseradish peroxidase, to produce resorufin, which is detected by its strong fluorescence. Calibration curves have been developed which show a linearity of fluorescence intensity versus hydrogen peroxide concentration in water over a reasonable concentration range of hydrogen peroxide, down to detection limits of submicromolar. Preliminary data shows the feasibility of measuring hydrogen peroxide production in cigarette smoke without prior separation from interfering substances. A μM level of hydrogen peroxide was found in aqueous solution resulting from several puffs of cigarette smoke for two different standard cigarettes. Further studies, to investigate which elements in the cigarette smoke contribute significantly to the production of hydrogen peroxide, are underway.

Effects of Dopamine D3R Receptor antagonist SB-277011-A on the Feeding Behavior and Locomotor Activity of Lean and Obese (fA/fA) Zucker Rats. *KATHARINE CHRISTIANSON (California State University Fresno, Fresno, CA 93710) PETER THANOS (Brookhaven National Laboratory, Upton, NY 11973).* Research has shown that the Dopamine D3 receptor (D3R) is important in mediating the addictive properties of various drug-seeking behaviors. D3R receptors allow the release of dopamine (DA) into CNS neural synapses creating feelings of pleasure. It is currently suspected that when a rewarding, or addictive, behavior is performed, an increase in synaptic dopamine causes the reward response to occur. Research has recently commenced investigations on obesity and eating behavior as an addictive behavior similar to drug and alcohol abuse. Thus, the DA and D3R function is being studied. As an antagonist to the D3R, the new drug SB-277011-A is a highly selective target for D3R and has been shown to alter midbrain DA activity in rats. The effects of this drug on addictive behaviors, including overeating, provide information about the actual role of the D3R in addiction. The present study seeks to examine the role of D3R in the eating behavior of lean and obese (fA/fA) Zucker rats. Male lean and obese Zucker rats were tested for changes in self-regulated food intake and locomotor activity when treated with D3R antagonist, SB-277011-A. All subjects had daily 2h access to food in operant conditioning chambers (Coulbourn Instruments) by way of lever pressing, while they had free access (24h) to water. Food intake and response behavior as well as locomotor activity were monitored throughout each 2h session via the automated computer system and software, Graphic State Notation version 1.0. Each animal established an individual vehicle baseline in eating behavior before treatments of each drug were performed. Injections of SB-277011-A in 3, 10 and 30 mg/kg doses were given prior to each session for three days per dose. The measured variables include total food intake (g/kg), water consumption, and counts of beam breaks for locomotor activity. Results showed that using SB-277011-A treatments of 3, 10, and 30 mg/kg, lean rats showed a significant dose-dependent decrease in the amount of food eaten within their two-hour access window. Genetically obese Zucker rats showed the same pattern, although less drastically. This study provides firm evidence for future sciences to follow in designing therapies, which would target the D3R receptors to aid in the fight for addiction control.

Motor Functioning in Drug Addicted Individuals: Chronic and Past Cocaine and Alcohol Abusers. *DANIELLE DELOSH (Stony Brook University, Stony Brook, NY 11790) RITA GOLDSTEIN (Brookhaven National Laboratory, Upton, NY 11973).* Research on the effects of cocaine on neuropsychological functioning has been reliable, but from the standpoint of motor functioning, there are inconsistencies. Neuropsychological test batteries, used to assess cognitive functioning in drug addiction, do not routinely assess motor functioning in drug-addicted individuals. Bauer (1994) found cocaine addicts to be slower on a vigilance reaction time task than normal controls and Lawrence-Craddock et. al., (2003) also found impairment in stimulant users on a reaction time task. The inconsistencies were mainly found in other tasks such as Finger-Tapping, Grooved Pegboard and Trails A, though Trails A is not classified as a pure motor task; it involves higher-order executive functioning. Timed Gait has not been used in previous research as a measurement of motor functioning in drug addicted individuals. Therefore, the current study focused on the impairment of motor functioning of drug-addicted individuals on Finger-Tapping (right and left hand), Grooved Pegboard (right and left hand) and Timed Gait. The sample consisted of 50 substance dependent individuals (42 cocaine, 8 alcohol), and 77 gender-matched controls. All subjects completed a standardized neuropsychological battery comprised of tests of attention, memory, decision-making and motor function. Analysis was only conducted on tasks of motor performance. Preliminary data indicated that substance dependent individuals (cocaine and alcohol combined) were older, less educated, lower estimates of general intellectual functioning, and reported higher rates of depression than normal controls. Results of the motor performance analysis revealed that although the substance dependent group showed impairment across four of the five motor tasks only Grooved Pegboard (Right Hand) was significantly different between the two groups. Limitation and future directions will also be discussed.

The Effects of Urine Toxicology on Motor Performance in Cocaine Addicted Individuals. *DANIELLE DELOSH (Stony Brook University, Stony Brook, NY 11790) RITA GOLDSTEIN (Brookhaven National Laboratory, Upton, NY 11973).* A majority of previous research on motor performance in addiction included abstinent cocaine addicts. However, there have been no known studies comparing the motor performance of cocaine addicts who tested positive for cocaine on the day of testing and those who did not. Moreover, the chronic and acute effects of cocaine on motor performance may differ and thus warrant investigation. The current study sought to clarify this issue by comparing the motor performance of cocaine addicts that tested positive (COC+; N=28) versus negative (COC-; N= 29) for cocaine at the time of the motor tasks (validated by a urine test). It was hypothesized that COC+ would exhibit impaired motor performance as compared to COC- because of the 'crash' following recent cocaine use (e.g., excessive sleepiness). All subjects were given the same neuropsychological battery, which included three tests of motor performance: Finger Tapping (right and left hand), Grooved Pegboard (right and left hand), and Timed Gait (only 12 COC+ and 14 COC-). Preliminary demographic findings revealed no group differences across age, education, socioeconomic status or depression. There were more African Americans and women in the COC+ group. Controlling for the appropriate possible confounding variables, results showed worse performance on Grooved Pegboard in the COC+ than COC- group. Timed Gait had a smaller sample size (N=26) and thus there may not have been enough subjects to produce a sizeable effect. Since Grooved Pegboard is not a simple motor task of speed or reaction time, but also tests fine motor dexterity and sequencing, it suggests a specific, higher-order motor impairment and not an overall gross motor impairment. Furthermore, these trends support a distinction between the acute and chronic effects of cocaine on motor functioning.

Tumor Necrosis Factor-Dependent Regulation of Inducible Nitric Oxide Synthase During the Host-Pathogen Immune Response. *MICHELLE DESIMONE (Northeastern University, Boston, MA 02115) BRIAN THRALL (Pacific Northwest National Laboratory, Richland, WA 99352).* During the host-pathogen response, immune cells such as macrophages release tumor necrosis factor (TNF), a signaling molecule whose primary role is the recruitment of other cells to the site of infection. TNF causes an array of biological effects, but elevated levels of circulating TNF can lead to chronic inflammation, which has been implicated in many disease states such as Alzheimer's, multiple sclerosis, arthritis, and cancer. In part, tissue damage during inflammation is due to the generation of free radicals, including nitric oxide. In this study, an in vitro macrophage model system was used to study the relationship between TNF-a and inducible nitric oxide synthase (iNOS), the enzyme responsible for the generation of nitric oxide. RAW 264.7 mouse macrophages were stimulated with *Escherichia coli lipopolysaccharide* (LPS) over a 24hr time course to induce signaling cascades and protein transcription associated with the immune response. The response curve showed that LPS caused the induction and shedding of TNF prior to the

induction of iNOS protein expression. When iNOS activity was inhibited with the pharmacological agent 1400W, it was found that enzyme activity had no effect on TNF shedding. To evaluate whether TNF caused the induction of iNOS, cells were treated with 100ng/mL recombinant TNF alone for 24hr. Western blot analysis showed that TNF alone was not sufficient to induce iNOS protein expression. Further studies using short-interfering RNA revealed that inhibiting TNF induction had no effect on iNOS protein expression in response to LPS. In contrast, iNOS activity was reduced by > 83 ± 11.7%. This suggests that TNF or TNF-stimulated pathways play a role in the regulation of iNOS activity. Future studies will examine the mechanism of iNOS activation and TNF's role in the regulation of this important inflammatory mediator.

In Vivo [3H]-Anandamide (AEA) Accumulation in Wild-Type and Fatty Acid Amide Hydrolase (FAAH) Knockout Mouse Brains. *CAMILE GOODEN (Stony Brook University, Stony Brook, NY 11790) ANDREW GIFFORD (Brookhaven National Laboratory, Upton, NY 11973).* Anandamide is an endogenous cannabinoid receptor ligand. The enzymatic degradation of anandamide and thus its regulation is facilitated by the action of FAAH. FAAH degrades anandamide into two product, arachidonic acid and ethanolamine. The uptake of anandamide has been related to the catalytic activity of FAAH. The concentration distribution of anandamide in regions of the mouse brain is correlated to the distribution of FAAH activity in those regions. Regions corresponding to high FAAH activity create a concentration gradient for anandamide uptake; the converse is true for low FAAH activity. In this study a solution consisting of tritiated anandamide is administered to mice (C57B16 wild type) via tail vein injections in a 10 mg/kg concentration and approximately 5 mCi/mouse. Following injection the mice were sacrificed at 2hr, 1hr, 30mins, and 5mins time intervals. A blood sample and the cerebellum, anterior cortex, posterior cortex, hippocampus and caudate putamen were dissected from each mouse and the radioactivity quantified. Deferential acccumulation of [3H]-AEA was observed in the brain regions of the C57B16 wild type mice. The purpose of this study was to determine an optimal time point at which to conduct experiments studying FAAH enzyme activity and the differentil accumulation of AEA and its metabolites in these brain regions. The accumalation of AEA and its metabolites in certain brain regions is highest at about 1 hr following injection. There appeared to be more [3H]-AEA uptake in the poterior cortex and the cerebellum at 1 hr relative to the 5 min time point. We also sought to reproduce the results obtained by Dr. Sherrye Glaser's method of determining regional accumalation by quantifying images obtained with the BetaImager by regionally disecting the brains of wild type mice injected with 10mg/kg [3H]-AEA and using beta scintillation counter.

Molecular Cage Construction for Use in Future Cancer Therapeutics. *ZACH HONTZ HONTZ (Columbia Basin College, Pasco, WA 99336) ROBERT SCHENTER (Pacific Northwest National Laboratory, Richland, WA 99352).* It is very important to develop new and improved methods to treat cancer in its many forms. Many cancer types are still not curable. Cancer kills over 1500 people per day in the United States. This project uses a computer code called MOPAC (Molecular Orbital PACkage) that will be used to build new types of molecules for cancer treatments (i.e. molecular cages). Molecular caging can be used in a new form of cancer treatment called cell-directed therapy, where a radioactive isotope decays and gives off an atomic particle that kills cancer cells. In MOPAC, molecules are constructed into a cage to hold the radioactive isotope that is attached to a monoclonal antibody. The monoclonal antibody finds cancer cells and attaches to them. Then the isotope, which is held in the molecule cage, decays and kills the cancer cell. Molecules are built (in MOPAC) by listing the amount of atoms and describing the bond lengths and angles. The molecule cage has to be stable enough to hold the isotope long enough for it to decay and kill the cancer. By killing only cancer cells, this treatment is safe and causes fewer side effects as other treatments. This project is currently in the process of building molecular cages.

The Quantification of Soldering Work at Thomas Jefferson National Accelerator Facility, the Health Risks Associated with Leaded Solder, and the Proposed Use of Lead-Free Solder. *TODD HUTNER (Florida State University, Tallahassee, FL 32306) PATTY HUNT (Thomas Jefferson National Accelerator Facility, Newport News, VA 23606).* Health risks associated with over exposure to lead are significant, and one of the ways that workers are exposed to lead is through leaded solder. Thus, the main focus of the research project is to quantify Jefferson Labs (JLab) soldering work, and to understand the health risks associated with leaded solder. Through this, recommendations on future solders work can be made. Current research on lead-free solder indicates that it does not flow to components as easily, requires higher temperatures, longer exposure times and more flux. In order to determine health risks, both surface and air samples were taken. To find surface concentrations, a wet wipe is swabbed over a $1ft^2$ area using a precut square. The wet wipe is then analyzed using atomic absorption spectroscopy to find the lead concentration. For air sampling, an MCE filter is placed upon an air pump, and placed in the breathing zone of the solderer. The filter is then analyzed using inductively coupled plasma-atomic emission spectroscopy to find the airborne concentrations of solder metals. Five samples of lead-free solder, along with a leaded solder, were obtained and distributed to two teams of soldering workers. Each sample of solder was labeled A-F respectively, and distributed with a survey regarding its effectiveness. When all 122 samples were returned, the mean concentration for surfaces was 276.83 ug/ft^2. The data fits a lognormal distribution, with the 90^{th} quantile at 576.2 ug/ft^2. The air samples returned some interesting results, with detectable levels of beryllium present in the air. It was suspected that the beryllium came from the components being soldered; however, further research is required on this matter. In conclusion, an acceptable surface contamination of $600ug/ft^2$ is proposed for JLab soldering stations. Survey results were unfavorable for all of the lead-free solders; it is also proposed for JLab that the use of lead-free solder not be implemented at this time.

Effect of the Cannabinoid CB1 Antagonist SR141716 on Food Intake and Ethanol Consumption in Female Lean and Obese Zucker Rats. *ABIGALE LADE (University of Wisconsin-Milwaukee, Milwaukee, WI 53211) PANAYOTIS K. THANOS (Brookhaven National Laboratory, Upton, NY 11973).* Several recent studies suggest an interaction between the endogenous cannabinoid system and both ethanol and food intake. Rats exposed to ethanol exhibit changes in endogenous cannabinoid levels in the brain, and increased food consumption is observed in animals treated with cannabinoids and cannabinoid agonists. Likewise, decreased ethanol and food consumption was observed in animals treated with a cannabinoid antagonist. The objective of the present study was to investigate the effects of the cannabinoid CB1 antagonist SR141716 on food intake and ethanol preference in obese (Ob) and lean (Le) Zucker rats, and thus to gain a better understanding of the role that this system plays in mediating food and ethanol consumption. These rats were chosen because of their unique phenotype of hyperphagia (Ob) and preferential ethanol consumption (Le) in the absence of any treatment. After a habituation period, rats were given ad libitum, 24-hour access to 10% ethanol as the only liquid available. Then food restriction was initiated for half of the obese and half of the lean rats, which continued throughout the study. In addition, for the next twelve days rats were given 4-hour per day access to 10% ethanol and water, and for the subsequent week rats were given 4-hour per day access to 10% ethanol and water every other day, with only water available on the alternate days. Next, rats were deprived of 10% ethanol, receiving access only to water for 4-hour day for one week to induce withdrawal. Finally, water and 10% ethanol were once again offered for 4h/day. At that point, animals that reached criteria were treated with 7.5 mg/kg SR141716. Weights, food intake, ethanol intake, and water intake were recorded daily. Results calculated include the following: percent ethanol preference, ethanol intake in grams per kilogram of body weight, food intake in grams per kilogram of body weight, and lick responses for ethanol and water.

Calculating the Absorbed Radiation Dose for Trabecular Bone from Radionuclides. *BENJAMIN LYNCH (Cedarville University, Cedarville, OH 45314) KEITH ECKERMAN (Oak Ridge National Laboratory, Oak Ridge, TN 37831) KARA KRUSE (Oak Ridge National Laboratory, Oak Ridge, TN 37831).* Radiation transport through trabecular bone has been studied to determine the energy deposited in sensitive regions of the skeleton. When a radionuclide enters the body some material may be deposited within individual bones of the skeleton. The energy deposited by the emitted radiation, e.g., beta particles, potentially places the person at risk for latent health effects, primarily cancer. It is believed the radiation does not do significant damage to the bone mineral itself, but causes damage to the bone marrow which lies within the cavities of trabecular bone. To simulate this phenomenon, a computer model has been developed that will determine the absorbed energy per unit mass (dose) to the marrow regions within the trabecular bone after the intake of a beta emitting radionuclide. Programs have been written that convert CT data of bone into the necessary input form for Monte Carlo N-Particle (MCNP). MCNP is a program developed at Los Alamos National Laboratory that uses the Monte Carlo statistical method to simulate radiation being passed through different materials. MCNP has been programmed to emit beta radiation from the bone mineral regions; the same way a radionuclide deposited in the bone would emit radiation. The program will then tally how much energy is deposited into the marrow regions of the trabecular bone. In a previous project,

researchers removed a lumbar vertebra from a cadaver. A vertebra was chosen because it is almost entirely trabecular bone with only a cortical bone shell. The cortical bone was removed from the sample, and the remaining trabecular bone was scanned with a Micro CT scanner. In the current project, work is still being done to determine how to segment the CT data into trabecular bone and marrow regions. Once the data is segmented, the simulation will be run for electrons of different energies ranging from 10 keV to 10 MeV. Current estimates of absorbed dose to the marrow are based on sampling chord length distributions created from studying cross sections of trabecular bone. The computer model simulating radiation transport through actual bone data should provide a more accurate estimate of absorbed dose. Combined with information from other research areas at Oak Ridge National Laboratory, this should provide an improved model for setting limits of exposure to bone seeking radionuclides. This data could be used for example in the field of nuclear medicine to set safe limits of exposure to radionuclides used for medical purposes.

Laser-Induced Fluorescence for Cancer Diagnosis. *MATTHEW MUSGRAVE (James Madison University, Harrisonburg, VA 22807) TUAN VO-DINH (Oak Ridge National Laboratory, Oak Ridge, TN 37831).* Esophageal cancer is one of the most deadly forms of cancer, and currently the most reliable way to diagnose esophageal cancer is by biopsy. A biopsy involves sending an endoscope down the patient's throat and cutting a piece of tissue out; then the sample must be analyzed, which could take several days. A new procedure is being developed to detect esophageal cancer that utilizes laser-induced fluorescence for in vivo cancer diagnosis. During the procedure a laser is sent down the biopsy channel of an endoscope and excites the tissue at five different wavelengths (400nm, 420nm, 440nm, 460nm, 480nm). The intensity of the fluorescence is measured over a broad range of wavelengths, normalized with respect to the total intensity measured, and graphed. The fluorescence signal for normal tissue is different than the signal for cancerous tissue. So by measuring how much the normalized data collected from a region of esophageal tissue differs from the spectrum of a standard normal graph, it can be determined whether or not the tissue is cancerous. The results collected so far using this technique are in agreement with the classifications made by a biopsy procedure. This technique has the potential to be a quick, cost-effective method to diagnose cancer.

Studies of the Glial Cells and Myelin in the Rat Spinal Cord Using Synchrotron-Generated X-ray Microplanar Beams (Microbeams). *AJANTHA NITHI (SUNY at Stony Brook, Stony Brook, NY 11794) AVRAHAM DILMANIAN (Brookhaven National Laboratory, Upton, NY 11973).* Microbeam radiation therapy is an experimental method that uses an array of parallel, microscopically thin planar beams of synchrotron generated x-rays. The method is based on the basic effect of sparing normal tissues, including those of the central nervous system (CNS) by microbeams up to very high doses. It is mediated in part by the recovery of the microvasculature from microbeam doses. Also, in the CNS the glial system seems to recover from microbeams. The current method of producing demyelination in the rat spinal cord, used in an effort to study the ensuing remyelination process, involves injection of gliotoxins into the spinal cord. The method is not only invasive (it requires surgery), but also can damage axons and the vasculature. However, due to the properties of microbeams mentioned above, it can be used as a novel tool for producing targeted, selective, axon-sparing demyelination much more efficiently. In order to follow the processes of myelination and demyelination, the spinal cord of adult rats were transaxially irradiated at the level of the T9 vertebra using a vertical microplanar beam 270-μm wide and 12 mm high with high incident doses of 500-1250Gy. The sensorimotor function was measured through the use of the accelerating rotor rod. The results obtained indicate that the rats recovered from an initial weight loss in the first two weeks which was cause by both the anesthesia effect and the radiation injury, and later followed normal weight gain. For most irradiation configurations we used, the rats returned to their original sensorimotor performance after about 4 days of recovery from the acute phase of the injury, although at some higher doses the recovery took a longer time. More histological results will soon be compiled by analyzing the tissue samples of the spinal cord rats.

Acute Effects of Low LET Radiation Exposure to Rat Brain: An Assessment Using MicroPET and Behavioral Models. *ELIZABETH RAFFI (Bronx Community College, Bronx, NY 10461) ONARAE RICE (Brookhaven National Laboratory, Upton, NY 11973).* Linear energy transfer (LET) radiation is the measurement of the number of ionizations which radiation causes per unit distance as it traverses the living cell or tissue. The difference between low and high LET is the non-linear relationship between range, atomic number and energy. Heavy ions (high linear energy transfer (HZE)) radiation is qualitatively different from those of low LET radiation. Alpha particles are an example of high LET radiation. X-ray and gamma rays are examples of low LET radiation. Low LET radiation is explored because it is a type of cosmic radiation. Cosmic radiation is discovered to be very harmful at chronic high doses to astronauts and the purpose for NASA being concern about their astronaut's health. Sprague-Dawley rats were exposed to low LET X-rays doses of 0 Gy, 15 Gy and 30 Gy. The objective was to assess behavioral models, particularly locomotor activity and Rotorod test to explore the effects of neurological damage in the brain that may have an affect on coordination and motor skills. Locomotor tested the rats for their spontaneous activity on the stimulant cocaine; and the number of beam breaks was recorded. The Rotorod test measured the rat's equilibrium on the rotating rod at 15 rotations per minute (RPM) and at 20 RPM. MicroPet imaging was used to observe and compare glucose metabolism in the rat's brain before and after exposure via the radioactive tracer FDG (fluorodeoxyglucose). MicroPet images were used to observe and explore global and regional changes in the FDG uptake in the brain that could possibly be affected by low LET exposure. In addition, MicroPET compliments the behavioral studies by providing a correlation between Locomotor, Rotorod tests and physiological aspects of this study. LET radiation had an effect on the glucose uptake regions of the brain: Striatum, Thalamus, and Hippocampus. Radiation affects glucose metabolism but has no definitive affects on locomotor or coordination. A significant amount of weight lost was present in the irradiated animals.

Measurement Bias Introduced From Non-Uniform Distributions of Radioactive Material in the Body. *JAMES RIVARD (Central Washington University, Ellensburg, WA 98926) TIM LYNCH (Pacific Northwest National Laboratory, Richland, WA 99352).* The purpose of this study was to evaluate the magnitude of uncertainties associated with the estimation of radioactive material that is heterogeneously distributed in the body using a calibration based on a uniform distribution. Measurements were performed inside of a room shielded with thirty centimeters (cm) of steel. Ten minute measurements were made using a scanning gamma ray spectroscopy detection system with an array of five 120% coaxial germanium detectors. Bottle-manikin-absorption (BOMAB) phantoms were used to simulate the geometry of a human subject. To simulate a non-uniform distribution of radioactive material within the body, both spiked and blank sections of BOMAB phantoms were combined. Five phantoms were used during the course of the study: reference male blank, reference female, reference male, 95th percentile male, and fission product. Three measurements were performed on each BOMAB section for each phantom. Data collection was performed with a computer algorithm. The calculated activity was compared to the decay corrected true activity. The measurement bias was evaluated over the energy range from 662 keV to 1408 keV. Activity was generally overestimated in all BOMAB phantom sections, except for the legs. Average percent bias for the pelvis was the smallest, while the legs were underestimated by -70%. The average percent bias for the simulated lung activity was found to be less than +7% for both 779 and 1408 keV energies. The negative bias for a simulated puncture wound ranged from a factor of 2x to a factor of 10x, depending on location. This work showed the significant bias that can be introduced into estimates of activity in the body for heterogeneous distributions of activity if the efficiency calibration is based on a uniform distribution.

Use of Diffraction Enhanced Imaging to Determine the X-ray Refractive Indices of Various Tissues at Select Energies. *MATTHEW TENG (Cornell University, Ithaca, NY 14853). ZHONG ZHONG (Brookhaven National Laboratory, Upton, NY 11973).* Diffraction enhanced imaging (DEI) was used to investigate the refractive indices of various organic tissues and water, at x-ray energies of 30, 32, 34, and 36 keV. These energies were chosen because of their similarity to medical imaging X-ray energies. This study was conducted so that future DEI studies of soft tissue would be able to make use of the refractive index information. The experiment was conducted using Silicon 333 reflection, typically used in DEI. In order to measure the small change in refractive index accurately across different samples and different energies, a sample holder which confines the sample to a 90-degree wedge was designed and constructed, and an experimental procedure was developed, to minimize systematic errors. The data for all four energies were analyzed and the refractive indices for several organic tissues and water were determined and fitted to a theoretical model. Clearly, each substance has a different refractive index; however, all substances showed the same inverse relationship between the energy and refractive index. This information will aid integration of DEI into clinical medicine in terms of optimization of DEI parameters in a clinical setting.

Treating Highly Malignant Rat Brain Tumors with Arrays of Parallel, Synchrotron-Generated X-ray Microplanar Beams (Microbeams). *SILMILLY TORIBIO (Hostos Community College, Bronx, NY 10451) DANIELLE WILLIAMS (Stony Brook University, Stony Brook, NY 11790) AVRAHAM DILMANIAN (Brookhaven National Laboratory, Upton, NY 11973).* Despite recent advances in conventional radiation therapy, including Intensity Modulated Radiation Therapy (IMRT) and Stereotactic Radiosurgery, the method still fails in treating highly malignant brain tumors such as high-grade gliomas (e.g., glioblastoma multiforme, GBM), and pediatric tumors of the central nervous system (CNS). The main limitations stems from the damage the therapy produces in the surrounding normal brain tissue. It has been shown in studies of the rat brain tumors that microbeam radiation therapy (MRT) addresses these limitations by a) sparing the normal brain tissue, and b) preferentially damaging the tumor, even when used from a single direction. Although the biological mechanisms underlying the sparing effects of microbeams on the CNS tissues is not well understood, it clearly involves recovery of the microvasculature and the glial system from the microbeam damage. The previous studies of MRT in the rat brain used the tumor model 9L gliosarcoma (9LGS), which is not a true representation of the high-grade gliomas in human beings. In particular, 9LGS tumors are encapsulated and have limited invasiveness, emulating more metastatic brain tumors rather than high-grade gliomas. We report here a recent experiment in which we applied MRT to a new rat tumor model, namely the F98 glioma. This tumor very closely simulates the characteristics of the human GBM due to its aggressive, highly proliferative with an infiltrative pattern of growth within the brain, and invasive nature. Furthermore, intracranial F98 tumors are reproducible. We irradiated rats with F98 tumors bilaterally (AP and laterally) with microbeams of dosage to produce single-exposure dosages of 45 Gy and 35 Gy and broad beams of 35 Gy and 25 Gy. The results indicate that a) the interlaced microbeams method failed because the 9 mm wide array of microbeams presumably did not cover the effective width of the F98 tumors; b) because non-interlaced microbeams have no therapeutic efficacy, any tumor margin left out of the interlaced volume will lead to rapid tumor regrowth and animal death; c) the broad beam method produced a better survival than microbeam for the same 35 Gy dose because, although the beam width was the same 9 mm, the non-crossed broad beams (17.5 Gy) have more therapeutic efficacy than the non-interlaced microbeams; and d) in both methods higher doses produced a better survival than lower ones.

An Evaluation of Multidomain Synthetic Peptide B2A2 by Detecting Calcium Deposition In Vitro with Calcein. *DARSHAN VAIRAVAMURTHY (Rice University, Houston, TX 77005) LOUIS PENA (Brookhaven National Laboratory, Upton, NY 11973).* Bone morphogenetic proteins (BMPs) are members of the transforming growth factor-beta (TGF-beta) gene superfamily of growth and differentiation factors. Members of the BMP family were originally cloned and characterized by their ability to induce ectopic bone formation. Of the various BMPs cloned, the inductive ability of BMP-2 has been well characterized. BMP-2 has been shown in clinical use to heal non-union fractures. However, in spite of the various advances in BMP research, clinical applications, such as spinal fusion kits, still require excessively high concentrations of exogenous rhBMP-2 to elicit proper bone formation. However, recently a multi-domain synthetic peptide B2A2 has been shown to synergistically enhance the bioactivity of the BMP-2 in two cell lines: C3H10T1/2 and C2C12. B2A2 in combination with BMP-2 increased alkaline phosphatase activity, and triggered Smad and MAPK signaling. In this study, we sought to confirm the synergetic effect of B2A2 by measuring calcium deposition of MC3T3-E1 in vitro using calcein. Additionally, we evaluated whether calcein staining can semi-quantitatively detect calcium deposition in MC3T3-E1 cell monolayers. MC3T3-E1 cell cultures were seeded in a 96 well microplate, and induced to differentiate with ‘Ñ-MEM induction medium (2% FBS, 50 ug/ml ascorbic acid, and 4 mM potassium phosphate) supplemented with 2.5 ng/ml rhBMP-2, varying concentrations of B2A2 (500 ng/ml-2000 ng/ml), or a combination of rhBMP-2 and B2A2. Current data does not confirm the synergistic effect of B2A2; however, results are not consistent. Experiments suggests that calcein detection of insoluble calcium in cell monolayers cultured in a 96 well microplate may not be a reliable method to quantitative mineralization by MC3T3-E1 cells.

Detection of Calcium Deposition in MC3T3-E1 Cell Monolayers by Calcein: A Study to Evaluate a Synthetic Peptide Analog of BMP-2. *DARSHAN VAIRAVAMURTHY (Rice University, Houston, TX 77005) LOUIS PENA (Brookhaven National Laboratory, Upton, NY 11973).* Bone morphogenetic proteins (BMPs) are members of the transforming growth factor-beta (TGF-beta) gene superfamily. Members of the BMP family were originally cloned and characterized due to their ability to induce ectopic bone formation. Of the various BMPs cloned, the inductive ability of BMP-2 has been best characterized. In clinical studies, BMP-2 has been shown to heal non-union fractures. However, in clinical applications, such as spinal fusion kits still require excessively high concentrations of exogenous recombinant BMP-2 (rhBMP-2) to elicit proper bone formation. Therefore, there is an interest to develop synthethic analogs or positive modulators of BMP-2 to reduce the costs of these applications. At Brookhaven National Laboratory a multi-domain synthetic peptide, designated B2A2, has been designed and shown to synergistically enhance the bioactivity of BMP-2 in two cell lines: C3H10T½ and C2C12. B2A2 combined with BMP-2 increased alkaline phosphatase activity, and triggered SMAD phosphorylation and suppressed MAPK signaling. In this study, we sought to confirm the synergistic effect of B2A2 on osteogenic differentiation by measuring calcium deposition in MC3T3-E1 cell monolayers in vitro using calcein, a calcium ion probe. Therefore, the major emphasis of this study was to evaluate whether calcein staining can quantitatively detect calcium deposition in MC3T3-E1 cell monolayers. MC3T3-E1 cell cultures were seeded in a 96 well microplate, and induced to differentiate with induction medium (a-MEM, 2% FBS, 50 ug/ml ascorbic acid, and 4 mM potassium phosphate) supplemented with rhBMP-2 (2.5 ng/ml) and varying concentrations of B2A2 (500 ng/ml-2000 ng/ml). Calcein fluorescence was read 10 and 14 days post induction. Due to high levels of intrasample variation, it seems that calcein staining may not be a feasible method to quantitatively detect calcium deposition in a 96 well microplate.

Nuclear Science

Radiation Detectors: An Analysis of Portal Monitors and Handheld Detectors. *EVA BAKER (Syracuse University, Syracuse, NY 13244) CARL CZAJKOWSKI (Brookhaven National Laboratory, Upton, NY 11973).* Portal monitors and handheld detectors were evaluated on their ability to detect nuclear radiation for the Department of Homeland Security to safeguard against the transportation of potentially dangerous nuclear sources into populated areas. Detector efficiency, ergonomics, identification success, and detection sensitivity were used to rate each detector. Sodium iodide crystals (NaI), germanium crystals, and polyvinyltoluene (PVT) were analyzed for gamma photon detection while lithium doped glass fibers and helium-3 tubes were tested for neutron detection. The efficiency is defined here as the ratio of the amount of nuclear particles recognized by the unit to the number of particles physically striking the detector. Three models have been proposed to determine this: a 3-dimensional geometry analysis, point source to square detector formula, and by using Monte Carlo N-Particle (MCNP) modeling software. Although the MCNP model appears to be the most promising, most of the calculations yielded abnormally high results.

Selecting RDUM Card Values in MCNP-PoliMi. *BROOKE BARGER (Ball State University, Muncie, IN 47306) SARRA POZZI (Oak Ridge National Laboratory, Oak Ridge, TN 37831).* MCNP-PoliMi is a modified version of the standard Monte Carlo N-Particle (MCNP) code that uses Monte Carlo Methods to simulate particle interactions in radiation detectors. The RDUM card is a unique feature of MCNP-PoliMi that filters out collisions that release small amounts of energy before the collisions are recorded in the data output file. The purpose of this investigation is to determine the RDUM card values that will eliminate low energy collisions without greatly impacting the accuracy of the final results. The advantage of eliminating these collisions is that less space is used to store the data output file. In the investigation, a wide range of values were tested for the RDUM card. The tests were compared to the control case in which the RDUM card is set at zero, and all of the collisions are recorded. An error was determined for each test based on the amount of data lost in comparison to the control case. This process of error calculation was repeated for different thresholds. The size of the data output file was also recorded. After obtaining the error estimates, the most efficient RDUM value was selected for each threshold so that a reasonably small error is produced. Using these recommended values reduces the size of the data output file by approximately forty five percent. While the recommended RDUM values are not the only reasonable values to use in MCNP-PoliMi, they have been tested and found to be good choices when an error of one percent is acceptable. If the user determines that more precision is needed in the simulation, tables are available to help the user find the RDUM values that match the desired level of accuracy.

Analysis of Neutron Flux in Preparation for Reaction Measurements with Radioactive Targets. *KATHERINE BAUER (Smith College, Northampton, MA 01063) MARGARET A. MCMAHAN (Lawrence Berkeley National Laboratory, Berkley, CA 94720).* At the 88-Inch

Cyclotron, in the Nuclear Science Division at Lawrence Berkeley National Laboratory in Berkeley, CA, researchers are trying to measure the cross section for the reaction $^{89}Zr(n,2n)^{88}Zr$. Knowing this cross-section accurately is important for the US Stockpile Stewardship Program; in addition, neutron cross-sections such as this one, are useful in order to understand nucleosynthesis. A large neutron flux is important for the SSP project because the ^{89}Zr target is radioactive, with a half-life of 78.41 hours. The resulting isotope, ^{88}Zr, is also radioactive with a half-life of 63.4 days. Without a large neutron flux, the material will decay too much, making if more difficult to calculate the cross-section. By replicating the experiment with activation foils that are not radioactive, using identical geometry the neutron flux can be evaluated and energy information can be obtained. The neutrons produced in the bombardment of the activation foils induces radioactivity within the foils. The decay of the radioactive material in these foils can be measured using a Ge-Li counter. The resultant information from counting radioactive decays is used to quantify the neutron flux. These same measurements of decay will also identify which reactions have energy thresholds that are too high to take place in the given beam-line. Neutron flux measurements for these non-radioactive foils will allow researchers to determine an expected neutron flux for the ^{89}Zr experiment—and if it will be high enough to effectively measure the (n,2n) cross-section. Results from this work showed a neutron flux measurement roughly 100 times smaller than expected, at 3×10^8 neutrons/cm^2/sec, which indicates that in the current conditions the ^{89}Zr experiment will not be possible. Also indicated from this work is that higher threshold reactions did not occur—reactions with thresholds above 12 MeV. Foils placed at different stances showed a steady and quantifiable difference in flux. These findings will allow future placements to be determined, as flux operates by a $1/r^2$ relationship with distance. Future work will include confirming these results related to distance, as well as producing a higher neutron flux, ideally around 3 x 10^10 neutrons/cm^2.

Conversion and Improvement of Time-Dependent Neutron Transport Code TDKENO. *ANDREW BIELEN (Pennsylvania State University, University Park, PA 16802) SEDAT GOLUOGLU (Oak Ridge National Laboratory, Oak Ridge, TN 37831).* In the world of nuclear engineering it is imperative that accurate and reliable computer codes exist to aid in the design and analysis of nuclear systems. TDKENO is a time-dependent three-dimensional neutron transport code that uses the improved quasistatic method. It can be used to model excursions, and calculate important parameters such as reactor period, peak power, and total power for a transient. The goal of this project was to convert TDKENO from Fortran 77 to Fortran 95 and then to make various other changes to the code to allow it to perform better. To perform the actual code conversion, a software package developed by Pacific-Sierra Research was used. A variety of other changes was then carried out to take further advantage of Fortran 95's improvements, including replacing all common blocks with modules, removing all large fixed-size container arrays in favor of more flexible allocatable arrays, implementing the SCALE free-form input routines rather than relying on a fixed input format, and taking out as many fixed parameters as possible. In addition, a new ordinary differential equations (ODE) solver for stiff systems was developed in place of the Livermore Solver of ODEs (LSODE) to solve the amplitude and precursor equations. It is felt that LSODE is too general and bulky a solver to be efficient; a new, more compact, more specific solver is required. This solver uses a second-derivative implicit method to solve the point kinetics equations. After the conversion and initial changes were carried out, extremely similar results were obtained when compared against previous cases run with the old version of the code. Results from the change in the ODE solver suggest that the code does not correctly predict local error, nor is it accurate enough. The results thus far indicate that the conversion was carried out very cleanly, which bodes well for the additional changes that will be made. For the ODE solver, further development is necessary, including modifying the error estimation and stepsize- and order-changing strategies. As well as a new ODE solver, there are several other improvements being considered, including developing an algorithm for determining flux shape calculation times, and adding support for anisotropic scattering. With these and other improvements, it is hoped that TDKENO will become a standard for time-dependent transport codes.

Creation of Theoretical Phase Diagrams to Model New Nuclear Fuel Alloys. *KRISTIN BRINEY (DePauw University, Greencastle, IN 46135) J. RORY KENNEDY (Argonne National Laboratory, Argonne, IL 60439).* The software Thermo-Calc is analyzed for its effectiveness in creating phase diagrams of transuranic fuel alloys. The software is found to be very powerful and flexible in creating diagrams, though rather database dependent. The lack of information on transuranic elements in the databases results in poor diagrams that do not match experimentally determined values. On a very basic level, however, data for single elements is shown to be accurate. The conclusion is made that a better, more thorough database is required to create useful diagrams. Also, some experimental data will need to be added to the program in order to verify the accuracy of the resulting diagrams.

Criticality Of Uranium Oxyflouride Solution In Bare Aluminum Cylindrical Vessels. *WADE BUTAUD (Texas A&M University, College Station, TX 77843) J. BLAIR BRIGGS (Idaho National Engineering & Environmental Laboratory, Idaho Falls, ID 83415).* The amount of fissile material that may be stored in one location is a concern that must be addressed by criticality safety experts who are responsible for the safety of nuclear operations. Many experiments were conducted in the mid 1900s involving criticality of a variety of fissile materials in a variety of different geometrical configurations. The measurement of critical solution heights were determined by J. K. Fox, L. W. Gilley, and D. Callihan for a uranium oxyflouride solution in a bare aluminum cylindrical vessel. In order to use these experiments, which were performed in the 1950's, as a benchmark for modern-day applications a more detailed evaluation of these experiments is required. By identifying and analyzing uncertainties in these experiments, the overall uncertainty in the neutron multiplication, kell, was found using Monte Carlo methods such as those implemented in KENO 5.a and MCNP. From these calculations, benchmark models were derived. The evaluation of these experiments, including benchmark models and their associated uncertainties, will be published in an OECD NEA publication entitled, "International Handbook of Evaluated Criticality Safety Benchmark Experiments" and will be available internationally to those who are seeking criticality safety information.

The Intensive Research Institute. *KEO CHHIM (California State University Fresno, Fresno, CA 93740) TOM KNIGHT (Lawrence Berkeley National Laboratory, Berkley, CA 94720).* The Intensive Research Institute consisted of four workshops: Natural Terrestrial Radioactivity, Cosmic Ray Detection, Neutron Activation Analysis, and Fingerprint Analysis. Each workshop was designed to expand knowledge in a certain area of science and guide in applying this knowledge to the classroom. The objective of Natural Terrestrial Radioactivity is that radioactivity is naturally occurring in our environment. Soil samples from different areas around the Berkeley lab were collected and analyzed. Yearly dosages of gamma ray exposure from Uranium, Thorium and Potassium were measured and compared to LBNL limits. Results showed that this exposure is insignificant. Primary cosmic rays are protons which react with the atmosphere and become secondary cosmic rays called muons. In the Cosmic Ray Detection workshop, we learned that the Earth is constantly being bombarded by cosmic rays. We built a cosmic ray detector that used scintillation paddles. By comparing count rate at different angles, we found that most muons come from directly above. By comparing count rate at different elevations, we found that as elevation increased, the number of muons detected increased. This shows that most muons have decayed at before reaching the Earth's surface. In the Neutron Activation Analysis workshop, stable isotopes of an element were bombarded with neutrons resulting in a radioactive isotope. Our objective in this workshop was to identify the elements present in an unknown pottery sample. Thirty-one of the 35 elements were found. Applications of NAA include: airplane/automobile part testing, forensics, and medical research. The objective in the Fingerprint Analysis workshop was to learn about the infrared spectrum and its use in infrared spectroscopy. One can analyze the chemical properties of a given sample such as different fingerprints using infrared spectroscopy. We found that the chemical compounds in different people's fingerprints could be characterized. IR fingerprint analysis is still in early development, but looks promising for forensic identification.

A Search for an Alternative Fuel for the Prismatic Next Generation Nuclear Plant. *RHETT CHRISTENSEN (University of Utah, Salt Lake City, UT 84108) JAMES W. STERBENTZ (Idaho National Engineering & Environmental Laboratory, Idaho Falls, ID 83415).* The Next Generation Nuclear Plant (NGNP) is a project to build a proof of concept nuclear powered plant that will co-generate electricity and hydrogen. A possible design is the prismatic NGNP reactor which is a graph moderated helium cooled reactor fueled with TRISCO coated particle fuel. This paper covers the study of an alternate fuel that could be used in the prismatic NGNP reactor. The fuel is a UO_2 ZrO_2 CaO mixture formed into a cylindrical rod clad with a high temperature carbide. The study was conducted using MCNP5 and a model of the prismatic NGNP core. Research began to see what k-effective values the UO_2 ZrO_2 CaO fuel could reach with the same dimensions as the TRISCO fuel rod. The UO_2 ZrO_2 CaO fuel was unable to reach the k-effective value of 1.32 needed by the prismatic reactor. Studies showed the particle fuel to be more reactive for two reasons: one, the carbon matrix the fuel particles

are dispersed in help moderate the neutrons, and two, the carbide cladding of the UO_2 ZrO_2 CaO fuel reduces its reactivity. Carbides with high melting temperature were compared and Silicon Carbide is the best cladding when reactivity and melting temperature are considered. To overcome the fuel's reactivity handicap the geometry of the fuel was changed by decreasing its radius. This led to a significant increase in reactivity. The behavior of 100% UO_2 fuel rods with different radii and enrichments of U-235 were examined, and 100% UO_2 fuel was able to produce the proper k-effective value of 1.32, but with too large of loadings of U-235. Therefore, a study was undertaken to see if ZrO_2 and CaO could replace the UO_2 and still get the same reactivity. It was found that this increased reactivity. The results of these studies show that the UO_2 ZrO_2 CaO fuel is a valid fuel that can meet the design requirements of the prismatic NGNP. This fuel gives the designers of the plant the ability to pick some parameters of the fuel and adjust the other fuel parameters to meet the design requirements of the reactor. Future studies will need to done to determine what fuel specifications can be fabricated and how the fuel holds up under the conditions that will be found in the reactor.

Investigating Low Gamma-Ray Spectrum Analysis in Soil and Rock Samples at Lawrence Berkeley National Laboratory (LBNL). *DONICHE DERRICK (Medgar Evers College, Brooklyn, NY 11216) AL SMITH (Lawrence Berkeley National Laboratory, Berkley, CA 94720).* About fifteen billion years ago the universe was created by a theory which scientists called the big bang. When the earth was created, matter along with radioactive elements were produced. The main radioactive elements found on earth are Uranium, Thorium, and Potassium. However, after world war two due to the fall- out from nuclear weapons testing long life Cesium was created and deposited on the earth's surface. Natural radioactivity is present around us whether it may be in the earth or the atmosphere. During the summer my objective was to study low gamma-ray emission from Uranium, Thorium, Potassium and Cesium present in soil and rock samples taken from around the hills of Berkeley at the LBNL site. In addition, calculations were performed to determine our annual dosage rate from these various radioactive elements. To perform this experiment we used a high-resolution germanium detector. So far, our results have shown that the amount of natural radioactive elements present in the samples is low in concentration and in effective dosage.

The Development of Finite Element Based Models to Predict the Performance of Proposed Generation IV Gas-Cooled Fast Reactor Fuels. *MARY ERNESTI (University of Missouri - Rolla, Rolla, MO 65401) DAN WACHS (Argonne National Laboratory, Argonne, IL 60439).* The thermal and mechanical performance of Gas-Cooled Fast Reactor (GFR) dispersion fuel forms for the Gen IV GFR reactor were evaluated using Finite Element Analysis (FEA) tools. FEA models of a 1/6 segment of a hexagonal element containing either hexagonal or cylindrical coolant flow channels were drawn in a 3-D modeling program. The model fuel elements were assumed to be composed of a SiC matrix and used to complete steady-state thermal and stress analysis. Due to the ceramic properties of SiC, tensile stress was considered the limiting factor in the analysis of the different geometries. A chosen maximum principal stress of 150 MPa was set as the material limit, with a safety factor of three. A goal of 50 MPa was set. After reviewing the model data from the numerous finite element models analyses, the cylindrical geometry was chosen as the more desirable design. Parametric studies on the density of coolant channels and web thickness were then performed on the cylindrical coolant flow models. As the density of the coolant channels increased, the maximum principal stress decreased. A full scale hexagonal core assembly with several different side lengths was also modeled. Future work will focus on more specific parametric studies of the cylindrical flow channel geometry concerning thermal conductivity, convection coefficients, and the thickness of the fuel elements.

The Mystery of Cosmic Rays is One of the Few Samples of Matter that Come from Outer Space. *JOSE GARCIA (Reedley College, Reedley, CA 93654) PEGGY MCMAHAN (Lawrence Berkeley National Laboratory, Berkley, CA 94720).* In 1912, a scientist named Victor Hess did an experiment with an electroscope and a balloon to understand where cosmic rays came from. He used an electroscope to detect charged particles. An electroscope works with two pieces a very thin foil suspended inside a glass jar. There is a brass ball on top, and a brass bar going down from it to the foil, the brass carries electricity to the foil, which becomes equally-charged. Since, like charges repel, the two foils will become separated. Victor Hess noticed over time the foil came back together, which meant that there must be charged particles hitting the electroscope and depolarizing the foil. As he increased his altitude the intensity of particles increased on his electroscope. Therefore, he concluded these particles came from outer space and not from Earth, so he called these particles cosmic rays. In 1936, he won the Nobel Prize for this scientific discovery. Here at the Lawrence Berkeley National Laboratory (LBNL), the Intensive Research Institute (I.R.I.), a group of Pre-Service Teachers wanted to prove Hess' experiment in a different way. The I.R.I built a detector to better understand the mystery of cosmic rays. Peggy McMahan, my mentor, explained how the muons came from a reaction in the atmosphere with the primary of cosmic rays. These muons hit a target, or one of the two scintillator paddles on the detector, and photons are created. Then, the photons bounce around into the next target, the photomultiplier tubes. The function of the photomultiplier tubes is to convert the photon signal to an electric signal and multiply it by a factor of 10,000. Then, the electric impulse goes to the circuit board which counts the number of cosmic rays per minute. After building the detector, the I.R.I. conducted an experiment at different locations as well as at different altitudes such as Berkeley Marina and Mt. Del Diablo. The results clearly illustrated that as the altitude increases, so does the number of cosmic rays detected. In conclusion, we supported Victor Hess original experiment.

Modification of MCNP-PoliMi Post-Processor to Account for Light Transport Effects in a Scintillator Detector. *MATTHEW HIATT (Texas A&M University, College Station, TX 77840) JOHN NEAL (Oak Ridge National Laboratory, Oak Ridge, TN 37831).* Time correlated photon and neutron counting is one of the best ways to detect nuclear materials in an active interrogation scenario. In order to do detailed simulation of these scenarios via Monte Carlo N-Particle - Politecnico di Milan (MCNP-PoliMi), the physics of the particle interactions and the light collection of the detector must be modeled correctly. As the detectors to be modeled grow in size, the simulations become less accurate due to increased light transport effects such as absorption and reflection. To examine and account for these effects and better model a 25 cm x 25 cm scintillator detector, a pulse height mapping of the scintillator was taken. A new section of code was added to the PoliMi post-processor that reduced the light collected from interactions based on their location within the scintillator. The amount of reduction was determined by data taken from a pulse height mapping of the scintillator with a lower pulse height resulting in a smaller light collection and vice versa. This reduction scheme did not reduce the number of counts significantly but during this process it was found that adjusting the simulated threshold could produce the desired effect. The change to the threshold in the code was able to reduce the overestimation of the counts per fission from ~40% to ~5% in the gamma and neutron peaks. Since this simulated threshold is significantly different than the experimental threshold, more work will have to be done to determine whether the experimental threshold is being extracted incorrectly or if some other effect causes the difference.

Algorithm Development for the Image Reconstruction of Tomography Data from Neutron Radiography. *SUSAN KING (University of Tennessee, Knoxville, TN 37916) JEFF SANDERS (Argonne National Laboratory, Argonne, IL 60439).* Neutron radiography is a unique method of nondestructively examining an object. Neutrons are suited to examine materials that other techniques, such as x-rays, cannot examine well. Like x-rays, they can give a very useful image of what the structure of an object looks like, but how neutrons and x-rays interact with matter is very different. Neutrons are attenuated preferentially by light materials, such as hydrogen and boron, while x-rays are attenuated by heavy, dense materials. As a result, neutrons are more suited to radiography of higher atomic number elements and in many cases, high radiation fields. This paper will examine the methods used to reconstruct tomography data gathered from neutron radiography, as well as explain how that data is collected. It will compare tomography reconstruction methods using standard phantoms and data used in x-ray radiography. Though the algorithms developed are intended to be used for neutron radiography in NRAD, the TRIGA neutron radiography reactor at Argonne National Laboratory West, the well defined x-ray data and phantoms will be used to perform initial evaluations of the reconstruction methods. Finally, suggestions on further improvements of the algorithms and descriptions of further work will be presented.

Active Pixel Sensor Characterization for the STAR Detector. *JAKE KING (University of Kansas, Lawrence, KS 66045) HOWARD MATIS (Lawrence Berkeley National Laboratory, Berkley, CA 94720).* The STAR collaboration is studying matter at high temperatures and densities. If a significant improvement to the measurement of particle trajectories can be made, charmed mesons that decay away from the primary collision point could be identified. To achieve this goal, STAR is building a vertex detector consisting of a new technology – active pixel sensors (APS). An APS is an implementation of standard CMOS technology in which each pixel has a photodiode directly above the epitaxial layer. Incident particles produce electron-hole pairs in the epitaxial

layer, and these electrons accumulate on the photodiode. Charge from the photodiode is digitized to identify the position of the incident particle. It is important to characterize the signal to noise, readout time, and resolution on several different pixel sizes so that the vertex detector can be optimized for cost and speed. Larger pixels result in a faster data acquisition, while smaller pixels have better resolution. We will present studies of 5, 10, 20 and 30 μm square pixel geometries that measure charge distribution and collection. We will also display the results of using a field emission scanning electron microscope with energies from 1 to 30 keV. This tool has the potential to probe regions of the APS integrated circuit and contribute to understanding its properties.

ORIGEN-S Gamma Decay Spectrum Characterization and Benchmarking. *JESSE KLINGENSMITH (Pennsylvania State University, State College, PA 16802) IAN C. GAULD (Oak Ridge National Laboratory, Oak Ridge, TN 37831).* The purpose of this project was to validate the recently revised ORIGEN-S master photon library, released with SCALE 5.0, and to benchmark the results against experiment. The experiment entailed the irradiation of small samples of ^{235}U, ^{239}Pu, and ^{241}Pu and the measurement of the resulting gamma decay spectra at discrete times after fission. An initial evaluation of the library found that the calculated gamma energy release based on evaluated Q values was not consistent with the calculated gamma spectrum energy. This was caused by instances of double accounting of gamma lines found in many parent / daughter pairs. These problems were generally observed when decay data and gamma spectrum data were obtained from different sources and for nuclides with short-lived metastable states. In order to correct these inconsistencies, the photon library was regenerated such that the photon spectrum data and decay data were always obtained from the same source. This ensures consistency among ORIGEN data libraries and between gamma decay power and spectral energy output. The resulting master photon library accounted for over 99.9% of the total gamma energy release, even at times as short as 2.7 seconds after fission. Spectrum accuracy is observed to increase at longer wait times, while nearly all peaks are resolved at the shortest times. Similarly, the total energy release rates fall within the experimental error for nearly 75% of all data points. These results represent dramatic improvements from SCALE 4.4, especially at very short times after fission.

The MIMOSA-5 Active Pixel Sensor for Studying Quark-Gluon Plasma. *LARA PIERPOINT (University of California, Los Angeles, Los Angeles, CA 90024) FABRICE RETIERE (Lawrence Berkeley National Laboratory, Berkley, CA 94720).* 51 universities are working in collaboration to study quark-gluon plasma (QGP) with the Solenoidal Tracker at RHIC (STAR) device at Brookhaven National Laboratory. Characterization of QGP, if it exists, can be accomplished by studying charm-quark hadrons in STAR, but more precise measurements are needed than those currently possible with the detectors in place. The relativistic nuclear collisions group (RNC) at Lawrence Berkeley Lab is designing a new detector that will utilize active pixel sensing (APS) technology to take data in STAR. Advantages of the active pixel sensor include high-speed readout capability and high pixel density. One disadvantage is that the technology employed by the sensor is new and requires characterization. We use as a baseline for our characterizations the MIMOSA-5 chip designed by LEPSI/IreS (Strasbourg, France), which represents a full-scale prototype at 512x512 pixels in a 2x2 cm area. The chip's properties render it inadequate for use in the final detector, but we utilize it for studying our data readout system and for comparison to the next-generation active pixel sensor expected to meet our detector specifications.

Comparison of Portal and Handheld Nuclear Radiation Detectors. *MICHAEL RILEY (University of Southern Maine, Portland, ME 04104) CARL CZAJKOWSKI (Brookhaven National Laboratory, Upton, NY 11973).* Portal monitors and handheld detectors were evaluated on their ability to detect nuclear radiation for the Department of Homeland Security to safeguard against the transportation of potentially dangerous nuclear sources into populated areas. Detector efficiency, ergonomics, identification success, and detection sensitivity were used to rate each detector. Sodium iodide crystals (NaI), germanium crystals, and polyvinyltoluene (PVT) were analyzed for gamma photon detection while lithium doped glass fibers and helium-3 tubes were tested for neutron detection. The efficiency is defined here as the ratio of the amount of nuclear particles recognized by the unit to the number of particles physically striking the detector. Three models have been proposed to determine this: a 3-dimensional geometry analysis, point source to square detector formula, and by using Monte Carlo N-Particle (MCNP) modeling software. Although the MCNP model appears to be the most promising, most of the calculations yielded abnormally high results.

Flow Testing for Reduced Enrichment Research and Test Reactors (RERTR) Fuel. *ADAM ROBINSON (Oregon State University, Corvallis, OR 97330) DAN WACHS (Argonne National Laboratory, Argonne, IL 60439).* The Reduced Enrichment Research and Test Reactor program was created to take the highly enriched uranium (HEU) fuel that operates many of today's research and test reactors and reduce them to low enriched uranium (LEU) fuels. Argonne National Lab has been a major part of this effort. They have designed and fabricated two types of fuels that they hope will satisfy this goal and plan on doing radiation testing on these fuels in the Advanced Test Reactor at Idaho National Engineering Laboratory. In order to model this new fuels behavior in the reactor, accurate thermal modeling must done first. In order to perform this thermal modeling, flow data had to be obtained for these fuels. A model of the fuel assembly was created and a system was built to test the flow over this fuel assembly as a function of differential core pressure, flow rate, and flow restriction due to orifices on the fuel assembly channel. This was also built at Argonne National Lab and was operated at the Idaho State University Thermal Hydraulics Laboratory. An array of orifice sizes were tested and loss coefficients were calculated for the different tested systems. With the obtained flow values and loss coefficients, accurate thermal models can now be created and analyzed before the fuel is sent for irradiation.

Using Neutron Activation Analysis to Identify Elements in an Unknown Sample. *CLAUDIA ROBLEDO (California State University Fresno, Fresno, CA 93728) ERIC NORMAN (Lawrence Berkeley National Laboratory, Berkley, CA 94720).* In 1936, neutron activation analysis (NAA) was discovered when a rare earth element became highly radioactive after exposure to a source of neutrons. NAA is a technique used to identify elements in unknown sample. For decades, NAA has been performed on art and historical artifacts to identify concentrations of chemical elements in the sample and to help confirm authenticity or origin of the art. During my time at Lawrence Berkeley Laboratory, my research objective was to identify elements in a sample of pottery. The sample was bombarded with neutrons in the core of the McClellan nuclear reactor, which made some of the nuclei radioactive. The process of neutron capture is necessary because a stable isotope gives no energy; therefore we are not able to identify the elements in a sample. When the isotope is radioactive it is unstable, thus emitting gamma rays which we can detect through a tool called a germanium detector. This allowed us to interpret the energies of the gamma rays emitted. Through NAA, my research group was able to identify thirty-two different chemical elements in the pottery sample.

Modeling Salt/Zeolite Ion Exchange. *JILL RYDALCH (Idaho State University, Pocatello, ID 83201) MICHAEL SIMPSON (Argonne National Laboratory, Argonne, IL 60439).* Ion exchange between molten chloride salt and zeolite-A is being developed as a possibility for the treatment of spent nuclear fuel. A two-site model for monovalent salt/zeolite-A ion exchange has been developed by Simpson and Gougar and a program written in matlab to test it against the experimental data. The results have been compared with the results of Simpson's excel spreadsheet. Parameters have been found that provide the best fit for the data. The solutions of the monovalent model have been compared with Gougar's multivalent model and the results plotted. Both Simpson's monovalent and Gougar's multivalent models adequately and comparably fit the monovalent data. In order to compare the two multivalent equations Simpson's multivalent model needs to put into a matlab code and the results generated from there.

Optimization of Hall A Optics Database Using C++ Software. *DIANE SCHOTT (Florida International University, Miami, FL 33199) DOUG HIGINBOTHAM (Thomas Jefferson National Accelerator Facility, Newport News, VA 23606).* In order to reconstruct the path of charged particles after a collision, Hall A at Thomas Jefferson National Accelerator Facility (TJNAF) uses two high-resolution spectrometers (HRS) that each contains a pair of vertical drift chambers (VDCs). The VDCs reconstruct the path of the scattered particles that have passed through the spectrometer magnets. In order to determine the properties of the particle, a matrix is used to convert the track at the VDC to the momentum and energy of the initial scattered particle. By taking elastic data with a carbon target, the momentum transformation matrix from the focal plane to the target plane, can be found by using the known correlation between scattering angle and momentum for elastic scattering. Improving this matrix will more accurately portray the momentum spectrum. To achieve this, the current database is used to find the initial elastic peaks in the momentum spectrum. These peaks are compared to values calculated by the Optimize++ program using the known scattering angle and beam energy. The program then tries to improve the database. Over multiple alterations with Optimize++, the matrix in the database will give a much better reconstruction of the incident

particles. This is seen in the narrowing of the elastic and excited state peaks in a plot of momentum versus counts. In the majority of the Hall A experiments, the VDCs are used, so as the experiments become more precise, it is necessary to achieve the best possible database in order to study the collision.

Fingerprint Analysis a the Infrared Beam Line. *JORGE SERVIN (West Hills College, Lemoore, CA 93245) MIKE MARTIN (Lawrence Berkeley National Laboratory, Berkley, CA 94720).* Fingerprint Analysis has been around for thousands of years. Samaritans were the first that we know of to use fingerprints as a way to sign a contract. Samaritans were not the only one's to use fingerprints as a way to do business, in the late 1800 century, Francis Galton used fingerprints in India because the majority of people there were illiterate. The most famous case in the history of fingerprinting occurred in the late 19th century when a man was spotted in the incoming prisoner line at the U.S. Penitentiary in Leavenworth, Kansas by a guard who 'knew' him and had just seen him already in the prison population. Upon examination, the incoming prisoner claimed to be named Will West, while the (not escaped) existing prisoner was named William West. According to their Bertillon Measurement they were essentially indistinguishable. As they were not twins, the Bertillon system came into some question. However, their fingerprints were different, and fingerprint identification received a significant boost in credibility. In our research at Lawrence Berkeley National Laboratory this summer, the Intensive Research Group did fingerprint analysis at the Infrared Beam line. Our project consisted of finding out what kind of chemical components were present in fingerprints. We put our fingerprints on a gold plated slide. Then, we used the FTIR (Fourier Transformation Infrared Red) Spectrometer to analyze the sample. The machine measures the absorbance of infrared radiation by the sample and records a spectrum. Then we search the computer library or known spectra and find the best match to the sample. This tells us the different types of molecules that are presented in the sample fingerprint. Now the boundaries of infrared forensics are being pushed into uncharted territories by researchers at Berkeley Lab, and the results are promising for criminal and antiterrorism investigations as well as for historians and archaeologists.

Initial Studies of $^{238}UO_2^{2+}$ and $^{248}Cm^{3+}$ Complexation by Potentiometry and Time Resolved Laser Fluorescence Spectroscopy (TRLFS). *KRISTINA SVENSSON (College of Marin, Kentfield, CA 94904) HEINO NITSCHE (Lawrence Berkeley National Laboratory, Berkley, CA 94720).* Understanding the chemical behavior of actinides' aqueous chemistry is necessary for designing cleanup and containment methods, predicting transport rates and preventing further contamination of areas to which actinides have been introduced. The determination of stability constants via potentiometric titrations or TRLFS provides fundamental chemical information which supplements data used for modeling actinide behavior in the environment. TRLFS was used to analyze micromolar concentrations of UO_2^{2+} and Cm^{3+} complexed with simple carboxylic acids of varying carbon chain lengths as well as with phosphoenol pyruvate (PEP) to attain fluorescence lifetime information. The modeling software Hyperquad 2000 aided in the determination of the stability constants of PEP, but additional experimentation is needed. The results show no correlation between carbon chain length and fluorescence lifetime. A blue shift is evident from that of free uranyl at pH 3.9 in the presence of 0.05M propionic acid. These shifts are evidence of a second fluorescent species in solution, but further characterization is required for identification. At pH 3, both UO_2^{2+} and Cm^{3+} show a red shift in the presence of 0.045M PEP. These shifts are evidence of a second fluorescent species in solution, but further characterization is required for identification.

Size and Weight Reduction Through the Use of Depleted Uranium Dioxide (DUO_2)-Steel Cermet Materials for Spent Nuclear Fuel Rail Transport and Storage System. *PAUL SWANEY (North Carolina State University, Raleigh, NC 27607) M. JONATHAN HAIRE (Oak Ridge National Laboratory, Oak Ridge, TN 37831).* Currently the US Department of Energy (DOE) has an inventory of ~500,000 MT of depleted uranium as a result of enrichment processes. The cost of disposing of this material has been estimated from $240million to 1.5 billion. Finding a practical use for the depleted uranium would save hundreds of millions if not billions of dollars. One possibility is using depleted uranium to make depleted uranium dioxide-steel cermet storage casks for spent nuclear fuel (SNF). Shielding analyses were conducted using the SAS1 Module of the SCALE4.4a code developed at Oak Ridge National Laboratory. The spent nuclear fuel radiation source term was obtained from Origen-ARP in the SCALE4.4a code package. The gamma shielding efficiency of the cermet material is compared to Holtec International's HI-STAR 100 cask system that uses conventional steel for radiation shielding. The HI-STAR 100 cask was modeled using information obtained from Holtec's Final Safety Analysis Report (FSAR). After modeling the HI-STAR 100 cask, the steel layers of the cask were replaced with a layer of cermet material. The thickness of the cermet shielding was adjusted to give the same radiation doses as the HI-STAR cask. The objective of this work is to reduce cask weight and size by using the cermet material to replace conventional steel. If no credit is taken for cermet mechanical properties during licensing, calculations show the cask weight reduced by 13.7% and the overall diameter of the cask reduced by 4.8%. However if the cermet can be relied upon for structural strength and more depleted uranium is used in the cermet material, then the effectiveness of the cermet is better utilized. When the cermet material is fully utilized the cask weight can be reduced up to 17.6% with a reduction in the cask diameter of 6.3%. A small study was performed to analyze the characteristics of a cask using cermet with embedded B4C neutron absorber. When this neutron absorber is embedded in the cermet, the cask diameter is reduced by over 10%. Smaller cask size will facilitate handling during SNF loading operations. If the cask size and weight become small enough, the cask can be put directly into the SNF storage pool for loading for transport, thereby eliminating the need for a separate pool transfer cask.

A Superabsorbing Hydrogel for Radiological Dispersal Device ("Dirty Bomb") Cleanup. *NADIA VASQUEZ (Richard J. Daley College, Chicago, IL 60652) MICHAEL KAMINSKI (Argonne National Laboratory, Argonne, IL 60439).* Radiological decontamination technologies are needed for non-destructive removal of radioactivity from porous surfaces such as concrete and marble. We are configuring a novel process for post-restoration of an RDD from porous materials in the event of a terrorist attack. The optimized process would involve three steps: (1) remove surface bound species and penetrate the pore structure to free radionuclide ions from the surface and into the pore water; (2) pull water from the pore structure with a superabsorbing hydrogel, and; (3) remove the radioactivity-loaded gel by wet vacuum. We studied decontamination properties in designing an optimal polymer gel formulation. We report performance parameters of polymer candidates for aqueous solution absorbency with a gravimetric analysis of swelling capacity of gel formulations ("tea bag test"). We found the polymer water absorbency is dependent on the effect of ions or chelators in the following wash solutions: NH_4Cl, $CaCl_2$, and deionized H_2O. We observed increased absorption capacity using smaller grain sized polymer than commercially distributed polymer. The resulting superabsorbent retention capacity calculations suggest that the critical absorption time of polymer formulations is within ten minutes of immersion. The absorbency of polymer candidates is affected by cross-linked and linear formulation ratios. Furthermore, double immersion did not affect subsequent retention of the polymer.

Nitrogen Solubility in Water. *WENDY WAGSTER (Texas A&M University-Kingsville, Kingsville, TX 78363) GRAYDON YODER (Oak Ridge National Laboratory, Oak Ridge, TN 37831).* Integral reactor concepts for new nuclear reactor designs with safety features that incorporate the pressurizer component as an integral part of the reactor core are being developed. Some of these designs use nitrogen to maintain the pressure within the reactor core. However, nitrogen dissolves in water and upon a pressure drop nitrogen pockets will develop in the primary system. Therefore, in order to analyze the integral reactors that use nitrogen pressurization it is important to understand how much nitrogen will dissolve into the water. The purpose of this research is to understand and determine the amount of nitrogen that dissolves in the water at various temperatures and pressures. Knowing the amount of dissolved nitrogen the second part of research is to determine the nitrogen concentration in the primary system as a function of time by establishing a nitrogen diffusion rate. The amount of nitrogen that dissolves in the water is calculated based on the partial pressure of nitrogen and the total pressure of the reactor core. It is well known that the amount of nitrogen that will dissolve is more dependent on temperature than pressure. Also, it is known that as water reaches its saturation point (at a specific pressure) the amount of nitrogen that dissolves will decrease and eventually reach zero. For the specified partial pressure of 24.673 atm (2.5 MPa) and 601 K the nitrogen concentration is 2.43 $g^{N2}/Kg\ H_2O$. For a total pressure of 148.038 atm (15 MPa) and a temperature of 601 K the nitrogen concentration is 2.564 $g^{N2}/Kg\ H_2O$. Transient diffusion calculations through the pressurizer/primary system interface will be used to determine the nitrogen concentration in the primary system. This information can then be used to determine the effect of dissolved nitrogen on the transient response of the reactor.

Studying the $^{11}C + d \rightarrow n + {}^{12}N$ Reaction for its Astrophysical Significance. *THAZIN WIN (University of Illinois at Chicago, Chicago, IL 60607) JOSEPH CERNY (Lawrence Berkeley National Laboratory, Berkley, CA 94720).* After the Big Bang there were only light nuclei up to boron in the early stages of development. For stars about the size

of our sun, energy is produced primarily by direct fusion of a sequence of reactions involving four hydrogen atoms into helium which is known as the p-p chain. However, for larger stars, the higher temperature and density occurrence allows for energy production by hydrogen burning of heavier elements. The CNO cycle is a hydrogen burning chain of proton reactions that can produce higher rates of energy generation in such massive stars; however the Big Bang did not directly produce CNO nuclei. One way this CNO cycle could have started is the creation of ^{12}C nuclei from a process beginning with hydrogen nuclei. Professor Cerny's group has led the effort to develop a radioactive ion-beam capability at the 88" Cyclotron via the Berkeley Experiments with Accelerated Radioactive Species (BEARS) initiative. Upon completion of the BEARS activity-handling system in August 1999, this coupled-cyclotron facility produced 1x108 ^{11}C ions/sec on target for nuclear experiments. The current experiment that the group is working on is to study ^{12}N by bombarding a CD2 target with a ^{11}C ($t_{1/2}$ =20 min) radioactive beam at 150 MeV. This d(^{11}C,^{12}N)n experiment requires the assembling of Si-strip detectors and a set up of nuclear electronics and the data acquisition system. The purpose of this reaction is to produce ^{12}N ($t_{1/2}$ = 11ms) which will rapidly ß decay to stable ^{12}C. Through this process, the group is hoping to contribute to the understanding of the production of ^{12}C in early generation stars. The d(^{11}C,^{12}N)n experiment at the 88-Inch cyclotron is completed; however, the detailed calculations of the differential cross section are continuing.

Physics

Velocity of Sound Measurements Using Multiple Reflections within a Stainless Steel Vessel. *JUSTUS ADAMSON (Brigham Young University, Provo, UT 84604) MARGARET GREENWOOD (Pacific Northwest National Laboratory, Richland, WA 99352).* An ultrasonic sensor to measure the velocity of sound for a liquid is under development at Pacific Northwest National Laboratory (PNNL) as part of a process to measure the adiabatic compressibility of the liquid. A rectangular stainless steel box with an open top was fabricated with an ultrasonic longitudinal transducer attached to one side to make the velocity measurements. To measure the velocity, an ultrasonic pulse is sent from the transducer and transmitted through the steel into the liquid and reflected back and forth between steel walls in the liquid. Fourteen reflections off the wall farthest from the transducer were used to calculate the velocity, equating to a path length of 1.43 meters. This method was used to measure the velocity of sound of distilled water and H_2O_2 solutions at various temperatures between 19.8 and 30.2 degrees Celsius. All of the velocity of sound measurements of distilled water came within ±0.5 m/s of the expected values given by Bilaniuk et al. The velocity measurements of the H_2O_2 solutions agreed with the measurements from a photo acoustic technique. The stainless steel apparatus method of measuring velocity could be significantly improved to make measurements of greater precision in the future.

Non-Intercepting Space-Charge Measurement of a Heavy Ion Beam. *MONSERRAT AMEZCUA (Contra Costa Community College, San Pablo, CA 94806) ENRIQUE HENESTROZA (Lawrence Berkeley National Laboratory, Berkley, CA 94720).* In the pursuit to find other means of generating commercial energy, the Heavy Ion Fusion program tests concepts for inertial fusion drivers in a series of experiments. One of which, the Neutralized Transport Experiment (NTX), is exploring the physics of focusing with plasma a space-charge-dominated beam, along with a way to accurately obtain a neutralized ion beam profile without disturbing the beam itself. Analysis of the NTX electron beam diagnostic system designed and developed by The Heavy Ion Fusion group at Lawrence Berkeley National Laboratory and intended to non-disturbingly measure the profile of a heavy ion beam, is needed. The diagnostics system consisting of an electron gun that provides a small spot electron beam that transversely crosses and is deflected by the space-charge of a 25mA potassium ion beam, has a camera installed beyond the electron beam path focused on a scintillator that gets optical image of the electron beam by extracting charges. To predict an ion beam profile from the experimental electron beam deflection measurements, simulations of the electron beam trajectories were carried out by a program created in the computer language Python. The ion beam profile was predicted to have the values of the ion beam parameters used in the simulation that best approximated the experimental data. A second program, traced electron trajectories using the electric field calculated from the charge distribution obtained from an image of the ion beam, thus, having the specific charge density distribution, electric potentials, and size of the actual ion beam. Comparing the non-intercepting diagnostic result with results obtained from image analysis, wire scanning, and slit cup experiments, showed the electron beam diagnostics is fairly accurate. Furthermore, the converging potassium ion beam was partially neutralized using a plasma source and the non-intercepting electron beam diagnostics predicted an accurate profile when compared to image analysis results. However, there are some factors interfering with the sensitive electron beam diagnostics making it hard to accurately predict the profile of a fully neutralized ion beam, and the plans to cover the NTX diagnostics box with µ-metal seem promising. The current NTX diagnostic system can scan an ion beam of up to 3 cm in radius providing information that helps us understand the physics of heavy ion beams and getting us closer to the ultimate goal of using inertial fusion as an energy source.

Adaption of the Equilibrium Stability Code to the Current Drive Experiment-Upgrade for Use in Creating Magnetic Reconstructions. *SARAH ANGELINI (Columbia University, New York, NY 10027) RICHARD MAJESKI (Princeton Plasma Physics Laboratory, Princeton, NJ 08543).* The Equilibrium and Stability Code (ESC) is a program being newly applied to creating magnetic reconstructions of spherical torus plasmas. For an experimental machine, magnetic reconstructions determine the locations of the magnetic flux surfaces. Because the flux surfaces reflect the magnetic fields that contain plasma, the location of the flux surfaces determines the distribution of the plasma. The most commonly used code available for magnetic reconstructions is the Equilibrium Fitting Code (EFIT). It was specifically written for one machine, the Doublet III D-Shape Tokamak (DIII-D) located at General Atomics, and cannot easily be used with another machine without fundamental, time-consuming changes. The ESC, however, was written to be compatible with a number of different machines. It is uniquely structured to take machine specifications and magnetics data from an experiment as simple input files. The ESC requires only smaller, data-related changes. Currently, these changes are being implemented so the ESC can be used with the Current Drive Experiment-Upgrade (CDX-U) at the Princeton Plasma Physics Laboratory. The data formats and collection programs of CDX-U are being edited so that they are compatible with ESC. The ESC also has a graphical interface and embedded documentation for the user. The adaption of ESC to CDX-U results in the ability to generate a reconstruction between plasma discharges. Because of the inherent adaptability of the ESC, it has a wide variety of machines to which it can be applied in the future.

On the Applicability of Phase Space Tomography to Reconstruct the Phase Space of a Space-Charge-Dominated Electron Beam. *JOSHUA AURIEMMA (University of Massachusetts Lowell, Lowell, MA 01854) PHILIPPE PIOT (Fermi National Accelerator Laboratory, Batavia, IL 60510).* Using data from the A0 Linac at the Fermi National Accelerator Laboratory, the main purpose of this project was to work backwards – given information about the path of the electron beam – to recreate a 2-dimensional histogram of the original beam at some previous point in phase space. The ultimate goal of this research is the task of finding the optimal amount of beam profiles required to recreate an accurate picture of the beam at the original point. Most tomographical reconstruction algorithms make the a priori assumption that the beam is Gaussian. The algorithm that we have utilized for this project was originally developed at the Deutsches Elektronen-Synchrotron (DESY) and makes no such assumption. As such, it is an excellent candidate for the tomographical reconstruction of most electron beams. It is clear from the generated histograms that the algorithm works very well with simulated data: a fairly accurate beam recreation can be seen with just three beam profiles at pi/3 radians apart. Further research is currently being carried out with actual data from the linac.

Electrochemical Process to Fabricate Ag-Cu Foils for Reactive Air Brazing. *JOEL BALE (Washington State University, Pullman, WA 99163) KENNETH SCOTT WEIL (Pacific Northwest National Laboratory, Richland, WA 99352).* Recently a new joining technique, referred to as reactive air brazing (RAB), has been developed for high temperature solid-state devices such as solid oxide fuel cells. Several brazing compositions have shown excellent long-term results in single atmosphere environments, in either oxidizing or reducing gas conditions. However in dual atmosphere conditions (i.e simultaneous exposure to both gases on opposing sides) the seal begins to break down after several hundred hours. Among the forms of braze material, foil is the most desirable form since it allows porosity within the joint to be mitigated. Alloy foils are conventionally fabricated by rolling the alloy bulk to desired thickness. However, this technique is not a convenient means of fabricating small quantities of various compositions. Attempting to find a specific sealing composition that will not degrade, different ratios of Ag to Cu were prepared in foil form via electroplating. In this study, electroplating was selected since it is relatively a simple process and easy to control amount of Cu deposited on Ag foils, in comparison with other deposition techniques such as sputtering. To avoid decomposing the water used in the copper sulfate solution into hydrogen and oxygen and to ensure that

only Cu was being oxidized and reduced, the applied potential was kept under 0.3 V and constant current condition was used during electroplating. Use of the Faraday equation for electrolysis allowed precise alloy compositions to be calculated and synthesized during electroplating. After Cu was deposited on Ag foils, the foils were heat-treated in reducing atmosphere (hydrogen) to diffuse Cu into Ag foils and homogenize the distribution of Cu in Ag foils. Finally, alloyed foils were rolled using a hand roll to have a desired thickness for brazing. Future research will employ this braze foil fabrication technique in attempting to identify a brazing composition that will not deteriorate under dual atmosphere conditions.

Marginal Stability Studies of Microturbulence Near Internal Transport Barrier ITB onset on Alcator C-Mod. *JESSICA BAUMGAERTEL (University of Washington, Seattle, WA 98105) MARTHA REDI (Princeton Plasma Physics Laboratory, Princeton, NJ 08543).* Insight into microturbulence and transport in tokamak plasmas is being sought using linear simulations of drift waves near the onset time of an internal transport barrier (ITB) on Alcator C-Mod. Microturbulence is likely generated by instabilities of drift waves and causes transport of heat and particles. This transport is studied because the containment of heat and particles is important for the achievement of practical nuclear fusion. We investigate marginal stability of ion temperature gradient (ITG) modes for conditions at the ITB region at the trigger time for ITB formation. Data from C-Mod, taken by TRANSP (a time dependent transport analysis code), is read by the code TRXPL and made into input files for the parallel gyrokinetic model code GS2. Ion temperature and density gradients in these input files are changed to produce new input files. Results from these simulations so far show that the weak ITG instability in the barrier region at the time of onset is above marginal stability; the normalized critical temperature gradient is 70% of the experimental temperature gradient. The growth rate increases linearly above the critical value, with the spectrum of ITG modes remaining parabolic up to a multiplicative factor of 2. The linear critical temperature gradient model breaks down for multiplicative factors of 4 and 8. Simulations were carried out on the NERSC IBM 6000 SP using 4 nodes, 16 processors per node. Predictive simulations were examined for converged instability after 10,000 timesteps in each case. Each simulation took approximately 30 minutes to complete on the IBM SP. Additional research on the effect of varied density gradients and of the roles of modified gradients for each of four plasma species is underway.

Heavy Ion Beam Optical Diagnostics. *BRYAN BELL (Shasta College, Redding, CA 96049) ALEX FRIEDMAN (Lawrence Berkeley National Laboratory, Berkley, CA 94720).* Heavy ion beam diagnostics consist of a slit that lets a portion of the heavy ion beam through and the scintillator that emits light when the ions strike it. Optical diagnostics are used to determine how 'good' a beam is. A beam needs to be spreading or contracting uniformly, if it's not, changes have to be made to the focusing magnetic and electric quadropules.In the High Current Experiment(HCX) at Lawrence Berkeley National Lab a potassium(k^+) ion beam is used. The ion beam injection energy is 1-1.6 MeV with a line charge density of 0.1-0.2μC/m. The goal of HXC is studying the transport of heavy ion beams the measuring the allowable "fill factor" (ratio of beam size to pipe size) improving the methods for determining the phase-space distribution of a beam. From an optical diagnostic station images are generated by the camera of the ion beam from the scintillator. When the ion beam passes through the slit it starts spreading out The spread is determined by the distance between the slit and the scintillator and the transverse velocity of the ions in the beam. From the spread we can obtain the transverse velocity of the ions in the beam x' =(u-x)/dz where u is a the horizontal coordinate of a pixel on the scinttilator x is the slit position and dz is the distance between the scintillator and the slit. By taking a small vertical slice of pixels on the scintillator and summing over the vertical axis f at x',x is obtained where x is the slit position. When this is done for all the vertical slices in the scintillor the distribution f(x') at the position the slit was at is formed. By making a composite of f(x') at each x another 2D image is made that shows the beam distribution as a function of x and x'. Similar things can be done to show the beam distribution as a function of y and y' from a slit that moves vertically. With the program that was written over the summer it will do all of the operations to derive the image that represents f(x,x') from a directory that contains the horizontal slit scan of the ion beam it also requires a text file describing the different properties of the experiment. The original goal of the project was to produce a 4D phase space distribution of the ion beam by synthesizing the to 2D data sets together. Unfortunately this wasn't accomplished in the ten week time frame but the program as it exists now does produce nice 2D results for f(x,x') f(y,y') and f(x,y) and does cubic and hermite interpolation on these 2D distributions.

Electronics Development for Free Electron Beam Diagnostics. *STUART BERGERON (Virginia Polytechnic Institute and State University, Blacksburg, VA 24060) KEVIN JORDAN (Thomas Jefferson National Accelerator Facility, Newport News, VA 23606).* New methods of signal processing of beam diagnostic systems for the Free Electron Laser (FEL) at Thomas Jefferson National Accelerator Facility will provide a better means to measure beam position and current. The existing Beam Position Monitor (BPM) system uses electronics adapted from the Continuous Electron Beam Accelerator Facility (CEBAF) machine for use in the FEL. This involves running large and expensive Radio Frequency (RF) cables out of the beam tunnel to high dynamic range electronics. The new BPM system will use embedded processors that take advantage of cell phone technology and the relative low dynamic range of the electron beam current in the FEL. Our team has tested the processors, filters, and amplifiers used in electronics chosen them according to their performance. This will allow complex BPM computation to be done more efficiently and with smaller, less expensive parts. The new processors are to be placed inside the tunnel, cutting down on the need for RF cable and running high-speed serial communication wires out of the tunnel. A circuit board designed by our team for RF to DC signal processing will also be built for the Beam Current Monitors (BCMs). Both BPM and BCM prototypes will be tested with signal from the FEL through Experimental Physics and Industrial Control System (EPICS) software and they will be calibrated. The new system, once in place, will allow for accurate beam measurement of beam position and beam current with simpler equipment.

Growth of Copper Oxide Nanorods on MgO (100). *LUKE BISSELL (Brigahm Young University, Provo, UT 84604) V. SHUTTHANADAN (Pacific Northwest National Laboratory, Richland, WA 99352).* We report the deposition of copper oxide films on MgO (100) and (110). The films were deposited by oxygen plasma assisted molecular beam epitaxy (MBE). The O_2 pressure was 1.0 x 10^{-5} torr. The deposition temperature was 675^{o}C. The films' chemistry, crystal structure, and morphology were characterized via in-situ x-ray photoelectron spectroscopy (XPS), atomic force microscopy (AFM), x-ray diffraction (XRD) and Rutherford backscattering spectroscopy (RBS). For the growth conditions listed above we observed the formation of oriented Cu_2O (110) nanorods on the MgO (100) substrate. The copper oxide deposited on the MgO (110) substrate exhibited grain structures.

Validation of a Dual-Head Scintimammography System in Early Detection of Small Breast Lesions. *RACHEL BLACK (Morgan State University, Baltimore, MD 21251) STAN MAJEWSKI (Thomas Jefferson National Accelerator Facility, Newport News, VA 23606).* Scintimammography is a nuclear medicine imaging method of breast cancer tumor detection that uses injected radiopharmaceuticals which carry a gamma ray emitting radioactive isotope to mark certain biological processes involved in breast cancer. This research was undertaken because of limitations in scintimammography using traditional single-headed gamma cameras in breast imaging. A single-headed system has several limitations that limit tumor detection. It is proposed that creating a system utilizing two gamma cameras to simultaneously image opposite sides of the breast will improve the imaging procedure by having one detector able to image lesions that the other detector may miss due to location of the lesion. The purpose of this study is to demonstrate that one can obtain more accurate readings with a dual-head system versus a single-head system. The Detector Group has designed and built a system that consists of two compact gamma cameras; the system is being tested at the University of Virginia (UVA) for testing. Each of the two gamma cameras are composed of a high resolution lead collimators and NaI(Tl) crystal scintillator arrays (crystal pixel size 3.0mm and intercrystal septa 0.2mm) which are optically coupled via a light guide to an 8x6 array of position sensitive photomultiplier tubes(PSPMTs). The Hamamatsu R7600-00-C8 PSPMTs are connected to a high voltage board with tube sockets that supply voltage to the tubes, and a signal conditioning board where the anode signal is amplified, shaped, and read into the computer. Results are obtained using a liquid filled plastic breast model known as a breast phantom. The breast phantom contains one or more radioactive lesions of various sizes. The typical contrast ratio of lesions in breast material has been found to be 6:1; therefore the breast phantom and lesion are filled to simulate this ratio. Initial experimental results showed substantial improvements in lesion imaging suggesting that two gamma cameras create a more sensitive system regardless of the lesion location or size. The system has potential to improve detection of small breast lesions and eventually to be implemented into a clinical environment for trial studies.

Analysis of the Stripper Foil for the Rare Isotope Accelerator. *HENRY BLAKES (Southern University A&M College, Baton Rouge, LA 70813) JERRY A. NOLEN, JR. (Argonne National Laboratory, Argonne,*

IL 60439). The Rare Isotope Accelerator (RIA) is the highest priority of the nuclear physics community in the United States for a major new facility. RIA is a next generation facility for basic research with radioactive beams that utilizes both standard Isotope-separator On-line (ISOL) and in-flight fragmentation methods with novel approaches to handle high primary-beam power and remove existing limitations in the extraction of short-lived isotopes. A versatile primary accelerator, a 1.4 GV, CW superconducting designed to simultaneously accelerate several heavy-ion charge states, will provide beams from protons at 900 MeV to uranium at 400 MeV/u at power levels of 400 kW. The wide variety of primary beams allows various production and extraction schemes to be used to optimize production of broad range of energies. By doing so they can be delivered at ion source energy for stopped-beam studies, reaccelerated by a second superconducting linac, or directly separated in-flight for use at energies up to 500 MeV/u.

Evidence for an Isomer in ^{254}No. *RYAN BLINSTRUP (Monmouth College, Monmouth, IL 61462) TENG LEK KHOO (Argonne National Laboratory, Argonne, IL 60439).* Nuclei with Z>92 are unstable due to fission. However, due to a large shell-correction energy, nuclei with Z up to 116 have be observed. The shell structure of 254No pulls its ground-state down and creates a barrier against fission. To further the study of super-heavy nuclei, the structural information of ^{254}No is studied by confirming an isomer and determining its spin in a ^{208}Pb(^{48}Ca,^{2}n) reaction. The double-sided silicon strip detector (DSSD) was calibrated for the electron data. Coincidence gates were set to only detect electron and alpha particles from the 254No isomer. The evidence for an isomer consisted of a sequence of three events: a ^{254}No implant, an electron detected 1.4s after the implant, and then an alpha particle within 2 min. The measured electron distribution spectrum was compared with model spectra of electrons from isomers with different spins. The measured electron distribution spectrum had a low yield of electrons beyond 306keV. The model of the 7- isomer decay spectrum had the same feature. Further observation of the gamma ray spectra will confirm the spin.

Investigation of Molecular Electrical Properties Using Au/Ge Thin Films. *TANINA BRADLEY (North Carolina A&T State University, Greensboro, NC 27411) MYRON STRONGIN (Brookhaven National Laboratory, Upton, NY 11973).* In this work we present the results of the nano-structural studies and electrical characterization of Gold (Au) films on ambient temperature or cooled amorphous Germanium (Ge) substrates. We were able to produce monolayers of Au that are 0.3-3 nm thick. These films were fabricated under high vacuum conditions (~10^{-8} Torr) using thermal evaporation. We used a simple series resistor circuit for in situ measurement of resistance of the film during deposition. This method allowed us to detect the continuous formation of the Au layers. The sheet resistance was measured as a function of temperature and thickness. The nano-structure of the films was determined using Atomic Force Microscopy (AFM). For the thinnest layers of Au on Ge we saw no structure in the AFM and we suspect that the thin Au layers alloy with the Ge. The temperature dependence of sheet resistance shows activated behavior. These initial experiments indicate that it may be possible to study thin layers of Au with sheet resistance approaching 10^{12} Ω/m^2. This possibility could result in experiments measuring the change in resistance when thiols and other molecules are put on the Au surface.

Array of Veto Counters for the World's Largest Neutron Detector. *CHRISTOPHER BRITTIN (The College of William and Mary, Williamsburg, VA 23187) BOGDAN WOJTSEKHOWSKI (Thomas Jefferson National Accelerator Facility, Newport News, VA 23606).* Veto counters for the scheduled E02-013 experiment at Jefferson Lab were evaluated. The JLab experiment will measure the electrical charge of the neutron at short distances. A veto detector will be implemented in order to distinguish neutrons from charged particles. The veto detector consists of 192 counters, with each counter consisting of a plastic scintillator optically coupled to a photomultiplier tube (PMT) via a light guide. It is important that the veto detector perform at a high efficiency, therefore characteristics such as signal amplitude attenuation, time resolution, and the required supply voltage must be known for each counter. Counters were evaluated on their ability to detect cosmic rays relative to the coincidence rate of two large scintillator counters placed vertically one above the other. Coincidence signals from the large counters were used to trigger events in the Analog-Digital-Converter (ADC) and the Time-Digital-Converter (TDC). Data was analyzed using the UNIX program Physics Analysis Workshop (PAW++). Attenuation characteristics were determined by investigating the signal amplitude as a function of the "position" of the upper counter. Time resolution characteristics were determined by investigating the difference between the coincidence time signals of the veto counter and the large counters. The required high voltage supply was determined (defined to be that voltage which places the ADC peak 100 channels above the pedestal, as dictated by the operational needs of E02-013). Analysis yielded the following mean values for the counters: a -1.08 kV required high voltage setting, a 14% signal amplitude attenuation per meter, and a time resolution of 0.4 ns. This is a sufficiently low high voltage setting and a sufficiently good time resolution. The attenuation is also sufficiently low, which will allow a high signal threshold to be implemented for the veto detector, increasing its efficiency. Based on these results it can be concluded that the counters satisfy the operational needs of the E02-013 JLab experiment.

Developing Control System of Electron Cyclotron Resonance Ion Source for Determining Ion Charge States. *KEVIN BROADNAX (North Carolina A&T State University, Greensboro, NC 27411) PETER OSTROUMOV (Argonne National Laboratory, Argonne, IL 60439).* Highly charged ions are being created by Electron Cyclotron Resonance Ion Sources (ECRIS) in laboratories for a wide range of studies. The goal of the ECRIS is to further explore the capabilities of the efficient production of the intermediate and high charge state ion beams that can be accelerated and used for the generation of rare ion beams. The ECRIS bending magnet can reach a maximum field strength of 13 kG. The G Programming language LabVIEW 6.1, developed by National Instruments, is the primary instrument controller that is used to regulate the control systems for the ECR ion source. LabVIEW's hardware linkage capabilities allow it to communicate with devices in order to properly acquire and analyze data from the ECRIS. The ECRIS bending magnet power supply receives a voltage signal from data acquisition cards which convert LabVIEW's digital communication into an analog signal. Serial communication is used to retrieve the magnetic field measurement from a digital gaussmeter. General Purpose Interface Bus (GPIB) interface cards sends and reads string data to a picoammeter, and all of this data is collected and organized by LabVIEW. From these measurements we should calculate the charge states of the various ions that are produced in the ECRIS ionization chamber.

Quantum Efficiency of Metal Photocathodes. *MAKINI BYRON (Columbia University, New York, NY 10027) TRIVENI RAO (Brookhaven National Laboratory, Upton, NY 11973).* Photoemission is a naturally occurring phenomenon in which photons striking a metal surface excite electrons and cause them to escape. The quantum efficiency (QE) of this process is defined as the ratio of electrons emitted from a surface to the number of photons that are incident on that surface. The purpose of this experiment was to measure the QE of photocathodes with different surface preparations using a continuous stream of ultraviolet light, and determine the best conditions for an optimum QE. The factors varied were the material of the cathode, the applied electric field, the wavelength of light incident on the cathode, and the "cleanliness" of the metal surface. The cathodes studied were polished copper, lead sputtered copper, and lead sputtered niobium. By using interference filters, the UV light was separated into narrow bandwidths of approximately 20nm, for wavelengths from 200nm to 300nm. A photodiode and meter were used to measure the power of the light incident on the photocathode. The emission of electrons was measured as a current using an electrometer. It was found that the quantum efficiency was greatest with light at shorter wavelengths. These wavelengths correspond to energies that are above the work function of the metal. There was a QE dependency on voltage, as well as the laser energy used in cleaning. Direct exposure of the cathode to the UV light source also had a cleaning effect on it, possibly removing surface impurities by a photochemical reaction instead of ablation. UV cleaning might prove to be useful in applications where a laser is not readily available for cleaning. The results of this experiment will be useful in determining the optimum conditions for producing high average current electron sources for high energy accelerators and high power light sources.

Statistical Analysis of the KOPIO Test Beam Data. *CRYSTAL CANTLEY (St. Joseph's College, Patchogue, NY 11772) JENNIFER MABANTA (St. Joseph's College, Patchogue, NY 11772) MICHAEL SIVERTZ (Brookhaven National Laboratory, Upton, NY 11973).* According to the Big Bang Theory, it is assumed that the creation of matter and antimatter would have been an equal distribution. However, if the laws governing matter and antimatter were symmetrical, then we would not have a universe today. The answer to this intriguing paradox may lie in what is known as charge parity (CP) symmetry violation. The purpose of the KOPIO experiment is to study rare decays of the neutral K-meson, which seems to display this CP symmetry violation. In order to observe these rare decays taking place, KOPIO makes use of the Alternating Gradient Synchrotron (AGS) accelerator, located at Brookhaven National Laboratory. The most recent test runs using the AGS took place in May of 2004. Through analyzing this data, the performance of the AGS will be improved enabling the KOPIO experiment to study these rare decays, providing useful insight into CP symmetry violation, which may

contribute to the dominance of matter over antimatter in the universe. With over two million events represented in the data from the test beam, powerful analytical tools such as the Physics Analysis Workstation (PAW), developed by the CERN laboratory in Geneva, Switzerland, will be used to manipulate the data effectively. This program will take into account the amount of uncertainty in these measurements. Using FORTRAN, a program was created to manage the large amounts of data, in order to make the calculations accessible to PAW. As more is discovered about how the data structures function, it will be necessary to make adjustments in the program to create the most useful histograms of the results. Understanding the findings of the KOPIO experiment may have the capability of testing our knowledge of some of the most basic laws of physics concerning the evolution of the early universe.

Structural and Magnetic Properties of the A-site Ordered Perovskite Manganites $RBaMn_2O_6$ (R = Pr, Nd, $Pr_{(1/2)}Nd_{(1/2)}$). *HUGH CHURCHILL (Oberlin College, Oberlin, OH 44074) YANG REN (Argonne National Laboratory, Argonne, IL 60439).* The temperature- and magnetic field-dependent structural properties of the half-doped A-site ordered manganites $RBaMn_2O_6$ (R = Pr, Nd, $Pr_{1/2}Nd_{1/2}$) have been studied using high energy X-ray powder diffraction. The antiferromagnetic to ferromagnetic phase transitions of all three materials are accompanied by first-order structural changes. The phase transition temperatures are shifted by 15–25 K in a magnetic field of 6 T. Both phases of $PrBaMn_2O_6$ and $Pr_{1/2}Nd_{1/2}BaMn_2O_6$ have tetragonal structures (space group P4/*mmm*), though the ferromagnetic phase of $Pr_{1/2}Nd_{1/2}BaMn_2O_6$ shows significant broadening of the (200) diffraction peak, suggesting a slight orthorhombic distortion of the tetragonal cell. $NdBaMn_2O_6$ is tetragonal (P4/mmm) in the antiferromagnetic phase and orthorhombic (Pmmm) in the ferromagnetic phase. This orthorhombic structure is considered in the context of the charge/orbital ordering found in ordered $RBaMn_2O_6$ (R = Y and rare-earths) with R^{3+} ionic radius less than that of Nd^{3+}. Orthorhombic strain is suggested as a critical parameter in the ferromagnetic to charge/orbital ordered transition in $RBaMn_2O_6$ as R^{3+} ionic radius decreases. Highly anisotropic thermal expansion is observed in $RBaMn_2O_6$ and is explained in terms of a change in orbital occupancy of the e_g electrons from the $d_{x^2-y^2}$ state to the $d_{3z^2-r^2}$ at the antiferromagnetic to ferromagnetic transition.

Emittance Measurement of an Oxygen-16 Beam. *SAMUEL CLAPP (Williams College, Williamstown, MA 01267) RICHARD PARDO (Argonne National Laboratory, Argonne, IL 60439).* With the Rare Isotope Accelerator (RIA), a Department of Energy-sponsored facility to be built in the near future, researchers will be able to create beams of unstable, neutron-rich nuclei that will help understand the processes by which heavy elements are created in catastrophic environments such as supernovae. Some of these beams will be created by a fragmentation process whereby a beam of stable nuclei is accelerated into a target where the nuclei are fragmented and converted into a beam of unstable nuclei. Understanding the optics of these kinds of the stable beams and learning how to control them are important parts of conducting research of this nature. One measurement that can help us understand these things is the emittance, a quantity that helps determine the quality of a beam. In this project we developed an emittance measuring system and conducted some initial measurements of a stable Oxygen-16 beam, which will help understand the initial stages of the acceleration process in RIA. The scanned wire emittance diagnostic was used, and software was developed with LabVIEW to conduct the procedure. The procedure involved doing a preliminary scan of the beam to determine its size and its center, and then measuring the emittance. The system worked very well at taking large amounts of data and formatting it properly. However, the system still needs to be optimized in order to produce higher quality data.

Detection and Suppression of Time-Varying Magnetic Fields that Adversely Affect a 100 keV Electron Beam Orbit. *JENNIFER COOPER (Clemson University, Clemson, SC 29632) JOSEPH GRAMES (Thomas Jefferson National Accelerator Facility, Newport News, VA 23606).* Magnetic fields both positively and negatively affect the electron beam orbit in a 100 keV beamline in the Test Lab, Injector Test Stand (ITS) at JLab. DC air-core magnets and iron solenoid magnets are used to steer and focus the electron beam throughout the beamline, but time-varying magnetic fields (prominent at power line frequency) adversely modulate the electron beam orbit. Concentrating on these problematic time-varying magnetic fields, a number of steps were taken to identify the sources of these fields and engineer a design to shield the beamline. Photographs of a viewer mounted inside the beamline were taken to estimate the displacement of the electron beam due to the varying magnetic fields. In addition, an Extech electromagnetic field adaptor (AC Gauss meter) was used to survey the beamline in a grid-like fashion to identify sources of time-varying magnetic fields. Non-essential power supplies were turned off and others relocated further away from the beamline. Little improvement was found when non-essential power supplies were eliminated because a power supply located beneath the beamline floor was detected and identified as the dominant source. Different metals, in a variety of shapes and designs, were tested to find the best way to redirect or suppress the fields from the beamline, while not interfering with the function of the DC steering magnets. Mumetal, a magnetic alloy, and enclosed shapes were found to best shield these magnetic fields. Bench tests for engineering solutions showed that by applying mumetal shields around beam pipe and steering magnets, time-varying magnetic fields could be greatly reduced. The time-varying magnetic fields were redirected and decreased the electron beam motion as measured using the viewer, without significantly altering the DC steering magnets.

Setup and Calibration of Stanford Linear Accelerator Center's (SLAC) Peripheral Monitoring Station (PMS) System. *CHRISTOPHER COOPER (Cornell University, Ithaca, NY 14853) JAMES LIU (Stanford Linear Accelerator Center, Stanford, CA 94025).* The goals of this project were to troubleshoot, repair, calibrate, and establish documentation regarding SLAC's (Stanford Linear Accelerator Center's) PMS (Peripheral Monitoring Station) system. The PMS system consists of seven PMSs that continuously monitor skyshine (neutron and photon) radiation levels in SLAC's environment. Each PMS consists of a boron trifluoride (BF_3) neutron detector (model RS-P1-0802-104 or NW-G-20-12) and a Geiger Müller (GM) gamma ray detector (model TGM N107 or LND 719) together with their respective electronics. Electronics for each detector are housed in Nuclear Instrument Modules (NIMs) and are plugged into a NIM bin in the station. All communication lines from the stations to the Main Control Center (MCC) were tested prior to troubleshooting. To test communication with MCC, a pulse generator (Systron Donner model 100C) was connected to each channel in the PMS and data at MCC was checked for consistency. All electronics from each non working station were brought into the lab for troubleshooting. Troubleshooting usually consisted of connecting an oscilloscope or scaler (Ortec model 871 or 775) at different points in the circuit of each detector to record simulated pulses produced by a pulse generator. The detectors and electronics were calibrated in the field using radioactive sources. Detector response for the BF_3 detector was dependent on the energy of the incident radiation. This was not needed for the GM detectors since GM detector response is only dependent on radiation energy below 100 keV; SLAC only produces a spectrum of gamma radiation above 100 keV. For the GM detector, calibration consisted of bringing a ^{137}Cs source and a NIST-calibrated RADCAL Radiation Monitor Controller (model 9010) out to the field; Calibration of the BF_3 detector was done using NIST certified neutron sources of known emission rates and energies. Five neutron sources ($^{238}PuBe$, ^{238}PuB, $^{238}PuF4$, $^{238}PuLi$ and ^{252}Cf) with different energies were used to account for the energy dependence of the response. Once the total dose rate (sum of the direct and scattered dose rates) was known, the response vs. energy curve was plotted. The first station calibrated (PMS6) was calibrated with these five neutron sources; all subsequent stations were calibrated with one neutron source and the energy dependence was assumed to be the same.

Testing a Prototype Lead Glass Calorimeter Using Studies of Electron Proton Elastic Scattering. *JUAN CORNEJO (California State University at Los Angeles, Los Angeles, CA 90032) MARK JONES (Thomas Jefferson National Accelerator Facility, Newport News, VA 23606).* Previous four-momentum transfer squared (Q2) measurements have not revealed perturbative Quantum ChromoDynamics helicity conserving scaling in the form factor ratios. Experiment E01-109, approved to run in Hall C at Jefferson Laboratory (JLab), will extend the form factor ratio studies to a Q2 of 9.0 GeV2 using elastic electron proton scattering. In the experiment the protons will be detected in the High Momentum Spectrometer (HMS) and the electron will be detected in a lead glass calorimeter which is currently under construction. A prototype calorimeter was created and tested using the HMS during the summer of 2004. This study tested the prototype calorimeter for its angular resolution using the over determined kinematics of the electron proton elastic scattering, and its ability to produce a clean coincidence peak using triggers from the HMS. Fortran 77 subroutines were created and entered into the Physics Analytical Workshop (PAW) program to calculate differences between predicted kinematics and measured kinematics. Positions and angles of coincidence electron were measured in the calorimeter by using a weighted average of the signals in each of the lead glass blocks in the calorimeter. This study has revealed a clean timing coincidence peak in the data. Though the resolution tests have not jet yielded a definite resolution. This test has also revealed rate is-

sues with the HMS triggers that need to be addressed for the upcoming experiment.

Analysis of the Stipper Foil for Rare Isotope Accelerator (RIA). *BRANDAN DARENSBOURG (Southern University, Baton Rouge, LA 70813) JERRY NOLEN (Argonne National Laboratory, Argonne, IL 60439).* The Rare Isotope Accelerator (RIA) is a facility with the ability to provide the highest-intensity beams of stable heavy ions for the production of rare isotopes. It does this through a method of accelerating the beam to a particular degree and then sending it though some type of foil. This foil will be some complementary element, which will then cause the striping of particles. These particles will scatter in an array of angles. What I have done in my stay here at Argonne National Laboratory is to take some estimated data as well as some crude form of data and analyze it through a number of different aspects. Optimizing this data according to the angle, energy, or particle type. The first data that received consisted of the incident number, the atomic number of the particle, particle weight, the angle in radians, and the energy in GeV/u. I was to convert this data into a form where it would be most feasible for us to see a specific amount of data on a particular element, in this case Uranium-238. First, I was to convert the energy from GeV to MeV and the angle from radians to mili-radians. With these units I was able to use more common formulas to reach the momentum of the particle incident particles throughout my data. Once I had the data in the correct units and momentum calculated we could then begin to exclude any data that was not necessary for plot we were trying to configure. We eliminated the unwanted data by removing all data that was outside a particular angle range of scattering, in this case all data less than negative seven mili-radians and all data greater than positive seven mili-radians. We also removed all data that was plus or minus a half a percent of the average energy of the Uranium-238 particles. From this data we were able to create a histogram which showed us the curve of counts (the number of incidents) versus the energy (in MeV/u). We also developed a plot from this data which showed the counts versus the momentum. From this data we were able to see different possibilities of the scattering, energy, and momentum of the Uranium 238 through the Carbon Stripping Foil.

Investigation of a Rotating Arc Spark Plug for use in a Stationary Power Lean-Burn Natural Gas Engine. *JOSEPH DURHAM (Carleton College, Northfield, MN 55057) JOHN ANDRIULLI (Oak Ridge National Laboratory, Oak Ridge, TN 37831).* The U.S. Department of Energy's Advanced Reciprocating Engine Systems (ARES) Program aims to reduce emissions from incomplete combustion and increase efficiency in natural gas power generator engines. Ultra-lean burn combustion would go a long way towards these goals but has been difficult to implement because of erratic combustion near the lean limit. The purpose of the Rotating Arc Spark Plug (RASP) portion of the ARES program is to reduce variability in ignition and potentially decrease wear on spark plugs. The RASP design utilizes an axial magnetic field imposed on a radial gap plug. The resulting Lorentz force causes the arc to rotate circumferentially between an inner and outer electrode, sweeping out a volume of space. Probability of ignition is increased by both increasing the volume of air-fuel mixture exposed to the arc and the increase in temperature of the arc plasma due to the magnetic field. A pressure chamber filled with instrument air was used to study RASPs at compression pressure. Properties of arc breakdown and rotation were studied at various pressures and gaps. The RASP design was also tested in a small, aluminum Kohler engine and the need for a final design iteration was discovered. The new design places the arc near a magnetic field peak outside of the cylindrical magnet and should allow the air/fuel mixture access to the arc location. The properties of the magnetic field in the new RASP configuration were studied to examine the viability of operating in a cast iron engine. Magnetic field studies indicate that around 50% of field strength is sacrificed under the new configuration, but methods of enhancing the external peak were discovered. This study also indicates that the RASP could function properly in a cast iron engine. Results from pressure chamber tests indicate total rotation and rotation rate decrease as pressure surrounding the RASP increases, and rotation is also decreased by gap size. It is believed that the new RASP configuration should provide substantial benefits to engine combustion reliability and plug erosion. Engine testing and analysis will commence once the new RASPs have been fabricated.

Reworking the CES Cluster Reconstruction Algorithm. *STEPHEN FEDELE (Yale University, New Haven, CT 06520) PAVEL MURAT (Fermi National Accelerator Laboratory, Batavia, IL 60510).* Tau leptons can decay either leptonically ($t \rightarrow e\ v\ v$) or hadronically ($t \rightarrow p\ v$ + any number of pi0s). The leptonic decay channel is difficult to detect due to the large amount of background caused by the very similar W-boson decay into an electron and neutrino. The importance of the hadronic decay channel in tau detection thus necessitates the ability to reconstruct such neutral pions. Such reconstruction occurs in CES, a strip chamber located within the electromagnetic calorimeter in the B0 detector at Fermi. Considering that high Pt pi0s decay into photon pairs, the ability to resolve overlapping clusters becomes very important in pi0 and thus tau reconstruction. The current reconstruction algorithm uses track and seed based windowing method. However, should a two clusters (perhaps overlapping) fall within the same window, one will fail to be reconstructed. A new method is proposed that uses a more advanced pattern matching algorithm to resolve clusters, even those that are overlapped. This new algorithm offers several benefits over the old one. It accomplishes reconstruction in a single pass, as opposed to the three passes required before. Further, the reconstruction is done completely within CES, independent of other portions of the detector. The ability to more accurately resolve clusters allows for tighter cuts on position. Ultimately, the new algorithm allows for more statistics as fewer events are suppressed or missed due to the old algorithm's shortcomings. In addition, due to the higher efficiency of the cuts with the new algorithm, such statistics will be cleaner with more desired events. This will allow better reconstruction of photons, pi0s and thus taus, thus giving more precise measurements of tau mass. At its current point, the algorithm does effectively resolve merged clusters. Early results from Monte Carlo simulations are promising, though more testing needs to be done to ensure proper reconstruction in the algorithm.

ATLAS Pixel: Quality Control of Front-End FE-I3 Chips. *ERIC FENG (University of California, Berkeley, Berkeley, CA 94720) MAURICE GARCIA-SCIVERES (Lawrence Berkeley National Laboratory, Berkley, CA 94720).* ATLAS is an international collaboration to build the next-generation high energy particle detector for the Large Hadron Collider (LHC) at CERN. The innermost of the three concentric detectors comprising ATLAS is a pixel detector that is positioned directly outside the LHC beam pipe. The pixel detector's building block is the module, which consists of a 250mm thick, finely pixilated silicon sensor tile that is bonded via indium bumps to 16 "Front End" silicon integrated circuits (FE-I3 chips). Each of the 50x400mm sensor pixels is read out by an independent channel on one of the FE-I3 chips. Quality control of these high-precision FE-I3 chips is vital to ensure the high detector efficiency required to distinguish individual tracks among the hundreds produced every 25ns by the LHC collisions. We describe electrical tests and visual inspections of 2,016 Front-End FE-I3 chips that were tested between 1/20/04-5/6/04 for use in module construction for the pixel detector. A host of electrical tests were performed on the wafers before and after they were diced into individual chips, which determined that there is a 1% degradation in the electrical quality of the chips that occurs during dicing and indium bump deposition. Visual inspections were performed on chips to filter out those with indium bump defects such as residual photoresist, merged bumps, smeared or missing bumps, and debris. These quality control checks resulted in an overall electrical yield of 62.7% and a visual yield of 86.8%. These figures compare favorably with the conservative projections of 50% and 85% that were used to purchase chips for the pixel detector.

An Exploration of Analysis Software at Stanford Linear Accelerator Center (SLAC) Through the Study of X(3872). *ANDREW FISCHER (Harvey Mudd, Claremont, CA 91711) VALERIE HALYO (Stanford Linear Accelerator Center, Stanford, CA 94025).* X(3872), a particle discovered by Belle Labs, has not yet been described in a sufficient enough way by any group to draw definitive conclusions about it. In order to verify the claims of Belle Labs and learn more about X(3872), Stanford Linear Accelerator Center (SLAC) has undertaken a project to analyze the particle, a subgroup of the BaBar project. The computing systems involved are complex; the tutorials for the software and new software releases both need constant testing and revision. Using a new software release, I tested tutorials for various software used by the BaBar group, including UNIX, Root, and CM2, in an effort to eventually analyze X(3872) data. The offline workbook for the BaBar software needs to be better maintained, and the CM2 tutorials need to be modified and updated. While none of my results contributed directly to the project (i.e., I have no results that add to information about X(3872)), improvement of the tutorials will streamline integration of new scientists into the BaBar group.

The Complexities of Environmental Tobacco Smoke and How They Affect Exposure Assessment. *DAVID FISHER (North Park University, Chicago, IL 60625) MICHAEL G. APTE (Lawrence Berkeley National Laboratory, Berkley, CA 94720).* Researchers have studied Environmental Tobacco Smoke (ETS) to quantify the dynamic behavior and toxicity of each constituent. Understanding the behavior of ETS constituents is critical to accurate exposure assessment for health effects studies. In trying to accurately assess exposure in a number of

smoking scenarios, researchers are finding that ETS is far more complex than once thought. The ultimate goal for researchers is to establish a set of tracers that successfully track the dynamic behavior of ETS for further field study in the health effects of ETS. In establishing the set, each marker constituent must represent characteristics of several other components of ETS. Problems in exposure assessment can because of the different dynamic behaviors of the constituents, such as differences in ETS gas and particle constituent behaviors. In particular, the use of nicotine as a tracer may cause exposure assessment misclassification because the dynamic behavior of nicotine is not similar to most other components of ETS. Research in component specific tracing has been deemed necessary for exposure and health effects to a given component. Two key factors affect the relative behavior of gas phase ETS tracers: ventilation and sorption. Sorption can be studied independently while ventilation experimentation must take sorption into consideration when interpreting data. Sorption experiments have been established to study ETS in real world conditions, meaning fully furnished rooms. Particle phase tracing must take into consideration particle size-dependent deposition rates as well as ventilation. Three particle size related classifications are studied. Functionally, these are lung alveoli absorbing particles, bronchial depositing particles, and nose and pharynx depositing particles. Particles also have more complex behavior considerations than gases, such as gravity, diffusion to surfaces, volatilization, and particle binding. This paper presents the complexity ETS and the limitations that tracers present in thorough exposure assessment

Empirical Bench-top Testing for Silicon Electron Beam Transmission Windows. *EVAN FRIIS (University of California, San Diego, La Jolla, CA 92093) CHARLES GENTILE (Princeton Plasma Physics Laboratory, Princeton, NJ 08543).* A silicon (Si) based electron beam transmission window is being developed for use in a KrF laser system in support of Inertial Fusion Energy. A 150 mm thick Si foil separates the KrF lasing medium from the electron beam source which is maintained at vacuum. Si has emerged as an excellent candidate due to its high strength, low Z, desirable thermal properties, and high electron transmission. The device must withstand cyclic (5 Hz) pressure differentials (2.3 atm), thermal load (300 C), and a highly corrosive environment with a minimum 80% e-beam transmission. To prevent corrosive degradation, one face of the window is coated with a 1.2μm diamond passivation barrier. This hostile environment presents a challenge in simulation. The high rate of change in the system preclude mass transfer techniques due to hysteric effects, and mechanical solutions prevent control of the pressure waveform. A novel solution to simulate the DP conditions is the use of a high displacement voice coil actuated diaphragm. The diaphragm and e-beam window constitute two walls of the chamber that simulates the lasing medium. A current applied through voice coil applies a force against the diaphragm, lowering the volume of the chamber and increasing the pressure. A chamber on the opposite window side is maintained at vacuum. Thermal loading is achieved via resistive heating elements, and a separate fluorine gas enclosure is utilized. The testing apparatus is currently being fabricated. Initial diaphragm reinforcement and excursion limit testing has indicated the diaphragm will be able to generate the requisite pressures. Ideas for creating an improved second generation apparatus and other potential applications for this technology are discussed.

Analysis of the Tiny Triplet Finder Algorithm for Track Segment Finding in BTeV's Level 1 Trigger System. *HENRY GARCIA (California State University, Sacramento, CA 95819) JIN YUAN WU (Fermi National Accelerator Laboratory, Batavia, IL 60510).* In order for the computer farms at Fermilab's C0 facility to be able to handle the data coming from the proposed BTeV detector, an efficient and reliable trigger needs to be developed to filter out any uninteresting data that does not need to be saved. Specifically, the level 1 trigger must execute once every 132 ns. The tiny triplet finder (TTF) algorithm is designed to replace the current BB33 algorithm for the pattern recognition stage of the BTeV level 1 trigger system. The TTF algorithm finds small segments of tracks within a rectangular volume whose two end faces are defined by the first and last pixel stations. Since pixel clusters in three adjacent stations are used to find these segments, these segments will be referred to as triplets. These triplets will then be combined to reconstruct the tracks due to a collision. The TTF algorithm improves the speed of this portion of the trigger from O(n2) to O(nlogn) while also freeing up space in the field-programmable gate arrays (FPGAs) which may be used for further analysis of the data. This research analyses the efficiency and reliability of the TTF algorithm by simulating the electronics using the C programming language and simulated proton/anti-proton collision Monte Carlo data. Although, various flavors of the algorithm have been implemented yielding a high percentage (99 - 100%) of track segments found, this research shows that this algorithm yields a large number of fake triplets as well. Various cuts have been implemented to try to reduce the number of fake triplets found. However, further cuts will need to be made to the data for the gain of speed and FPGA space to outweigh the cost of such a high increase in fake triplets. With further analysis of the triplet data, it may be possible to reduce the number of fake triplets enough to justify the use of the TTF algorithm in BTeV's level 1 trigger.

Data Acquisition System for Fluorescence Testing of ^{225}Ra. *ANDREW GIAGNACOVA (Lincoln Univsersity, Lincoln University, PA 19352) ZHENG-TIAN LU (Argonne National Laboratory, Argonne, IL 60439).* The permanent Electric Dipole Moment of Ra-225 will be measured to test the time reversal invariance violation. An atomic beam of Ra-225 will be trapped with a magneto optical trap. To effectively trap the atoms the trapping lasers must be tuned to a resonant frequency of the Ra-225. To measure this frequency a laser will be positioned transverse to the atomic beam. We will vary the wavelength of the laser and use a photodiode to measure the light intensity of the laser atomic beam interaction. A system was devised to collect the data from the photodiode as well as render that analog signal into a TTL logic pulse to be acquired by a PC based data acquisition system.

Noise Reduction in the Solid-State Neutral Particle Analyzer. *MATTHEW GOMEZ (University of Michigan, Ann Arbor, MI 48109) A. LANE ROQUEMORE (Princeton Plasma Physics Laboratory, Princeton, NJ 08543).* A solid-state neutral particle analyzer (SSNPA) is being used to detect the escape of high-energy particles on the National Spherical Torus Experiment (NSTX). The SSNPA has four surface-barrier detectors, which view the horizontal midplane of NSTX. The output pulse amplitude of the detectors is proportional to radiation energy. Neutral particles with energies up to 100 keV can be observed. The SSNPA is used to link changes in energetic particle flux with plasma events, but the present noise level prevents this. Two solutions are being tested to fix this problem: 1) Increase the signal to noise ratio (S/N) in the system or 2) Ultra-fast digitization (UFD) of the signal. In an effort to increase the signal before noise is introduced, a preamplifier with 3x gain and a close-coupled second stage amplifier are being tested. These new electronics are battery powered to eliminate excess ground loops and they increase the signal by a factor of ~1000 before noise is introduced in the cable. With UFD the signal is input to the digitizer, and post-shot analysis separates the signal from the noise using pulse height analysis software. Improving the analog electronics has increased the S/N by a factor of two using the increased gain preamplifier and the original amplifier. This indicates that most noise is entering the system at or before the preamp. Further testing is being performed to confirm this. UFD is being used on NSTX but time constraints prohibit a significant amount of data from being collected. The limited results indicate that UFD will likely improve signal interpretation. In a similar experiment, UFD has been implemented on a test reactor at MIT with promising results. At MIT different sources of electronic noise were confirmed with UFD, and then reduced or eliminated. This indicates that while improving traditional analog electronics may make some progress, digital signals will yield better results. In the future UFD will be further utilized on NSTX to identify types of noise, which will aid in the elimination of that noise.

Creating a Non-invasive Technology to Move Magnetic Particles in the Brain Using High Temperature Superconductors. *ANAND GOPALSAMI (The University of Chicago, Chicago, IL 60637) JOHN HULL (Argonne National Laboratory, Argonne, IL 60439).* High temperature superconductors have the ability to trap a permanent magnetic field as long as its temperature remains below 77 degrees Kelvin. By pulsing the superconductor with a large current, a magnetic field can be induced and negated. Setting up a series of superconductors will allow the movement of a magnetic particle across them by turning on and off the magnetic field of each superconductor. This technology can be utilized to non-inversely treat ailments inside the human brain; antitoxins can be placed onto a magnetic particle which will be guided to the specific area of cancer. This research involves testing and understanding the complexities of high temperature superconductors and how they work in various environments. By simulating blood flow rate in the human body using plastic tubing filled with water and glycerin, a superconductor could hold a small magnetic particle (a few millimeters in diameter) at a distance of three centimeters and a flow rate of 350 ml/min. These numbers need to be increased to a distance of ten centimeters and a flow rate of about 1000 ml/min to account for optimal conditions in the human brain. Moving the magnetic particle from one superconductor to another was achieved with the flow and against the flow. Refinement of this process is underway, because there is no room for error when transporting chemical agents in the body. There is much to do still, but the potential of this research is limitless.

Second Order Effects in Beam Position Monitor (BPM) Response. *ADAM GRAY (University of Georgia, Athens, GA 30609) THOMAS RUSSO (Brookhaven National Laboratory, Upton, NY 11973).* Six of The Department of Energy's laboratories are teaming together to build the Spallation Neutron Source (SNS) at Oak Ridge National Laboratory. The SNS project will focus on research using intense pulsed neutron beams. Brookhaven National Laboratory's Collider-Accelerator Department is responsible for the designing, building, and testing of the Ring System for the SNS project. Beam Position Monitors (BPMs) are used to determine beam position in particle accelerators. Magnets with adjustable magnetic fields, called dipoles and quadrupoles, are built and strategically placed in accelerators to manipulate the beam's position so that it is in the center of the beam pipe. These magnets bend and focus the beam. The electrical center of the BPM, the point where current from the beam is the same on all BPM electrodes, should be extraordinarily close to the mechanical center, the center of the aperture. Using a scanning apparatus, the coordinates of these centers are determined. A raster scan, a scan that spans the entire aperture in 1.0 mm increments, is performed. The aperture that the scan spans is dependent on the diameter of the BPM. A larger BPM has a larger aperture. The results from the scan are recorded in a spreadsheet. This scan reveals how well the BPM was designed and built. As the wire of the scanning apparatus gets closer to a particular electrode, the signal in that electrode should increase proportionally to the decrease in signal of the opposite electrode. The goal is to calculate a regression function that improves the accuracy of the data.

Technical and Economic Feasibility of a Renewable Energy System at Summit Station, Greenland. *CRYSTAL HARDY (University of Indianapolis, Indianapolis, IN 46227) ANDY WALKER, OTTO VANGEET, ROBI ROBICHAUD (National Renewable Energy Laboratory, Golden, CO 89401).* Summit Station is a research facility supported by the National Science Foundation (NSF) located at the peak of the Greenland ice cap at an elevation of 3249 meters. The mission of the station is to make sensitive measurements of the atmosphere and the ice cap. Exhaust from the 87-kilowatt (kW) diesel generator that powers the facility adversely affects the quality of these measurements. The NSF asked the U.S. Department of Energy's Federal Energy Management Program (FEMP) to conduct a technical and economic analysis of options for using renewable energy at the station. The goal is to optimize the life-cycle cost while reducing fuel consumption and exhaust gas production. FEMP considered several system configurations for the analysis. Each system was evaluated using the Hybrid Optimization Model for Electric Renewables, a software program developed at the National Renewable Energy Laboratory that models system cost and performance using power requirements, wind and solar resources, component performance characteristics, component costs, fuel costs, and maintenance and operation costs as inputs. Currently, transportation of equipment, manpower, and fuel to Summit's remote location is only by air. Transportation, therefore, is very expensive, and it limits the size and weight of material transported and limits the frequency of deliveries. The ice terrain and winter temperatures below -60ºC are challenges for existing wind turbine, storage battery, and photovoltaic tracking technologies. Site-specific wind and solar resource data make modeling renewable power systems possible, but transportation, construction, maintenance, and climate challenges make it difficult to estimate exact system design and costs. However, our analysis determined that a hybrid renewable system consisting of a 25 kW photovoltaic array, three 100 kW wind turbines, 120 2.0 volt storage batteries, and a 110 kW converter would reduce generator run time by 49 percent and provide a simple payback of 12.28 years, for a 60 kW average load (1440 kWh/d).

Event Simulation Using Monte Carlo Methods. *RENEE HARTON (Massachusetts Institute of Technology, Cambridge, MA 02139) STEPHEN MRENNA (Fermi National Accelerator Laboratory, Batavia, IL 60510).* This project is a study of event simulation using Monte Carlo Methods. Using Pythia, an event generator, and Monte Carlo Methods, the collision of fundamental particles was simulated. After simulation, histograms of the cosine of the angle between the resulting quark and the initial particle's path were measured using the Physics Analysis Workstation (PAW). In the first case, a simulation of the ideal collision of an electron and positron, two leptons, was performed. A string, which is a result of the two particles fusing together after colliding, was formed. This later decayed into quarks that did not scatter. This simulation being a pretty picture, was far from the truth, because it did not take into account parton scattering, where the color of a quark is spread throughout space via gluons and other quarks. Simulations incorporating parton scattering were later performed and evaluated. After simulating the collision of two leptons, the collision between two hadrons was performed. With the increasing energy required by present day experiments, the colliding particles are often hadrons, since it is easier to get them to the high energy required. As a result, the simulated collision of hadrons is relevant. In this simulation, the hadrons collided and formed a Z boson which decayed into specific quarks. These quarks then formed colorless systems by creating other hadrons, such as pi(0) mesons, pi(+) mesons, and pi(-) mesons. Since hadrons have no net color and are made of several quarks and gluons, the end result which is sensed by the detector is clouded, which makes analysis more difficult. Using PAW, the amounts of each resulting hadron were measured to create a picture similar to the one measured by the detector. Although, this cluttered picture will complicate research efforts for physicists, there is a more energetic realm where forces may merge and particles may appear and hadrons allow us to enter that world.

Highly Efficient Selective Photodetachent of Negative Ions. *AARON HAVENER (University of Tennessee, Knoxville, TN 37909) YUAN LIU (Oak Ridge National Laboratory, Oak Ridge, TN 37831).* Highly Efficient Selective Photodetachent of Negative Ions in an RF Quadrupole Ion Cooler The Holifield Radioactive Ion Beam Facility (HRIBF) provides accelerated radioactive ion beams (RIBs) for experimental research in nuclear physics and nuclear astrophysics. The purity of the accelerated RIB is of crucial importance to many experiments. But very often RIBs produced at the HRIBF using the isotope separation on-line (ISOL) technique have large isobaric contamination that complicates and sometimes compromises experiments. Separating isobaric contaminants from RIBs has been a challenging problem. The HRIBF tandem post-accelerator requires negatively charged RIBs as input. The use of lasers to selectively remove unwanted isobars by electron photodetachment from negative ion beams has been reported. However, the degree of isobar suppression has been very low due to lack of high laser power or insufficient interaction time or distance between the photons and the negative ions. This experiment investigates a novel scheme of efficient suppression of isobar contaminants by photodetachment in a gas-filled RF-only quadrupole (RFQ) ion guide. Stable negative nickel and cobalt ion beams produced by a cesium sputter negative ion source are extracted from the ion source, mass analyzed using a dipole magnet, then decelerated to less than 100eV energies and focused into a RFQ ion guide filled with helium buffer gas. A laser beam is directed into the RFQ along the axis. Inside the RFQ, the ions can be cooled by collisions with the buffer gas molecules to such a degree that ion energies in both longitudinal and transverse directions can be reduced to the thermal energy of the buffer gas. Once cooled, the ions will move many times slower through the RFQ. Therefore, much longer interaction time between the photons and the ions inside the RFQ can be achieved. Thus, high efficiency of photodetachment is expected. A Nd:YAG laser beam at 1064 nm wavelength is used for selectively removing the Co- ions. The energy of the 1064 nm photon is 1.165 eV, much larger than the electron affinity of Co (0.661 eV) but slightly above the electron affinity of Ni (1.156 eV). It is therefore expected that Co- ions will be strongly depleted. A detailed description of the experimental setup along with expected measurements of photodetachment efficiencies and suppression factors for the Co- ions will be provided in the poster presentation.

X-Ray Reflectivity Results of Multi-layered thin film of Si/Cu/Permalloy/Pt/SiO_2. *VIRGINIA HAYES (Chicago State University, Chicago, IL 60628) CHINEDUM IBEABUCHI (Chicago State University, Chicago, IL 60628) JUSTIN AKUJIEZE (Argonne National Laboratory, Argonne, IL 60439).* In order to design more efficient write heads in information technology it is necessary to satisfy the condition for increasing the bit size density in magnetic disk drives. This would require increasing the anisotropy of media so that magnetic information is unaltered as a result of increase current enabling thermal stability. To make this possible materials of high magnetic permeability u , high saturation Magnetization (having high memory) and low Magnetic field remanent must be found to enable easy transitions. This will entail making thin films of desired thickness, known compositions and structure, and of known magnetic structure, and of low surface roughness. To do this we must first find a combination of materials that will allow for a high magnetization and low anisotropy. For our work we will explore multi-layers of rare earths 4fn with high magnetization and possibly low anisotropy with transition elements 3dn of ferromagnetic characteristic. Here permalloy (Py = $Ni_{80}Fe_{20}$) is a good candidate. The experiment started by using the multi-layered design of materials through the process of sputtering. This is to layer thin films, which are of nano-thickness, onto one another in a vacuum tight system with the help of Ar gas. Several samples were deposited at their lowest power and dynamic vacuum pressure to ensure smoothness of surfaces. In this process we layered a Si [001] substrate with 200Å of copper, 40Å of permalloy (Py = $Ni_{80}Fe_{20}$), and a variance of Platinum instead of gadolinium which may be used as a standard ranging from 0, 3, 10, 20, 30, 40, 50 Å and a super-lattice of Py/Pt, and

Gd. This was covered by 60 Å of Silicon oxide as a capping layer. Using x-ray analysis enabled initial analysis for average chemical composition in these multi-layered structures. And through the use of Paratt program which involved the fitting of theoretical reflectivity curves derived from Paratts recursive formula, the individual layer thickness and the roughness of the interface were found. Analysis showed that the sputtering conditions were optimal in making smooth thin films of these materials. Controlled chemical compositions and magnetic structures, desired thickness, and smoothness can be assembled as desired. The average obtained compositions expectedly differ from the actual simulated results bearing in mind that there was absence of layer to layer analysis hence complete absence of roughness of the interfaces.

Studies of the STAR Endcap Electromagnetic Calorimeter. *JACQUELYN HOSTLER (Berea College, Berea, KY 40404) ROBERT CADMAN (Argonne National Laboratory, Argonne, IL 60439).* The Endcap Electromagnetic Calorimeter (EEMC) is used to detect particles at the Solenoidal Tracker at RHIC (STAR) where the spin of gluons is being studied. Photons produced in proton-proton collisions will be used to measure the polarization of the gluons within protons. A Shower Maximum Detector (SMD) built by scientists at Argonne recently has been installed that distinguish between single photons and those produced from π^0 decay. The SMD has recently been installed, so it must be first calibrated. We checked the mapping between SMD strips and electronics channels and studied whether decays of K^+ mesons could be used as a tool to calibrate the EEMC. Using some of the first data from the SMD, we searched for correlations due to particles passing through neighboring strips to determine if strips were misrouted. For the K+ study we developed and studied a method of distinguishing two types of K^+ decay ($K^+ \rightarrow \pi^+ + \pi^0$ and $K^+ \rightarrow \mu^+ + \nu\mu$) from the momenta of the kaon and its charged daughter particle. We also studied whether photons detected in the calorimeter could easily be correlated with the K^+ decay. We tested our program for both high energy kaons (around 10 GeV) and low energy kaons (about 500 MeV). For the low energy kaons the decay type was easily determined, but the resulting photons were located in a wide angle range. The high energy kaons have photons that could be more easily located in a small angle; however it was almost impossible to determine the type of kaon decay the kaon underwent.

Determination of Accurate Collision Energies for Near-Thermal Electron Capture Studies Using Merged Beams. *STEVEN HOUGH (University of Tennessee, Knoxville, TN 37996) CHARLES C. HAVENER (Oak Ridge National Laboratory, Oak Ridge, TN 37831).* Electron capture is an important process in plasma environments, such as in astrophysics with relation to gaseous nebulae. Herrero produced a theoretical, oscillatory structure of the cross section for near-thermal collision energies (0.01 - 1 eV/amu) that has not yet been fully tested. Currently, the electron-capture cross section for $N^{2+}+H \rightarrow N^{+}+H^{+}$ is being measured for energies in this near-thermal region. The merged-beams technique used in this experiment is an accurate tool for studying electron capture for a broad range of collision energies, especially low energies. For the current experiment, a 6.97 keV H beam is merged with a N^{2+} beam whose energy ranges from 40 to 46 keV producing the desired low relative collision energies. A challenge with merged-beams is determining accurate collision energies. To establish this energy, a definite merge angle and angular spread must first be determined. A program has been developed in Matlab that automatically and efficiently calculates the merge angle based on horizontal and vertical beam profiles. Previously, this had been done visually. Another Matlab program has been developed to simulate the ion and neutral beam interactions using typical merge angles and angular divergences. By studying how the various beam parameters affect the actual collision energy, the simulations have shown that a correction needs to be added to the merge angle due to angular spread. Measurements for $N^{2+}+H$ are currently in progress, and the correction will be applied to this data. The new method for determining merge angles has increased the accuracy of the collision energies.

Measuring Physical Properties of Various Materials Using Lasers. *DOMINIC HOWARD (Universitiy of Maryland, Adelphi, MD 20783) RICK RUSSO (Lawrence Berkeley National Laboratory, Berkley, CA 94720).* Part of my research for the summer included using lasers to measure properties of various materials. I shot a 1064nm Pulsed laser at a sample of material to be analyzed. The impact of the light pulse on the sample produces waves of certain characteristics that are based on the physical properties of the material. This is similar to the surface waves generated in water by throwing a rock into a calm lake. Those waves are analyzed by using a Mach-Zehnder interferometer connected to a computer using Labview software. It is therefore possible to find the flexural stiffness and shear rigidity of various samples including many different types of metals and papers. The results agreed with expected values. The advantage of this method is the sample can be moving while it is tested and has the capacity to give more accurate data.

Simulation of Transmission and Attenuation of Photons in a Labyrinth. *KAI HUDEK (Colorado School of Mines, Golden, CO 80401) ALBERTO FASSO (Stanford Linear Accelerator Center, Stanford, CA 94025).* Neutrons travel through tunnels and ducts (labyrinths) according to curves that are universally applicable, regardless of labyrinth geometry or particle energy. Photons were believed to follow this manner, but this has been found not to be the case. Photons transmit through labyrinths with a definite functional dependence upon both particle energy and labyrinth geometry. In the first leg of a two-legged labyrinth, photons attenuate according to the function $\text{Dose}=1/(1+Ax^2)$. In the second leg, photons attenuate according to the function $\text{Dose}=1/(1+Bx^3)$, in which A and B are functions of energy and labyrinth geometry, and x is a dimensionless unit of d/sqrt(a) in which d is the distance from the labyrinth mouth and a is the cross-sectional area. Dose is an attenuation factor. The A and B values have not been analyzed sufficiently to determine their functional dependence upon energy and cross-sectional area, however they have been tabularized which allows for interpolation of the data for use in calculations. These results were determined by simulating a mono-energetic beam incident upon a two-legged labyrinth with angular spread to cover the mouth. Work was begun on utilizing a real spectrum to determine a functional dependence by placing an iron target at the mouth of the labyrinth, and striking it with an electron beam. However, the techniques used to gather the mono-energetic beam data were not sufficient to effectively gather a complete set of real spectrum data and analyze its functionality.

Searching for Gravitational Lensing by Cosmic Strings in Hubble Great Observatories Origins Deep Survey (GOODS) Data. *CATHERINE IHM (Northwestern University, Evanston, IL 60208) GEORGE SMOOT (Lawrence Berkeley National Laboratory, Berkley, CA 94720).* Cosmic strings are linear topological defects that may have formed during phase transitions of the early universe. Their existence has not yet been proven; their discovery could deeply affect cosmology and particle physics. To detect cosmic strings, their lensing effects can be exploited. If a string lies between an observer and a galaxy, light from the galaxy will then travel in two paths around the string. The observer will see an identical pair of galaxies, one image on each side of the string. Our detection method involves finding pairs of similar galaxies within a wide-field sky survey and analyzing the distribution of their separations. In the presence of a GUT-scale cosmic string, the number of pairs is expected to pile up at around 5 arcseconds of separation. Images from the Great Observatories origins Deep Survey (GOODS), which surveyed Hubble Deep Field-North and Chandra Deep Field-South, were searched for lensed pairs. Similarity between two galaxies is assessed by cross-correlating the objects and finding their correlation coefficients. All pairs within a certain range of appropriate correlation values were selected, and their separation distribution was plotted. No “piling up” of pairs occurred; a cosmic string was not detected. However, this technique for detection has not yet been applied to all of the sections in the GOODS fields. The rest of the data must be searched, and many other wide-field surveys investigated before the existence of cosmic strings is conclusively ruled out or confirmed.

Argon Ion Production Following a K-Shell Vacancy Cascade. *CORI JACKSON (Solano Community College, Suisun, CA 94534) FRED SCHLACHTER (Lawrence Berkeley National Laboratory, Berkley, CA 94720).* Electron reconfiguration following photoionization of an atom is a complex process when the vacancy is created in an inner shell of the atom. Ionization of an inner-shell electron creates a cascade of electronic transitions to fill the vacancy or vacancies produced. An atom with a K-shell vacancy is unstable, often resulting in an emission of an electron. An electron from a higher level rushes to fill the void left after the departure of the K-shell electron. Transitions continue to occur until all lower shells have been filled with electrons. The entire vacancy cascade may follow any number of paths and each may produce a variety of highly ionized ions. Experimental investigation is performed to test quantum mechanical calculations regarding ion abundance following K-shell photoionization and resulting vacancy cascades. Charge state distribution and total ion yield resulting from a vacancy cascade following photoionization of a K-shell electron in argon has been measured as a function of photon energy using synchrotron radiation and magnetic mass spectroscopy. K-shell ionization of argon was produced by intense, monochromatic x rays supplied by beamline 9.3.1 at the Advanced Light Source (ALS) located at Lawrence Berkeley National Laboratory (LBNL). Argon was injected into a 180 magnetic mass analyzer and then bombarded with x rays to produce photoionization. Photons with energies ranging from 3200 to 3220 eV were used to ionize the K-shell electrons. The analyzer separated the resultant argon

ions according to charge state. Argon-ion charge states Ar^{+} through Ar^{7+} were measured and normalized to existing abundance ratios for ion production at 3213 eV. Ion production was dependent on photon energy. Above the argon K-shell ionization threshold of 3206.3 eV, the Ar^{4+} ion is most prevalent. Ar^{4+} comprises approximately 42% of all ions produced above this photon energy. Below the K-shell ionization threshold, only small quantities of ions are produced. Future work will examine ion production as a function of reconfiguration pathway in order to explain these abundance results.

Investigation of Molecular Electrical Properties Using Au/Ge Thin Films. *CHRISTOPHER JESSAMY (North Carolina A&T State University, Greensboro, NC 27411) MYRON STRONGIN (Brookhaven National Laboratory, Upton, NY 11973).* In this work we present the results of the nano-structural studies and electrical characterization of Gold (Au) films on ambient temperature or cooled amorphous Germanium (Ge) substrates. We were able to produce monolayers of Au that are 0.3-3 nm thick. These films were fabricated under high vacuum conditions (~10^{-8} Torr) using thermal evaporation. We used a simple series resistor circuit for in situ measurement of resistance of the film during deposition. This method allowed us to detect the continuous formation of the Au layers. The sheet resistance was measured as a function of temperature and thickness. The nano-structure of the films was determined using Atomic Force Microscopy (AFM). For the thinnest layers of Au on Ge we saw no structure in the AFM and we suspect that the thin Au layers alloy with the Ge. The temperature dependence of sheet resistance shows activated behavior. These initial experiments indicate that it may be possible to study thin layers of Au with sheet resistance approaching 10^{12} Ω/m^2. This possibility could result in experiments measuring the change in resistance when thiols and other molecules are put on the Au surface.

Characterization and Analysis of the Negative Feedback Loop Laser Pointing and Stabilization System for the Laser Optics and Accelerator Systems Integrated Studies (L'OASIS) Group. *ZAC JUDKINS (College of Marin, Kentfield, CA 94904) CSABA TOTH (Lawrence Berkeley National Laboratory, Berkley, CA 94720).* The L'OASIS Ti: Sapphire laser system involves multiple laser beams propagated over hundreds of meters, ultimately converging within a volume of a few cubic millimeters. Mechanical and electrical noise within the laser sources and optics, along with air-currents on the tables, create small vibrations of the beam. Over long propagation distances these micron sized vibrations manifest as deviations from a known centroid by up to one fifth the laser beam's diameter (and up to a full beam diameter in the focused area of the target chamber). Stabilizing the effects of these vibrations would greatly reduce wasted time and increase the success rate of experiments done by the group. The negative feedback loop stabilization system under testing this summer consists of a Hamamatsu Position Sensitive Detector (PSD) and a piezoelectric actuator (PZT) placed upstream from the PSD. The PSD relays information about the beam's movment about a set centroid to the PZT; the PZT makes micron sized pointing adjustments to reject these movements. The main problems with this stabilization method arise due to the laser system. The main pulse beam of the L'OASIS system has a repetition rate of 10 Hz, with each pulse lasting approximately 200 ps (50 fs inside the target chamber). The problem is that the frequencies of the problematic vibrations occur at a much higher rate. So, the PZT attempts to correct pulse N+1 using information about pulse N, but recent tests have shown that there is no position correlation between consecutive pulses at a rep rate of 10 Hz. A possible solution may be to inject a low intensity continuous wave (CW) laser collinearly with the main pulse beam, such that the two beams encounter the same optics and air-currents, and their centroids fluctuate in the same manner. The PSD would then have continuous information about the position of both laser beams and could simultaneously correct for the CW and the main pulse beam. Attempts to implement this solution have shown poor results due to the diverse nature of the vibrations to be rejected. The feedback loop successfully corrects the CW beam while decreasing the stability of the pulse beam by approximately 30%. Expecting collinearity of the beam paths seems implausible; increasing the repetition rate of the pulse beam to 1 kHz, may show improvement.

Measuring Glass Thickness of a Reference Cell Used in a Polarized ^{3}He Experiment. *NATHAN JUSTIS (Brigham Young University, Provo, UT 84602) JIAN-PING CHEN (Thomas Jefferson National Accelerator Facility, Newport News, VA 23606).* Studies of the spin structure of the neutron are often conducted using a polarized 3He target due to its close spin resemblance to that of a free neutron. Experiments are conducted by bombarding polarized 3He nuclei with high-energy electrons from a linear accelerator. The polarized ^{3}He gas is contained in a glass tube-like cell called the target cell. In addition to the target cell, a reference cell is also used for calibration purposes. The thicknesses of each cell must be accurately determined for the analysis of the scattering data of the experiment. The thickness of a reference cell named Janine was determined by using a tunable infrared laser to create a thin-film interference pattern by reflecting the laser light off of the glass cell. The intensity of the pattern is known to vary sinusoidally as the wavelength of the laser changes. Such variation was recorded as an array of numbers by a LabView program at 26 different points on the cell. Each of the 26 sets of data were then fitted to an equation containing the thickness variable in order to determine the thickness of the glass. Janine was found to have side, or wall, thicknesses ranging from 1.42 mm to 1.65 mm, with an uncertainty of less than 5% in every case. End, or window, thickness measurements were also successfully taken, but have yet to be fitted to the derived equation. Window thickness measurements had not been previously attempted at JLab. Because of this research, wall thickness measurements of Janine can be used in the analysis of experiment E01-012 and window thickness measurements can be considered possible at JLab.

Open Channel Liquid GaInSn Alloy Flow in Transverse Magnetic Field. *SCOTT KATHREIN (University of Illinois, Urbana, Champaign, IL 61820) HANTAO JI (Princeton Plasma Physics Laboratory, Princeton, NJ 08543).* One of the most exciting new developments in tokamak design is the possibility of a liquid lithium first wall. Our experiment simulates this using a wide rectangular open channel liquid metal flow and a transverse magnetic field. Velocity profiles of this flow are measured. The dimensionless Hartman number which describes our flow (~160) approaches that of liquid lithium applications in fusion devices. Simulation of the channel was completed using the magnetohydrodynamic Navier-Stokes equation, under the assumption of laminar flow. The equations were evolved in time until an equilibrium state was found. In the initial design of the experiment, the flow was measured using 2 diagnostics: a paddle submerged in the liquid to measure the force of the flow, and a Hall probe consisting of two submerged electrodes that measure a potential difference. In the past, open air magnetic coils were used, but these are being replaced with new coils with a soft iron core. We are also finding a larger pump that is compatible with gallium, indium, and tin. In the results of the previous experimental design, the simulation results agree qualitatively with the experimental results, but only after the viscosity parameter in the simulations is quadrupled. The results differed from conventional Hartmann flow in both stimulations and experiments. The velocity at the center was found to increase, while in typical Hartmann flow, the velocity profile flattens out at the center. This effect is attributed to the wide nature of the flow, and the effect this has on current paths in the flow. In normal Hartmann flow, current flows downward at the center of the flow. It produces a J x B force which retards the flow. However, in our wide channel experiment, these currents are limited to the edge regions, and fluid velocity at the center actually increases to account for the retarded flow elsewhere. Once the design and construction of the revised experiment is completed, more data will be taken and compared to simulation.

Using Weak Gravitational Lensing to Compare Filters and Study Tomography of a Massive Galaxy Cluster. *JOHN KEHAYIAS (Columbia University, New York, NY 10027) MORGAN MAY (Brookhaven National Laboratory, Upton, NY 11973).* We have been working with data from the Deep Lens Survey used in Wittman et al' s paper "Weak Lensing Discovery and Tomography of a Cluster at z = 0.68" (2003) to study the same galaxy cluster with different weighting/filter functions. When there is a large mass between an observer and distant background galaxies, General Relativity predicts a bending of the light – weak gravitational lensing. By studying this small effect over an entire field, it is statistically feasible to "see" an otherwise dark mass (sensitive to baryonic and dark matter) through a tangential shear (proportional to mass) map. Weighting and filtering are used to optimize the shear maps, and we have studied four different filter functions: NFW (Navarro, Frenk & White 1997), modified Gaussian, aperture mass, and TMF (Tomographic Matched Filtering, Hennawi & Spergel 2004). We have looked at maps produced from the different filters, and calculated signal to noise (by randomizing galaxy ellipticities) to optimize each filter and find the best one. We find that all the filters can be optimized by varying their cutoff parameter and perform nearly equally well. However, TMF performs slightly better, even with the non-optimal NFW as its base filter. In addition, we have used TMF to find redshift information of the cluster. Our results have agreed with what Wittman has found for a redshift estimate and mass maps. Additionally, we used TMF on simulation data from Martin White, where we identified several massive clusters and successfully found their redshifts with tomography.

Performance of Two New Clover High-purity Germanium Gamma-ray (HPGe) Detectors. *MICHAEL KING (Purdue University, West Lafayette, IN 47906) ROBERT JANSSENS (Argonne National Laboratory, Argonne, IL 60439).* High-purity germanium gamma-ray detectors consisting of one or more crystals of high purity germanium are extensively used in the detection of gamma decay events. Two new detectors of this form, called clovers, consisting of four closely packed axially parallel germanium crystals were just acquired by the Physics Division of Argonne National Laboratory. Before these detectors can be used in nuclear physics experiments, however, it is necessary to characterize them to assure their accuracy under a variety of operating conditions. This was the main purpose of this work. Analysis was performed on the resolution, peak to total ratio, and efficiency of the clovers for varying radiation intensities and energy ranges simulating potential experimental conditions. Notable problems were found in both detector 1 and detector 2. Comparisons of the data with Monte Carlo simulations were also carried out.

Chemical Vapor Deposition (CVD) Growth of Vertically Aligned Single Wall Carbon Nanotube Arrays. *ANIKA KINKHABWALA (Columbia University, New York City, NY 10027) GYULA ERES (Oak Ridge National Laboratory, Oak Ridge, TN 37831).* The carbon nanotube has potential uses in various technological fields. However, before new applications can be realized, the carbon nanotube growth process must be better understood and controlled. Nanotube growth experiments were performed using a modified chemical vapor deposition (CVD) apparatus in which the tube furnace is replaced with a vacuum chamber and a graphite filament heater. Carbon containing gas molecules enter the chamber as a high-pressure gas expansion through a 100-micron diameter nozzle directed toward the heated substrate. This molecular beam approach provides better control capabilities, thus allowing for synthesis of new forms of carbon nanotube structures. In this case, the molecular beam collides with catalyst particles, previously deposited on a substrate, at an elevated temperature (500°C-700°C) and forms nanotubes. Of the carbon gases tested (propylene, acetylene, methane, ethylene), only acetylene proved effective in growing vertically aligned nanotube arrays. Using acetylene, vertically aligned arrays of nanotubes up to 300 microns tall were grown at 650°C. Raman spectroscopy, scanning electron microscope (SEM), and transmission electron microscope (TEM) images confirm that these arrays are made of single wall nanotubes (SWNT's) and are free of catalyst particle contamination.

Characterization of an Electro-Optical Modulator for Next Linear Collider Photocathode Research. *MATTHEW KIRCHNER (Colorado School of Mines, Golden, CO 80401) AXEL BRACHMANN (Stanford Linear Accelerator Center, Stanford, CA 94025).* The Stanford Linear Accelerator Center (SLAC) Next Linear Collider design parameters call for a polarized electron source capable of outputting bunches of electrons 1.4 ns apart (714 MHz). SLAC currently uses a pulsed Ti: Sapphire laser incident on a GaAs photocathode to produce polarized electrons. The pulses produced by this laser are approximately 300 ns in duration and occur at a frequency of 60 or 120 Hz. The purpose of this research is to find a way to modulate the 300 ns pulse into a high-frequency pulse train. High-frequency modulation of the 300 ns laser pulses was achieved with an electro-optical (EO) modulator, which uses the Pockel's Effect to change the polarization of incoming light. The highest frequency possible was 200 MHz (limited by the RF amplifier). For this reason, the SLAC 119MHz timing signal was selected for input into the amplifier. The output of the amplifier was passed through the EO modulator to induce an alternating half-wave phase shift of the incident laser light. The cube polarizer at the exit of the modulator rejects any laser light not parallel to its polarization axis. These two effects coupled together produce amplitude modulation of the laser pulse. The modulation can be changed by several variables. The linearly polarized light incident into the modulator can be rotated by a half-wave plate to any polarization angle. The DC Bias could be changed to give the RF signal an offset. The input signal can also be changed to vary the voltage across the crystals. Finally, the RF setup (attenuators, splitters, cables, terminators) can be changed. This paper examines how all of these variables change the modulation characteristics of the EO modulator used. The rotation of the half-wave plate was found to change the percent modulation from 10% to 90%. Adding a DC Bias to the half-wave plate rotation caused the modulated signal to change shape as modulation depth still ranged from 10-90%. The modulation depth was shown to increase with increased input voltage. RF setup was only varied slightly but small changes still gave drastic changes in percent modulation. The EO modulator examined showed that high-frequency modulation of a Ti:Sapphire laser pulse is possible with a high percent modulation. This research should be extended up to 714 MHz and the RF setup should be optimized for maximum modulation in future studies.

Measurement of g1p at a Future Electron Ion Collider. *MINDY KOEHLER (Kansas State University, Manhattan, KS 66506) ANTJE BRUELL (Thomas Jefferson National Accelerator Facility, Newport News, VA 23606).* After more than 30 years of experiments, many questions have been left unanswered about the structure of the nucleon, including the contributions of the different partons to the spin of the nucleon. To answer these questions, the nucleon needs to be probed with higher resolution and higher luminosity than available in current experiments. A future Electron-Ion Collider (EIC) would allow for collisions at high center-of-mass energies, high luminosities and high beam polarizations. As a result, one can expect the probing of the nucleon on much smaller distance scales, allowing for a clear interpretation within perturbative Quantum Chromodynamics (QCD). Before such a collider can be approved, one must optimize the parameters of the collider with respect to the various physics processes of interest. One quantity of extreme interest is the spin-dependent structure function of the proton, g1p (and of the neutron, g1n) and its behavior at very low values of x. The focus of this study was to anticipate the kinematic coverage and statistical precision of the data on g1 at a future collider by performing Monte Carlo simulations. The information from these simulated events was then analyzed, enabling predictions to be made about the behavior of g1 at low values of x. Using various energy scenarios of a future electron ion collider, it was found that g1 can be measured at x values as low as $5x10^{-4}$, which is much lower than values previously obtained. It was also found that values for g1p can be obtained over a wide range in Q2, allowing the gluon polarization to be determined from the scaling violation of g1. The simulations performed in this study strongly indicate that the beam energies for the two proposed designs of the EIC will give similar precision in the measurements of the gluon polarization. Precision measurements of the spin structure function of the nucleon at low x will provide a better understanding of the polarization of gluons inside the nucleon, thus helping to complete the picture of the structure of the nucleon. This information, combined with direct measurements of the gluon polarization at the EIC, will help to complete the model of the building blocks of matter. Moreover, the determination of the integral of the difference between the spin structure functions of the proton and the neutron (the Bjorken Sum Rule) will allow a precision test of one of the most fundamental quantities in QCD.

A Nondestructive Method of Grain Microstructure Determination. *JOYCE LAI (University of California, Berkeley, Berkeley, CA 94720) APURVA MEHTA (Stanford Linear Accelerator Center, Stanford, CA 94025).* Customarily, a material has been sectioned to study its internal grain microstructure and thus in the process is destroyed. Using x-rays, however, there are two nondestructive methods of determining the sources of diffraction spots and hence the internal grain microstructure of a sample. One technique consists of placing a wire in the path of a diffracted ray so that its image is prevented from appearing on the detector screen. Ray-tracing is then done to locate the source within the sample from whence the rays emanate. In this experiment, we investigate the other technique of determining source location by recording diffraction patterns at ten equally-spaced detector distances and then graphing the data with reasonable-fit lines using the least-squares fitting routine. We then perform a ray-tracing triangulation technique to pinpoint the location of the source from which the rays are coming. Cluster analyses are employed and plots of ray number versus pixel position of certain points at some particular detector distances are created. An error propagation analysis is then carried out as a check to the cluster analyses and graphs of error deviation along the detector path versus ray number are constructed. With statistical error analyses and construction of error boxes using chosen pixel error deviations and delta z error values, the best error measurement using the detector method was found to be plus/minus 100 microns. In this study, it was found that the detector method provided a much poorer resolution than the traditional wire technique of which there is a source size precision of within 1-5 microns. The detector method, though, is sufficient for large-grain material studies.

Evaluation of Various Methods of Neutron Dosimetry. *ETHAN LAKE (Tennessee Technological University, Cookeville, TN 38501) PEGGY MCMAHAN (Lawrence Berkeley National Laboratory, Berkley, CA 94720).* As ionizing radiation, neutrons can be very destructive. Normally, the earth's atmosphere and magnetic field act as a shield from large amounts of dangerous radiation. However, in the harsh environment of space and the upper atmosphere, there is little, or no, protection. Scientists wish to study the effects of neutrons on both living cells and microelectronics in order to better understand the effects of neutron radiation, and to improve shielding and safety precautions. At Lawrence

Berkeley National Laboratory a large-area detector sensitive to fast neutrons is being developed which will incorporate new technology in scintillators and electron multipliers. Scintillators are being researched and will be tested to determine which is best for the application; selection criteria and characteristics will be discussed. The Gas Electron Multiplier consists of a series of foils which will multiply the scintillation induced photoelectrons. It will be assembled and tested to determine its operating characteristics, and results will be discussed. Using these components and others, the neutron detector will be able to give a 2-D picture of neutron flux incident on any sample.

Erosion and Failure: A Spectroscopic Analysis of High Pressure Natural Gas Engine Spark Plugs. *DAVID LAYTON (North Georgia College, Dahlonega, GA 30597) R.K. RICHARDS (Oak Ridge National Laboratory, Oak Ridge, TN 37831).* Due to recent advances in design, natural gas engines are becoming increasingly popular in industry as a clean, efficient, reliable source of power. However, greater efficiency means higher cylinder pressures, and, at high pressures, the voltage necessary to induce ignition becomes greater causing spark plugs to erode much more quickly. Since the erosion mechanism is unknown, spark plug failure unexpectedly halts production causing industry to lose millions annually. To understand this erosion process, a spectroscopic analysis of the plasma generated by electrical arcs of natural gas engine spark plugs, both used (various hours of use) and unused, was conducted. Differences between the emission spectra of used and unused plugs suggest a mechanism for erosion involving Ni, which composes the base of the ground electrode of the plug, and Ca, present in engine lubricant. Interestingly, emissions due to the sputtering of the Ir and Pt tips have not been observed. Other elements which play secondary roles in the erosion mechanism can be observed through more rigorous analyses of the spectra. Metallurgical analysis confirms these findings, as well as, the presence of various glassy calcium-metallic oxides on the surface of used spark plugs-this glassy coat accounts for the suppression of nickel sputtering observed in the spectra of used plugs. Once these oxides become embedded in the surface of the spark plug tips, inconsistencies in the thermal expansion rates between the material and this contaminant lead to surface cracking and, inevitably, ignition failure. Variations in the emission spectra also raised many interesting questions which led to the discovery of a distinct pattern in spark plug behavior characteristic of all plugs-the implications of this are as yet unknown. Although none of these findings isolate a single causal agent for erosion, they illuminate the concerns regarding spark plug failure. The task is now to determine which mechanism causes failure first and to circumvent it.

Absolute Photoionization Cross Sections of Kr^{4+} and Kr^{5+} Ions. *ERIKA LEVENSON (University of California, Berkeley, Berkeley, CA 94720) FRED SCHLACHTER (Lawrence Berkeley National Laboratory, Berkley, CA 94720).* The abundance and charge-state distribution of ions inside planetary nebulae can tell scientists a great deal about the evolution of stars. Photoionization models are used in the analysis of emission lines of ions from nebulae, and atomic data such as photoionization cross sections are needed for input. Krypton ions are created in planetary nebulae, but no atomic data exists for their ionization. Absolute photoionization cross-section measurements were made for Kr^{4+} and Kr^{5+} ions at beamline 10.0.1 at the Advanced Light Source (ALS), using third generation synchrotron radiation from the ALS and the merged-beams technique. Interference of the direct and indirect photoionization processes produces resonances at several photon energies. The number of photoions detected and all measured experimental variables are used to calculate the absolute cross section at various photon energies to put the measurements on an absolute scale. Absolute photoionization cross-section measurements as a function of nominal photon energy for Kr4+ from 85-92 eV, Kr^{4+} from 121-134 eV, and Kr^{5+} from 88-95 eV were made. These data will serve as benchmarks for theory and will be available for input to astrophysical models.

Analysis of Beam Position Monitor Data for the Spallation Neutron Source Using Various Statistical Methods. *ERICA LEWIS (Tennessee State University, Nashville, TN 37209) GEORGE DODSON (Oak Ridge National Laboratory, Oak Ridge, TN 37831).* The use of the Spallation Neutron Source (SNS) accelerator will soon provide an instrument to investigate stronger, lighter and cheaper materials for scientific research and industrial development. The SNS Linear Accelerator (Linac) is used to accelerate negatively charged hydrogen ions (H^-) for the purpose of generating intense beams of neutrons from a mercury target. One challenge of the SNS is to maintain the alignment of the H^- pulsed beam through the Linac. As the H^- pulsed beam travels through the Linac there are M number of Beam Position Monitors (BPM) to determine the vertical and horizontal movement as well as the phase and amplitude of the beam. The results obtained from the use of histograms, Gaussian plots, and a technique called Singular Value Decomposition (SVD), will be closely examined to determine the beamline motion resolution. Histograms and Gaussian plots were cross referenced with each other to determine if there was a deviation in the beam's centroid motion which could be due to correlated or uncorrelated events. SVD was employed to separate the system and diagnostic properties needed to accurately analyze the beam centroid motion. The preliminary results obtained from the SVD analysis can be correlated with the ion pulse beam parameters and machine properties to serve as a diagnostic tool for characterizing the dynamic beamline motion in the Linac.

General Testing Procedures of Pulsar Boards. *ANGELA LITTLE (Seattle Pacific University, Seattle, WA 98119) TED LIU (Fermi National Accelerator Laboratory, Batavia, IL 60510).* Pulsar Boards are currently used as part of the Level 2 Trigger system at CDF (Collider-Detector at Fermilab) and are being used in the L2 Trigger Upgrade. Since additional boards will be produced over the next few years, it is important to have proper documentation on how to test new boards and maintain ones currently in use. New production boards were tested and the procedure for testing was documented. One of the goals of the documentation is to allow those less familiar with the setup the ability to test Pulsar boards. Much of the information included involves the setup of the teststand, from plugging in and cabling up the boards to running specific tests on them. The procedures outlined in the document give one the ability to test all the board interfaces as well as the hardware.

Growth of Gallium Phosphide on Silicon Wafers. *JEREMY MAY (Fort Lewis College, Durango, CO 81301) JERRY OLSON (National Renewable Energy Laboratory, Golden, CO 89401).* Gallium Phosphide on a silicon wafer has the potential to be an efficient solar cell or layer of a tandem cell. However, before the GaP crystals can be grown, the Si wafer must be cleaned and dangling bonds filled with acceptable chemical species. For growth without anti phase domains, the right amounts of Ga and PH3 must be used at the right temperatures. To clean the Si wafers we used a 2:1:10 solution of ammonium hydroxide: hydrogen peroxide: water, distilled water, and hydrofluoric acid in that order. Ammonia (from the 2:1:10) stayed on the Si through the water rinse and reacted with the HF to create particles NH_4F. The longer the substrates were rinsed in water, the fewer particles remained at the end of the cleaning process. This suggests that ammonia was gradually being washed off the surface during the H_2O rinse. A reactor was used to grow the GaP. We report on the effects of varying the starting and ending temperatures in the reactor, the amount of time the temperature was graded from start to end temperature, and the amount of TEGa and PH_3 allowed into the reactor. A light scattering test was used to quantify the smoothness of the resulting epilayers and compare them. Optimal growth conditions were around 925 degrees Celsius continuous or grading from 950 to 1000 degrees Celsius in six minutes. Future work could focus on varying the length of the growth time and the annealing process.

The Universe Adventure: Public Education in Cosmology and Astrophysics. *MELISSA MCCLURE (University of Rochester, Rochester, NY 14627) MICHAEL BARNETT (Lawrence Berkeley National Laboratory, Berkley, CA 94720).* In the past few years, the lack of public comprehension of scientific concepts and discoveries has become a concern. If people do not understand science, they are less likely to appreciate it; students and young people are an essential part of the future of science, but if they are not informed about the new and exciting innovations being made in technical fields, they may fail to be inspired to consider a career in one of them. At the very least, because government grants for science come from money from taxpayers, scientists wish to inform the public about the discoveries which their money is financing. The result has been an increase on the part of the scientific community to provide the public with information and education aimed towards a non-technical audience. To this end, scientists must use the latest information technologies and educational techniques to convey abstract concepts in ways that are accessible to a wide spectrum of learning styles.

Mapping the Magnetic Field in the PHENIX Detector at the Relativistic Heavy Ion Collider. *ANDREW MCCORMICK (University of Illinois at Urbana-Champaign, Urbana-Champaign, IL 61801) ACHIM FRANZ (Brookhaven National Laboratory, Upton, NY 11973).* The PHENIX experiment at the Relativistic Heavy Ion Collider (RHIC) at Brookhaven National Laboratory studies the properties of the strong nuclear force and the nature of hadronic matter under extreme conditions. The PHENIX detector consists of four independent magnetic spectrometers which are used to identify the reaction products of ion-ion and polarized proton-proton collisions and to measure their momenta. The goal of this

research project was to accurately map the magnetic fields generated by the magnet systems in the central PHENIX spectrometer arms. When a charged particle passes through a magnetic field its trajectory is bent an amount proportional to the strength of the magnetic field. The amount the particle bends is also dependent on the exact charge and mass of the particle. Thus, if a detailed map of the magnetic field is available, it is possible to compare the actual path of a particle with the theoretically predicted path of a certain type of particle. These comparisons can then be used to help identify the particle in question.

Reduction of Wave-Guide Effects and Measurement of Work Functions of Novel TCOs and Ink-Jet Printed Conducting Polymers for Organic Semiconductor Devices. *BONNIE MCLAUGHLIN (Brigham Young University, Provo, UT 84602) SEAN SHAHEEN (National Renewable Energy Laboratory, Golden, CO 89401).* Alternative structures, compositions, and methods of fabrication were investigated to improve the performance of organic photovoltaic cells and organic light emitting diodes (OLEDs). For OLEDs, researchers examined the effects of roughening the outer surface of the glass substrate through chemical etching and nanostructuring the polymer/substrate interface through the growth of ZnO nanofibers to reduce losses due to waveguide effects in the polymer and glass substrate. The angular dependence of the emission spectra in the new structures is characterized. Roughening the glass enhances the intensity of forward-emitted light and reduces the angular dependence of the emission. Incorporation of ~200 nm long nanofibers also reduces angular dependence, and we expect longer nanofibers to have a larger effect. Researchers thus expect OLEDs with an etched outer glass surface and/or nanofibers inserted at the polymer/substrate interface will exhibit enhanced performance. The potential for two alternative transparent conductive oxide (TCO) materials, Indium titanium oxide (ITiO) and indium zinc oxide (IZO) was investigated. ITiO can be fabricated with approximately twice the conductivity of ITO, which is the most commonly used TCO at present. IZO has conductivity between that of ITO and ITiO, and can be deposited at temperatures as low as 200ºC. Investigations using the Kelvin Probe technique show a systematic increase in work function as the indium content of the IZO is increased. Work functions for ITiO are largest where conductivity is the greatest. Having high work functions in TCOs reduces the drive voltage required for the device and allows for higher photovoltages to be produced in solar cells. IZO and ITiO are potentially better TCOs. Researchers again employed the Kelvin Probe technique to characterize films of the conducting polymer poly(ethylenedioxythiophene) (PEDOT) that have been deposited through either spin coating or ink-jet printing. Ink-jet printing is a technique that is better suited for industrial-scale film deposition, since there is no loss of material during the printing process, and the material can be deposited with micron scale spatial resolution. Results indicate that ink jetting produces lower work functions than spin coating. Researchers are currently investigating the effects of varying the solvent of PEDOT. Preliminary measurements have shown this to be an important parameter in determining the properties of the printed film.

Vacuum Chamber Pressure Optimization for the Muon-to-Electron Conversion Experiment (MECO). *ANDREW MCUMBER (Binghamton University, Binghamton, NY 13902) WILLIAM MORSE (Brookhaven National Laboratory, Upton, NY 11973).* The term MECO describes the multidisciplinary experiment of finding a rare, symmetry-violating process (RSVP). The strict conversion of a muon particle into an electron is of great interest to high-energy physicists, as it is a prediction of Supersymmetry Theory. To meet the challenge of sensing this minute interaction, key components of the reaction chamber must be optimized, with regard to efficiency and cost. While desiring an optimum record of such processes, excessive levels of interference from ambient particles serve to inhibit the obtainment of crucial data. Thus, in observing this elusive effect within the detecting apparatus, a partial vacuum chamber is used. It is in this arena where human factors come into play, as costs are considered. To achieve a maximally evacuated chamber, while acknowledging financial constraints, an analysis of the trajectories at hand becomes necessary. The Maple 9.5 mathematical utility is well suited for the MECO case. Access to its vast collection of functions allows for the plotting of muon paths (pre-reaction). Two material mediums in the reaction center, standard atmosphere and carbon hexafluorane (CF_6), both at a variety of pressures (P < 1 atm), are studied for their energy-reducing effects upon the leptons. Initially, adiabatic systems are considered, at first with a constant B-field along the z-axis, and then with a field that decreases in strength with approximate linearity. Finally, gas characteristics are added to the algorithm. Ultimately, the investigation gives forth the most cost-effective vacuum pressure for the experiment.

Beam Aborts in PEP-II Rings and Lingering Drift Chamber Currents. *NICOLETTE MESHKAT (University of California, Berkeley, Berkeley, CA 94709) THOMAS GLANZMAN (Stanford Linear Accelerator Center, Stanford, CA 94025).* The BABAR detector at Stanford Linear Accelerator Center was designed to study CP-violation in B-meson decays from electron-positron collisions in the PEP-II electron-positron storage rings. Background radiation in the High Energy Ring (HER) and Low Energy Ring (LER) of PEP-II has the potential to damage the sensitive equipment in the BABAR detector. As a result, the beams in the HER and LER can be aborted to prevent such damage. In the span of a few microseconds, the HER and LER currents drop from, for example, 1450 micro Amps and 2300 micro Amps, respectively, to zero. At this time the voltage in the Drift Chamber is rapidly ramped down from a potential of 1930 V to a safe potential of 800 V, thus we would expect the currents in the Drift Chamber to quickly go to zero once the beams are aborted. However, we observe an average 15 second delay in the measured time it takes for all current in the Drift Chamber to fall below 1 micro Amp. This delay has been hypothesized as an instrumentation issue and not as a physical phenomenon. The specific sources of this error are still not completely known, but analysis suggests that it results from the interplay of the CAEN High Voltage supplies and the EPICS system and/or limitations within those systems.

Testing and Debugging of Sector Crossing Trigger Modifications on the MT2A Trigger Board at E949. *DANIEL MINER (Brandeis University, Waltham, MA 02454) GEORGE REDLINGER (Brookhaven National Laboratory, Upton, NY 11973).* E949 is a rare kaon decay experiment designed to measure the magnitude of the matrix element V_td in the CKM quark mixing matrix in weak interactions. Recently, an upgrade to a component of the lowest level trigger used in the experiment, known as MT2A (for Meantimer levels T and 2, revision A) was made to increase the acceptance rate of the experiment by introducing the acceptance of sector-crossing events in the T and 2 layer detector arrays. The work done during the course of the project included the testing of the logic and the timing of the three new logic modes introduced by the upgrade as well as the original mode. It also included making any necessary repairs to the board when problems were discovered in the testing process. In the course of the testing, it was determined, after a few repairs, that all the logic modes were fully functional, and the system timing was, depending on the logic mode, either within operational parameters, or able to be made to be so through the use of a minimal amount of time trimming cables.

Building and Analysis of the First Octant of the Octagonal Detector for the G0 Backward Angle Measurement. *RYAN MONSON (Central Michigna University, Mount Pleasant, MI 48859) DAVID GASKELL (Thomas Jefferson National Accelerator Facility, Newport News, VA 23606).* The G0 backward angle measurements measure the elastic scattering of electrons off both hydrogen and deuterium targets at backward angles. In order to isolate the elastic electrons from other scattered particles (such as inelastic electrons and pions), three types of detectors are needed: Focal Plane Detectors (FPD), Cryostat Exit Detectors (CED), and Aerogel Cherenkov Detectors (Cherenkov). Due to previous G0 measurements, the FPDs are already mounted on a detector frame, but a new frame is needed to house the CEDs and the Cherenkov. This frame will attach to the FPD frame for the backward angle measurements. The G0 detector was designed in an octagonal structure with a separate frame for each octant. This project focuses on the construction of the first octant built for the backward angle measurements. In this project, the first octant was built, methods of construction were determined, tools that could be used in the construction of the frame were manufactured and tested, and design schematics were modified. As the first backward angle octant was constructed, each step was analyzed and adjusted so the detectors are aligned correctly relative to the electron trajectory. The exterior frame was built first. Then a box was made to house the CED scintillators in their proper alignments. This box was placed precisely in the frame. The CED scintillators were glued to light guides, which were in turn glued to photomultiplier tube adaptors. Once the CED box was put in place and the light guides were glued to the scintillators, the Cherenkov was filled with aerogel and placed in the frame. While the first frame was being built, construction methods for the remaining seven octants were being determined. Tools that could be used in the construction of the remaining octants, including measurement tools designed to place the CED box in the correct location within the frame, were being manufactured and tested. Design schematics were being modified, including a modification to the dimensions of the CED box that came about when the CED box and the Cherenkov box were placed in the frame and found to interfere with each other spatially. Using all of the design modifications, tools, and construction methods that resulted from building the first octant frame,

the remaining seven octant frames can be constructed quickly and precisely.

Parallelization and Optimization of the EMIR4 Code. *RYAN MOORE (Georgia Institute of Technology, Atlanta, GA 30332) MARK CARTER (Oak Ridge National Laboratory, Oak Ridge, TN 37831).* The Variable Specific Impulse Magnetoplasma Rocket (VASIMR) concept creates thrust by accelerating ionized gasses through magnetic and electric fields. A helicon antenna produces plasma that is further heated by electromagnetic waves at the Ion Cyclotron Range of Frequencies. The fortran95 EMIR code simulates the underlying physics behind the plasma rocket. It is aiding in the design of a Radio Frequency (RF) antenna that maximizes heating efficiency. EMIR solves Maxwell's equations over the domain by setting up a large system of algebraic equations in a complex, ill-conditioned, and non-symmetric matrix that is solved using the Multifrontal Massively Parallel Sparse direct solver (MUMPS). The remainder of EMIR will be sped by further using the same Message Passing Interface (MPI) that MUMPS uses. EMIR was analyzed to determine where further parallelization would be most effective. Each part of the code was subjected to scaling studies by varying grid size and resolution to show memory usage, time elapsed, and resolution-specific errors. This information was used in debugging and deciding which sections to parallelize using MPI. Initial tests revealed the minimum effective grid size to be approximately 0.10 cm radially and 1.02 cm axially. Under these boundary conditions, the building of the matrix was the slowest part of the serial code. An MPI test program was developed that mimics the build matrix section of the EMIR code. Timing and memory studies on this test program showed that MPI would improve speed and distribute memory usage. The MPI test program divides blocks of the matrix between the different processors, packs those blocks into buffers, and has the master gather the slaves' buffers into its own. The master then reassembles the matrix into its intended form. The buffers are flexible to allow for different numbers of equations and various sizes of matrix components. MPI is not effective when the matrix build is fast (under 0.5 seconds) because the overhead of initializing MPI outweighs the time saved by splitting up the matrix. For lengthy matrix builds, MPI reduces time greatly and distributes memory usage. This will be an important implementation in the EMIR4 code. Making EMIR4 more parallel will allow the VASIMR rocket to be modeled on a broader range of computer architectures with greater grid size, resolution, and accuracy. The scaling studies involved made EMIR more robust by identifying errors that were promptly debugged.

Viability of Confined Magnetic Radiation Shielding for Human Mars Mission. *MICHAEL MOORE (College of the Redwoods, Eureka, CA 99501) STEPHEN GOURLAY (Lawrence Berkeley National Laboratory, Berkley, CA 94720).* The possibility of a human mars mission is greater than ever after the successes of the two robotic rovers and the discovery of tantalizing evidence that water once existed on the red planet. Among the many problems to overcome while traversing the inner solar system on a voyage to Mars is how to best shield future astronauts from the onslaught of radiation found in interplanetary space. The effects of ionizing radiation are well studied at low LET (linear energy transfer), but for the highly charged particles with high kinetic energy (very high LET) very little is known about the risk to humans. It is clear from measurements taken by several science instruments that interplanetary space contains more radiation than current shielding technologies can handle. Consisting mainly of protons, the radiation environment is most dangerous due to positive ions from solar particle events and galactic cosmic radiation. The kinetic energy of these ions varies from 2 keV to 1020 eV. By plotting the radius of curvature of charged particles through a constant magnetic field against kinetic energy and strength of field it is shown that a large part of the most dangerous ions will pass through even the strongest magnetic field producible using Superconducting NbTi.

Spin Dependence in Proton-Proton Elastic Scattering at Relativistic Heavy Ion Collider (RHIC). *DAVID MORSE (University of Rochester, Rochester, NY 14627) WLODEK GURYN (Brookhaven National Laboratory, Upton, NY 11973).* The pp2pp experiment, which finished taking data in May of 2003 at Brookhaven National Lab at the Relativistic Heavy Ion Collider, is investigating the spin dependence of elastic proton-proton collisions at the center of mass energy range 50 < vs < 500 GeV. Because an elastic collision is one where the sum of the momenta of the outgoing protons is zero, the scattering angles F of the two protons are equal and have opposite signs, with the partial components Fx , Fy and Fz following the same relationship. The experiment is in the final stages of analysis. To this end, software must be developed to understand the data. My task is to develop and implement various C++ programs in ROOT, an object oriented data analysis framework. These programs have two main applications. The first is the development of software to determine the spin asymmetry An. Spin asymmetry arises from an electromagnetic interaction between the protons and an interference term from a hadronic interaction, which has never before been measured experimentally at these energies. The errors on these results must also be calculated very carefully, taking into account all possible systematic errors in the experiment. This leads to the other main application, which is to determine which events are truly elastic, thus minimizing the error due to background noise. A useful way to achieve this is to produce a visual aid for reconstructing events. For this I developed an Event Display program, which recognizes and displays the data points on the Si strip detectors. This not only lets us discriminate between elastic and background events, but also helps in understanding the background events themselves. More error analysis will be done by changing parameters in the analysis and examining how the results change. We will not be ready to obtain the final results until all the possible errors have been accounted for.

High Resolution X-Ray Spectroscopy with a Microcalorimeter. *JOHANNES NORRELL (Birmingham-Southern College, Birmingham, AL 35209) IAN M. ANDERSON (Oak Ridge National Laboratory, Oak Ridge, TN 37831).* Energy-dispersive spectrometry (EDS) is often the preferred choice for X-ray microanlysis, but there are still many disadvantages associated with EDS, the most significant of which is the relatively poor energy resolution, which limits detection sensitivity and the ability to distinguish among closely spaced spectral features, limiting even qualitative analysis. A new type of EDS detector that operates on the principle of microcalorimetry has the potential to eliminate this shortcoming, reaching resolutions an order of magnitude better. The detector consists of an absorber in thermal contact with a transition edge sensor (TES). An X-ray from the specimen hits the absorber and manifests itself as a change in temperature. Because the system is kept at 80 mK, the heat capacity is low and the temperature spike is observable. The TES responds to the increase in temperature by transitioning from its superconducting to its normal conducting state, thus sharply raising the overall resistance of the circuit. The circuit is kept at a constant voltage, so the increase in resistance is manifested as a decrease in current flow. This decrease in current is measured by a superconducting quantum interference device (SQUID), and by integrating the current over time, the energy of the incident X-ray is determined. The prototype microcalorimeter was developed by NIST, and this technology is now available commercially through a partnership between Vericold Technologies and EDAX International. ORNL has received the first of these commercial microcalorimeters in the United States. The absorber in this detector is gold, and the TES consists of a gold-iridium bilayer. It is designed to offer spectral resolution of 10-15 eV at a count rate of ~150 s^{-1}. The goal of this project was to analyze and document the performance of the detector, with particular attention given to the effects of an X-ray optic used to improve collection efficiency, the multiple window system and any other sources of spectral artifacts. It was found that the detector is capable of distinguishing many L'Ñ and L'Ò spectral lines, with a resolution between 13 and 17 eV. It was also observed that the background has an unusual shape, and this is largely being attributed to the variable transmission coefficient of the X-ray optic. These preliminary results suggest that the microcalorimeter has a high potential for use in microanalysis, but more work to quantify its capabilities must still be done.

Aspects of Strange Particle Electroproduction. *TANYA OSTAPENKO (Gettysburg College, Gettysburg, PA 17325) M.D. MESTAYER (Thomas Jefferson National Accelerator Facility, Newport News, VA 23606).* The Hall B Physics Division at Thomas Jefferson National Accelerator Facility (JLab) uses the CEBAF Large Acceptance Spectrometer (CLAS) and offline techniques to study the strong force interaction. We specifically analyzed the reaction e p → e' K^+ Λ (1405), where Λ (1405) → Σ^- p^+ and Σ^- → (n) p^-. Physicists have assumed that Λ(1405) is a uds quark triplet, but recent analysis has indicated that Λ (1405) may consist of a kaon nucleon bound state, known as a molecular state. Comparing the decay rates of Λ (1405) to S- p+ with its decay to S+ p- will help distinguish between these two models. In order to study Λ (1405), we must reconstruct the events that occur between the initial collision between the electron beam and the target proton, and the detected particles. For our particular reaction, CLAS detects e', K+, p+ and p-, but the neutron is identified by calculating the missing mass of the reaction using the missing energy and missing momentum. From there, a neutron cut is made on the data and a p- is included to determine the invariant np- mass. We have two ways of calculating the invariant np- mass; we can use the missing momentum and missing energy as the neutron's momentum and energy or we can use the missing momentum and the accepted value to define its total 4-momentum. Intuitively, we know that using the known value of the neutron mass takes

into account prior information and places a neutron mass constraint on the data, so such results should yield a smaller error. To prove this, we compared histogram plots of the S- invariant mass using the unconstrained neutron 4-momentum and the other using the 4-momentum constrained by the known neutron mass. By inspection, one can see the difference that previous knowledge makes in the experimental width (error) of the S- mass. From our methods, we deduced that the smaller error is indeed yielded by the constrained data. This analysis is a just one step in studying Λ (1405) and it is hoped that the complete process leading back to (1405) will aid physicists in discovering the true quark structure of Λ (1405) which has been shrouded in mystery and, in turn, give physicists a more complete theory of the strong force interaction.

Using Synchrotron Light Techniques to Study a Native American Artifact: The Wolf's Head Pouch. *ANGELA PADILLA (Hunter College, New York, NY 10021) VIVIAN STOJANOFF (Brookhaven National Laboratory, Upton, NY 11973).* Hair samples of a Native American Indian wolf's head pouch were analyzed using x-ray fluorescence, small angle x-ray scattering, infrared microspectroscopy, and powder diffraction at the National Synchrotron Light Source at Brookhaven National Laboratory, Upton NY. The wolf's head pouch is one of eight Native American Indian artifacts now preserved in the armorial collections of the Skokloster Museum in Sweden. There is interest in the study of such perishable artifacts. Perishable artifacts contain cognitive components that identify a culture greater than do artifacts made of stone or bone. The Skokloster artifacts are important because they are made mostly of perishable materials. Perishable materials do not survive in the acidic soils of Southeastern Pennsylvania, in which they are believed to derive, according to Marshall J. Becker of the Department of Anthropology, West Chester University, West Chester, Pennsylvania, the owner of the samples. High lead and zinc content was detected by x-ray fluorescence. Small angle x-ray scattering, infrared microspectroscopy, and powder diffraction all showed evidence that the hairs are mammal and will be discussed. However it remains unclear from which mammal they derived. The wolf's head pouch was an intricate fabrication of a wolf's head with only the jaws confirmed to be that of a wolf. All other components were dyed and sewn on. Speculation regarding the mammal hair origin will continue to be researched.

Determining Muon Detection Efficiency Rates of Limited Streamer Tube Modules using Cosmic Ray Detector. *MAGGIE PAN (Cornell University, Ithaca, NY 14853) PETER KIM, CHARLIE YOUNG, MARK CONVERY (Stanford Linear Accelerator Center, Stanford, CA 94025).* In the Babar detector at the Stanford Linear Accelerator Center, the existing muon detector system in the Instrumented Flux Return gaps is currently being upgraded. Limited Streamer Tubes (LST) have been successful in other projects in the past, and are thus reliable and sensible detectors to use. The tubes have been assembled into modules to strengthen the mechanical structure. Before installation, numerous tests must be performed on the LST modules to ensure that they are in good condition. One important check is to determine the muon detection efficiency rates of the modules. In this study, a cosmic ray detector was built to measure the efficiency rates of the LST modules. Five modules themselves were used as muon triggers. Two z strip planes were also constructed as part of the setup. Singles rate measurements were done on the five modules to ensure that high voltage could be safely applied to the LST. Particle count vs. voltage graphs were generated, and most of the graphs plateau normally. Wire signals from the LST modules as well as induced signals from the strip planes were used to determine the x-y-z coordinates of the muon hits in a stack of modules. Knowing the geometry of the stack, a plot of the potential muon path was generated. Preliminary results on muon detection efficiency rates of the modules in one stack are presented here. Efficiencies of the modules were determined to be between 80% and 90%, but there were large statistical errors (7%) due to the limited time available for cosmic data runs. More data samples will be taken soon; they will hopefully provide more precise measurements, with 1-2% errors for most modules before installation. Future work includes systematic studies of muon detection efficiency as a function of the operating voltage and threshold voltage settings.

Intra-molecular Fluorescence Resonance Energy Transfer Within the NMDA Receptor. *DAVID PANTHER (George Fox University, Newberg, OR 97132) GALYA ORR (Pacific Northwest National Laboratory, Richland, WA 99352).* Several methods are available for studying protein-protein interactions in vitro, but only a few methods can be used in the living cell. Fluorescence resonance energy transfer (FRET) is one such method. A donor fluorophore is excited and non-radiatively transfers its energy to an acceptor. There are several ways to calculate the efficiency of the transfer, which reports the distance between the donor and acceptor, but the most reliable way is to measure it directly. To do so, one must use a CCD camera to measure donor and acceptor fluorescence intensities with direct excitation, then measure the acceptor intensity with non-direct excitation, which is the FRET image. Since spectral overlap is necessary for FRET to occur, donor and acceptor emission cannot be completely separated, therefore some donor and acceptor emission "bleedthrough" is present in the FRET image. The appropriate percentage of donor and acceptor signal must then be subtracted from the FRET image. Accurately determining the appropriate percentage is the problem addressed here. Typically, a single value is calculated for each percentage. However, since the bleedthrough was not constant as intensity varied, an equation was derived here to describe the bleedthrough of the donor and the acceptor into the FRET channel. FRET was measured between enhanced cyan fluorescent protein (eCFP) and enhanced yellow fluorescent protein (eYFP), expressed on two subunits within the NMDA receptor in HEK-293 cells. When tested, this equation performed better than single-valued bleedthrough percentages when calculating FRET.

A New Device for Relative Luminosity Measurements at PHENIX. *HARSHIL PARIKH (University of Illinois at Urbana-Champaign, Urbana-Champaign, IL 61801) WEI XIE (Brookhaven National Laboratory, Upton, NY 11973).* The PHENIX collaboration probes spin dependent nucleon structure in polarized proton collisions at the Relativistic Heavy Ion Collider at Brookhaven National Laboratory. These measurements include the study of the gluon spin contribution to the proton spin through the longitudinal double spin asymmetries which requires a precise measurement of relative luminosities. During the proton-proton run in 2002 and 2003, a beam-beam counter (BBC) was used as the relative-luminosity monitor. In future high luminosity runs, the probability of multiple proton-proton collisions per bunch crossing will be too significant to allow for accurate measurement of relative-luminosity using the BBC. We propose a new relative luminosity telescope (RLT) which consists of three layers of pad chambers and is installed in the vicinity of the beam-pipe in the PHENIX interaction region. The new instrument is expected to provide measurements with high resolution in high luminosity environment at RHIC. Monte Carlo simulations are being performed to optimize the detector configuration. The acceptance of the proposed RLT will be small enough to avoid the problem of multiple collisions per bunch crossing. The RLT is also expected to be able to determine the collision vertex through the correlation of channels in the three pad-chamber stations and thus will help to measure precisely acceptance variations as function of the collision vertex. This has been one of the major uncertainties in measuring the relative luminosity in the previous runs.

Study of a Direction Sensitive Photo-Sensor. *ZACH PARSONS (University of South Dakota, Vermillion, SD 57069) MILIND DIWAN (Brookhaven National Laboratory, Upton, NY 11973).* A charged particle traveling through a medium will polarize the medium creating radiation. If the speed of the particle is greater than the speed of light in that medium, the radiation is emitted as a coherent wave front known as Cherenkov radiation. The photons all have the same angle with respect to the direction of the particle. This radiation is similar to the sonic boom heard from supersonic aircraft. This Cherenkov radiation can be detected by photo sensors to understand properties of the charged particles. Today's large water Cherenkov detectors, like Super Kamiokande in Japan, use photomultiplier tubes (PMT's) to detect the photons. In this report, we studied a new kind of photo detector, a direction sensitive PMT, which uses a lens to transfer the incident photon angle to a position on a detecting surface. We have studied a basic wide angle lens design. The lens was altered to make it cost effective, while at the same time efficient. The resolution of the lens was relaxed in exchange for the tightening of several other parameters. The parameters that were studied included lens thickness, image plane area, system aperture, and distance from lens to image plane.

Cooling the Linear Radio Frequency Quadrupole (RFQ) Trap for More Efficient Ion Transfer at the Canadian Penning Trap. *ILANA PERCHER (Oberlin College, Oberlin, OH 44074) GUY SAVARD (Argonne National Laboratory, Argonne, IL 60439).* High-precision mass measurement at the Canadian Penning Trap (CPT) relies upon the work of two traps, the first of which is a linear radio frequency quadrupole (RFQ) that collects, cools, and stores ions for ejection into the second Penning, trap. This paper describes the role of the RFQ trap at the CPT and its redesign for operation at cryogenic temperatures for improved efficiency. A simple heat transfer model is discussed, as are changes to part geometry and material in order to minimize heat transfer and achieve the desired temperature gradient.

Detection of Galaxy Clusters with the XMM-Newton Large Scale. *JOSEPH PIACENTINE (California State University Chico, Chico, CA 95929) PHIL MARCHALL (Stanford Linear Accelerator Center, Stanford, CA 94025).* For many years the power of counting clusters of galaxies as a function of their mass has been recognized as a powerful cosmological probe; however, we are only now beginning to acquire data from dedicated surveys with sufficient sky coverage and sensitivity to measure the cluster population out to distances where the dark energy came to dominate the Universe's evolution. This project uses the XMM X-ray telescope to scan a large area of sky, detecting the X-ray photons from the hot plasma that lies in the deep potential wells of massive clusters of galaxies. These clusters appear as extended (not point-like) objects, each providing just a few hundred photons in a typical observation. The detection of extended sources in such a low signal-to-noise situation is an important problem in astrophysics: we propose to solve it by using as much prior information as possible, translating our experience with well-measured clusters to define a ''template'' cluster that can be varied and matched to the features seen in the XMM images. Using analysis code, that can be straightforwardly adapted to this problem: the template was defined, and then the method applied to real XMM data. Presented are the findings based on the the software's ability to distinguish astronomical objects in a series of test runs and finally on real XMM data. The results of these series of experiments suggests a level of confidence for the software to be used in future eandevors to indentify clusters.

Commissioning of New Hybrid Calorimeter and Associated Data Acquisition System for the Primakoff Experiment. *DANIEL POMEROY (University of Massachusetts Amherst, Amherst, MA 01003) DAVID LAWRENCE (Thomas Jefferson National Accelerator Facility, Newport News, VA 23606).* The hybrid calorimeter (HYCAL) constructed for the Primakoff Experiment at Thomas Jefferson National Accelerator Facility has a completely unique design. It consists of an outer layer of lead-glass detectors that surround an inner layer of high-resolution lead-tungstate ($PbWO_4$). It will be used to measure photons produced by the decay of a neutral pion (π^0) particle created via the Primakoff effect, in order to reconstruct the π^0 lifetime. Because HYCAL and its associated data acquisition system (DAQ) have yet to be used in actual experiments, it is important to test the capabilities of each. In this study, we verified the functionality of HYCAL and investigated the live time properties of the associated DAQ. For HYCAL a measurement of a well-established value, such as the lifetime of a muon (μ) particle, was used to verify the functionality of the detector. The most recent study of the μ lifetime measured the value to be 2.197078 $\pm$ 0.000073 μs (Bardin, 1984), and the world average is 2.19703 $\pm$ 0.004 μs (Eidelman et al., 2004). By setting a somewhat simplistic trigger, we were able to use HYCAL to make a measurement of the μ lifetime. Our measured value is 2.1 $\pm$ 0.7 μs. In the case of the DAQ, it is important to know how a loss of live time due to increased event rate and size affects the output data rate. To do this, the maximum data rate, which could be read out without significant loss in live time, was measured for three separate situations. The first involved a full readout of every channel while varying the trigger rate. In the second case, the number of channels read out was varied while the trigger rate was kept constant. Finally, the DAQ was set to read out 100 channels, the approximate event size produced by the decay photons of the π^0, while the trigger rate was varied. In all three cases, the maximum data rates could be achieved with a minimum live time of 90%. The agreement in measurement of the μ lifetime to previously measured values shows the effectiveness of the HYCAL detector. In addition, the live time analysis of the DAQ showed the live time to be stable for values above 90%. It was also shown that the DAQ system could operate above this limit with the expected run conditions for the Primakoff Experiment. These two results are good evidence that the new detector will be effective in a high precision measurement of the π^0 lifetime.

A Scintillating Possibility. *THOMAS RAND-NASH (University of California, Berkeley, Berkeley, CA 94720) BOB JACOBSEN (Lawrence Berkeley National Laboratory, Berkley, CA 94720).* Accurate neutrino-nuclei cross sections are critical for understanding the dynamics of supernovae collapse. Further, supernovae models based on current cross section estimates have been unsuccessful in predicting the abundances of heavy elements produced during these events. To address these concerns, a new detector is required. The goal of the group is the selection of materials for, and construction of, prototypes for this detector. Several scintillating calorimeter paddles are constructed using sheets of solid scintillator, wavelength shifted optical fibers, and photomultiplier tubes. All aspects of the designs are explored, from electronics configurations, to data analysis methods, in an effort to understand the system while maximizing its function. The optimal configuration will resolve energies up to several hundred MeV, and will serve as the prototype for a segemented, upgradeable, and portable detector to be housed at the Spallation Neutron Source at Oak Ridge National Laboratory. Ultimately, the detector will be able to search for neutrino oscillations, measure the neutrino-proton scattering cross sections, and measure neutrino-nucleus cross sections.

Calibrating a Zeeman Slower to Search for the Electric Dipole Moment of Radium-225. *NATHAN RASSI (University of Illinois at Urbana-Champaign, Urbana, IL 61820) ELAINE SCHULTE (Argonne National Laboratory, Argonne, IL 60439).* The violation of time-reversal symmetry is a fundamental issue in particle physics related to the Standard Model. Time-reversal symmetry prohibits a permanent non-zero atomic Electric Dipole Moment (EDM). The discovery of a non-zero atomic EDM would indicate an explicit violation of time-reversal symmetry. EDM is measured with a laser after the atoms have been slowed and trapped. The atoms are slowed with a laser and a Zeeman slower, which must be calibrated to the specific atom, in this experiment Radium-225. The Zeeman slower was calibrated by taking spatial magnetic maps of the Zeeman slower and comparing them to the desired fields. Consistency and reproducibility tests were also done on the Zeeman slower. The desired fields were achieved, and the Zeeman slower passed the consistency and reproducibility tests. The calibration was successfully completed, and the Zeeman slower is ready to slow Radium-225 atoms to permit their EDM to be measured.

Photomultiplier Calibration for Measuring Proton Extinction Rate for KOPIO Experiment. *BLENDELL REGISTER-WHEATLE (Broward Community College, Davie, FL 33314) CAROL SCARLETT (Brookhaven National Laboratory, Upton, NY 11973).* As part of the KOPIO Beam Monitor, small Photo Multiplier Tubes(PMTs) were calibrated so that they could be used in proton extraction rate measurements. In analyzing the response of the PMT's, two different studies were done. The first was the single photoelectron response of the PMTs; then a high voltage scan study was conducted. Two additional sources were also measured and recorded for comparison. The findings based on the study of single photoelectrons showed that both PMTs produced a gain of about 5×10^6 with a high voltage setting at 1400. Also the findings showed that the Ruthenium source produced 7 photoelectrons and 0 for the cosmic rays.

Testing of High-Resolution Si and Ge Analyzers for X-ray Emission Spectroscopy and X-ray Raman Scattering. *KEVIN REYNOLDS (Norfolk State University, Norfolk, VA 23504) UWE BERGMANN (Stanford Linear Accelerator Center, Stanford, CA 94025).* A project at Stanford Linear Accelerator Center (SLAC) is currently underway for the building of a new multi-crystal x-ray spectrometer that will be used to probe the fundamental structures of light elements, including water, as well as 3d transition metals, such as metalloproteins, in dilute systems. Experimentation for determining the focal lengths for the prospective high-resolution, spherically-curved silicon (Si) and germanium (Ge) analyzers for the instrument and the energy resolutions at their respective focal points is described in this paper. The focal lengths of the Si and Ge analyzers being sampled are found by minimizing the focal size made from a diffused helium-neon (HeNe) gas laser operating at 632 nm (0.95 meV). Afterwards, the energy resolutions are determined by using synchrotron radiation (SR), in the range from 6-16 keV energies. The experiments were performed at Beamline 10-2 at the Stanford Synchrotron Radiation Laboratory (SSRL), a division of SLAC. This data, along with the energies of the incident beams, is used to determine which samples are most effective at focusing x-rays to the highest spatial and energy resolution. Sample Si (440)A, with a focal length of 1015.2 mm, is concluded to have the best energy resolution. Furthermore, a new multi-crystal goniometer was tested and commissioned. As part of this work, the device was prealigned into Rowland geometry, in order to facilitate the process of finding a single high-energy resolution x-ray focus for all 7 analyzers.

Let There be (More) Light: Modeling Superconducting Magnets to Optimize Luminosity for Large Hadron Collider (LHC). *RAPHAEL ROSEN (Harvard University, Cambridge, MA 02138) STEVE GOURLAY (Lawrence Berkeley National Laboratory, Berkley, CA 94720).* Realizing luminosity levels necessary to operate the Large Hadron Collider (LHC) at maximum potential requires sharp advances in the development of superconducting magnets. The larger the aperture of a magnet, the greater the luminosity—the number of collisions per second per cross section. Larger apertures, however, decease the gradient—an essential parameter for steering beams. Our group modeled magnetic fields of quadrupole magnets, considering Nb_3Sn and NbTi cables. We generated a plot of gradient as a function of magnet bore radius to determine how large one could construct a magnet without making the gradient

flag too abruptly. The model we used employed a theoretical framework to describe magnetic field as a function of current, while it applied empirical equations to describe the current's dependence upon field. We used Mathematica 5.0 to solve these two functions of one another. The ultimate, most accurate gradient model used four thick rings of superconducting cable. As expected, we found that Nb_3Sn at 1.8 K had the highest gradient of our materials, though we were surprised to learn that the curves were not linear, but instead resembled a 1/x graph. Experimental measurements of gradient for Nb_3Sn matched our plot well, though our field values appeared high when compared with our older lab data, but not so high when compared with our latest research. Predictions we made for NbTi matched existing data well, lending credence to the accuracy of our model's theoretical component. Future research might look to improve the empirical formula for Nb_3Sn. Additionally, physicists can, when given a necessary gradient, use our plot to determine the maximum possible bore radius, clearing the way for a new breed of magnets that may achieve still greater luminosities.

Analysis of Wire Tracking Algorithms Through Use of Simulated Data. *KENNETH ROSSATO (University of Maryland, College Park, MD 20742) OLE HANSEN (Thomas Jefferson National Accelerator Facility, Newport News, VA 23606).* Hall A of the Continuous Electron Beam Accelerator Facility (CEBAF) at Jefferson Lab (JLab) employs two high resolution spectrometers (HRS) to examine the dynamics of nuclear interactions. Tracking information for each HRS is provided by two vertical drift chambers (VDC), each a sealed box with two perpendicular planes of 368 parallel sense wires, filled with an easily ionizable gas. Particle travel through a VDC causes electrical signals on nearby sense wires, which can be interpreted by data acquisition equipment and analysis software to reconstruct the track. A computer program was written and used to simulate VDC data, which can then be interpreted by a specially modified version of the analysis software. From this data, many attributes of the track reconstruction algorithm can be tested, including accuracy, precision, and efficiency. Flaws can be found quickly and accurately as reconstructed tracks are compared against the simulated originals. Using this method, the current ROOT-based analysis software used by Hall A successfully reproduced over 99.9% of a series of 5000 test tracks, yielding a mean theta and phi in the detector plane that were consistent with the original simulated data. The simulator package (simulator program and modifications to the Hall A analyzer) is now ready to be used in tests of track reconstruction algorithms. Future plans include modifying the simulator to introduce noise and spurious tracks, testing the ability of the analyzer to reconstruct tracks efficiently. Futhermore, an older track reconstruction algorithm, used by ESPACE, will be reimplemented in C++ and tested as well. The performance of this ESPACE-based algorithm may expose further flaws or strengths in the ROOT-based algorithm and give direction for further work on the analyzer.

Analysis of Beam Position Monitor Data for the Spallation Neutron Source Using Various Statistical Methods. *ARIEL RUFFIN (Tennessee State University, Nashville, TN 37209) THEO YEBUAH (Tennessee State University, Nashville, TN 37209) TED WILLIAMS (Oak Ridge National Laboratory, Oak Ridge, TN 37831) GEORGE DODSON (Oak Ridge National Laboratory, Oak Ridge, TN 37831).* The use of the Spallation Neutron Source (SNS) accelerator will soon provide an instrument to investigate stronger, lighter and cheaper materials for scientific research and industrial development. The SNS Linear Accelerator (Linac) is used to accelerate negatively charged hydrogen ions (H^-) for the purpose of generating intense beams of neutrons from a mercury target. One challenge of the SNS is to maintain the alignment of the H^- pulsed beam through the Linac. As the H^- pulsed beam travels through the Linac there are M number of Beam Position Monitors (BPM) to determine the vertical and horizontal movement as well as the phase and amplitude of the beam. The results obtained from the use of histograms, Gaussian plots, and a technique called Singular Value Decomposition (SVD), will be closely examined to determine the beamline motion resolution. Histograms and Gaussian plots were cross referenced with each other to determine if there was a deviation in the beam's centroid motion which could be due to correlated or uncorrelated events. SVD was employed to separate the system and diagnostic properties needed to accurately analyze the beam centroid motion. The preliminary results obtained from the SVD analysis can be correlated with the ion pulse beam parameters and machine properties to serve as a diagnostic tool for characterizing the dynamic beamline motion in the Linac.

A Simulation Study for a Prototype of a Multipurpose Segmented Neutrino Detector. *LESLIE SANFORD (Southern University A&M College, Baton Rouge, LA 70813) A. R. FAZELY (Lawrence Berkeley National Laboratory, Berkley, CA 94720).* We report Monte Carlo simulation studies of a small one-ton fine segmented detector with plastic scitinllator strips and x-y scintillating fibers for tracking. The Monte Carlo simulation is designed to simulate low energy neutrino interactions within a volume of one cubic meter. All Monte Carlo calculations were performed using Geant-3.21 code. The purpose of this research is to study the properties of low energy neutrino interactions. The segmented detector is capable of fine sampling and calorimetry in order to perform measurements of energy and momentum with good resolution for low energy neutrino interactions. The detector is composed of alternating planes of thin plastic scintillator and tracking devices. These planes are of sufficient height and width to allow full calorimetry of Michel electrons. The detector could serve as a prototype for a larger 200 - ton detector to search for neutrino oscillations, measure neutrino-proton scattering cross sections, search for rare decays of po and h and measure neutrino nucleus interaction cross sections, all of interest to nuclear, particle and astrophysics.

Development of ORBIT Data Generation and Exploration. *GEOFFREY SHELBURNE (Augsburg, Minneapolis, MN 55454) KESHAVAMURTHY INDIRESHKUMAR (Princeton Plasma Physics Laboratory, Princeton, NJ 08543).* In the evaluation of particle confinement and diffusion in Tokamak plasmas, it is desirable to approach the problem in terms of the guiding center of particle orbits. The ORBIT code is a dynamic numerical code, written in Fortran 90, which integrates the Hamiltonian equations of the guiding center motion for particles. Previously, ORBIT used the National Center for Atmospheric Research (NCAR) graphics package and did not produce data files that were accessible after processing. This was problematic and did not allow comparison of ORBIT configurations or adaptation for more flexible visualization software. Different configurations of ORBIT access different subroutines and variables, therefore a dynamic subroutine capable of differentiating between the various configurations was necessary. We replaced NCAR graphics calls with a subroutine that stores all resulting data from each run in a binary network common data format (netCDF) file using the easy CDF (ezCDF) libraries. During each run, the variables' data is sent to a single subroutine which determines characteristics of each data array. According to the ORBIT parameters of each run, data are labeled and stored as scalar variables, time indexed profiles, or parameter specific arrays. Data is then accessed directly by the ElVis graphics software and can be viewed in all operating systems. We examine the limitations of the previous data generating configuration as well as the updated version. We find that the newly developed data generation and exploration methods allow greater portability across platforms as well increased ability to explore data generated from various ORBIT configurations. The netCDF format allows greater accessibility, flexibility, and smaller file sizes than ASCII format data. Future work will focus on simplifying the code and moving away from the use of the ezCDF libraries, which are only capable of storing arrays of 3 dimensions or less.

Asymmetries of a Ponderomotive Potential Near Resonance. *DAVID SIEGEL (Cornell University, Ithaca, NY 14853) NATHANIEL FISCH (Princeton Plasma Physics Laboratory, Princeton, NJ 08543).* Ponderomotive forces with spatially varying magnetic fields have previously been predicted at Princeton Plasma Physics Laboratory as useful for current drive in a plasma. However, it is difficult in practice to impose a spatially varying magnetic field sufficiently localized to produce high efficiency. To overcome this limitation, a new idea was proposed, namely, the possibility of creating the current drive with the sharp spatial variations in the electric field. The predictions of this new implementation of the ponderomotive current drive effect were then checked numerically. The differential equations governing single particle motion were found, and solved computationally with Matlab pre-programmed ODE solvers and finally a simple fourth-order Runge-Kutta algorithm in the significantly faster C++ programming language. The case of a two-Gaussian potential was examined. The possibility of unidirectional particle transmission through regions of high ponderomotive potential was hypothesized as a current generating mechanism in this configuration. While results often conform to expectations, particles have been observed to become trapped in potential wells, which can result in excessive heating. A higher transmission rate than expected (up to 90%) has also been indicated over a range of parameters, creating more of a simulated current than expected. The parameters that result in these high transmission rates also result in low trapping probabilities. Future work will need to be done to explore this relationship and to determine the exact mechanism for these higher transmission rates.

VbnlTrak: An Interactive Graphical Post Processor for the TriComp™ Particle Accelerator Modeling Suite. *ANDREW SIEMION (Sierra College, Rocklin, CA 95677) AHOVI KPONOU (Brookhaven National Laboratory, Upton, NY 11973).* We present the development of the application VbnlTrak, an interactive graphical post-processor

for some components of Field Precision's TriComp 2D™ suite of finite element (FE) electrostatic and magnetostatic field solution and charged particle orbit tracking programs. Although the TriComp suite produces accurate data, the visualization components, which perform functions such as graphing of electric equipotential lines, plotting of particle trajectories and graphical labeling of solution space components, lack certain features that the Brookhaven Preinjector Group's electron beam ion source (EBIS) team would like to have access to. VbnlTrak serves as an alternative post-processing tool to VTrak, one of the visualization routines distributed with the TriComp suite. The plotting process has been streamlined to allow the complete configuration of plot characteristics before plotting is explicitly executed. Several new plot types have been added which allow the display of axial electric potential, axial magnetic field magnitude, and beam emittance. In addition, a full range of customization options have been added which allow the user much improved control over plot style, annotation and inclusions. New output options, including additional file export selections and the integration of a common windows print dialog have also been added. The user now has the ability to overlay any and all plot types onto a single graph, and all plot components have been made interactively resizable via the implementation of a graphical windowing/layering system. VbnlTrak was written for the Windows environment using a combination of Compaq Visual Fortran and the Winteracter Graphics Libraries. Here we describe the upgrades and additions instituted in VbnlTrak. Selected mathematical and geometric methods used to interpret TriComp solution files and visualize conformal mesh FE data are detailed. Illustrations of the program interface and labeled sample plots are included.

Developing of Software for Calculating the Ionization Cross-sections and Simulating Evolution of Ionic Charge States in an Ion Trap. *PARMINDER SINGH (Monroe Community College, Rochester, NY 14623) ALEXANDER PIKIN (Brookhaven National Laboratory, Upton, NY 11973).* My activity was related to modifying the existing and writing new software for simulating charge states distribution of ions confined within the electron beam. The existing program SUK was limited to 10 elements and was not able to simulate a variety of elements, which BNL ion source group was planning to produce. Currently the data on ionization cross-sections are very scarce and scattered in different sources. These data are frequently needed for atomic physics analysis, especially for analysis of ionization. Therefore, developing of the program, which can calculate the ionization cross-section for different ion species and charge states were very useful for the atomic physics analysis of the group. The task: 1. Extension of the range of program SUK, which calculates dynamics of ionic charge states in the electron beam to 10 new elements. 2. Writing a separate program for calculating the ionization cross-sections of ions by electron impact for the specific electron energy. 3. Modifying this program for calculating the ionization cross-sections in a defined energy range of electrons for specified number of points.

Gas-Filled Recoil Separation of Heavy Ions at Intermediate Energies. *MATTHEW STERNBERG (University of Oregon, Eugene, OR 97403) GUY SAVARD (Argonne National Laboratory, Argonne, IL 60439).* Current capabilities for the capture of fusion products used for mass measurements at the Canadian Penning Trap are limited. The facility can only capture reaction products with a small range of angles. The setup has the ability to capture products up to 4 degrees off axis in one direction and 2 degrees off axis along the other direction. The reaction products are then separated from the primary beam by using a velocity filter. In many reactions that take place most recoil products are emitted at angles within 4 degrees of the axis. However, there are many desirable reactions where the majority of products fall outside this window. The use of a large bore solenoid magnet has been investigated as a means of capturing a larger range of recoil products. A Monte Carlo simulation was developed to model the transport of ions through a gas-filled solenoid magnet. Different means of disposing of the primary beam have also been investigated, such as using various beam stops as well as velocity filters. A method was developed in which a large range of recoil products at various energies could be efficiently separated from the primary beam. Monte Carlo simulations suggest that recoil products could be captured at angles as large as 12 degrees, improving the current efficiency by as much as 1000%.

Examining the Oxygen Isotope Effect on Phase Transitions as a Function of Temperature and Magnetic Field for $Sm_{0.5}Sr_{0.5}MnO_3^{16,18}$. *ANNE STYKA (University of Illinois at Chicago, Chicago, IL 60607) YANG REN (Argonne National Laboratory, Argonne, IL 60439).* Magnetic field (MF) dependence of the phase separation (PS) in the manganites $Sm_{0.5}Sr_{0.5}MnO_3^{16}$ and $Sm_{0.5}Sr_{0.5}MnO_3^{18}$ was studied using high-energy X-ray powder diffraction. These compounds show intrinsic inhomogeneities in the form of coexisting competing phases below a temperature Tps. The oxygen isotope effect is examined under differing applied fields and temperature raging from 4.2 to 240K. The critical temperature is about 110K from which it is apparent that above this only a single phase is present, dotted with forming particles of ferromagnetic phase. The T_{ps} varies, though slightly, as a function of the strength of the MF applied to the sample. Determining the role of the oxygen isotope effect in these manganites will provide important answers to the governing physics behind the colossal magnetoresistance effect.

Coupling Mode Locked Femtosecond Laser Pulses into Photonic Crystal Fibers. *JONAH VAN BOURG (Columbia University, New York, NY 10027) ROBERT KAINDL (Lawrence Berkeley National Laboratory, Berkley, CA 94720).* An important device in the realm of modern optics is a nonlinear interferometer - an optical array which can be used to determine the phase of a mode locked oscillated 800nm femtosecond laser operating at 80 megahertz and thereby stabilize it. To build such a device, the spectrum of the laser's gaussian pulse must be broadened in such a way that it remains collimated and intense. To do so, the infrared laser light is focused into a complex microstructure fiber, also known as a photonic crystal fiber (PCF) by using an extremely precise five axis fiber mount (~0.2 um precision). After the beam was focused into the fiber, a direct correlation between the intensity of the input gaussian pulse and the breadth of the output spectrum was observed, confirming the important formula which governs self-phase modulation in nonlinear optics.

Concepts in Wind Energy Production as Applied in a Cross-Curriculum Educational Setting. *JENNIFER VOLLMER (North Dakota State University, Fargo, ND 58105) GARY SEIFERT (Idaho National Engineering & Environmental Laboratory, Idaho Falls, ID 83415).* Trends in education today call for links between subjects, and for teaching these subjects in a hands-on, constructivist, and exciting way. Wind energy is an issue interesting to children and adults alike, and offers a link between many different fields, such as physics, environmental science, and economics, as well as providing a wealth of enjoyable inquiry-based hands-on activities. An educational unit focused on basic guidelines for these cross-curricular ideas was formed with a physics focus to help fill a gap in physics curricula where usable, age appropriate, hands-on lessons are lacking. The curriculum involves using environmental science and social perspectives initially to show students why studying wind energy is important, followed by concepts involving induction, aerodynamics, power in the wind, and how Betz's law affects wind power capture. Factors influencing the flow of wind are considered for a wind farm design, followed by an economic analysis of a real site using publicly available wind energy data. As a final project, students are asked to propose a wind farm design suitable for an energy need of their choice, whether it is a supplemental small turbine for residential needs, or a large megawatt commercial farm. The curriculum is supported by work of INEEL engineers Kurt Meyers and Gary Seifert, which involves promoting public knowledge of wind energy as a resource for rural communities and providing technical assistance in prospecting for suitable wind sites and analyzing data from wind anemometers. This data then assists landowners in making well-informed decisions on how and if to proceed in developing wind energy on their property. The data is public and used in the curriculum's final activity. The end goal of this project is to make the curriculum package available to educators nationwide as an on-line resource.

Black Hole Accretion and X-Ray Variability in AGN. *ZACHARY VOLLRATH (Clemson University, Clemson, SC 29634) GREG MADEJSKI (Stanford Linear Accelerator Center, Stanford, CA 94025).* Active Galactic Nuclei (AGN) have very luminous centers which are so bright that the surrounding stars can not adequately account for the energy emission of AGN. One of the most accepted explanations for this energy release is black hole accretion. These black holes accrete near by gas and dust, and as a result gravitational potential is converted to energy which is released. In order to probe the accretion mechanism which lies close to the black hole, short time scale X-ray variability is analyzed. The very short time scale variability will increase understanding of the processes that occur in the heart of galaxies. Data from the ASCA X-ray telescope was reduced and analyzed using the programs FTOOLS, XSELCT, and ASCASCREEN. Light curves and event lists were generated for long term observations of different AGN which were sent to collaborators for further analysis using the event time arrivals. The analysis will compare accretion and jet dominated AGN and will provide use with an understanding of how short scale time variability can relate to the mechanism very close to black holes buried within AGN.

A Decoupling Box for Spectral Readout in the Dissociative Electron Attachment of Nitric Oxide. *ALEXANDER WARKENTIN (Fresno City College, Fresno, CA 93741) ALI BELKACEM (Lawrence Berkeley National Laboratory, Berkley, CA 94720).* The Dissociative Electron Attachment (DEA) of nitric oxide (NO) will be studied with the use of a femtosecond titanium sapphire laser and a position sensitive, delay line detector with the use of micro-channel plates (MCP) to aid in the search and study of reported dissociation channels. The position and time of flight (TOF) of the O^- anions collected on a detector can be used with conservation of energy equations to determine the internal energy of the dissociated nitrogen atoms. However, One of the problems inherent to complex detection systems is limitations imposed by the presence of electronic noise. To address this problem the detector splits up the signal into two wires: one with a signal pulse and noise, and one with just noise. A high-pass filter decoupling circuit box was designed and built that allows an efficient subtraction of these contributing noise waveforms between wires. A test of the decoupling box's performance was carried out using similar noise vibrations and signal pulses. The tests show that when the time delay is set correctly between the noise and noise/signal wires from the detector's anode, that the out-of-phase noise cancels at the transformer in the decoupling box to yield a clean signal pulse that can be used in the data readout.

Experimental Setup to Characterize Various Pressurized Gases Using Ultrasonic Attenuation. *BRUCE WATSON (Columbia Basin College, Pasco, WA 99301) MORRIS S. GOOD (Pacific Northwest National Laboratory, Richland, WA 99352).* High accuracy monitoring of gas composition using ultrasonic sensors to characterize a gas or mixture of gases promises to have many benefits in cost, speed, accuracy, and flexibility for a wide range of gases and applications in the process industry. The experimental setup described will measure ultrasonic attenuation of a gas or mixture of gases at a pressure up to 3 bar using an inexpensive pressure chamber and micromachined air-coupled capacitance transducers. Polyatomic gases display a characteristic relaxation attenuation specific to the gas. Monatomic gases only display the classical attenuation characteristic. Measurements could be taken that would show these characteristics for polyatomic gases, monatomic gases, and gas mixtures. To show the proof of this concept, an experimental apparatus was assembled and measurements were acquired using argon at a pressure of 3 bar and varying the transducer separation from 0.632 in. (1.605 cm) to 7.632 in. (19.385 cm) in 1.0 in. (2.54 cm) increments. A conclusion is that this setup can measure attenuation; however a more robust, cost-effective sensor with similar broad bandwidth, sensitivity, and accuracy is required for successful commercial applications. Future work will measure attenuation of a gas and of gas mixtures. An assumption is that measured ultrasonic attenuation of a gas mixture combined with wave velocity would identify an unknown gas and the percentages of the gases.

A Search for Variable Sources in the Sloan Digital Sky Survey. *ALLISON WIDHALM (University of Southern California, Los Angeles, CA 90007) MASAO SAKO (Stanford Linear Accelerator Center, Stanford, CA 94025).* The Sloan Digital Sky Survey (SDSS) is an ambitious ongoing project, which is mapping in detail one quarter of the entire sky to study the properties of over a 100 million astronomical objects. A fraction of the sky is observed more than once, which allows us to search for transient objects (sources that vary in brightness), some of which may be associated with supernovae, afterglows of gamma-ray bursts, as well as activity of material near a super-massive black hole in a quasar. The project will involve photometric analyses of a large amount of data from the SDSS archive. Accurate photometric measurements over the entire survey area will allow us to search for transient events that occur on timescales ranging from days to years. We will identify the types of objects, and possibly execute follow-up observations with other observatories.

Characterization of Limited Streamer Tubes (LST) Z Plane Signals. *NATHANIEL WILLIAMS (Whitworth College, Spokane, WA 99251) CHARLES YOUNG, PETER KIM, MARK CONVERY (Stanford Linear Accelerator Center, Stanford, CA 94025).* The Resistive Plate Chambers (RPCs) used to detect muons in the BaBar detector are losing efficiency and are being replaced by Limited Streamer Tubes. Z planes are a component of the detector that gathers detects muons. It is desired to know how Z signals vary from across the plane. Using an Oscilloscope and Scintillator triggers, the output signals of the Z plane can be characterized at various points on the plane and analyzed. The results of this study indicate an approximate signal speed of .58c with signals decreasing in pulse height and staying constant in pulse width for strips further down the output cable.

X-Ray Reflectivity Results of Multi-layered Thin Film of Si/Cu/Permalloy/Pt/SiO_2. *TRACY WILLIAMS (Chicago State University, Chicago, IL 60628) JUSTIN AKUJIEZE (Argonne National Laboratory, Argonne, IL 60439).* Design more efficient write heads for applications in the information technology. Necessary to satisfy the condition for increasing the bit size density in magnetic disk drives. This would require increasing the anisotropy of media so that magnetic information is unaltered as a result of increase current enabling thermal stability. Goal to enhance the capability of write heads by finding materials of high magnetic permeability u , high saturation Magnetization (having high memory) and low Magnetic field remanent to enable easy transitions. This will entail making thin films of desired thickness, known compositions and structure, and of known magnetic structure, and of low surface roughness. To do this we must first find a combination of materials that will allow for a high magnetization and low anisotropy. For our work we will explore multi-layers of rare earths 4fn with high magnetization and possibly low anisotropy with transition elements 3dn of ferromagnetic characteristic. Here permalloy is a good candidate.

Setup and Calibration of SLAC's Peripheral Monitoring Stations. *ABBIE WOOD (University of New Orleans, New Orleans, LA 70148) JAMES LIU (Stanford Linear Accelerator Center, Stanford, CA 94025).* The goals of this project were to troubleshoot, repair, calibrate, and establish documentation regarding SLAC's (Stanford Linear Accelerator Center's) PMS (Peripheral Monitoring Station) system. The PMS system consists of seven PMSs that continuously monitor skyshine (neutron and photon) radiation levels in SLAC's environment. Each PMS consists of a boron trifluoride (BF_3) neutron detector and a Geiger Müller (GM) gamma ray detector together with their respective electronics. Electronics for each detector are housed in Nuclear Instrument Modules (NIMs) and are plugged into a NIM bin in the station. All electronics from each station were brought into the lab for troubleshooting. Troubleshooting usually consisted of connecting an oscilloscope or scaler at different points in the circuit of each detector to record simulated pulses produced by a pulse generator; the input and output pulses were compared to establish the location of any problems in the circuit. Once any problems were isolated, repairs were done accordingly. The detectors and electronics were then calibrated in the field using radioactive sources. Calibration is a process that determines the response of the detector. Detector response is defined as the ratio of the number of counts per minute interpreted by the detector to the amount of dose equivalent rate (in mrem per hour, either calculated or measured). For the GM detector, calibration consisted of bringing a Cs-137 source and a NIST-calibrated RADCAL Radiation Monitor Controller (model 9010) out to the field; the absolute dose rate was determined by the RADCAL device while simultaneously irradiating the GM detector to obtain a scaler reading corresponding to counts per minute. Detector response was then calculated. Calibration of the BF_3 detector was done using NIST certified neutron sources of known emission rates and energies. Five neutron sources (PuBe, PuB, PuF_4, PuLi and Cf-252) with different energies were used because BF_3 detector response is very sensitive to the energy of the incident radiation. The actual neutron dose rate was calculated by considering the direct dose rate and scattered dose rate. Once the total dose rate was known, the response vs. energy curve was plotted. The first station calibrated (PMS6) was calibrated with these five neutron sources; all subsequent stations were calibrated with one neutron source and the energy dependence was assumed to be the same.

Pressure Drop Versus Flow Rate Analysis of the Limited Streamer Tube Gas System of the BaBar Muon Detector Upgrade. *MING YI (Massachusetts Institute of Technology, Cambridge, MA 02139) CHARLES YOUNG, PETER KIM, MARK CONVERY (Stanford Linear Accelerator Center, Stanford, CA 94025).* It has been proposed that Limited Streamer Tubes (LST) be used in the current upgrade of the muon detector in the BaBar detector. An LST consists of a thin silver plated wire centered in a graphite-coated cell. One standard LST tube consists of eight such cells, and two or three such tubes form an LST module. Under operation, the cells are filled with a gas mixture of CO2, argon and isobutane. During normal operation of the detector, the gas will be flushed out of the system at a constant low rate of one volume change per day. During times such as installation, however, it is often desired to flush and change the LST gas volumes very rapidly, leading to higher than normal pressure which may damage the modules. This project studied this pressure as a function of flow rate and the number of modules that are put in series in search of the maximal safe flow rate at which to flush the modules. Measurements of pressure drop versus flow rate were taken using a flow meter and a pressure transducer on configurations of one to five modules put in series. Minimal Poly-Flo tubing was used for all connections between test equipments and

modules. They contributed less than 25% to all measurements. A ratio of 0.00022±0.00001 mmHg per Standard Cubic Centimeter per Minute (SCCM) per module was found, which was a slight overestimate since it included the contributions from the tubing connections. However, for the purpose of finding a flow rate at which the modules can be safely flushed, this overestimate acts as a safety cushion. For a standard module with a volume of 16 liters and a known safe overpressure of 2 inches of water, the ratio translates into a flow rate of 17000±1000SCCM and a time requirement of 56±5 seconds to flush an entire module.

Limited Streamer Tube Testing Module Assembly of the BaBar Muon Detector Upgrade. *BRENDA ZARATE (Dartmouth College, Hanover, NH 03755) CHARLES YOUNG, PETER KIM, MARK CONVERY (Stanford Linear Accelerator Center, Stanford, CA 94025).* It has been proposed that Limited Streamer Tubes (LST) be used in the current upgrade of the muon detector in the BaBar detector. An LST consists of a thin silver plated wire centered in a graphite-coated cell. One standard LST tube consists of eight such cells, and two or three such tubes form an LST module. The goal of this project is to assemble two fully functional small scale LST modules for testing and monitoring purposes. Two LST tubes have already been assembled and sealed, each having the same width as a regular tube, but with a length of 50cm, approximately one seventh of a regular tube. Pieces such as high voltage boxes and signal-reading electronics that are necessary for a module to fully function were added onto each tube, so that each one was made into an electrically shielded and self-contained unit. All channels of the two units were able to pick up signals from passing cosmic ray particles. The modules' small scale, easy portability, and the fact that they contain all the necessary components of normal LST modules give them a number of practical uses such as testing the composition of the gas mixtures before the gas is piped to real modules in BaBar as well as testing the effects of new gas compositions.

Science Policy

Chinese Energy Security Focus on Oil and Gas including Brief Overview of Nuclear Energy. *GONZALO GUZMAN (University of Washington, Seattle, WA 98195) KRISTI BRANCH (Pacific Northwest National Laboratory, Richland, WA 99352).* For the past several years, China's rapid economic development has necessitated increased use of energy resources in China making China for the first time a net importer of petroleum. China is currently the number two oil importer in the world, second to the U.S. China's import of petroleum has greatly influenced its current energy strategy which is linked to its current foreign policy relations. The Pacific Northwest Center for Global Security had indicated interest in assessing China's current energy strategy and its impact on the future of the US-Sino relations. The focus of my research was on China's energy strategy for the oil and gas sector. I have also assessed the status and the outlook of the nuclear sector as it stands in China's plans for achieving diversification and independence of its energy resources. In the course of my research, I have targeted literature and article research at the University of Washington libraries, met with and interviewed energy and China experts at the National Bureau of Asian Research (NBR) and solicited information from the PNNL staff. My research confirmed that in the last several years China has aggressively pursued a strategy that is aimed at self-reliance and resource and supplier diversification. The paper assesses China's pro-active foreign policy in diversifying its petroleum suppliers who range from countries like Angola, Sudan and Kazakhstan to the more traditional suppliers such as Saudi Arabia and Iran. The research also looks at creation of strategic reserves and the expansion of nuclear industry as means of attaining self-reliance. The research has demonstrated the potential conflict in foreign policy between US and China as the two major oil importers are vying for the same oil suppliers. The findings also point to the rise of potential proliferation threat as China's quid pro quo dealings with countries such as Iran and Sudan include arms trade and could potentially include trade in nuclear technology in exchange for access to oil. In all, this paper aims at educating and providing useful information to any policy maker who deals with issues of energy security and nonproliferation in China and East Asia region.

Waste Management

Caustic Side Solvent Extraction Of Radioactive Cesium From Nuclear Waste: Boric Acid As A New Stripping Solution. *MARY DITTO (Knox College, Galesburg, IL 61401) LAETITIA DELMAU (Oak Ridge National Laboratory, Oak Ridge, TN 37831).* Caustic-Side Solvent Extraction (CSSX) has been approved as the technique to extract radioactive cesium from nuclear waste being stored at the US DOE (Department of Energy) Savannah River Site. Currently, nitric acid is being used to strip the cesium from the calix[4]crown-6 ether-base solvent. This project was done to assess whether boric acid would be a more effective stripping solution. The quality of a stripping solution is determined by the corresponding cesium distribution ratio: the ratio of the total concentration of cesium extracted into the organic phase by the total concentration of cesium remaining in the aqueous phase. A very low cesium distribution ratio is required for a successful strip to provide adequate assurance that all of the cesium has been removed from the organic phase. Previous results have shown that H_3BO_3 (1 mM), after three strips, could reach a distribution ratio of 0.004. This could be a significant improvement over HNO_3 (1 mM) that exhibits cesium distribution ratios after three strips of 0.05. This project tried to confirm the stripping ability of H_3BO_3. However, these preliminary results could not be reproduced. Anions such as chloride and oxalate were also used instead of $CsNO_3$ and yet the distribution ratio for H_3BO_3 as the aqueous stripping solution never went lower than 0.0125. This did not prove to be consistent with previous results and it was determined that some dissociation must be occurring in the system raising the distribution ratio higher than was previously expected.

The Creation of a Process Flow Diagram and Mass Balance Sheet for the Remote Treatment Project. *BRAD DRANSFIELD (Brigham Young University - Idaho, Rexburg, ID 83460) STEVEN HERRMANN (Argonne National Laboratory, Argonne, IL 60439).* Creation of a process flow diagram for the Remote Treatment Project is necessary to detail the functional and all other requirements of a facility for segregation and treatment of radioactive waste. Waste needing treatment is remote handled and as so the facility will need to be shielded for the protection of the workers. A process flow diagram and associated mass balance sheet provide essential information for justification of a proposed facility and related equipment. Informational records on the waste that is stored at both Argonne National Laboratory and the Idaho National Engineering Laboratory is limited, thus limiting the accuracy of a mass balance sheet. In creating mass balance sheets for the waste many assumptions were made and great effort was taken to record how assumptions were made. The process flow diagram and mass balance content are bases on the best available information. Taking into account the types of assumptions and the lack of hard facts about the waste contents the information collected is meant to only be used as rough estimates. It is believed that the only way to definitively know the volumes and masses of waste streams is to open, segregate, and repackage all waste containers. Such is the primary objective of the proposed facility.

Index of Authors

C

D

E

F

G

H

I

J

K

L

M

N

O

P

Q

R

S

T

U

V

W

X

Y

Z

Index of Schools

R

S

T

U

V

W

Y

PROGRAMS OFFERED BY THE U.S. DEPARTMENT OF ENERGY'S OFFICE OF SCIENCE

http://www.scied.science.doe.gov

UNDERGRADUATE RESEARCH PROGRAMS

CCI: *The Community College Institute of Science and Technology.* This internship program is open to students attending community colleges.

PST: *Pre-Service Teacher Program.* This internship program is designed for students aspiring to become K-12 science, math, and technology educators.

SULI: *Science Undergraduate Laboratory Internship.* This internship program is open to all undergraduate students attending 2 or 4 year colleges or universities.

GRADUATE AND FACULTY PROGRAMS

Albert Einstein Distinguished Educator Fellowship: This program brings K - 12 Science, Math, and Technology teachers to Washington, D.C. for a ten-month fellowship with a federal agency or legislative office.

Faculty Sabbatical Program: This program offers opportunities for faculty members from minority serving institutions to serve a half or full sabbatical doing reserach with a DOE scientist.

Faculty and Student Teams: This internship program is open to teams of college faculty members and 2 or 3 undergraduate students.

Laboratory Science Teacher Professional Development Program: This summer fellowship program is open to K-14 teachers.

OTHER PROGRAMS

Energy Research Laboratory Equipment Program: This program grants available used equipment to institutions of higher education for energy-related research.

Science Bowl: This program is a national math and science competition for teams of public and private high school and middle school students.